



SOUTHERN PLAINS
TRANSPORTATION CENTER

Characterization of Asphalt Binders Exposed to Extreme Temperatures through Simple and Effective Test Methods

Nazimuddin M. Wasiuddin, Ph.D.
Waleed B.M. Omer, M.Sc.
Zahid Hossain, Ph.D., P.E.
Mohammad Ziaur Rahaman, M.Sc.
Rouzbeh Ghabchi, Ph.D.
Musharraf Zaman, Ph.D., P.E.
Syed Ashik Ali, M.Sc.

SPTC14.1-80-F

**Southern Plains Transportation Center
201 Stephenson Parkway, Suite 4200
The University of Oklahoma
Norman, Oklahoma 73019**

SPTC/UTC Disclaimer

The contents of this report reflect the views of the authors, who are responsible for the facts and accuracy of the information presented herein. This document is disseminated under the sponsorship of the Department of Transportation University Transportation Centers Program, in the interest of information exchange. The U.S. Government assumes no liability for the contents or use thereof.

TECHNICAL REPORT DOCUMENTATION PAGE

1. REPORT NO. SPTC14.1-80	2. GOVERNMENT ACCESSION NO.	3. RECIPIENTS CATALOG NO.	
4. TITLE AND SUBTITLE Characterization of Asphalt Binders Exposed to Extreme Temperatures Through Simple and Effective Test Methods	5. REPORT DATE November 2018		
	6. PERFORMING ORGANIZATION CODE		
7. AUTHOR(S) Nazimuddin M. Wasiuddin, Waleed Mohammed Omer Zahid Hossain, Mohammad Ziaur Rahaman, Rouzbeh Ghabchi, Musharraf Zaman, Syed Ashik Ali.	8. PERFORMING ORGANIZATION REPORT		
9. PERFORMING ORGANIZATION NAME AND ADDRESS Louisiana Tech University, Arkansas State University, The University of Oklahoma.	10. WORK UNIT NO.		
	11. CONTRACT OR GRANT NO. DTRT13-G-UTC36		
12. SPONSORING AGENCY NAME AND ADDRESS Southern Plains Transportation Center 201 Stephenson Pkwy, Suite 4200 The University of Oklahoma Norman, OK 73019	13. TYPE OF REPORT AND PERIOD COVERED Final March 2014 – May 2018		
	14. SPONSORING AGENCY CODE		
15. SUPPLEMENTARY NOTES University Transportation Center			
16. ABSTRACT <p>In the ASU study, Superpave and MSCR tests were performed to evaluate viscoelastic properties of selected asphalt binders approved in Arkansas and Texas. A total of 65 binder samples were tested in the laboratory. Of these, eight were unmodified binders, 24 were PMBs, 27 were WMA-additive modified, and 6 were RAP modified binders. The non-recoverable compliance and MSCR percent recovery data of the tested binders were analyzed for grading and establishing the MSCR percent recovery criteria for local service temperature and traffic conditions. The developed guidelines are expected to be helpful for transportation agencies in Arkansas and Texas to adopt the MSCR test method in their quality control process. In the OU study, the polymer-modified binders were found to meet the Superpave® specifications and exhibited satisfactory rutting and fatigue resistance. The high- and low-temperature PG grades of the RAP binder blends were observed to increase with an increase in the RAP binder content. From the MSCR test results, the minimum %Recovery requirement based on the J_{nr} criteria suggested in AASHTO TP 70 was found to be appropriate for differentiating polymer-modified binders from non-polymer modified binders. Also, the addition of a higher stress level, such as 10 kPa to the MSCR test method, was found to help understand the nonlinear viscoelastic behavior of the polymer-modified binders. Furthermore, the J_{nr} value decreased and MSCR grades increased with an increase in the amount of RAP binder, which indicated an improved resistance to rutting for the RAP binder blends. The rutting and moisture susceptibilities of the asphalt mixes with high RAP content were found to be satisfactory from Hamburg Wheel Tracking (HWT) tests. A comparison of the Superpave®, MSCR and HWT test results is also presented in this report. In the LTU study, the extensional deformation behavior of PG binders 58-28, PG 64-22, and PG 76-22 and its parameters including geometry and temperature were investigated through an extensional rheological approach using a DSR-based Sentmanat Extensional Rheometer (SER). A test method and a sample preparation procedure for asphalt binders were developed as a replacement to the conventional force ductility test. With a more reproducible, significantly less material and time consuming, and with a more mechanistic approach, the developed novel test method can help improve the durability of modified asphalt pavements.</p>			
17. KEY WORDS Multiple Stress Creep and Recovery (MSCR), Polymer-Modified Asphalt Binder, Sentmanat Extensional Rheometer (SER)		18. DISTRIBUTION STATEMENT No restrictions. This publication is available at www.sptc.org and from the NTIS.	
19. SECURITY CLASSIF. (OF THIS REPORT) Unclassified	20. SECURITY CLASSIF. (OF THIS PAGE) Unclassified	21. NO. OF PAGES 376 + cover	22. PRICE

SI* (MODERN METRIC) CONVERSION FACTORS

APPROXIMATE CONVERSIONS TO SI UNITS

SYMBOL	WHEN YOU KNOW	MULTIPLY BY	TO FIND	SYMBOL
LENGTH				
in	inches	25.4	millimeters	mm
ft	feet	0.305	meters	m
yd	yards	0.914	meters	m
mi	miles	1.61	kilometers	km
AREA				
in ²	square inches	645.2	square millimeters	mm ²
ft ²	square feet	0.093	square meters	m ²
yd ²	square yard	0.836	square meters	m ²
ac	acres	0.405	hectares	ha
mi ²	square miles	2.59	square kilometers	km ²
VOLUME				
fl oz	fluid ounces	29.57	milliliters	mL
gal	gallons	3.785	liters	L
ft ³	cubic feet	0.028	cubic meters	m ³
yd ³	cubic yards	0.765	cubic meters	m ³
NOTE: volumes greater than 1000 L shall be shown in m ³				
MASS				
oz	ounces	28.35	grams	g
lb	pounds	0.454	kilograms	kg
T	short tons (2000 lb)	0.907	megagrams (or "metric ton")	Mg (or "t")
TEMPERATURE (exact degrees)				
°F	Fahrenheit	5 (F-32)/9 or (F-32)/1.8	Celsius	°C
ILLUMINATION				
fc	foot-candles	10.76	lux	lx
fl	foot-Lamberts	3.426	candela/m ²	cd/m ²
FORCE and PRESSURE or STRESS				
lbf	poundforce	4.45	newtons	N
lbf/in ²	poundforce per square inch	6.89	kilopascals	kPa
APPROXIMATE CONVERSIONS FROM SI UNITS				
SYMBOL	WHEN YOU KNOW	MULTIPLY BY	TO FIND	SYMBOL
LENGTH				
mm	millimeters	0.039	inches	in
m	meters	3.28	feet	ft
m	meters	1.09	yards	yd
km	kilometers	0.621	miles	mi
AREA				
mm ²	square millimeters	0.0016	square inches	in ²
m ²	square meters	10.764	square feet	ft ²
m ²	square meters	1.195	square yards	yd ²
ha	hectares	2.47	acres	ac
km ²	square kilometers	0.386	square miles	mi ²
VOLUME				
mL	milliliters	0.034	fluid ounces	fl oz
L	liters	0.264	gallons	gal
m ³	cubic meters	35.314	cubic feet	ft ³
m ³	cubic meters	1.307	cubic yards	yd ³
MASS				
g	grams	0.035	ounces	oz
kg	kilograms	2.202	pounds	lb
Mg (or "t")	megagrams (or "metric ton")	1.103	short tons (2000 lb)	T
TEMPERATURE (exact degrees)				
°C	Celsius	1.8C+32	Fahrenheit	°F
ILLUMINATION				
lx	lux	0.0929	foot-candles	fc
cd/m ²	candela/m ²	0.2919	foot-Lamberts	fl
FORCE and PRESSURE or STRESS				
N	newtons	0.225	poundforce	lbf
kPa	kilopascals	0.145	poundforce per square inch	lbf/in ²

*SI is the symbol for the International System of Units. Appropriate rounding should be made to comply with Section 4 of ASTM E380. (Revised March 2003)

CHARACTERIZATION OF ASPHALT BINDERS EXPOSED TO EXTREME TEMPERATURES THROUGH SIMPLE AND EFFECTIVE TEST METHODS

**Final Report
SPTC14.1-80**

**Nazimuddin M. Wasiuddin, Ph.D.
Waleed B.M. Omer, M.Sc.
Zahid Hossain, Ph.D., P.E.
Mohammad Ziaur Rahaman, M.Sc.
Rouzbeh Ghabchi, Ph.D.
Musharraf Zaman, Ph.D., P.E.
Syed Ashik Ali, M.Sc.**

Louisiana Tech University
Arkansas State University
The University of Oklahoma

ACKNOWLEDGEMENTS

The authors at the Arkansas State University are thankful to the Sothern Plains Transportation Center (SPTC) for providing financial support for this study. The authors sincerely appreciate suppliers of asphalt binder, reclaimed asphalt pavement (RAP), and warm mix asphalt (WMA) additives used in this study. The authors are also thankful to research partners from the University of Oklahoma and Louisiana Technological University for their technical support for this study.

The authors at the University of Oklahoma would like to express their sincere gratitude to all the staff of the School of Civil Engineering and Environmental Science and the Southern Plains Transportation Center (SPTC) for their help and support. Special thanks are extended to Mr. Michael Schmitz (Mike) for his technical support in the laboratories. The authors want to thank every member of Dr. Zaman's Research Group specially Ms. Shivani Rani who helped unselfishly throughout this project. Also, the authors want to offer special thanks to Dr. Amir Arshadi for his great help and cooperation throughout this project. The authors are grateful to Dr. Zahid Hossain and his research group at Arkansas State University for their support in conducting this project. The authors are also grateful to Jackson Autrey for his assistance with the laboratory testing. The financial support provided by the Oklahoma Department of Transportation (ODOT) and the Southern Plains Transportation Center (SPTC) are gratefully acknowledged. The authors are thankful to ODOT staff, especially Mr. Kenneth Hobson, for their assistance. Thanks are also extended to all the material suppliers in Oklahoma, New Mexico and Texas for their help throughout this study.

The authors at the Louisiana Tech University gratefully acknowledge the funding and support provided by the Southern Plains Transportation Center (SPTC) for this project. The authors are thankful to Professor Musharraf Zaman of University of Oklahoma and Professor Louay Mohammad of Louisiana State University for their technical help during the project. The authors would also like to thank LTRC Materials Research Administrator Dr. Samuel Cooper III for his support in performing some force ductility tests and data analyses.

TABLE OF CONTENTS

CHAPTER 1 INTRODUCTION	1
1.1 BACKGROUND	1
1.2 PROBLEM STATEMENT	2
1.3 SIGNIFICANCE OF THE STUDY	3
1.4 OBJECTIVES	4
1.5 REPORT OUTLINE	5
1.5.1 Part ONE	5
1.5.2 Part TWO.....	5
1.5.3 Part THREE.....	6
CHAPTER 2 PART ONE LITERATURE REVIEW	7
2.1 VISCOELASTIC BEHAVIOR OF ASPHALT BINDER	7
2.2 POLYMER MODIFIER	8
2.3 WMA TECHNOLOGY.....	9
2.3.1 Organic-based WMA Technologies (Sasobit®)	10
2.3.2 Water Bearing Additive Technologies (Advera®).....	11
2.3.3 Chemical Additive-based Technologies (Evotherm® 3G).....	11
2.3.4 Reclaimed Asphalt Pavement	11
2.4 TESTING METHODS	12
2.4.1 Superpave AASHTO M 320	12
2.4.2 MSCR Test.....	12
2.5 DISADVANTAGES OF DSR TEST METHOD.....	14
2.6 DISADVANTAGES OF “PG PLUS” TESTS.....	15
2.7 IMPLEMENTATION OF MSCR METHOD.....	15
2.8 MSCR STUDY RELATED TO PMBS.....	18
2.9 STUDY RELATED TO WMA	23
2.10 STUDY RELATED TO RECLAIMED ASPHALT PAVEMENT	26
2.11 INTERPRETATION OF MSCR TEST RESULTS	27
2.11.1 Polymer Method	27
2.11.2 Quadrant Method	27
CHAPTER 3 PART ONE METHODOLOGY	31
3.1 INTRODUCTION	31
3.2 MATERIAL SELECTION AND PREPARATION	31
3.2.1 Unmodified and Modified Binder	31
3.2.2 Reclaimed Asphalt Pavement (RAP)	31
3.3 BINDER EXTRACTION AND RECOVERY	34
3.4 MIXING OF THE RAP BINDERS.....	35

3.5 WMA.....	36
3.6 MIXING OF WMA	36
3.7 LABORATORY TESTING	37
3.7.1 Aging Procedure of Binder	37
3.7.2 Physical Testing	39
CHAPTER 4 PART ONE RESULTS AND DISCUSSIONS	45
4.1 SUPERPAVE TEST RESULTS.....	45
4.1.1 Viscosity Results of Unmodified and Polymer Modified Binders.....	45
4.1.2 Effect of WMA on the Viscosity of Unmodified Binders and PMBs.....	46
4.1.3 Effect of RAP on the Viscosity of Unmodified Binders	47
4.2 DSR TEST RESULT OF UNMODIFIED BINDERS AND PMBS	49
4.3 BBR TEST	50
4.4 EFFECT OF WMAS ON RUTTING FACTORS OF UNMODIFIED BINDERS AND PMBS	54
4.5 EFFECT OF RAP ON RUTTING FACTORS OF UBS	55
4.6 SUPERPAVE PG GRADING.....	58
4.7 AASHTO M 332 SPECIFICATION.....	62
4.8 MSCR DATA OF UNMODIFIED BINDERS	64
4.8.1 MSCR Database.....	64
4.8.2 Polymer Method	65
4.8.3 MSCR Grade	66
4.8.4 Stress Sensitivity	67
4.9 ARKANSAS' POLYMER-MODIFIED BINDER	68
4.9.1 MSCR Database.....	68
4.9.2 Investigating the Polymer Modification.....	70
4.9.3 MSCR Grade	72
4.9.4 Elastic Recovery vs. Percent Recovery	74
4.9.5 Stress Sensitivity	76
4.9.6 Elastic Recovery vs. Percent Recovery	82
4.9.7 Stress Sensitivity	84
4.10 NON-CONVENTIONAL MSCR TEST FOR PMBS.....	84
4.10.1 Effect of Higher Stress levels and temperature on PMBs.....	85
4.11 EFFECTS OF WMA ADDITIVES.....	90
4.11.1 MSCR Database	90
4.11.2 Polymer Method	91
4.11.3 Effect of WMA additives on the MSCR Grades	93
4.12 EFFECTS OF WMA ADDITIVES ON THE POLYMER MODIFIED BINDERS	94
4.12.1 MSCR Database	94

4.12.2	Polymer Method	97
4.12.3	Effect of WMA additives on the PMBs of MSCR Grades.....	98
4.13	EFFECTS OF RAP	100
4.13.1	MSCR Database	100
4.13.2	Polymer Method	101
4.13.3	Effect of the RAP on the Unmodified Binders of MSCR Grades	102
CHAPTER 5 PART TWO LITERATURE REVIEW		105
5.1	RHEOLOGICAL AND MECHANICAL PROPERTIES OF POLYMER-MODIFIED BINDERS	105
5.2	RHEOLOGICAL AND MECHANICAL PROPERTIES OF RAP BINDER BLENDS	108
5.3	ASPHALT MIXES WITH HIGH AMOUNTS OF RAP	110
5.4	CONVENTIONAL ASPHALT BINDER TEST METHODS	113
5.4.1	Superpave® Performance Grade (PG) and Its Limitation.....	113
5.4.2	Other Test Methods and Their Limitations	115
5.5	MULTIPLE STRESS CREEP RECOVERY (MSCR) METHOD.....	117
5.5.1	Development of MSCR Test Method.....	117
5.5.2	Studies Related to MSCR Test	120
5.6	INTERPRETATION OF MSCR TEST DATA	127
5.6.1	Polymer Method	127
5.6.2	Stress Sensitivity	128
5.6.3	MSCR Grading	128
5.7	IMPLEMENTATION OF MSCR METHOD.....	129
5.8	HAMBURG WHEEL TRACKING TEST	130
5.9	SUMMARY	132
CHAPTER 6 PART TWO METHODOLOGY.....		133
6.1	INTRODUCTION	133
6.2	MATERIAL COLLECTION AND SAMPLE PREPARATION	133
6.2.1	Collection of Asphalt Binders	133
6.2.2	Extraction of Binder from RAP	135
6.2.3	RAP Binder Blends.....	135
6.2.4	Collection of Asphalt Mixes	135
6.3	LABORATORY TESTING	137
6.3.1	Superpave® Grading of Asphalt Binders	137
6.3.2	Short-term and Long-term Aging of Asphalt Binders	137
6.3.3	Dynamic Shear Rheometer (DSR) Test.....	138
6.3.4	Rotational Viscosity (RV) Test.....	140
6.3.5	Bending Beam Rheometer (BBR) Test	141
6.3.6	Multiple Stress Creep Recovery (MSCR) Test.....	143

6.3.7	Hamburg Wheel Tracking (HWT) Test.....	144
6.4	COMPARATIVE ANALYSIS OF THE SUPERPAVE®, MSCR AND HWT TEST RESULTS.....	146
CHAPTER 7	PART TWO RESULTS AND DISCUSSIONS.....	149
7.1	TEST RESULTS OF ASPHALT BINDERS.....	149
7.1.1	Introduction.....	149
7.1.2	Superpave® Test Results	149
7.1.3	MSCR Test Results.....	173
7.1.4	Comparison of DSR and MSCR Test Results.....	209
7.1.5	Summary	214
7.2	TEST RESULTS OF ASPHALT MIXES.....	214
7.2.1	Introduction.....	214
7.2.2	Volumetric Properties of Asphalt Mixes	214
7.2.3	Hamburg Wheel Tracking (HWT) Test Results.....	220
7.2.4	Evaluation of Rutting and Resistance to Moisture-induced Damage of the Mixes	221
7.2.5	Comparison of HWT, DSR and MSCR Test Results	224
7.2.6	Summary	226
CHAPTER 8	PART THREE LITERATURE REVIEW	229
8.1	INTRODUCTION.....	229
8.1.1	Background	229
8.1.2	Overview on the Polymer Modified Asphalt Binder Characterization.....	233
8.2	ADVANTAGES OF USING SER FOR CHARACTERIZATION OF POLYMER IN ASPHALTIC MATERIALS REPLACING FORCE DUCTILITY TESTS.....	234
8.3	DESCRIPTION OF THE SER.....	235
8.4	VALIDATION OF SER RESULTS WITH PREVIOUS EXTENSIONAL RESULTS	236
8.4.1	Extension Experiment with Commercial poly-isobutylene (PIB) (BASF Oppanol (B15) [2].....	236
8.4.2	Extensional Experiment with Natural Rubber [231].....	237
8.4.3	Shear Rheology of Lupolen 1840H [236].....	239
CHAPTER 9	PART THREE METHODOLOGY	241
9.1	INTRODUCTION.....	241
9.2	EXTENSIONAL TEST PARAMETERS	241
9.3	SELECTION OF ASPHALT BINDER GRADES	241
9.4	SELECTION OF GEOMETRY.....	242
9.5	SELECTION OF TEMPERATURE	242
9.6	EXPERIMENTAL PLAN	242
9.7	SAMPLE PREPARATION	245
9.7.1	Preparing the Binder	245
9.7.2	Controlling the Sample Thickness.....	245

9.7.3	Cutting the Sample to the Desired Dimensions	246
9.8	TEST PROCEDURE	254
CHAPTER 10	PART THREE RESULTS AND DISCUSSIONS	261
10.1	SIMULATING SECOND AND FIRST PEAK ELONGATION FORCE	261
10.1.1	Introduction	261
10.1.2	Simulating Second Peak Elongation Force	261
10.1.3	Simulating First Peak Elongation Force	262
10.2	SELECTION OF GEOMETRY	267
10.2.1	Correlation between Sample Initial X-Sectional Area and Elongation Force	267
10.2.2	Width and Thickness Effect in the Elongation Force	271
10.3	SELECTION OF A TEMPERATURE	278
10.3.1	Temperature Effect in the Second Peak Elongation Force	278
10.3.2	Temperature Effect in the Elongation Force vs Step Time Curve Characteristics	281
10.4	TEST PARAMETERS AND SPECIFICATIONS	285
CHAPTER 11	CONCLUSIONS AND RECOMMENDATIONS	287
11.1	PART ONE CONCLUSIONS AND RECOMMENDATIONS	287
11.1.1	Conclusions	288
11.1.2	Recommendations	291
11.2	PART TWO CONCLUSIONS AND RECOMMENDATIONS	292
11.2.1	Conclusions	292
11.2.2	Recommendations	295
11.2.3	Guidelines	296
11.3	PART THREE CONCLUSIONS AND RECOMMENDATIONS	297
11.3.1	Conclusions	297
11.3.2	Recommendations	299
CHAPTER 12	IMPLEMENTATION/ TECHNOLOGY TRANSFER	301
12.1	PART ONE	301
12.1.1	Conferences and Other Presentations	301
12.2	PART TWO	302
12.2.1	Implementation and Technology Transfer Workshop	302
12.2.2	Peer-Reviewed Journal and Conference Papers	302
12.3	PART THREE	303
12.3.1	Peer-Reviewed Journal and Conference Papers	303
ACRONYMS, ABBREVIATIONS, AND SYMBOLS		305
REFERENCES.....		307
APPENDIX.....		335

LIST OF TABLES

Table 1. Types and source-location of binders	33
Table 2. Non-conventional MSCR Test Matrix	43
Table 3. Viscosity result of WMA	48
Table 4. Viscosity Test Results of RAP Modified Binders	49
Table 5. PG grading of PMBs	60
Table 6. PG grading of WMA.....	61
Table 7. PG grading of unmodified binders.....	62
Table 8. PG grading of RAP modified binders	62
Table 9. Minimum J_{nr} value range for MSCR grading	63
Table 10. Stress sensitivity criteria of MSCR Test.....	64
Table 11. MSCR data base of PG 64-22 (from Arkansas) at 64°C	65
Table 12. MSCR database for PG 70-22 (Arkansas) at 64°C and 70°C.....	69
Table 13. MSCR database for PG 76-22 (Arkansas) at 64°C, 70°C and 76°C	71
Table 14. MSCR database of PG 70-22 (Texas)	80
Table 15. MSCR database of PG 76-22 (Texas)	80
Table 16. MSCR database of PG 64-22 with WMA additives at 64°C.....	91
Table 17. Change of MSCR grade of PG 64-22 with addition of WMA additives	93
Table 18. MSCR watabase of PG 70-22 with and without WMA additives.....	95
Table 19. MSCR database of PG 76-22 with and without WMA additives	96
Table 20. Change of MSCR grading of PG 70-22 with WMA additives.....	99
Table 21. Change of MSCR grading of PG 76-22 with WMA additives.....	100
Table 22. MSCR database of RAP modified binders	101
Table 23. MSCR grades based on J_{nr} [184].....	129
Table 24. Sources and types of the binders collected for study	134
Table 25. Properties of selected asphalt mixes	136
Table 26. Test matrix for Superpave® tests	138
Table 27. Test matrix for MSCR test	144
Table 28. HWT test matrix	146
Table 29. Continuous high-temperature PG grades of PG 70-XX and PG 76-XX binders	161
Table 30. Continuous low-temperature PG grades of PG 70-XX and PG 76-XX binders	163

Table 31. Continuous high-temperature PG grades of 0%, 25%, 40% and 60% RAP1 and RAP2 binder blends	171
Table 32. Continuous low-temperature PG grades of 0%, 25%, 40% and 60% RAP1 and RAP2 binder blends	172
Table 33. MSCR test results for PG 70-XX and PG 76-XX binders at 64 °C	174
Table 34. MSCR test results for PG 70-XX and PG 76-XX binders at 64 °C and 0.1, 3.2 and 10 kPa	182
Table 35. MSCR test results of 0%, 25%, 40% and 60% RAP1 and RAP2 binder blends	195
Table 36. MSCR test results of 0%, 25%, 40% and 60% RAP1 and RAP2 binder blends at 64 °C and 0.1, 3.2 and 10 kPa	201
Table 37. Ranking of PG 70-XX binders with respect to rut performance	210
Table 38. Ranking of PG 76-XX binders with respect to rut performance	210
Table 39. Ranking of the RAP binder blends with respect to rut performance	211
Table 40. Coefficient of variation of the DSR and MSCR test of PG 70-XX binders	212
Table 41. Coefficient of variation of the DSR and MSCR test of PG 76-XX binders	213
Table 42. Subjective comparison of the DSR and MSCR tests	213
Table 43. Summary of aggregates' gradation of MIX-1	216
Table 44. Summary of aggregate properties and volumetric properties of MIX-1	216
Table 45. Summary of aggregates' gradation of MIX-2	217
Table 46. Summary of aggregate properties and volumetric properties of MIX-2	217
Table 47. Summary of aggregates' gradation of MIX-3	218
Table 48. Summary of aggregate properties and volumetric properties of MIX-3	218
Table 49. Summary of aggregates' gradation of MIX-4	219
Table 50. Summary of aggregate properties and volumetric properties of MIX-4	219
Table 51. Rut depths of asphalt mix specimens at different number of wheel passes	224
Table 52. Performance parameters of asphalt mix specimens obtained from the HWT tests	224
Table 53. Comparison of HWT, DSR and MSCR test results	225
Table 54. PG plus requirement for performance graded asphalt binder (modified) for four different states	231
Table 55. Summary of materials and experimental plan	244
Table 56. Statistical analysis of the selected geometry	286

LIST OF FIGURES

Figure 1. Viscoelastic response of bitumen under creep loading [18]	7
Figure 2. (a) Schematic diagram of a 1-second creep and 9 -seconds recovery curve at 3.2 kPa for nonlinear viscoelastic curve; (b) Permanent strain of the creep and recovery curve of polymer-modified binder [20].....	9
Figure 3. Showing the determination of the percent recovery and J_{nr} value	13
Figure 4. Loading scheme of MSCR test method [10].....	14
Figure 5. Current status of MSCR test method implementation [63].....	18
Figure 6. J_{nr} vs. ALF rutting [10]	19
Figure 7. $G^*/\sin\delta$ vs. ALF rutting [10].....	20
Figure 8. Polymer curve for detecting the polymer based on the MSCR % R at $J_{nr,3.2kPa}$	28
Figure 9. Quadrant plot for analyze the MSCR % R based on the ER value	29
Figure 10. Flow chart of this study	32
Figure 11. Location of binder's sources	32
Figure 12. Collection of RAP coarse from the existing pavement	33
Figure 13. Centrifuge machine with extraction bowl and filters	34
Figure 14. Recovery assembly	35
Figure 15. A Rolling Thin-Film Oven (RTFO) from James Cox and Sons	38
Figure 16. A Pressure Aging Vessel (PAV) from ATS.....	39
Figure 17. A DV-II+ Pro Rotational Viscometer (RV)	40
Figure 18. A DSR Machine with Bottom and Upper Plate.....	41
Figure 19. Viscosity test results of the few unmodified and polymer modified binders	45
Figure 20. Viscosity test results of the few WMA	47
Figure 21. Viscosity vs. temperature of RAP modified binders	49
Figure 22. $G^*/\sin\delta$ vs. temperature for: (a) Unaged PG 64-22; (b) RTFO-aged PG 64-22.....	51
Figure 23. $G^*/\sin\delta$ vs. temperature for: (a) Unaged PG 70-22; (b) RTFO-aged PG 70-22.....	52

Figure 24.	$G^*/\sin\delta$ vs. temperature for: (a) Unaged PG 76-22;	
	(b) RTFO-aged PG 76-22.....	53
Figure 25.	(a) Stiffness vs temperature for PMBs and unmodified binders	
	(b) M-value vs. Temperature for PMBs.....	56
Figure 26.	$G^*/\sin\delta$ vs. Temperature for (a) Unaged and RTFO PG 76-22	
	(b) Unaged and RTFO-aged PG 64-22	57
Figure 27.	Passing temperature (at $G^*/\sin\delta = 1$ kPa or $G^*/\sin\delta = 2.2$ kPa)	
	of PMBs.....	58
Figure 28.	$G^*/\sin\delta$ values of unaged and RTFO aged RAP modified binders.....	58
Figure 29.	MSCR %R vs. J_{nr} @ 3.2 kPa for PG 64-22 (Arkansas) at 64°C.....	66
Figure 30.	MSCR grades of tested PG 64-22 (Arkansas) binders	67
Figure 31.	R_{diff} , % vs. $J_{nr,diff}$, % for PG 64-22 (Arkansas).....	68
Figure 32.	MSCR %R vs. J_{nr} @ 3.2 kPa for PG 70-22 (Arkansas) at 64°C.....	72
Figure 33.	MSCR %R vs. J_{nr} @ 3.2 kPa for PG 76-22 (Arkansas) at 64°C	73
Figure 34.	Frequency of sample vs. J_{nr} @ 3.2 kPa for PG 70-22	
	(Arkansas) binders	74
Figure 35.	Frequency of sample vs. J_{nr} @ 3.2 kPa for PG 76-22	
	(Arkansas) binders	74
Figure 36.	Quadrant plot for PG 70-22 (Arkansas)	76
Figure 37.	Quadrant plot for PG 76-22 (Arkansas)	76
Figure 38.	R_{diff} , % vs. $J_{nr,diff}$, % for PG 70-22 (Arkansas).....	77
Figure 39.	R_{diff} , % vs. $J_{nr,diff}$, % for PG 76-22 (Arkansas).....	77
Figure 40.	MSCR %R vs. J_{nr} @ 3.2 kPa for PG 70-22 (Texas) at 64°C	81
Figure 41.	Frequency of sample vs J_{nr} @3.2 kPa for PG 70-22 from Texas.....	82
Figure 42.	Frequency of sample vs J_{nr} @3.2 kPa for PG 76-22 from Texas.....	82
Figure 43.	Quadrant plot for PG 70-22 (Texas)	83
Figure 44.	Quadrant plot for PG 76-22 (Texas)	84
Figure 45.	(a) Change of J_{nr} with stress level for (a) PG 70-22 (Arkansas)	
	at 64°C (b) PG 70-22 (Arkansas) at 70°C	86
Figure 46.	%R vs stress levels for PG 70-22 (Arkansas) at 70°C	87

Figure 47. Change of J_{nr} with stress level for SBS modified PMBs at: (a) 64°C (b) 70°C (c) 76°C	89
Figure 48. %R vs stress levels of PG 76-22 at 76°C.....	89
Figure 49. MSCR %R values PG 64-22 with and without WMA additives at 3.2 and 64°C.....	92
Figure 50. J_{nr} values of PG 64-22 with and without WMA additives at 3.2 and 64°C.....	92
Figure 51. MSCR %Recovery vs. J_{nr} at 3.2 kPa for PG 64-22 with WMA additives at 64°C.....	93
Figure 52. MSCR %R values PG 70-22 with and without WMA additives at 3.2 kPa and 64°C.....	97
Figure 53. MSCR %R values PG 76-22 with and without WMA additives at 3.2 kPa and 64°C.....	97
Figure 54. MSCR %R vs. J_{nr} @ 3.2 kPa for PG 70-22 at 64°C.....	98
Figure 55. MSCR %R vs. J_{nr} @ 3.2 kPa for PG 76-22 With and Without WMA Additives at 64°C	99
Figure 56. MSCR %R vs. J_{nr} @ 3.2 kPa for RAP modified binders at 64°C	103
Figure 57. Schematic of the colloidal structure of binder and the effect of polymer modification: (a) base binder; (b) polymer-modified binder [120]	106
Figure 58. Schematic of DSR test setup [143]	114
Figure 59. Schematic of MSCR test method (a) strain vs time and (b) stress vs time [163]	119
Figure 60. Polymer method of MSCR analysis [56]	128
Figure 61. Work flow of the present study.....	134
Figure 62. (a) Collection of aggregates for laboratory produced asphalt mixes; (b) collected aggregates and asphalt binder.....	136
Figure 63. Test setup for DSR test on asphalt binder samples: (a) DSR apparatus; (b) asphalt binder samples for DSR test.....	139
Figure 64. Typical plots from DSR tests on asphalt binder samples: (a) $ G^* /\sin\delta$ vs temperature; (b) $ G^* \cdot\sin\delta$ vs temperature	140
Figure 65. Rotational Viscosity test setup for asphalt binder	141

Figure 66.	A typical plot of the RV test conducted on asphalt binder sample	141
Figure 67.	Test setup for BBR test on asphalt binder sample: (a) BBR apparatus; (b) asphalt beam sample	142
Figure 68.	Typical plots from BBR test on asphalt binder sample: (a) m_{60} vs temperature: (b) S_{60} vs temperature	142
Figure 69.	Example of stress response of a binder in MSCR test.....	143
Figure 70.	(a) Asphalt mix sample before HWT test; (b) Sample after test; (c) HWT test setup.....	145
Figure 71.	A typical plot of HWT rut depths vs. number of wheel passes [106]	146
Figure 72.	Variation of $ G^* $ with temperature for unaged and RTFO-aged conditions: (a) PG 70-XX binders; (b) PG 76-XX binders	151
Figure 73.	Variation of phase angle with temperature for unaged and RTFO-aged conditions: (a) PG 70-XX binders; (b) PG 76-XX binders	152
Figure 74.	Variation of $ G^* /\sin\delta$ with temperature for unaged and RTFO-aged conditions: (a) PG 70-XX binders; (b) PG 76-XX binders	154
Figure 75.	Variation of $ G^* \cdot\sin\delta$ with temperature for PAV-aged condition: (a) PG 70-XX binders; (b) PG 76-XX binders	155
Figure 76.	Variation of viscosity with temperature for unaged condition: (a) PG 70-XX binders; (b) PG 76-XX binders	157
Figure 77.	Variation of m_{60} with temperature for PAV-aged condition: (a) PG 70-XX binders; (b) PG 76-XX binders	158
Figure 78.	Variation of S_{60} with temperature for PAV-aged condition: (a) PG 70-XX binders; (b) PG 76-XX binders	159
Figure 79.	Superpave® PG grading of binders: (a) PG 70-XX; (b) PG 76-XX	160
Figure 80	Variation of $ G^* $ with temperature for unaged and RTFO-aged conditions and 0%, 25%, 40% and 60% RAP1 and RAP2 binder blends.....	165
Figure 81	Variation of phase angle with temperature for unaged and RTFO-aged conditions and 0%, 25%, 40% and 60% RAP1 and RAP2 binder blends.....	165
Figure 82.	Variation of $ G^* /\sin\delta$ with temperature for unaged and RTFO-aged conditions and 0%, 25%, 40% and 60% RAP1 and RAP2 binder blends.....	166

Figure 83.Variation of viscosity with temperature for unaged condition and 0%, 25%, 40% and 60% RAP1 and RAP2 binder blends	167
Figure 84.Variation of m_{60} with temperature for PAV-aged condition and 0%, 25%, 40% and 60% RAP1 and RAP2 binder blends	168
Figure 85.Variation of S_{60} with temperature for PAV-aged condition and 0%, 25%, 40% and 60% RAP1 and RAP2 binder blends	169
Figure 86.Superpave® PG grading of 0%, 25%, 40% and 60% RAP1 and RAP2 binder blends.....	173
Figure 87.Effect of source on J_{nr} values at 64 °C: (a) PG 70-XX binders; (b) PG 76-XX binders	176
Figure 88.Effect of Source on %Recovery values at 64 °C: (a) PG 70-XX binders; (b) PG 76-XX binders	177
Figure 89.Variation of $J_{nr\ diff}$ with R_{diff} at 64 °C: (a) PG 70-XX binder; (b) PG 76-XX binder	179
Figure 90.Polymer curve analysis at 64 °C and 3.2 kPa stress level: (a) PG 70-XX binders; (b) PG 76-XX binders.....	181
Figure 91.Change in J_{nr} value with stress levels at 64 °C: (a) PG 70-XX binders; (b) PG76-XX binders	184
Figure 92.Change in %Recovery with stress levels at 64 °C: (a) PG 70-XX binders; (b) PG 76-XX binders	185
Figure 93.Plot of $J_{nr\ diff}$ and R_{diff} with increasing stress levels at 64 °C: (a) PG 70-XX binders; (b) PG 76-XX binders	186
Figure 94.Changes in J_{nr} values with temperature for PG 70-XX binders: (a) 0.1 kPa stress level; (b) 3.2 kPa stress level.....	187
Figure 95.Changes in J_{nr} values with temperature for PG 76-XX binders: (a) 0.1 kPa stress level; (b) 3.2 kPa stress level.....	188
Figure 96.Changes in %Recovery with temperature for PG 70-XX binders: (a) 0.1 kPa stress level; (b) 3.2 kPa stress level.....	189
Figure 97.Changes in %Recovery with temperature for PG 76-XX binders: (a) 0.1 kPa stress level; (b) 3.2 kPa stress level.....	190

Figure 98. Polymer curve analyses at higher temperatures and 3.2 kPa stress level: (a) PG 70-XX binders; (b) PG 76-XX binders	191
Figure 99. Changes in J_{nr} values with stress level: (a) PG 70-XX binders at 70 °C; (b) PG 76-XX binders at 70 °C; (c) PG 76-XX binders at 76 °C	193
Figure 100. Changes in %Recovery with stress levels: (a) PG 70-XX binders at 70 °C; (b) PG 76-XX binders at 70 °C; (c) PG 76-XX binders at 76 °C	194
Figure 101. J_{nr} values of 0%, 25%, 40% and 60% RAP1 and RAP2 binder blends	196
Figure 102. %Recovery values of 0%, 25%, 40% and 60% RAP1 and RAP2 binder blends at 64 °C	197
Figure 103. $J_{nr\ diff}$ values of 0%, 25%, 40% and 60% RAP1 and RAP2 binder blends	198
Figure 104. R_{diff} values of 0%, 25%, 40% and 60% RAP1 and RAP2 binder blends at 64 °C	198
Figure 105. Polymer curve analysis for 0%, 25%, 40% and 60% RAP1 and RAP2 binder blends at 64 °C and 3.2 kPa stress level	199
Figure 106. Changes in J_{nr} values with stress levels for 0%, 25%, 40% and 60% RAP1 and RAP2 binder blends at 64 °C	201
Figure 107. Changes in %Recovery values with stress levels for 0%, 25%, 40% and 60% RAP1 and RAP2 binder blends at 64 °C	202
Figure 108. Variation in $J_{nr\ diff}$ with stress levels for 0%, 25%, 40% and 60% RAP1 and RAP2 binder blends at 64 °C	202
Figure 109. Variation in R_{diff} with stress levels for 0%, 25%, 40% and 60% RAP1 and RAP2 binder blends at 64 °C	203
Figure 110. Changes in J_{nr} values with an increase in temperature for 25%, 40% and 60% RAP1 and RAP2 binder blends: (a) 0.1 kPa stress level; (b) 3.2 kPa stress level	204
Figure 111. Changes in %Recovery values with an increase in temperature for 25%, 40% and 60% RAP1 and RAP2 binder blends: (a) 0.1 kPa stress level; (b) 3.2 kPa stress level	205
Figure 112. Polymer curve analysis for 0%, 25%, 40% and 60% RAP1 and RAP2 binder blends at different temperatures and 3.2 kPa stress level	206

Figure 113.Changes in J_{nr} values with stress level for 25%, 40% and 60% RAP1 and RAP2 binder blends at 70° and 76 °C	207
Figure 114.Changes in %Recovery values with stress level for 25%, 40% and 60% RAP1 and RAP2 binder blends at 70° and 76 °C	208
Figure 115.HWT test results of the asphalt mixes: (a) NMA= 12.5 mm; (b) NMA= 19 mm.....	223
Figure 116.Comparison of DSR and HWT test results	226
Figure 117.Comparison of MSCR and HWT test results	226
Figure 118.Force ductility results of non-polymer modified asphalt emulsion [230]	232
Figure 119.Force ductility results of polymer modified asphalt emulsion [230].....	232
Figure 120.a) Side view of the Sentmanat Extensional Rheometer (SER) during Operation. Inside Squares: A. Master Drum, B. Slave Drum, C. Bearings, D. Intermeshing Gears, E. Chassis, F. Drive Shaft, G. Torque Shaft, H. Sample, I. Securing Clamps. b) Elevation the SER during an experiment. Symbols: L_0 Unsupported Length, Ω Drive Shaft Rotation Rate, T Torque, F Tangential Force.	236
Figure 121.Comparison of tensile stress growth curves data from SER and another extensional rheometer technology [220].....	237
Figure 122.Extensional stress relaxation modulus for NR-RSS2 at 23°C [231]	238
Figure 123.Tensile stress growth curves for NR-RSS2 for constant Hencky strain rates ranging from 0.001s ⁻¹ to 10 s ⁻¹	238
Figure 124.Tensile stress growth curves at 130°C for Affinity PL 1880 LLDPE obtained from the SER. Also shown LVE given by $\eta_g^+ = 3\eta^+$ generated by the cone and the plate measurements in start-up steady shear flow.....	239
Figure 125.The binder placed in to the small can.....	247
Figure 126.The binder poured in to the silicon mold	248
Figure 127.The binder was removed from the silicon mold	248
Figure 128.Binder placed between two stainless steel plates	249
Figure 129.Silicon mat placed above the binder	249
Figure 130.The thick glass placed over the silicon mat.....	250
Figure 131.The loads placed over the thick glass	250

Figure 132.The binder’s shape after removing the loads	251
Figure 133.Cracked during the cutting process due to a long cooling period	251
Figure 134.Sticking to the metal edge due to a short cooling period	252
Figure 135.Cutting the binder to the desired length	252
Figure 136.Sample with desired dimensions.....	253
Figure 137.Sample with desired dimensions.....	253
Figure 138.Inserting the smart swap.	255
Figure 139.Fixing the SER bracket.....	255
Figure 140.The SER fixture prior to the sample loading.....	256
Figure 141.SER fixture after loading the sample	256
Figure 142.Length of the sample 12.75 mm.....	257
Figure 143.Clamps kicked out due to the hard stresses.....	257
Figure 144.Double-sided adhesion tape fixed to the drums	258
Figure 145.Loading the sample post to the double-side adhesion tape	258
Figure 146.Software screenshot shows the test Parameter	259
Figure 147.Software screenshot shows the DSR control panel	259
Figure 148.Sample during the extensional deformation test	260
Figure 149.Sample after the end of the test	260
Figure 150.Elongation force vs. step time for PG 76-22 geometry of 9.0 mm x 0.72 mm.....	263
Figure 151.Elongation force vs. step time for PG 64-22 geometry of 9.0 mm x 0.72 mm.....	263
Figure 152.Elongation force vs. step time for PG 58-28 geometry of 9.0 mm x 0.72 mm.....	264
Figure 153.Elongation force vs. step time for PG 76-22 geometry of 6.0 mm x 0.83 mm.....	264
Figure 154.Elongation force vs. step time for PG 64-22 geometry of 6.0 mm x 0.83 mm.....	265
Figure 155.Elongation force vs. step time for PG 58-28 geometry of 6.0 mm x 0.83 mm.....	265

Figure 156.Elongation force vs. step time for PG 76-22 geometry of 7.5 mm x 0.4 mm.....	266
Figure 157.Elongation force vs. step time for PG 64-22 geometry of 7.5 mm x 0.40 mm.....	266
Figure 158.Elongation force vs. step time for PG 58-28 geometry of 7.5 mm x 0.40 mm.....	267
Figure 159.Second peak elongation force vs. initial area	268
Figure 160.Average second peak elongation force vs. initial area	269
Figure 161.First peak elongation force vs. initial area	270
Figure 162.Average first peak elongation force vs. initial area	270
Figure 163.Average second peak elongation force vs. width	273
Figure 164.Average second peak Elongation force vs. thickness, for the different initial areas	273
Figure 165.Average second peak elongation force vs. width, for the different thicknesses.....	274
Figure 166.Average second peak elongation force vs. thickness, for different widths	274
Figure 167.Average first peak elongation force vs. Width	276
Figure 168.Average first peak elongation force vs. thickness	277
Figure 169.Average first peak elongation force vs. thickness	277
Figure 170.Average first peak elongation force vs. width.....	278
Figure 171.Second Peak Elongation Force vs. Temperature.....	279
Figure 172.Average Second Peak Elongation Force vs. Temperature	280
Figure 173.Second Peak Elongation Force vs. Temperature.....	280
Figure 174.Average Second Peak Elongation Force vs. Temperature	281
Figure 175.Elongation Force vs. Step Time for PG 76-22 geometry of 8 mm x 0.72 mm at 4°C.....	282
Figure 176.Elongation Force vs. Step Time for PG 76-22 geometry of 8 mm x 0.72 mm at 10°C.....	282
Figure 177.Elongation Force vs. Step Time for PG 76-22 geometry of 8 mm x 0.72 mm at 16°C.....	283

Figure 178.Elongation Force vs. Step Time for PG 76-22 geometry of 9 mm x 0.72 mm at 4°C.....	283
Figure 179.Elongation Force vs. Step Time for PG 76-22 geometry of 9 mm x 0.72 mm at 10°C.....	284
Figure 180.Elongation Force vs. Step Time for PG 76-22 geometry of 9 mm x 0.72 mm at 16°C.....	284

EXECUTIVE SUMMARY

Part ONE

For quality assurance and quality control purposes, suppliers and users of asphalt binders follow the widely used dynamic shear rheometer (DSR) test method (AASHTO T 315) to capture viscoelastic properties of polymer-modified binders (PMBs), warm mix asphalt (WMA)- and reclaimed asphalt pavement (RAP)-modified binders. However, AASHTO T 315 has been designed for unmodified asphalt binders, and it is inadequate to characterize modified binders because of the relatively small impact of the phase angle and strain levels on the rutting and fatigue factors, respectively. On the other hand, the recently balloted multiple stress creep recovery (MSCR) test (AASHTO T 350) results can better relate the laboratory-based and field rutting of PMBs and additive-modified binders. In the current study, Superpave and MSCR tests were performed to evaluate viscoelastic properties of selected asphalt binders approved in Arkansas and Texas. A total of 65 binder samples were tested in the laboratory. Of these, eight were unmodified binders, 24 were PMBs, 27 were WMA-additive modified, and 6 were RAP modified binders. The non-recoverable compliance and MSCR percent recovery data of the tested binders were analyzed for grading and establishing the MSCR percent recovery criteria for local service temperature and traffic conditions. The developed guidelines are expected to be helpful for transportation agencies in Arkansas and Texas to adopt the MSCR test method in their quality control process.

Part TWO

In recent years, asphalt modifications have become increasingly popular in asphalt pavement construction. In view of technical, environmental, and economic benefits, the pavement industry is in favor of using high amounts of Reclaimed Asphalt Pavement (RAP) in asphalt mixes for pavement construction. Consequently, accurate rheological characterization of asphalt binders containing polymer modifiers and RAP binder is important because pavement performance is largely influenced by asphalt binder properties.

Numerous test methods have evolved over the last three decades for evaluating the rutting susceptibility of asphalt binders. The objective of the current study was to use a simple Dynamic Shear Rheometer (DSR) based test method as an alternative to the Superpave® Performance Grade (PG) tests or “PG plus” tests to accurately evaluate high-temperature performance of asphalt binders. To achieve this objective, the rheological characteristics of asphalt binders were evaluated using the Multiple Stress Creep Recovery (MSCR) and Superpave® test methods. MSCR is usually pronounced as the word “massacre”. For this purpose, polymer-modified binders were collected from different sources located in Oklahoma, New Mexico, and Texas. Also, binders were extracted from two RAPs and blended with a commonly used PG 64-22 binder at selected rates, namely 0%, 25%, 40%, and 60% by the weight of the binder. Furthermore, four different asphalt mixes containing polymer-modified binders and different amounts of RAP were tested for rutting performance in the laboratory. The rutting parameter ($|G^*|/\sin\delta$), fatigue parameter ($|G^*|\cdot\sin\delta$), viscosity, high- and low-temperature PG grades of all modified and unmodified binders were evaluated based on the Superpave® test methods. The MSCR tests were conducted to determine high-temperature MSCR grades and to evaluate the effects of the addition of polymer and RAP binder on non-recoverable creep compliance (J_{nr}) and %Recovery values of the binders.

The polymer-modified binders were found to meet the Superpave® specifications and exhibited satisfactory rutting and fatigue resistance. The high- and low-temperature PG grades of the RAP binder blends were observed to increase with an increase in the RAP binder content. From the MSCR test results, the minimum %Recovery requirement based on the J_{nr} criteria suggested in AASHTO TP 70 was found to be appropriate for differentiating polymer-modified binders from non-polymer modified binders. Also, the addition of a higher stress level, such as 10 kPa to the MSCR test method, was found to help understand the nonlinear viscoelastic behavior of the polymer-modified binders. Furthermore, the J_{nr} value decreased and MSCR grades increased with an increase in the amount of RAP binder, which indicated an improved resistance to rutting for the RAP binder blends. The rutting and moisture susceptibilities of the asphalt mixes with

high RAP content were found to be satisfactory from Hamburg Wheel Tracking (HWT) tests. A comparison of the Superpave[®], MSCR and HWT test results is also presented in this report.

Part THREE

Modification of asphalt binders is essential to improve the physical and rheological properties of asphalt and to reduce the aging effect. The use of polymers to modify asphalt is the most common approach in asphalt modification. Force ductility test has been a challenging topic as an indicator of asphalt performance, especially for the modified asphalt binders. The significance of the force ductility test as a measure of fatigue and thermal cracking has been debated because of its low reproducibility, empirical nature and the unclear relationship with the fundamental asphalt properties, especially with modified asphalt binders [1]. Extensional deformations tests where converging flows occur have been used by many for polymer characterizations (2). In this study, the extensional deformation behavior of binders Performance Graded 58-28, PG 64-22, and PG 76-22 and its parameters including geometry and temperature were investigated through an extensional rheological approach using a DSR-based Sentmanat Extensional Rheometer (SER). Furthermore, a test method and a sample preparation procedure for asphalt binders were developed as a replacement to the conventional force ductility test. The sample preparation method has been simplified and detailed in a way that it can be performed in all asphalt labs. A detailed analysis indicates that the average second peak and first peak elongation forces increase due to the increase of the sample's area, with R^2 values of 0.85 and 0.84, respectively. However, the same areas with different dimensions derived different values of elongation force that is due to the dominant role of the width. The elongation force of all samples with the same area but different dimensions increases due to the width's increment even though the thickness decreases.

Based on this study, the recommended test specifications are as follow: the selected geometry is 9 mm x 0.72 mm (width x thickness). The second peak elongation force F_2 value was chosen as a recommended force ductility parameter. The minimum F_2 value recommended is 14 N, which was lower than the lowest limit of 99% confidence

interval (14.45N – 15.99 N). Also, the minimum ratio of the second peak elongation force over the first peak elongation force F_2/F_1 of 1.25 is recommended for PG 76-22. This is also lower than the lowest value of 99% confidence interval (1.29-1.51). The recommended temperature is 4°C, the recommended strain rate is 0.1s^{-1} , and the recommended final strain is 3.4 rad. Therefore, with a more reproducible, significantly less material and time consuming, and with a more mechanistic approach, the developed novel method can help improve the durability of modified asphalt pavements.

CHAPTER 1

INTRODUCTION

1.1 BACKGROUND

According to the Federal Highway Administration (FHWA), the United States (U.S.) has over 4 million miles public centerline roads. Of these, about 2.50 million miles of roads are paved [0]. About 95% of the paved roads in the US are comprised of asphalts [2]. Since asphalt is a viscoelastic material, it can resist permanent deformation or rutting of flexible pavements [3-4]. Heavy traffic loads and high summer temperatures in the flexible pavements are responsible for the rutting. For last several years, different agencies including state Departments of Transportation (DOTs) have been trying to identify different laboratory-based test procedures and parameters for predicting field rutting.

In 1987, the U.S. congress approved the Strategic Highway Research Program (SHRP) to develop techniques to improve the performance, durability, safety, and efficiency of the U.S. highways [3]. One of the main objectives of the 1987 SHRP study was to develop specifications for asphalt binders. Thus, the SHRP study carried out a vast research program to develop Superpave test methods and specifications for asphalt binders. In 1993, the Performance Grade (PG) specifications were introduced as a part of the Superpave system to grade asphalt binders. These specifications were adopted by the American Association of State Highway and Transportation Officials (AASHTO) and balloted in AASHTO M 320. To measure the contribution of the asphalt binder to rutting under high service temperatures and to fatigue at intermediate temperatures, the Superpave PG grade system introduced a Dynamic Shear Rheometer (DSR)-based test method, AASHTO T 315.

The AASHTO T 315 method recommends the rutting factor ($G^*/\sin\delta$) for predicting the field rutting. But, from field experience researchers found the rutting factor was inadequate for predicting the field of rutting [4-7]. The AASHTO T 315 method and AASHTO M 320 specifications were mainly developed on the basis of unmodified

binders. The rutting factor was unable to adequately capture the benefits of elastomeric modification because of a relatively small impact of the phase angle (δ) on the overall value of $G^*/\sin\delta$ [8]. However, most of the DOTs currently use polymer modified binders (PMBs) to sustain heavy traffic loads and extreme climate conditions. To address this issue, many highway agencies routinely conduct additional tests such as the elastic recovery (ER) test (AASHTO T 300) to identify the existence of polymers in PMBs, and these are often called the PG-Plus tests. However, the PG Plus tests do not have any specific standards among the DOTs, and they vary from one DOT to another.

The aforementioned issues caused researchers to continue to look for an improvement to the high temperature parameter, $G^*/\sin\delta$, used in AASHTO M 320. To measure the accumulated strain in PMBs as well as in unmodified binders, Bahia et al. [4] proposed a test method named Repeated Creep Recovery Test (RCRT). The RCRT method has some limitations as well. One of these limitations is that it considers low stress levels only to measure the permanent strain of binders. At low stress levels, most of the PMBs do not show their nonlinear behavior. To overcome this problem, the FHWA modified the RCRT method by increasing stress levels and renamed it Multiple Stress Creep Recovery (MSCR) test [9]. Non-recoverable creep compliance (J_{nr}) and percent creep recovery (%R) obtained from the MSCR test results have been reported to show good correlations with field rutting [9].

1.2 PROBLEM STATEMENT

Several highway agencies have raised some concerns of using the MSCR test as a quality control tool for the performance of asphalt binders. The Asphalt Institute (AI) has taken the flagship in establishing the MSCR guidelines through various presentations and technology transfer meetings. The current study is expected to address the following issues for conditions prevailing in Arkansas and Texas:

- The commonly used DSR test method (AASHTO T 315) is incapable of capturing the viscoelastic properties of polymer modified binders (PMBs) [10-14], because unlike neat binders, PMBs response to applied stress levels and demonstrate nonlinear responses relating to rutting parameter. To mitigate this issue, many DOTs perform extra tests in addition of the regular Superpave tests calling them the PG Plus tests. However, there are some drawbacks of the PG Plus tests. For

instance, the PG Plus tests are not reflective of actual field performances, rather finding the presence of a particular modifier. Further, there does not exist a specific test methodology that all DOTs can follow while performing the PG Plus tests.

- In AASHTO M 320, the binder characterization is achieved by bumping up the high PG temperature of the binder, which is a major difference from the MSCR test specifications (AASHTO MP 332). In the bumped grading system, binders are tested at 6 to 18°C above the high PG temperature, which results in the usage of highly modified binders than actually needed for a project. On the other hand, the MSCR test procedure uses a more practical high temperature during the testing process than this bumped grading system [15, 16].
- The PG specification, AASHTO M 320, is unable to identify poor polymer structures, which could result in disastrous pavement performance, because binders with weak polymer structure could collapse under high stress levels. On the other hand, the proposed MSCR test procedure is able to characterize polymer structures, which are susceptible of collapsing under higher stresses [15,16].

1.3 SIGNIFICANCE OF THE STUDY

The Arkansas State Highway and Transportation Department (AHTD) and Texas Department of Transportation (TxDOT) have been using the PMBs, WMA, and Reclaimed Asphalt Pavement (RAP) to sustain heavy traffic loads and extreme climate conditions. Data obtained from this study will help AHTD and TxDOT to develop the MSCR test protocols and guidelines. This study will also help both DOTs to eliminate the costly test method known as the ER test, which they routinely use for characterizing PMBs.

Also, the present study was pursued to generate useful test results of polymer-modified binders and RAP binder blends available in Oklahoma as-well-as in New Mexico and Texas. The test results are expected to help in the implementation of the MSCR test methods by the DOTs of Oklahoma, New Mexico and Texas by replacing the time-

consuming and costly “PG Plus” tests. The rutting performances of the polymer-modified binders are expected to be better understood by using the MSCR parameters. The Superpave® and MSCR grades of the RAP binder blends, determined in the present study, are expected to help pavement engineers in selecting the proper RAP content for asphalt mixes. In addition, the outcomes of this study are expected to help the pavement engineers gain an understanding when using high amounts of RAP on the rutting potential of asphalt mixes commonly used in Oklahoma.

Force Ductility (AASHTO T300) has been in use in Louisiana as a PG Plus test. In this study, a new extensional deformation test has been developed to replace the force ductility test using a Sentmanat Extensional Rheometer (SER) fixture inside the DSR. With a more reproducible, significantly less material and time consuming, and with a more mechanistic approach, the developed novel test method can help improve the durability of modified asphalt pavements.

1.4 OBJECTIVES

Part ONE

The main objectives of Part One are as follows:

- Determination of the MSCR %Recovery and non-recoverable creep compliance relationships of the selected asphalt binders from Arkansas and Texas.
- Determination of MSCR %Recovery and Jnr limits for commonly used binders in Arkansas and Texas.
- Assessment of the presence of polymer through MSCR %Recovery of PMBs and binders recovered from RAPs.

Part TWO

The specific objectives of Part Two are as follows:

- Evaluating the MSCR parameters i.e., Jnr and MSCR %Recovery for polymer-modified asphalt binders available in Oklahoma, New Mexico and Texas.
- Characterizing the rheological properties of the polymer-modified binders using the MSCR test method.

- Assessing the effects of the addition of RAP binder on the properties of RAP binder blends using the Superpave® and MSCR test methods.
- Determining the relationship between the MSCR parameter (Jnr) and rutting performance of asphalt mixes containing polymer-modified binders and RAP.

Part THREE

The primary objective of Part Three is to develop a new extensional deformation test method using a Sentmanat Extensional Rheometer (SER) inside the dynamic shear rheometer (DSR) to fulfill the acknowledged gap in the current PG System by replacing the force ductility test.

The specific objectives are as follows:

- Develop a sample preparation method
- Perform a parametric study for the effect of sample geometry (thickness and width), and select the final geometry
- Investigate the effect of temperature and select the test temperature
- Analyze the reproducibility of the results
- Recommend test parameters and specifications for the new method

1.5 REPORT OUTLINE

1.5.1 Part ONE

Chapter 1 provides a brief history of PG system and MSCR test methods. The problem statement, significance, and objectives are also included in this chapter. Chapter 2 deals with the details literature review of the MSCR test method and MSCR implementation status in the USA. Chapter 3 presents the selection, collection, mixing procedure, and testing of the different types of the binders used in this study. Chapter 4 analyses and discusses the results obtained from Superpave and MSCR test data of unmodified, PMBs, WMA, and RAP-modified binders. Finally, Chapter 11 provides conclusions and recommendations for future study.

1.5.2 Part TWO

The presentation of the materials in Part Two is organized in the following order:

Chapter 5: The first part of this chapter presents a summary of the literature review conducted with a focus on the rheological and mechanical properties of polymer-modified binders and RAP binder blends. This chapter also summarizes previous studies related to the conventional binder characterization methods and their limitations. A review of literature focusing on the development, advantages, implementation and interpretations of the MSCR test method is presented in the last part.

Chapter 6: This chapter describes the selection, collection and preparation of polymer-modified binders and RAP binder blends and asphalt mixes. Descriptions of various test methods such as Superpave® tests, conventional and non-conventional MSCR tests and Hamburg Wheel Tracking (HWT) tests are also presented in this chapter.

Chapter 7: Analyses of the Superpave® and MSCR test results conducted on polymer-modified binders and RAP binder blends are presented in this chapter. Also, comparisons between the Superpave® and MSCR test results, the applicability of the MSCR test methods to characterize polymer-modified binders and RAP binder blends and effects of the addition of high amount of RAP are described in Chapter 7. The HWT test results conducted on the asphalt mixes containing polymer-modified binders and RAP are also presented in this chapter. The relations of the HWT test with the Superpave® and MSCR test methods are also discussed in this chapter.

Chapter 11: Important findings of this study and the recommendations based on these findings are presented in this chapter. The recommendations for future studies are also included in this chapter.

1.5.3 Part THREE

Part Three of this report is organized as follows. A detailed literature review of related research is included in Chapter 8. Chapter 9 contains methodology and materials used for development of the novel DSR-based extensional deformation test. Finally, Chapter 10 contains results and discussions related to temperature effect, geometry effect and reproducibility. Chapter 11 contains conclusions and recommendations from Part One, Two and Three.

CHAPTER 2

PART ONE LITERATURE REVIEW

2.1 VISCOELASTIC BEHAVIOR OF ASPHALT BINDER

Viscoelastic asphalt is a thermoplastic liquid that behaves as an elastic and plastic material. At higher temperatures an asphalt binder behaves like a Newtonian fluid, and at lower temperatures it behaves like an elastic material. At normal pavement service temperatures, the asphalt shows viscoelastic behavior [17]. Hence, at these temperatures, the asphalt shows a time dependent relationship between applied stress and resultant strain [18]. According to Airey [18] at intermediate ranges of temperature and loading times, asphalt represents three types (Figure 1) of strain, namely, linear elastic, delayed elastic and viscous strains.

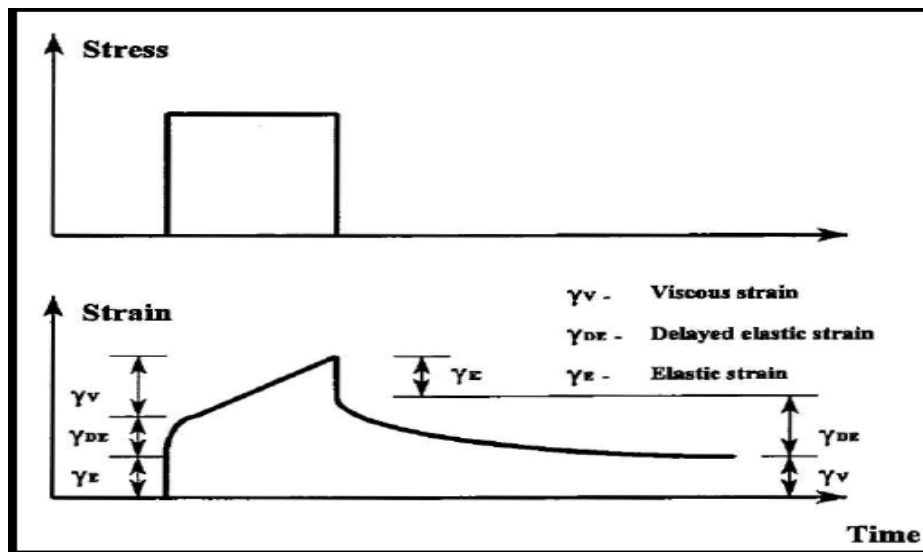


Figure 1. Viscoelastic response of bitumen under creep loading [18]

Among the three strains, viscous strain only results in the non-recoverable deformation when creep is applied on the asphalt binder. However, the other two strains are completely recoverable when the applied stress is released. At short loading durations and/or high testing temperatures, the asphalt binder reveals elastic response, and at intermediate loading durations and/or high testing temperatures it shows the delayed elastic response. Purely viscous and delayed elastic strain or deformations are time

dependent deformations [18]. Purely elastic deformation is recovered when the load is removed and the delayed elastic deformation is recovered, but the effect is not immediate.

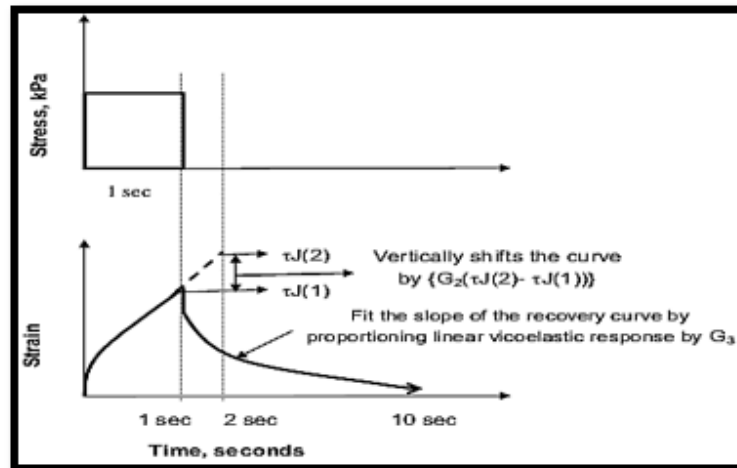
Shirodkar et al. [19] performed MSCR tests on different PMBs to characterize the MSCR curve. Based on this study, it was concluded that the creep and recovery curve could be categorized in three components: linear viscoelastic, non-linear viscoelastic, and permanent strain, as illustrated in Figure 2. These researchers also found that viscoelastic properties of the binder and effects of polymer in the binder can be characterized from the MSCR curve.

2.2 POLYMER MODIFIER

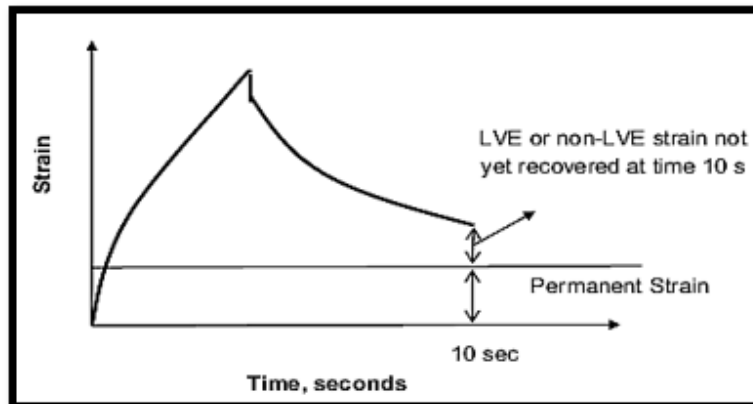
Traffic loads on pavements have increased in recent years. To sustain the increased loads, state DOTs are searching for the binders with improved performance compared to typical PG asphalt binders. In recent years, polymers are playing important roles in the asphalt industry to enhance the strength of the binders. Polymers make a secondary network or change the colloidal structure of the asphalt binders by molecular reaction within the asphalt binder. The physical properties like strength, stiffness, and adhesion of asphalt binders are responsible for enhancing or sustaining the pavement performance. Polymers not only increase the physical properties but also increase the mechanical and rheological properties of the binder. Polymers used for asphalt binder modification are divided into two groups, namely, plastomers and elastomers. Roughly 75% of the modifier are classified as elastomers, 15% as plastomers, and 10% either rubber or miscellaneous modifiers [21, 22].

Elastomers increase the elastic properties of the binders and decrease the permanent deformation of the pavement. As a result, the binder returns to its original state when the load is released. Different types of elastomers such as styrene-butadiene-styrene (SBS), natural rubber, reclaimed tire rubber/crumb rubber, polybutadiene, polyisoprene, isobutene isoprene copolymer, polychloropren, and styrene butadiene rubber (SBR) are used for modifying the binders [23,24].

Plastomers are used in binder to extend high rigidity and reduce the deformations under the traffic load. The addition of plastomers also increases the viscosity of the binder. Plastomers have high early strength under deformation, but they are less flexible compared to elastomers and tend to rupture under heavy loads [25].



(a)



(b)

Figure 2. (a) Schematic diagram of a 1-second creep and 9 -seconds recovery curve at 3.2 kPa for nonlinear viscoelastic curve; (b) Permanent strain of the creep and recovery curve of polymer-modified binder [20]

2.3 WMA TECHNOLOGY

Considering environmental impacts and overall construction costs of asphalt pavements, paving industries in many countries including the U.S. often use WMA

mixes in lieu of Hot Mix Asphalt (HMA) mixes. Additives used in WMA technologies reduce asphalt binders viscosity, which reduces the plant mixing and field compaction temperatures of asphalt mixes. The WMA additives can reduce the production and compaction temperatures from 20°C to 55°C [26-27]. Most of the existing studies on WMA are based on the Superpave tests. In the current study, selective WMAs are evaluated by using the MSCR test methods. Three commonly used WMA additives, namely, Sasobit® (an organic modifier), Evotherm® (a chemical additive), and Advera® (a water bearing agent), were evaluated in this study.

Considering environmental impacts and overall construction costs of asphalt pavements, paving industries in many countries including the U.S. often use WMA mixes in lieu of Hot Mix Asphalt (HMA) mixes. Additives used in WMA technologies reduce asphalt binders viscosity, which reduces the plant mixing and field compaction temperatures of asphalt mixes. The WMA additives can reduce the production and compaction temperatures from 20°C to 55°C [26-27]. Most of the existing studies on WMA are based on the Superpave tests. In the current study, selective WMAs are evaluated by using the MSCR test methods. Three commonly used WMA additives, namely, Sasobit® (an organic modifier), Evotherm® (a chemical additive), and Advera® (a water bearing agent), were evaluated in this study.

2.3.1 Organic-based WMA Technologies (Sasobit®)

Sasobit® is manufactured by Sasol Wax in South Africa. It is a synthetic wax that is produced in the coal gasification process [28]. Synthetic waxes are different from paraffin waxes, which are normally considered objectionable in asphalt. Synthetic waxes contain long chemical chains, which help to keep the waxes in solution.

Therefore, synthetic waxes help to reduce the viscosity of binder at conventional asphalt binder mixing and compaction temperatures. The melting point of the synthetic waxes is below 100°C, which helps reduce the viscosity of the binder above 100°C. According to Damm et al. [29], blending of 3 to 4% Sasobit® by weight allows a reduction in mixing temperature from 20°C to 40°C. The current study used 1.5% Sasobit® by the weight of the binder.

2.3.2 Water Bearing Additive Technologies (Advera®)

Advera® is available in the form of a very white powder, which is supplied by PQ Corporation. It contains finely powered sodium aluminum silicate hydrate (zeolite), which release water when Advera® is mixed with the binder. The released water makes a foaming effect in the asphalt binder, which increases the volume of the binder and decreases the viscosity. Advera® can release up to 20% of water when it is heated around 85°C to 182°C. The release operation of the water from zeolite happens very slowly which helps to extend time of workability for enabling the aggregate to be rapidly coated and compactable at temperatures significantly lower than those typically used for HMA [30]. According to the manufacture, the minimum dosage of Advera® in the asphalt mix is 0.25% by the weight of the mix. The current study used 6% Advera® by the weight of the binder that is around 0.3% (assume 5% asphalt binder in the asphalt mix) of the weight of the mix.

2.3.3 Chemical Additive-based Technologies (Evotherm® 3G)

Three types of Evotherm®, namely, Evotherm® 3G (third generation), Evotherm® ET (Emulsion Technology) and Evotherm® DAT (Dispersed Asphalt Technology) are available in the market. Evotherm® 3G was used in the current study as it was readily available to the research team. Evotherm® 3G is a chemical package, which was developed by MeadWestavaco Asphalt Innovations, Charleston, South Carolina [31]. Unlike Evotherm® DAT, this WMA additive is water-free. It can reduce the internal friction between the binder and coated aggregate during the mixing and compaction processes [32]. It can also reduce the mixing temperatures from 33°C to 45°C [32]. For this study, Evotherm® 3G was used at a rate of 0.5% by the weight of the asphalt binder, as recommended by the manufacturer.

2.3.4 Reclaimed Asphalt Pavement

Due to the increasing price of the asphalt binders, most of the DOTs and Hot Mix Asphalt (HMA) industries have been using the RAP as a replacement of virgin asphalt binders and aggregates in recent years. According to a NCHRP project [33], an asphalt mixture containing up to 20% RAP performs similar to that of a mixture with 100% virgin binder. Researchers of the NCHRP project reported that HMA mixtures with high

percentages of RAP showed higher resistance to rutting at high temperatures and lower resistance to fatigue cracking at low temperatures. Due to the disadvantages of the high percentages of RAP in fatigue cracking, high amounts of RAP are not usually recommended by researchers [34]. Swiertz et al. [35] and Mallick et al. [36] reported that a majority of the transportation agencies have use RAP in asphalt mixtures at percentages ranging from 10% to 20%. According to Copeland [37] and Jones [38], most of the DOTs including AHTD and TxDOT allow up to 30% of RAP in base courses and 10% RAP in surface courses.

2.4 TESTING METHODS

2.4.1 Superpave AASHTO M 320

In 1987, the U.S. congress approved the SHRP study to develop the techniques to improve the performance, durability, safety, and efficiency of the U.S highways (3). Initially, the SHRP study had a total of three objectives; one of which was to develop the asphalt binder specifications. To this end, the SHRP carried out a vast research program to develop the Superpave specifications and test methods for unmodified asphalt binders. In 1993, the PG asphalt binder specifications were introduced as a part of the Superpave system. These specifications were released as AASHTO M 320. The Superpave specifications provided a significant amount of information for evaluating and understanding the mechanism of rutting and fatigue behavior of asphalts. To measure the contribution of the binder to rutting under high service temperatures and fatigue at intermediate temperatures, the Superpave PG system introduced the Dynamic Shear Rheometer (DSR)-based test method (AASHTO T 315).

2.4.2 MSCR Test

The aforementioned literature review illustrated that the current PG specification was developed for unmodified binders. Thus, the PG specifications are inadequate to characterize the rutting and fatigue behavior of the PMBs. Bahia et al. [6] was initiated NCHRP Project No. 9-10, "Superpave Protocols for Modified Asphalt Binders," and reported that Superpave test methods were not suitable for characterizing the PMBs. The underlying reason was that the Superpave specifications were mainly developed on

the basis of unmodified binders. To resolve this issue, Bahia et al. [7] proposed a test method called the RCRT method. The RCRT method has some limitations. One of the limitations is that RCRT considers lower stress levels than the actual traffic loading to measure the permanent strain of binders. At lower stress levels, a majority of the PMBs do not show the nonlinear behavior. To overcome this problem, the FHWA modified the RCRT method by increasing stress levels and renamed it the MSCR test method [9]. The MSCR test method (AASHTO T 350) uses the well-established creep and recovery test concept. In the MSCR test method, one second shearing creep load is applied to the RTFO-aged asphalt binder by using a DSR. After the one second load is removed, the test sample is allowed to release the creep load for nine seconds. The test is started with the application of a low stress 0.1 kPa for 10 creep/recovery cycles, and then the stress is increased to 3.2 kPa, which is repeated for an additional 10 cycles. Figures 3 and 4 represent how the loads are applied in the MSCR test method. The MSCR test gives two major output parameters, namely, J_{nr} and percent creep recovery (%R), as shown in Figure 3. The J_{nr} value indicates the amount of residual strain left in the binder within the linear and nonlinear viscoelastic range at high temperatures and high stress levels. The percent creep recovery measures how much the asphalt specimen returns to its original position after the load is released.

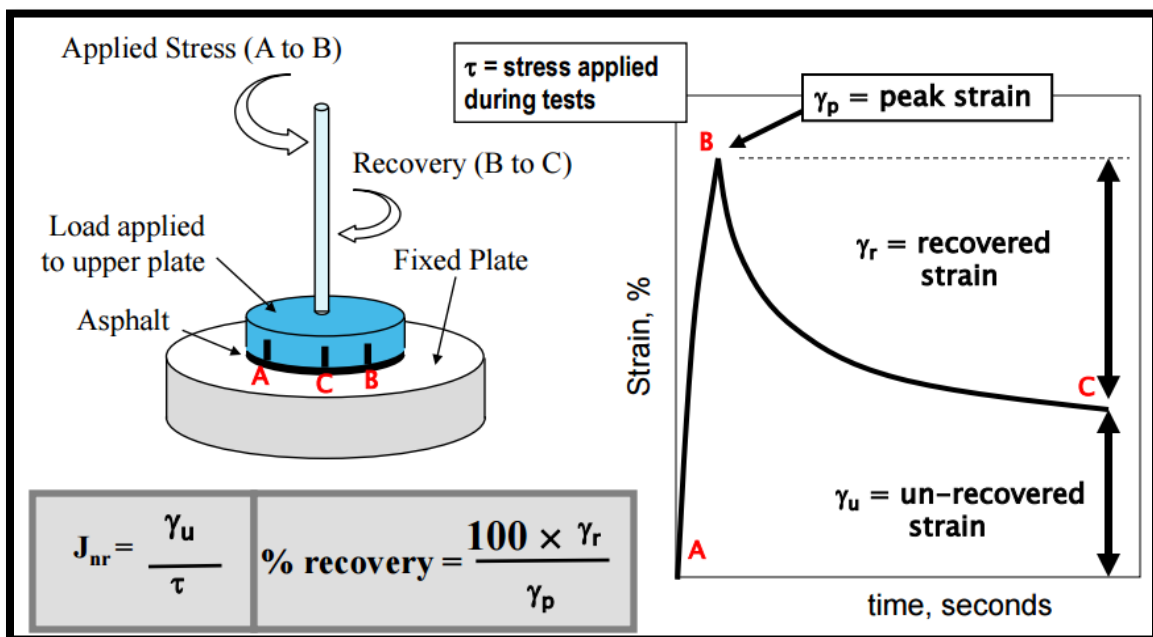


Figure 3. Showing the determination of the percent recovery and J_{nr} value

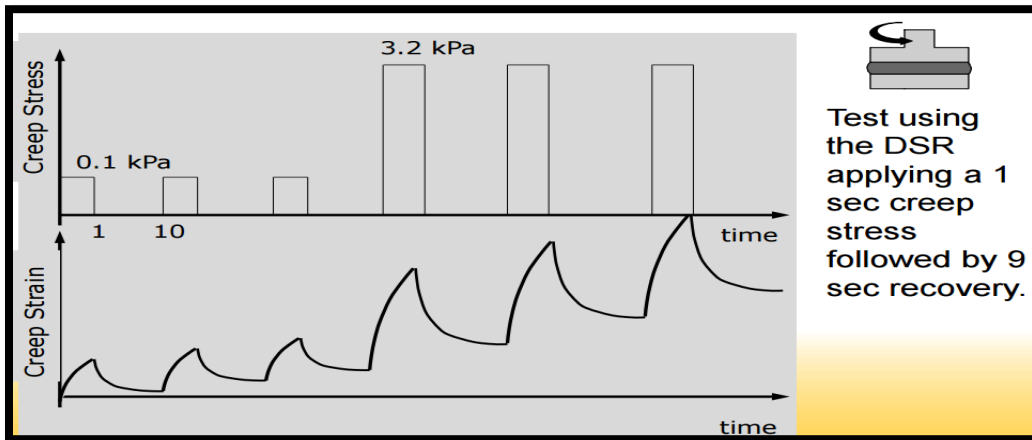


Figure 4. Loading scheme of MSCR test method [10]

2.5 DISADVANTAGES OF DSR TEST METHOD

The DSR test method is conducted in accordance to AASHTO T 315 (Determining the Rheological Properties of Asphalt Binder Using a DSR). This test method provides the rutting and fatigue behavior of the asphalt binder at very low strain level. From the various field study researchers found that the rutting and fatigue parameters obtain from this method does not well correlate with the actual field rutting [14]. At low strain levels, unmodified binders show the non-linear behavior. A majority of the PMBs are modified by using elastomers, which show the linear behavior at low strain level. Under low strain levels, the secondary network (which form by the molecular interactions of polymer) in the PMBs is never activated [39].

In the MSCR test, high levels of creep load and strain are applied to the binder that reflect the actual field condition. The FHWA Accelerated Loading Facility (ALF) study revealed a very poor correlation between rutting parameter of DSR test and field rutting with a R^2 value of only 0.13. The relationship of J_{nr} to rutting was significantly better, with a R^2 value of 0.82.

2.6 DISADVANTAGES OF “PG PLUS” TESTS

Many agencies have introduced additional tests to characterize polymer-modified binders, such as ER, tenacity, and forced ductility (FD). These tests along with their specifications, are called the Superpave “PG Plus” specifications [14]. Like other state agencies, the AHTD and TxDOT use the ER test to determine the presence of polymer in the asphalt binder. The recommended ER value varies from one state DOT to another state DOT. The ER test is time consuming as a single ER test requires about 4 hours. But, the MSCR test can be performed only within 1 hour. Also, the MSCR test can be performed by using a DSR machine, which is used for AASHTO T 315. Additional equipment called a ductilometer is needed for conducting the ER test. The ductilometer is an expensive piece of equipment that imposes additional cost to the agency. Another PG Plus test called the forced ductility is also used by some state agencies. Tabatabaee et al. [40] found that there was no correlation between the ductility test data and fatigue, and between the former and rutting resistance of asphalt pavements.

2.7 IMPLEMENTATION OF MSCR METHOD

The Asphalt Institute (AI) has been working with the New England Asphalt/User Producer group (NEAUPG), Southeastern Asphalt User/Producer Group (SEAUPG), North Central Asphalt User/Producer Group (NCAUPG), Rocky Mountain Asphalt User/Producer group (RMAUPG), and Pacific Coast Conference on Asphalt Specifications (PCCAS) to develop the MSCR implementation strategies across the U.S.

The MSCR test can be implemented in two ways, one is Full Implementation (FI) and other is Partial Implementation (PI) [41]. The FI process includes complete replacement of AASHTO M 332 [42] instead of AASHTO M 320. The FI is a revised grading system based on climate and loading, and it eliminates grade bumping and PG Plus tests. Whereas, both AASHTO M 332 and AASHTO M 320 are to be considered for grading the binders in the PI process. The current Superpave specification, AASHTO M 320, is completely based on the climate condition, and it does not relate the traffic conditions.

For example, a state that does not follow AASHTO M 332 will use a same binder (e.g. PG 70-22) for a county road as well as for an Interstate, where the maximum 7-day consecutive pavement temperature (98% reliability) is 64°C and the minimum pavement temperature (98% reliability) is greater than -22°C. AASHTO M 332 solves this issue as this specification considers the traffic condition as well as the climate condition. But, some agencies are still avoiding the FI of MSCR because of they are trying to avoid the “major task” of a name change [43] (e.g. according to new specification, the MSCR grade of a PG 70-22 binder will be PG 64E-22, PG64V-22, PG64H-22, or PG64S-22).

There are some obstacles in accepting the MSCR test specifications by the highway agencies. One of the obstacles is the nomenclature of asphalt binders. As typically the MSCR test is performed at 64°C, a PG 70-22 binder might be called a PG 64H-22 binder. To avoid this naming issue, the AI suggested using this naming technique as an interim solution. As soon as both the users (agencies) and suppliers (refineries) are comfortable with this naming convention, the naming technique can be implemented in FI. Moreover, a survey conducted in 2010 revealed additional difficulties in implementing the MSCR specification. These obstacles include insufficient DSR equipment and software, lack of resources to perform transitional tests, lack of guidance from suppliers and other states, and uncertainty about the effects on binder supply and modification processes.

In the U.S., various user groups and agencies have implemented or are using the MCSR test method to characterize the PMBs. Such initiatives have governed a few state groups to verify the reproducibility of MSCR tests and the specification criteria [44, 45]. The New England Asphalt/User Producer group (NEAUPG), Southeastern Asphalt User/Producer Group (SEAUPG), North Central Asphalt User/Producer Group (NCAUPG), Rocky Mountain Asphalt User/Producer group (RMAUPG), and Pacific Coast Conference on Asphalt Specifications (PCCAS) are conducting an inter-laboratory study (ILS) to determine the precision of AASHTO T 350 for DOTs. The SEAUPG in 2011, Expert Task Group (ETG) in 2009, PCCAS in 2013, and the NEAUPG in 2010 and 2012 have also initiated ILSs through participation of multiple

laboratories to evaluate the repeatability and reproducibility of AASHTO T 350 test results [46-48]. The AI is trying to make the DOTs conscious of the advantages of the MSCR test method over the time consuming “PG Plus” tests [49-61]. A summary of the MSCR test method implementation pathways of these state DOTs are given below [48, 62-66]:

- New York, Maryland, Connecticut, Virginia, Oklahoma, Florida, Dist. of Columbia, Louisiana and Missouri have adopted FI of AASHTO M 332 for all grades binder.
- New Hampshire, Maine, Rhode Island, New Jersey have adopted the FI of AASHTO M 332 for modified grades binder.
- North Dakota, South Dakota, Nebraska, Iowa, Minnesota, and Wisconsin will adopt the FI of AASHTO M 332 within a year.
- Pennsylvania and Delaware have allowed a substitution of PG 64E-22 in 2015.
- Kentucky, South Carolina, Illinois and Tennessee have replaced the PG-Plus test with %R of MSCR test.
- Georgia currently uses the MSCR parameters for Ground Tire Rubber (GTR) modified binder [66].
- Utah has been using %R of MSCR test on micro surfacing emulsion.
- Washington (WA) has also implemented the MSCR parameters for all types of binder. But this state will use only Heavy (H), Very Heavy (V), and Extreme (E) grades for grading the WA’s binders.
- Nevada has accepted the AASHTO M 332 specification only for PG 76-22 binder.
- MS, NC, and WV have considered the implementation of some form, and they are still working on that.
- Some states have accepted or will accept the FI of AASHTO M 332 for one or two types of binder or for special modified binder like modify by Reclaimed Asphalt Pavement (RAP).

Figure 5 represents the state of implementation of the MSCR test, as of 2014. Since no analyses have been done for commonly used binders and conditions prevailing in

Arkansas other than the present study, no guidelines are currently available for Arkansas. TxDOT has done the MSCR test only for PG 58-28, PG 64-22, and PG 70-34 binders [62], but they did not perform any MSCR tests on PG 70-22 and PG 76-22 binders. In this study, Texas' PG 70-22 and PG 76-22 binders were also considered for developing the MSCR guidelines for TxDOT.

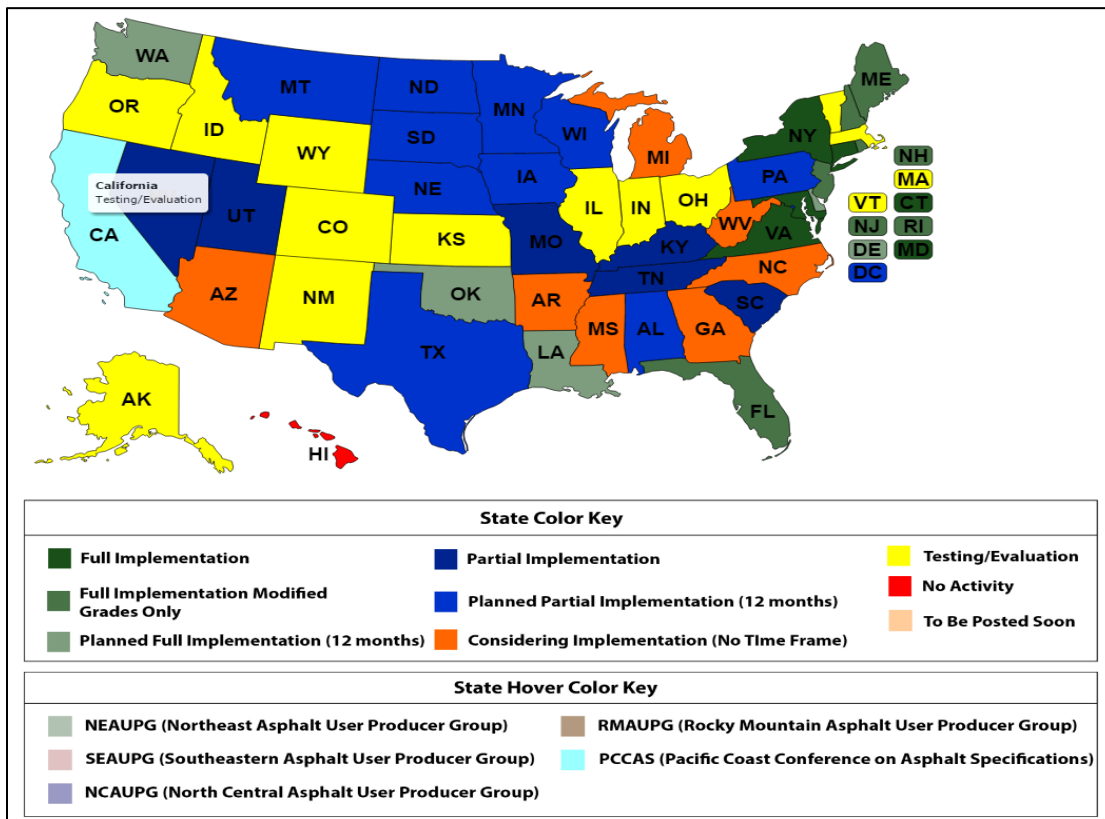


Figure 5. Current status of MSCR test method implementation [63]

2.8 MSCR STUDY RELATED TO PMBS

Various studies have been done on topics related to the MSCR test method. Based on previous studies [e.g., 14] researchers reported that the MSCR test was a better tool for characterizing PMBs and other stiff binders than other test methods such as ER. While validating the MSCR test method, D'Angelo [10] considered a few MnROAD test sections, the FHWA's ALF study, and an I-55 Mississippi Field study for different types of binders and mix designs. The MnROAD study used three binders: an unmodified binder (PG 58-28), and two PMBs (PG 58-34 and PG 58-40). DSR tests were done on

RTFO- aged binders for measuring the $G^*/\sin\delta$ value at 58oC, and MSCR tests were done at stress levels from 0.025 to 25.6 kPa at 58oC, and the field rut depths were estimated by using a Hamburg Wheel tester. It was reported that the field rutting did not correlate well with the rutting factor when rutting value was greater than 15 mm. But, the MSCR-based J_{nr} and the field rutting in the cases of the MnROAD mixes provided a much better correlation with field rutting. In the ALF study, total seven types of PMBs and twelve types of mix designs were tested for DSR rutting factors, MSCR non-recoverable compliance at 640C, and field rutting at service temperatures. At low stress levels up to 1.00 kPa, the J_{nr} values of most of the binders exhibited a linear response and the J_{nr} values remained constant with an increasing stress level. Figures 6 and 7 clearly show that the J_{nr} value from the MSCR test is better correlated ($R^2= 0.82$) with rutting in ALF study compared to the $G^*/\sin\delta$ value from SHRP criteria ($R^2= 0.2$). In the I-55 Mississippi field study, total 8 PMBs and one control binder were used for mix designs. In this study, MSCR tests were done at 3.2 kPa and at 70oC. The MSCR test results were found to be better correlated with field rutting compared to the SHRP test results.

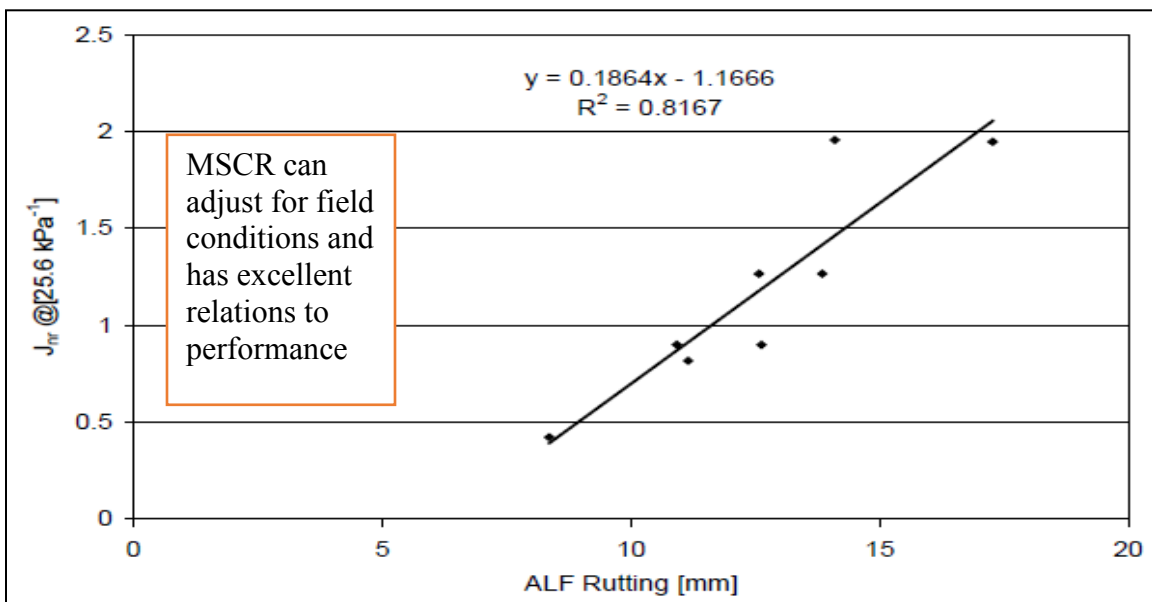


Figure 6. J_{nr} vs. ALF rutting [10]

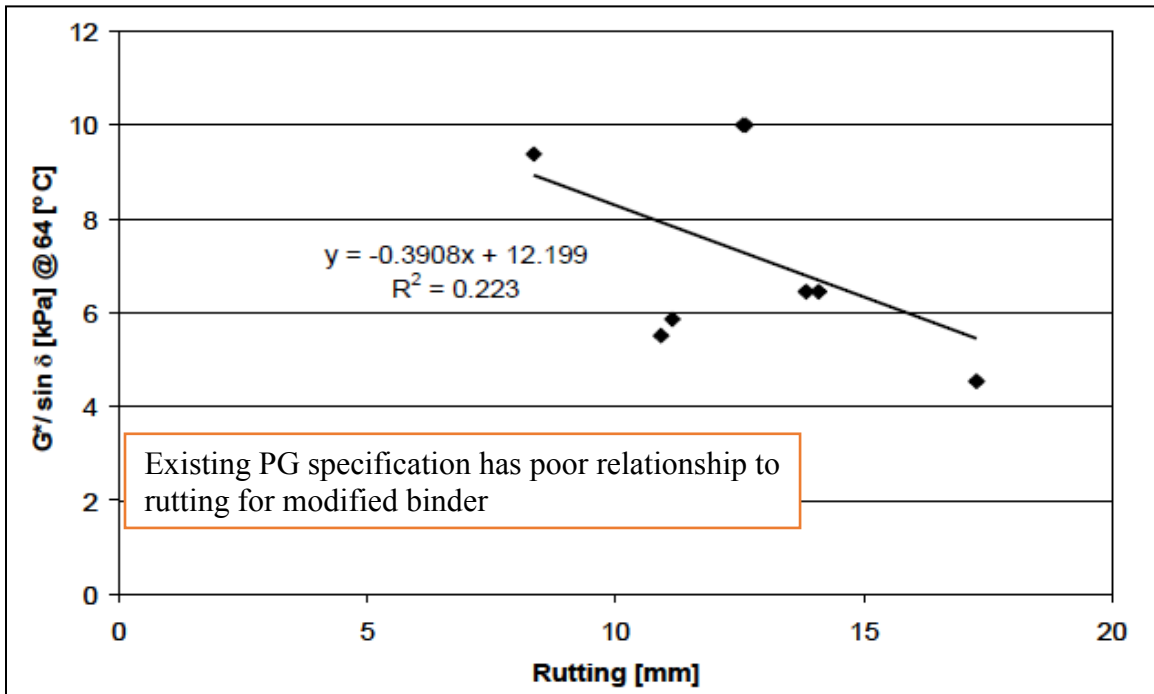


Figure 7. $G^*/\sin \delta$ vs. ALF rutting [10]

DuBois et al. [64] performed PG, MSCR, forced ductility, dynamic complex modulus tests and flow tests on the PMBs and unmodified binders to determine the feasibility of using the MSCR test method in New Jersey Department of Transportation (NJDOT) construction projects. From this study, the authors found that the MSCR elastic recovery curve requirement appears to be more precise requirement to evaluate elastic response as compared to the ER test results at 25⁰C. Binders with Jnr values of less than 0.5 kPa-1 appear to show better high temperature performance. The authors also reported that the MSCR recovery of 40% or more at 3.2 kPa will ensure that it is above the MSCR elastic recovery curve. This could serve as specification to the MSCR test method. This study also reported that the MSCR test method was more economical compared to the ER test. This study would be useful for NJDOT because using the MSCR parameter in the binder specification would have the potential to allow the New Jersey to open the market to abroad range of modified binders.

Wasage et al. [65] tested unmodified, PMBs and crumb rubber modified binders by following the MSCR test method at stress levels from 0.025 to 25.60 kPa and at temperatures ranging from 30°C to 70°C. Based on the laboratory test results, the authors reported that the %R for unmodified binder was very low compared to that of the PMBs. Crumb rubber modified binder and PMB showed nonlinear viscoelastic properties at higher stress levels. It was also observed that the value of J_{nr} for the unmodified binder depended on the temperature, but for PMB or crumb rubber modified binders mainly depended on the temperature as well as the stress level. The best correlation between J_{nr} and rut depth was obtained at the highest MSCR stress level of 12.8 kPa.

For analyzing and describing the creep recovery behavior of asphalt binders, Domingos et al. [66] performed MSCR tests on a PG 76-XX binder modified with different additives. MSCR tests were conducted on these binder samples at temperatures varying from 52°C to 76°C. These researchers found that the MSCR test parameters were helpful to characterize the polymer modified binders.

Santagata et al. [67] used the MSCR test method to evaluate the rutting resistance of different PMBs and also investigated the effects of several factors such as polymer type, composition, structure and the dosage of modifiers. The effect of the short-term aging condition was also investigated in this study. PMBs were tested by applying 0.1 kPa shear stress, with a temperature variation of 40°C, 60°C and 80°C. They found that the polymer structures changed due to the change of temperature; as a result, the aging effect changed relative rankings of asphalt binders.

Nejad et al. [68] performed the MSCR and Zero shear viscosity (ZSV) tests, and estimated a rutting parameter ($G^*/(1-(1/\tan\delta\sin\delta))$) proposed by Shenoy [69] for evaluating the effect of high density polyethylene (HDPE) on the rutting properties of a penetration (85/100) grade binder. It was observed that that the Shenoy's rutting parameter gave a negative result, which means that the rutting parameter proposed by Shenoy [69] was unable to measure the rutting characteristics of highly modified

binders. Based on the three test parameters, these researchers concluded that the MSCR test method was easier for predicting the rutting resistance of highly modified binder compared to other two test methods. The ZSV method was time consuming and the Shenoy's proposed rutting parameter gave the negative result for highly modified binder.

Laukkanen et al. [70] performed MSCR tests for predicting the rutting behavior of three unmodified, three elastomer-modified, two elastomer with wax-modified, and one wax modified binders. The MSCR tests were conducted on unaged binders and at 50°C. Based on the test results, researchers concluded that wax alone and wax with elastomer modified binders showed higher stress sensitivity and higher percent recovery compared to other modified and unmodified binders. These researchers also found that the change of percent recovery as well as the non-recoverable compliance values of unmodified binders are very small compare to the modified binders (wax alone and wax with elastomer). From the result of the LPC wheel tracking device and MSCR parameters, researchers indicated that Jnr and %R values were well correlated with the rutting value.

For comparing the accuracy of the AASHTO M 320 PG and the AASHTO M 332 MSCR grade, Davidson et al. [71] conducted MSCR and DSR tests on selected SBS modified binders. All binder samples were tested at 64°C. Based on the test results, the authors concluded that Jnr decreased and %R increased with the increase of the SBS in the unmodified binder. The addition of 2% SBS would increase the binder's MSCR grade by one traffic level, from S to H, or from H to V. From this study, the authors decided that MSCR is the better test method for characterizing the PMBs.

To evaluate the effects of stress levels, temperature, and percentage addition of a polymer on the Jnr value of MSCR test parameters, Hafeez et al. [72] conducted the MSCR test on two types of unmodified binders, and five types of modified asphalt binders, which is modified by different percentages of Elvaloy. MSCR tests were performed at 58, 64, 70, 76°C and at a stress levels ranging from 0.025 to 25.6 kPa.

The test results revealed that J_{nr} value for all binders except the 2% Elvaloy modified binder were linear up to a stress level of 3.2 kPa. After the 3.2 kPa stress level, the J_{nr} values gradually increased. The percentage of modifier has an effect on the J_{nr} value. Based on the test results, the researchers concluded that stress sensitivity of the binders decreased with an increase the percentage of Elvaloy with the unmodified binder. In this study, the authors also found that the J_{nr} value was well correlated ($R^2 = 0.96$) with the mixers rut depth, which was obtained from a Hamburg Wheel Tracking (HWT) tester. Zoorob et al. [73] reported that stress sensitivity of PMBs are more apparent and distinguishable at higher stress levels.

Zhang et al. [74] pursued a laboratory study to compare the rutting parameters of the DSR and MSCR tests along rut depths from the HWT and Repeated Loading Permanent Deformation (RLPD) tests. The coefficient of correlation (R^2) between the DSR-based $G^*/\sin\delta$ (at 64°C, 70°C, and 76°C) and rut depth from the HWT was below 0.5, and the coefficient of correlation between $G^*/\sin\delta$ and rut depth from the RLPD was around 0.6. The J_{nr} values at 0.1 kPa and 3.2 kPa showed good correlation ($R^2 > 0.75$) with the HWT rut depth. The rut depth from the RLPD was also well correlated with the J_{nr} value at 0.1 kPa ($R^2 > 0.9$) compared to the J_{nr} value at 3.2 kPa.

Stevens et al. [75] analyzed the Arizona's Department of Transportation (ADOT) MSCR database to evaluate potential implications of the adoption of the AASHTO M 332 specification based on MSCR test parameters: J_{nr} and %R. The ADOT's MSCR database prepared on the basis of more than 375 different asphalt binder samples. By using the MSCR method, Arizona's binders were graded at multi high temperatures as specified in AASHTO M 320. The authors reported that the current numbers of binder grade would increase from 8 to 13 if the ADOT used AASHTO M 332 without any changes of binder properties in the specifications.

2.9 STUDY RELATED TO WMA

Considering environmental impacts and overall construction costs of asphalt pavements, paving industries in many countries, including the U.S. often use WMA

mixes in lieu of HMA mixes. Additives used in the WMA technologies reduce asphalt binders viscosity, which reduces the plant mixing and field compaction temperatures. Researchers have invested a great deal of study to characterize the PMBs by using the MSCR test. But, in the case of WMA, the amount of study related to MSCR is very negligible. So, in this study, WMA also considered for characterizing selected WMA binders by following the MSCR test method.

To evaluate the applicability of Sasobit® in WMA applications, including the effect of WMA in the environment, Hurley et al. [76] performed a laboratory study on the asphalt mixtures, which were made by two types of aggregate and two asphalt binder grades (PG 64-22 and PG 58-28) with Sasobit®. In this study, the PG 64-22 binder was produced in the laboratory by adding 2.5% Sasobit® with PG 58-28, The PG 70-22 binder was produced by adding 4% Sasoflex with PG 58-28, and the PG 76-22 binder was produced by adding 4% Sasoflex with PG 64-22. The addition of Sasobit® or Sasoflex reduced the amount of design asphalt binder content as well as air voids (up to 0.87%) in the mix design. From the Asphalt Pavement Analyzer (APA) and Hamburg test data, these researchers observed that Sasobit® increased the rutting potential compared to control mixtures. The APA test results showed that Sasobit® did not affect the resilient modulus of asphalt mixes. For determining the tensile strength ratio and moisture susceptibility of mixtures, the tensile strength and Hamburg tests were conducted in the lab. Test results showed that without an anti-stripping agent, Sasobit® increased the moisture susceptibility of the asphalt mixtures compared to control mixtures. As the MSCR test did not evolve during the study period, it was out of the scope of this study.

To evaluate the applicability of Evotherm® in warm mix asphalt (WMA) applications including the effect of WMA in the environment, Hurley et al. [77] performed a laboratory test on the asphalt mixes which were made by two types of aggregate (granite and limestone) and two asphalt binder grades (PG 64-22 and PG 76-22). The addition of Evotherm® reduced the amount of design asphalt binder content as well as air voids (up to 1.4%) in the mix design. From the APA and Hamburg tests, these researchers

observed that Evotherm® increased the rutting potential compared to a control mixture. The APA test results showed that Evotherm® increased the resilient modulus of asphalt mixes when compared to the control mixture. The tensile strength ratio (TSR) and moisture susceptibility test results of asphalt mixtures showed that Evotherm® decreased the moisture susceptibility of the mixtures when compared to the control mixture.

To investigate the effect of WMA additives on the performance of PMBs, Kim et al. [78] conducted Superpave tests on same PG grade of PMBs from different types of WMA additives. In this study, PG 76-22 binders were collected from three different sources, and they were modified by Sasobit® and Asphamin® at rates of 1.5% and 0.3%, respectively by weight of the asphalt binder. From the DSR test results for the unaged binder, the authors observed that binders with WMA exhibited higher resistance to rutting at a higher temperature when compared to the neat PMBs. At intermediate temperatures, the values of $G^* \cdot \sin \delta$ for PMBs with WMA were higher compared to the PMBs without WMA, meaning that the addition of the additives in the PMBs being less resistant to fatigue cracking. The warm PMBs were found to have significantly higher stiffness values which relates to possible lower resistance on low temperature cracking. The PMBs with Sasobit® showed significantly lower m-values than the control PMBs.

Ziari et al. [79] performed MSCR tests to evaluate the effect of Sasobit® in a 60/70 penetration grade binder. MSCR test result showed that the percent recovery value of WMA modified binder was higher compared to the original binder.

To evaluate the effect of the two WMA additives (Sasobit® and Asphamin®) on the viscosity and rutting properties of rubber modified asphalt (RMA) binders, Akisetty et al. [80] prepared the WMA by adding 10% RMA. Binders from five different sources were studied in this research. The viscosity of the RMA with Asphamin® was higher compared to the control binders (without Asphamin®). Authors mentioned that the cause of higher viscosity of binders by addition of Asphamin® is due to the filling effect of the additive. But the addition of Sasobit® with RMA reduced the viscosity compared

to the control binders. The rutting parameters of the unaged and RTFO-aged WMA were higher compared to the control binders.

Morea et al. [81] prepared five types of mixtures for evaluating the effect of WMA and tensoactive additives on the conventional asphalt (CA) and PMB. Rheological tests including DSR and MSCR tests were performed for determining properties of extracted binders from asphalt mixes. The Hamburg wheel tracking test was also performed on asphalt mixes for evaluating their rutting and moisture susceptibility. Creep stresses (0.1 kPa and 3.2 kPa) were applied for 2 sec and subsequently the load was removed; then the extracted binders were allowed to relax for 18 sec during the MSCR test. Based on the DSR test results, the change of rheological properties of binders from HMA and WMA (without additives) with CA was negligible compared to the HMA and WMA (without additives) with PMB. For the extracted binders from the asphalt mix of WMA (with additives) with PMB, the accumulated strains during the MSCR test decreased compared to the extracted binders from control WMA mix (without additives) with PMB. The rutting resistance of blends without additives was better for HMA (with CA and PMB) compared to the WMA (with CA and PMB). The authors found that the addition of additives to the conventional asphalt did not change the rutting performance of the binders. In the case of PMB, the authors did not find significant effect of additives on the rutting resistance.

2.10 STUDY RELATED TO RECLAIMED ASPHALT PAVEMENT

Mannan [82] performed the MSCR test to evaluate the effect of recycled asphalt shingles (RAS) on the physical and chemical properties of the asphalt binders. She found that, the addition of RAS into the virgin binder decreased the J_{nr} value, which indicated that the addition of RAS binders increases the resistance of permanent deformation. Wu et al. [83] investigates the performance of HMA with and without RAS and RAP based on the evaluation of field cores drilled from four experimental sections of Washington State. They also used the MSCR test to evaluate the rutting performance of the virgin binder with RAP and RAS. Based on the laboratory study, Wu et al. [83]

found that the addition of RAP and RAS increased the %R of the MSCR test. Similar kind of result also found other researchers [84-87].

2.11 INTERPRETATION OF MSCR TEST RESULTS

2.11.1 Polymer Method

Based on the aforementioned literature review, strain response of the PMB is nonlinear and depends on the stress levels. MSCR parameters are not only used for measuring the stress sensitivity but also used for measuring the elasticity of the asphalt binder by measuring the recovery percentage from peak loading [88]. Unmodified binders tend to recover a lower percentage of the imposed strain than modified binders due to the absence of elastomeric polymer. The polymer method is similar to the elastic recovery test in respect to elasticity response of PMB. The FHWA conducted MSCR tests on different types PMBs and has correlated the %R and J_{nr} values [89]. Figure 8 shows the standard MSCR curve, relating to the %R and J_{nr} value at 3.2 kPa [42]. AASHTO M 332 proposed a relationship for detecting the polymer in the asphalt binders, which is shown in Equation 1. In Figure 8, the curved line represents the minimum %R value (Y-axis) corresponding to J_{nr} value (X-axis) at 3.2 kPa. Asphalt binders that fall above the curve are considered to have sufficient delayed elastic response; those which are below the curve are considered of low elasticity. The % R value at J_{nr} value greater than 2.0 is not considered for evaluating the presence of elastomer into the PMB [90].

$$R = \begin{cases} 29.37 (J_{nr, 3.2 \text{ kPa}})^{-0.2633} & J_{nr, 3.2 \text{ kPa}} \geq 0.1 \\ 55 & J_{nr, 3.2 \text{ kPa}} < 0.1 \end{cases} \dots \dots \dots (1)$$

2.11.2 Quadrant Method

The quadrant method is a simple way to analyze the %R and ER data of the binders, which helps to organize customer satisfaction data. Hossain et al. [91] applied this method to measure the minimum %R value for Oklahoma department of transportation (ODOT) and set the minimum %R value for PG 70-22 and PG 76-22 as 50% and 80%, respectively without penalizing suppliers or risking users. The quadrant diagram is

obtained by plotting the agency or DOT recommended ER data in the X axis and %R at 3.2 kPa, which is 15% less than the state recommended ER [92] value in the Y axis. A typical quadrant plot is shown in Figure 9. The minimum %R value depends on the binder types. Each DOT has minimum ER value or phase angel for particular binders. AHTD allows the minimum ER value at 25°C for PG 70-22 and PG 76-22 are 40% and 50%, respectively. TxDOT allows the minimum ER value at 25°C for PG 70-22 and PG 76-22 are 30% and 50% respectively. The quadrant plot has a total of four quadrants, namely, Pass (1st quadrant), User Risk (2nd quadrant), Fail (3rd quadrant), and Supplier Risk (4th quadrant). Any point falling in the first, second, third and fourth quadrants indicates that the binder meets both ER and %R targets, (neither user nor supplier is at risk), meets %R but fails on ER, fails on both %R and ER, and fails on %R but meets ER, respectively. The term “Pass” is used to indicate a situation where both MSCR %R value and ER value meet the MSCR %R specification and DOT’s recommended criterion, respectively. As first quadrant meets both criteria, it is in the safe zone for suppliers as well as for users. The diagonal opposite term is called “Fail,” which is used to indicate neither %R nor ER value meets the MSCR %R specification and DOT’s recommended criterion, respectively. The other two terms, called User Risk and Supplier Risk are used for comparison between the ER or phase angel and MSCR %R value. In this study, %R recovery data from the laboratory testing and ER value from the binder’s supplier were analyzed on the basis of the AHTD’s minimum ER value.

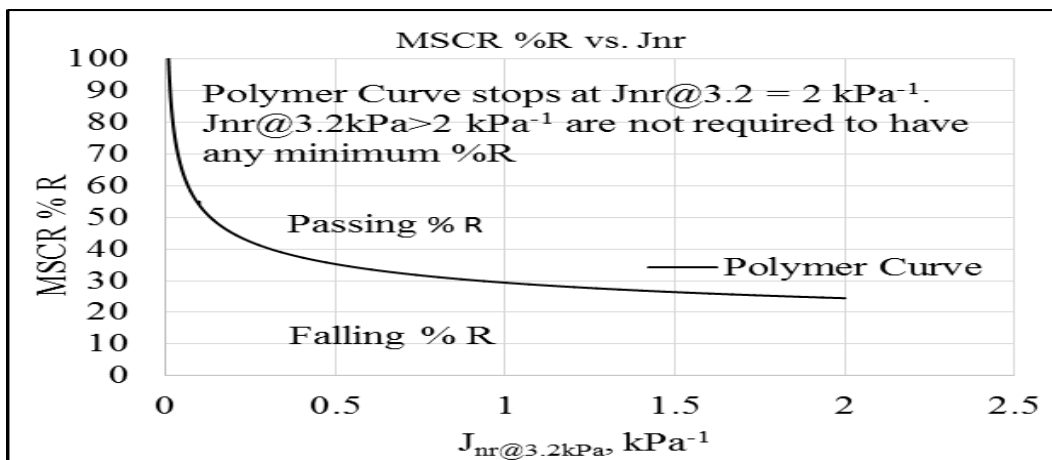


Figure 8. Polymer curve for detecting the polymer based on the MSCR % R at $J_{nr,3.2kPa}$.

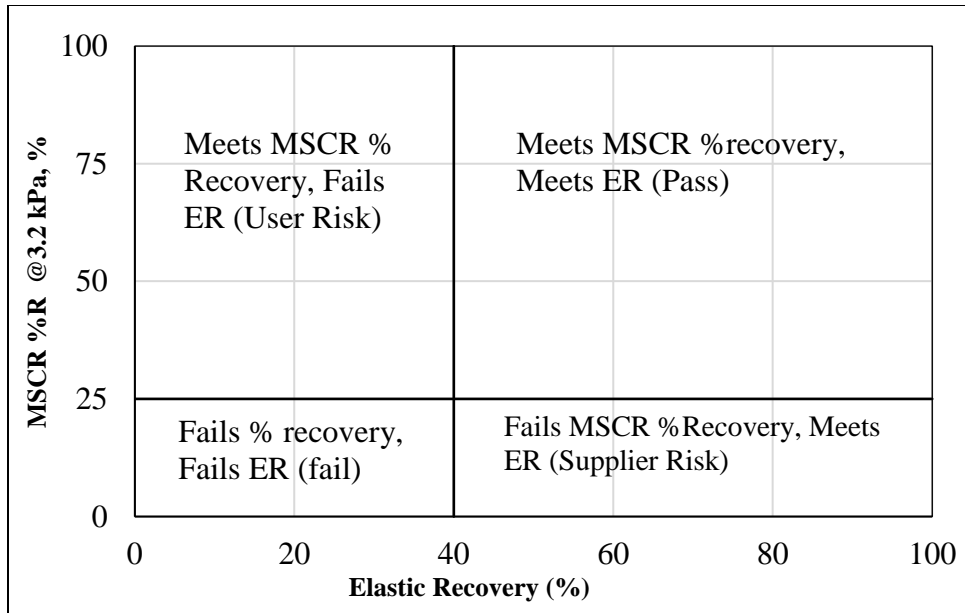


Figure 9. Quadrant plot for analyze the MSCR % R based on the ER value

THIS PAGE IS INTENTIONALLY BLANK

CHAPTER 3

PART ONE METHODOLOGY

3.1 INTRODUCTION

This chapter includes details and the overall approach of the study. It is comprised of a description of the materials used in this study, extraction and recovery of the binder from RAP, mixing procedures of the RAP and WMA additives with the virgin binder, the experimental plan to complete the proposed research, and the experimental procedures to complete the research objectives. The flow chart of this study is shown in Figure 10. Laboratory-based tests conducted in this study are: MSCR, DSR, Rotational Viscometer (RV), and Bending Beam Rheometer (BBR). Each of these tests along with their details procedures is discussed in this chapter.

3.2 MATERIAL SELECTION AND PREPARATION

3.2.1 Unmodified and Modified Binder

Two types of PMBs (PG 70-22, PG 76-22) and one unmodified binder (PG 64-22) from 9 sources and two types of PMBs from three sources were collected to achieve the objectives of this study. Table 1 represents the selected refinery locations along with the types of binders collected from each refinery. The refinery locations are also shown in Figure 11.

3.2.2 Reclaimed Asphalt Pavement (RAP)

Two types of coarse RAP samples namely, RAP1 and RAP2, were collected from I-40 in Forrest City, Arkansas and from I-40 near Alma, Arkansas, respectively. According to the AHTD's record book (J file-page 350 and page 88/21), the construction of sections from which RAP1 and RAP2 were collected, finished on Mar. 29, 2002 and Apr. 22, 2003, respectively. Those RAP (cylindrical core) samples are about 13 years old. Figure 12 shows the details procedure of collection of the cylindrical cores.

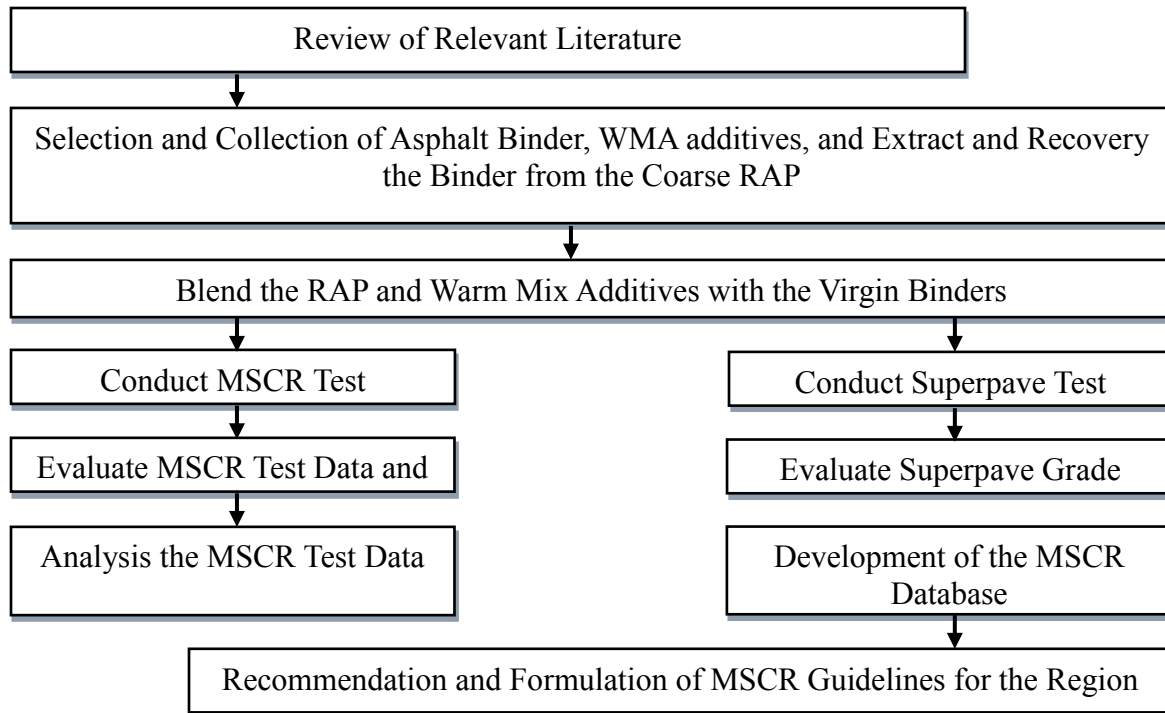


Figure 10. Flow chart of this study

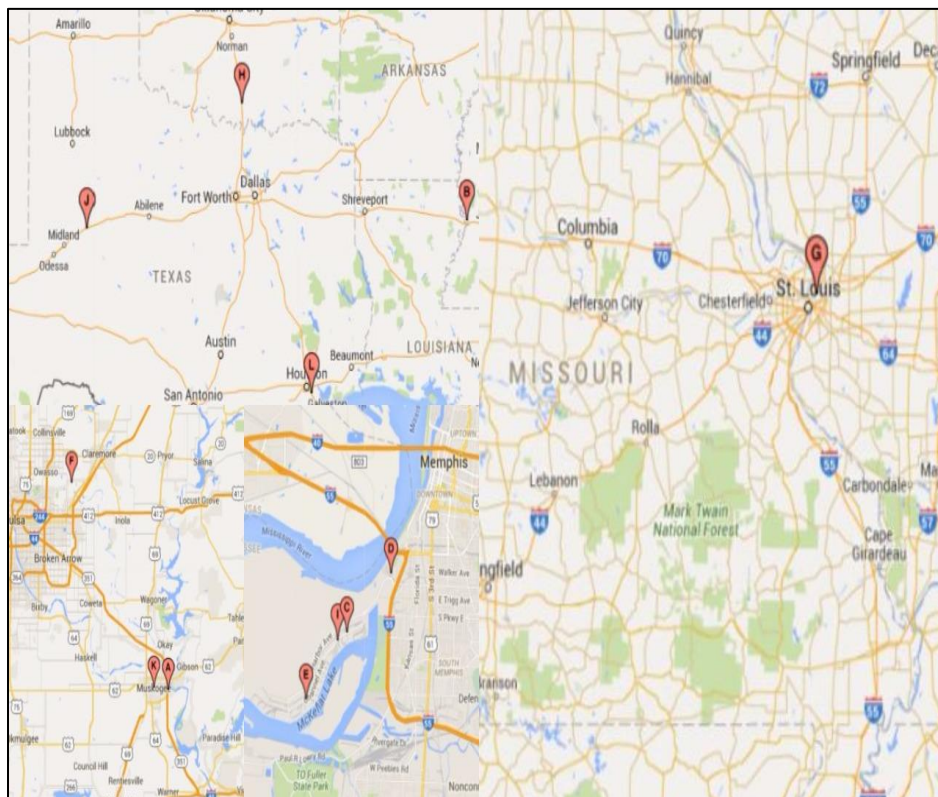


Figure 11. Location of binder's sources

Table 1. Types and source-location of binders

Source	Source	Source Approved	Binder types
S1	A	AHTD	PG 64-22, PG 70-22,PG 76-22
S2	B	AHTD	PG 64-22, PG 70-22,PG 76-22
S3	C	AHTD	PG 64-22, PG 70-22,PG 76-22
S4	D	AHTD	PG 64-22, PG 70-22,PG 76-22
S5	E	AHTD	PG 64-22, PG 70-22,PG 76-22
S6	F	AHTD	PG 64-22, PG 70-22,PG 76-22
S10	G	AHTD & TXDOT	PG 64-22, PG 70-22,PG 76-22
S11	H	AHTD & TXDOT	PG 64-22, PG 70-22,PG 76-22
S12	I	AHTD & TXDOT	PG 64-22, PG 70-22,PG 76-22
S7	J	TxDOT	PG 70-22,PG 76-22
S8	K	TxDOT	PG 70-22,PG 76-22
S9	L	TxDOT	PG 70-22,PG 76-22



Figure 12. Collection of RAP coarse from the existing pavement

3.3 BINDER EXTRACTION AND RECOVERY

The RAP binder was extracted from the coarse RAP samples followed by AASHTO T 164 (Quantitative Extraction of Asphalt Binder from Hot Mix Asphalt) and recovered using ASTM D 5404 (Recovery of Asphalt from Solution Using the Rotary Evaporator). The collected RAP samples (cores) were heated in an oven of $110 \pm 5^{\circ}\text{C}$, and then they were broken down, and about 800-1000 gm of samples were placed into an extraction bowl as shown in Figure 13. The bowl containing test samples were then placed into an extraction apparatus (centrifuge). N-propyl bromide (n-PB) solvent was used for separating the RAP binder from the aggregate. The loose samples were soaked into the 500 ml of n-PB for about 5-6 hours. A dried filter, also shown in Figure 13 was placed around the rim of a bowl and over on the bowl is tightly clamped. A beaker was set up to collect the extracted solution. After 5-6 hours, the centrifuge was slowly started and the speed was gradually increased (maximum up to 3600 r/min) until solvent ceased to flow from the drain.



Figure 13. Centrifuge machine with extraction bowl and filters

The Rotary Evaporator used in this study is shown in Figure 14. It consists of a heating oil bath, a vacuum, and a chiller. Recovery was accomplished by following the ASTM D5404 method. A 53 mbar vacuum pressure with low nitrogen flow was applied for extracting the n-PB from the solution (n-PB and RAP binder). The temperature of the water bath was maintained at 143°C during the separation of n-PB from the solution. In

the final step, 800 mbar of vacuum pressure with low nitrogen flow was applied where the temperature of water bath was 153°C. Final step was finished after 50 minutes. At the end of the 50 minute, the distillation flask was removed from the apparatus and the flask was wiped for cleaning the oil. The flask was inverted and placed into an oven at 160°C for one hour to let the asphalt be poured into a properly sized container.



Figure 14. Recovery assembly

3.4 MIXING OF THE RAP BINDERS

The recovered binder was mixed with the virgin binder (PG 64-22 from S1) to produce RAP blended binders containing 25%, 40%, and 60% of RAP binder by the weight of the virgin (neat) binder. To prepare the RAP blended asphalt specimens, about 300g of virgin binder was heated to 150°C. The recovered binder from RAP was heated in an oven at 160°C for 90 minutes, and after heating the recovered binder from RAP, it was mixed with the preheated neat binder. The RAP blended binders were stirred by using a glass rod for one minute at ten minute intervals. After one minute of stirring the RAP blended mixture was put into the oven for 10 minutes and the process continued for 1 hour.

3.5 WMA

Sasobit®: Sasobit® is manufactured by Sasol Wax, South Africa. It is a synthetic wax that is produced in the coal gasification process. The melting point of the synthetic waxes is below 100°C that is why Sasobit® reduces the viscosity of the binder after 100°C. According to Damm et al. [29], blending 3 to 4% Sasobit® by weight allows a reduction in mixing temperature of 20°C to 40°C. In this study used a 1.5% Sasobit® by weight of the binder.

Advera®: Advera® is available in the form of a very white powder which is supplied by PQ Corporation. It is a manufactured synthetic zeolite. Advera® can be released up to 20% of water when it is heated around at 85°C to 182°C. The release operation of the water from zeolite happens very slowly which helps to extend time of workability for enabling the aggregate to be rapidly coated and compactable at temperatures significantly lower than those typically used for HMA [30]. According to the manufacturer, the minimum dosage of Advera® in the mix is 0.25% by the weight of the mix. The current study used a 6% Advera® by the weight of the binder.

Evotherm®: Evotherm® 3G is a chemical package which was developed by MeadWestvaco Asphalt Innovations, Charleston, South Carolina. It can reduce the mix temperatures 33-45°C [32]. In this study, Evotherm® 3G was used at a rate of 0.5% by the weight of the asphalt binder.

3.6 MIXING OF WMA

An amount of 1.50 % Sasobit®, 0.50 % Evotherm® and 6.00 % Advera® were mixed with all three types of binders collected from S1, S2, and S3. To prepare the WMA, about 300 g of virgin binder was heated to 150°C. The aforementioned percentages of WMA additives were mixed with the preheated neat binder. The WMA additive and neat binder mixtures were stirred by using a glass rod for one minute at ten minute intervals. After every one minute of stirring, the WMA additive and neat binder mixture was put into the oven for 10 minutes (at 150°C Temperature) and the process continued for 1 hour.

3.7 LABORATORY TESTING

To fulfill the objectives of this study, a number of rheological tests were performed on the PMBs, unmodified binders, RAP modified binders, and WMA. The rheological evaluation included measuring the percent recovery and non-recoverable creep compliance using the MSCR test, evaluating the dynamic shear modulus (G^*) and phase angle (δ) by following the DSR tests, measuring binder's viscosity by following the rotational viscometer (RV) test, and estimating the low-temperature stiffness ($S(t)$) and m -values by conducting bending beam rheometer (BBR) tests. AASHTO T 240 and AASHTO R 28 were followed to simulate the short-term and long-term aging, respectively.

3.7.1 Aging Procedure of Binder

To simulate the short-term and long-term aging of binders, a Rolling Thin-Film Oven (RTFO) and a Pressure Aging Vessel (PAV), respectively were used in this study. The residue from the RTFO test was used to make long-term aged binder.

Rolling Thin-Film Oven (RTFO): The RTFO test was performed for changing the aging condition of binder from unaged to short-term aged by following the AASHTO T 240 (Standard Method of Test for Effect of Heat and Air on a Moving Film of Binder) test method. The apparatus along with an RTFO bottle is shown in Figure 15. It simulates the binder's aging during manufacturing and placement in the field. In this test 35 ± 0.5 gm of heated liquid binder was poured into each of the RTFO bottles. The bottles were allowed to cool for 60 to 180 minutes. During this time, the RTFO chamber was preheated at 163°C . After cooling, the bottles were carefully placed into the RTFO oven carousel. The carousel rotates at constant speed of 15 RPM for 85 minutes. During the rotating of the carousel, the temperature of the oven and the rate of airflow into the bottle was maintained at 163°C and 4 lit/min respectively. After 85 minutes, the bottles were removed from the carousel and stored the residue from the bottle was kept into the tin can for future purposes. The RTFO residue was tested within 72 hours.



Figure 15. A Rolling Thin-Film Oven (RTFO) from James Cox and Sons

Pressure Aging Vessel (PAV) Test: The residue from the RTFO test was used for performing the PAV test for changing the aging condition of the binder from short-term to long-term aging. The apparatus is shown in Figure 16 along with the PAV pans. This aging process is done in accordance to AASHTO R 28 (Accelerated Aging of Asphalt Binder Using a Pressurized Aging Vessel). It helps to the binder simulate in-service aging over a 7 to 10 year period. In this test, 50 ± 0.5 gm of RTFO-aged binder was poured into a preheated pan. After pouring the asphalt into the pans, the pans were placed into the pan holder and put into the preheated PAV machine. When the PAV's temperature was reached at the desired temperature (100°C), the PAV chamber was pressurized to 305 psi and the sample kept at this condition for 20 hours. At the end of the aging period, the pressure was released gradually. When the PAV was depressurized, pans from the pans holder were removed and placed in an oven set to 170°C for 15 min. Then the residue from the pans were scraped into tin containers to keep the PAV-aged binder for future purposes. The PAV aging was an automated process.



Figure 16. A Pressure Aging Vessel (PAV) from ATS

3.7.2 Physical Testing

3.7.2.1 Rotational Viscosity (RV) Testing

The RV test was used to measure the viscosity of asphalt binders according to AASHTO T 316 (Standard Method of Test for Viscosity Determination of Asphalt Binder Using Rotational Viscometer). The RV test is normally performed at high temperatures (135 to 180°C). The viscosity of asphalt binder indicates the workability, pumpability, and mixability of the binder. The amount of torque required to maintain the constant speed (20 RPM) of the cylindrical spindle calculates the viscosity of the binder. According to AASHTO T 316, the recommended maximum viscosity of the binder at 135°C is 3 Pa.s.

A DV-II+ Pro rotational viscometer (RV) (Figure 17) from Brookfield Engineering Inc. was used for measuring the viscosity of asphalt binders. A sufficient amount of binder was heated to a desired temperature until fluid poured into the sample chamber. About 10 gm of heated liquid binder was poured into the sample chamber and the chamber putted into the environmental chamber. The environmental chamber with sample

chamber was heated for about 30 minutes to bring the temperature of the environmental chamber to test temperature. After reaching to test temperature, another 10 minutes time was allowed to equilibrate at the desired test temperature and the procedure was followed for each test temperature. After equilibrating the test temperature, spindle was allowed to rotate at constant speed of 20 RPM. The amount of torque required to maintain the constant speed (20 RPM) of the cylindrical spindle indicates the viscosity of the binder. In this study all types of binder were tested at four different temperatures (135°C, 150 °C, 165 °C, and 180 °C) for measuring the viscosity of the binder.



Figure 17. A DV-II+ Pro Rotational Viscometer (RV)

3.7.2.2 Dynamic Shear Rheometer (DSR)

The DSR tests are conducted in accordance to AASHTO T 315 (Standard Method of Test for Determining the Rheological Properties of Asphalt Binder Using a DSR). The apparatus along with silicon molds shown in Figure 18 was used in this study. DSR method follows for measuring the rheological properties of unaged, short-term aged, and long-term aged asphalt binders. The DSR measures the dynamic shear modulus (G^*) and phase angle (δ) of the asphalt binder. It is used to measure the viscoelastic

properties of an asphalt binder at high and intermediate temperatures. The G^* and δ values indicate the elastic and viscous properties of the asphalt binder, respectively.

In this study, a Modular Compact Rheometer MCR 302, Version: Rheoplus\32 V3.62 was used. Two important parameters are obtained from the DSR test: rutting factor ($G^*/\sin\delta$) and fatigue factor ($G^*.\sin\delta$). The rutting factor is measured for unaged and short-term aged binders and it indicates the rutting resistance of asphalt binder. In AASHTO T 315, a minimum $G^*/\sin\delta$ of 1.0 kPa is mentioned for unaged binder and a minimum $G^*/\sin\delta$ value of 2.2 kPa is mentioned for short-term aged binder. The fatigue factor is measured for long-term aged binders, and it indicates the fatigue resistance of asphalt binder. In AASHTO T 315, a maximum $G^*.\sin\delta$ value of 5000 kPa is mentioned for PAV-aged binders.



Figure 18. A DSR Machine with Bottom and Upper Plate.

Two parallel plates (the bottom plate is fixed and the top plate oscillates) were used for applying the shear load on the asphalt sample at 10 rad/sec. A 25 mm diameter and 1 mm thickness of asphalt binder's specimen was used for measuring the rutting parameters of the asphalt binder at high temperatures. For measuring the rutting parameters, all PG 70-22 binders with and without WMA were tested at 67°C, 70°C, and 73°C, and PG 76-22 binders with and without WMA were tested at 73°C, 76°C, and 76°C. And, 61°C, 64°C, and 67°C temperature were followed for PG 64-22 with 25%, 40%, and 60% RAP, and PG 64-22 with WMA. Three replicates were tested for each material and the average value of three replicates was reported as the test result.

3.7.2.3 Bending Beam Rheometer Testing

The Bending Beam Rheometer (BBR) tests were conducted in accordance to AASHTO T 313 (Determining the Flexural Creep Stiffness of Asphalt Binder Using the Bending Beam Rheometer). The BBR test method is used for measuring the creep stiffness (S) and stress relaxation (m-value) of asphalt binders at lower temperatures. The parameters obtained from the BBR test help to measure the resistance of low temperature cracking of the asphalt binder. The S-value should be ≤ 300 MPa and the m-value should be ≥ 0.300 .

The liquid asphalt sample was poured into the small simple beam (127 mm X 12.7 mm X 6.35 mm) mold. After pouring the liquid binder sample into the mold, the mold was allowed to cool for 45 to 60 minutes. The beam sample was placed in a fluid (methanol) bath at a test temperature for 60 minute. After 60 minutes, constant load of (980 \pm 50 mN) was applied on the sample beam for 240 seconds. The stiffness (S) and the m-value were recorded at 8, 15, 30, 60, 120, and 240 seconds. The S- and m- values at 60 seconds were considered as the design values. In this study, all binders were tested at -9°C and -12°C temperatures. The BBR tests were conducted at the Asphalt Binder Laboratory of the University of Oklahoma, which is a research partner of this study.

3.7.2.4 MSCR testing

To evaluate the permanent strain of asphalt binders, the MSCR test uses the well-established creep and recovery test concept. In the MSCR test method, one second

shearing creep load is applied to the RTFO-aged asphalt binder by using the DSR machine. After the one second load is removed, the samples are allowed to release the creep load for nine second. The test is started with the application of a low stress 0.1 kPa for 10 creep/recovery cycles and then the stress is increased to 3.2 kPa and repeated for an additional 10 cycles.

In this project, a Modular Compact Rheometer MCR 302, Version: Rheoplus\32 V3.62 was used for measuring the MSCR parameters. The samples measured 25 mm in diameter and 1 mm in thickness. All samples were tested at 64°C according to AASHTO T 350. But, some researchers followed higher temperatures and higher stress levels if the difference of % recovery value at 0.1 kPa and 3.2 kPa stress level and at 64°C is very small [4, 84-87]. The MSCR test at 64°C and at 0.1 kPa and 3.2 kPa stress levels is called conventional MSCR test and if the test temperature or stress levels is higher or lower than 64°C or the stress level is different from 0.1 kPa or 3.2 kPa, then it is called the non-conventional MSCR test. Both conventional and non-conventional MSCR tests were followed in this study. In this study, all binders tested at three stress levels (0.1 kPa, 3.2 kPa, and 10 kPa) and at different temperatures. Table 2 shows the test matrix for the non-conventional MSCR tests.

Table 2. Non-conventional MSCR Test Matrix

Asphalt Binder	Binder Source	Temperature (°C)	Stress Level (kPa)
PG 64-22	S1 to S9	64	0.1, 3.2, 10
PG 64-22 + 25% (RAP1 and RAP2)	S1	64	0.1, 3.2, 10
PG 64-22 + 40% (RAP1 and RAP 2)	S1	64, 70,76	0.1, 3.2, 10
PG 64-22 + 60% (RAP1 and RAP 2)	S1	64, 70,76	0.1, 3.2, 10
PG 64-22 + WMA	S1-S3	64	0.1, 3.2, 10
PG 70-22	S1-S12	64, 70	0.1, 3.2, 10
PG 70-22 + WMA	S1-S3	64, 70	0.1, 3.2, 10
PG 76-22	S1-S12	64, 70,76	0.1, 3.2, 10
PG 76-22 + WMA	S1-S3	64, 70,76	0.1, 3.2, 10

THIS PAGE IS LEFT INTENTIONALLY BLANK

CHAPTER 4

PART ONE RESULTS AND DISCUSSIONS

4.1 SUPERPAVE TEST RESULTS

4.1.1 Viscosity Results of Unmodified and Polymer Modified Binders

Unmodified binders and PMBs from all sources met the Superpave specification (viscosity must be below 3 Pa.s at 135°C) except PG 76-22 from the S5. Figure 19 shows the RV test results of a few unmodified binders and PMBs from S1, S5, and S7. From Figure 19, it is seen that the viscosity of unmodified binders are lower than the PMBs, which was expected. The viscosity of all binders decreased with the increase of the testing temperature, which was also expected. The viscosity values of the unmodified binders were lower than those of the PMBs. This kind of trend was also reported by other researchers [e.g., 23, 93]. The viscosity values of same PG grade binders varied from source to source. For instance, the viscosity of PG 76-22 (S1) at 135°C was 1.11 Pa.s and the viscosity of same PG binder at the same test temperature from S5 was 3.21 Pa.s.

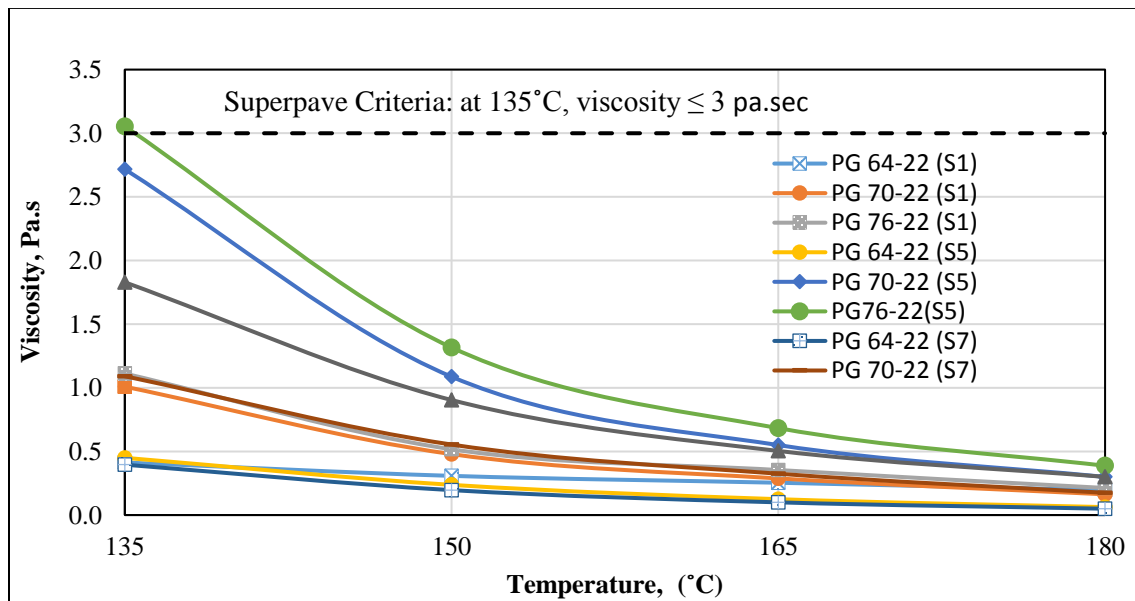


Figure 19. Viscosity test results of the few unmodified and polymer modified binders

4.1.2 Effect of WMA on the Viscosity of Unmodified Binders and PMBs

A 1.5% Sasobit[®], 6% Advera[®], and 0.50% Evotherm[®] (by weight of the binder) were mixed with unmodified binders and PMBs from S1 to S3. All WMA-modified binders were tested at 135°C to 180°C at 15°C interval. Warm mix additives with binders from the aforementioned sources were the Superpave specification (viscosity at 135°C is below the 3 Pa.s). Based on data presented in Figure 20, the viscosity values of all PG binders with Sasobit[®] and Evotherm[®] were lower than those of the control binders. However, Advera[®] showed an opposite trend of Sasobit[®] and Evotherm[®]. This kind of trend was also observed by other researchers [e.g., 78, 94]. According to Akisetty et al. [94], an increase in the viscosity of unmodified binders and PMBs with Advera[®] is caused by the addition of fine powder to the binder, which acts as a filler. In reality, when Advera[®] is added to the mixture, a very fine water spray is created as all the crystalline water is released, which causes volume expansion, thereby increasing the workability and compatibility of the mixture [94]. Figure 20 shows that the viscosity of the control PG 76-22 from S2 at 135°C is 1.517 Pa.s, which is higher than that of PG 76-22 (from S2) with Sasobit[®] and Evotherm[®] at same test temperatures. The viscosity reduction efficiency of Sasobit[®] is higher than Evotherm[®]. This trend was observed for all types of control binders from S1 through S3. At 135°C, the incorporation of Advera[®] into the control PG 76-22 (S2) increased the viscosity from 1.517 Pa.s to 1.692 Pa.s. The viscosity results of binders from S1 to S3 with warm mix additives at different temperatures are presented in Table 3.

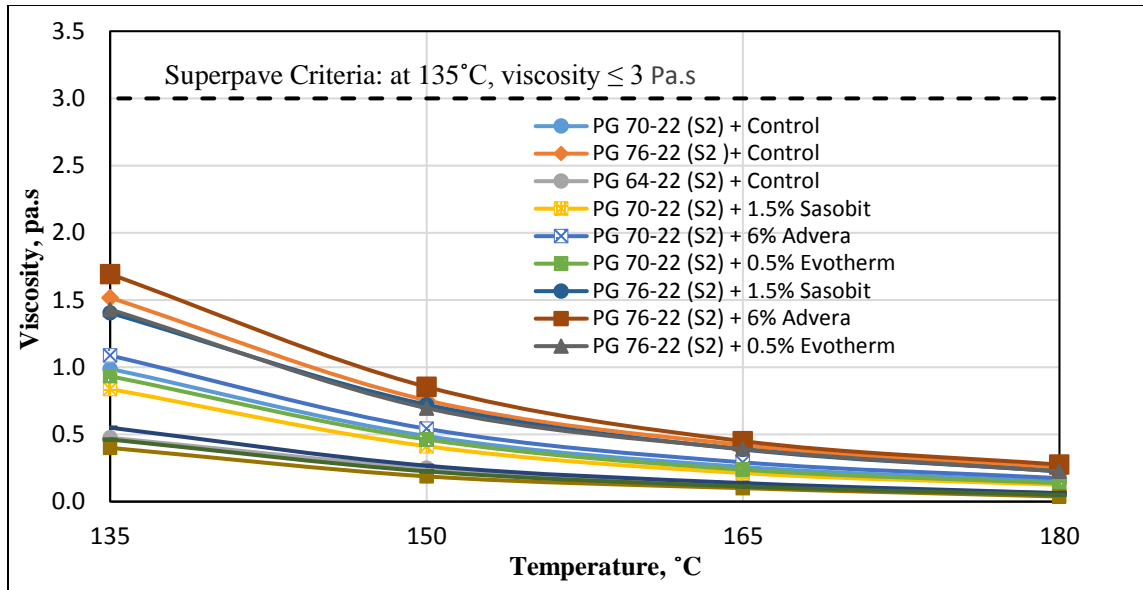


Figure 20. Viscosity test results of the few WMA

4.1.3 Effect of RAP on the Viscosity of Unmodified Binders

Table 4 and Figure 21 show the viscosity data of the unaged RAP- modified asphalt binders at different high temperatures, as measured using the RV test. From this figure it can be seen that at different testing temperatures the viscosity values of RAP1 and RAP2 modified binders were higher than that of the control binder (without RAP). For example, at 135°C, the viscosity of the control binder was about 0.413 Pa.s and that of 60% RAP1 modified binder was 2.171 Pa.s, which was about 5 folds of the control binder. At 180°C, the viscosity changes from 0.196 Pa.s to 0.258 Pa.s due to 60% RAP1 addition, which is about 1.3 times of that of the control binder. Such increase in viscosity marks an increased stiffness due to the addition of RAP in the unmodified binder. Colbert et al. [93] reported that the addition of RAP increased the viscosity of the unmodified binder, which is similar to the findings of the current study. The viscosity of 60% RAP2 with control binder was more than 3 Pa.s, which did not meet the Superpave specification. Thus, up to 40% of RAP1 and RAP2 can be used as replacement of the unmodified binder without violating the Superpave specification for viscosity.

Table 3. Viscosity (Pa.s) result of WMA at different temperature

Source	Binder type	WMA additives	% Additives	Sample Condition	Viscosity at 135° C	Viscosity at 150° C	Viscosity at 165° C	Viscosity at 180° C
S1	PG 64-22	Sasobit®	1.5	Unaged	0.404	0.196	0.096	0.046
S1	PG 64-22	Advera®	6	Unaged	0.529	0.267	0.129	0.067
S1	PG 64-22	Evotherm®	0.5	Unaged	0.488	0.225	0.113	0.050
S1	PG 70-22	Sasobit®	1.5	Unaged	0.792	0.408	0.217	0.125
S1	PG 70-22	Advera®	6	Unaged	1.004	0.504	0.275	0.163
S1	PG 70-22	Evotherm®	0.5	Unaged	0.875	0.413	0.213	0.088
S1	PG 76-22	Sasobit®	1.5	Unaged	0.929	0.458	0.242	0.129
S1	PG 76-22	Advera®	6	Unaged	0.929	0.442	0.238	0.125
S1	PG 76-22	Evotherm®	0.5	Unaged	0.825	0.388	0.188	0.100
S2	PG 64-22	Sasobit®	1.5	Unaged	0.400	0.188	0.100	0.038
S2	PG 64-22	Advera®	6	Unaged	0.550	0.267	0.138	0.063
S2	PG 64-22	Evotherm®	0.5	Unaged	0.463	0.225	0.113	0.050
S2	PG 76-22	Sasobit®	1.5	Unaged	1.404	0.721	0.388	0.225
S2	PG 76-22	Advera®	6	Unaged	1.692	0.854	0.450	0.275
S2	PG 76-22	Evotherm®	0.5	Unaged	1.429	0.696	0.392	0.225
S2	PG 70-22	Advera®	6	Unaged	1.087	0.542	0.292	0.175
S2	PG 70-22	Evotherm®	0.5	Unaged	0.933	0.463	0.238	0.138
S2	PG 70-22	Sasobit®	1.5	Unaged	0.838	0.413	0.213	0.125
S3	PG 64-22	Sasobit®	1.5	Unaged	0.413	0.213	0.125	0.075
S3	PG 64-22	Advera®	6	Unaged	0.579	0.288	0.150	0.075
S3	PG 64-22	Evotherm®	0.5	Unaged	0.438	0.200	0.100	0.050
S3	PG 70-22	Sasobit®	1.5	Unaged	0.763	0.400	0.213	0.125
S3	PG 70-22	Evotherm®	0.5	Unaged	0.825	0.400	0.200	0.125
S3	PG 70-22	Advera®	6	Unaged	0.900	0.454	0.288	0.188
S3	PG 76-22	Sasobit®	1.5	Unaged	1.300	0.600	0.325	0.200
S3	PG 76-22	Advera®	6	Unaged	1.471	0.679	0.375	0.213
S3	PG 76-22	Evotherm®	0.5	Unaged	1.100	0.538	0.288	0.175

Table 4. Viscosity (Pa.s) Results of RAP Modified Binders

Source	Binder type	RAP source	% RAP	Sample Condition	Viscosity at 135° C	Viscosity at 150° C	Viscosity at 165° C	Viscosity at 180° C
S1	PG 64-22	No RAP	0	Unaged	0.413	0.308	0.254	0.196
S1	PG 64-22	RAP 1	25	Unaged	0.771	0.392	0.213	0.125
S1	PG 64-22	RAP 1	40	Unaged	0.954	0.454	0.237	0.129
S1	PG 64-22	RAP 1	60	Unaged	2.171	0.954	0.483	0.258
S1	PG 64-22	RAP 2	25	Unaged	0.983	0.479	0.246	0.138
S1	PG 64-22	RAP 2	40	Unaged	1.521	0.704	0.354	0.204
S1	PG 64-22	RAP 2	60	Unaged	3.209	1.354	0.654	0.354

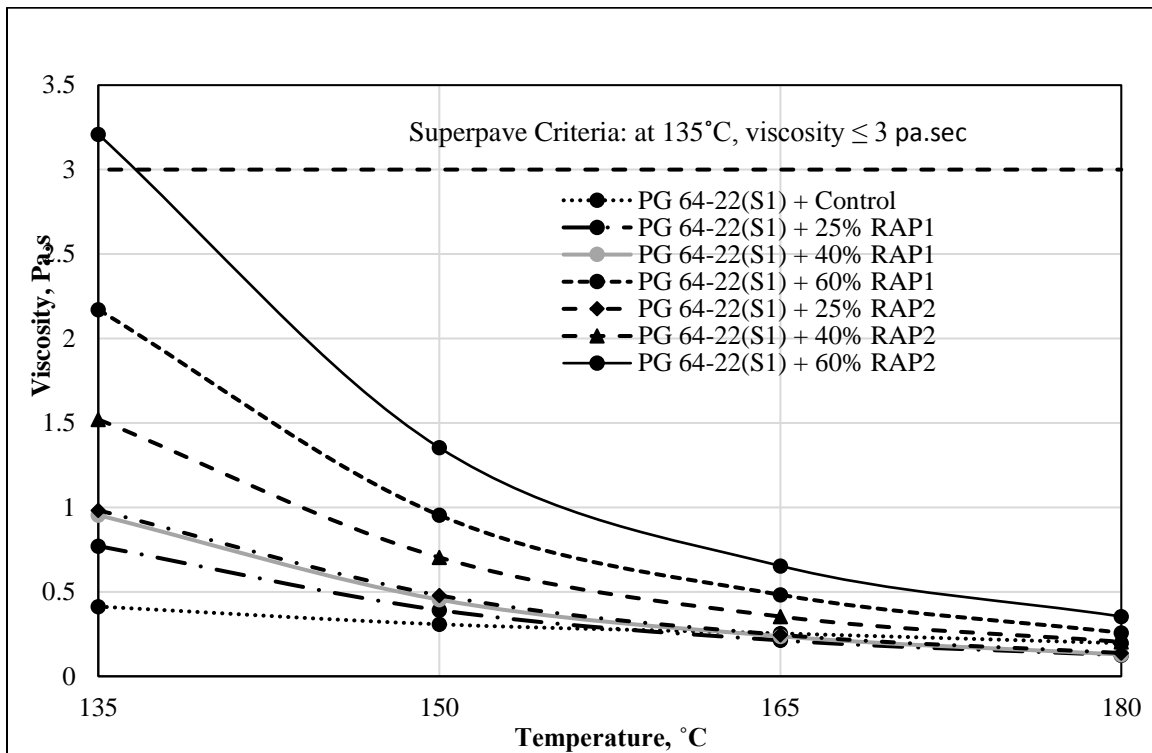


Figure 21. Viscosity vs. temperature of RAP modified binders

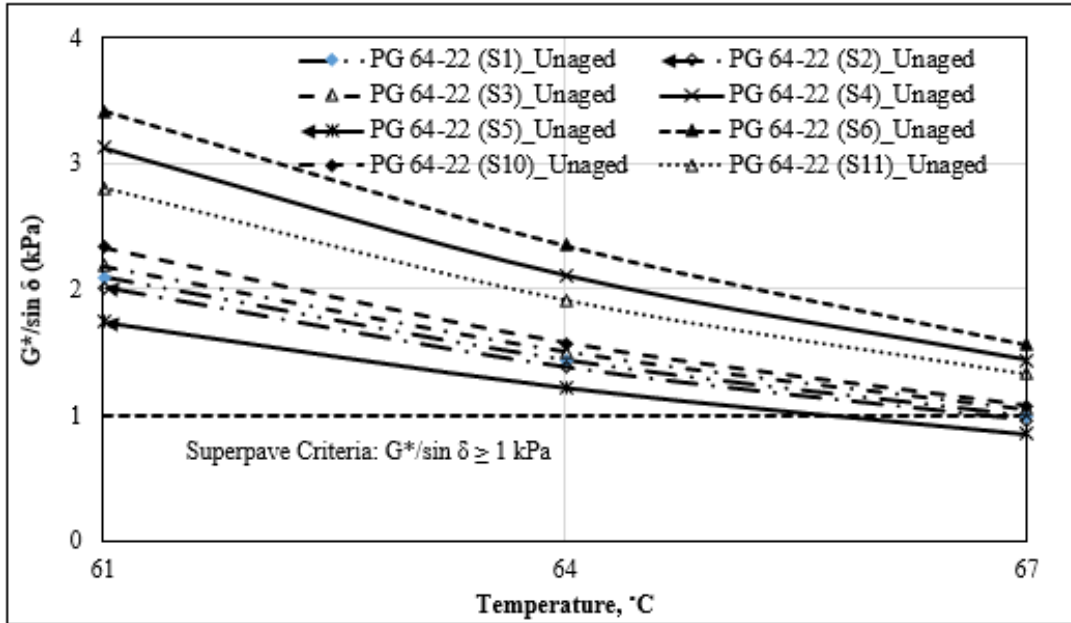
4.2 DSR TEST RESULT OF UNMODIFIED BINDERS AND PMBS

Figures 22, 23, and 24 show the rutting parameters of unaged and RTFO-aged binders of PG 64-22, PG 70-22, and PG 76-22, respectively. From the results, it can be noticed that PG 64-22 binder shows the lowest rutting resistance and PG 76-22 was shown the

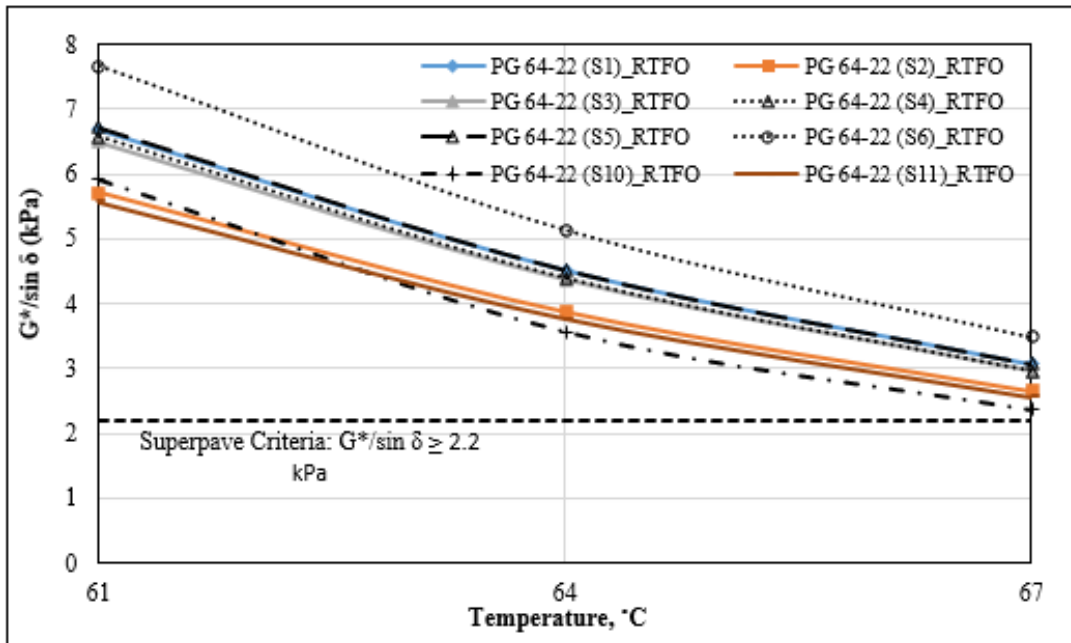
highest rutting resistance, which was expected. For instance, the $G^*/\sin\delta$ value of unaged PG 70-22 binder from S1 at 73°C is 1.12 kPa, and at same temperature and from the same source, the $G^*/\sin\delta$ value of unaged PG 76-22 binder is 1.86. At 64°C, the unaged and RTFO aged PG 64-22 binders met the Superpave criteria. Like PG 64-22 binder, PG 70-22 and PG 76-22 binders also met the Superpave criteria at 70°C and 76°C, respectively. As expected, the $G^*/\sin\delta$ value decreased with an increase of the DSR testing temperature (Figures 22, 23, and 24). For instance, the $G^*/\sin\delta$ values of the RTFO aged PG 64-22 binder from S1 are 6.68 kPa, 4.52 kPa, and 3.07 kPa at 61°C, 64°C and 67°C, respectively. Consequently, the $G^*/\sin\delta$ value of RTFO-aged PG 64-22 binder from S1 is increased to 2 times when the testing temperature is increased from 61°C to 67°C.

4.3 BBR TEST

According to the Superpave specifications, at 60 seconds, the m-value must be equal or greater than 0.300, and the S-value must not exceed 300 MPa. The temperatures corresponding to these values were determined through interpolation or extrapolation. Asphalt binders that are not too stiff at low temperatures are able to return to original position at relaxation time. Based on Figure 25 (a), some PMBs show lower stiffness values compared to the unmodified binders. For example, PG 76-22 and PG 64-22 (from S1) binders showed the same S-value (300 MPa) at -20.3°C and -24.4°C, respectively. But, some PG 70-22 binders showed an opposite trend. It can be noted that all of these binders are of the same low PG temperature of -22°C. From Figure 25, it is also observed that the S-value decreased and m-value increased with an increase of the BBR testing temperature, as expected. For instance, the m-values of the PG 70-22 binder from S3 are 0.35 and 0.34 corresponding to low critical temperatures of -12°C and -15°C, respectively.

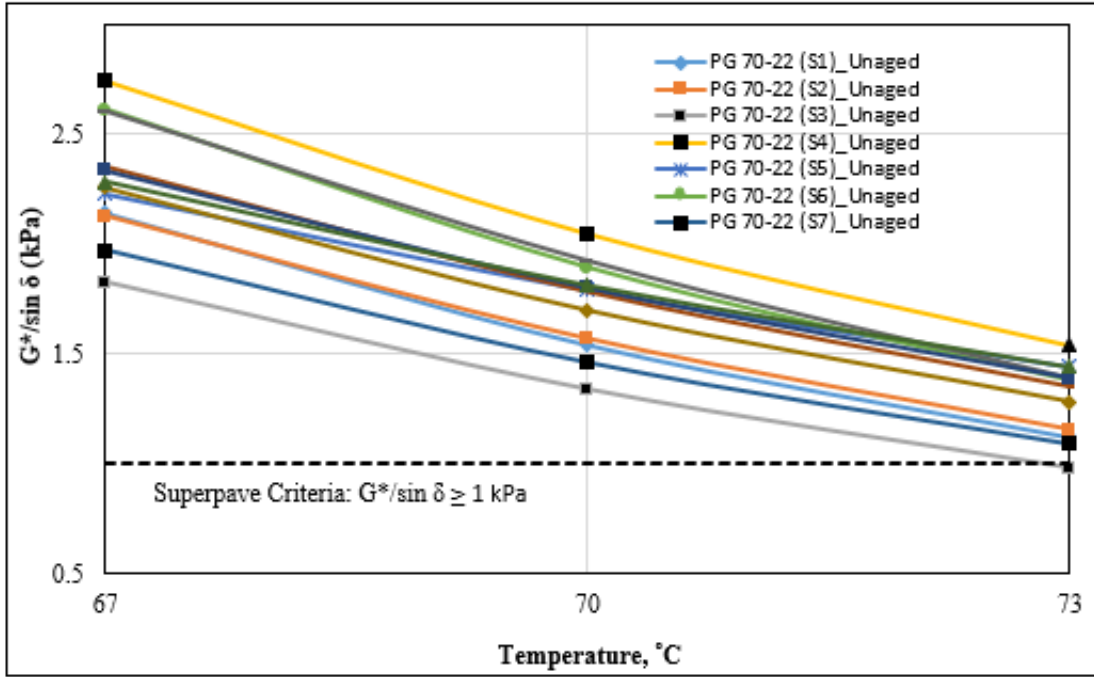


(a)

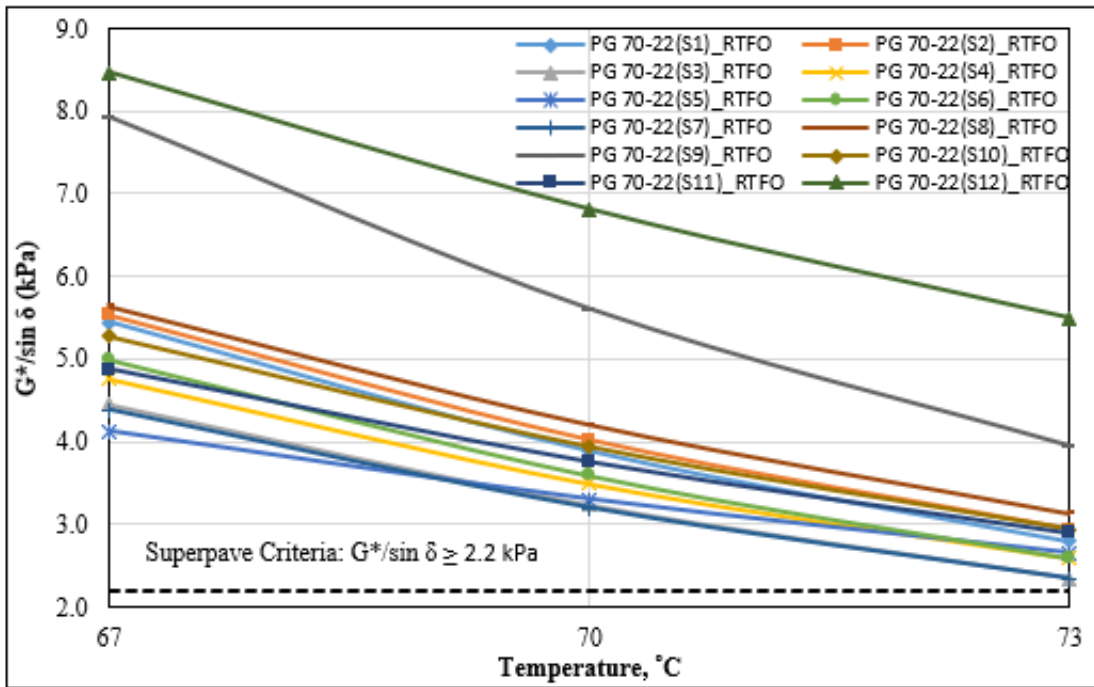


(b)

Figure 22. $G^*/\sin \delta$ vs. temperature for: (a) Unaged PG 64-22; (b) RTFO-aged PG 64-22

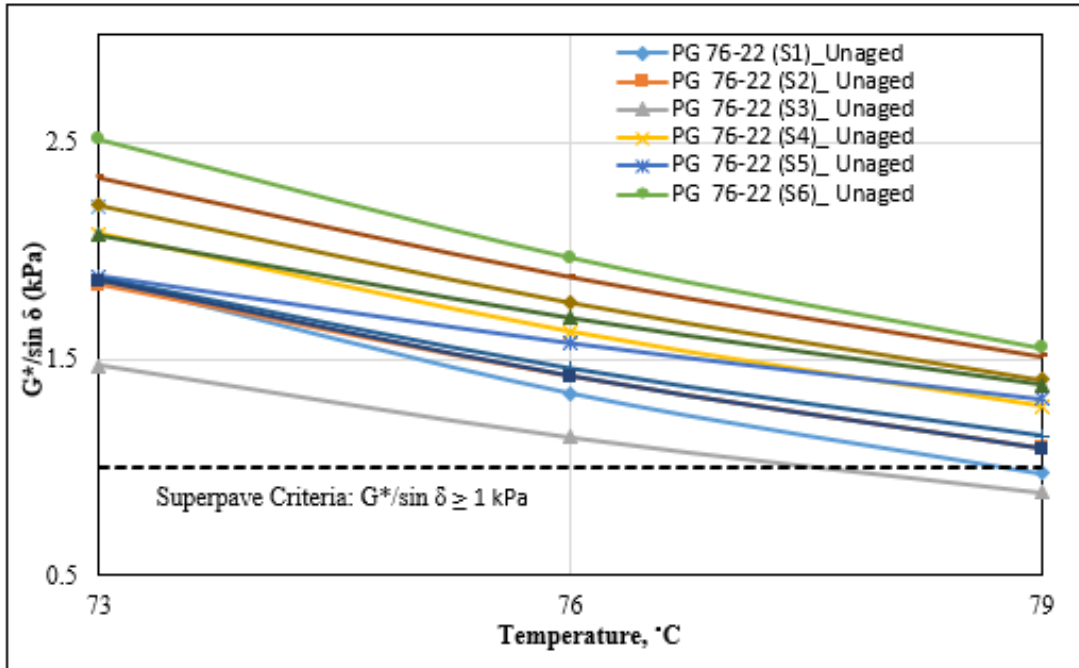


(a)

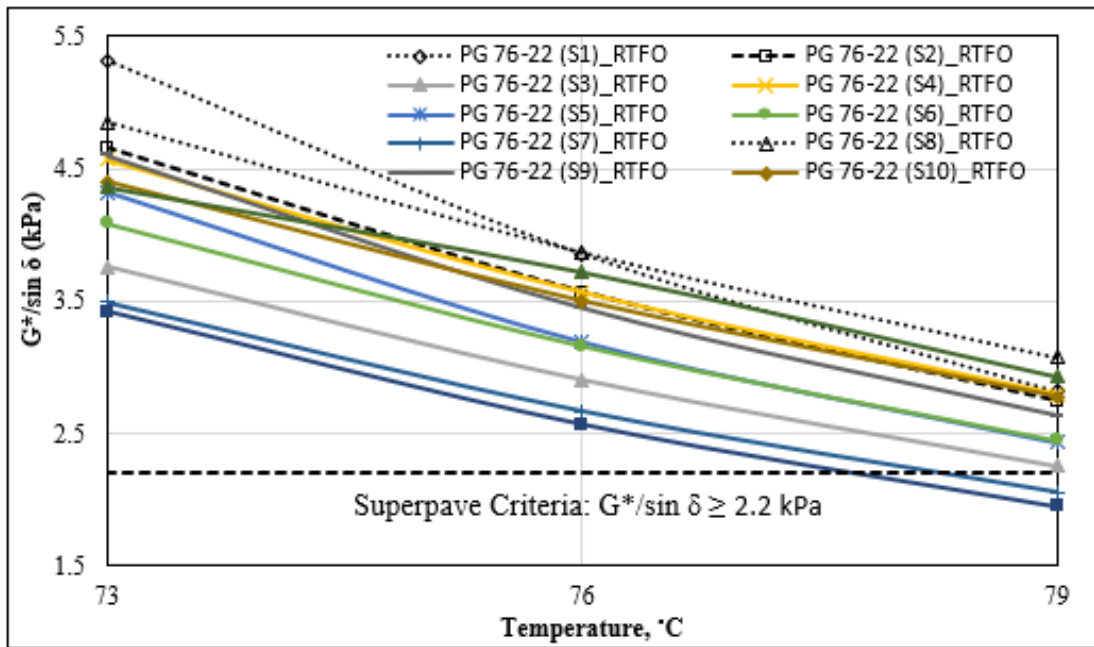


(b)

Figure 23. $G^*/\sin \delta$ vs. temperature for: (a) Unaged PG 70-22; (b) RTFO-aged PG 70-22



(a)



(b)

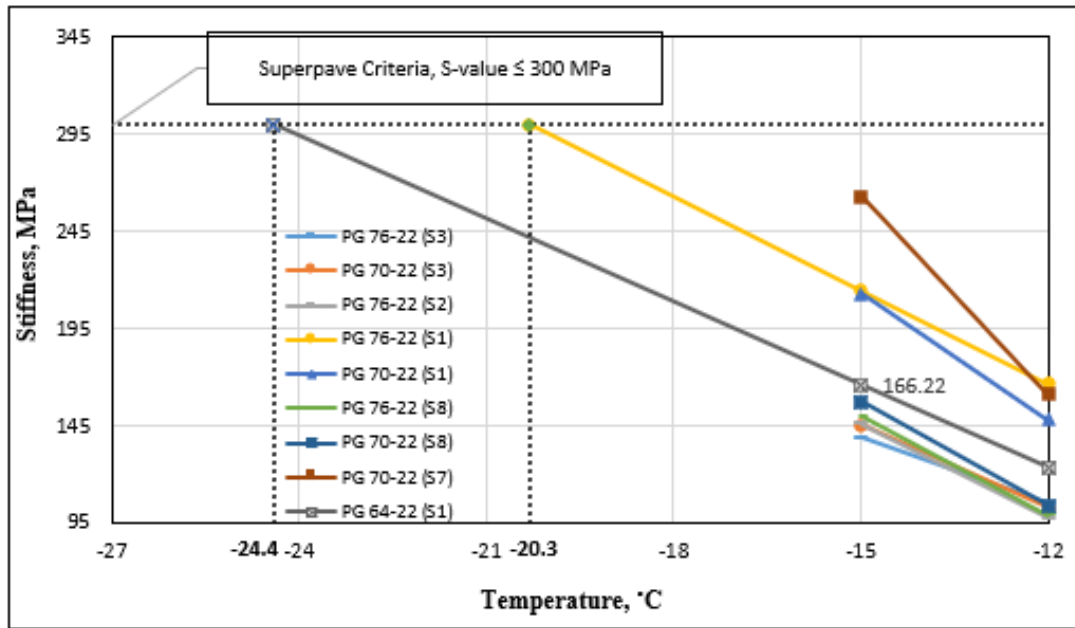
Figure 24. $G^*/\sin \delta$ vs. temperature for: (a) Unaged PG 76-22; (b) RTFO-aged PG 76-22

4.4 EFFECT OF WMAS ON RUTTING FACTORS OF UNMODIFIED BINDERS AND PMBS

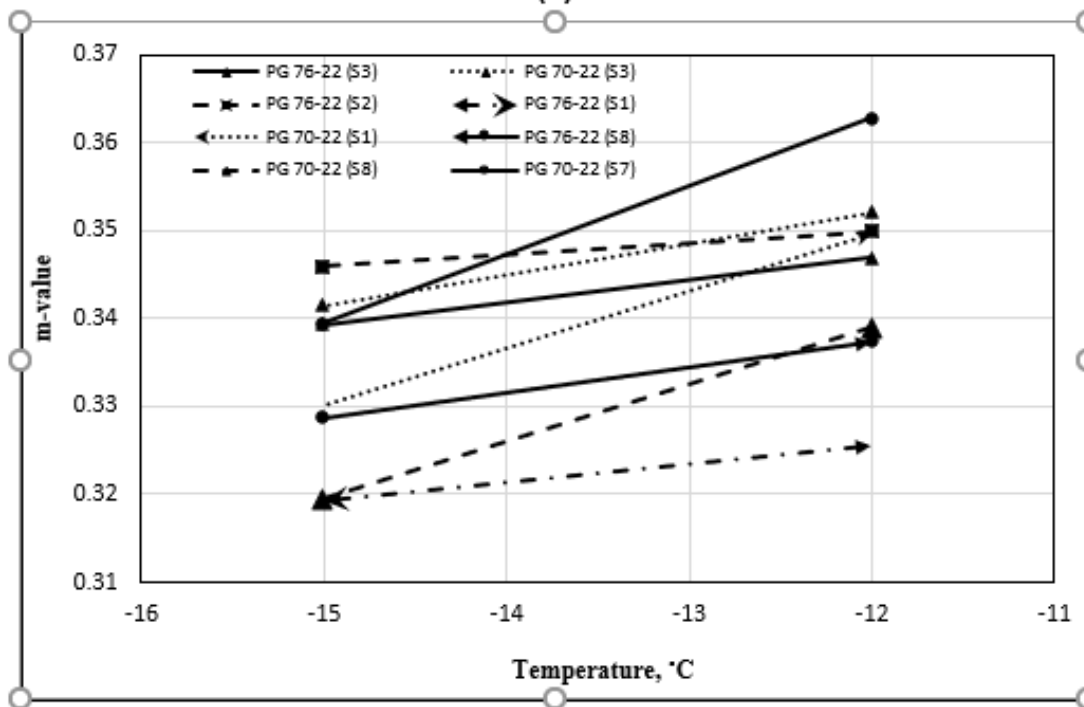
Amounts of 1.5% Sasobit[®], 6% Advera[®], and 0.50% Evotherm[®] (by the weight of the binder) were mixed with binders from S1, S2, and S3. Figure 26 shows a graphical representation of $G^*/\sin\delta$ values of PG 76-22 (from S2) and PG 64-22 (from S2) with and without WMA additives for a better understanding. Figure 26 reveals that the addition of the Sasobit[®] significantly increases the rutting resistance of the PMBs, which is followed by Evotherm[®] and then Advera[®]. Figure 26 (b) shows that PG 64-22 with and without WMA additives shows a similar trend as the PMBs (PG 76-22 and PG 70-22). Based on data presented in Figure 26 (a), at 73°C, the $G^*/\sin\delta$ value of the unaged control PG 76-22 is about 1.84 kPa and the unaged PG 76-22 binder modified with 1.5% Sasobit[®] is up to 2.51 kPa, which is significantly higher than the control binder. The addition of Advera[®] and Evotherm[®] increased the rutting factors from 1.84 kPa to 2.06 kPa, and from 1.84 kPa to 1.91 kPa, respectively. In addition, Figure 26 (a) illustrates that control PG 76-22 binder passed the Superpave rutting criterion at 78°C and the same binder with Sasobit[®] passed at 81°C, which is 3°C higher than the control binder. This is indicative that with the addition of Sasobit[®] increases the rutting resistance of PG 76-22 from S2. For the same binder, the addition of Advera[®] also increased the high PG temperature from 78°C to 80°C. This kind of trend was also observed for PG 64-22 and PG 70-22 binders from S2. The addition of Evotherm[®] decreased the high PG temperature of PG 76-22 binder from S1 to S3. Hurly et al. (77) also found that the addition of Evotherm[®] generally decreased the rutting potential of the asphalt mixes. For PG 64-22 from S1 to S3, the passing temperature (at $G^*/\sin\delta = 1.00$ kPa for unaged and $G^*/\sin\delta = 2.20$ kPa for RTFO-aged) increased when the Evotherm[®] was added with control binder. A similar kind of trend was also observed for PG 70-22 binders from S1 to S3. Among three of WMA additives, the capability of increasing the passing temperature is higher for Sasobit[®], which is shown in Figure 27. Thus, it can be concluded that the addition of Sasobit[®] has a significant effect on the PG grade of the tested binders.

4.5 EFFECT OF RAP ON RUTTING FACTORS OF UBS

Binders in the amounts of 25%, 40%, and 60% recovered from RAP1 and RAP2 samples were mixed (by the weight of the binder) with the PG 64-22 binder from S1. The DSR tests were performed on the Unaged and RTFO-aged of binders modified with RAP. Figure 28 shows that the Superpave test criteria for rutting were satisfied for both unmodified and RAP-modified binders. RAP1 and RAP2 were aged for a long period of times (about 13 years) in the field. As a result, these RAP binders were stiffer compared to the unmodified binder. As expected, a lower value of $G^*/\sin \delta$ was obtained at higher temperature and vice versa. Figure 28 also shows that with an addition of RAP content, the $G^*/\sin \delta$ values also increased significantly, which indicates a better resistance to permanent deformation. For example, at 61 °C, the $G^*/\sin \delta$ value of unaged PG 64-22 increased from 2.09 kPa to 22.83 kPa when this binder was blended with 60% RAP1 binder, which is about 10 times higher than that of the unmodified (PG 64-22) binder. Therefore, an addition of RAP provided would improve the rutting resistance of the asphalt pavement.

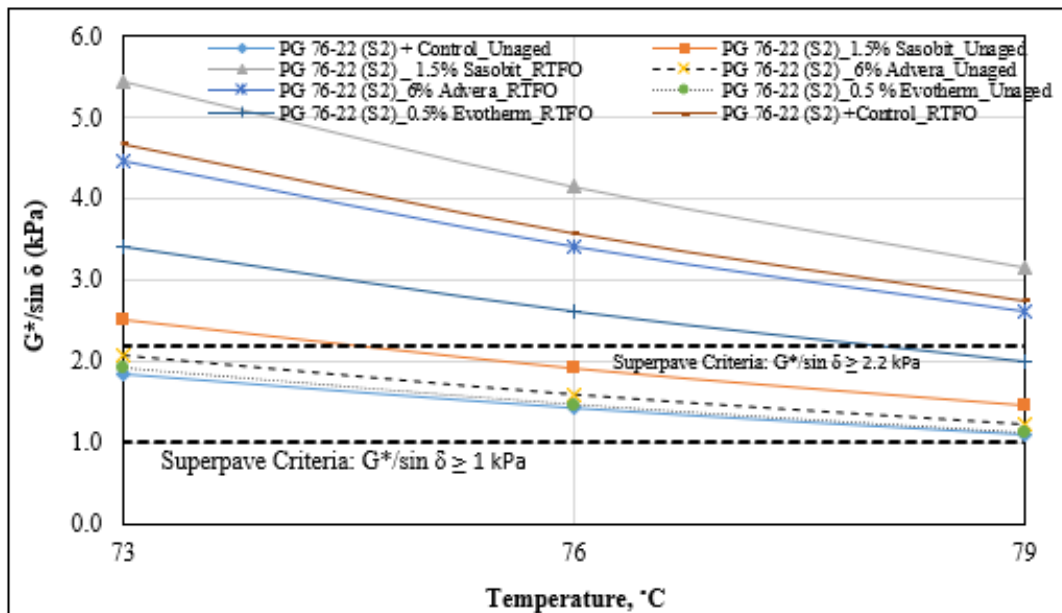


(a)

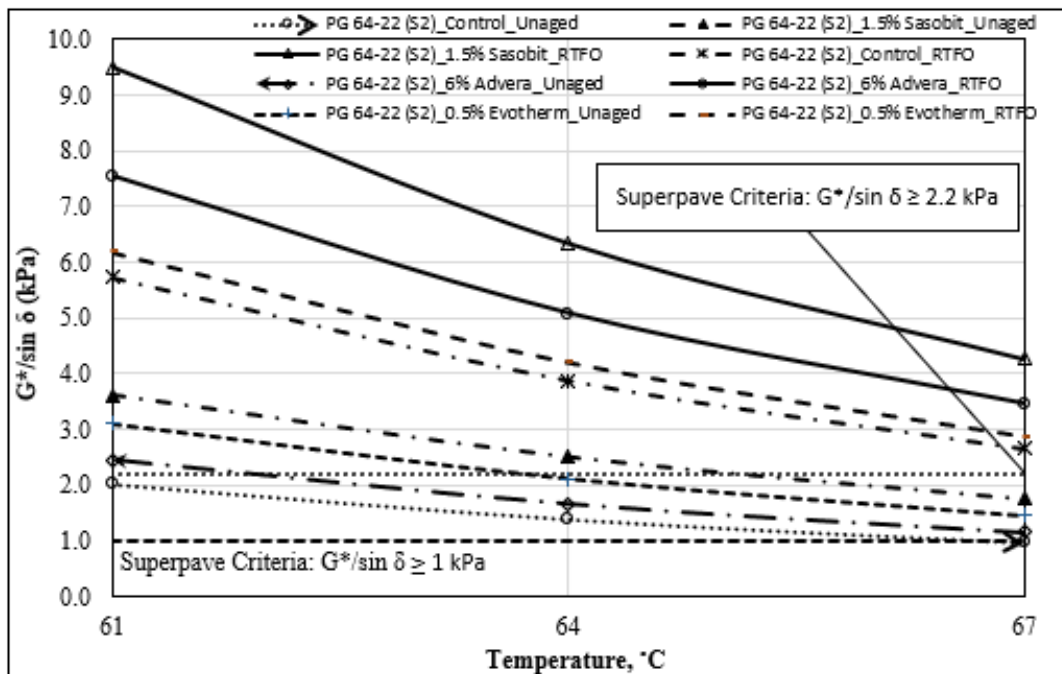


(b)

Figure 25. (a) Stiffness vs temperature for PMBs and unmodified binders, (b) M-value vs. Temperature for PMBs



(a)



(b)

Figure 26. $G^*/\sin \delta$ vs. Temperature for (a) Unaged and RTFO PG 76-22 (b) Unaged and RTFO-aged PG 64-22

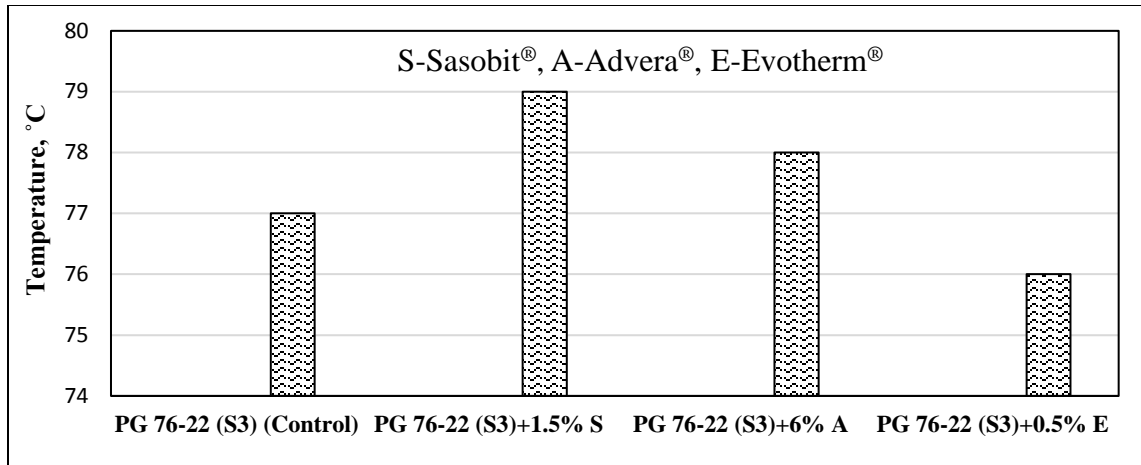


Figure 27. Passing temperature (at $G^*/\sin\delta = 1$ kPa or $G^*/\sin\delta = 2.2$ kPa) of PMBs

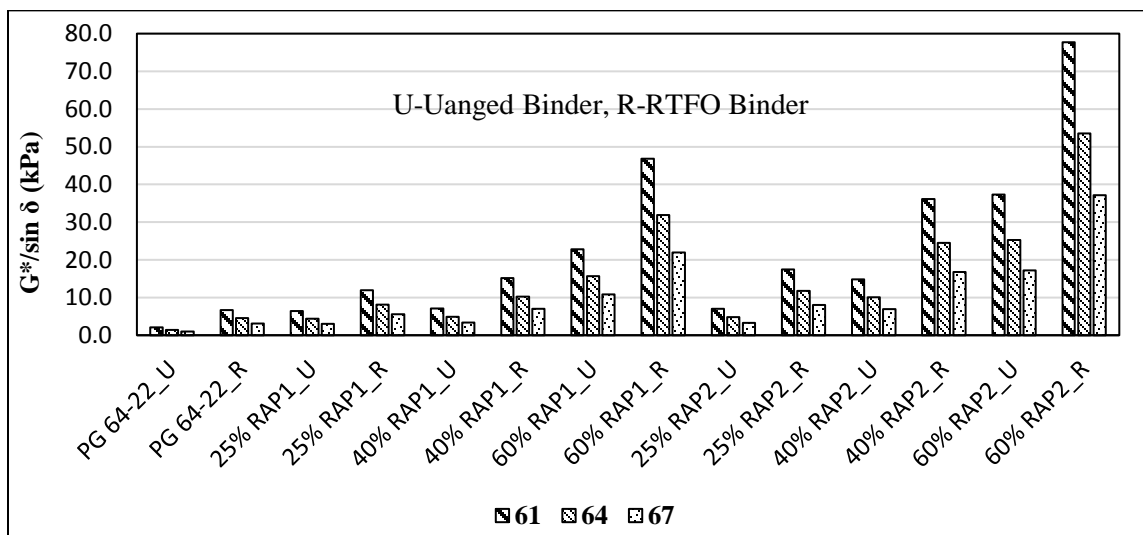


Figure 28. $G^*/\sin\delta$ values of unaged and RTFO aged RAP modified binders

4.6 SUPERPAVE PG GRADING

In this study, all selected binders were graded based on their high temperature test results of the DSR test as the primary focus of this study was the high service temperatures. For a few selected binders, low PG grades were also evaluated in a partner university (the University of Oklahoma) laboratory. The high temperature grading was done based on the Superpave rutting criteria (for unaged condition, $G^*/\sin\delta \geq 1$ kPa; and for RTFO-aged condition, $G^*/\sin\delta \geq 2.2$ kPa) of unaged and RTFO-aged

binders and low temperature cracking criteria (S-value no more than 300 MPa and m-value at least 0.300) of PAV-aged binders. The actual high PG temperatures corresponding to these values were determined through interpolation or extrapolation of results of laboratory tests conducted at three temperatures. The S-value and m-value were measured at two different temperatures for measuring the actual low PG temperatures of the binder. Due to a large amount of data present in the PG grading, snapshots of the PG grades of the PMBs and WMA are presented in Tables 5 and 6, respectively. Tables 7 and 8 represent PG grades of the unmodified and RAP modified binders, respectively. Based on data presented in Tables 5 through 8, all tested binders passed the manufacturer's labeled PG grades except the Evotherm[®] containing PG 76-22 from S1. For example, the actual PG grades of PG 76-22, PG 70-22, and PG 64-22 from S1 were found to be PG 78-30, PG 73-29, and PG 66-29, respectively. Earlier it was mentioned that Evotherm[®] reduced the high temperature grades. The addition of Evotherm[®] with the PG 76-22 from S1 reduced its PG grade to PG 74-22. The addition of RAP significantly increased the high temperature PG grades. An addition of 60% RAP (from RAP2) bumped the PG grades of PG 64-22 to PG 92-XX. Here, XX denotes that the low PG grade was not determined due to the limitation of resource (equipment) available to the research team.

Table 5. PG grading of PMBs

Source	Binder type	Sample Condition	G*/sin δ (kPa) at 67°C	G*/sin δ (kPa) at 70°C	G*/sin δ (kPa) at 73°C	G*/sin δ (kPa) at 76°C	G*/sin δ (kPa) at 79°C	Temperature (°C) at, G*/sin δ = 1 or 2.2 kPa	Temperature (°C) at, m = 0.3, s = 300 MPa (when t= 60 sec)	Actual PG Grading
S1	PG 70-22	Unage	2.14	1.54	1.12	X	X	73.49		PG 73-29
S1	PG 70-22	RTFO	5.44	3.89	2.80	X	X	74.15		PG 73-29
S1	PG 70-22	PAV	X	X	X	X	X	X	-29	PG 73-29
S3	PG 70-22	Unage	1.82	1.34	0.98	X	X	72.69		PG 72-36
S3	PG 70-22	RTFO	4.45	3.23	2.35	X	X	73.24		PG 72-36
S3	PG 70-22	PAV	X	X	X	X	X	X	-36	PG 72-36
S7	PG 70-22	Unage	1.97	1.46	1.09	X	X	73.43		PG 73-26
S7	PG 70-22	RTFO	4.39	3.20	2.35	X	X	73.24		PG 73-26
S7	PG 70-22	PAV	X	X	X	X	X	X	-26	PG 73-26
S8	PG 70-22	Unage	2.35	1.78	1.35	X	X	74.91		PG 74-28
S8	PG 70-22	RTFO	5.63	4.21	3.13	X	X	75.06		PG 74-28
S8	PG 70-22	PAV	X	X	X	X	X	X	-28	PG 74-28
S1	PG 76-22	Unage	X	X	1.86	1.34	0.97	78.60		PG78-30
S1	PG 76-22	RTFO	X	X	5.32	3.86	2.82	80.28		PG78-30
S1	PG 76-22	PAV	X	X	X	X	X	X	-30	PG78-30
S2	PG 76-22	Unage	X	X	1.84	1.42	1.09	78.60		PG78-34
S2	PG 76-22	RTFO	X	X	4.66	3.57	2.75	80.55		PG78-34
S2	PG 76-22	PAV	X	X	X	X	X	X	-34	PG78-34
S3	PG 76-22	Unage	X	X	1.47	1.14	0.88	77.65		PG77-39
S3	PG 76-22	RTFO	X	X	3.76	2.91	2.26	79.07		PG77-39
S3	PG 76-22	PAV	X	X	X	X	X	X	-39	PG77-39
S8	PG 76-22	Unage	X	X	2.34	1.88	1.51	82.56		PG81-33
S8	PG 76-22	RTFO	X	X	4.85	3.87	3.07	81.81		PG81-33
S8	PG 76-22	PAV	X	X	X	X	X	X	-33	PG81-33

Table 6. PG grading of WMA

Source	Binder type	WMA additives	% Additives	Sample Condition	G*/sin δ (kPa) at 73° C	G*/sin δ (kPa) at 76° C	G*/sin δ (kPa) at 79° C	Temperature (°C) at, G*/sin δ = 1 or 2.2 kPa	Actual High Temperature PG Grading
S1	PG 76-22	Sasobit®	1.5	Unaged	2.49	1.77	1.27	75.48	PG 75-XX
S1	PG 76-22	Sasobit®	1.5	RTFO	7.76	5.55	3.93	75.52	PG 75-XX
S1	PG 76-22	Advera®	6	Unaged	1.28	0.91	0.58	74.61	PG 74-XX
S1	PG 76-22	Advera®	6	RTFO	3.24	2.27	1.60	75.13	PG 74-XX
S1	PG 76-22	Evotherm®	0.5	Unaged	1.33	0.95	0.69	74.41	PG 74-XX
S1	PG 76-22	Evotherm®	0.5	RTFO	2.36	1.67	1.05	74.48	PG 74-XX
S2	PG 76-22	Sasobit®	1.5	Unaged	2.51	1.91	1.45	81.43	PG 81-XX
S2	PG 76-22	Sasobit®	1.5	RTFO	5.44	4.14	3.15	81.35	PG 81-XX
S2	PG 76-22	Advera®	6	Unaged	2.06	1.58	1.21	80.37	PG 80-XX
S2	PG 76-22	Advera®	6	RTFO	4.46	3.40	2.60	80.15	PG 80-XX
S2	PG 76-22	Evotherm®	0.5	Unaged	1.91	1.46	1.12	79.78	PG 78-XX
S2	PG 76-22	Evotherm®	0.5	RTFO	3.40	2.61	2.00	78.03	PG 78-XX
S3	PG 76-22	Sasobit®	1.5	Unaged	2.00	1.52	1.15	79.95	PG 79-XX
S3	PG 76-22	Sasobit®	1.5	RTFO	4.06	3.12	2.38	79.53	PG 79-XX
S3	PG 76-22	Advera®	6	Unaged	1.62	1.25	0.97	78.58	PG 78-XX
S3	PG 76-22	Advera®	6	RTFO	3.63	2.77	2.13	78.86	PG 78-XX
S3	PG 76-22	Evotherm®	0.5	Unaged	1.56	1.20	0.92	78.19	PG 76-XX
S3	PG 76-22	Evotherm®	0.5	RTFO	2.87	2.20	1.69	76.28	PG 76-XX

Table 7. PG grading of unmodified binders

Source	Binder type	Sample Condition	G*/sin δ (kPa) at 61°C	G*/sin δ (kPa) at 64°C	G*/sin δ (kPa) at 67°C	Temperature (°C) at, G*/sin δ = 1 or 2.2 kPa	Actual High Temperature PG Grading
S1	PG 64-22	Unaged	2.09	1.43	0.99	66.72	PG 66-XX
S1	PG 64-22	RTFO	6.68	4.52	3.07	68.19	PG 66-XX
S2	PG 64-22	Unaged	2.01	1.38	0.96	66.54	PG 66-XX
S2	PG 64-22	RTFO	5.72	3.88	2.65	67.63	PG 66-XX
S3	PG 64-22	Unaged	2.18	1.50	1.04	66.98	PG 66-XX
S2	PG 64-22	RTFO	6.48	4.37	2.97	68.06	PG 66-XX
S4	PG 64-22	Unaged	3.13	2.11	1.44	68.28	PG 68-XX
S4	PG 64-22	RTFO	6.57	4.40	2.97	68.02	PG 68-XX
S5	PG 64-22	Unaged	1.74	1.22	0.85	65.80	PG 65-XX
S5	PG 64-22	RTFO	6.71	4.52	3.07	68.17	PG 65-XX
S6	PG 64-22	Unaged	3.41	2.35	1.56	68.63	PG 68-XX
S5	PG 64-22	RTFO	7.68	5.14	3.48	68.35	PG 68-XX
S10	PG 64-22	Unaged	2.33	1.57	1.07	67.08	PG 67-XX
S10	PG 64-22	RTFO	5.91	3.56	2.35	66.84	PG 67-XX
S11	PG 64-22	Unaged	2.81	1.91	1.32	68.03	PG 67-XX
S11	PG 64-22	RTFO	5.56	3.77	2.55	67.46	PG 67-XX

Table 8. PG grading of RAP modified binders

Source	Binder type	RAP source	% RAP	Sample Condition	G*/sin δ (kPa) at 61°C	G*/sin δ (kPa) at 64°C	G*/sin δ (kPa) at 67°C	Temperature (°C) at, G*/sin δ = 1 or 2.2 kPa	Actual High Temperature PG Grading
S1	PG 64-22	RAP 1	25	RTFO	11.93	8.11	5.53	74.4	PG74-XX
S1	PG 64-22	RAP 1	25	Unaged	6.46	4.36	2.99	74.03	PG74-XX
S1	PG 64-22	RAP 1	40	Unaged	7.11	4.92	3.4	75.97	PG 75-XX
S1	PG 64-22	RAP 1	40	RTFO	15.2	10.28	7.04	76.8	PG 75-XX
S1	PG 64-22	RAP 1	40	Unaged	22.83	15.63	10.83	90.2	PG 87-XX
S1	PG 64-22	RAP 1	40	RTFO	46.8	31.867	21.933	87.2	PG 87-XX
S1	PG 64-22	RAP 2	25	Unaged	7.02	4.78	3.28	79.33	PG 77-XX
S1	PG 64-22	RAP 2	25	RTFO	17.433	11.8	8.063	77.67	PG 77-XX
S1	PG 64-22	RAP 2	40	Unaged	14.8	10.08	6.9	71.19	PG 71-XX
S1	PG 64-22	RAP 2	40	RTFO	36.133	24.5	16.8	84.23	PG 71-XX
S1	PG 64-22	RAP 2	60	Unaged	37.317	25.253	17.227	92.6	PG 92-XX
S1	PG 64-22	RAP 2	60	RTFO	77.697	53.533	37.133	92.13	PG 92-XX

4.7 AASHTO M 332 SPECIFICATION

The main differences between AASHTO M 320 and AASHTO M 332 are the traffic loading and the pavement temperature. The AASHTO M 320 specifications are based

on the climate temperature, but AASHTO M 332 specifications consider the climate as well as the traffic condition. Like AASHTO M 320, AASHTO M 332 follows the same rules and procedures for unaged and PAV-aged binders, but, for RTFO-aged binders AASHTO M 332 specifications consider J_{nr} values instead of $G^*/\sin\delta$ on the basis of the traffic condition. Table 9 shows the specific traffic loading conditions for specific J_{nr} limits. The high and low critical temperatures of the asphalt binders are represented by XX and YY, respectively. Traffic conditions are represented by S (Standard), H (Heavy), V (Very Heavy), and E (Extreme).

Table 9. Minimum J_{nr} value range for MSCR grading

J_{nr} (kPa ⁻¹) Criteria	MSCR Grading
$J_{nr} \leq 4.5$ and >2.0	PG XXS-YY (S: Standard)
$J_{nr} \leq 2.0$ and >1.0	PG XXH-YY (H: Heavy)
$J_{nr} \leq 1.0$ and >0.5	PG XXV-YY (V: Very Heavy)
$J_{nr} \leq 0.5$	PG XXE- YY (E: Extreme)

According to AASHTO M 332, if the number of load repetition is less than 10 million Equivalent Single Axle Load (ESAL) then the traffic condition is called Standard, if the ESAL is between 10-30 million ESALs then it is designated as Heavy, if the ESAL is greater than 30 million then it is called Very Heavy, and if the ESAL is greater 30 million along with standing traffic it is designated as Extreme. Stress sensitivity is an important parameter for prediction of the performance of PMBs at high stress levels, which is also included in AASHTO M 332. The condition of stress sensitivity is that the difference between J_{nr} values at 0.1 kPa and 3.2 kPa must be less than or equal to 75% of J_{nr} values at 0.1 kPa, as expressed in Equation 2. Table 10 represents the stress sensitivity criteria of the MSCR test method.

$$J_{nr\text{diff}} = \frac{J_{nr,3.2 \text{ kPa}} - J_{nr,0.1 \text{ kPa}}}{J_{nr,0.1 \text{ kPa}}} * 100 \leq 75\% \dots \dots \dots (2)$$

Table 10. Stress sensitivity criteria of MSCR Test

$J_{nr,diff} = (J_{nr,3.2} - J_{nr,0.1} / J_{nr,0.1}) * 100$ Error! Digit expected.	Stress Sensitivity (AASHTO M 332 Criterion)
$\leq 75\%$	Yes
$> 75\%$	No

4.8 MSCR DATA OF UNMODIFIED BINDERS

4.8.1 MSCR Database

The developed MSCR database of PG 64-22 (from Arkansas) is shown in Table 11. None of the unmodified binders met the %R criterion of AASHTO M 332. Therefore, all tested PG 64-22 binders were anticipated to demonstrate very low rutting resistance because of their low %R value at 3.2 kPa. Further, Table 11 shows that the J_{nr} values increased and %R values decreased with the increase of stress levels. For example, the %R values of PG 64-22 binders (from S1) at 0.1 kPa, 3.2 kPa, and 10 kPa are 7.96, 1.91, and -0.16, respectively. Based on the data presented in Table 11, except PG 64-22 from S5, none of PG the 64-22 binders showed any %R values at 10 kPa. As mentioned earlier, the rate of strain accumulation increases with an increase of the stress level, which shows poor rutting resistance. As a result, PG 64-22 binders cannot sustain high traffic load due to a low %R and high J_{nr} values.

Table 11. MSCR data base of PG 64-22 (from Arkansas) at 64°C

Source	$J_{nr0.1}$, kPa	$J_{nr3.2}$, kPa	$J_{nr\ diff}$, (3.2-0.1) %	Stress Sensitivity (Meets AASHTO M 332)	R100, %	R3200, %	R_{diff} (0.1-3.2) %	% R (Meets AASHTO T 350)	J_{nr10} kPa	R10000, %	MSCR GRADE
S1	1.86	2.14	14.79	Yes	7.96	1.91	76.04	No	2.51	-0.16	PG 64S-22
S2	2.04	2.31	13.39	Yes	7.27	2.08	71.49	No	2.67	-0.07	PG 64S-22
S3	1.84	2.12	15.39	Yes	8.16	1.88	77.01	No	2.44	-0.14	PG 64S-22
S4	2.25	2.45	8.53	Yes	3.72	0.60	83.89	No	2.69	-0.50	PG 64S-22
S5	1.70	2.03	19.37	Yes	14.92	4.59	69.21	No	2.36	0.77	PG 64S-22
S6	1.79	1.97	9.82	Yes	5.46	1.37	74.73	No	2.21	-0.23	PG 64H-22
S10	1.94	2.27	14.53	Yes	9.69	1.93	80.08	No	2.87	-0.37	PG 64S-22
S11	2.45	1.33	8.41	Yes	3.44	0.55	83.89	No	2.97	-0.69	PG 64H-22

4.8.2 Polymer Method

MSCR test results of PG 64-22 binders were analyzed by following the polymer method. From Figure 29, it is evident that all tested PG 64-22 binders are plotted below the polymer curve, indicating the absence of polymer. Further, the J_{nr} values of about 75% of tested binders were higher than 2 kPa⁻¹. Only 25% of the tested PG 64-22 binders were above the polymer curve. This kind of scenario was also observed by Wasage et al. [65], Hafeez et al. [72] and Hossain et al. [91] in their respective studies, which reported low %R value and high J_{nr} values for unmodified binders.

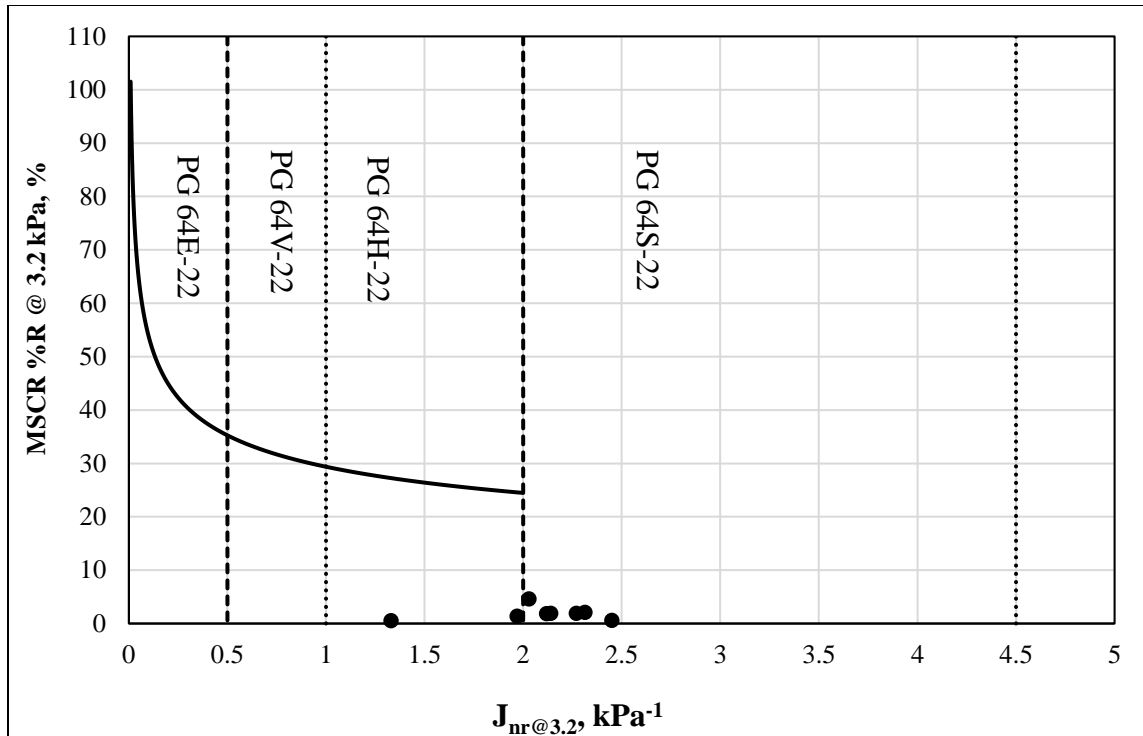


Figure 29. MSCR %R vs. J_{nr} @ 3.2 kPa for PG 64-22 (Arkansas) at 64°C

4.8.3 MSCR Grade

As illustrated earlier, AASHTO M 332 grades a binder based on its J_{nr} value. Figure 30 shows the frequency distribution of the MSCR grades of tested PG 64-22 binders. MSCR grades of PG 64-22 are also shown in Table 11. Based on data presented in Figures 29 and 30, and Table 13, only 25% of the tested binders were graded as a PG 64H-22, and rest of the binders were graded as a PG 64S-22. Thus, 75% of tested binders were sufficient to support standard traffic, as expected, having J_{nr} values in the range from 2 kPa^{-1} to 4.5 kPa^{-1} .

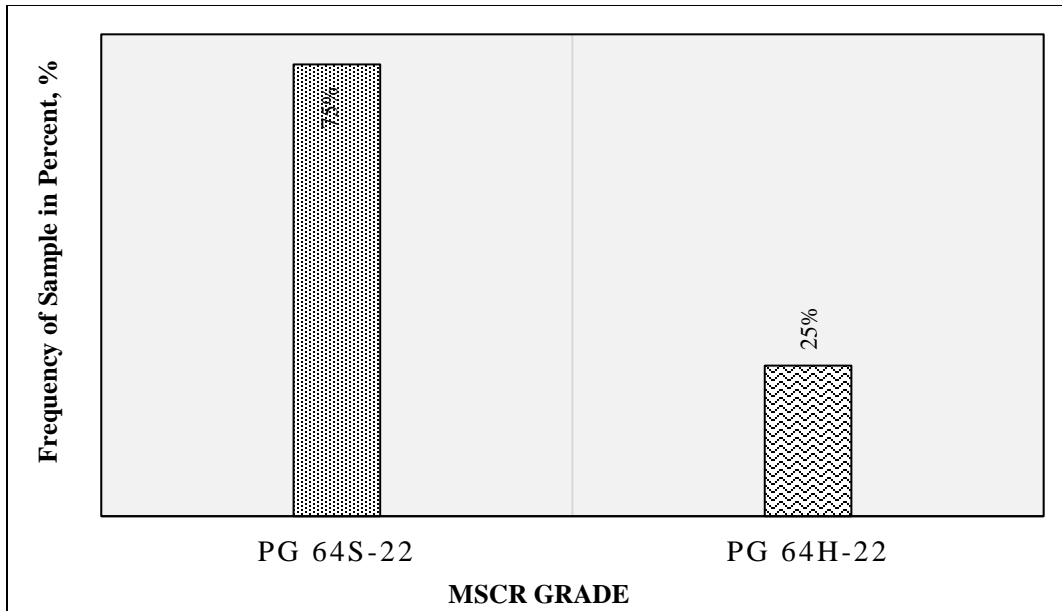


Figure 30. MSCR grades of tested PG 64-22 (Arkansas) binders

4.8.4 Stress Sensitivity

Stress sensitivity was estimated using Equation 2 and data presented in Table 11. It is seen that all tested binders met the AASHTO M 332 stress sensitivity criteria. For all PG 64-22 binders, the difference between J_{nr} values at 0.1 kPa and 3.2 kPa (while increasing the stress level from 0.1 kPa to 3.2 kPa) was less than 75% of the J_{nr} at 0.1 kPa. Thus, the findings of this study indicate that PG 64-22 binders are not excessively stress sensitive to unexpected heavy loads or unusually high temperatures. In Figure 31, $J_{nr\text{diff}}$ is the difference of J_{nr} value at stress levels between 0.1 kPa and 3.2 kPa, and R_{diff} is the difference of the %R values at 0.1 kPa and 3.2 kPa. The tested data were fitted by using Microsoft Excel and the resulting coefficient of determination (R^2) was found to be about 0.35. From Table 11, it is seen that when the stress level increases from 3.2 kPa to 10 kPa, the %R values of unmodified binders was almost zero or negative, which marked that unmodified binders are not stress sensitive.

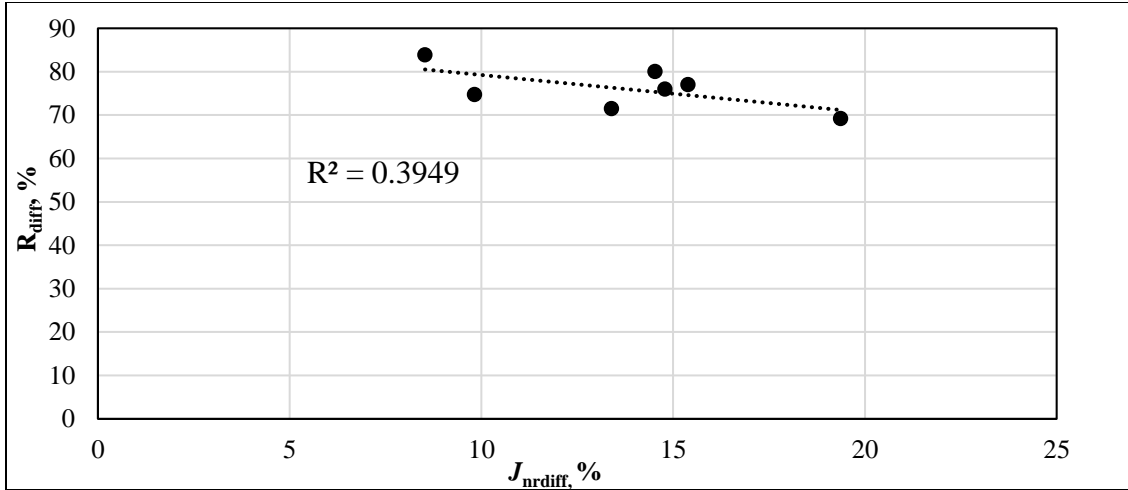


Figure 31. $R_{diff}, \%$ vs. $J_{nr,diff}, \%$ for PG 64-22 (Arkansas)

4.9 ARKANSAS' POLYMER-MODIFIED BINDER

4.9.1 MSCR Database

In this study, two types of PMBs were used for evaluating the MSCR test method. The MSCR test results of PG 70-22 and PG 76-22 binders are presented in Tables 12 and 13, respectively. All tested PMBs met the AASHTO M 332 criterion for stress sensitivity.

Table 12. MSCR database for PG 70-22 (Arkansas) at 64°C and 70°C

Source	Testing Temperature (°C)	$J_{nr,0.1}$, kPa	$J_{nr,3.2}$, kPa	$J_{nr,diff}$, (3.2-0.1) %	Stress Sensitivity (Meets AASHTO T 332)	R100, %	R3200, %	R_{diff} (0.1-3.2) %	$J_{nr,10}$, kPa	R10000, %	$J_{nr,diff}$, (10-3.2) %	$J_{nr,diff}$, (10-0.1) %	R_{diff} (3.2-10) %	R_{diff} (0.1-10) %	MSCR GRADE
S1	64	0.52	0.64	22.10	Yes	40.02	29.51	26.27	0.78	18.80	21.95	48.91	36.29	53.03	PG 64V-22
S1	70	1.30	1.70	31.34	Yes	30.63	15.78	48.48	2.07	6.22	21.47	59.54	60.56	79.68	PG70H-22
S2	64	0.54	0.67	24.81	Yes	46.88	37.03	21.03	0.86	24.05	28.60	60.51	35.11	48.73	PG 64V-22
S2	70	1.25	1.74	39.38	Yes	38.28	22.07	42.37	2.27	8.50	30.47	81.85	61.63	77.83	PG70H-22
S3	64	0.61	0.79	30.57	Yes	42.29	28.11	33.52	1.03	12.94	30.35	70.19	53.97	69.40	PG 64V-22
S3	70	1.43	2.03	42.21	Yes	32.87	13.73	58.22	2.65	3.24	30.18	85.12	76.43	90.15	PG70S-22
S4	64	0.33	0.35	6.65	Yes	64.53	63.45	1.67	0.49	48.79	39.42	48.68	23.10	24.39	PG 64E-22
S4	70	0.65	0.88	34.40	Yes	63.88	54.16	15.23	1.34	30.40	53.03	105.66	43.86	52.41	PG70V-22
S5	64	0.05	0.05	-8.92	Yes	94.05	93.84	0.22	0.08	88.04	55.20	41.38	6.19	6.39	PG 64E-22
S5	70	0.08	0.09	5.98	Yes	94.30	92.50	1.91	0.38	66.78	332.18	357.71	27.80	29.18	PG70E-22
S6	64	0.79	1.00	27.11	Yes	36.76	24.63	33.09	1.20	14.69	20.25	52.84	40.57	60.16	PG 64V-22
S6	70	1.81	2.46	35.78	Yes	28.88	13.23	54.31	3.00	3.91	21.70	65.25	70.95	86.57	PG70S-22
S10	64	0.22	0.21	3.98	Yes	74.12	74.07	0.08	0.35	53.32	63.87	57.34	28.01	28.07	PG 64E-22
S10	70	0.48	0.62	27.61	Yes	69.68	59.67	14.36	1.16	26.06	88.75	140.86	56.32	62.59	PG70V-22
S11	64	0.16	0.16	2.97	Yes	80.68	79.73	1.19	0.37	54.02	132.18	125.29	32.24	33.04	PG 64E-22
S11	70	0.38	0.52	36.86	Yes	75.11	63.96	14.85	1.28	24.77	147.97	239.36	61.27	67.02	PG70V-22
S12	64	0.04	0.03	10.69	Yes	92.83	92.77	0.06	0.05	86.24	60.20	43.08	7.04	7.10	PG 64E-22
S12	70	0.06	0.06	4.23	Yes	92.62	91.30	1.43	0.27	63.24	350.07	331.01	30.73	31.72	PG70E-22

The %R values decreased with an increase of the stress level. For example, at 3.2 kPa and 64°C, the %R of PG 70-22 (from S2) was about 21% lower than that at 0.1 kPa and at the same temperature. Unlike unmodified binders, all PG 70-22 and PG 76-22 binders showed high %R values, this may be a sign that these binders were modified with polymers. However, the exact type of modifier used in modifying the asphalt binders was unknown to the research team. Previously it was mentioned that elastomers increase the elastic properties of the binders and decrease the permanent deformation of the asphalt binders. As a result, binders return to the original position when the load is released. Plastomer has high early strength under deformation but they are less flexible compared to elastomers and tend to rupture under heavy loads [25]. Thus, the suppliers of those PMBs may have used the elastomeric polymer for modifying the unmodified binders. Tables 13 and 14 show that the J_{nr} and %R values are mainly dependent on the testing stress levels and temperatures. For instance, the J_{nr} values of PG 76-22 (from S1) increased abruptly (from 0.88 to 2.21) when the temperature was increased from 70°C to 76°C. The effect of stress level and temperature will be discussed later in this chapter.

4.9.2 Investigating the Polymer Modification

The %R values of PG 70-22 and PG 76-22 binders at 64°C and 3.2 kPa were calculated by Equation 1 for investigating presence of elastomers. Figures 32 and 33 show the %R values at $J_{nr,3.2\text{ kPa}}$ for PG 70-22 and PG 76-22 binders, respectively. The %R values of all PG 76-22 binders were above the polymer curve except PG 76-22 from source S1. Five out of nine PG 70-22 binders were also above the polymer curve. As previously mentioned, if the %R values of binders fall above the polymer curve then these binders have elastomers. This statement is found true for a majority of PMBs tested in this study.

Table 13. MSCR database for PG 76-22 (Arkansas) at 64°C, 70°C and 76°C

Source	Testing Temperature(°C)	J _{nr 0.1} , KPa	J _{ns 2} , KPa	J _{nr diff} , (3.2-0.1) %	Stress Sensitivity (Meets AASHTO T 332)	R100, %	R3200, %	R _{diff} (0.1-3.2) %	J _{nr 10} , KPa	R10000, %	J _{nr diff} , (10-3.2) %	J _{nr diff} , (10-0.1) %	R _{diff} (3.2-10) %	R _{diff} (0.1-10) %	MSCR GRADE
S1	64	0.27	0.32	20.10	Yes	41.07	30.63	25.43	0.44	15.25	37.24	64.83	50.20	62.86	PG 64E-22
S1	70	0.66	0.88	32.35	Yes	32.01	16.28	49.13	1.23	5.84	38.99	83.96	64.12	81.75	PG 70V-22
S1	76	1.57	2.21	40.35	Yes	23.57	6.81	71.09	3.22	0.72	45.75	104.58	89.48	96.96	PG 76S-22
S2	64	0.14	0.15	5.68	Yes	75.85	74.75	1.46	0.20	66.33	30.98	38.44	11.28	12.57	PG 64E-22
S2	70	0.31	0.39	25.48	Yes	70.75	64.29	9.14	0.62	44.28	57.94	98.21	31.15	37.43	PG 70E-22
S2	76	0.71	1.11	55.38	Yes	62.21	45.29	27.20	1.79	19.57	61.35	150.75	56.83	68.55	PG 76H-22
S3	64	0.16	0.17	2.72	Yes	76.12	75.28	1.11	0.24	61.37	46.16	50.14	18.48	19.38	PG 64E-22
S3	70	0.33	0.40	22.34	Yes	72.89	66.63	8.60	0.77	37.23	89.83	132.23	44.13	48.93	PG 70E-22
S3	76	0.72	1.17	61.87	Yes	66.62	47.58	28.58	2.24	13.89	91.61	210.16	70.80	79.15	PG 76H-22
S4	64	0.08	0.09	3.60	Yes	85.86	85.73	0.15	0.09	84.46	1.04	4.69	1.48	1.63	PG 64E-22
S4	70	0.12	0.15	21.64	Yes	88.14	85.92	2.51	0.23	75.63	56.84	90.57	11.97	14.19	PG 70E-22
S4	76	0.24	0.30	25.25	Yes	85.90	82.38	4.09	0.87	50.45	184.39	255.97	38.77	41.27	PG 76E-22
S5	64	0.03	0.03	1.47	Yes	96.28	96.23	0.05	0.02	95.74	8.94	10.27	0.51	0.56	PG 64E-22
S5	70	0.04	0.05	4.20	Yes	96.11	95.57	0.56	0.06	92.63	34.52	40.18	3.08	3.62	PG 70E-22
S5	76	0.10	0.11	10.00	Yes	93.98	93.29	0.74	0.41	71.79	321.70	298.66	23.05	23.62	PG 76E-22
S6	64	0.13	0.14	7.69	Yes	79.02	78.42	0.76	0.15	74.19	14.34	20.74	5.41	6.12	PG 64E-22
S6	70	0.23	0.27	20.11	Yes	78.99	75.57	4.33	0.49	55.71	77.77	113.53	26.30	29.48	PG 70E-22
S6	76	0.52	0.74	40.90	Yes	72.68	63.48	12.66	1.54	28.83	109.29	194.91	54.59	60.34	PG 76V-22
S10	64	0.04	0.04	8.84	Yes	92.45	92.15	0.33	0.03	91.96	15.77	23.22	0.54	0.21	PG 64E-22
S10	70	0.07	0.07	3.58	Yes	92.37	91.72	0.71	0.11	83.91	57.23	51.60	8.52	9.17	PG 70E-22
S10	76	0.16	0.14	10.60	Yes	89.68	88.79	0.99	0.64	52.59	341.82	295.01	40.77	41.36	PG 76E-22
S11	64	0.20	0.22	8.74	Yes	71.38	69.39	2.78	0.35	50.50	63.37	77.65	27.23	29.26	PG 64E-22
S11	70	0.44	0.62	40.54	Yes	65.46	53.69	17.98	1.11	24.66	77.63	149.65	54.07	62.33	PG 70V-22
S11	76	1.06	1.82	71.64	Yes	55.29	30.89	44.13	3.16	5.06	73.33	197.50	83.62	90.85	PG 76H-22
S12	64	0.02	0.02	7.10	Yes	94.79	94.63	0.17	0.03	91.92	21.99	13.34	2.86	3.03	PG 64E-22
S12	70	0.04	0.04	4.63	Yes	94.73	93.90	0.88	0.10	82.37	160.41	148.34	12.28	13.05	PG 70E-22
S12	76	0.08	0.07	7.79	Yes	93.21	91.69	1.63	0.69	43.58	892.83	815.47	52.47	53.24	PG 76E-22

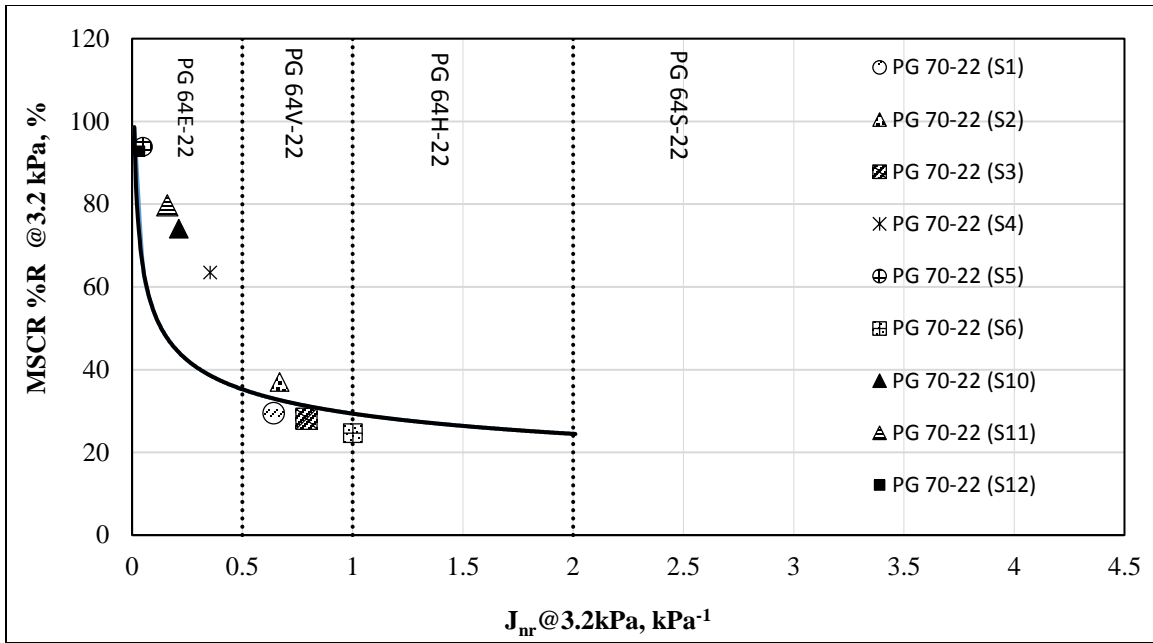


Figure 32. MSCR %R vs. $J_{nr} @ 3.2 \text{ kPa}$ for PG 70-22 (Arkansas) at 64°C

4.9.3 MSCR Grade

All PG 70-22 and PG 76-22 binders were graded on the basis of $J_{nr,3.2\text{kPa}}$ at the aforementioned testing temperature. Tables 12 and 13 show a summary of the test results obtained of these PMBs. Figures 34 and 35 show the frequency distribution of the MSCR grades of PG 70-22 and PG 76-22 binders, respectively. For PG 70-22 binders, at 64°C, 55% of binders could be graded as PG 64E-22 and other 45% could be graded as PG 64V-22 on the basis of J_{nr} value at 3.2 kPa. For the same asphalt binders, at 70°C, 22% of binders could be graded as PG 70H-22, PG 70E-22 and PG 70S-22, and 33% of binders could be graded as PG 70V-22. All PG 76-22 binders could be graded as PG 64E-22 at 64°C. At 70°C, about 22% and 78% of PG 76-22 binders could be graded as PG 70V-22 and PG 70E-22, respectively. At 76°C, PG 76-22 binders could be graded as PG 76E-22, PG 76V-22, PG 76H-22, and PG 76S-22. Based on the observed data, at 0.1 kPa and 3.2 kPa, the effect of temperature was negligible for changing the J_{nr} values. For example, 4 out of 9 PG 76-22 binders could sustain more than 30 million (plus standing traffic) ESALs at 64°C, 70°C, and 76°C. This

could happen due to the presence of high percentage of elastomers in the PG 76-22 binders.

From the previous discussion, PMBs could be used at different locations on the basis of climate temperatures and traffic conditions. For instance, PG 70-22 from S1, could be used where the climate temperature is 64°C and traffic loading is greater than 30 million ESAL, and same binders could also be used where the climate temperatures is 70°C and traffic loading is between 10-30 million ESALs. According to AASHTO M 320, PG 70-22 could be used where at 98% reliability the maximum pavement temperature would be 70°C or lower. This specification is valid on the basis of temperature, it fails when the traffic conditions were considered. AASHTO M 332 could be helped to select the specific binders for specific area on the basis of climate as well as the traffic condition of that area.

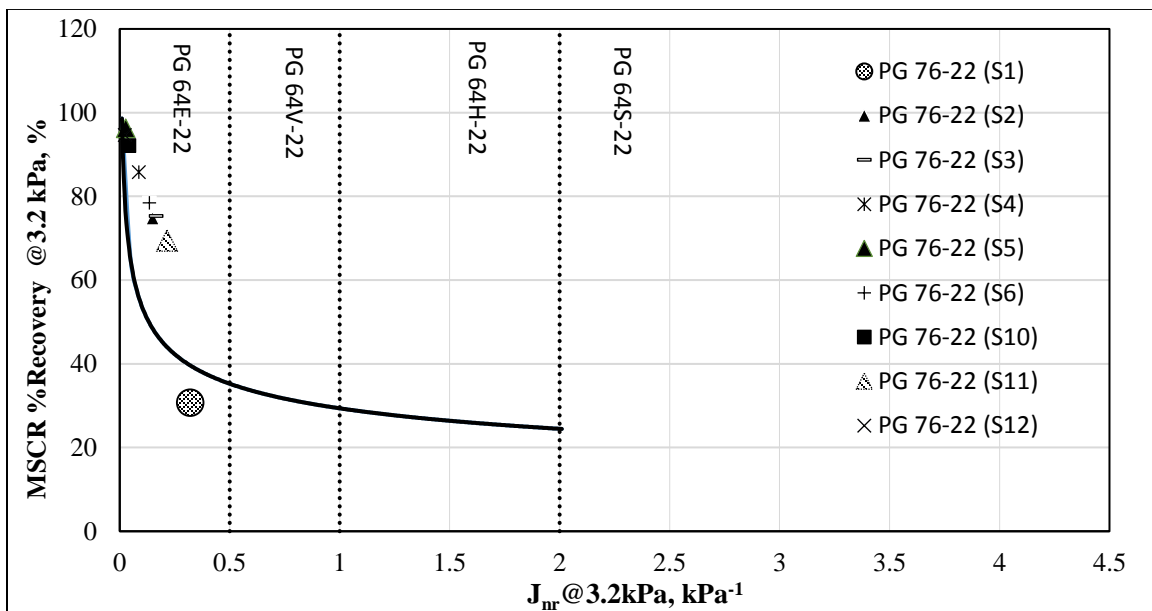


Figure 33. MSCR %R vs. J_{nr} @ 3.2 kPa for PG 76-22 (Arkansas) at 64°C

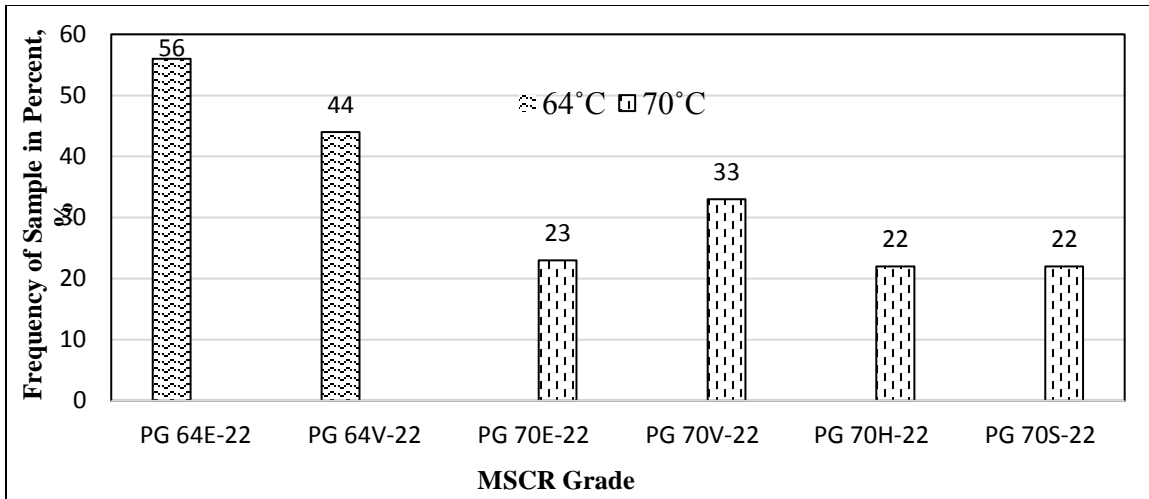


Figure 34. Frequency of sample vs. J_{nr} @ 3.2 kPa for PG 70-22 (Arkansas) binders

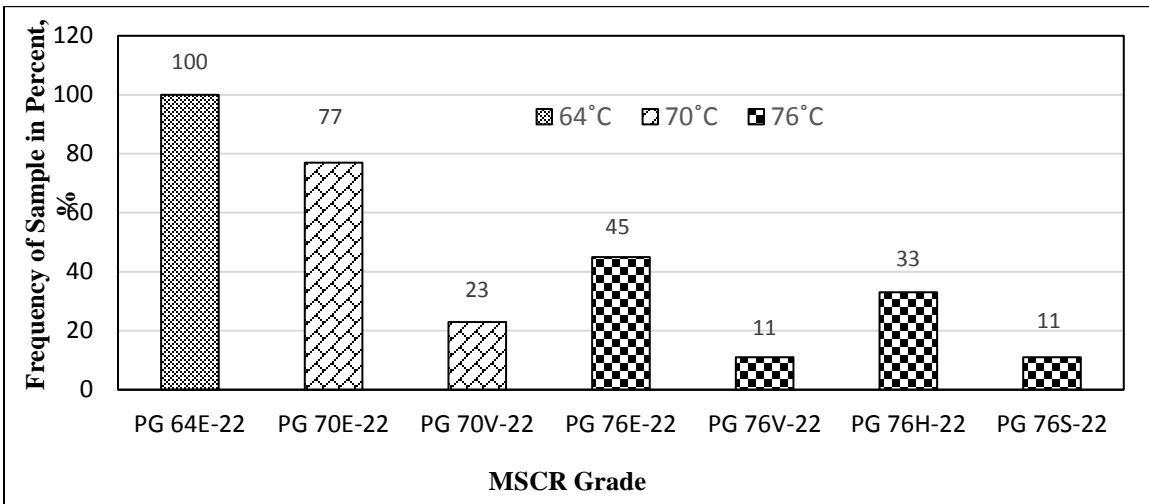


Figure 35. Frequency of sample vs. J_{nr} @ 3.2 kPa for PG 76-22 (Arkansas) binders

4.9.4 Elastic Recovery vs. Percent Recovery

The quadrant plot of the PG 70-22 and PG 76-22 are shown in Figures 36 and 37, respectively. The elastic recovery values for PMBs were obtained from the certification data provided by the binder suppliers. Previously it was mentioned that a quadrant plot helps to disclose whether the binders could be categorized as “User Risk,” “Supplier Risk,” “Both at Risk,” or “None at Risk.” The AHTD recommends that the minimum elastic recovery values for PG 70-22 and PG 76-22 are 40% and 50%, respectively. The

quadrant diagram is obtained by plotting the agency or DOT recommended ER data in the X axis and %R at 3.2 kPa along the Y axis. The AI also recommends using the ER value while estimating the minimum required %R value, which is 15% less than the agency recommended minimum ER value [92]. Thus, according to the AI, the minimum %R value for PG 70-22 and PG 76-22 binders will be 25% and 35%, respectively. The ranges of %R at 3.2 kPa and 64°C, and ER at 25°C of tested PG 76-22 binders were between 30.63% and 96.23%, and between 80% and 94%, respectively. All PG 76-22 binders fall in the first quadrant except the PG 76-22 binder from S1, which fall in the fourth quadrant. Therefore, a %R value of 35% is applicable for PG 76-22 binders. So, the minimum %R value of 35% will be S1 at Supplier Risk. For a more conservative approach, a value of 60% for the MSCR %R can be recommended for PG 76-22 binders, and this will still put one supplier at risk but no user is at risk.

From Figure 36, it is seen that all PG 70-22 binders fall in the first quadrant. Therefore, all suppliers met the AI recommended minimum %R values (25%) and AHTD's current ER limit for PG 70-22 binders. Based on the quadrant plot, the minimum MSCR %R value of 25% is recommended for the PG 70-22 binders, without putting any supplier or user at risk. To be conservative, a value of 70% for the MSCR %R can be recommended for PG 70-22 binders, and this will put four suppliers at risk but no user is at risk.

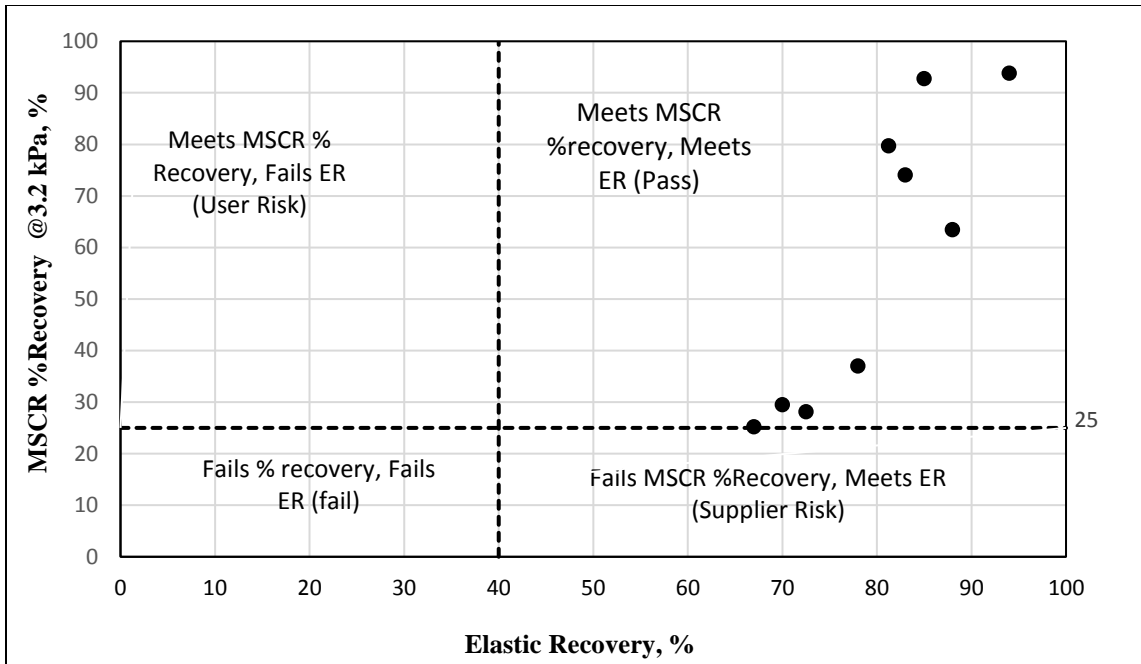


Figure 36. Quadrant plot for PG 70-22 (Arkansas)

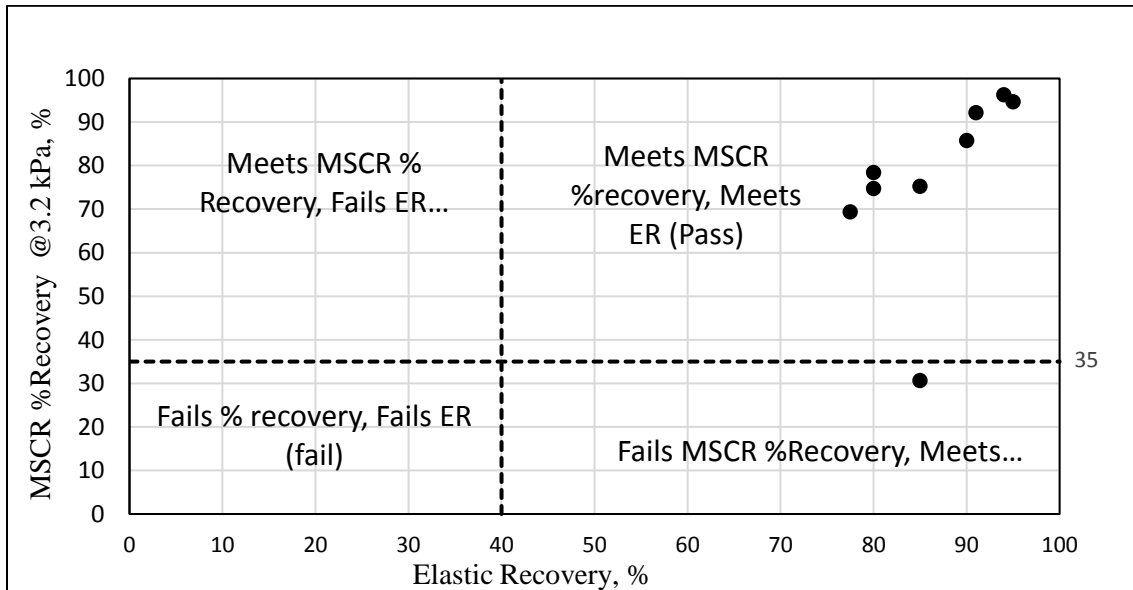


Figure 37. Quadrant plot for PG 76-22 (Arkansas)

4.9.5 Stress Sensitivity

Based on data shown here, all tested PMBs met the AASHTO M 332 stress sensitivity criteria. For all PMBs, the difference of J_{nr} values at 0.1 kPa and 3.2 kPa (while

increasing the stress level from 0.1 kPa to 3.2 kPa) was less than 75% of the J_{nr} at 0.1 kPa. The rate of change of %R values of PG 76-22 binders with changing the stress levels from 0.1 kPa to 3.2 kPa was lower than those of the PG 70-22 binders. Thus, the findings of this study indicate that PG 70-22 binders are more stress sensitive than the PG 76-22 binders. In Figures 38 and 39, $J_{nr,diff}$ is the difference of J_{nr} value at stress levels between 0.1 kPa and 3.2 kPa, and R_{diff} is the difference of the %R values at 0.1 kPa and 3.2 kPa. The tested data were fitted by using the Microsoft Excel and the coefficient of determination (R^2) values of PG 70-22 and PG 76-22 binders were found to be about 0.83 and 0.79, respectively. Further, unlike unmodified binders, PMBs showed less stress sensitivity than others in terms of R_{diff} . It is also observed that when the stress levels increased from 3.2 kPa to 10 kPa, the %R of PMBs were higher compared to the low stress levels, which marked that sensitivity of asphalt binders increased with an increase of the stress level.

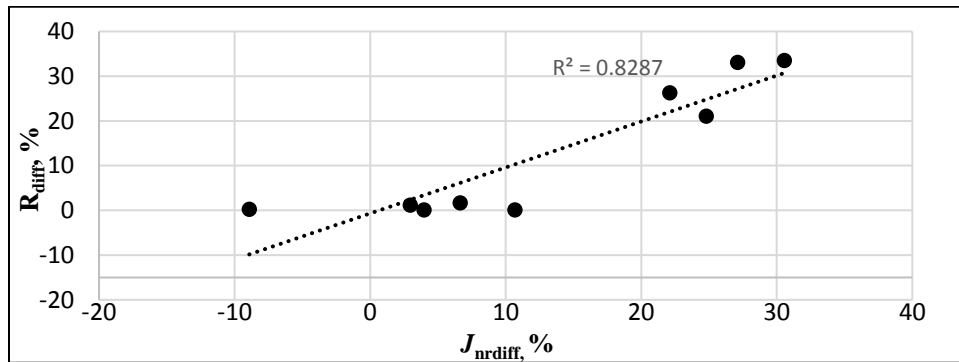


Figure 38. R_{diff} , % vs. $J_{nr,diff}$, % for PG 70-22 (Arkansas)

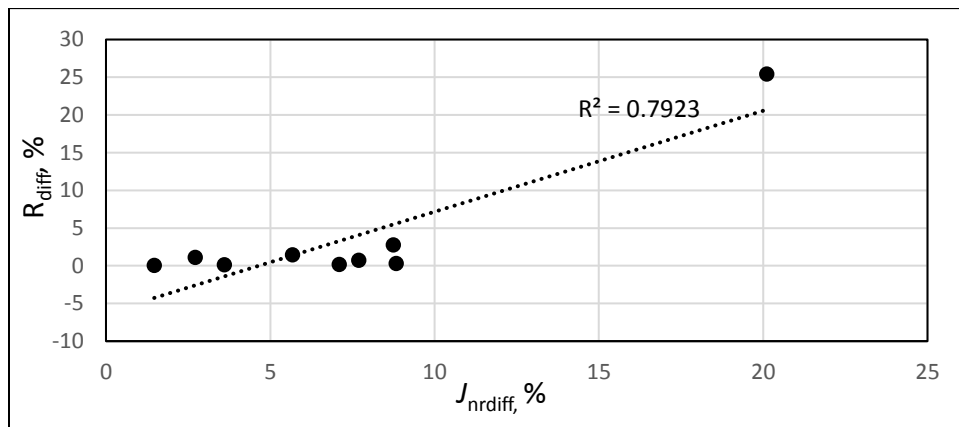


Figure 39. R_{diff} , % vs. $J_{nr,diff}$, % for PG 76-22 (Arkansas)

4.10 Texas' Polymer-Modified Binders

The MSCR test results for the PG 70-22 and PG 76-22 binders are presented in Tables 14 and 15, respectively. All tested PMBs met the AASHTO M 332 criterion for stress sensitivity. The J_{nr} values increased with an increase of the stress level. For example, at 0.1 kPa and at 64°C, a J_{nr} value of PG 70-22 (from S7) was about 22% lower than that at 3.2 kPa and at the same temperature. Unlike unmodified binders, PMBs showed lower J_{nr} values, which may be a sign that these binders were modified with polymers. It could be noted that the types of polymer used in the PMBs were unknown to the research team. Previously it was mentioned that elastomers increase the elastic properties of the binders and decrease the permanent deformation of the asphalt binders. As a result, binders return to their original position when the load is released. Plastomer has high early strength under deformation but they are less flexible compared to elastomers, and they tend to rupture under heavy loads [25]. Thus, the suppliers of those PMBs might have used the elastomeric polymer for modifying the binders. Tables 14 and 15 show that the J_{nr} and %R values are mainly dependent on the testing stress levels and temperatures. For instance, at 3.2 kPa, the %R values of PG 76-22 binder from S9 decreased abruptly from 56.80% to 45.65% when the testing temperature increased from 64°C to 70°C.

Figure 40 shows the %R values at $J_{nr,3.2\text{ kPa}}$ for PMBs. The %R values of all PG 70-22 binders were above the polymer curve except PG 70-22 from S9. Like Arkansas' binders, all PMBs from Texas were also graded on the basis of $J_{nr,3.2\text{ kPa}}$ at different testing temperatures. The frequency distribution of the MSCR grades of PG 70-22 and PG 76-22 binders are shown in Figures 41 and 42, respectively. At 64°C, all PG 76-22 binders from S7, S8 and S9 would sustain more than 30 million ESAL plus standing traffic as their MSCR grade is PG 64E-22. PG 76-22 binder from S8 was found stiffer than other sources as the MSCR grade of this binder was under the extreme load categories (ESAL greater than 30 million plus standing traffic) at three testing temperatures. This might have happened due to the presence of high percentage of elastomers in PG 76-22 binder from S8. For PG 70-22 binder, at 64°C, two third of the tested binders would be graded as PG 64V-22 and other one third of tested binders

could be graded as PG 64E-22 on the basis of J_{nr} value at 3.2 kPa. For the same asphalt binders, at 70°C, 75% of binders could be graded as PG 70H-22, and 25% of binders could be graded as PG 70E-22.

Table 14. MSCR database of PG 70-22 (Texas)

Source	Testing Temperature (°C)	J _{nr 0.1} , kPa	J _{nr 3.2} , kPa	J _{nr diff, (3.2-0.1)} %	Stress Sensitivity (Meets AASHTO T 229)	R100, %	R3200, %	R _{diff (0.1-3.2)} %	J _{nr 10} , kPa	R10000, %	J _{nr diff, (10-3.2)} %	J _{nr diff, (10-0.1)} %	R _{diff (3.2-10)} %	R _{diff (0.1-10)} %	MSCR GRADE
S7	64	0.53	0.65	22.67	Yes	53.08	44.28	16.59	0.85	28.65	29.45	58.80	35.30	46.03	PG 64V-22
S7	70	1.19	1.72	44.87	Yes	47.48	28.99	38.94	2.21	11.98	28.50	86.16	58.66	74.76	PG70H-22
S8	64	0.17	0.16	7.84	Yes	75.56	75.61	-0.06	0.28	52.84	77.28	63.36	30.11	30.06	PG 64E-22
S8	70	0.38	0.46	22.95	Yes	71.64	61.99	13.47	0.99	24.36	113.9	163.02	60.72	66.00	PG70E-22
S9	64	0.44	0.55	25.72	Yes	34.91	23.65	32.29	0.75	12.89	34.83	69.51	45.52	63.10	PG 64V-22
S9	70	1.11	1.50	35.32	Yes	25.59	11.43	55.37	2.03	3.95	35.33	83.14	65.50	84.59	PG70H-22

80 Table 15. MSCR database of PG 76-22 (Texas)

Source	Testing Temperature (°C)	J _{nr 0.1} , kPa	J _{nr 3.2} , kPa	J _{nr diff, (3.2-0.1)} %	Stress Sensitivity (Meets AASHTO T 332)	R100, %	R3200, %	R _{diff (0.1-3.2)} %	J _{nr 10} , kPa	R10000, %	J _{nr diff, (10-3.2)} %	J _{nr diff, (10-0.1)} %	R _{diff (3.2-10)} %	R _{diff (0.1-10)} %	MSCR GRADE
S7	64	0.18	0.18	1.00	Yes	76.76	77.09	-0.43	0.23	68.63	29.76	29.30	10.98	10.60	PG 64E-22
	70	0.34	0.41	19.64	Yes	75.72	71.36	5.76	0.77	45.43	88.95	126.05	36.33	40.00	PG 70E-22
	76	0.76	1.31	71.69	Yes	69.67	50.85	27.00	2.37	18.03	81.23	211.18	64.55	74.12	PG 76H-22
S8	64	0.04	0.04	3.39	Yes	91.79	91.97	-0.20	0.03	92.58	22.45	25.08	-0.67	-0.87	PG 64E-22
	70	0.07	0.07	0.94	Yes	91.70	91.36	0.37	0.08	87.97	12.89	12.13	3.72	4.08	PG 70E-22
	76	0.15	0.14	3.70	Yes	89.06	88.35	0.79	0.38	66.45	166.39	156.83	24.85	25.43	PG 76E-22
S9	64	0.13	0.25	91.02	No	75.32	56.80	24.61	0.35	45.44	42.29	171.81	20.02	39.69	PG 64E-22
	70	0.25	0.67	167.72	No	75.82	45.65	39.82	1.01	29.69	50.61	303.22	35.06	60.90	PG 70V-22
	76	0.71	1.90	169.34	No	64.58	27.95	56.83	2.77	11.97	45.73	292.68	57.40	81.55	PG 76H-22

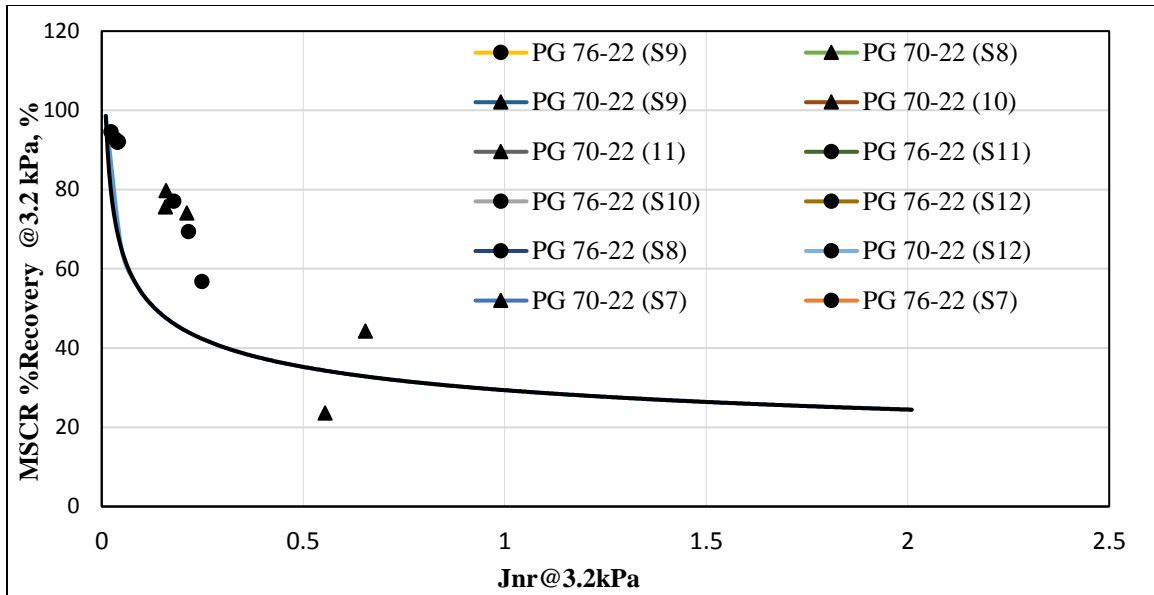


Figure 40. MSCR %R vs. J_{nr} @ 3.2 kPa for PG 70-22 (Texas) at 64°C

From the aforementioned discussion, it is apparent that the same asphalt binder could be used at different locations on the basis of climate temperatures and traffic conditions (e.g., PG 70-22 from S7 could be used where the climate temperature is 64°C and traffic loading is greater than 30 million ESALs, and same binders could be used where the climate temperatures is 70°C and traffic loading is between 10-30 million ESALs).

According to AASHTO M 320, PG 76-22 can be used where with a 98% reliability the maximum pavement temperature is 76°C or lower. This specification is valid on the basis of temperature, but it failed when the traffic conditions were considered. AASHTO M 332 could be helpful in selecting the specific binders for specific area on the basis of climate as well as traffic condition.

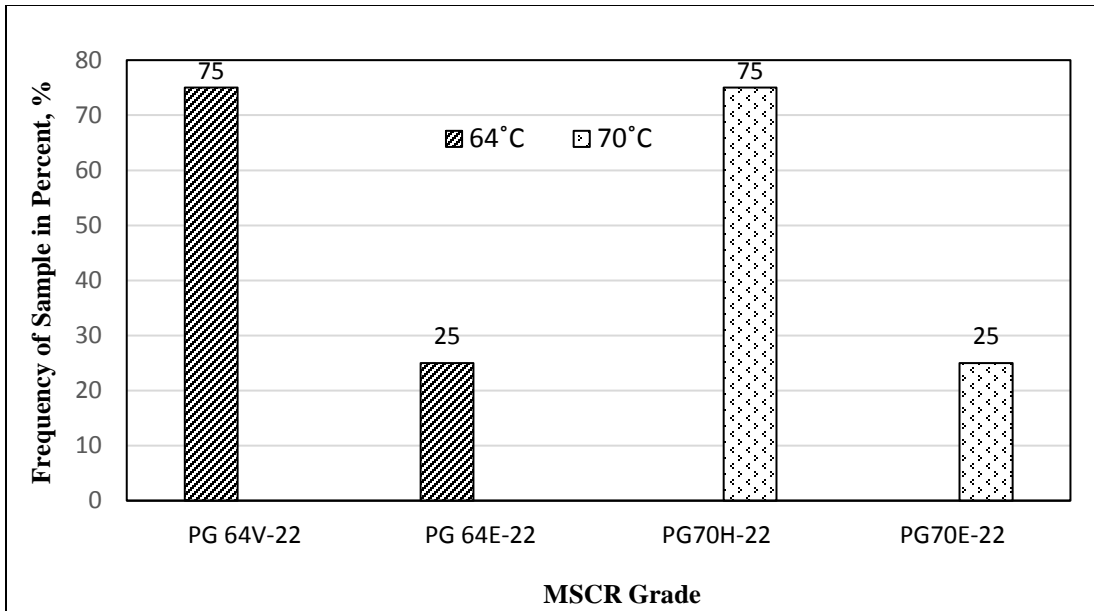


Figure 41. Frequency of sample vs J_{nr} @3.2 kPa for PG 70-22 from Texas

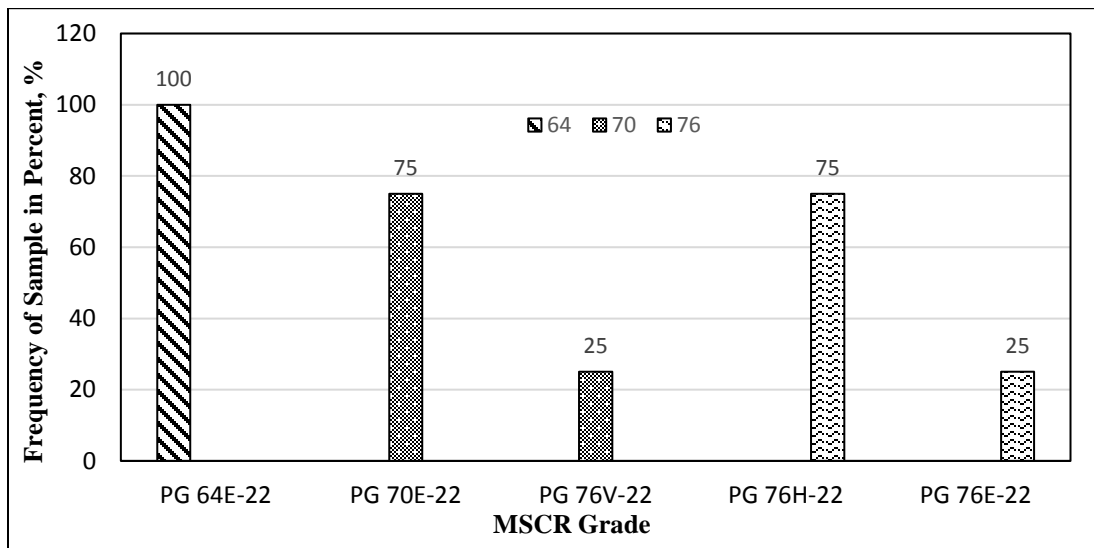


Figure 42. Frequency of sample vs J_{nr} @3.2 kPa for PG 76-22 from Texas

4.9.6 Elastic Recovery vs. Percent Recovery

The quadrant plot of the PG 70-22 and PG 76-22 are shown in Figures 43 and 44, respectively. TxDOT recommends the minimum elastic recovery values for PG 70-22 and PG 76-22 to be 30% and 50%, respectively. The ranges of %R value at 3.2 kPa

and at 64°C, and the elastic recovery value at 25°C of PG 70-22 were found to be between 23.64% to 92.77%, and 70% to 89%, respectively. All binders met the MSCR %R values and the AI recommended ER values. However, a value of 42% as the %R for a PG 76-22 binder appears to be a very conservative approach for conditions prevailing in Texas. At %R value of 42%, only one (S9) out of 6 suppliers was at risk of not meeting the recommended %Recovery. Therefore, based on the AI's recommendations and TxDOT's current ER limit, except for the PG 70-22 from S9, a %R value of 42% is applicable for PG 70-22 binders. Therefore, a value of 42% for the MSCR %R is recommended for PG 70-22 binders while putting one supplier at risk. This supplier will be required to adjust their plant processes to meet the %R requirement. It is evident that all PG 76-22 binders fall in the first quadrant. Therefore, all suppliers met the AI recommended minimum %R values (35%) and TxDOT' current ER limit for PG 76-22. Based on the quadrant plot, the research team recommends a minimum MSCR %R value of 55% for PG 76-22 binders without putting any suppliers or users at risk.

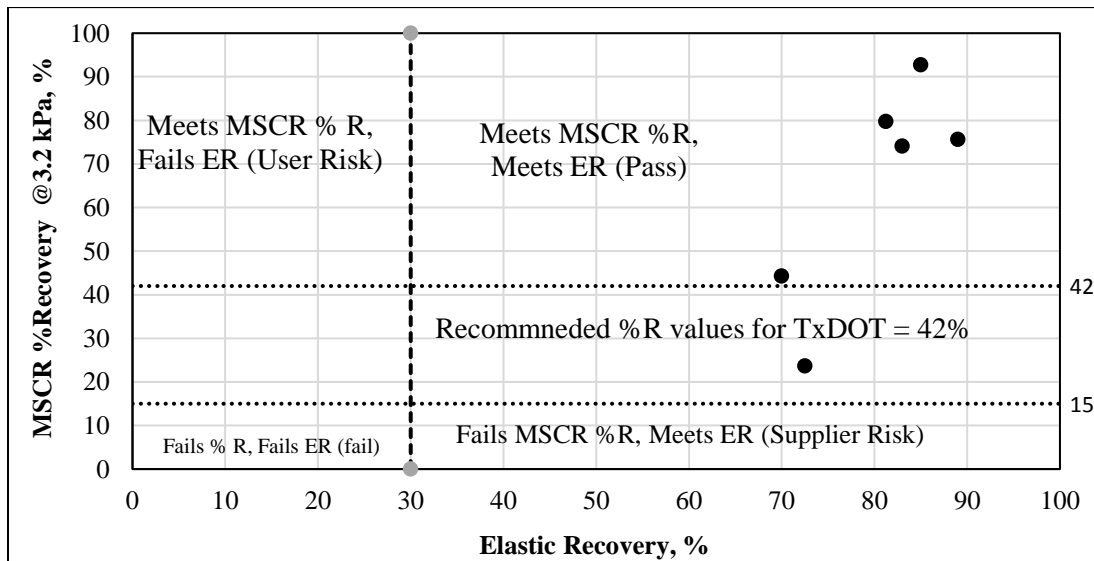


Figure 43. Quadrant plot for PG 70-22 (Texas)

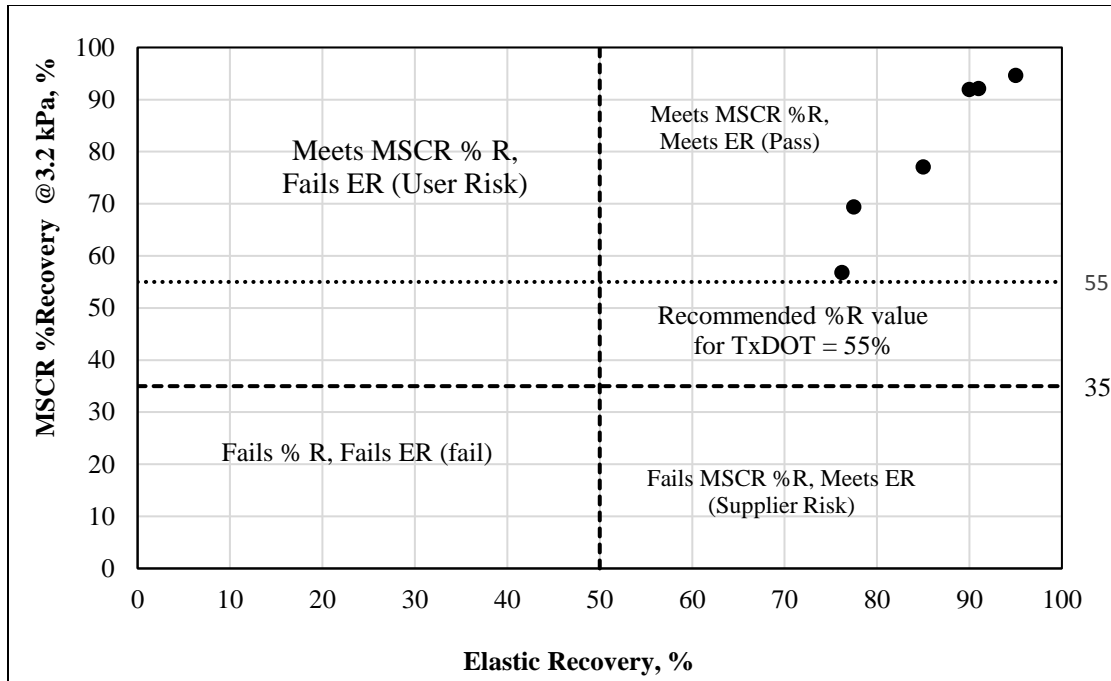


Figure 44. Quadrant plot for PG 76-22 (Texas)

4.9.7 Stress Sensitivity

All tested PMBs met the AASHTO M 332 stress sensitivity criteria except PG 76-22 from S9. The rate of change of J_{nr} values of PG 70-22 with changing the stress levels from 0.1 kPa to 3.2 kPa was higher than that of the PG 76-22 binders (except PG 76-22 from S9). Thus, the findings of this study indicate that PG 70-22 binders are more stress sensitive than PG 76-22 binders.

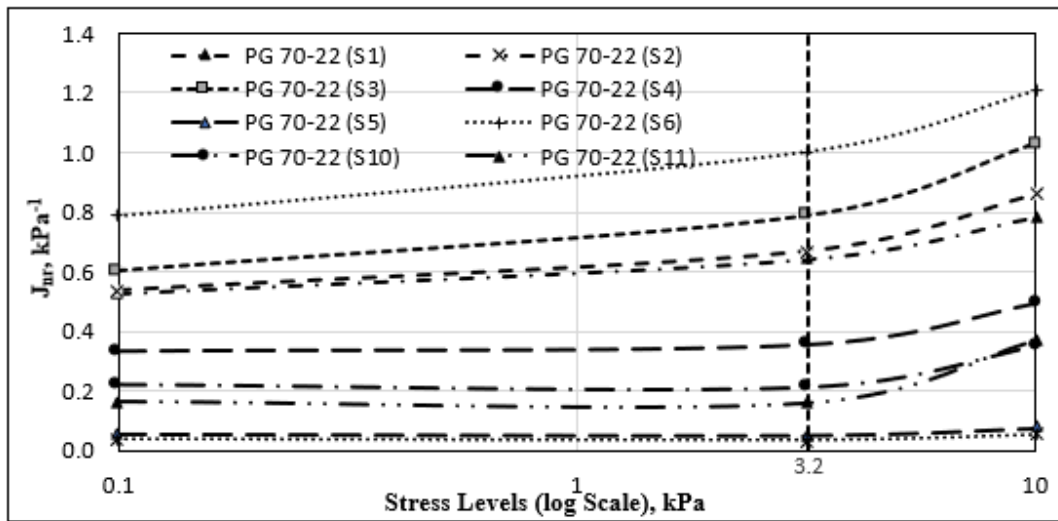
4.10 NON-CONVENTIONAL MSCR TEST FOR PMBS

Even though the MSCR test method is a better tool than AASHTO T 315 for characterizing RTFO-aged PMBs, researchers do not agree with the stress levels in the test [5, 12, 14, 95, 96]. At the currently recommended MSCR stress levels, PMBs do not show a nonlinear behavior. Thus, high stress levels are suggested by researchers to get clear pictures of rutting, which is a nonlinear phenomenon. [97-99]. Wasage et al. [65] tested unmodified, PMB and crumb rubber modified binder by following the MSCR test method at stress levels from 0.025 to 25.6 kPa and at temperatures ranging from 30°C

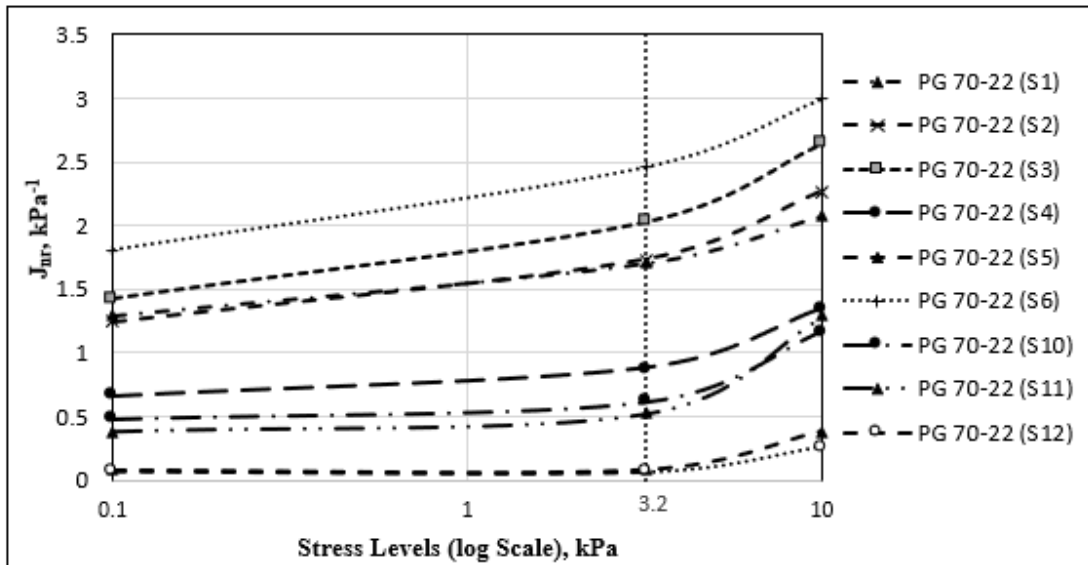
to 70°C. These researchers found the best correlation between J_{nr} and rut depth from a Hamburg Wheel track at the MSCR stress level of 12.8 kPa. .

4.10.1 Effect of Higher Stress levels and temperature on PMBs

Figure 45 shows that the J_{nr} values of PG 70-22 binders at different stress levels and at two testing temperatures (64°C and 70°C). The J_{nr} values of 77% of the tested PG 70-22 binders, except those from S3 and S6, were nearly independent of the stress level up to 3.2 kPa at both testing temperatures (64°C, 70°C). The stress sensitivity was clear at 10 kPa irrespective of the testing temperature. As a result, the AHTD could consider 10 kPa or a higher stress level at 64°C for measuring the nonlinear properties of PG 70-22 binders. However, at a higher stress level of 10 kPa and at 70°C, the %R values of a few PG 70-22 binders from S1, S3, and S6 were almost zero (Figure 45). On the other hand, at a stress level of 3.2 kPa, the nonlinearity behavior of PG 70-22 binders was insignificant. Jafari et al. [100] also reported that the MSCR %R value decreased and the J_{nr} value increased with an increasing the testing temperature. Hence, at 70°C, the AHTD could consider a stress level between 3.2 kPa and 10 kPa for measuring the nonlinear properties of PG 70-22 binders.



(a)



(b)

Figure 45. (a) Change of J_{nr} with stress level for (a) PG 70-22 (Arkansas) at 64°C (b) PG 70-22 (Arkansas) at 70°C

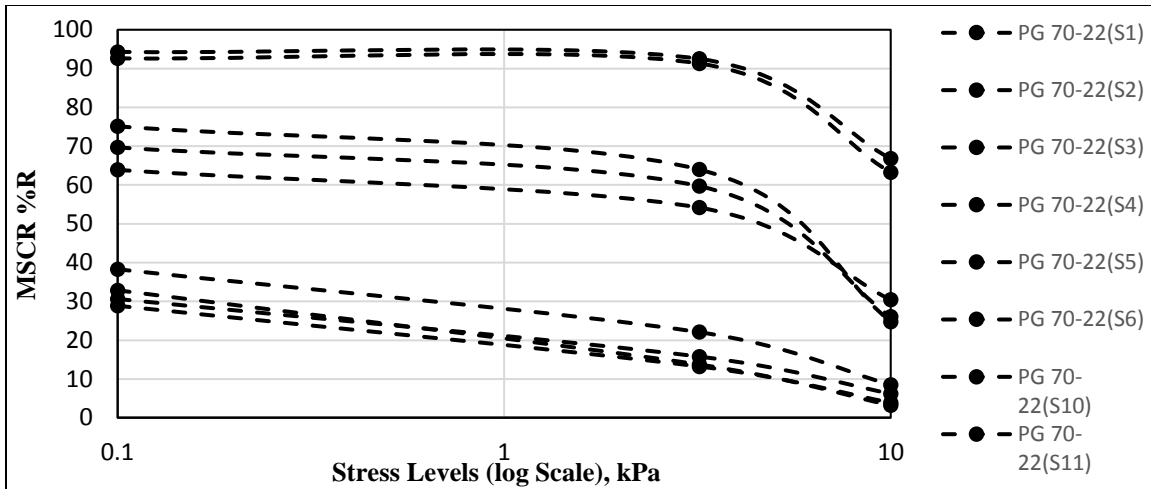
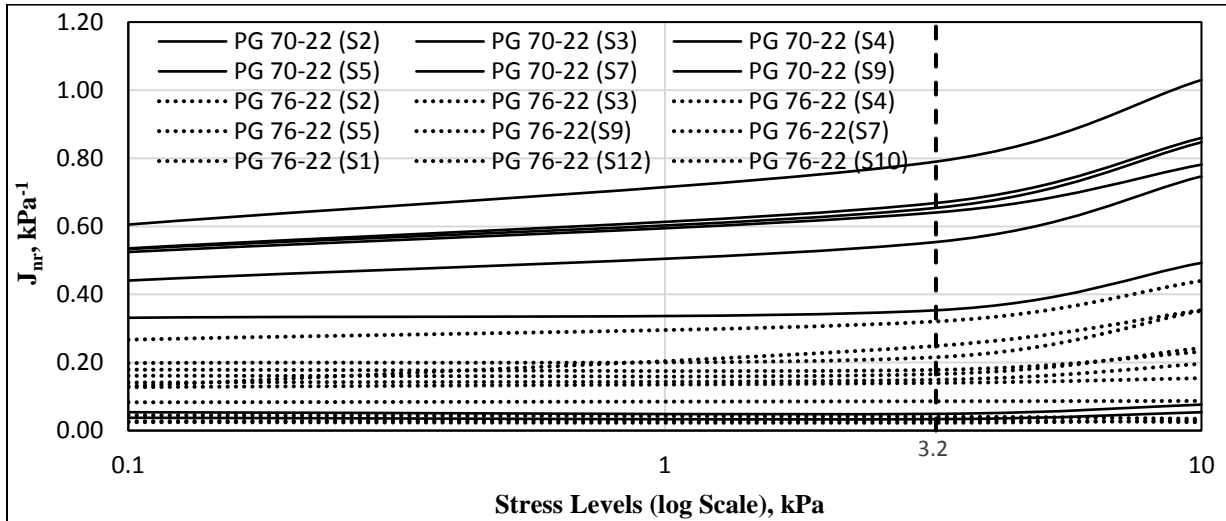


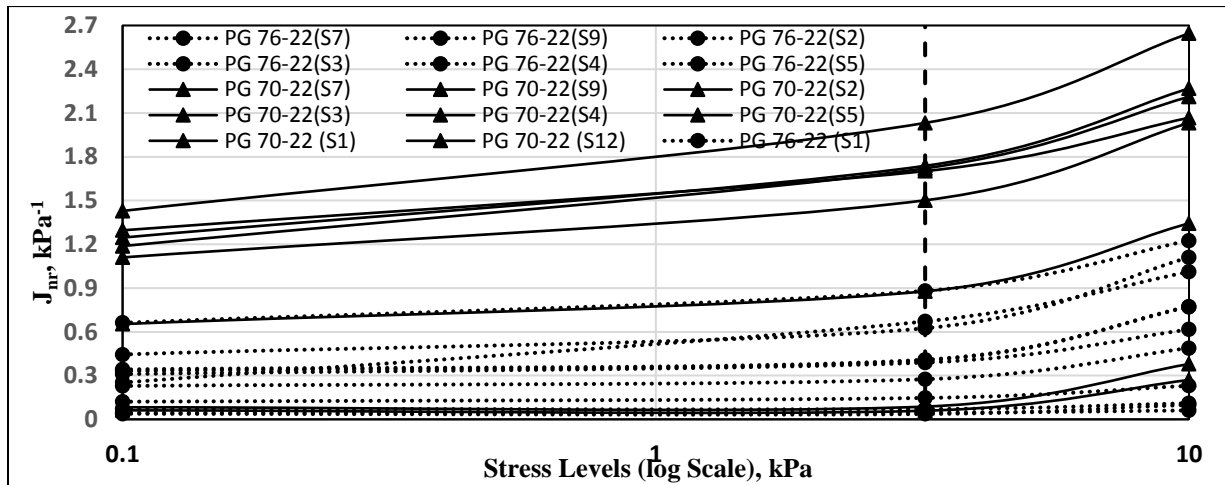
Figure 46. %R vs stress levels for PG 70-22 (Arkansas) at 70°C

Figure 45 shows the J_{nr} values of SBS-modified PMBs at different stress levels at different testing temperatures (64°C, 70°C, and 76°C). In this figure, the dotted lines represent the J_{nr} values of PG 76-22 binders at different stress levels. At 64°C and a stress level up to 3.2 kPa, all dotted lines are almost straight and it was difficult to distinguish them. However, most of the dotted lines are also straight at higher stress levels. Thus, SBS-modified PG 76-22 binders did not show a nonlinear behavior at higher stress levels at 64°C. Therefore, at 64°C, further investigation is needed for capturing the stress level at which SBS-modified PG 76-22 binders would show the nonlinear response. At 70°C, the stress sensitivity of PG 76-22 binders was also not clear at 0.1 kPa and 3.2 kPa. The stress sensitivity slightly revealed at a stress level of 10 kPa, but it was insignificant. Jafari et al. [100] reported that at 12.8 kPa and at 70°C, SBS-modified binders showed a significant amount of nonlinear behavior. Thus, a stress level of 12.8 kPa can be added to the MSCR standard procedure to measure the nonlinearity of SBS-modified binders at 70°C. Stress sensitivity of the asphalt binders are also dependent on the temperature, which is shown in Figure 45(c). The stress sensitivity or nonlinear behavior of PG 76-22 was insignificant at 3.2 kPa and at 70°C and 64°C. But, at the same stress levels and at 76°C, PG 76-22 binders started to show nonlinear responses. The stress sensitivity and J_{nr} values of the PMBs also increased with an increase of the testing temperatures in other studies [84, 91, 100].

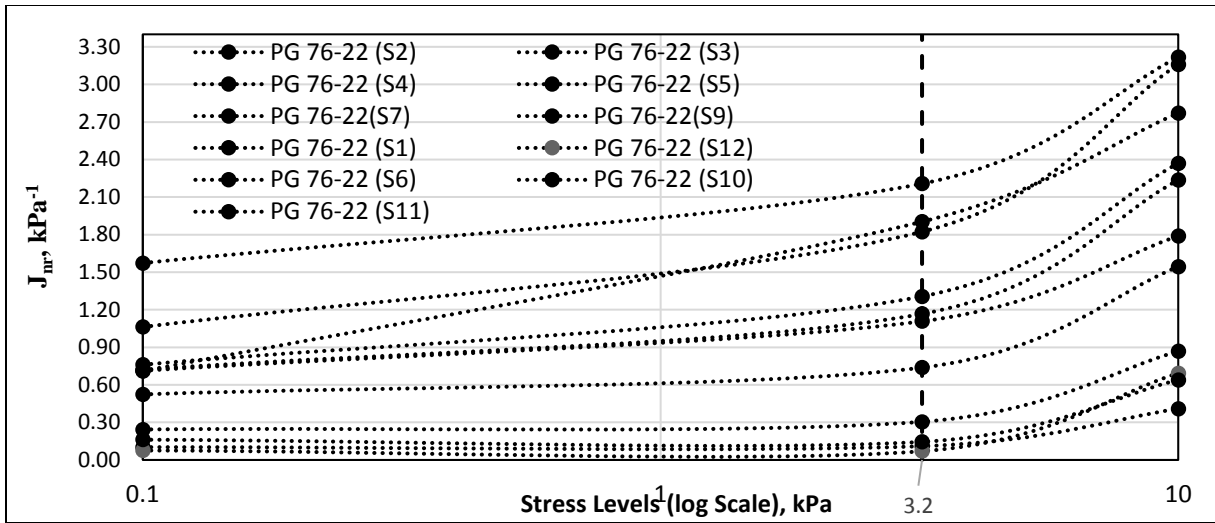
The nonlinear behavior of the binders was more visible at a stress level of 10 kPa. However, the %R values of PG 76-22 from S1 and S11 were nearly zero (Figure 46) at 10 kPa and at 76°C. Hence, at a testing temperature of 76°C, the AHTD can consider a stress level between 3.2 kPa and 10 kPa for measuring the nonlinear properties of SBS-modified PG 76-22 binders.



(a)



(b)



(c)

Figure 47. Change of J_{nr} with stress level for SBS modified PMBs at: (a) 64°C (b) 70°C (c) 76°C

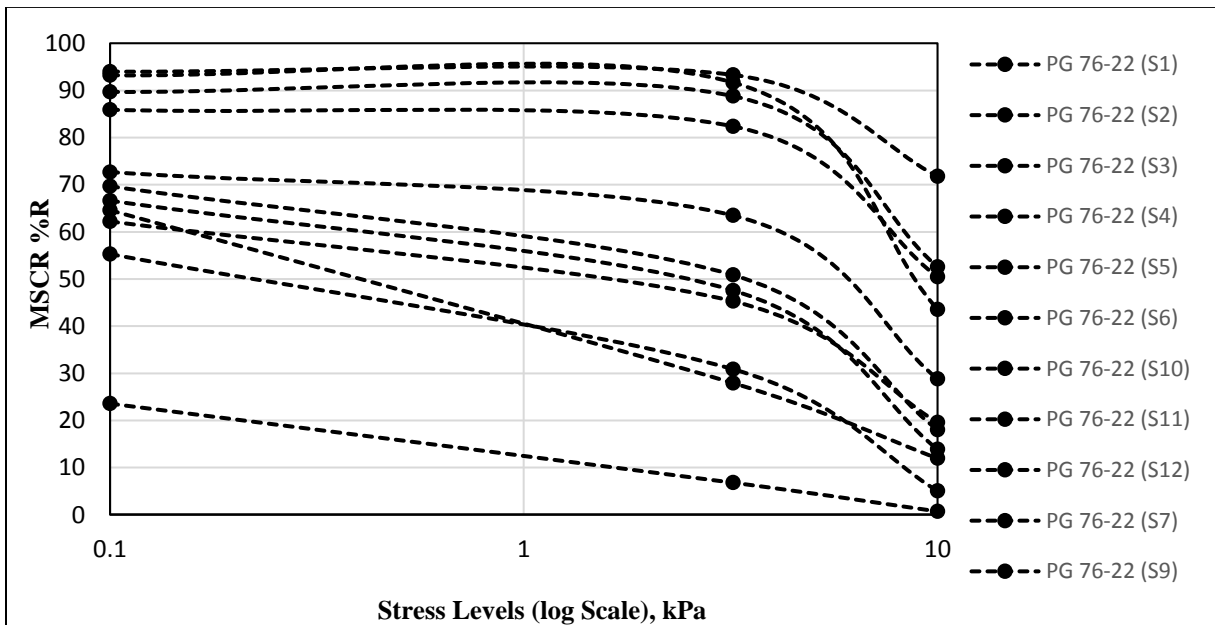


Figure 48. %R vs stress levels of PG 76-22 at 76°C

4.11 EFFECTS OF WMA ADDITIVES

4.11.1 MSCR Database

Based on data presented in Table 16, the addition of Sasobit[®] increased the %R value of the unmodified binders from S1 to S3. All unmodified binders with and without WMA met the stress sensitivity criteria except for the PG 64-22 (from S3) with Sasobit[®]. Like unmodified binders, WMA containing binders showed very negligible amount of %R values at a stress level of 10 kPa. Figures 49 and 50 represent the J_{nr} and %R values of the unmodified and WMA-modified binders. Unlike Sasobit[®], the addition of Advera[®] and Evotherm[®] decreased the rutting resistance of the unmodified binders from S2 and S3. The decreasing trend of %R values with the addition of Advera[®] and Evotherm[®] in binders from S2 and S3 were different from those S1. For binders from S1, %R values increased with the addition of Advera[®] and Evotherm[®]. However, the change of %R values of the Advera[®] modified binders was negligible compared to the unmodified binders (without Advera[®]). Kvasnak et al. [101] found that Evotherm[®] increased the creep compliance values of the WMA compared to the HMA. Kvasnak et al. [101] and Jamshidi et al. [102] also reported that the addition of Sasobit[®] contributed to the increase of the %R, which is an indication of greater rutting resistance for Sasobit[®]-modified binders, compared to unmodified binders. For example, at 3.2 kPa, the addition of Sasobit[®] increased the %R values of the PG 64-22 binders (from S2) from 2.08% to 4.05%, which was about 2 folds of the unmodified binders. On the other hand, at 3.2 kPa, Evotherm[®] decreased the %R values of the PG 64-22 (from S2) binders from 2.08% to 1.15%. It could be mentioned that all unmodified binders with and without WMA additives were tested at 64 °C and this temperature was below the melting point temperature of the Sasobit[®]. Thus, at 64 °C, the effect of the Sasobit[®] was negligible on the viscosity properties of the binders, and Sasobit[®] could have formed a lattice structures in the binder and provided better stability to the binder. Zaumanis et al. [103] also reported that Sasobit[®] made lattice structures into the asphalt binder at service temperatures and increased the rutting performance of the binders in their corresponding study.

4.11.2 Polymer Method

It was observed from Figure 51 that the unmodified binders from all sources were below the polymer curve. A similar kind of scenario was also observed for unmodified binders with WMA additives. The addition of WMA additives did not significantly change the %R values of the unmodified binders at 3.2. Thus, the %R values (at 3.2 kPa) of PG 64-22 binders from S1 to S3 with and without WMA plotted below the polymer curve. Sasobit® containing plastomers is responsible for reducing the viscosity of the binders at working temperatures and it stiffens the binder at the service temperatures [104-105].

Table 16. MSCR database of PG 64-22 with WMA additives at 64°C

Source	WMA additives	% Additives	$J_{nr,0.1}$, kPa	$J_{nr,3.2}$, kPa	J_{nr} diff, (3.2-0.1) %	Stress Sensitivity (Meets AASHTO T	R100, %	R3200, %	Rdiff (0.1-3.2) %	$J_{nr,10}$, kPa	R10000, %	MSCR Grade
S1	N	0	1.86	2.14	14.79	Yes	7.96	1.91	76.04	2.51	-0.16	PG 64S-22
S1	S	1.5	1.26	1.66	31.78	Yes	16.27	3.81	76.58	2.22	0.30	PG 64H-22
S1	A	6	1.54	1.76	14.43	Yes	8.91	2.54	71.54	2.03	0.23	PG 64H-22
S1	E	0.5	1.58	1.84	15.72	Yes	9.43	2.63	72.16	2.18	0.07	PG 64H-22
S2	N	0	2.04	2.31	13.39	Yes	7.27	2.08	71.49	2.67	-0.07	PG 64S-22
S2	S	1.5	1.11	1.44	29.74	Yes	14.62	4.05	72.20	2.00	0.29	PG 64H-22
S2	A	6	1.72	1.93	12.25	Yes	6.56	1.86	71.62	2.20	0.03	PG 64H-22
S2	E	0.5	2.18	2.44	11.65	Yes	5.13	1.15	77.58	2.79	-0.46	PG 64S-22
S3	N	0	1.84	2.12	15.39	Yes	8.16	1.88	77.01	2.44	-0.14	PG 64S-22
S3	S	1.5	0.58	1.08	86.21	No	32.16	6.85	78.67	1.86	0.49	PG 64H-22
S3	A	6	1.77	1.94	9.98	Yes	4.87	1.23	74.83	2.17	-0.17	PG 64H-22
S3	E	0.5	2.22	2.46	10.42	Yes	4.77	0.94	80.24	2.76	-0.54	PG 64S-22

N.B: N-No WMA, S-Sasobit®, A-Advera®, E-Evotherm®

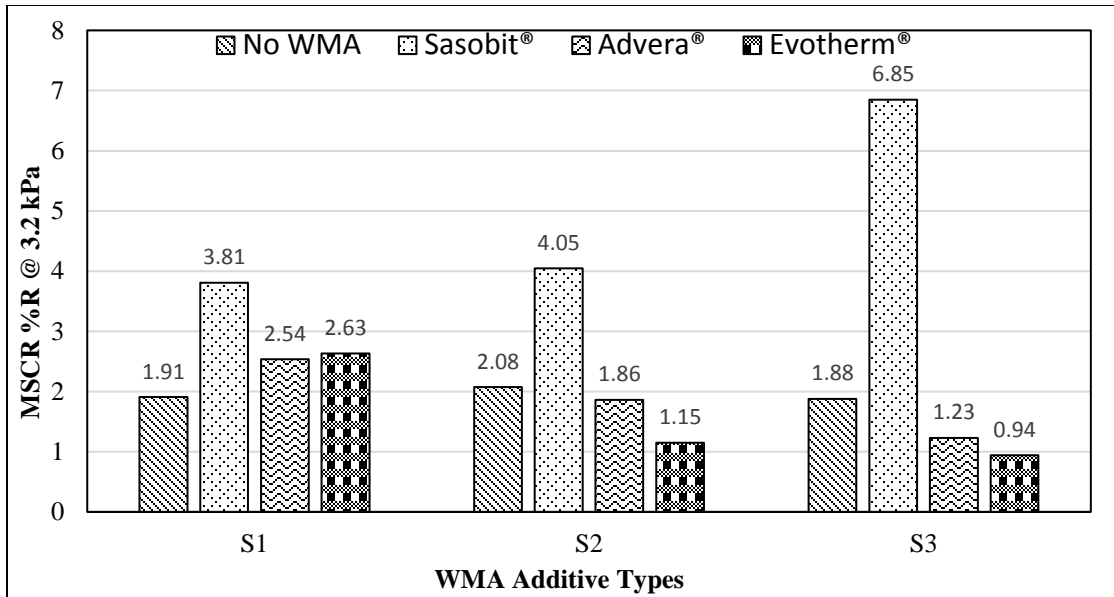


Figure 49. MSCR %R values PG 64-22 with and without WMA additives at 3.2 and 64°C

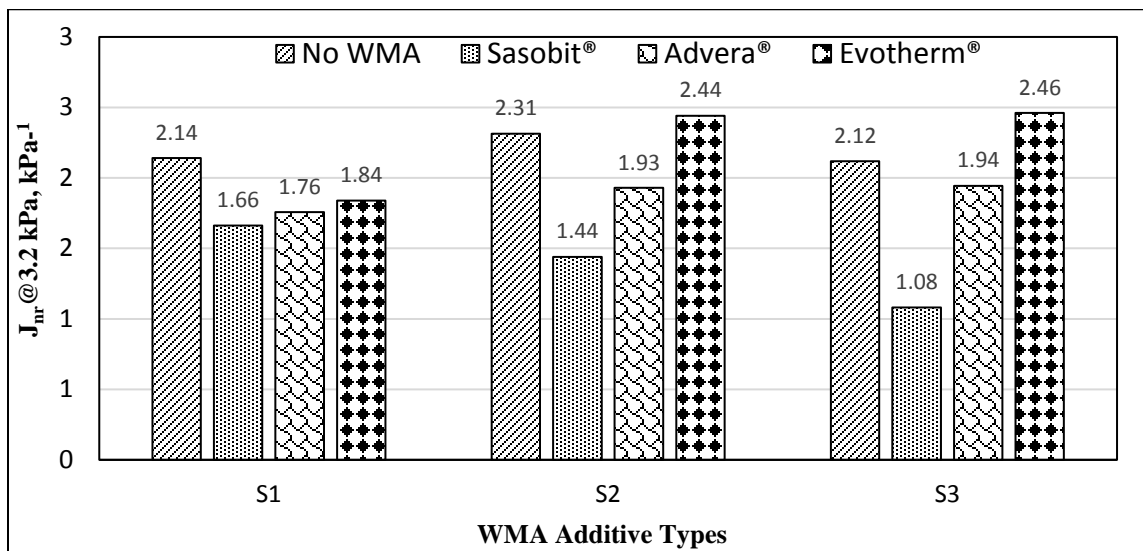


Figure 50. J_{nr} values of PG 64-22 with and without WMA additives at 3.2 and 64°C

Xiao et al. [106] reported that Evotherm® and Advera® containing binders generally showed a similar kind of rutting resistance as those of the control binders. Therefore, on the basis of the findings of the existing literature and current study, it is reasonable for the Evotherm® and Advera® containing unmodified binders to fall below the polymer curve as the unmodified binders also is fell under the polymer curve.

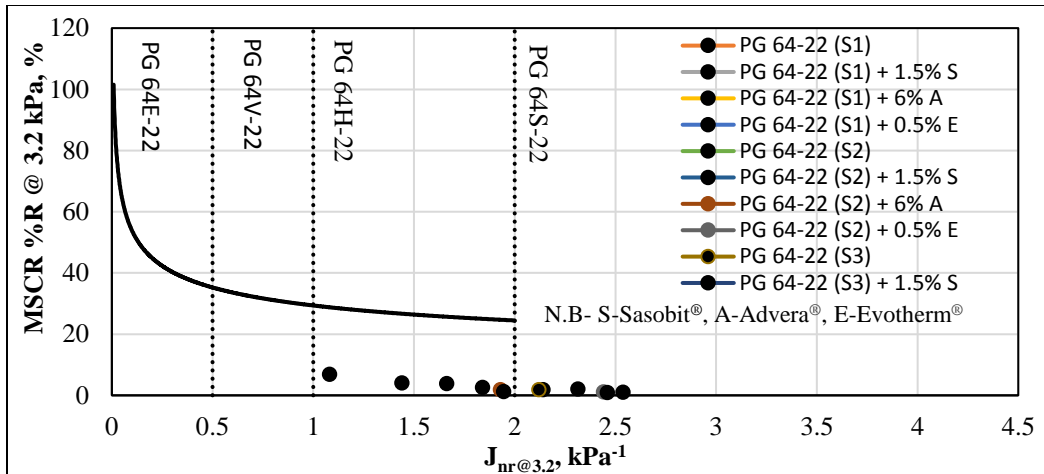


Figure 51. MSCR %Recovery vs. J_{nr} at 3.2 kPa for PG 64-22 with WMA additives at 64°C

4.11.3 Effect of WMA additives on the MSCR Grades

Binders from all three sources modified with Sasobit[®] and Advera[®] showed a better MSCR grade than the neat binder, as reflected by a lower J_{nr} value. For example, the addition of Sasobit[®] and Advera[®] with the PG 64-22 binder from S2 increased the MSCR grade from PG 64S-22 to PG 64H-22, as shown in Table 17. Unlike Sasobit[®] and Advera[®], Evotherm[®] did not change the MSCR grades of the unmodified binders from S2 and S3. For instance, MSCR grades of the PG 64-22 (from S2 and S3) with and without the addition of the Evotherm[®] was PG 64S-22. However, the addition of Evotherm[®] increased the MSCR grade of the PG 64-22 binders from S1.

Table 17. Change of MSCR grade of PG 64-22 with addition of WMA additives

Source	MSCR Grade No WMA Additives	MSCR Grade Sasobit [®]	MSCR Grade Advera [®]	MSCR Grade Evotherm [®]
S1	PG 64S-22	PG 64H-22	PG 64H-22	PG 64H-22
S2	PG 64S-22	PG 64H-22	PG 64H-22	PG 64S-22
S3	PG 64S-22	PG 64H-22	PG 64H-22	PG 64S-22

4.12 EFFECTS OF WMA ADDITIVES ON THE POLYMER MODIFIED BINDERS

4.12.1 MSCR Database

Due to a large amount of data present in the MSCR database of PG 76-22 with WMA, a snapshot of the MSCR database is presented in Table 18. The %R values of PG 70-22 and PG 76-22 binders at 3.2 kPa and at 64°C are shown in Figures 52 and 53, respectively. The MSCR test results of the PG 70-22 from S1 to S3 with and without WMA additives are shown in Table 19. Based on data presented in Tables 18 and 19, all tested binders met the AASHTO M 332 stress sensitivity criteria. For all binders, the difference of J_{nr} values at 0.1 kPa and 3.2 kPa stress was less than 75% of the J_{nr} at 0.1 kPa. Thus, the findings of this study indicate that PMBs with and without WMA additives are not excessively stress sensitive to unexpected heavy loads or unusually high temperatures. Like unmodified binders, the addition of Sasobit® increased the %R and decreased the J_{nr} values of the PG 70-22 and PG 76-22 binders. For example, at 64°C and 3.2 kPa, the addition of Sasobit® increased the %R values of the PG 70-22 (from S1) from 15.78% to 29.51%. The effects of the Advera® and Evotherm® on the %R and J_{nr} values of PG 70-22 binders varied from source to source. At all stress levels and two selected testing temperatures, the addition of Advera® increased the %R values of the PG 70-22 from S1 and decreased the %R values of those binders from different sources (S2 and S3). This kind of trend was also apparent for Evotherm® as well. For instance, Evotherm® increased the %R values of the PG 70-22 from S2 and decreased the %R values of PG 70-22 from S1 and S3. However, the effects of those additives were consistent for PG 76-22 binders at all stress levels and three testing temperatures. The addition of Evotherm® and Advera® decreased the %R and increased the J_{nr} values of PG 76-22 binders from S1 to S3. Thus, the effects of the Evotherm® and Advera® on the %R and J_{nr} values, were consistent with findings for PG 76-22 but inconsistent for PG 64-22 and PG 70-22 binders. Since no chemical tests on the PMBs and WMA, was done in this study, the variation of the effects of WMA additives on the MSCR parameters of the asphalt binders were unknown to the research team. Thus, chemical analyses of these binders are recommended to get a better understandings of WMA-modified binders.

Table 18. MSCR database of PG 70-22 with and without WMA additives

Source	WMA additives	% Additives	Testing Temperature	J _{nr 0.1} , KPa	J _{nr 3.2} , KPa	J _{nr diff} , (3.2-0.1) %	Stress Sensitivity (Meets AASHTO T 332)	R100, %	R3200, %	Rdiff (0.1-3.2) %	J _{nr 10} , KPa	R10000, %	J _{nr diff} , (10-3.2) %	J _{nr diff} , (10-0.1) %	Rdiff (3.2-10) %	Rdiff (0.1-10) %	MSCR GRADE
S1	N	0	64	0.52	0.6	22.1	Yes	40.02	29.5	26.27	0.7	18.80	21.95	48.91	36.29	53.03	PG 64V-22
S1	N	0	70	1.30	1.7	31.3	Yes	30.63	15.7	48.48	2.0	6.22	21.47	59.54	60.56	79.68	PG70H-22
S1	S	1.5	64	0.35	0.4	27.0	Yes	45.62	34.6	24.09	0.6	21.64	44.37	83.39	37.51	52.57	PG 64E-22
S1	S	1.5	70	0.35	0.4	29.7	Yes	34.04	19.3	43.27	1.7	8.04	32.20	71.59	58.36	76.38	PG 70E-22
S1	A	6	64	0.41	0.5	22.1	Yes	40.59	31.2	22.89	0.6	20.90	20.04	45.71	33.23	48.51	PG 64E-22
S1	A	6	70	1.00	1.2	28.3	Yes	31.95	18.4	42.19	1.5	8.48	19.57	53.52	54.05	73.44	PG 70H-
S1	E	0.5	64	0.63	0.7	22.2	Yes	37.06	26.2	29.20	0.9	15.91	21.80	48.91	39.42	57.10	PG 64V-22
S1	E	0.5	64	1.48	1.9	30.2	Yes	28.52	14.0	50.85	2.3	4.86	22.46	59.48	65.36	82.97	PG 70H-
S2	N	0	64	0.54	0.6	24.8	Yes	46.88	37.0	21.03	0.8	24.05	28.60	60.51	35.11	48.73	PG 64V-22
S2	N	0	70	1.25	1.7	39.3	Yes	38.28	22.0	42.37	2.2	8.50	30.47	81.85	61.63	77.83	PG70H-22
S2	N	1.5	64	0.25	0.3	24.4	Yes	56.77	49.0	13.56	0.4	35.15	47.59	83.68	28.37	38.08	PG 64E-22
S2	S	1.5	70	0.71	0.9	35.3	Yes	45.66	31.4	31.03	1.3	16.37	38.66	87.73	48.01	64.14	PG70V-22
S2	S	6	64	0.52	0.6	24.3	Yes	45.74	35.6	22.04	0.8	23.15	24.86	55.29	35.10	49.40	PG 64V-22
S2	A	6	70	1.24	1.6	35.5	Yes	36.49	20.9	42.62	2.1	8.13	24.94	69.41	61.19	77.73	PG 70H-
S2	A	0.5	64	0.49	0.6	24.5	Yes	47.83	38.2	20.10	0.7	25.35	28.49	59.98	33.66	46.99	PG 64V-22
S2	E	0.5	70	1.15	1.6	38.4	Yes	38.83	23.0	40.66	2.1	9.42	31.60	82.23	59.12	75.74	PG 70H-
S3	E	0	64	0.61	0.7	30.5	Yes	42.29	28.1	33.52	1.0	12.94	30.35	70.19	53.97	69.40	PG 64V-22
S3	N	0	70	1.43	2.0	42.2	Yes	32.87	13.7	58.22	2.6	3.24	30.18	85.12	76.43	90.15	PG70S-22
S3	N	1.5	64	0.46	0.6	40.1	Yes	46.22	30.2	34.60	0.9	13.11	55.79	118.32	56.62	71.63	PG 64V-22
S3	N	1.5	70	1.38	1.9	44.4	Yes	33.84	13.6	59.55	2.7	3.07	38.46	99.95	77.55	90.92	PG 70H-
S3	S	6	64	0.69	0.9	31.1	Yes	38.82	23.9	38.38	1.1	10.69	24.84	63.66	55.38	72.49	PG 64V-22
S3	S	6	70	1.64	2.2	39.4	Yes	29.51	11.0	62.59	2.8	2.55	22.99	71.54	76.99	91.38	PG 70S-22
S3	A	0.5	64	0.92	1.2	33.3	Yes	35.38	19.5	44.76	1.5	7.43	26.88	69.20	61.98	78.99	PG 64H-
S3	A	0.5	70	2.12	3.0	41.4	Yes	26.32	8.02	69.51	3.7	1.01	25.83	78.00	87.45	96.17	PG 70S-22

N.B: N-No WMA, S-Sasobit®, A-Advera®, E-Evotherm®

Table 19. MSCR database of PG 76-22 with and without WMA additives

	WMA additives	% Additives	Testing Temperature	J _{nr 0.1} , KPa	J _{nr 3.2} , KPa	J _{nr diff} , (3.2-0.1) %	Stress Sensitivity (Meets AASHTO T 332)	R100, %	R3200, %	R _{diff} (0.1-3.2) %	J _{nr 10} , KPa	R10000, %	J _{nr diff} , (10-3.2) %	J _{nr diff} , (10-0.1) %	R _{diff} (3.2-10) %	R _{diff} (0.1-10) %	MSCR GRADE
S1	N	0	64	0.27	0.32	20.10	Yes	41.07	30.63	25.43	0.44	15.25	37.24	64.83	50.20	62.86	PG 64E-22
S1	N	0	70	0.66	0.88	32.35	Yes	32.01	16.28	49.13	1.23	5.84	38.99	83.96	64.12	81.75	PG 70V-22
S1	N	0	76	1.57	2.21	40.35	Yes	23.57	6.81	71.09	3.22	0.72	45.75	104.58	89.48	96.96	PG 76S-22
S1	S	1.5	64	0.16	0.21	31.54	Yes	49.34	37.88	23.30	0.31	21.03	50.68	98.22	44.58	57.45	PG 64E-22
S1	S	1.5	70	0.46	0.63	38.33	Yes	38.32	21.56	43.86	0.97	8.62	52.64	111.15	60.15	77.59	PG 70V-22
S1	S	1.5	76	1.20	1.77	47.88	Yes	28.05	9.43	66.49	2.78	1.77	56.42	131.31	81.58	93.76	PG 76H-22
S1	A	6	64	0.64	0.75	16.88	Yes	18.14	11.61	35.99	0.85	5.90	13.55	32.68	49.19	67.49	PG 64V-22
S1	A	6	70	1.62	1.87	15.55	Yes	22.17	4.54	69.66	2.16	1.45	15.10	32.99	68.09	90.50	PG 70H-22
S1	A	6	76	3.73	4.35	16.55	Yes	6.39	1.02	83.94	5.10	-1.10	17.04	36.42	210.10	117.28	PG 76S-22
S1	E	0.5	64	0.90	1.03	14.32	Yes	15.70	8.35	46.84	1.20	3.26	16.79	33.53	60.94	79.24	PG 64H-22
S1	E	0.5	70	2.18	2.55	16.74	Yes	9.46	2.67	71.75	3.03	-0.08	18.81	38.70	103.03	100.86	PG 70S-22
S1	E	0.5	76	4.90	5.75	16.99	Yes	4.89	-0.29	105.85	7.02	-2.35	22.19	42.96	-720.85	148.22	NA
S2	N	0	64	0.14	0.15	5.68	Yes	75.85	74.75	1.46	0.20	66.33	30.98	38.44	11.28	12.57	PG 64E-22
S2	N	0	70	0.31	0.39	25.48	Yes	70.75	64.29	9.14	0.62	44.28	57.94	98.21	31.15	37.43	PG 70E-22
S2	N	0	76	0.71	1.11	55.38	Yes	62.21	45.29	27.20	1.79	19.57	61.35	150.75	56.83	68.55	PG 76H-22
S2	S	1.5	64	0.08	0.09	12.49	Yes	79.94	78.59	1.68	0.11	74.00	24.87	40.48	5.85	7.43	PG 64E-22
S2	S	1.5	70	0.20	0.24	20.27	Yes	74.72	70.42	5.75	0.40	53.01	63.76	96.96	24.73	29.06	PG 70E-22
S2	S	1.5	76	0.50	0.75	51.58	Yes	66.51	52.29	21.39	1.27	26.54	68.91	156.05	49.25	60.10	PG 76V-22
S2	A	6	64	0.15	0.15	3.52	Yes	73.79	72.98	1.11	0.20	64.03	28.99	33.53	12.27	13.24	PG 64E-22
S2	A	6	70	0.33	0.41	24.21	Yes	68.07	61.10	10.25	0.61	41.44	48.72	84.72	32.18	39.13	PG 70E-22
S2	A	6	76	0.78	1.18	51.23	Yes	58.67	41.06	30.02	1.75	17.30	48.19	124.11	57.88	70.53	PG 76H-22
S2	E	0.5	64	0.17	0.18	6.14	Yes	73.27	71.97	1.76	0.25	61.53	36.14	44.49	14.51	16.02	PG 64E-22
S2	E	0.5	70	0.39	0.50	29.47	Yes	67.25	59.11	12.11	0.78	38.09	55.03	100.72	35.56	43.36	PG 70E-22
S2	E	0.5	76	0.92	1.45	58.07	Yes	57.63	38.45	33.27	2.27	13.73	56.76	147.78	64.29	76.17	PG 76H-22

N.B: N-No WMA, S-Sasobit®, A-Advera®, E-Evotharm®

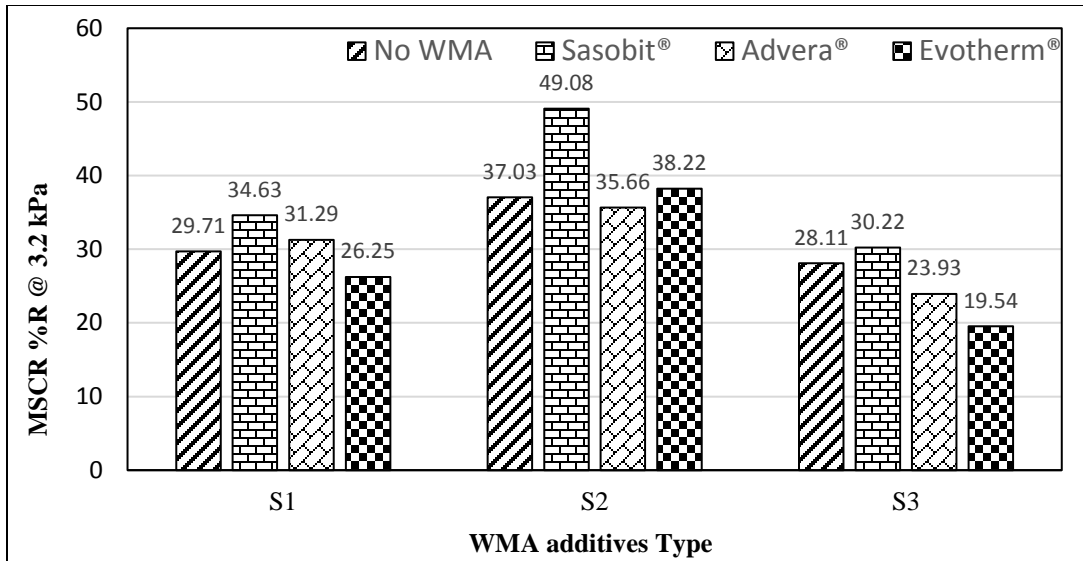


Figure 52. MSCR %R values PG 70-22 with and without WMA additives at 3.2 kPa and 64°C

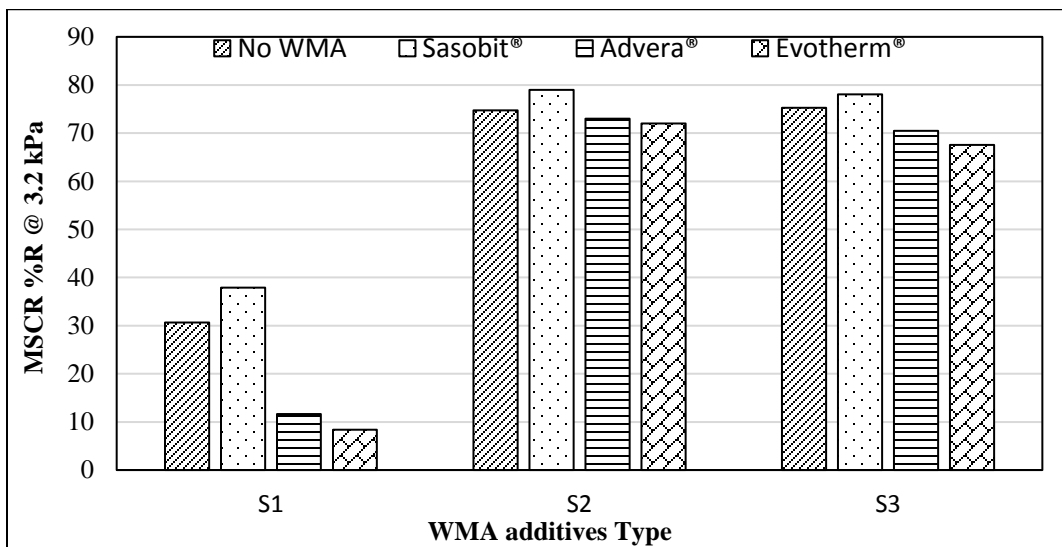


Figure 53. MSCR %R values PG 76-22 with and without WMA additives at 3.2 kPa and 64°C

4.12.2 Polymer Method

From Figures 54 and 55, it is evident that the locations of the PMBs in the polymer curve did not change with the addition of the WMA additives. Earlier it was mentioned

that Evotherm[®] and Advera[®] reduced the %R values, and Sasobit[®] increased the %R values of the PMBs. However, the changes of %R value at 3.2 kPa of PMBs with the addition of Advera[®] or Evotherm[®] was negligible, which was reflected on the polymer curve as well as of the binders MSCR grades. For instance, PG 76-22 binders from S2 with and without the addition of the WMA additives were above the polymer curve. A similar type of trend was also observed for the Sasobit[®]-modified binders.

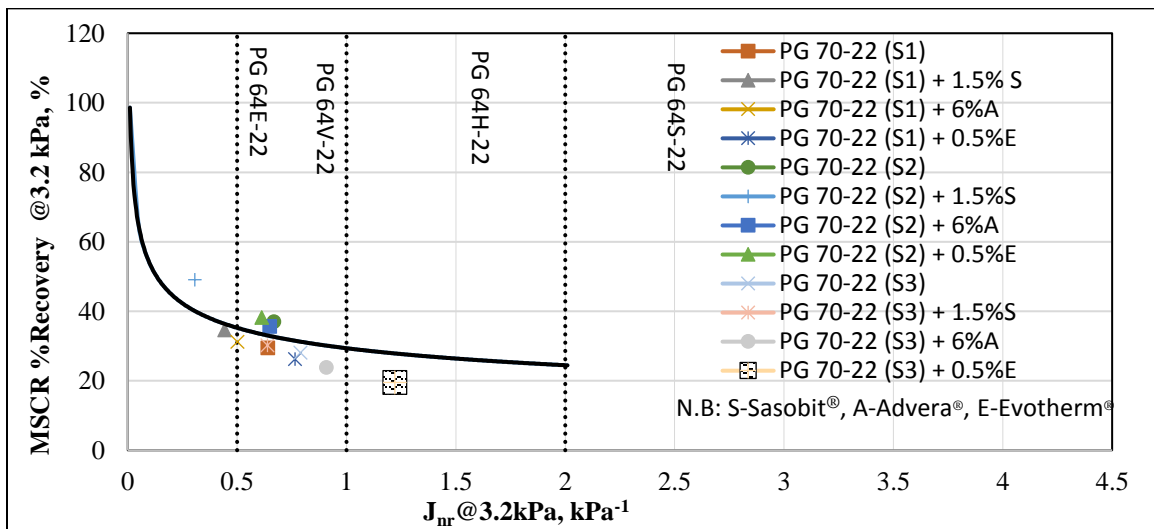


Figure 54. MSCR %R vs. J_{nr} @ 3.2 kPa for PG 70-22 at 64°C

4.12.3 Effect of WMA additives on the PMBs of MSCR Grades

The MSCR grades of the asphalt binders have been evaluated based on the J_{nr} values at 3.2 kPa. As described earlier, the effect of the Evotherm[®] and Advera[®] on the MSCR %R and J_{nr} was consistent for PG 76-22 and but the inconsistent for PG 64-22 and PG 70-22 binders. This kind of trend was also observed for MSCR grading. At all testing temperatures, the addition of Sasobit[®] either increased or did not change the MSCR grades of the PMBs as shown in Tables 20 and 21.

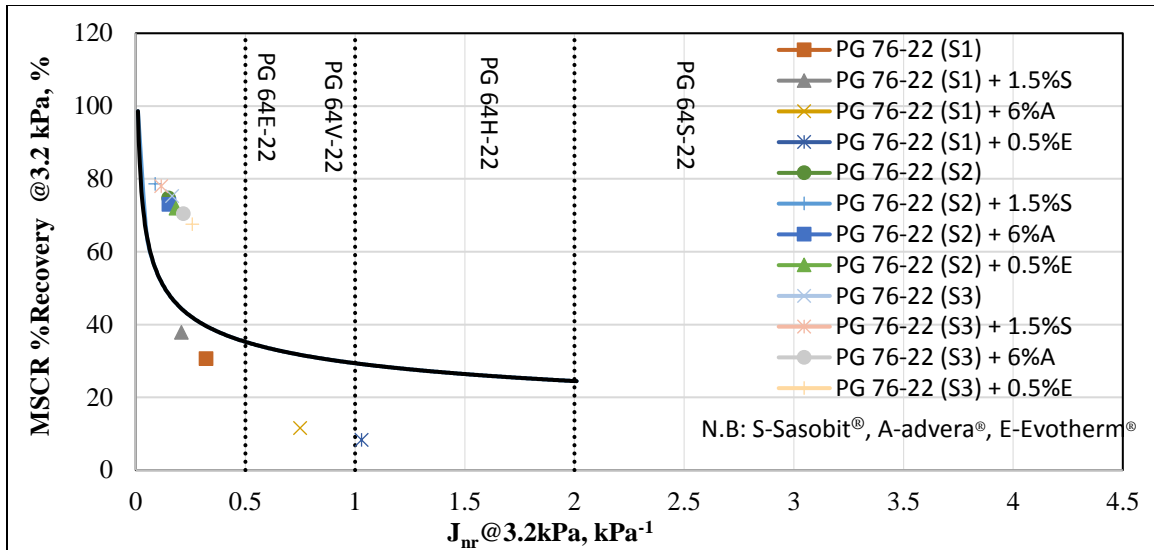


Figure 55. MSCR %R vs. J_{nr} @ 3.2 kPa for PG 76-22 With and Without WMA Additives at 64°C

Table 20. Change of MSCR grading of PG 70-22 with WMA additives

Source	MSCR Grade at 64°C N	MSCR Grade at 64°C S	MSCR Grade at 64°C A	MSCR Grade at 64°C E	MSCR Grade at 70°C N	MSCR Grade at 70°C S	MSCR Grade at 70°C A	MSCR Grade at 70°C E
S1	PG 64V-22	PG 64E-22	PG 64E-22	PG 64V-22	PG 70H-22	PG 70E-22	PG 70H-22	PG 70H-22
S2	PG 64V-22	PG 64E-22	PG 64V-22	PG 64V-22	PG 70H-22	PG 70V-22	PG 70H-22	PG 70H-22
S3	PG 64V-22	PG 64V-22	PG 64V-22	PG 64H-22	PG 70S-22	PG 64H-22	PG 70V-22	PG 70S-22

N.B: S- Sasobit®, A-Advera®, E-Evotherrm®, N-No WMA additives

Table 21. Change of MSCR grading of PG 76-22 with WMA additives

Source	MSCR Grade at 64°C N	MSCR Grade at 64°C S	MSCR Grade at 64°C A	MSCR Grade at 64°C E	MSCR Grade at 70°C N	MSCR Grade at 70°C S	MSCR Grade at 70°C A	MSCR Grade at 70°C E	MSCR Grade at 76°C N	MSCR Grade at 76°C S	MSCR Grade at 76°C A	MSCR Grade at 76°C E
S1	PG 64E-22	PG 64E-22	PG 64V-22	PG 64H-22	PG 70V-22	PG 70V-22	PG 70H-22	PG 70S-22	PG 76H-22	PG 76V-22	PG 76H-22	PG 76H-22
S2	PG 64E-22	PG 64E-22	PG 64E-22	PG 64E-22	PG 70E-22	PG 70E-22	PG 70E-22	PG 70E-22	PG 76S-22	PG 76H-22	PG 76S-22	NA
S3	PG 64E-22	PG 64E-22	PG 64E-22	PG 64E-22	PG 70E-22	PG 70E-22	PG 70V-22	PG 70V-22	PG 76H-22	PG 76V-22	PG 76H-22	PG 76H-22

N.B: S-Sasobit®, A-Advera®, E-Evotherm®, N-No WMA additives

4.13 EFFECTS OF RAP

4.13.1 MSCR Database

Table 22 presents the MSCR database of the RAP modified binders. From the viscosity and DSR tests, it was expected that RAP modified binders will show higher %R and lower J_{nr} values compare to the control binders. This expectation was met for binders containing RAP, as shown in Table 22. An addition of RAP with the control binder increased the %R values of the modified binders. Previously it was mentioned that recovered RAP binders were from pavements of about 13 years old from I-40. Thus, RAP 1 and RAP 2 showed lower J_{nr} and higher %R values compare to the control binder. For instance, at 64°C and 3.2 kPa, the %R values of PG 64-22 from S1 (control binders) increased from 1.91% to 45.68% due to the addition of 60% RAP1. Among the two RAP sources, RAP2 binder showed the higher %R values and lower J_{nr} values at all testing temperatures and stress levels. For example, at 64°C and 3.2 kPa, the %R values of 60% RAP1 and 60% RAP2 modified binders were 45.68% and 49.52%, respectively. It can be noted that the mix design sheet of aforementioned pavement sections were not available to the research team. Thus, the properties of the original binders used in the pavements of these RAPs were unknown to the research team.

Table 22. MSCR database of RAP modified binders (Binder Type: PG 64-22 from S1)

RAP Source	RAP (%)	Testing Temperature	$J_{nr,0.1}$, kPa	$J_{nr,3.2}$, kPa	$J_{nr,diff}$ (3.2-0.1) %	Stress Sensitivity (Meets AASHTO)	R100, %	R3200, %	R_{diff} (0.1-3.2) %	MSCR GRADE
No	0	64	1.87	2.14	14.79	Yes	7.96	1.91	76.04	PG 64S-22
RAP1	25	64	0.89	1.04	16.32	Yes	17.4	8.22	52.83	PG 64H-XX
RAP1	40	64	0.47	0.55	16.12	Yes	27.14	17.81	34.38	PG 64V-XX
RAP1	40	70	1.18	1.44	22.41	Yes	18.47	7.06	61.78	PG 70V-XX
RAP1	40	76	2.82	3.53	25.27	Yes	11.33	1.84	83.74	PG 76S-XX
RAP1	60	64	0.1	0.11	10	Yes	49.26	45.68	7.27	PG 64E-XX
RAP1	60	70	0.28	0.33	15.83	Yes	39.6	31.17	21.32	PG 70E-XX
RAP1	60	76	0.69	0.87	26.22	Yes	30.57	17.06	44.2	PG 76V-XX
RAP2	25	64	0.47	0.53	12.54	Yes	23.79	16.16	32.06	PG 64V-XX
RAP2	40	64	0.19	0.21	10.52	Yes	37.26	32.14	13.74	PG 64E-XX
RAP2	40	70	0.48	0.57	16.86	Yes	27.98	18.22	34.88	PG 70V-XX
RAP2	40	76	1.17	1.46	24.59	Yes	19.33	7.11	63.26	PG 76H-XX
RAP2	60	64	0.05	0.09	100	No	54.52	49.52	9.17	PG 64E-XX
RAP2	60	70	0.14	0.15	8.13	Yes	46.41	42.05	9.4	PG 70E-XX
RAP2	60	76	0.34	0.4	17.1	Yes	37.14	27.51	25.93	PG 76E-XX

4.13.2 Polymer Method

The %R value of RAP modified binders at 64°C were calculated by using Equation 1 for investigating the polymers. Figure 55 shows the %R value at $J_{nr,3.2 kPa}$ for RAP modified binders. Like the unmodified binders all percentages of RAP modified binders were scattered below the polymer curve. As previously mentioned, if a binder plotted above the polymer curve then it has polymers. This statements is true for RAP modified binders if the RAP binders contain plastomers, as plastomers increase the toughness. The research team could not make any conclusive remarks, why the RAP modified

binders were scattered under the polymer curve, as the mix design properties of the pavement sections (where from RAP1 and RAP2 were collected) was unknown. However, such behavior could be due to two possible reasons: (1) The polymers used in the original binders of these pavements degraded their quality due to the exposure of heat and other environmental conditions for a long time, and (2) Since traces of the solvents (nPB) used in the recovery process may have been entrapped in the binder that makes the binders soft. Similar observations were made by other researchers [e.g., 84]

4.13.3 Effect of the RAP on the Unmodified Binders of MSCR Grades

All RAP modified binders were graded on the basis of $J_{nr,3.2kPa}$ at 64°C, 70°C, and 76°C. Table 22 provides a summary of the test results obtained for RAP modified binders. The MSCR grade of the control binder (PG 64-22 from S1) was PG 64S-22 at 64°C. The MSCR grades of the binders with 25% RAP1 and 25% RAP2 were PG 64H-XX and PG 64V-XX, respectively, which indicate that an addition of RAP could increase the MSCR grade of the unmodified binder. Previous studies [e.g., 106-108] also reported that higher percentages (greater than 20%) of RAP increased the rutting resistance and stiffness of the asphalt mix. The MSCR grades of 40% RAP2 modified binders at 64°C, 70°C, and 76°C were PG 64E-XX, PG 70V-XX, and PG76H-XX, respectively. At the same testing temperatures and with 40% RAP1, the MSCR grades were different from those of RAP2. Regardless of the RAP source, the performance of RAP modified binders were superior to PG 64-22 binders. A high percentage of RAP with the virgin binder will reduce the overall cost of the project. However, 60% of RAP2 modified binders did not meet the viscosity requirement set by AASHTO T 316. So, based on this study, the research team recommended that AHTD can increase the current limit of the RAP binder up to 40%. In this study, research team did not investigate the performance of PMBs modified with RAP.

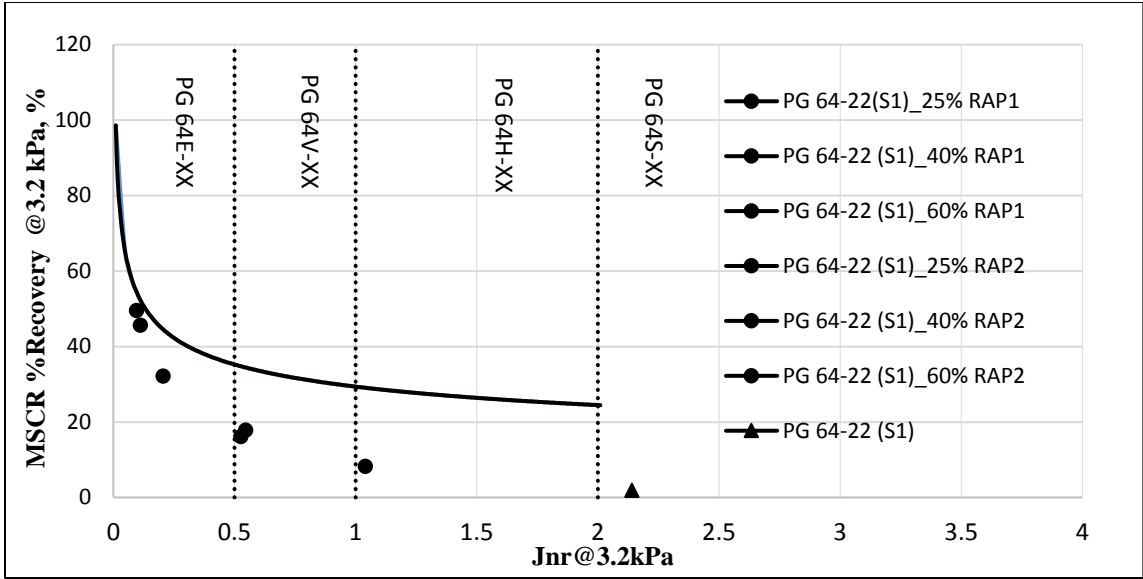


Figure 56. MSCR %R vs. Jnr @ 3.2 kPa for RAP modified binders at 64°C

THIS PAGE IS INTENTIONALLY BLANK

CHAPTER 5

PART TWO LITERATURE REVIEW

5.1 RHEOLOGICAL AND MECHANICAL PROPERTIES OF POLYMER-MODIFIED BINDERS

Over the past three decades, the asphalt industry has used asphalt binder modification with polymers as an effective tool for producing mixes with better performance and improved service life. Continuously increasing traffic and axle load in recent years have led to the search for new types of asphalt binders with better performance [109-112]. For this reason, researchers have started to evaluate, develop and use a wide range of modifiers to improve characteristics of asphalt binders and enhance performance of asphalt pavements [111-113].

Several studies have been conducted to characterize the viscoelastic properties and to evaluate performance of polymer-modified asphalt binders [114-116]. Plastics, elastomers, fibers and additives are the four major groups of polymer used for the modification of asphalt binders. In general, elastomers (75%) are known to be the most popular modifiers followed by plastomers (15%). Rubber, fibers and other polymer products are also used for asphalt binder modification, but to a limited degree [117].

Asphalt binder consists of three major fractions, namely asphaltenes, resins, and oils. According to Airey [118], some portions of maltenes (consisting of resins and oils) can be absorbed by the polymer during mixing and experience swelling. Due to the chemical dissimilarities of the binder and polymer, a two-phase structure (a “polymer-rich phase” and an “asphaltene-rich phase”) can be observed in the blended binder at service temperature. The polymer-rich phase contains all of the polymers added to the binder, while the “asphaltene-rich phase” contains all of the heavy fractions (i.e., asphaltenes). However, these two phases can exhibit properties that are different from those of the base binder. Performance of blended binders is reported to be affected by the distribution, continuity and homogeneity of these phases. According to Airey [118] and Elseifi et al. [119], at sufficient high polymer concentrations, a continuous polymer-rich

phase can be developed that would dominate performance of the binder. A dominating polymer-rich phase can make a binder soft, flexible, and elastic, whereas the asphaltene-rich phase can make it hard, brittle, and inelastic. Figure 57 shows a schematic of the colloidal structure of the binder and the effect of polymer modification.

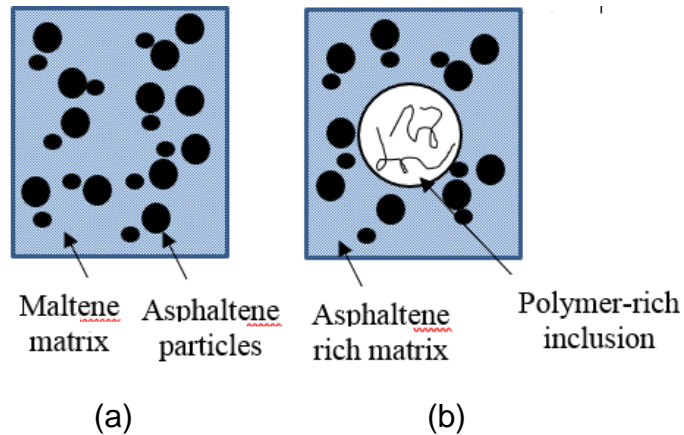


Figure 57. Schematic of the colloidal structure of binder and the effect of polymer modification: (a) base binder; (b) polymer-modified binder [120]

Airey [121] evaluated the effects of binder source, polymer content, binder–polymer compatibility and aging on the rheological properties of the polymer-modified binders. Significant improvements in the rheological properties of binders were observed due to SBS polymer modification from the penetration, softening point, elastic recovery and DSR test results. It was also reported that the nature of the network established within the binder due to polymer modification depends on the nature of the base binder, the nature and content of the polymer and the binder-polymer compatibility. Furthermore, the binder with a high polymer content was observed to exhibit a more viscous behavior than the elastic response after oxidative aging.

Several studies have been conducted to determine the effect of modifiers on the rheological properties of asphalt binders and asphalt mixes [122, 123]. It has been observed that addition of polymers to asphalt binders helps mitigate major pavement distresses such as rutting at high temperature, low-temperature cracking, and fatigue cracking [124].

The effects of aging and polymer content on the performance of the binders were investigated by Elseifi et al. [119]. The rheological and physical changes associated with the modification of two elastomeric polymers, namely SBS linear block copolymers and Styrene Ethylene Butylene Styrene (SEBS) linear block copolymers, were analyzed. The dynamic mechanical tests were performed using a DSR apparatus at temperatures ranging from 5° to 75 °C. The binders modified with both SBS and SBES were found to exhibit an increase in the rutting resistance at service temperatures above 45 °C. A significant improvement in the fatigue resistance was observed for SBS-modified binders at intermediate service temperatures. The low-temperature performance grade was found to remain unchanged after binder modification.

Kumar et al. [125] studied the effect of addition of Crumb Rubber (CR), Ethylene Vinyl Acetate (EVA) and SBS modifiers to neat binder on its aging, temperature susceptibility and fatigue life. It was observed that the temperature susceptibility of the binder decreased as the modifier content increased. A SBS-modified binder was found to exhibit a lower viscosity temperature susceptibility than EVA- and CR-modified binders. The EVA-modified binder was observed to show a higher rutting resistance value than SBS- and CR-modified binders, while adding each of the modifiers in the same amount. In addition, the SBS-modified binder exhibited maximum elastic recovery than the CR- and EVA-modified binders. The results of the Tensile Strength Ratio (TSR) of asphalt mixes showed that the asphalt mix containing EVA was more resistant to moisture-induced damage than any other modified binders. From wheel-tracking test results, the EVA- and SBS-modified asphalt mixes were found to exhibit a better resistance to rutting than mixes containing neat binder.

The high-temperature rheological properties of SBS-, oxidized polyethylene-, propylene-maleic anhydride-, and recycled crumb rubber-modified binders with and without PPA were investigated by Xiao et al. [126]. It was observed that the rubber-modified binder containing PPA showed greater viscosity than the binders modified using other compounds. The polymer-modified binders produced with oxidized polyethylene and propylene-maleic anhydride was found to exhibit the potential of reducing the energy

demand during mixing and compaction of the mixes. The failure temperature and $|G^*|/\sin\delta$ of tested polymer-modified binders were found to be dependent on the binder source. Furthermore, from the phase angle results it was found that the polymer type had a significant effect on the viscoelastic characteristics of the modified binders. Moreover, the results of viscometry, amplitude sweep, frequency sweep, creep and creep recovery, and relaxation spectrums of polymer-modified binders were found to get affected by polymer types, asphalt sources, and test temperatures.

Rahi et al. [127] evaluated the effectiveness of the Styrene-ethylene/propylene-styrene (SEPS) modification of asphalt binders with respect to two different specification parameters, namely the $|G^*|/\sin\delta$ and the Zero Shear Viscosity (ZSV). The frequency sweep test was conducted at 40°, 50°, and 60 °C under controlled-strain conditions at frequencies between 0.1 and 100 Hz to determine the high-temperature characteristics of the asphalt binders. The results of the $|G^*|/\sin\delta$ and ZSV indicated that the rutting resistance of the asphalt binders increased constantly with an increase in SEPS concentration in asphalt binder.

5.2 RHEOLOGICAL AND MECHANICAL PROPERTIES OF RAP BINDER BLENDS

The use of RAP has become an important part of the pavement construction practice in recent years due to environmental concerns, scarcity of high-quality aggregates and increased cost of virgin asphalt binder. The Annual Asphalt Pavement Industry Survey (2013) reported a significant growth in the use of RAP from 2009 to 2012. It was also reported that the asphalt industry remained the country's number-one recycler by reusing RAP at a rate of over 99 percent. More than 98 percent contractors were reported to use RAP in 2012. The amount of RAP used in asphalt mixes increased from 56 million tons in 2009 to 68.3 million tons in 2012. Approximately, 3.4 million tons of asphalt binder was conserved during 2012. The amount of savings in asphalt binder was estimated to worth over \$2 billion [128]. As the use of RAP is increasing rapidly, it is important to evaluate the performance of asphalt mixes containing RAP.

A number of studies have been conducted to evaluate performance of asphalt binders with the addition of different amounts of RAP binder [129-132]. The high-temperature PG grades of the RAP binder blends were observed to increase or remain unchanged compared to that of the neat binder. However, the low-temperature PG grades of the RAP binder blends were found to remain the same or increase maximum by one grade compared to the unmodified binder [129].

Kim et al. [130] investigated the rutting and fatigue performances of RAP binder- and SBS-modified binders. The rutting and fatigue parameters were found to increase with an increase in the amount of RAP binder. The indirect tensile strength of asphalt mixes containing RAP was also found to increase with an increase in RAP content. All mixes containing RAP showed relatively low creep compliance values. It was also reported that a mix containing RAP and SBS polymer may lead to a better resistance to fatigue cracking.

Colbert and You [131] studied the performance of the RAP binder blends using Superpave® binder characterization tests. Effects of short-term and long-term aging on the binders' viscosity and stiffness were evaluated. A PG 58-28 binder was used as the neat binder to blend with different amounts of RAP binder, namely 50%, 70% and 100% by weight of the binder. It was found from the Rotational Viscosity (RV) test results that the workability and pumping potential of the RAP binder blends reduced as the amount of RAP binder increased. Low-temperature frequency sweep tests were conducted at six different frequencies: 0.01, 0.1, 1, 5, 10, and 25 Hz at reference temperatures of 13°, 28°, 40°, 58° and 70 °C to develop shear modulus master curves for the RAP binder blends. The results showed that the shear modulus of the binder blends increased with an increase in RAP binder in the blend. The shear moduli of the blended binders were observed to remain unchanged as the amount of RAP binder increased from 50% to 70%. Also, the shear moduli of the blended binders were found to increase significantly due to RTFO- and PAV-aging.

The rutting susceptibility of asphalt binders and asphalt mixes containing different polymer modifiers and RAP binder from different sources was evaluated by Bernier et al. [132]. The rutting resistance of the asphalt mixes was determined from Asphalt Pavement Analyzer (APA) testing and was compared with the binder performance measured using MSCR and frequency sweep tests. The Fourier Transform Infrared Spectroscopy (FTIR) tests were also conducted to determine oxidation levels of different RAP binders. It was found that the binder from a basalt RAP source exhibited significantly higher $|G^*|$ values than any other binders at low frequencies. It was also observed that the addition of 10% RAP binder exhibited greater rutting resistance than other binder blends.

5.3 ASPHALT MIXES WITH HIGH AMOUNTS OF RAP

In view of the benefits associated with incorporating RAP in asphalt mixes, the paving industry is in favor of using higher amounts of RAP in asphalt pavement construction. However, concerns of state DOTs over the long-term effects of using high amounts of RAP on the performance of asphalt pavements have limited its use [129, 133-135]. These concerns are mainly due to the lack of enough mechanistic performance data and proper specifications for mixes containing RAP [133]. The Oklahoma Department of Transportation (ODOT) specifications limit the maximum amount of binder replacement by RAP or Recycled Asphalt Shingles (RAS) for surface courses and other Superpave[®] mixes as 12% and 30%, respectively [136].

West et al. [137] evaluated the performance of asphalt mixes containing moderate (i.e., 20%) and high (i.e., 45%) amounts of RAP under accelerated loading and determined the applicability of laboratory tests to predict field performance of asphalt mixes containing RAP. Test sections were constructed at the National Center for Asphalt Technology (NCAT) test track using a 50-mm thick surface course mix. The test sections constructed using asphalt mixes containing RAP were found to perform well for rutting under heavy loading conditions. It was also concluded from the indirect tensile strength test results that the use of RAP improved the tensile strength of asphalt mixes.

A New Hampshire Department of Transportation (NHDOT) study examined the effect of high percentages of RAP binder on the properties of the binder blends. Tests were conducted on asphalt binders extracted from 28 different asphalt mixes to determine their PG grades and critical cracking temperatures. The high- and low-temperature PG grades were observed to remain the same or increase by only one PG grade with the addition of different amounts of RAP binder. It was also observed that the high temperature PG grades for several RAP binder blends exhibited a grade bump with the addition of 20% RAP binder. The change in the failure temperature with respect to the percent binder replacement was found to decrease as the amount of RAP binder increased in the RAP binder blends [129].

Another study conducted by Hong et al. [128] evaluated the long-term performance of Hot Mix Asphalt (HMA) containing high percentages of RAP. For this purpose, FHWA's Long-Term Pavement Performance (LTPP) test sections in Texas were investigated for transverse cracking, rut depth and ride quality over sixteen years. With regards to transverse cracking, it was observed that, using 35% RAP in the HMA led to faster pavement deterioration than that with only virgin materials. Also, the asphalt mix with 3% latex-modified binder was found to exhibit less transverse cracks than asphalt mixes containing RAP. However, the asphalt mixes with 35% RAP were found to be more rut resistant than the asphalt mixes with virgin binders. Furthermore, the addition of RAP to the asphalt mixes was found to have no significant effect on the ride quality. It was reported that the pavement with high RAP content (e.g., 35%) are expected to perform well during its life span.

Ghabchi et al. [139] evaluated the effect of addition of different amounts of RAP binder to virgin binders on the moisture-induced damage potential of the asphalt mixes using the Surface Free Energy (SFE) approach. For this purpose, two binders (a PG 64-22 and a PG 76-28) were blended with different amounts of RAP binder (0%, 10%, 25% and 40%). A Dynamic Contact Angle (DCA) analyzer was used to determine the SFE components (non-polar, acid and base) of the binder blends. It was found that, for both the binders, the addition of RAP binder increased the acid SFE components of the RAP

binder blends, while the base SFE components remained almost unchanged. Also, the wettability, work of adhesion, work of debonding and energy parameters of the RAP binder blends with six different types of aggregates were evaluated in that study. The wettability and the work of adhesion of the RAP binder blends over the aggregates were found to increase with an increase in the amount of RAP binder. However, the blending of RAP binder with the PG 64-22 binder was found to result in a higher work of adhesion. Evaluating the energy parameters of the asphalt aggregate system, it was observed that the moisture-induced damage potential of the both binders reduced with an increase in the RAP binder content.

Sabouri et al. [140] investigated the performance of the asphalt mixes containing RAP with respect to amount of RAP, total asphalt content and various base binders. The rutting performance of the asphalt mixes was evaluated with a permanent deformation model developed by Choi and Kim [141]. The Simplified Viscoelastic Continuum Damage (S-VECD) model was used to evaluate the fatigue properties of asphalt mixes. Nine laboratory-produced asphalt mixes were tested for this purpose. The Triaxial Stress Sweep test, Dynamic Modulus (DM) test and the Cyclic Direct Tension tests were also used to evaluate the rutting and fatigue properties of the asphalt mixes. The high- and low-temperature PG grades of the binder blends were found to increase with an increase in RAP binder. The use of soft binder with RAP in the asphalt mixes resulted in improved fatigue resistance without compromising the rutting resistance of the mixes. These researchers suggested to use either a soft base binder, maintain the optimum asphalt binder content or increase asphalt layer thickness while incorporating high amounts of RAP in asphalt mixes.

In a recent study, Ghabchi et al. [135] evaluated the effects of RAS and RAP on the fatigue cracking, low-temperature cracking and stiffness of HMA mixes. A nation-wide survey was conducted among the DOTs to find out the major concerns of incorporating RAP and RAS in asphalt mixes. The fatigue cracking was found to be a major concern among all the state DOTs while using RAP and RAS. The resistance to fatigue cracking, low-temperature cracking and stiffness of the asphalt mixes containing different

amounts of RAS (0 to 6%) and/or RAP (0 to 30%) with two types of binders (PG 64-22 and PG 70-28) were evaluated in the laboratory using Four-point Bending Beam Fatigue, DM test, Creep Compliance, and Indirect Tensile Strength tests. The maximum increase in the fatigue life was observed for the asphalt mixes with PG 64-22 binder and 5% RAS and 5% RAP. Also, the dynamic moduli of the asphalt mixes were observed to increase with the addition of RAS and/or RAP indicating a better rutting performance of mixes. However, the low-temperature cracking potential of the asphalt mixes was found to increase with an increase in the RAP and RAS content in the mixes.

5.4 CONVENTIONAL ASPHALT BINDER TEST METHODS

5.4.1 Superpave® Performance Grade (PG) and Its Limitation

Before implementation of the Superpave® system, characterization of asphalt binders was mainly based on empirical methods. Different empirical tests such as penetration, ductility, softening point and viscosity were used for the characterization of asphalt binders. These empirical tests were reported to have no direct correlations with the HMA pavement performance. Also, these tests were conducted at one standard temperature without considering binder properties at other temperatures pertaining to climatic conditions. Furthermore, there was no scope for testing binder properties at low temperatures to determine binders' resistance to thermal cracking. To address these limitations, the Superpave® PG system was developed to characterize asphalt binders based on their performance [142].

The DSR test, introduced by the Superpave®, is used to characterize the rheological properties of the asphalt binders. In the DSR test, a cylindrical binder sample of desired shape is sandwiched between two parallel plates (Figure 58). Torque is applied to the plate to create sinusoidal, oscillatory stresses or strains on the binder sample at required temperatures and loading frequencies. The DSR test is conducted at a relatively low stress level to ensure linear viscoelastic behavior of the asphalt binder [143]. Figure 58 presents a schematic of the DSR test. The total dissipated energy can be calculated from the stress-strain curve of the DSR test using Equation 3. According to Anderson et al. [144] the rutting can be related to the total dissipated energy keep

from a DSR test. The term $|G^*|/\sin \delta$ was identified as the rutting parameter and was used to determine the high-temperature performance grade of the binder being tested [145].

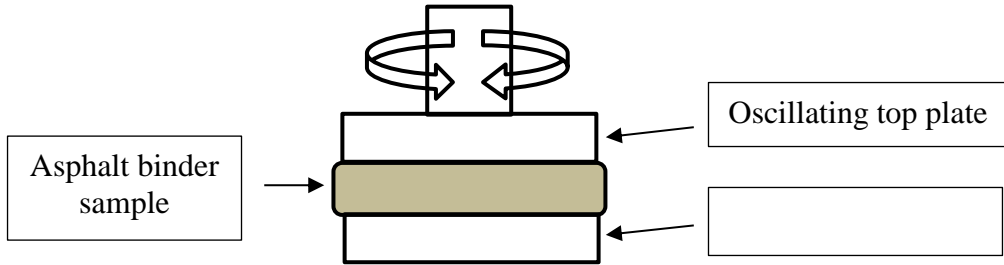


Figure 58. Schematic of DSR test setup [143]

$$W_i = \Pi * \tau_0^2 * \frac{1}{|G^*|/\sin \delta} \dots \dots \dots (3)$$

where,

W_i = Total dissipated energy,

τ_0 = Maximum applied stress,

$|G^*|$ = Shear modulus of asphalt binder, and

δ = Phase angle of asphalt binder.

The NCHRP project 9-10 (2001), “Superpave® Protocols for Modified Binders,” was conducted to investigate the suitability of the test protocols proposed in the Superpave® specifications for characterizing modified asphalt binders. A wide range of commonly used modified asphalt binders were tested in that study. It was observed that the mechanical behavior of many modified binders could be highly non-linear and very sensitive to stress level, speed, and traffic volume. It was also reported that the simplifying assumptions used for the Superpave® test methods restricted their applicability for modified asphalt binders. The Superpave® test methods such as AASHTO T 315 [146] was found to be inadequate for measuring the non-linear viscoelastic properties of polymer-modified binders. The correlation between rutting properties of asphalt mixes and the $|G^*|/\sin \delta$ of asphalt binders was found to be poor (with a coefficient of determination, R^2 , equal to 23.77%). It was concluded that the

Superpave[®] specifications that were mainly developed for characterizing unmodified asphalt binders are inadequate for proper characterization of modified binders [147].

5.4.2 Other Test Methods and Their Limitations

Consequently, many researchers and DOTs started searching for additional test methods for characterizing polymer-modified binders. This quest resulted in the introduction of Superpave[®] “PG Plus” test methods such as ER [148], Tenacity [149], and Forced Ductility (FD) [150] tests [151].

Shenoy [152] proposed a refinement of the Superpave[®] high-temperature specification parameter using basic principles. A new high-temperature parameter called Shenoy's parameter ($|G^*| / (1 - 1 / (\tan \delta \cdot \sin \delta))$) was proposed to replace the $|G^*| / \sin \delta$. It was proposed that the permanent deformation could be minimized by maximizing Shenoy's parameter. Experimental data of some typically used binders with widely different rheological characteristics were used for the verification of the prediction. It was observed that the Shenoy's parameter correlated well with actual experimental data more than the $|G^*| / \sin \delta$, suggested by Superpave[®] specifications.

Dongré and D'Angelo [153] correlated high-temperature specification parameters obtained from different asphalt binder tests with the rutting performance data from an Accelerated Loading Facility (ALF) at the FHWA's Turner-Fairbank Highway Research Center located in Virginia. The ZSV was determined using the Carreau model [154] at different creep stress levels and by conducting multicycle creep-recovery test on the asphalt binders [153]. The frequency sweep data at the high temperature PG grades were also used to obtain the ZSV values. Among these parameters, the ZSV determined from the Carreau model was found to exhibit a good correlation with the rutting performance of the asphalt mixes. However, this method was found to be time-consuming. It was recommended that the ZSV determined from the single frequency sweep test can be used as a possible replacement of rutting parameter.

Dongré et al. [155] conducted another study to evaluate the adequacy of storage viscosity (η') as a replacement for the Superpave[®] high-temperature rutting parameter

($|G^*|/\sin\delta$). It was found that the accumulated strain, ZSV, and η' showed reasonable correlations with rut depths measured in a HWT test. The η' value was found to be the most promising binder parameter for characterizing the rutting resistance of asphalt mixes. The temperature at which η' becomes equal to a viscosity of 220 Pascal-seconds (Pa-s) was proposed as a new specification criterion.

A study conducted by Virginia Department of Transportation (VDOT) identified the presence of polymer modifiers in binders by Fourier Transform Infrared (FTIR) Spectroscopy and Elastic Recovery (ER) techniques. It was found that both of these techniques were not capable of identifying polymers in modified binders [156].

Zoorob et al. [157] investigated the effects of frequency sweep test on the penetration grade binders (40/50 and 20/30) and a SBS block copolymer-modified binder at different temperatures. The measured shear modulus ($|G^*|$) and phase angle (δ) values were found to indicate the differences between the SBS-modified binder with other non-modified binders. A Low Shear Viscosity (LSV) temperature sweep test was also conducted to obtain Equi-Viscous Temperature (EVT) at 2 kPa·s viscosity. Frequency sweep tests conducted at EVT on SBS-modified binders showed that the LSV concept was not applicable to modified binders in which no viscosity plateau can be obtained.

The advantages and disadvantages of different test parameters namely, penetration, softening point, $|G^*|/\sin\delta$, Shenoy's parameter, zero-shear viscosity, storage viscosity (η) and the J_{nr} were investigated by Domingos and Faxina [158]. A 50/70 penetration grade asphalt binder was used as the base binder and to prepare crumb rubber-, SBS-, and Poly Ethylene (PE)-modified asphalt binders of similar high-temperature PG grade (PG 76-XX). The rutting resistance of these binders were evaluated using different parameters at 64° and 70 °C. It was observed that the $|G^*|/\sin\delta$ exhibited more conservative results in predicting rutting susceptibility than the Shenoy's parameter. Some similarities in the ranking of the asphalt binders' susceptibility to rutting were observed while considering the $|G^*|/\sin\delta$, Shenoy's parameter and J_{nr} parameter. However, the creep and recovery test method was found to detect substantial

differences among the rheological responses of the modified binders, which were not clearly observed in other test procedures.

5.5 MULTIPLE STRESS CREEP RECOVERY (MSCR) METHOD

5.5.1 Development of MSCR Test Method

Outcomes of the NCHRP project 9-10 suggested that the repeated loading can be used for the characterization of the PMA binders [159]. Consequently, a new test method, called the Repeated Creep and Recovery Test (RCRT), was proposed by Bahia et al. [159]. The rate of permanent strain accumulation in the asphalt binder due to repeated loading was estimated by this test method. In this method, a creep load of 0.3 kPa was applied for 1 second to the asphalt binder, followed by a recovery period of 9 seconds. The main drawback of the RCRT test method was its low stress level compared to the actual field conditions [160].

The stress dependency of binders in the RCRT and the relationship of this test method with the asphalt mixes' performance were evaluated by Delgadillo et al. [143]. Different polymer-modified and aged asphalt binders were used to evaluate the non-linearity of the RCRT test. Binders were tested at six different stress levels, namely 0.025, 0.1, 0.4, 1.6, 6.4 and 10 kPa. The stress sensitivity of the RCRT test was found to vary with asphalt binder type, modification type and temperature. Also, the RCRT test was found to be more sensitive to stress level than the stress sweep test. Furthermore, the permanent deformation of the asphalt mixes was found to have a good correlation with the RCRT parameter. Moreover, it was observed that the behavior of the binder at a high stress level may be used as an indicator of the rutting resistance of the asphalt mixes.

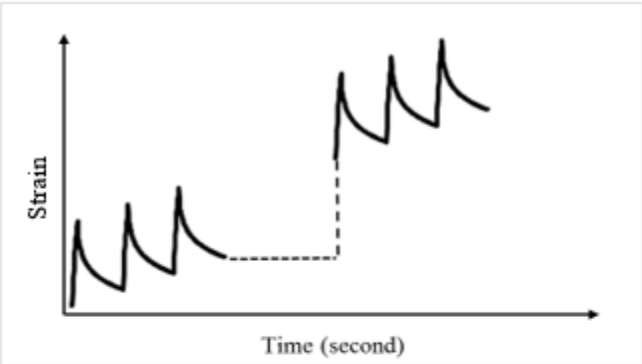
D'Angelo et al. [160] evaluated the applicability of the RCRT method on modified binders as an alternative to Superpave[®] PG plus tests. A complete RCRT protocol was developed for testing asphalt binders. In that study, two stress levels (0.1 and 3.2 kPa) were proposed for testing. Binders with less networked structure were found to exhibit an increase in compliance at 3.2 kPa stress level. It was also observed that the analysis

of RCRT data can provide useful information on the polymer network within the binder. It was reported that a relationship existed between percent recovery values obtained from the RCRT and elastic recovery tests. Also, tests on the field cores indicated that unlike the elastic recovery test, the RCRT can identify the presence of polymer(s) in a binder. A new parameter called non-recoverable creep compliance (J_{nr}) was introduced to determine the rutting potential of the polymer-modified asphalt binders.

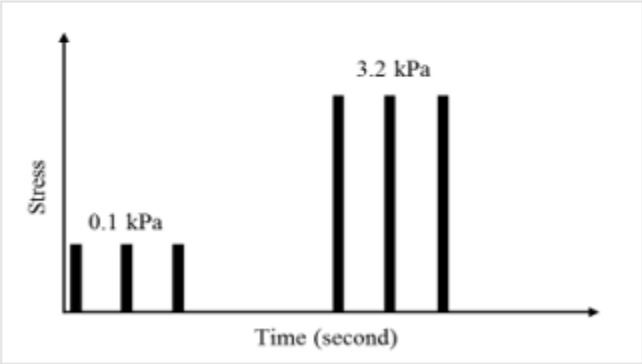
A study conducted by D'Angelo [161] evaluated the high-temperature rutting properties of both unmodified and polymer-modified asphalt binders. The outcomes of that study were used for the development of the MSCR test method. The relationship between the existing Superpave[®] grading and the J_{nr} parameter at 3.2 kPa stress level was evaluated using multiple unmodified and polymer-modified asphalt binders. Unmodified binders used in this study exhibited a linear behavior up to a stress level of 3.2 kPa, whereas the polymer-modified binders showed a non-linear behavior at a low stress level. The two-phase nature of the polymer-modified binders was reported to be responsible for this phenomenon. Also, the variation of rutting with J_{nr} was exhibited using the results from other studies. A new high-temperature binder specification, based on MSCR test method, was proposed for asphalt binders as a replacement for grade bumping procedure. It was also observed that the stress dependency of polymer-modified binders was affected by the stiffness of base binder, amount of polymer and extent of the polymer network in the binder.

Reinke [162] investigated the suitability of the J_{nr} parameter to predict the high-temperature performance of asphalt mixes. The J_{nr} values of all modified binders tested in that study were found to increase with an increase in the stress level. It was also found that the different polymer systems responded differently to the applied stress. It was concluded that an understanding of the stress sensitivity of the asphalt binders would be necessary to evaluate their rutting potential. It was also recommended that the J_{nr} value of the binders be determined at the climatic temperature using a range of stress levels to evaluate their rutting resistance.

Figure 59 presents a schematic of the MSCR test at 0.1 and 3.2 kPa stress levels [163]. The non-recoverable creep compliance is calculated by dividing the non-recoverable strain after each creep and recovery cycle with the corresponding applied stress. For example, the J_{nr} at 0.1 kPa is calculated by dividing the non-recoverable strain after each creep and recovery cycle by 0.1 kPa. Equations 4 and 5 present the calculation procedure for the J_{nr} at 0.1 kPa. The J_{nr} for 3.2 kPa stress level can be calculated using similar procedure [164].



(a)



(b)

Figure 59. Schematic of MSCR test method (a) strain vs time and (b) stress vs time [163]

$$J_{nr} = \frac{\varepsilon_{10}}{0.1} \dots \dots \dots (4)$$

$$J_{nr,0.1} = \frac{\sum(J_{nr,0.1}, N)}{10} \dots \dots \dots (5)$$

where,

$$\varepsilon_{10} = \varepsilon_r - \varepsilon_0,$$

ε_r = Strain at the end of the recovery portion of each cycle, and

ε_0 = Initial strain at the beginning of the creep portion of each cycle.

5.5.2 Studies Related to MSCR Test

D'Angelo and Dongré [163] evaluated the compatibility of the linear and radial SBS polymers with the binders using MSCR and ER test methods. It was found that the ER tests could not differentiate between different levels of polymer modifications, whereas the MSCR test was able to determine the extent of the polymer network in the binders. Also, the binder with radial SBS polymer was found to exhibit a higher recovery than the binder with linear SBS modification. Furthermore, the MSCR test results were verified with the fluorescence micrographs of the binders. It was found that the MSCR test was a convenient and less time-consuming test for optimum polymer-modified binders.

Tabatabaee and Tabatabaee [165] evaluated the effectiveness of the current Superpave® specifications, time sweep and MSCR tests with respect to the performance of the asphalt mixes. A PG 58-22 binder was modified by adding 3%, 6%, 9%, 12%, and 15% ground crumb rubber using a laboratory scale mixer. The highly Crumb Rubber-Modified (CRM) binders were observed to exhibit a better rut resistance from the MSCR results. It was observed that both MSCR and $|G^*|/\sin\delta$ parameters can be used in predicting permanent deformation behavior of asphalt binders modified with the CRM.

Adorjányi, and Füleki [166] studied the performances of different hard, polymer-modified and penetration grade (35/50, 50/70) binders typically used in Hungary using MSCR test. The MSCR tests were conducted on RTFO-aged binders at high temperature (60 °C) and three different stress levels, namely 0.1, 3.2, and 6.4 kPa. It was found that the average recoverable strains of the polymer-modified and hard binders were independent of the stress level. However, the binder with a higher penetration value exhibited a lower recoverable strain and higher stress sensitivity. Significant differences in the non-recoverable creep compliance values were also observed for the asphalt binders with the same penetration grade. A good correlation was found between the average recoverable strain and average non-recoverable compliance at all stress levels for tested binders.

Wasage et al. [167] investigated the results of the MSCR test for several conventional, polymer- and crumb rubber-modified asphalt binders to evaluate the suitability of J_{nr} as a new parameter for the prediction of rutting. Four different asphalt binders within same high-temperature PG grade were selected. Asphalt mixes were prepared using the same aggregate gradation, asphalt content and air voids. Relatively low recovery was observed for the conventional binder while polymer-modified binder showed a high recovery at all stress levels. The J_{nr} of polymer-modified binder was found to be weakly dependent on the stress up to a level of 12.8 kPa at a temperature of 40 °C. After that stress level, an increased stress dependency was observed with an increase in stress level. A stress of about 1 kPa at 40 °C was found as a common lower boundary of the linear viscoelastic behavior for all of the tested binders. The best correlation between the rut depth and the J_{nr} value was observed at a stress level of 12.8 kPa. Also, a linear viscoelastic model was developed for MSCR test. The model was reported to be capable of describing the MSCR test for all binders.

Shirodkar et al. [168] studied the behavior of both in-house and industry-produced polymer-modified binders by characterizing creep and recovery curves obtained from the MSCR test. A methodology was developed to determine the different components, such as linear viscoelastic, non-linear viscoelastic, and permanent strain from the creep

and recovery curve. Cycle 6 of 0.1 kPa stress level and cycles 1, 6, and 10 of 3.2 kPa stress level were used to determine the linear and non-linear viscoelastic parameters, respectively. It was found that the non-linear viscoelastic parameters and permanent strain were not affected by the cycles of the MSCR test but were influenced by the type of base binder. Also, the MSCR parameter, J_{nr} was found to be affected by the type of base binders and polymers.

A study funded by the New Jersey Department of Transportation was conducted to verify the suitability of MSCR parameters as a standard measure to evaluate the performance of polymer-modified binders [169]. It was found that the MSCR test could be used as a replacement of more time intensive elastic recovery and force ductility tests. It was also reported that using the MSCR test resulted in a reduction of capital cost and expenses associated with characterization of asphalt binders. Furthermore, a database containing properties of asphalt binders and mixes properties was developed to help engineers in selecting appropriate binders and mixes that can meet the required criteria in the specifications. A J_{nr} value of less than 0.5 kPa^{-1} showed a better high-temperature performance. It was also reported that an MSCR %Recovery value greater than 40% at 3.2 kPa stress level might meet the elastic recovery requirements of the binder. It was further suggested that a low J_{nr} value with a high MSCR %Recovery and a high $|G^*|/\sin\delta$ value would ensure the binders' capability to withstand heavy and extreme traffic loads.

DuBois et al. [170] conducted a study to establish correlations between the parameters from the MSCR test with the laboratory measured high-temperature properties of asphalt mixes. A total of ten different asphalt mixes were evaluated for this purpose. Binder of each mix was tested in accordance with the Superpave[®] and MSCR tests to measure $|G^*|/\sin\delta$ and J_{nr} . The J_{nr} values were found to correlate well with the rutting performance of asphalt mixes measured using a flow time test. It was also observed that the rutting resistance of the asphalt mixes improved as the J_{nr} value of the binder decreased. Asphalt binders were found to exhibit a better rutting performance as the J_{nr}

values approached 0.5 kPa^{-1} or lower. Furthermore, the flow time result was found to exhibit poor correlations with the $|G^*|/\sin\delta$ and MSCR %Recovery.

The high-temperature performance of highly modified asphalt binders was investigated by Mohseni and Azari [171] using the Incremental Repeated Load Permanent Deformation (iRLPD) and the MSCR test method. The MSCR and iRLPD tests were conducted at PG, PG-6 °C and PG-12 °C temperatures. The iRLPD tests were performed at 1.0, 3.2, and 5.0 kPa shear stress levels, each consisting of 20 cycles. The relationship between the loading time and permanent strain was found to be linear for neat binders, whereas it was observed to be highly non-linear for polymer-modified binders. It was also observed that the permanent strain of polymer-modified binders was time-dependent and the non-linearity of strain increased with the level of modification. A comparison of average recovery values between both tests showed that the MSCR %Recovery was significantly less than that of the iRLPD test. The variability of the MSCR test on highly modified binders was found to be dependent on the binder type. The MSCR, LTPPBind and iRLPD Traffic Models were developed to relate the binders' test parameters to Equivalent Single Axle Load (ESAL). The iRLPD and LTPPBind estimated similar ESAL values for most of the modified binders, whereas the iRLPD and MSCR traffic estimates were found to be different for the modified binders.

Domingos and Faxina [172] evaluated the effect of longer creep-recovery times on the MSCR test parameters using a number of modified asphalt binders. A 50/70 penetration grade binder which is equivalent to a PG 64-XX binder was used as a base binder to prepare PPA-, SBS- and SBS+PPA-modified binders. The modifier contents were selected to achieve a binder grade of PG 76-XX. Standard MSCR tests along with non-conventional tests were conducted at a creep and recovery times of 2 and 18 seconds, respectively. It was found that the PPA-modified binders exhibited the highest %Recovery and the lowest J_{nr} values. However, the highest $J_{nr \text{ diff}}$ values were observed for the PPA-modified binder. It was also observed that an increase in creep-recovery time decreased the %Recovery and increased the non-recoverable compliance of all modified binders. The effect of an increase in both creep and recovery times was found

to be more pronounced for SBS-modified binders. It was suggested that the addition of PPA might be a good alternative to reduce the susceptibility to rutting at longer creep-recovery times.

Zhang et al. [173] evaluated the MSCR and DSR test methods in characterizing the rutting properties of asphalt binders used in HMA mixes. A good correlation ($R^2 > 0.75$) was found between the J_{nr} values of binders and the rut depths of HMA obtained from a HWT test. Also, the rutting parameter, $|G^*|/\sin\delta$, was found to exhibit a relatively poor correlation ($R^2 < 0.5$) with the rut depths. This study showed that the MSCR test has potential to serve as a surrogate for the rutting parameter, $|G^*|/\sin\delta$.

A study was conducted by Hossain et al. [174] to produce a MSCR database for different types of polymer-modified binders used in Oklahoma. Asphalt binders from different sources in Oklahoma were collected and tested at 64 °C and at 0.1 and 3.2 kPa stress levels. The asphalt binders were then graded using the MSCR grading system. The results from the quadrant plot indicated that both supplier and user may not be at risk if they use PG 76-28 asphalt binders. It was also recommended that an MSCR %Recovery value of 50% could be adopted for PG 70-28 binders without putting many suppliers at risk. The MSCR %Recovery value of 80% for PG 76-28 was recommended. The MSCR %Recovery was found to decrease with temperature but increase with aging. It was suggested that the MSCR test method could be adopted by ODOT in its quality assurance process to characterize the high-temperature performance of asphalt binders.

Stevens et al. [175] developed a MSCR database for Arizona DOT to determine the impacts of changing the grading system from Superpave® to MSCR-based system. The AASHTO T 350 [176] test method and AASHTO M 332 [178] specification were followed for conducting the DSR and MSCR tests, respectively. The database of three separate groups (A, B, and C) of asphalt binders consisting of 375 individual asphalt binder samples were evaluated in this study. It was observed that although the binders used in Arizona were produced according to AASHTO M 320 [179] specification, they met the standard traffic requirements of the AASHTO M 332 [177]. Adopting the MSCR

specification for grading of asphalt binders was found to increase the number of asphalt binder grades used by Arizona DOT from 8 to 13.

A study conducted by Yang and You [179] used both DSR and MSCR tests to determine the high-temperature performance of bio-oil modified asphalt binders. A PG 58-28 binder was blended with 5% and 10% of three types of bio-oils generated from waste woods, namely untreated bio-oil, treated bio-oil and polymer-modified bio-oil. From the DSR test results it was found that the addition of bio-oil to binder increased the $|G^*|$ value and reduced the phase angle. The rutting resistance of the binder was found to increase with the addition of bio-oil. A decrease in the J_{nr} value and an increase in the %Recovery were also observed with the addition of bio-oil to binder. The MSCR test results showed that the polymer-modified bio-oil performed worse than untreated and treated bio-oil-modified binders.

The effect of stress level on the creep and recovery behavior of SBS- and PPA-modified binders was investigated by Jafari et al. [180]. Asphalt binders of same continuous PG grade were selected as base binder and mixed with 2%, 4%, and 6% SBS and required amounts of PPA to achieve the same continuous high temperature PG grade. The MSCR tests were conducted at 55°, 70 °C and at the high temperature PG grade of each binder and at a stress level of 12.8 kPa in addition to the standard MSCR procedure. It was found that the J_{nr} values at low stress levels (0.1 and 3.2 kPa) were almost independent of stress at any temperature indicating linear viscoelastic characteristics of asphalt binders. However, the stress sensitivity of the modified binders was observed to be more prominent at a high temperature and a high stress level (12.8 kPa). The SBS-modified binders were found to exhibit significantly less sensitivity to stress levels than the PPA-modified binders of the same PG grade. It was also observed that the asphalt binder modified with PPA exhibited a higher stress-sensitivity than others. Furthermore, the PPA-modified binders exhibited much lower recovery values than the corresponding SBS-modified binders. It was recommended that a stress level higher than 3.2 kPa be used to evaluate the J_{nr} values of the SBS- and PPA-modified binders in the non-linear viscoelastic region.

The creep-recovery behavior of various elastomer and/or wax modified binders was evaluated by Laukkanen et al. [181]. Different linear viscoelastic parameters, namely $|G^*|/\sin\delta$, ZSV and LSV were calculated for tested asphalt binders. It was observed that, all the rutting parameters except $|G^*|/\sin\delta$, ranked highly modified binders as the most rut resistant and unmodified binders as the most rut susceptible binders. From the MSCR ranking, it was found that the modified binders were much more rut resistant compared to the unmodified binders of same penetration grade. It was observed that the non-recoverable creep compliance at 3.2 kPa and the accumulated strain at the end of the MSCR test could predict binder's contribution to rutting of asphalt mixes. Also, the relationships between these two parameters and rutting of asphalt mixes were found to be linear. It was reported that the highly modified binders, especially those modified with wax, were more stress sensitive compared to unmodified and moderately modified binders.

Saboo and Kumar [182] evaluated the rutting performance of unmodified and polymer-modified asphalt binders using different rut prediction parameters and compared their results with the rutting performance of the associated asphalt mixes. Two viscosity graded binders and two polymer-modified binders (SBS- and EVA-modified) were selected for that study. The temperature sweep test at 10 rad/s, steady-shear viscosity test at a shear rate varying from 0.1 to 100 s⁻¹ and MSCR test were conducted to evaluate various rutting susceptibility parameters. A laboratory wheel-tracking device was used to measure the rutting performance of prepared HMA. From the binder tests results, it was found that the polymer-modified binders showed a better rutting performance than conventional binders. It was also observed that the rutting performance of the binders evaluated using different methods provided similar rankings. However, the amount by which one binder was superior to the other varied with the method. The MSCR test was found to be the more fundamental test method and was reported to provide more information about the viscoelastic nature of the asphalt binder than other test methods.

5.6 INTERPRETATION OF MSCR TEST DATA

5.6.1 Polymer Method

A %Recovery vs. J_{nr} plot is a very useful tool for characterizing asphalt binders at high temperature. This plot is known as the “polymer method” of MSCR data analysis [183]. In the present study, the MSCR test data was analyzed using the polymer method. The MSCR parameters, namely J_{nr} and %Recovery obtained from the 3.2 kPa stress level at 64 °C, were plotted to characterize the binders by locating it on the polymer plot. The AASHTO TP 70 [164] provisional specification introduced a typical curve called the “MSCR curve” as a borderline between elastomeric polymer-modified and unmodified binders [183]. The equation of the MSCR curve is given in Equation 6.

$$y = 29.37x^{-0.2633} \dots \dots \dots (6)$$

where,

y = MSCR %Recovery at 3.2 kPa, and

x = Non-recoverable creep compliance at 3.2 kPa.

An asphalt binder can be defined as a highly elastic binder if the plot of the %Recovery vs. J_{nr} falls above the MSCR curve. This highly elastic binder can be modified with high amounts of elastomeric polymers. If the plot of %Recovery vs. J_{nr} falls below the MSCR curve, then it indicates that the binder will exhibit low elasticity. Such a binder is not expected to be modified with enough elastomeric polymers. Figure 60 presents a typical plot of the polymer method.

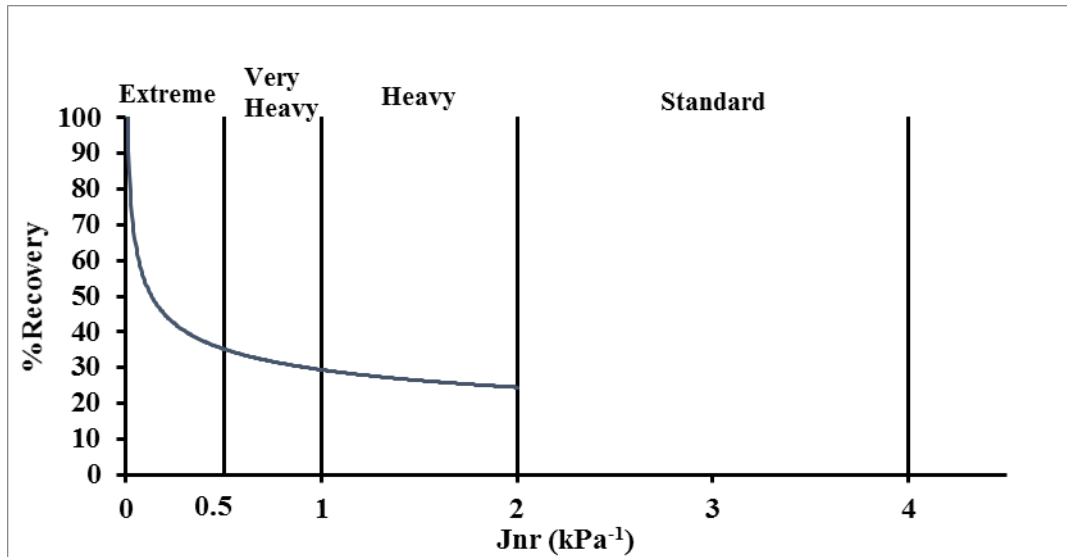


Figure 60. Polymer method of MSCR analysis [56]

5.6.2 Stress Sensitivity

Stress sensitivity ($J_{nr \text{ diff}}$) is another important parameter that can be determined from the MSCR test results. A binder's performance at a higher temperature or at a higher stress level than expected can be evaluated with the help of the stress sensitivity parameter [174] In the MSCR test method, the $J_{nr \text{ diff}}$ is calculated based on the difference in J_{nr} values at two stress levels. According to the AASHTO MP 19 [184], the increase in J_{nr} due to an increase in stress level from 0.1 kPa to 3.2 kPa must be less than or equal to 75% of the J_{nr} at 0.1 kPa. The equation for calculating $J_{nr \text{ diff}}$ is given below:

$$J_{nr \text{ diff}} = \frac{J_{nr, 3.2 \text{ kPa}} - J_{nr, 0.1 \text{ kPa}}}{J_{nr, 0.1 \text{ kPa}}} 100 \leq 75\% \dots \dots \dots (7)$$

5.6.3 MSCR Grading

The MSCR grading system can be used to characterize the performance of unmodified and polymer-modified binders. The MSCR grade of a binder is calculated based on the J_{nr} values at 3.2 kPa stress level. In this grading system, the J_{nr} values are used as an indicator of the level of traffic that a binder can sustain at a given temperature. Four traffic levels are considered in the J_{nr} -based grading system, namely Standard (S), Heavy (H), Very Heavy (V) and Extreme (E). For example, at 64 °C, the four MSCR

grades are PG 64S-XX (Standard), PG 64H-XX (Heavy), PG 64V-XX (Very Heavy), and PG 64E-XX (Extreme). Table 23 presents the MSCR grading of binders according to the AASHTO MP 19 [184] provisional specification.

Table 23. MSCR grades based on J_{nr} [184]

J_{nr} (kPa ⁻¹) criteria	MSCR Grading
$2.0 < J_{nr} \leq 4.0$	PG 64S-XX (S: Standard)
$1.0 < J_{nr} \leq 2.0$	PG 64H-XX (H: Heavy)
$0.5 < J_{nr} \leq 1.0$	PG 64V-XX (V: Very Heavy)
$J_{nr} \leq 0.5$	PG 64E- XX (E: Extreme)

5.7 IMPLEMENTATION OF MSCR METHOD

Publications by the Asphalt Institute (AI) have identified the benefits of adopting the MSCR test method over the “PG Plus” tests. For example, the AI published an implementation document for the MSCR test, named “*Implementation of the Multiple Stress Creep Recovery Test and Specification,*” to help the asphalt industry with the implementation of the MSCR test method [185]. Although the ultimate goal of the AI was the full implementation of this relatively new binder specification, the Asphalt Institute Technical Advisory Committee recognized that many agencies might be uncomfortable in transitioning to a system that uses different grade names [185]. A number of meetings, presentations and webinars were conducted by the AI, FHWA, and state DOT engineers to facilitate implementation of the MSCR test method [183, 186-193]. A number of inter-laboratory studies were also conducted by the AI to determine the precision of the AASHTO TP 70 [164] test method for the Southeastern Asphalt User/Producer Group (SEAUPG) and the North East Asphalt User/Producer Group (NEAUPG). The Inter-Laboratory Study (ILS) by NEAUPG to evaluate the repeatability and reproducibility of the AASHTO TP 70 [164] test method involved twenty-eight laboratories located in the NEAUPG region. In addition to the 2010 ILS, the NEAUPG also conducted a second ILS involving twenty-eight laboratories from users, producers

and industry/academia [193]. In 2011, the SEAUPG conducted a similar study involving twenty-three laboratories located in the SEAUPG region [194].

The implementation status of the MSCR test method of each state can be found in the AI's interactive database [195]. A highlight of the status of implementation in Oklahoma, New Mexico and Texas DOTs is presented below [195].

The Oklahoma Department of Transportation (ODOT) is in the process of full implementation of the MSCR test method for all PG binders. The minimum MSCR %Recovery requirements for PG 70-28 OK (PG 64V-28), PG 76-28 OK (PG 64E-28), and PG 76E-28 binders have been set in the specifications. The Texas Department of Transportation (TxDOT) is in the process of setting minimum %Recovery requirements for different binders. The TxDOT is planning to replace the elastic recovery with the MSCR %Recovery. Currently, the New Mexico Department of Transportation (NMDOT) is testing all binders under the MSCR specification. The NMDOT has been conducting MSCR tests for several years as a part of the Western Co-ops efforts with University of Wisconsin [195].

5.8 HAMBURG WHEEL TRACKING TEST

To identify the rutting potential of HMA mixes, many transportation agencies have started using Loaded Wheel Testers (LWT) as a supplement to their mix design procedure. It was found that the LWTs allow for an accelerated evaluation of rutting potential of the designed asphalt mixes. Several LWTs are currently being used in the United States, which include the following: Georgia Loaded Wheel Tester, Asphalt Pavement Analyzer (APA), Hamburg Wheel Tracking device (HWT), Laboratoire Central des Ponts et Chaussées (French) Wheel Tracker, and Purdue University Laboratory Wheel Tracking Device (PURWheel) [197-201]. Results obtained from the wheel tracking devices were found to correlate well with the actual field performance when the loading and environmental conditions of a given location were considered [197, 199, 201].

The capability of the HWT test to determine the moisture sensitivity of asphalt mixes were evaluated by Lu and Harvey [202]. For this purpose, both laboratory test and field performance data were used on a large scale. Asphalt mixes were prepared using two types of aggregates, two types of binders and three different additive contents. The HWT test was found to overestimate the performance of the asphalt mixes containing the conventional binders and underestimate the performance of mixes containing polymer-modified binders.

Grebenschikov and Prozzi [203] compared the rut depths obtained from the HWT test with the rut depths from the Mechanistic-Empirical Pavement Design Guide (MEPDG). The results of two types of asphalt mixes (Type C and Type D) from a previous TxDOT project were used for this purpose. Each mix was prepared using three aggregate gradation levels, namely fine, target and coarse and five binder contents. It was found that both the MEPDG and the HWT test ranked the mixes in the same order with respect to rutting.

Walubita et al. [204] evaluated three laboratory tests, namely the DM test, Repeated Load Permanent Deformation (RLPD) test, and HWT test, for characterizing the permanent deformation response of HMA mixes relative to the field performance under both conventional traffic loading and Accelerated Pavement Testing (APT). It was observed that all three test methods provided consistent results in terms of rutting behavior. Also, the Superpave[®] mixes were generally found to exhibit higher moduli values with greater rutting resistance potential than the conventional mixes. The HWT test was found to exhibit the best repeatability and the lowest variability in the test results, compared to the DM and RLPD tests. It was suggested to use the HWT test for routine stripping assessment and rutting performance prediction of HMA.

Differences in rutting performance between laboratory and field compacted asphalt mixes were studied by Howard and Doyle [205] using APA and HWT devices. A total of 398 field cores and laboratory produced samples were tested in that study. No significant differences were observed between the rut depths of plant produced and laboratory produced mixes determined by APA rut tests. However, the rut depths of

plant produced mixes obtained from the HWT test were observed to be higher than that of the laboratory produced mixes. Also, the rutting performance of laboratory produced mixes was found to decrease significantly with a reduction in mixing temperature.

Sel et al. [206] evaluated the effect of test temperature on the rut depths of asphalt mixes obtained from a HWT test. The Hamburg test database and Aggregate Quality Monitoring Program database of TxDOT were used for this purpose. Statistical analyses of the collected data showed that the binder grade influenced the HWT rut performance of asphalt mixes. Binders with a higher PG grade were found to accumulate less deformation than the binders with a lower PG grade. Significant differences in the performance were observed when the samples were tested at 40° and 50 °C. The average deformation was found to exhibit an increasing trend in rutting with an increase in test temperature.

5.9 SUMMARY

Polymer-modified binders have been reported to exhibit better rutting and fatigue performances in the pavement than the unmodified binders. The MSCR test method was developed by recognizing the limitations of traditional test methods to characterize polymer-modified binders. The current MSCR test method and specification are the results of many laboratory and field investigations. The MSCR test method has been found to be capable of characterizing the rheological properties of binders modified with different types and amounts of polymers. Also, the MSCR parameters have been found to better reflect field rutting performance than the Superpave® test method parameters. The scarcity and increased cost of the components of asphalt mixes has led to the incorporation of high amounts of RAP in asphalt mixes. The RAP binder blends have been reported to exhibit better rutting resistance than the unmodified binders. Also, the pavement sections with high RAP content have been found to perform well during their service life. Furthermore, the HWT test was reported to be appropriate for evaluating the rutting performance of asphalt mixes.

CHAPTER 6

PART TWO METHODOLOGY

6.1 INTRODUCTION

This chapter presents an overview of the material selection process, test matrices, and performance tests for both asphalt binders and asphalt mixes. The test matrices included testing polymer-modified binders, RAP binder blends and asphalt mixes containing polymer-modified binders and different RAP contents. The major tasks of this study are to: (i) collect unmodified and polymer-modified asphalt binders from different refineries in Oklahoma, New Mexico and Texas; (ii) extract binder from selected RAPs; (iii) prepare asphalt binder samples containing RAP binder; (iv) determine Superpave[®] performance grade (PG) of unmodified and polymer-modified binders; (v) perform MSCR tests on unmodified and polymer-modified binders and analyze the test results; (vi) collect plant produced asphalt mixes with different RAP contents; and (vii) perform HWT tests on collected mixes and analyze the test results. A flow chart of the work flow pursued for this study is given in Figure 61.

6.2 MATERIAL COLLECTION AND SAMPLE PREPARATION

6.2.1 Collection of Asphalt Binders

As noted previously, some commonly used asphalt binders in Oklahoma, Texas and New Mexico were evaluated in this study. Asphalt binders were collected from seven different sources; four of these sources were located in Oklahoma, one in New Mexico and two in Texas. Since the main focus of this study was to evaluate the polymer-modified binders, PG 70-XX and PG 76-XX binders were collected from these sources. The type and amount of polymer modification were not shared by the suppliers with the research team. An unmodified asphalt binder, PG 64-22, was also collected from an Oklahoma refinery for blending with the RAP binder. It is important to note that the PG grading system of the asphalt binder represents the maximum high and low temperatures it can sustain. For example, for a PG 64-22 binder, the number 64 indicates that the binder can be used in areas where the maximum seven-day average pavement temperature could be as high as 64 °C. The number -22 means that the

binder is capable of withstanding a temperature as low as -22 °C, without experiencing any low-temperature cracking [207]. Table 24 presents the types and locations of the collected binders.

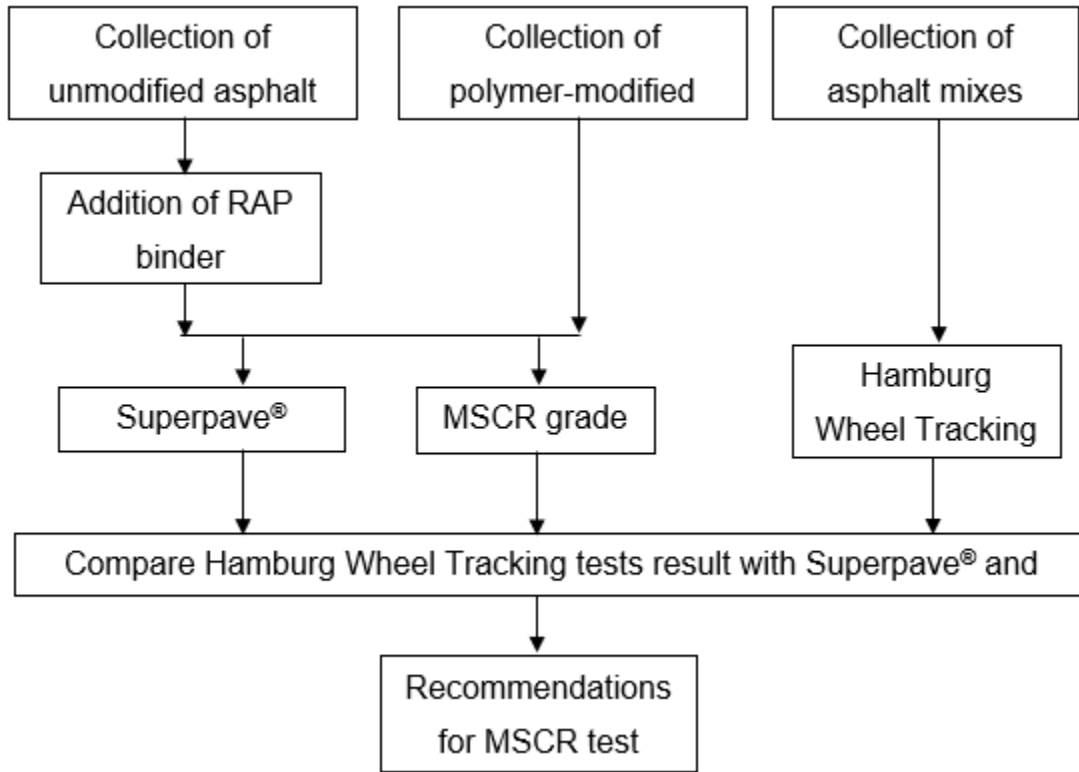


Figure 61. Work flow of the present study

Table 24. Sources and types of the binders collected for study

Source	Source locations	Binder types
S1	Oklahoma	PG 64-22, PG 70-28, PG 76-28
S2	Oklahoma	PG 70-28, PG 76-28
S3	Oklahoma	PG 70-28, PG 76-28
S4	Oklahoma	PG 76-28
S5	New Mexico	PG 70-28, PG 76-28
S6	Texas	PG 70-28, PG 76-28
S7	Texas	PG 70-22

6.2.2 Extraction of Binder from RAP

Approximately 25 kg of fine RAP was collected from two local suppliers in Oklahoma for extraction of binder. The RAP samples were collected from two sources, namely Silver Star Construction Co., located in Moore, OK and Haskell Lemon Construction Co., located in Norman, OK. For convenience, these materials were designated as RAP1 and RAP2, respectively. The collected RAPs were shipped to Arkansas State University (ASU) for binder extraction. The binder recovery from RAP was performed using a Rotary Evaporator available at the ASU Materials Laboratory in accordance with the AASHTO T 319 (Standard Method of Test for Quantitative Extraction and Recovery of Binder from Asphalt Mixtures) method [208]. Approximately 320 g of RAP1 and 258 g of RAP2 binders were obtained after extraction. The RAP binders were shipped back to the OU Asphalt Binder Laboratory.

6.2.3 RAP Binder Blends

The RAP binders (RAP1 and RAP2) were blended with the unmodified PG 64-22 binder at four different amounts, namely 0%, 25%, 40% and 60% (by weight of total binder). The blending of the PG 64-22 binder and RAP binders was performed using a hand mixing process. For this purpose, the PG 64-22 binder and the RAP binders were heated to 150 °C for an hour prior to blending. The required amount of RAP binder was then weighed and added to the unmodified binder. The binder blend was mixed for one minute at every 10 minutes for an hour to consistency. For future reference in this study, the 25%, 40% and 60% RAP1 binder blends are defined as PG 64-22-R1-25, PG 64-22-R1-40 and PG 64-22-R1-60 binder, respectively. Similarly, PG 64-22-R2-25, PG 64-22-R2-40 and PG 64-22-R2-60 are used to represent 25%, 40% and 60% RAP2 binder blends, respectively.

6.2.4 Collection of Asphalt Mixes

Asphalt mixes containing polymer-modified binders and different amounts of RAP were selected to evaluate the rutting susceptibility of the asphalt mixes. For this purpose, asphalt mix design sheets required for the production of asphalt mixes were collected from Silver Star Construction Co. After evaluating these mix designs, a total of four asphalt mixes were selected for this study. Table 25 presents the properties of the

selected asphalt mixes. Since the production of asphalt mixes with high RAP content (e.g., 35% RAP) is not very common in Oklahoma, the asphalt mixes with polymer-modified binder (MIX-1) and 25% RAP (MIX-2) were collected from the aforementioned asphalt plant, but those containing 35% RAP (MIX-3 and MIX-4) were produced in the laboratory. For laboratory produced mixes, asphalt binders, RAP and aggregates were collected from the same plant to maintain consistency. Figure 62 presents the photographs of the collection of the asphalt mixes and aggregates from the asphalt plant.



Figure 62. (a) Collection of aggregates for laboratory produced asphalt mixes; (b) collected aggregates and asphalt binder.

Table 25. Properties of selected asphalt mixes

Asphalt plant	Mix ID	Mix type	Nominal maximum aggregate size NMAS (mm)	Binder type	RAP content (%)
Silver Star	MIX-1	S4	12.5	PG 76-28	0%
Construction Co. (Moore, OK)	MIX-2	S3	19	PG 64-22	25%
	MIX-3	S3	19	PG 64-22	35%
	MIX-4	S4	12.5	PG 64-22	35%

6.3 LABORATORY TESTING

6.3.1 Superpave® Grading of Asphalt Binders

The polymer-modified binders and the RAP binder blends were evaluated using the Superpave® grading system. The Superpave® test methods consist of conducting DSR tests, Rotational Viscometer (RV) test, and Bending Beam Rheometer (BBR) test, in accordance with AASHTO M 320 [178]. The test matrix used for this purpose is presented in Table 26.

6.3.2 Short-term and Long-term Aging of Asphalt Binders

The short-term aging of the asphalt binders was simulated in the laboratory by conducting Rolling Thin Film Oven (RTFO) tests according to the AASHTO T 240 [209] test method (Standard Method of Test for Effect of Heat and Air on a Moving Film of Binder). The RTFO-aging simulates the oxidation and aging of asphalt binders during mixing in the asphalt plant and compacting in the field. During RTFO-aging, the oven temperature was kept constant at 163 °C and the air flow rate was maintained at 4 liters/minutes for 85 minutes. The AASHTO R 28 [210] (Standard Practice for Accelerated Aging of Binder Using a Pressurized Aging Vessel) was followed to simulate long-term aging of asphalt binders in the field using a Pressure Aging Vessel (PAV). This aging is intended to simulate 5 to 10 years of service life in the field. The PAV-aging was conducted on binder residues obtained from the AASHTO T 240 [209] (RTFO) test method. The RTFO-aged binder samples were placed in stainless steel pans and were aged in a pre-heated vessel at 100 °C for 20 hours under an air pressure of 2.10 MPa.

Table 26. Test matrix for Superpave® tests

Test name and designation	Test conditions	Binder from Oklahoma PG 64-XX from (S1)	Binder from Oklahoma PG 70-XX from (S1, S2, S3)	Binder from Oklahoma PG 76-XX from (S1, S2, S3, S4)	Binder Outside of Oklahoma PG 70-XX from (S5, S6, S7)	Binder Outside of Oklahoma PG 76-XX from (S5, S6)
RAP blending		RAP1 and RAP2 (25%, 40% and 60%)	No	No	No	No
Superpave® grade: AASHTO M 320		Yes	Yes	Yes	Yes	Yes
RV: AASHTO T 316	Unaged	From 135 °C to 180 °C @ 15 °C	From 135 °C to 180 °C @ 15 °C	From 135 °C to 180 °C @ 15 °C	From 135 °C to 180 °C @ 15 °C	From 135 °C to 180 °C @ 15 °C
DSR: AASHTO T 315	Unaged and RTFO-aged	@61 °C, 64 °C, 67 °C	@ 67 °C, 70 °C, 73 °C	@73 °C, 76 °C, 79 °C	@ 67 °C, 70 °C, 73 °C	@73 °C, 76 °C, 79 °C
	PAV-aged	@ 19 °C, 22 °C, 25 °C	@ 25 °C, 28 °C, 31 °C	@25 °C, 28 °C, 31 °C	@ 25 °C, 28 °C, 31 °C	@25 °C, 28 °C, 31 °C
RTFO: AASHTO T 240		Yes	Yes	Yes	Yes	Yes
PAV: AASHTO R 28		Yes	Yes	Yes	Yes	Yes
BBR: AASHTO T 313	PAV-aged	@ -9 °C, -12 °C	@ -18 °C, -21 °C	@ -18 °C, -21 °C	@ -18 °C, -21 °C	@ -18 °C, -21 °C

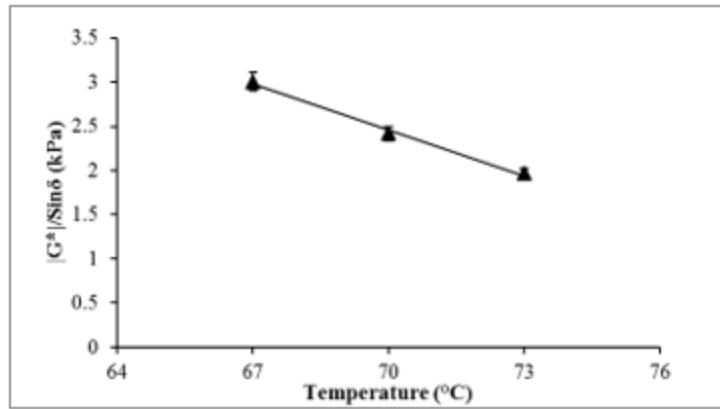
6.3.3 Dynamic Shear Rheometer (DSR) Test

The DSR test was conducted in accordance with the AASHTO T 315 [146] (Standard Method of Test for Determination of Rutting and Fatigue Factors Using a Dynamic Shear Rheometer) test method. The DSR test was conducted in a thermally-controlled test chamber with a temperature tolerance of ± 0.1 °C. It is an oscillatory test which is conducted at a loading frequency of 10 rad/s [146]. For this purpose, unaged and

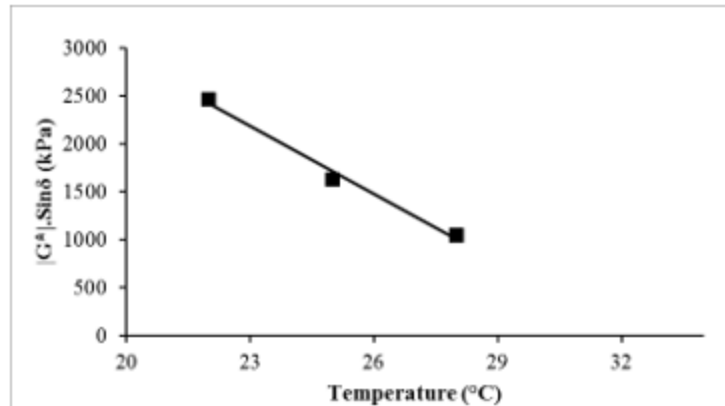
RTFO-aged binder samples were prepared by using a silicon rubber mold having a diameter of 19 mm and a thickness of 1.5 mm. A mold with 8 mm diameter and 3 mm thickness was used to prepare PAV-aged binder samples for DSR testing. The unaged and RTFO-aged samples were tested using 25 mm diameter parallel plates with 1 mm gap, while PAV-aged samples were tested using 8 mm diameter parallel plates with 2 mm gap. The asphalt binder sample for DSR test and the test setup are presented in Figure 63. The DSR tests on unaged and RTFO-aged binders were conducted under three different temperatures, namely performance grade (PG), PG+3°, and PG-3 °C. The PAV-aged samples were tested under three different temperatures, namely intermediate PG, intermediate PG+3°, and intermediate PG-3 °C. The shear modulus ($|G^*|$) and phase angle (δ) were calculated using the software supplied by the instrument manufacturer. The rutting parameter ($|G^*|/\sin\delta$) of unaged and RTFO-aged binders at high temperatures were determined. In addition, the fatigue parameter ($|G^*|\cdot\sin\delta$) for PAV-aged binders at intermediate temperatures were determined as well. Generally, a higher value of $|G^*|/\sin\delta$ is an indication of higher rutting resistance and a higher $|G^*|\cdot\sin\delta$ value is an indicator of lower fatigue resistance (Bahia, and Anderson, 1995). The lowest temperature corresponding to a $|G^*|/\sin\delta$ value of 1.0 kPa for unaged or 2.20 kPa for RTFO-aged binders was considered as the continuous high PG temperature for the tested asphalt binders [178]. Figure 64 presents typical plots of DSR test results.



Figure 63. Test setup for DSR test on asphalt binder samples: (a) DSR apparatus; (b) asphalt binder samples for DSR test



(a)



(b)

Figure 64. Typical plots from DSR tests on asphalt binder samples: (a) $|G^*|/\sin\delta$ vs temperature; (b) $|G^*|\cdot\sin\delta$ vs temperature

6.3.4 Rotational Viscosity (RV) Test

The Rotational Viscosity (RV) tests were conducted on unaged asphalt binders using a Brookfield Rotational Viscometer. The AASHTO T 316 [211] (Standard Method of Test for Viscosity Determination of Binder Using Rotational Viscometer) test method was followed to conduct the RV tests. The workability of the asphalt binders during mixing and compaction in the field was evaluated using this test method. The RV test setup used for this study is presented in Figure 65. Approximately 10 g of asphalt binder sample is needed for conducting a RV test. For this purpose, a standard cylindrical spindle was submerged in the liquid asphalt binder and was rotated at a constant speed of 20 revolutions/minute (rpm). The torque required for the spindle to maintain a constant rotational speed of 20 rpm was measured and reported as the rotational

viscosity. In this study, the rotational viscosities of the binders were determined at 135°, 150°, 165° and 180 °C. Figure 66 presents a typical plot of RV test results.



Figure 65. Rotational Viscosity test setup for asphalt binder

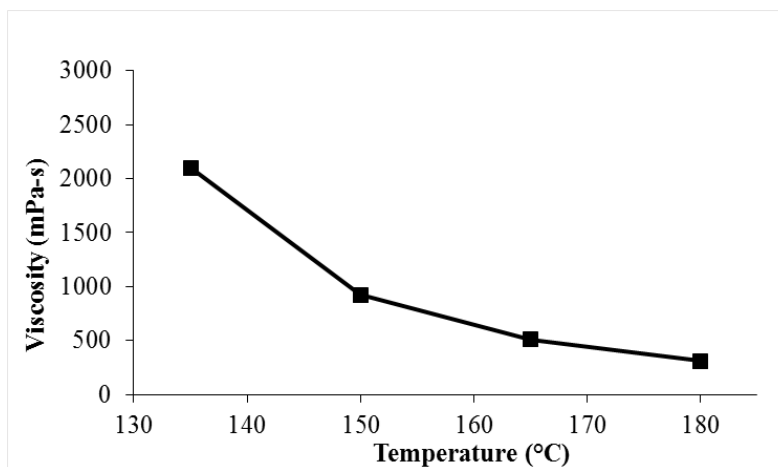


Figure 66. A typical plot of the RV test conducted on asphalt binder sample

6.3.5 Bending Beam Rheometer (BBR) Test

The AASHTO T 313 [212] (Standard Method of Test for Determining the Flexural Creep Stiffness of Binder Using the Bending Beam Rheometer) test method was followed to conduct the BBR test on asphalt binders. The BBR test was performed on the PAV-aged asphalt binders to determine their resistance to thermal cracking at low temperature. An Asphalt beam sample having a length of 127 mm, width 12.7 mm, and thickness 6.35 mm was prepared for this test. The sample was subjected to a constant load of 980 ± 50 mN applied at the mid-span of the beam for 240 seconds. The

stiffness, S_{60} (maximum bending stress divided by the maximum strain), and the rate of stress relaxation, m_{60} (slope of stiffness versus time), were calculated for specified loading times (t) of 8, 15, 30, 60, 120, and 240 seconds. The values of the stiffness and the rate of stress relaxation at $t = 60$ seconds were used to quantify the thermal cracking resistance of the binders. The continuous low-temperature PG grade of the binders were determined based on the results from the BBR tests, following the Superpave® specifications [178]. The highest temperature corresponding to an m_{60} of 0.30 or a S_{60} of 300 MPa was reported as the low temperature PG grade. Figure 67 and 68 present the test setup and typical plots of BBR test on asphalt binder, respectively.

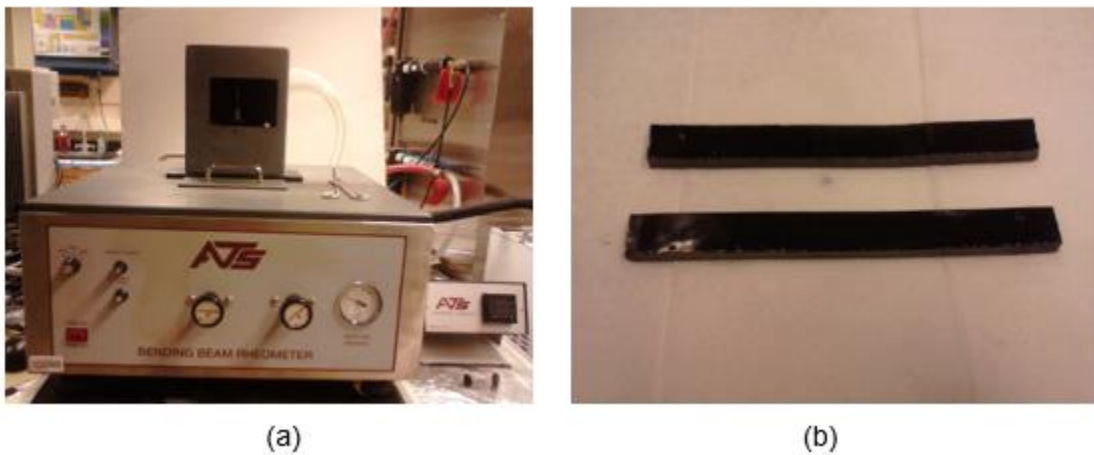


Figure 67. Test setup for BBR test on asphalt binder sample: (a) BBR apparatus; (b) asphalt beam sample

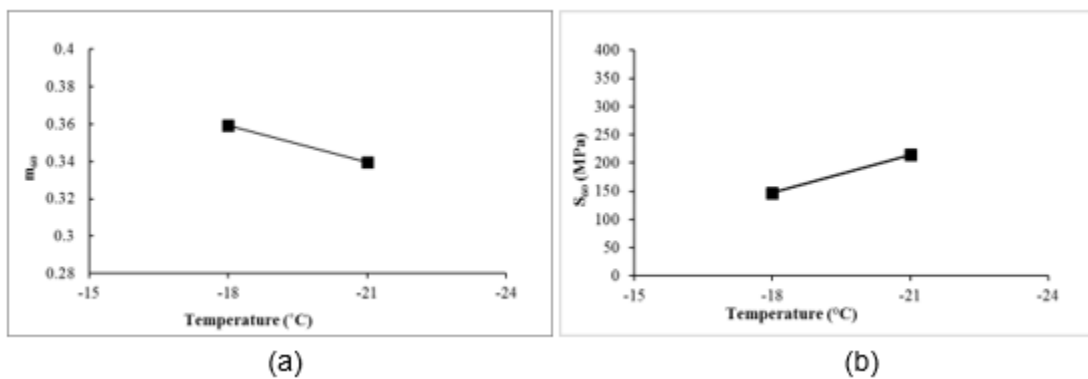


Figure 68. Typical plots from BBR test on asphalt binder sample: (a) m_{60} vs temperature; (b) S_{60} vs temperature

6.3.6 Multiple Stress Creep Recovery (MSCR) Test

The MSCR tests were conducted on asphalt binders, following both “conventional” and “non-conventional” procedures. The “conventional” method refers to the MSCR test performed using the AASHTO TP 70 procedure [164] (Standard Method of Test for Multiple Stress Creep Recovery (MSCR) Test of Binder Using a Dynamic Shear Rheometer) at a high environmental temperature. The high environmental temperature of Oklahoma (64 °C), as noted by Hossain et al. [174], was used in this study.

The “non-conventional” MSCR test method refers to conducting the MSCR tests at a higher stress level (10 kPa) and at high temperatures (70° and 76 °C) to characterize the non-linear viscoelastic properties of polymer-modified binders and RAP binder blends [111]. Each stress level consists of ten loading-unloading cycles. Each cycle consists of a one-second creep loading and a nine-second recovery period. The non-recoverable creep compliance (J_{nr}) and the %Recovery were calculated from the MSCR test results. Figure 69 shows a typical plot of MSCR test conducted on asphalt binder. The test matrix for MSCR test followed in this study is presented in Table 27. The MSCR parameters of the binders were determined using both conventional and non-conventional MSCR test methods.

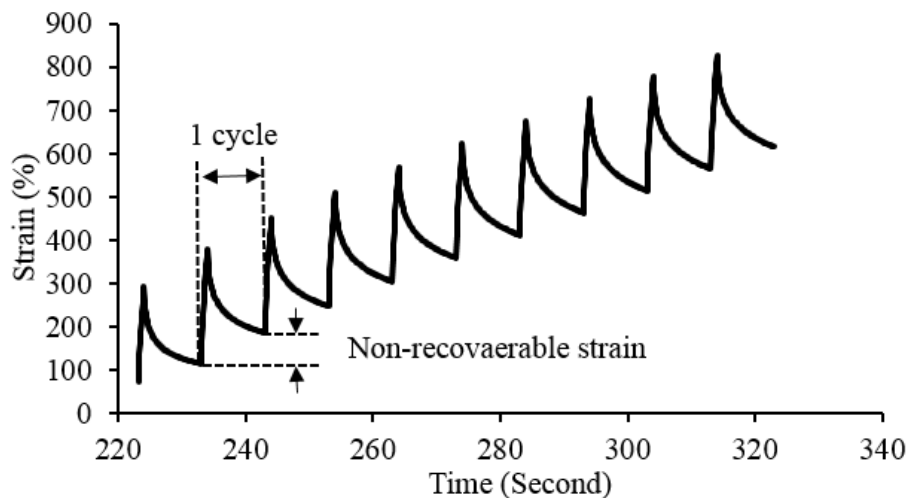


Figure 69. Example of stress response of a binder in MSCR test

Table 27. Test matrix for MSCR test

Test name and designation	Test conditions	Binders from Oklahoma PG 64-XX from (S1)	Binders from Oklahoma PG 70-XX from (S1, S2, S3)	Binders from Oklahoma PG 76-XX from (S1, S2, S3, S4)	Binders outside of Oklahoma PG 70-XX from (S5, S6, S7)	Binders outside of Oklahoma PG 76-XX from (S5, S6)
MSCR: conventional AASHTO TP 70 (AASHTO, 2013)	RTFO-aged	0.1 kPa and 3.2 kPa @ 64 °C	0.1 kPa and 3.2 kPa @ 64 °C	0.1 kPa and 3.2 kPa @ 64 °C	0.1 kPa and 3.2 kPa @ 64 °C	0.1 kPa and 3.2 kPa @ 64 °C
MSCR: Non-conventional	RTFO-aged	10 kPa @ 64 °C, 70 °C and 76 °C	10 kPa @ 64 °C, 70 °C and 76 °C	10 kPa @ 64 °C, 70 °C and 76 °C	10 kPa @ 64 °C, 70 °C and 76 °C	10 kPa @ 64 °C, 70 °C and 76 °C

6.3.7 Hamburg Wheel Tracking (HWT) Test

The HWT tests were conducted on samples of asphalt mixes collected and produced for this study, in accordance with the AASHTO T 324 (AASHTO, 2014), to determine their rutting susceptibility and moisture-induced damage potential. Samples for the HWT test were prepared in the laboratory by using a Superpave® gyratory compactor. The diameter and height of the compacted samples were 150 mm and 60 mm, respectively. The bulk specific gravity values (G_{mb}) of the compacted cylindrical samples were determined in accordance with the AASHTO T 269 (Standard Method of Test for Percent Air Voids in Compacted Dense and Open Asphalt Mixtures) test method [213]. The compacted samples with an air void of $7 \pm 0.5\%$ were selected for conducting HWT tests. In this method, two cylindrical samples were cut to a desired shape to place them in the plastic molds and mounting tray. The mounting tray was then placed in the HWT machine for testing. In this study, the HWT tests were conducted at 50 °C with a wheel pass frequency of 52 passes/minute and a wheel load of 705 N. The average linear speed of the wheel was approximately 1.1 km/h and traveling approximately 230 mm (9.05 in.) before reversing the movement direction. The test was automatically terminated after reaching a maximum rut depth of 20 mm or 20,000 wheel passes,

whichever reached first. Figure 70 presents the HWT test setup and the asphalt mix samples before and after test. Deformations were measured along the length of the wheel path at 11 equally-spaced points. The rut depth at the mid-point of the sample was considered for further analysis. From the HWT test result, the post-compaction consolidation, creep slope, stripping slope, and stripping inflection point were determined. Figure 71 shows a typical plot of a HWT test. Important parameters such as the post-compaction consolidation, creep slope, stripping slope and stripping inflection point are noted in Figure 71. Table 28 presents the test matrix for the HWT test. Two sets of samples were tested for each mix type to ensure repeatability.

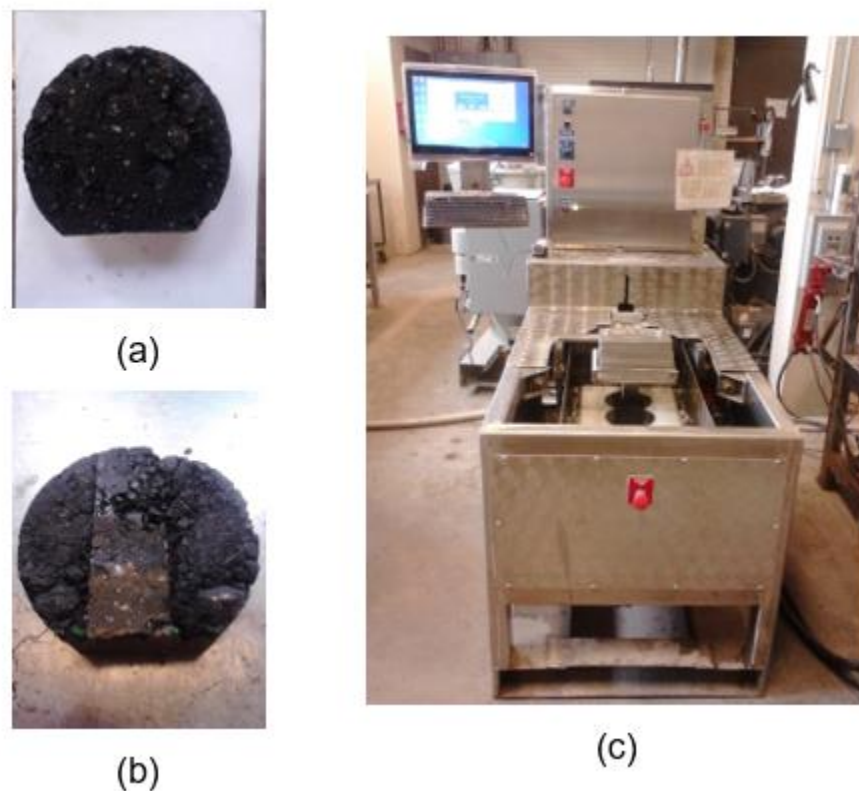


Figure 70. (a) Asphalt mix sample before HWT test; (b) Sample after test; (c) HWT test setup

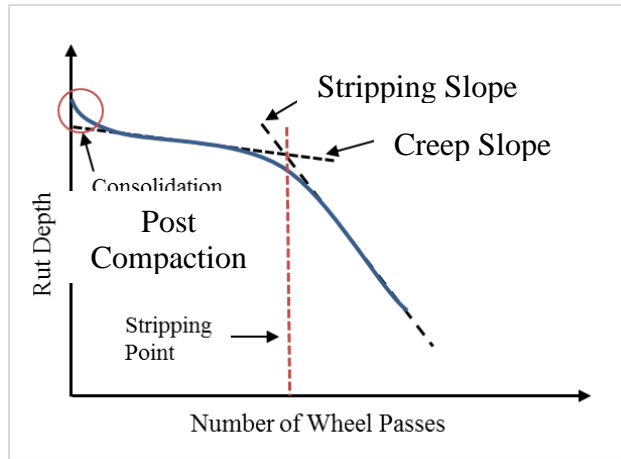


Figure 71. A typical plot of HWT rut depths vs. number of wheel passes [106]

Table 28. HWT test matrix

Mix ID	Mix type	Binder type	RAP content (%)	Sample dimensions (mm)	No. of samples	Test temp (°C)	Failure criteria
MIX-1	S4	PG 76-28	0%	Diameter: 150 Height: 60	2	50	Max. rut depth 20 mm or 20,000 wheel passes
MIX-2	S3	PG 64-22	25%	Diameter: 150 Height: 60	2	50	Max. rut depth 20 mm or 20,000 wheel passes
MIX-3	S3	PG 64-22	35%	Diameter: 150 Height: 60	2	50	Max. rut depth 20 mm or 20,000 wheel passes
MIX-4	S4	PG 64-22	35%	Diameter: 150 Height: 60	2	50	Max. rut depth 20 mm or 20,000 wheel passes

6.4 COMPARATIVE ANALYSIS OF THE SUPERPAVE®, MSCR AND HWT TEST RESULTS

In order to compare the results of the Superpave® and MSCR tests for evaluating the rutting resistance of an asphalt mix, the HWT rut results were used as a benchmark of the rutting performance. For this purpose, the $|G^*|/\sin\delta$ parameter obtained from the DSR test and the J_{nr} parameter obtained from the MSCR tests conducted under

different temperatures and different stress levels were used for the comparative analyses. An attempt was made to find a parameter that best predicts the rutting performance of the asphalt mixes. Also, a one-to-one comparative assessment of the DSR and MSCR test methods was conducted in this study. Some testing aspects such as test repeatability, variability of results, and advantages and limitations of the test methods were also assessed.

THIS PAGE IS LEFT INTENTIONALLY BLANK

CHAPTER 7

PART TWO RESULTS AND DISCUSSIONS

7.1 TEST RESULTS OF ASPHALT BINDERS

7.1.1 Introduction

This chapter presents the Superpave[®] and MSCR test results conducted on polymer-modified binders and RAP binder blends. A comprehensive analysis of the Superpave[®] and MSCR test results is also presented. Furthermore, the suitability of both methods for characterizing the polymer-modified binders and RAP binder blends was evaluated.

7.1.2 Superpave[®] Test Results

7.1.2.1 Polymer-modified Asphalt Binders

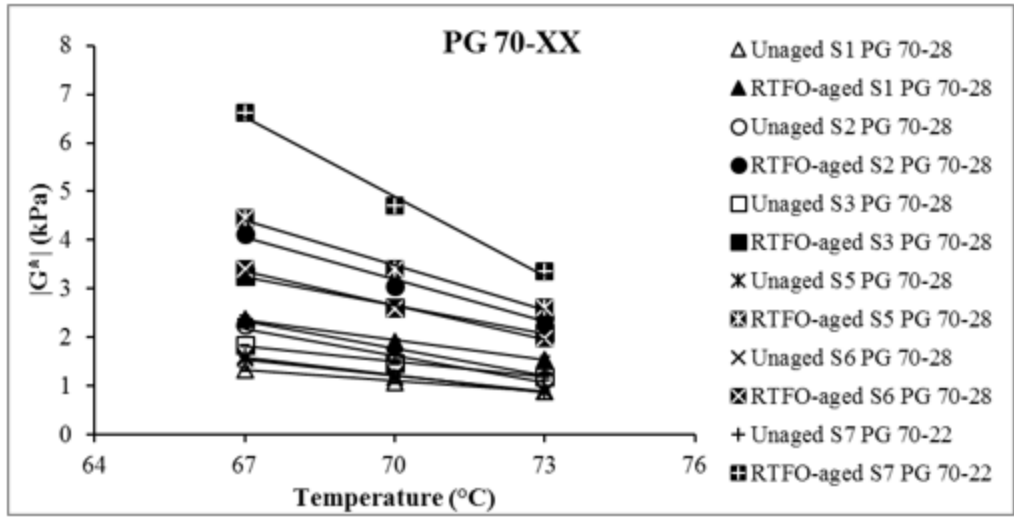
DSR test results

Figures 72 (a) and 72 (b) present the variation of $|G^*|$ values of the polymer-modified PG 70-XX and PG 76-XX binders, respectively, at different temperatures. The DSR test on unaged and RTFO-aged binders were conducted at their corresponding high performance grade (PG), PG+3° and PG-3 °C temperatures. From Figures 72 (a) and 72 (b), it was observed that the $|G^*|$ values decreased with an increase in temperature for all aging conditions and binder types. For example, the $|G^*|$ value of the unaged S1 PG 70-28 binder was found to be 1.34 kPa at 67 °C, where S1 indicates Source 1. The $|G^*|$ values for the same binder were 1.08 kPa (19% reduction) and 0.89 kPa (34% reduction) at 70 °C and 73 °C, respectively. In the case of the PG 76-XX binders, a similar trend of reducing $|G^*|$ with increasing temperature was observed. Also, the RTFO-aged binders exhibited a similar reducing trend of $|G^*|$ with temperatures although the $|G^*|$ values measured for the RTFO-aged binders were found to be higher than unaged binders, as expected. The $|G^*|$ value of the RTFO-aged S1 PG 70-28 binder was found to increase by approximately 91% of that for the unaged binder at high PG temperature (70 °C). Therefore, it can be concluded that the shear modulus as well as the stiffness of the asphalt binder are expected to increase with aging. Furthermore, the $|G^*|$ values for the PG 70-XX binders were found to vary from 1.08 to

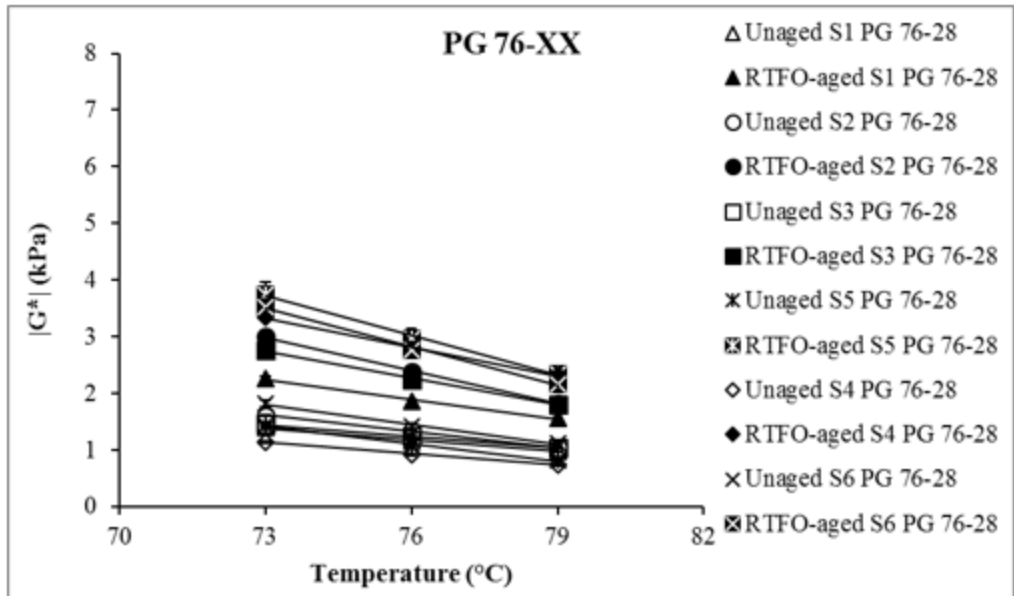
1.70 kPa under unaged condition and from 1.91 to 4.72 kPa under RTFO-aged condition at high PG temperature (70 °C). The S7 PG 70-22 binder, where S7 indicates Source 7, was found to exhibit the highest $|G^*|$ values under both unaged and RTFO-aged conditions among all of the PG 70-XX binders. For the PG 76-XX binders, the $|G^*|$ values varied from 0.92 to 1.42 kPa under unaged conditions and from 1.86 to 2.97 kPa under RTFO-aged conditions at 76 °C.

As shown in Figures 73 (a) and 73 (b), the phase angles of the PG 70-XX and PG 76-XX binders, respectively, were found to increase with an increase in temperature. The phase angles measured for the unaged S1 PG 70-28 at 67°, 70° and 73 °C were found to be 54.83°, 54.87° and 54.90°. However, the level of increase was not the same for all binders. Also, from Figures 73 (a) and 73 (b), the phase angles of the PG 70-XX and PG 76-XX binders were found to reduce with aging. For example, the phase angle measured for the RTFO-aged S1 PG 70-28 binder was found to be 52.03° at 70 °C, which is 5% lower than that of the unaged S1 PG 70-28 binder at the same temperature. Thus, it can be concluded that, asphalt binders become stiffer with aging, as reported by other researchers.

The phase angles of the PG 70-XX binders were found to vary from 54.87° to 75.20° under unaged conditions, and from 52.03° to 69.73° under RTFO-aged conditions at a high PG temperature (70 °C). The S7 PG 70-22 binder was found to exhibit the highest and the S1 PG 70-28 binder exhibited the lowest phase angle values among all of the tested PG 70-XX binders under both aging conditions. For the PG 76-XX binders at 76 °C, the phase angle values were observed to vary from 47.47° to 68.83° under unaged conditions and from 45.17° to 59.17° under RTFO-aged conditions.

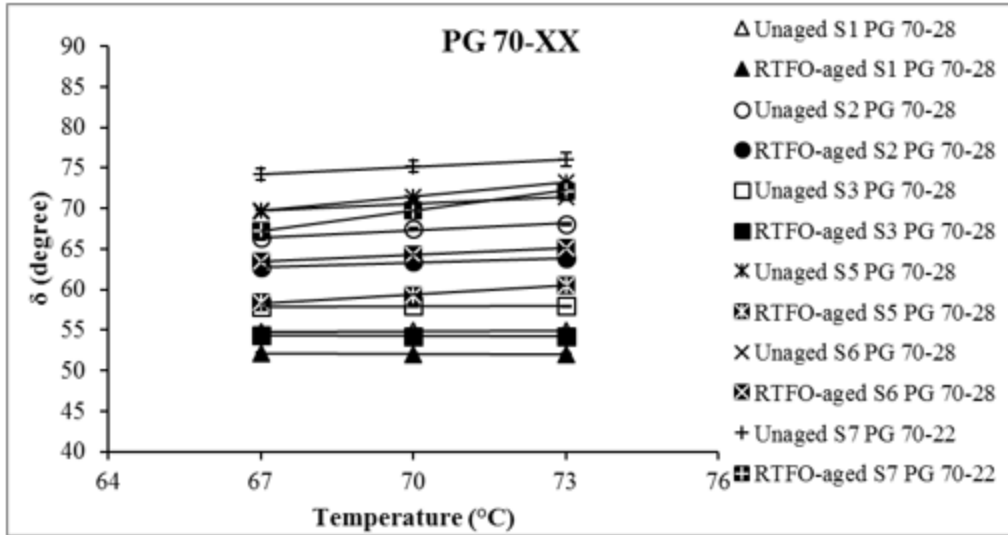


(a)

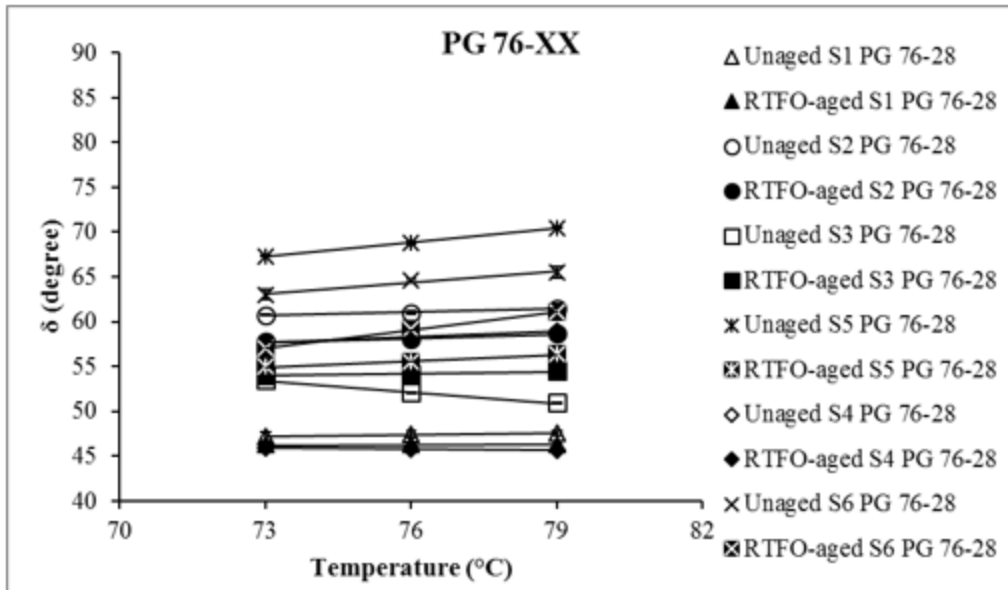


(b)

Figure 72. Variation of $|G^*|$ with temperature for unaged and RTFO-aged conditions: (a) PG 70-XX binders; (b) PG 76-XX binders



(a)

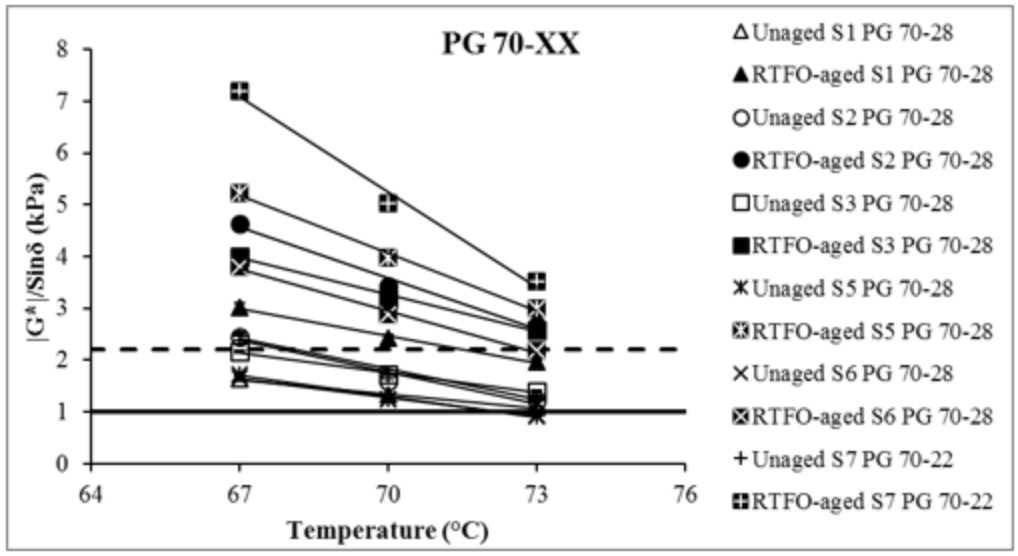


(b)

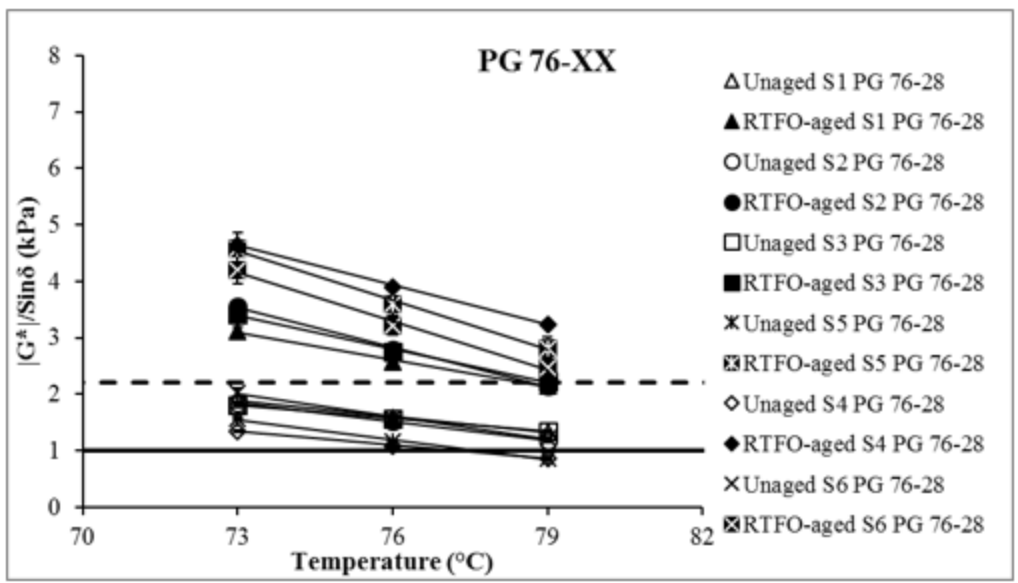
Figure 73. Variation of phase angle with temperature for unaged and RTFO-aged conditions: (a) PG 70-XX binders; (b) PG 76-XX binders

Figures 74 (a) and 74 (b) present the variations of rutting parameters for the PG 70-XX and PG 76-XX binders at their corresponding high PG, PG+3° and PG-3 °C temperatures, respectively. It was observed that the $|G^*|/\sin\delta$ value decreased with an

increase in testing temperature for all aging conditions and binder types. From Figures 74 (a), the $|G^*|/\sin\delta$ values of the unaged S1 PG 70-28 binder at 67 °C was found to be 1.63 kPa. However, the $|G^*|/\sin\delta$ values were 1.32 kPa (19% reduction) and 1.08 kPa (38% reduction) at 70° and 73 °C temperatures, respectively. Generally, a higher value of $|G^*|/\sin\delta$ is an indicator of a higher rutting resistance [145]. According to the Superpave® binder specifications, the $|G^*|/\sin\delta$ values of the binder under unaged and RTFO-aged conditions should be greater than or equal to 1.0 and 2.2 kPa at high PG temperature, respectively. All tested binders were found to meet these Superpave® specifications requirements under unaged and RTFO-aged conditions. The $|G^*|/\sin\delta$ values for the unaged PG 70-XX binders were found to vary from 1.24 to 1.76 kPa. For the same binders (PG 70-XX) under RTFO-aged condition, the $|G^*|/\sin\delta$ values varied from 2.42 to 5.03 kPa at high PG temperature (70 °C). The S7 PG 70-22 binder was found to exhibit the highest and the S1 PG 70-28 binder showed the lowest $|G^*|/\sin\delta$ values under RTFO-aged condition, among all of the tested PG 70-XX binders. Also, all of the polymer-modified PG 76-XX binders were found to meet the Superpave® specifications requirement of rutting parameter at high PG temperature. For the PG 76-XX binders at 76 °C, the $|G^*|/\sin\delta$ values were found to vary from 1.08 to 1.58 kPa under unaged condition and from 2.57 to 3.90 kPa under RTFO-aged condition. Among all of the PG 76-XX binders tested in this study, the S4 PG 76-28 binder was found to exhibit the highest and the S1 PG 76-28 binder exhibited the lowest $|G^*|/\sin\delta$ values under RTFO-aged condition. Therefore, the polymer-modified S7 PG 70-22 and S4 PG 76-28 binders, are expected to exhibit relatively better rutting resistance than the other PG 70-XX and PG 76-XX binders, respectively, when used in a mix. An improvement in the rutting resistance of polymer-modified binders was also reported by others [119, 126, 170]. According to Airey [121], the rheological characteristics of the polymer-modified binders are functions of the combined effects of the composition of the binder and polymer and the amount of polymer used in the binder. It was also observed that the binders modified with highly elastomeric polymer, such as SBS exhibited a better rutting performance at high temperatures due to the formation of a continuous polymer network when dissolved/dispersed in the binder [121]



(a)

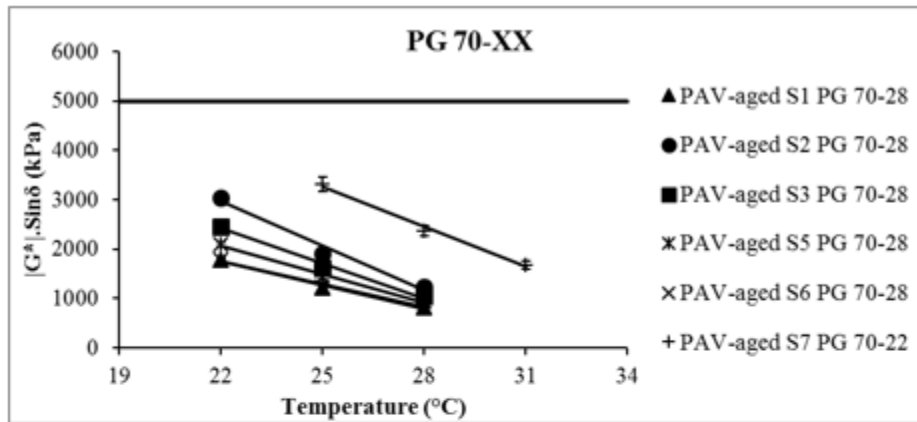


(b)

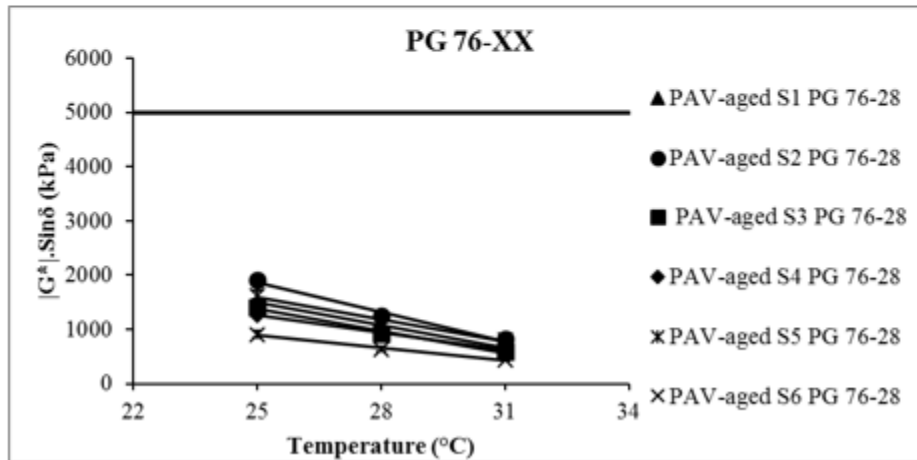
Figure 74. Variation of $|G^*|/\sin\delta$ with temperature for unaged and RTFO-aged conditions: (a) PG 70-XX binders; (b) PG 76-XX binders

Figures 75 (a) and 75 (b) present the variation of fatigue parameter ($|G^*| \cdot \sin\delta$) with temperature for the PAV-aged PG 70-XX and PG 76-XX binders, respectively. A lower value of fatigue parameter is an indicator of a higher fatigue resistance [145]. The Superpave® binder specifications require that the $|G^*| \cdot \sin\delta$ value of the PAV-aged

binders be less than 5,000 kPa at intermediate PG temperature. From Figures 75 (a) and 75 (b), the $|G^*| \cdot \sin \delta$ values were found to decrease with an increase in temperature. For example, from Figure 75 (a), the average $|G^*| \cdot \sin \delta$ for the S1 PG 70-28 binder at 22 °C was observed as 2,330 kPa. However, at 25 °C and 28 °C, the average $|G^*| \cdot \sin \delta$ values were 1,743 kPa (25% reduction) and 1,123 kPa (52% reduction), respectively. Also, the $|G^*| \cdot \sin \delta$ values for the PG 70-28 binders collected from S1, S2, S3, S4, S5, and S6 sources were found to vary between 1,217 and 1,900 kPa at 25 °C. The $|G^*| \cdot \sin \delta$ values for the S7 PG 70-22 binder was measured as 2,370 kPa at 28 °C.



(a)



(b)

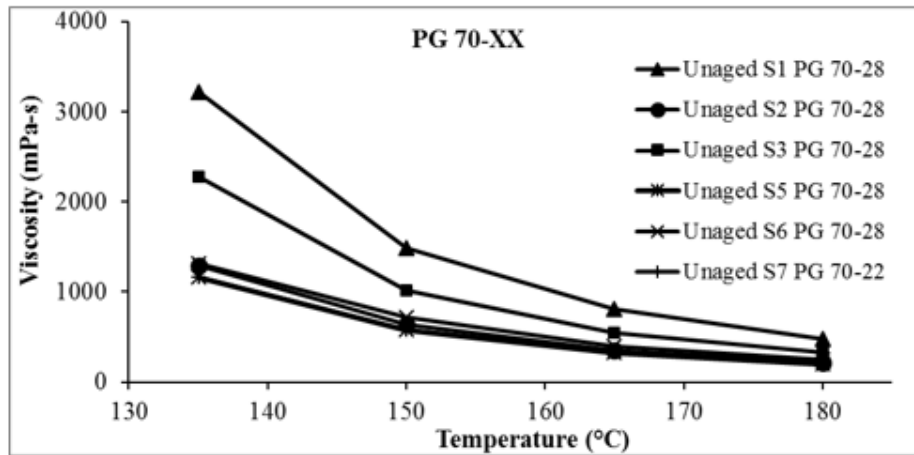
Figure 75. Variation of $|G^*| \cdot \sin \delta$ with temperature for PAV-aged condition: (a) PG 70-XX binders; (b) PG 76-XX binders

Therefore, the S7 PG 70-22 binder was found to exhibit the highest and the S1 PG 70-28 binder was found to show the lowest $|G^*| \cdot \sin \delta$ values among all of the PG 70-XX binders at their corresponding intermediate temperatures. This indicates that the S1 PG 70-28 binder is expected to have a better fatigue performance than the other PG 70-XX binders. Also, the $|G^*| \cdot \sin \delta$ value of the PG 76-XX binders were found to vary from 910 to 1,250 kPa at 28 °C. Among the tested PG 70-XX binders, the S4 PG 76-28 binder was found to exhibit the lowest $|G^*| \cdot \sin \delta$ value at intermediate temperature. The results indicate that the S4 PG 76-28 binder is expected to provide a better fatigue resistance when used in a mix. All the PG 70-XX and 76-XX binders were found to satisfy the Superpave® specifications requirement of the fatigue parameter.

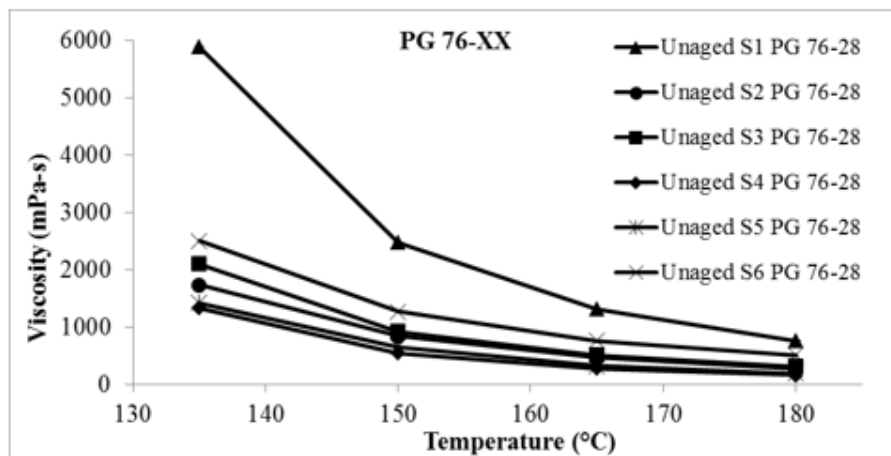
RV test results

Figures 76 (a) and 76 (b) present the results of the rotational viscosity test conducted on the unaged PG 70-XX and PG 76-XX binders, respectively. From Figures 76 (a) and 76 (b), it is evident that the viscosity of all tested binders reduced with increasing test temperatures. For example, the viscosity of the S1 PG 70-28 binder was found to be 3213 mPa·s at 135 °C, and it decreased to 1487 mPa·s (54% reduction), 812.5 mPa·s (75% reduction) and 475 mPa·s (85% reduction) at 150°, 165° and 180 °C, respectively. Also, comparing Figures 76 (a) and 76 (b) reveals that, except binders from S3 source, the viscosities of the PG 76-XX binders are higher than those measured for the PG 70-XX binders from identical sources, as expected. For example, the viscosity of the S1 PG 76-28 binder at 135 °C was found to be 83% higher than that of the S1 PG 70-28 binder at the same temperature. Furthermore, the viscosities of the PG 70-XX binders were found to vary from 1163 to 3213 mPa·s at 135 °C, while the S1 PG 70-28 binder exhibited the highest and both the S5 PG 70-28 and S7 PG 70-22 binders exhibited the lowest viscosity values. Therefore, it can be concluded that the S1 PG 70-28 and S1 PG 76-28 binders are expected to require more compaction efforts in the field among other tested binders when used in a mix. These observations were found to be consistent with the findings reported in previous studies [121]. Also, a number of studies have reported that the viscosities of the modified binders are influenced by the polymer structure and binder source [121, 126]. As reported by Lu and Isacsson (1997), the relatively high

viscosity observed for the polymer-modified binders are due to a strong interaction between the polymer particles in the binder.



(a)



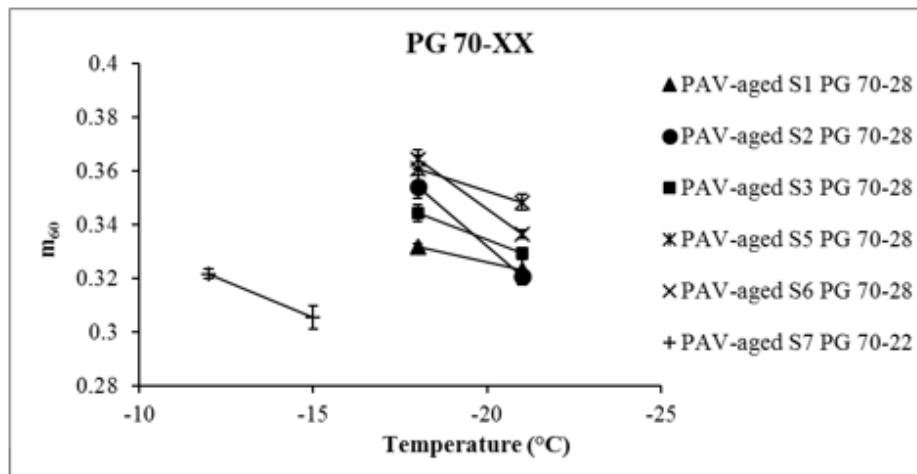
(b)

Figure 76. Variation of viscosity with temperature for unaged condition: (a) PG 70-XX binders; (b) PG 76-XX binders

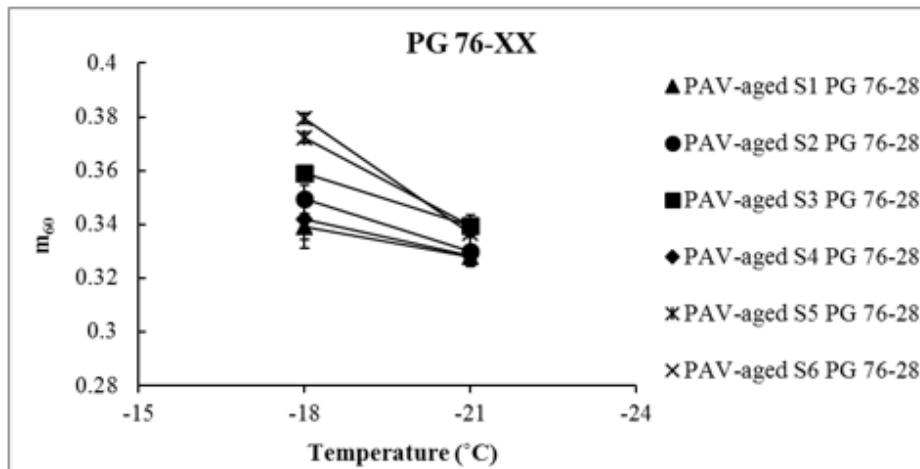
BBR test results

Figures 77 (a) and 77 (b) present the m_{60} values and Figures 78 (a) and 78 (b) present the S_{60} values measured from BBR tests conducted on the PAV-aged PG 70-XX and PAV-aged PG 76-XX binders, respectively. From Figures 77 and 78, it can be observed that the m_{60} values reduced and the S_{60} values increased with a reduction in testing temperatures. For example, the m_{60} value of the S1 PG 70-28 binder was found to be 0.332 at -18 °C, while it decreased to 0.323 at -21 °C. The S_{60} values of the same binder were observed to increase from 131.4 MPa to 192.10 MPa when the temperature

changed from -18° to -21 °C. According to the Superpave® binder specifications, the m_{60} values should be minimum 0.300 and the S_{60} values should be less than 300 MPa at low PG temperature. All the tested binders were found to meet the Superpave® specifications requirement at low PG temperature. The improved low-temperature rheological properties of the modified binders were also reported by Lu and Isacson (1997). It was reported that, at low temperature, polymer-modified binders exhibited a lower complex modulus and a lower reduction rate in phase angle with temperature than unmodified binders. This, in turn, helps to improve the low-temperature rheological properties of polymer-modified binders.

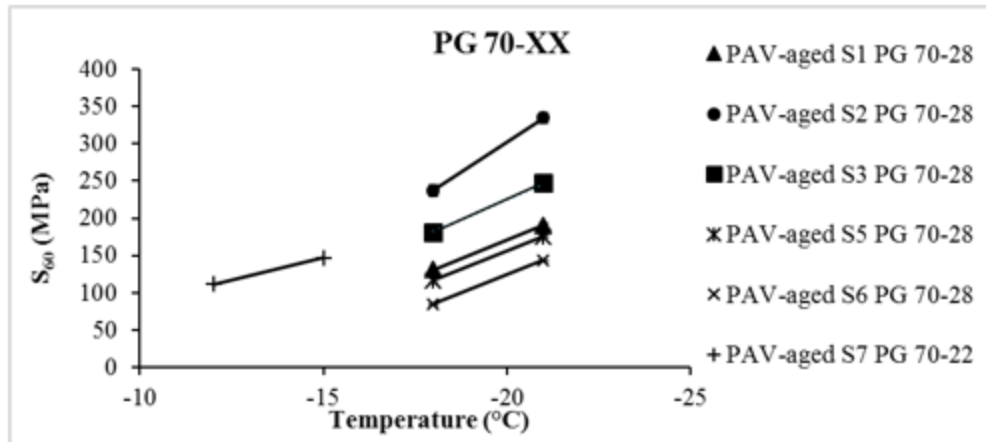


(a)

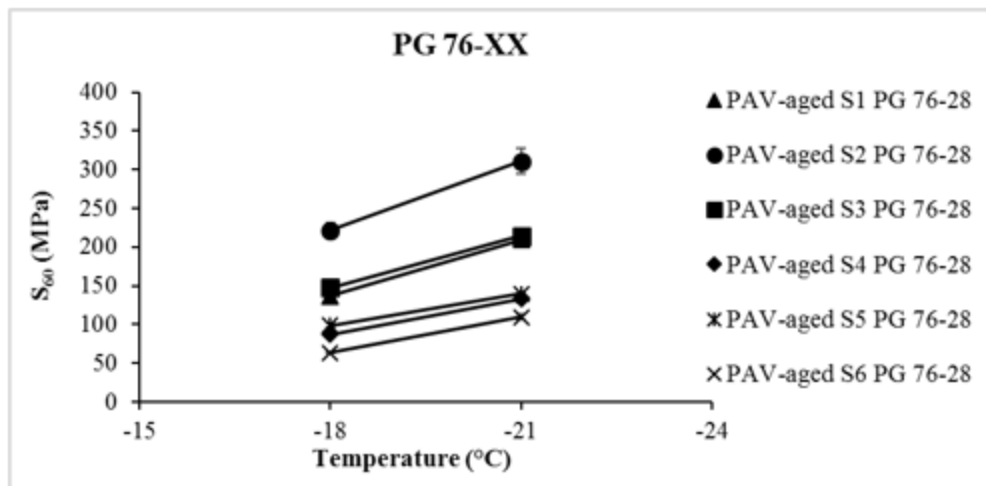


(b)

Figure 77. Variation of m_{60} with temperature for PAV-aged condition: (a) PG 70-XX binders; (b) PG 76-XX binders



(a)



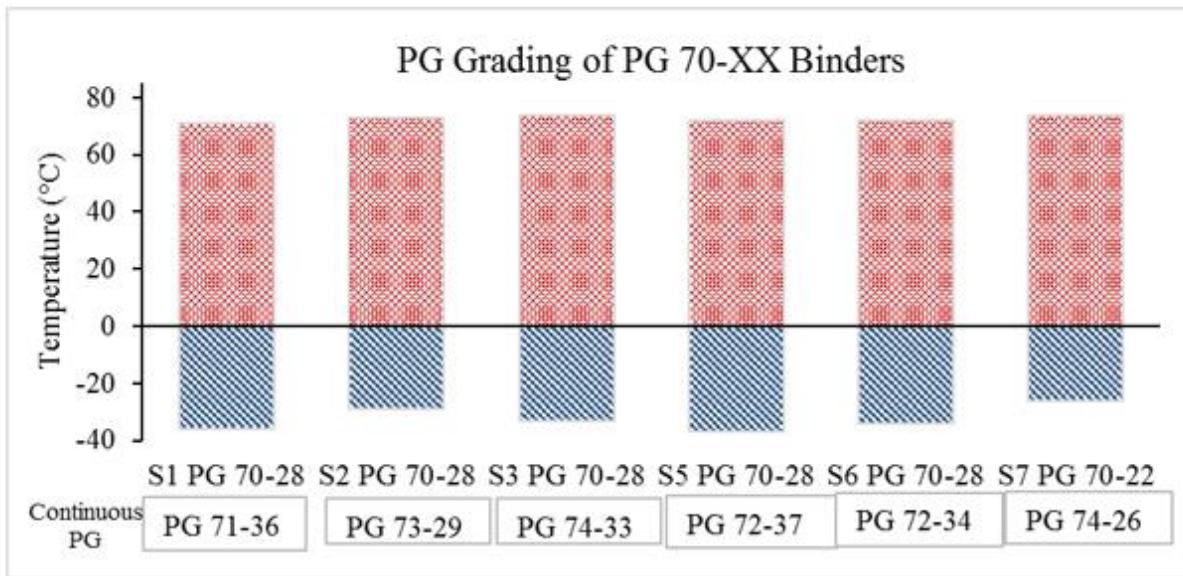
(b)

Figure 78. Variation of S_{60} with temperature for PAV-aged condition: (a) PG 70-XX binders; (b) PG 76-XX binders

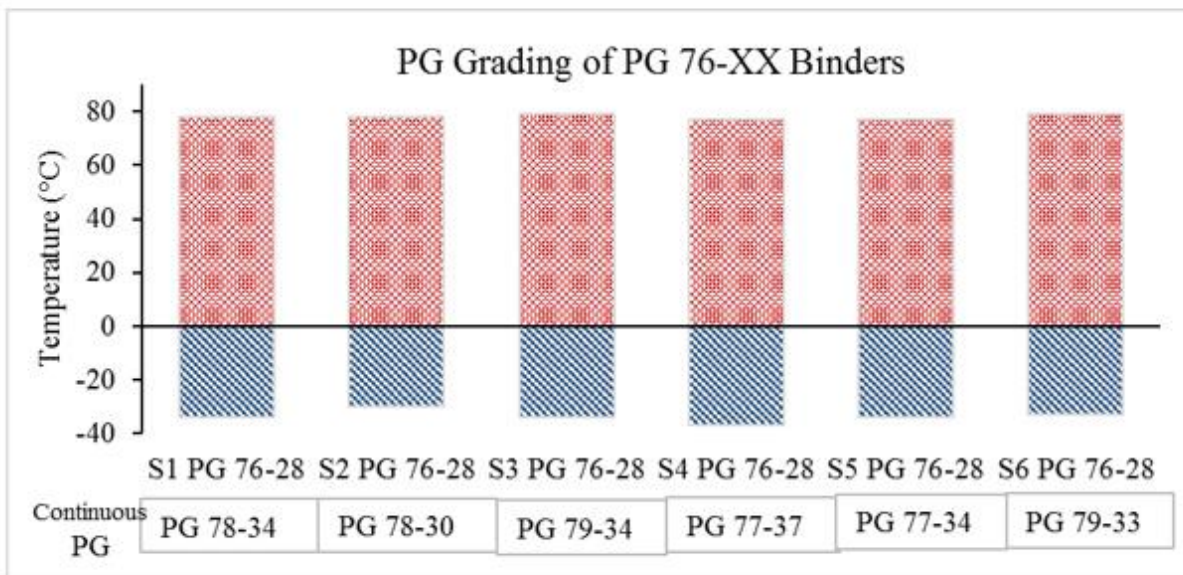
Superpave® PG grading

The continuous high- and low-temperature PG grades of the binders were determined based on the results of the DSR and BBR tests, respectively. According to the Superpave® specifications, the temperature corresponding to a $|G^*|/\sin\delta$ value of 1.0 kPa for unaged or 2.20 kPa for RTFO-aged asphalt binders (whichever is the lowest) was considered as the continuous high-temperature PG grade. From the BBR test results, the temperature corresponding to an m_{60} value of 0.300 or S_{60} value of 300 MPa (whichever is the highest) was considered as the low PG temperature. Tables 29 and 30 present the continuous high- and low- temperature PG grades of the tested

binders. Figures 79 (a) and 79 (b) show graphical representations of the continuous PG grades of the PG 70-XX and PG 76-XX binders, respectively. From Figures 79 (a) and 79 (b), it can be observed that the label used by the manufacturer meets the minimum specifications requirements to be graded as advertised. For instance, the continuous PG temperature of the S1 PG 70-28 binder was found to be PG 71-36.



(a)



(b)

Figure 79. Superpave® PG grading of binders: (a) PG 70-XX; (b) PG 76-XX

Table 29. Continuous high-temperature PG grades of PG 70-XX and PG 76-XX binders

Source	Binder Type	Aging Condition	Temp. (°C)	$ G^* /\sin\delta$ (kPa)	Superpave [®] requirement $ G^* /\sin\delta$ (kPa)	PG Temp. (°C)	Continuous high-temperature PG
S1	PG 70-28	Unaged	67	1.63	1		
S1	PG 70-28	Unaged	70	1.32	1		
S1	PG 70-28	Unaged	73	1.08	1	73.8	
S1	PG 70-28	RTFO-aged	67	3.01	2.2		
S1	PG 70-28	RTFO-aged	70	2.42	2.2		
S1	PG 70-28	RTFO-aged	73	1.96	2.2	71.5	PG 71
S1	PG 76-28	Unaged	73	1.90	1		
S1	PG 76-28	Unaged	76	1.58	1		
S1	PG 76-28	Unaged	79	1.33	1	82.4	
S1	PG 76-28	RTFO-aged	73	3.11	2.2		
S1	PG 76-28	RTFO-aged	76	2.57	2.2		
S1	PG 76-28	RTFO-aged	79	2.15	2.2	78.5	PG 78
S2	PG 70-28	Unaged	67	2.46	1		
S2	PG 70-28	Unaged	70	1.60	1		
S2	PG 70-28	Unaged	73	1.23	1	73.6	
S2	PG 70-28	RTFO-aged	67	4.64	2.2		
S2	PG 70-28	RTFO-aged	70	3.43	2.2		
S2	PG 70-28	RTFO-aged	73	2.67	2.2	74.1	PG 73
S2	PG 76-28	Unaged	73	1.84	1		
S2	PG 76-28	Unaged	76	1.52	1		
S2	PG 76-28	Unaged	79	1.17	1	80.6	
S2	PG 76-28	RTFO-aged	73	3.55	2.2		
S2	PG 76-28	RTFO-aged	76	2.80	2.2		
S2	PG 76-28	RTFO-aged	79	2.14	2.2	78.7	PG 78
S3	PG 70-28	Unaged	67	2.16	1		
S3	PG 70-28	Unaged	70	1.73	1		
S3	PG 70-28	Unaged	73	1.40	1	76	
S3	PG 70-28	RTFO-aged	67	4.00	2.2		
S3	PG 70-28	RTFO-aged	70	3.20	2.2		
S3	PG 70-28	RTFO-aged	73	2.58	2.2	74.4	PG 74
S3	PG 76-28	Unaged	73	1.80	1		
S3	PG 76-28	Unaged	76	1.56	1		
S3	PG 76-28	Unaged	79	1.34	1	83.3	
S3	PG 76-28	RTFO-aged	73	3.41	2.2		
S3	PG 76-28	RTFO-aged	76	2.75	2.2		
S3	PG 76-28	RTFO-aged	79	2.22	2.2	79	PG 79
S4	PG 76-28	Unaged	73	1.34	1		
S4	PG 76-28	Unaged	76	1.08	1		
S4	PG 76-28	Unaged	79	0.87	1	77.2	
S4	PG 76-28	RTFO-aged	73	4.65	2.2		
S4	PG 76-28	RTFO-aged	76	3.90	2.2		
S4	PG 76-28	RTFO-aged	79	3.24	2.2	83.4	PG 77

Table 29. (continue) Continuous high-temperature PG grades of PG 70-XX and PG 76-XX binders

Source	Binder Type	Aging Condition	Temp. (°C)	$ G^* /\sin\delta$ (kPa)	Superpave® requirement $ G^* /\sin\delta$ (kPa)	PG Temp. (°C)	Continuous high-temperature PG
S5	PG 70-28	Unaged	67	1.72	1		
S5	PG 70-28	Unaged	70	1.25	1		
S5	PG 70-28	Unaged	73	0.93	1	72.2	
S5	PG 70-28	RTFO-aged	67	5.22	2.2		
S5	PG 70-28	RTFO-aged	70	3.97	2.2		
S5	PG 70-28	RTFO-aged	73	3.00	2.2	75	PG 72
S5	PG 76-28	Unaged	73	1.56	1		
S5	PG 76-28	Unaged	76	1.16	1		
S5	PG 76-28	Unaged	79	0.86	1	77.7	
S5	PG 76-28	RTFO-aged	73	4.57	2.2		
S5	PG 76-28	RTFO-aged	76	3.60	2.2		
S5	PG 76-28	RTFO-aged	79	2.82	2.2	81	PG 77
S6	PG 70-28	Unaged	67	1.65	1		
S6	PG 70-28	Unaged	70	1.24	1		
S6	PG 70-28	Unaged	73	0.94	1	72.3	
S6	PG 70-28	RTFO-aged	67	3.79	2.2		
S6	PG 70-28	RTFO-aged	70	2.88	2.2		
S6	PG 70-28	RTFO-aged	73	2.18	2.2	72.8	PG 72
S6	PG 76-28	Unaged	73	2.04	1		
S6	PG 76-28	Unaged	76	1.56	1		
S6	PG 76-28	Unaged	79	1.22	1	80.4	
S6	PG 76-28	RTFO-aged	73	4.20	2.2		
S6	PG 76-28	RTFO-aged	76	3.22	2.2		
S6	PG 76-28	RTFO-aged	79	2.47	2.2	79.8	PG 79
S7	PG 70-22	Unaged	67	2.46	1		
S7	PG 70-22	Unaged	70	1.76	1		
S7	PG 70-22	Unaged	73	1.27	1	74.1	
S7	PG 70-22	RTFO-aged	67	7.19	2.2		
S7	PG 70-22	RTFO-aged	70	5.03	2.2		
S7	PG 70-22	RTFO-aged	73	3.53	2.2	74.9	PG 74

Table 30. Continuous low-temperature PG grades of PG 70-XX and PG 76-XX binders

Source	Binder type	BBR parameters	Temp. (°C) -18	Temp. (°C) -21	Superpave® specification requirement	Temp. (°C)	Temp. - 10 (°C)	Continuous low- temperature PG grade
S1	PG 70-28	m ₆₀	0.332	0.323	0.3	-29.22	-39.22	
S1	PG 70-28	S ₆₀ (kPa)	131.1	190.68	300	-26.5	-36.5	PG XX-36
S1	PG 76-28	m ₆₀	0.339	0.328	0.3	-28.58	-38.58	
S1	PG 76-28	S ₆₀ (kPa)	136.77	209.67	300	-24.72	-34.72	PG XX-34
S2	PG 70-28	m ₆₀	0.354	0.321	0.3	-23.16	-33.16	
S2	PG 70-28	S ₆₀ (kPa)	237.46	334.58	300	-19.93	-29.93	PG XX-29
S2	PG 76-28	m ₆₀	0.35	0.33	0.3	-24.33	-34.33	
S2	PG 76-28	S ₆₀ (kPa)	221.74	310.99	300	-20.68	-30.68	PG XX-30
S3	PG 70-28	m ₆₀	0.344	0.33	0.3	-26.84	-36.84	
S3	PG 70-28	S ₆₀ (kPa)	181.71	246.93	300	-23.44	-33.44	PG XX-33
S3	PG 76-28	m ₆₀	0.359	0.34	0.3	-27.1	-37.1	
S3	PG 76-28	S ₆₀ (kPa)	147.26	212.81	300	-24.83	-34.83	PG XX-34
S4	PG 76-28	m ₆₀	0.342	0.328	0.3	-27.33	-37.33	
S4	PG 76-28	S ₆₀ (kPa)	87.25	133.47	300	-31.81	-41.81	PG XX-37
S5	PG 70-28	m ₆₀	0.361	0.348	0.3	-32.59	-42.59	
S5	PG 70-28	S ₆₀ (kPa)	116.6	175.22	300	-27.39	-37.39	PG XX-37
S5	PG 76-28	m ₆₀	0.372	0.339	0.3	-24.6	-34.6	
S5	PG 76-28	S ₆₀ (kPa)	98.3	139.28	300	-32.77	-42.77	PG XX-34
S6	PG 70-28	m ₆₀	0.364	0.337	0.3	-24.93	-34.93	
S6	PG 70-28	S ₆₀ (kPa)	84.98	144	300	-28.93	-38.93	PG XX-34
S6	PG 76-28	m ₆₀	0.379	0.337	0.3	-23.57	-33.57	
S6	PG 76-28	S ₆₀ (kPa)	63.36	109.51	300	-33.38	-43.38	PG XX-33
S7	PG 70-22 ^a	m ₆₀	0.322	0.305	0.3	-16.00	-26.00	
S7	PG 70-22 ^a	S ₆₀ (kPa)	111.38	146.85	300	-27.95	-37.95	PG XX-26

^a S7 PG 70-22 was tested at -12° and -15 °C as per specification requirement.

7.1.2.2 RAP Binder Blends

The effect of the addition of different amounts of RAP binder to the neat binder was evaluated using the Superpave® test method. The Superpave® test results of PG 64-22, PG 64-22-R1-25, PG 64-22-R1-40, PG 64-22-R2-25, PG 64-22-R2-40 binders were adopted from a previous project performed by the OU research team.

DSR test results

Figure 188 presents the variation of the $|G^*|$ with temperature for unaged and RTFO-aged RAP binder blends. From Figure 188, it can be found that the addition of RAP binder increased the $|G^*|$ value of the PG 64-22 binder, as expected. For example, the $|G^*|$ values of the unaged PG 64-22 binder at 61° and 64 °C were found to be 2.39 and 1.70 kPa, respectively. However, the $|G^*|$ values of the PG 64-22-R1-25 binder at 61° and 64 °C were found to be 4.28 and 2.80 kPa, respectively. Also, the PG 64-22-R1-40 and PG 64-22-R1-60 binders were found to exhibit an increasing trend of $|G^*|$ values with an increase in RAP1 binder. Furthermore, a similar trend of increasing $|G^*|$ values with increased amount of RAP binder was observed for the RAP2 binder blends. These results indicate that the shear modulus as well as the stiffness of the PG 64-22 binder are expected to increase with an increase in the amount of RAP binder irrespective of the RAP source [131, 132, 215].

Figure 81 presents the variation of δ values of the RAP binder blends with temperature. From Figure 81, it can be observed that the phase angles of the PG 64-22 binder exhibited a reducing trend with an increase in the amount of RAP binder for both RAP sources. For example, the phase angle of the unaged PG 64-22 binder was found to be 84.63° at 64 °C, whereas the same for the PG 64-22-R2-25 and PG 64-22-R2-40 binders were 84.00° and 79.50° at 64 °C at the same temperature, respectively. Therefore, it can be concluded that addition of RAP binder is expected to reduce the phase angle and change the viscoelastic properties of asphalt binders. Hossain et al. [215] reported a similar increasing trend of $|G^*|$ and a reducing trend of δ values with an increase in the amount of RAP in the binder blends. The oxidative hardening experienced by the RAP binder throughout its service life was reported to be the reason of such observations.

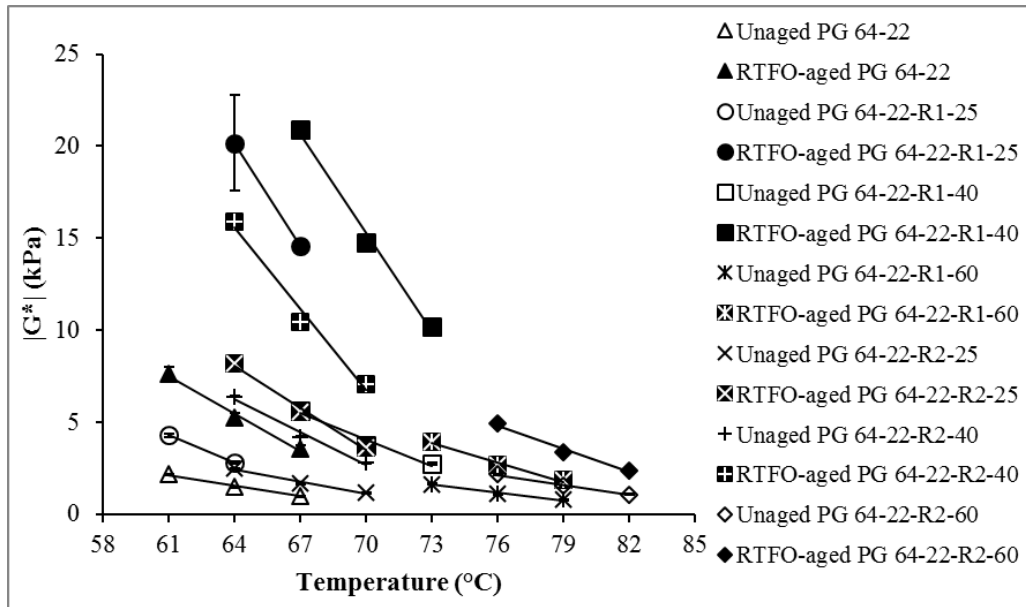


Figure 80 Variation of $|G^*|$ with temperature for unaged and RTFO-aged conditions and 0%, 25%, 40% and 60% RAP1 and RAP2 binder blends

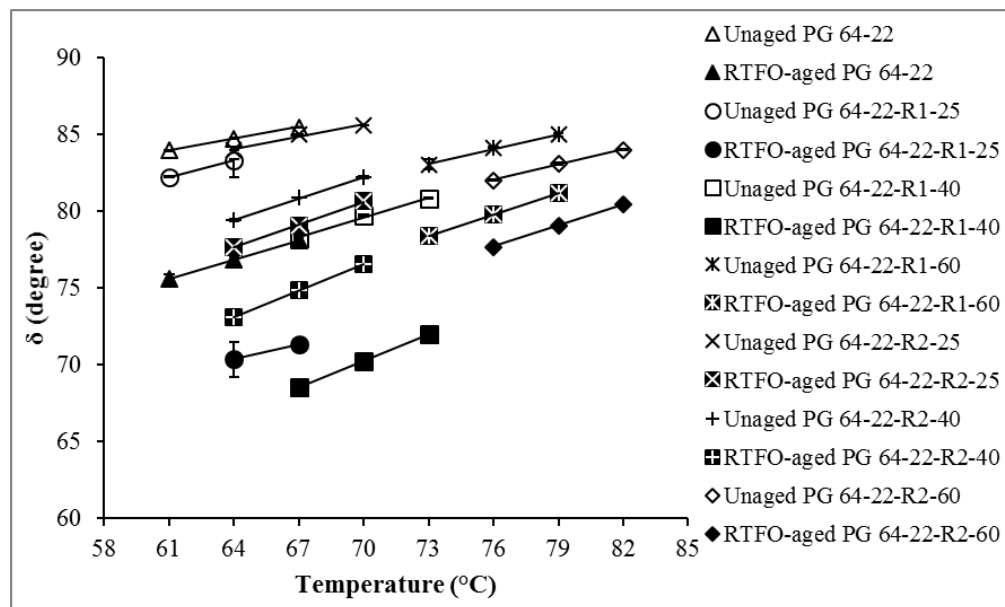


Figure 81 Variation of phase angle with temperature for unaged and RTFO-aged conditions and 0%, 25%, 40% and 60% RAP1 and RAP2 binder blends

Figure 82 presents the effect of blending RAP1 and RAP2 binders on the $|G^*|/\sin\delta$, under unaged and RTFO-aged conditions and at different temperatures. As mentioned earlier, a higher $|G^*|/\sin\delta$ value is an indicator of a higher rutting resistance [145]. The $|G^*|/\sin\delta$ values were found to increase with the blending of RAP binder to the PG 64-22

binder. For example, the $|G^*|/\sin\delta$ values of the PG 64-22-R1-25 and PG 64-22-R1-40 binders were found to be 2.82 and 3.81 kPa at 64 °C. These values were approximately 65% and 125% higher than the $|G^*|/\sin\delta$ of unaged PG 64-22 binder, respectively. A similar increase in the $|G^*|/\sin\delta$ values was also observed for RAP2 binder blends. However, the level of increase in the $|G^*|/\sin\delta$ with addition of RAP binder was found to be dependent on the RAP sources. Therefore, the RAP binder blends are expected to exhibit a higher rutting resistance than those without any RAP binder, as reported by other researchers [131, 132, 215].

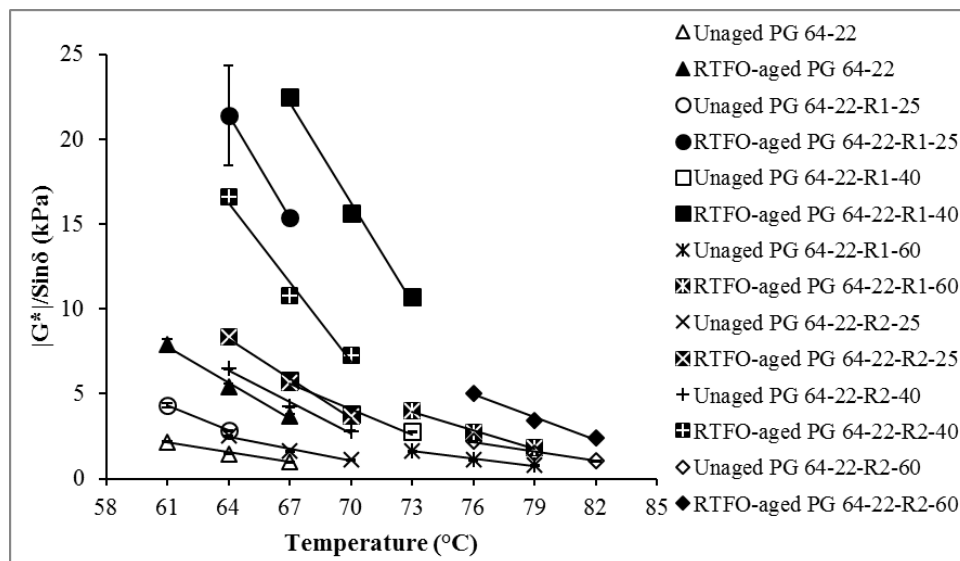


Figure 82. Variation of $|G^*|/\sin\delta$ with temperature for unaged and RTFO-aged conditions and 0%, 25%, 40% and 60% RAP1 and RAP2 binder blends

RV test results

Rotational viscosity test results of the RAP binder blends are presented in Figure 83. From Figure 83, the viscosities of the RAP binder blends are higher than that of the neat PG 64-22 binder. This is due to the fact that the RAP binder experienced oxidative hardening and aging throughout its service life [215]. The viscosities of the PG 64-22 binder exhibited a continuous increasing trend with an increase in the amount of RAP binder. For example, the viscosity of the PG 64-22 binder was found to be 518.75 mPa·s at 135 °C and it increased to 1,054.5 mPa·s (103% increase) and 1237 mPa·s (138% increase) for the PG 64-22-R1-25 and PG 64-22-R1-40 binders, respectively. However, the PG 64-22-R1-60 binder was observed to exhibit a lower viscosity than

those of the PG 64-22-R1-25 and PG 64-22-R1-40 binders. With the addition of RAP2 binder to the neat binder, the viscosity follows a similar increasing trend, as observed for RAP1 binder blends. The viscosity values were approximately 25%, 105% and 153% higher than that of the neat binder for PG 64-22-R2-25, PG 64-22-R2-40 and PG 64-22-R2-60 binders. This indicates that the RAP binder blends are expected to result in a reduced workability, when used in a mix. Colbert and You [131] also reported that the amount of RAP binder added to the neat binder influenced the viscosity and pumping ability of associated asphalt mixes. It was also reported that the workability and the pumping potential based on viscosity of the binder significantly reduced as the amount of RAP binder increased.

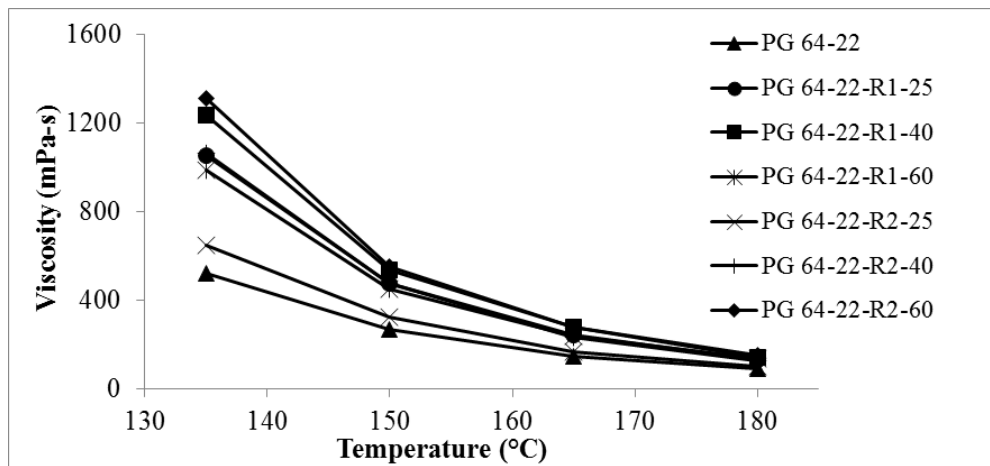


Figure 83. Variation of viscosity with temperature for unaged condition and 0%, 25%, 40% and 60% RAP1 and RAP2 binder blends

BBR test results

For an improved resistance to low-temperature cracking, binders should not be too stiff at low temperatures and need to have the ability to relax of built-up stresses in a reasonable amount of time [145]. Figures 84 and 85 present the m_{60} and the S_{60} values measured by conducting the BBR tests on RAP binder blends. From Figures 84 and 85, it was observed that the m_{60} values reduced and the S_{60} values increased with the addition of RAP1 and RAP2 binder to the PG 64-22 binder. For example, the m_{60} value for neat binder was found to be 0.329 at -12 °C. It reduced to 0.315, 0.299 and 0.302 for the PG 64-22-R2-25, PG 64-22-R2-40 and PG 64-22-R2-60 binders, respectively, at the

same testing temperature. Also, the S_{60} values of the neat binder were found to increase from 127.24 MPa to 142.24, 155.67 and 196.10 MPa for the PG 64-22-R2-25, PG 64-22-R2-40 and PG 64-22-R2-60 binders, respectively, at -12 °C. Similar trends of variation in m_{60} and S_{60} values were observed for RAP1 binder blends except for the PG 64-22-R1-60 binder. It is suspected that some anomalies related to operator, machine or a combination of both had some roles behind such discrepancies in the test results for the PG 64-22-R1-60 binder. As the stiffness of the binder increased and the stress relaxation factor reduced with the addition of RAP binder, the binder blends are expected to exhibit a higher susceptibility to low-temperature cracking. These observations comply with the findings of an earlier study conducted by Daniel et al. [129].

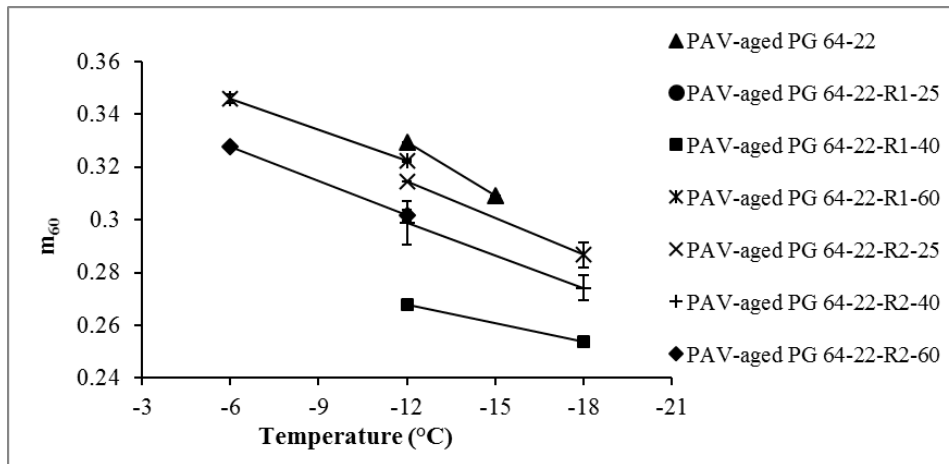


Figure 84. Variation of m_{60} with temperature for PAV-aged condition and 0%, 25%, 40% and 60% RAP1 and RAP2 binder blends

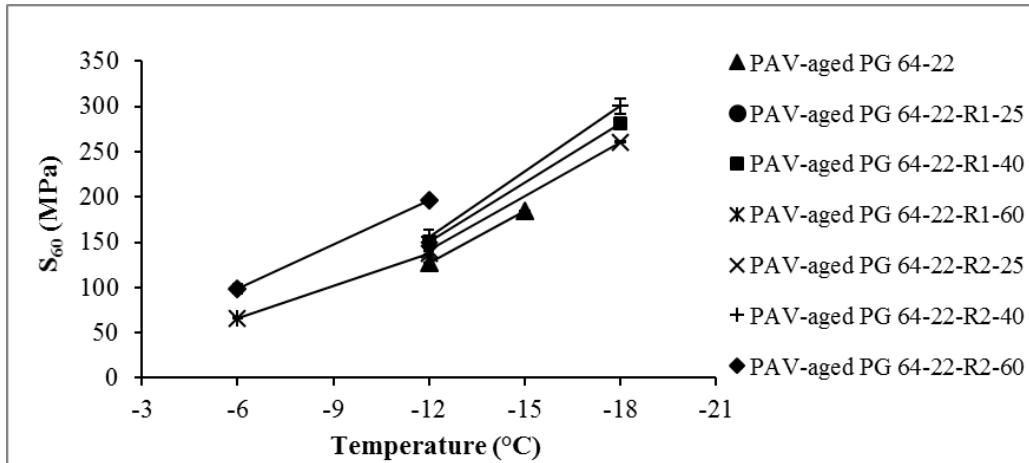


Figure 85. Variation of S_{60} with temperature for PAV-aged condition and 0%, 25%, 40% and 60% RAP1 and RAP2 binder blends

Superpave® PG grading

The continuous PG grades of the RAP binder blends were determined based on the DSR and BBR test results in accordance with the Superpave® specifications. Tables 31, 32 and Figure 86 present the continuous high-and low-temperature PG grades of the RAP binder blends. It can be observed that the high-temperature PG grade increased with an increase in the RAP binder. As seen in Figure 86, the high-temperature PG grade of neat binder changes from PG 66 to PG 67, PG 76 and PG 77 with the addition of 25%, 40% and 60% RAP1 binder, respectively. Also, the high-temperature PG grades were found to be PG 69, PG 71 and PG 82 for the PG 64-22-R2-25, PG 64-22-R2-40 and PG 64-22-R2-60 binders, respectively. Therefore, the change in the high-temperature PG grades was found to be insignificant for the PG 64-22-R1-25 and PG 64-22-R2-25 binders. However, the addition of 40% and 60% RAP1 binders to the neat binder resulted in a bump of about two PG grades. Also, the high-temperature PG grades were observed to be one and three grades higher than that of neat binder for the PG 64-22-R2-40 and PG 64-22-R2-60 binders, respectively. Furthermore, it was found that the continuous low-temperature PG grade of the PG 64-22 binder increased from PG -26 to PG -22 and PG -8 (three PG grade reduction) with the addition of 25% and 40% RAP1 binder. The PG grade of the PG 64-22-R1-60 binder was found not to follow this trend as a new batch of neat binder was used for blending. The low-temperature PG grades of the PG 64-22-R2-25, PG 64-22-R2-40 and PG 64-22-R2-60 binders were found to be PG -25, PG -21 and PG -22, respectively. Therefore, only one grade

increase in the low-temperature PG grade was observed due to the addition of 60% RAP2 binder to the PG 64-22 binder. Overall, these results indicate that the addition of RAP binder to neat binder is expected to decrease the rutting susceptibility of the binder blends and increase the possibility of low-temperature cracking of the binder, when used in a mix [129, 132, 215].

Table 31. Continuous high-temperature PG grades of 0%, 25%, 40% and 60% RAP1 and RAP2 binder blends

Binder type	RAP type	RAP binder (%)	Aging condition	Temp. (°C)	$ G^* /\sin\delta$ (kPa)	Superpave [®] requirement $ G^* /\sin\delta$ (kPa)	Temp. (°C)	Continuous high-temp. PG grade
PG 64-22		0	Unaged	61	2.16	1		
PG 64-22		0	Unaged	64	1.47	1		
PG 64-22		0	Unaged	67	1.00	1	66.7	
PG 64-22		0	RTFO aged	61	7.88	2.2		
PG 64-22		0	RTFO aged	64	5.38	2.2		
PG 64-22		0	RTFO aged	67	3.66	2.2	69.6	PG 66
PG 64-22	RAP1	25	Unaged	61	4.31	1		
PG 64-22	RAP1	25	Unaged	64	2.82	1		
PG 64-22	RAP1	25	Unaged	67	9.52	1	67.7	
PG 64-22	RAP1	25	RTFO aged	61	19.57	2.2		
PG 64-22	RAP1	25	RTFO aged	64	21.40	2.2		
PG 64-22	RAP1	25	RTFO aged	67	15.40	2.2	73.6	PG 67
PG 64-22	RAP1	40	Unaged	67	5.77	1		
PG 64-22	RAP1	40	Unaged	70	3.81	1		
PG 64-22	RAP1	40	Unaged	73	2.78	1	76.0	
PG 64-22	RAP1	40	RTFO aged	67	22.50	2.2		
PG 64-22	RAP1	40	RTFO aged	70	15.67	2.2		
PG 64-22	RAP1	40	RTFO aged	73	10.73	2.2	77.1	PG 76
PG 64-22	RAP1	60	Unaged	73	1.64	1		
PG 64-22	RAP1	60	Unaged	76	1.12	1		
PG 64-22	RAP1	60	Unaged	79	0.79	1	77.25	
PG 64-22	RAP1	60	RTFO aged	73	4.00	2.2		
PG 64-22	RAP1	60	RTFO aged	76	2.71	2.2		
PG 64-22	RAP1	60	RTFO aged	79	1.85	2.2	77.81	PG 77
PG 64-22	RAP2	25	Unaged	64	2.53	1		
PG 64-22	RAP2	25	Unaged	67	1.66	1		
PG 64-22	RAP2	25	Unaged	70	1.15	1	69.26	
PG 64-22	RAP2	25	RTFO aged	64	8.38	2.2		
PG 64-22	RAP2	25	RTFO aged	67	5.64	2.2		
PG 64-22	RAP2	25	RTFO aged	70	3.66	2.2	71.65	PG 69
PG 64-22	RAP2	40	Unaged	64	6.49	1		
PG 64-22	RAP2	40	Unaged	67	4.25	1		
PG 64-22	RAP2	40	Unaged	70	2.82	1	71.35	
PG 64-22	RAP2	40	RTFO aged	64	16.60	2.2		
PG 64-22	RAP2	40	RTFO aged	67	10.75	2.2		
PG 64-22	RAP2	40	RTFO aged	70	7.27	2.2	72.89	PG 71
PG 64-22	RAP2	60	Unaged	76	2.19	1		
PG 64-22	RAP2	60	Unaged	79	1.53	1		
PG 64-22	RAP2	60	Unaged	82	1.08	1	82.21	
PG 64-22	RAP2	60	RTFO aged	76	5.02	2.2		
PG 64-22	RAP2	60	RTFO aged	79	3.45	2.2		
PG 64-22	RAP2	60	RTFO aged	82	2.39	2.2	82.2	PG 82

Table 32. Continuous low-temperature PG grades of 0%, 25%, 40% and 60% RAP1 and RAP2 binder blends

RAP type	RAP binder (%)	Test Temp. (°C)	m60 (Spec.:0.3)	S60 (kPa) (Spec.: 300)	Temp. (°C)	Temp. – 10 (°C)	Continuous low-temp. PG grade
	0	-12	0.329	-			
	0	-15	0.309	-	-16.4	-26.4	
	0	-12	-	127.24			
	0	-15	-	184.19	-21.1	-31.1	PG XX-26
RAP 1	40	-12	0.268	-			
RAP 1	40	-18	0.254	-	1.8	-8.17	
RAP 1	40	-12	-	151.27			
RAP 1	40	-18	-	280.92	-18.9	-28.9	PG XX-8
RAP 1	60	-6	0.346	-			
RAP 1	60	-12	0.322	-	-17.7	-27.7	
RAP 1	60	-6	-	66.6			
RAP 1	60	-12	-	136.47	-25.6	-35.6	PG XX-27
RAP 2	25	-12	0.315	-			
RAP 2	25	-18	0.287	-	-15.1	-25.1	
RAP 2	25	-12	-	142.2			
RAP 2	25	-18	-	260.51	-20	-30	PG XX-25
RAP 2	40	-12	0.299	-			
RAP 2	40	-18	0.274	-	-11.7	-21.7	
RAP 2	40	-12	-	155.6			
RAP 2	40	-18	-	300.56	-18	-28	PG XX-21
RAP 2	60	-6	0.328	-			
RAP 2	60	-12	0.302	-	-12.4	-22.4	
RAP 2	60	-6	-	98.6			
RAP 2	60	-12	-	196.1	-18.4	-28.4	PG XX-22

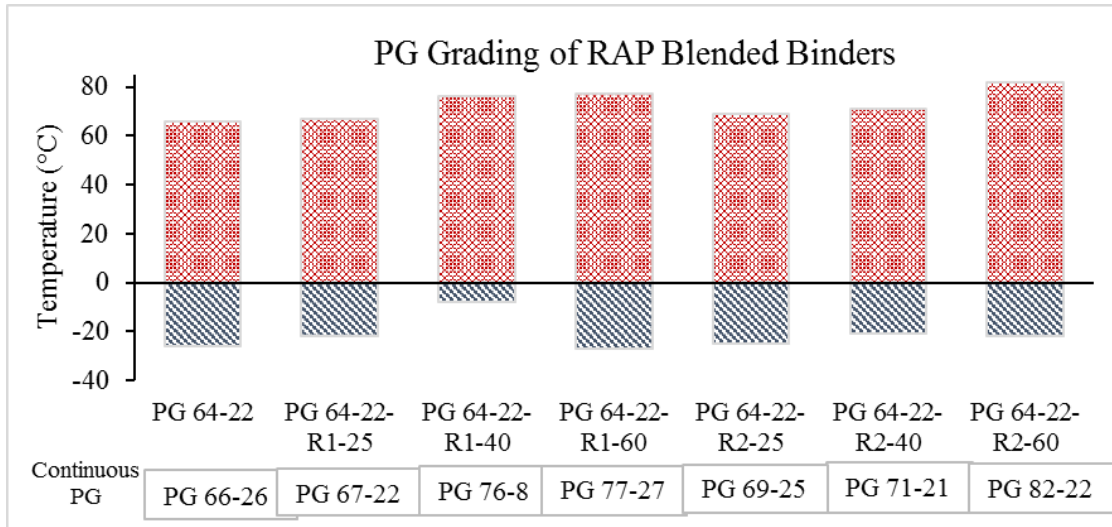


Figure 86. Superpave® PG grading of 0%, 25%, 40% and 60% RAP1 and RAP2 binder blends

7.1.3 MSCR Test Results

7.1.3.1 Polymer-modified Binders

The MSCR tests on the RTFO-aged polymer-modified PG 70-XX and PG 76-XX asphalt binder samples were conducted at a temperature of 64 °C. Pertinent results of the J_{nr} (0.1 kPa), J_{nr} (3.2 kPa), $J_{nr\ diff}$, R_{100} and R_{3200} values, as well as the R_{diff} of the PG 70-XX and PG 76-XX binders, are presented in Table 33. The term “ R_{100} ” denotes the MSCR %Recovery at 0.1 kPa, whereas J_{nr} (0.1 kPa) refers to the non-recoverable creep compliance obtained from the MSCR test at 0.1 kPa. The $J_{nr\ diff}$ refers to the percent difference in J_{nr} values as the stress level changes from 0.1 kPa to 3.2 kPa.

Non-recoverable creep compliance (J_{nr})

The results of the J_{nr} values of the PG 70-XX and PG 76-XX binders at 0.1 and 3.2 kPa stress levels and 64 °C are presented in Figures 87 (a) and 87 (b). Generally, a lower J_{nr} value for binder represents a higher rutting resistance when used in a mix (D’Angelo, 2010). From Figures 87 (a) and 87 (b), relatively low J_{nr} values were observed for both PG 70-XX and PG 76-XX binders and they fell below 0.5 kPa^{-1} . For both PG 70-XX and PG 76-XX binders, it can be observed that the J_{nr} value measured at 3.2 kPa stress level was unchanged or higher compared to that measured at 0.1 kPa stress level. For

example, the J_{nr} for the S5 PG 70-28 binder was found to increase from 0.25 to 0.33 kPa^{-1} when the stress level increased from 0.1 to 3.2 kPa. However, the J_{nr} value of the S1 PG 76-28 remained unchanged with a change in the stress level.

Table 33.MSCR test results for PG 70-XX and PG 76-XX binders at 64 °C

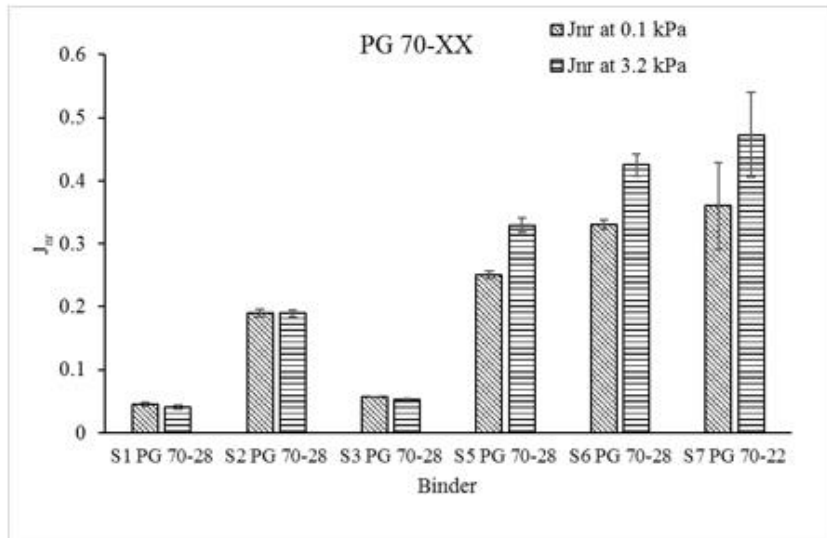
Binder Type	Temp (°C)	J_{nr} (0.1 kPa) kPa^{-1}	J_{nr} (3.2 kPa) kPa^{-1}	$J_{nr \text{ diff}}$ (0.1-3.2)	Stress sensitivity (Meets AASTHO MP 19)	R_{100} (%)	R_{3200} (%)	R_{diff} (0.1-3.2)	%Recovery (Meets AASTHO TP 70)	MSCR grade
S1 PG 70-28	64	0.05	0.04	-8.95	Yes	96.15	95.8	0.36	Yes	PG 64E-XX
S1 PG 76-28	64	0.02	0.02	-6.30	Yes	97.29	97.24	0.05	Yes	PG 64E-XX
S2 PG 70-28	64	0.19	0.19	2.10	Yes	77.79	77.4	0.44	Yes	PG 64E-XX
S2 PG 76-28	64	0.06	0.06	-1.65	Yes	89.56	89.8	-0.32	Yes	PG 64E-XX
S3 PG 70-28	64	0.06	0.05	-5.75	Yes	94.05	94	0.05	Yes	PG 64E-XX
S3 PG 76-28	64	0.06	0.06	1.94	Yes	91.89	91.9	-0.05	Yes	PG 64E-XX
S4 PG 76-28	64	0.03	0.03	-2.35	Yes	94.71	94.45	0.28	Yes	PG 64E-XX
S5 PG 70-28	64	0.25	0.33	31.89	Yes	71.41	63.8	10.60	Yes	PG 64E-XX
S5 PG 76-28	64	0.08	0.10	28.03	Yes	81.84	76.4	6.63	Yes	PG 64E-XX
S6 PG 70-28	64	0.33	0.43	28.66	Yes	71.31	64.68	9.29	Yes	PG 64E-XX
S6 PG 76-28	64	0.11	0.14	30.02	Yes	80.32	75.74	5.69	Yes	PG 64E-XX
S7 PG 70-22	64	0.36	0.47	31.21	Yes	42.77	30.27	29.22	No	PG 64E-XX

Therefore, selecting the right stress level of the MSCR test is important to predict the rutting susceptibility of the binder with respect to the J_{nr} value. Furthermore, from Figures 87 (a) and 87 (b), variations in J_{nr} values can be observed for the binders of same PG grade but different sources. For example, the PG 70-XX binders were found to exhibit J_{nr} values ranging from 0.05 kPa^{-1} (S1 PG 70-28) to 0.36 (S7 PG 70-22) at 0.1

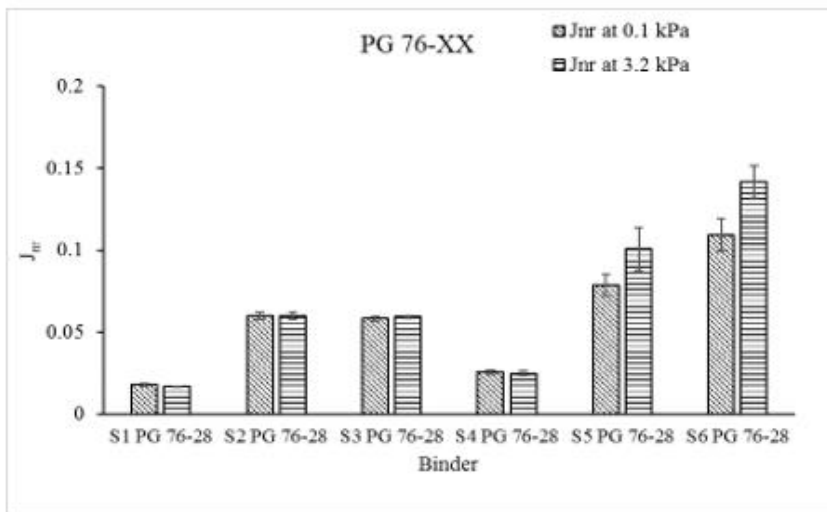
kPa and from 0.04 kPa^{-1} (S1 PG 70-28) to 0.47 (S7 PG 70-22) at 3.2 kPa stress levels. Also, the J_{nr} values for the PG 76-XX binders were observed to vary from 0.02 kPa^{-1} (S1 PG 76-28) to 0.11 (S6 PG 76-28) at 0.1 kPa and from 0.02 kPa^{-1} (S1 PG 76-28) to 0.14 (S6 PG 76-28) at 3.2 kPa stress levels. Thus, it can be concluded that, the J_{nr} values as-well-as the rutting performance of the binders can vary although they have the same Superpave® PG grade. These observations were found to be consistent with the findings of the other studies [180].

MSCR %Recovery

Figures 88 (a) and 88 (b) present the %Recovery values of the PG 70-XX and PG 76-XX binders from MSCR tests conducted at a temperature of $64 \text{ }^\circ\text{C}$. According to D'Angelo (2010), the %Recovery value obtained from the MSCR test at high temperatures can be used to evaluate the rutting performance of a pavement. This parameter can also provide useful information regarding the reaction of base binder with polymer and formation of the polymer network [161]. The %Recovery value measured at the 3.2 kPa stress level was found to be unchanged or lower than that measured at the 0.1 kPa stress level for both polymer-modified binders. For example, the S1 PG 70-28 binder was found to exhibit an insignificant reduction (0.36% difference) in the %Recovery with an increase in the stress level from 0.1 kPa to 3.2 kPa . A reason for such a low reduction in the %Recovery may be attributed to the linear viscoelastic behavior of the binder at both stress levels. Another reason can be the shortness of the rest period in the test procedure, which may cause the binder not to have enough time to fully recover at the end of loading and unloading cycles at 0.1 kPa stress level [216].



(a)

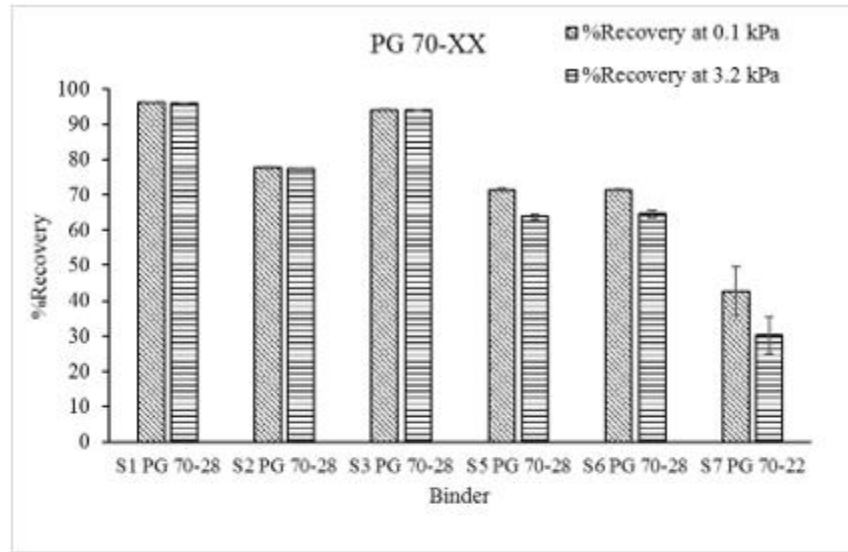


(b)

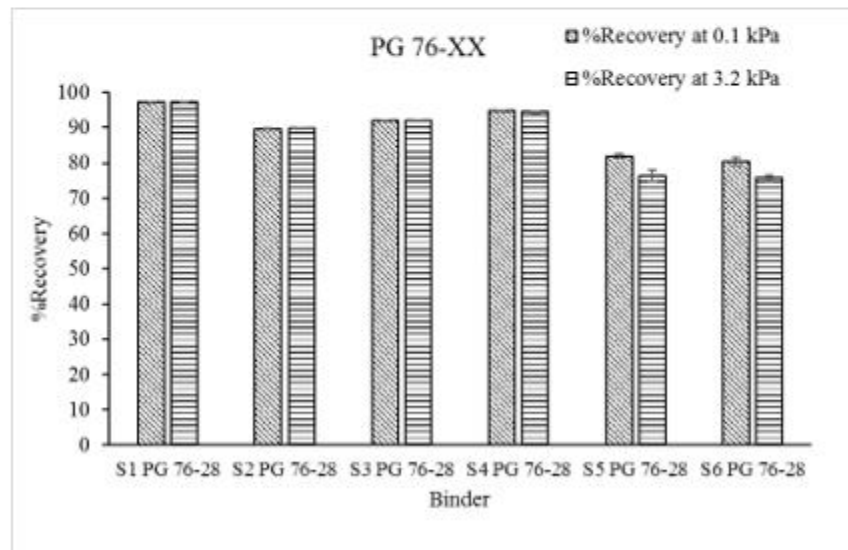
Figure 87. Effect of source on J_{nr} values at 64 °C: (a) PG 70-XX binders; (b) PG 76-XX binders

However, the %Recovery value of the S7 PG 70-22 binder was found to reduce by approximately 29.22% when the stress level increased from 0.1 to 3.2 kPa. Also, from Figures 88 (a) and 88 (b), relatively high %Recovery values were observed for both PG 70-XX and PG 76-XX binders from all sources except for the S7 PG 70-22. D'Angelo [161] reported that a high %Recovery value obtained from an MSCR test can be used as an indication of strong polymer network in the binder at the corresponding high temperature. D'Angelo [161] also tested the PPA-, SBS linear polymer- and SBS radial

polymer-modified binders under fluorescence micrographs to establish relationship between %Recovery and polymer network. The polymers in the binders with low %Recovery were found to simply float in the asphalt. On the other hand, the binders with a high %Recovery were found to exhibit a strong polymer network with a leathery look indicating extensive cross-linking and well-dispersed concentrations of polymers [161].



(a)



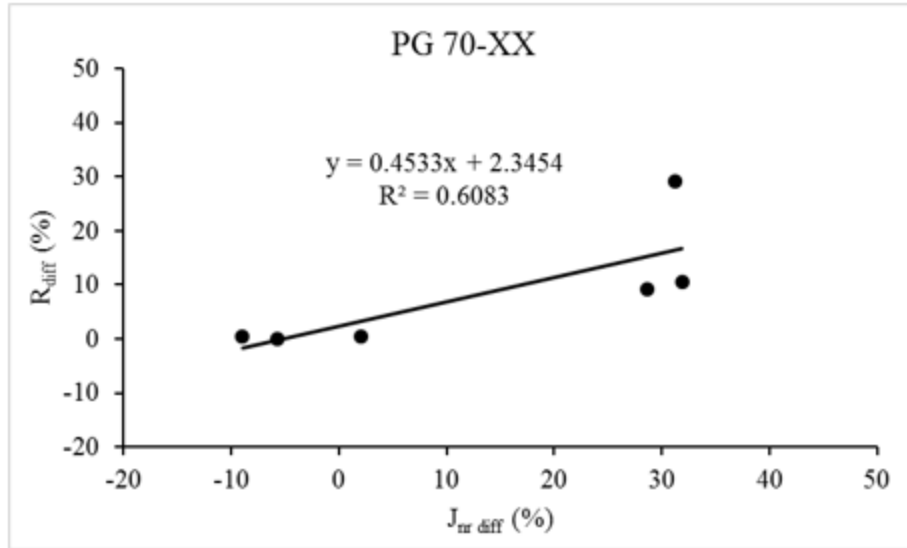
(b)

Figure 88. Effect of Source on %Recovery values at 64 °C: (a) PG 70-XX binders; (b) PG 76-XX binders

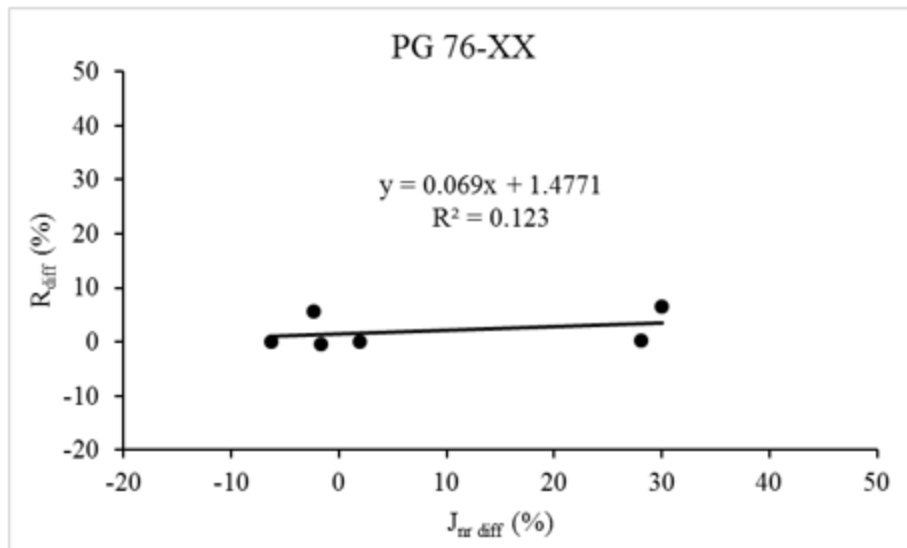
Therefore, it can be concluded that all the PG 70-XX and PG 76-XX binders except S7 PG 70-22 are expected to have a strong polymer network at 64 °C. Furthermore, similar to J_{nr} values, binders with the same PG grade were found to exhibit variations in %Recovery values. For example, the %Recovery of PG 70-XX binders were found to vary from 96.15% (S1 PG 70-28) to 42.77% (S7 PG 70-22) at 0.1 kPa and from 95.8% (S1 PG 70-28) to 30.27% (S7 PG 70-22) at 3.2 kPa stress levels. The %Recovery values for the tested PG 76-XX binders were observed to be as high as 97.24% for the S1 PG 76-28 binder and as low as 75.74% for the S6 PG 76-28 binder at 3.2 kPa stress level. Therefore, despite having the same PG grade, the %Recovery values at certain stress levels and temperatures can vary depending on the viscoelastic behavior of a particular binder and binder source. These observations support the findings of other studies [161, 180, 175]

Stress sensitivity

Table 33 presents the percentage difference in J_{nr} values ($J_{nr \text{ diff}}$) while the stress level changes from 0.1 kPa to 3.2 kPa at 64 °C. From Table 33 it can be observed that all the polymer-modified binders met the minimum stress sensitivity requirement ($J_{nr \text{ diff}} < 75\%$) proposed by the AASHTO MP 19 (AASHTO, 2010) specification. The maximum increase in J_{nr} values for the PG 70-XX and PG 76-XX binders were found to be 31.89% and 28.03%, respectively. Therefore, it can be concluded that the tested polymer-modified binders were not overly stress sensitive. This means that the binders are expected not to undergo high amount of strain when subjected to unexpected heavy loads or unusually high temperatures. Figures 89 (a) and 89 (b) show the variation of $J_{nr \text{ diff}}$ with R_{diff} values for the tested polymer-modified binders. These plots provide an insight on the trend of changes in J_{nr} with %Recovery values when subjected to a high stress level. From Figures 89 (a) and 89 (b), it can be observed that the rate of increase in %Recovery of the PG 70-XX binder has a relatively good correlation with the rate of increase in J_{nr} value. Comparatively, the PG 76-XX binder did not exhibit a good correlation. Therefore, it can be concluded that the changes in %Recovery of the PG 76-XX binders are expected to be less sensitive to the change in stress level than that of the J_{nr} value.



(a)



(b)

Figure 89. Variation of $J_{nr\ diff}$ with R_{diff} at 64 °C: (a) PG 70-XX binder; (b) PG 76-XX binder

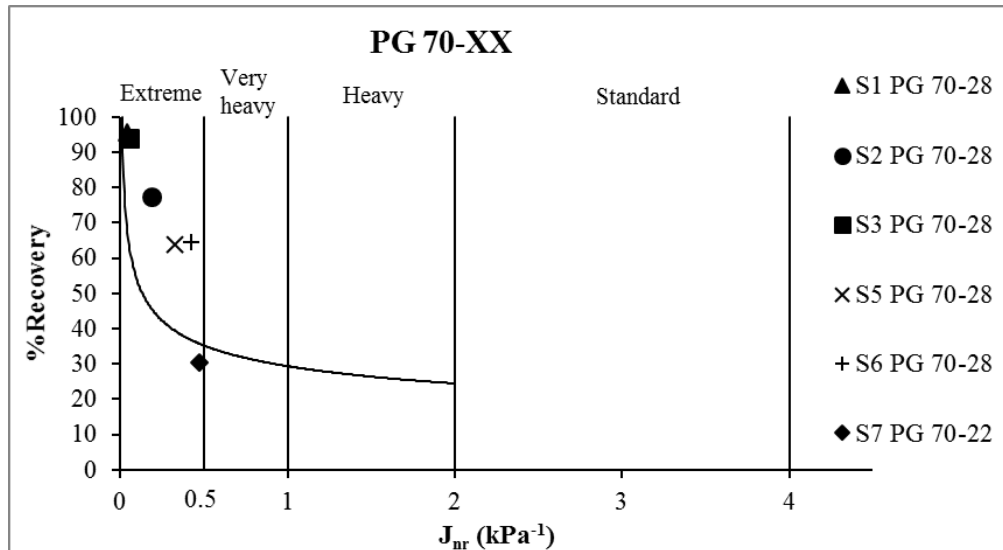
Polymer method

The analysis of the results of the MSCR tests conducted on the PG 70-XX and PG 76-XX binders using polymer curve are presented in Figures 90 (a) and 90 (b), respectively. In these figures, the %Recovery values at the 3.2 kPa stress level and 64 °C temperature were plotted against the corresponding J_{nr} values. From Figure 90 (a),

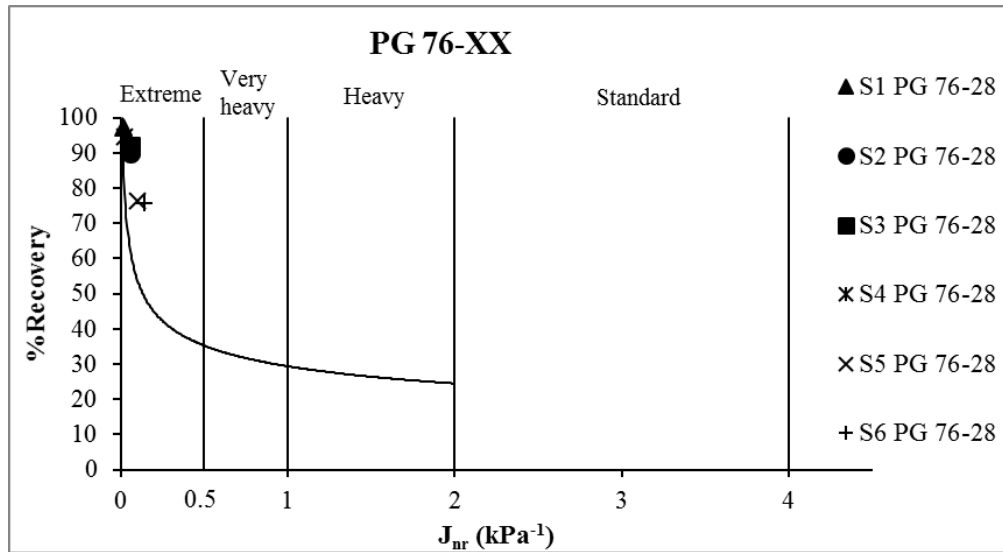
all the PG 70-XX binders were found to meet the %Recovery requirement proposed by the AASHTO TP 70 [164] specification, except the S7 PG 70-22 binder. The %Recovery of S7 PG 70-22 binder was found to fall below the MSCR curve, which means either the binder was not modified with elastomeric modifiers or the modification level was low. As evident from Figure 90 (b), the data points for the PG 76-XX binders were found to be clustered above the MSCR curve. These results indicate that the PG 76-XX binders were modified with elastomeric polymers. No conclusive comment could be made on the effect of a particular polymer on the performance properties of the asphalt binder as the types and the amounts of polymers used by the refineries were unavailable.

MSCR grading system

The MSCR grades of the PG 70-XX and PG 76-XX binders were determined according to the AASHTO MP 19 [184] specification and are presented in Table 4.5 and Figures 90 (a) and 90 (b). From Table 33, it is evident that the grades of all the tested PG 70-XX and PG 76-XX binders were found to be PG 64E-XX. This means that the tested PG 70-XX and PG 76-XX binders can sustain extreme traffic level at 64 °C without significant permanent deformation, when used in a mix. The results of the MSCR binder grade indicates that the tested polymer-modified binders are expected to exhibit high rutting resistance at 64 °C temperature and at extreme level of traffic, when used in a mix [174].



(a)



(b)

Figure 90. Polymer curve analysis at 64 °C and 3.2 kPa stress level: (a) PG 70-XX binders; (b) PG 76-XX binders

Effect of increased stress level

In addition to the stress levels recommended by AASHTO TP 70 [164], the MSCR tests were also conducted at the 10 kPa stress level to determine the stress sensitivity and non-linearity of the polymer-modified binders. Table 34 presents the results of the MSCR tests conducted at three different stress levels, namely 0.1, 3.2 and 10 kPa, at 64 °C.

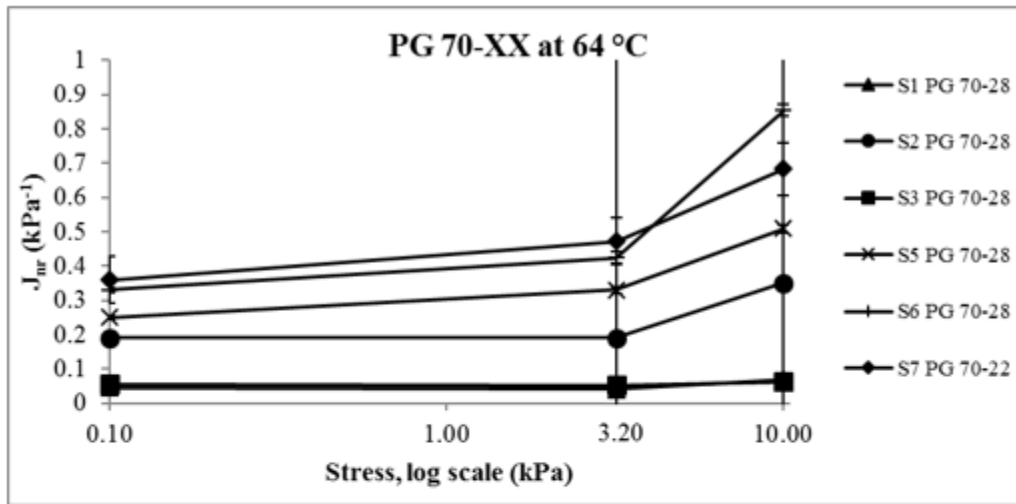
Table 34. MSCR test results for PG 70-XX and PG 76-XX binders at 64 °C and 0.1, 3.2 and 10 kPa

Binder Type	Temp (°C)	J _{nr} (0.1 kPa) kPa ⁻¹	J _{nr} (3.2 kPa) kPa ⁻¹	J _{nr} (10 kPa) kPa ⁻¹	J _{nr diff} (0.1-3.2)	J _{nr diff} (3.2-10)	R ₁₀₀ (%)	R ₃₂₀₀ (%)	R ₁₀₀₀₀ (%)	R _{diff} (0.1-3.2)	R _{diff} (3.2-10)
S1 PG 70-28	64	0.05	0.04	0.07	-8.95	67.34	96.15	95.8	91.14	0.36	4.864
S1 PG 76-28	64	0.02	0.02	0.02	-6.3	-1.98	97.29	97.24	96.57	0.05	0.69
S2 PG 70-28	64	0.19	0.19	0.35	2.1	82.67	77.79	77.4	58.34	0.44	24.66
S2 PG 76-28	64	0.06	0.06	0.07	-1.65	3.61	89.56	89.8	88.41	-0.32	1.59
S3 PG 70-28	64	0.06	0.05	0.06	-5.75	17.24	94.05	94	91.21	0.05	2.97
S3 PG 76-28	64	0.06	0.06	0.06	1.94	-3.87	91.89	91.9	91.13	-0.05	0.87
S4 PG 76-28	64	0.03	0.03	0.03	-2.35	16.97	94.71	94.45	92.177	0.28	2.40
S5 PG 70-28	64	0.25	0.33	0.51	31.89	54.46	71.41	63.8	47.92	10.6	24.93
S5 PG 76-28	64	0.08	0.1	0.28	28.03	180.16	81.84	76.4	49.55	6.63	35.16
S6 PG 70-28	64	0.33	0.43	0.85	28.66	101.01	71.31	64.68	34.56	9.29	46.57
S6 PG 76-28	64	0.11	0.14	0.21	30.02	45.73	80.32	75.74	65.78	5.69	13.15
S7 PG 70-22	64	0.36	0.47	0.68	31.21	44.57	42.77	30.27	17.28	29.22	42.92

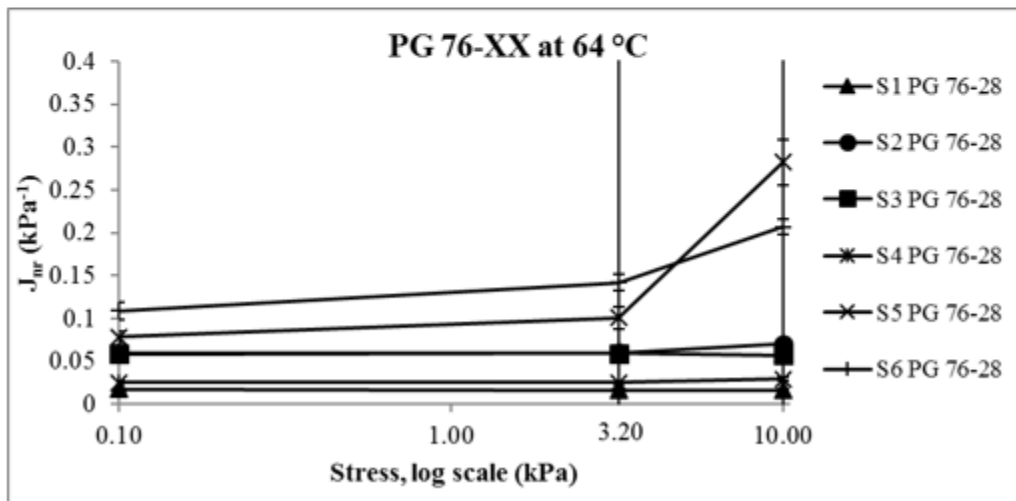
Figures 91 (a) and 91 (b) show the changes in J_{nr} values with stress levels at 64 °C. According to Golalipour [111] the use of increased stress levels can help to differentiate the rutting performance of the binders and identify the performance of the binders when used in a mix. For example, the J_{nr} values of the PG 70-XX binders were observed to remain unchanged with an increase in the stress level from 0.1 to 3.2 kPa. However, significant changes in the J_{nr} values were observed for most of the PG 70-XX binders while increasing the stress level from 3.2 to 10 kPa. According to Golalipour [111], this rapid changing in J_{nr} value can be used as an indicator of non-linear behavior of asphalt binder. Therefore, it can be concluded that the PG 70-XX binders started exhibiting non-linear viscoelastic behavior at the 10 kPa stress level. The transition between linear and non-linear viscoelastic region of the tested binders are expected to lie at a stress level between 3.2 and 10 kPa. However, the variation in the J_{nr} values of the PG 70-XX binders from S1 and S2 sources were found to be insignificant at different stress levels. From Figure 91 (b), it can be observed that four out of six sources of the tested PG 76-XX binders were found not to exhibit any significant change in J_{nr} values with an increase in stress level from 3.2 to 10 kPa. This indicates that the stress sensitivities of the binders were relatively low when they were tested at stress levels up to 10 kPa. Therefore, the PG 76-XX binders were observed to behave as a linear viscoelastic material up to the 10 kPa stress level. However, the PG 76-XX binders from S5 and S6 sources exhibited a relatively high amount of change (55% for S5 and 180% for S6) in J_{nr} with an increase in the stress level from 3.2 to 10 kPa. This means that the binders from S5 and S6 sources became overly stress sensitive with an increase in stress level. The high non-linearity of these binders might result in poor performance when subjected to high stress levels in pavements [111].

The variation in %Recovery of the PG 70-XX and PG 76-XX binders at 64 °C with an increase in the stress levels is presented in Figures 92 (a) and 92 (b). As can be seen in Figure 92 (a), the %Recovery values of the PG 70-XX binders from S1 and S2 sources remained unchanged with an increase in stress level. However, significant changes in the %Recovery values were observed for the PG 70-XX binders from other sources (Source S3, S4, S5 and S6). Also, a sharp reduction in the %Recovery value was

observed only for the S5 PG 76-28 and S6 PG 76-28 binders with an increasing stress level. Furthermore, the %Recovery of the PG 76-28 binders from other sources (S1, S2, S3 and S4) was found to exhibit a relatively low stress sensitivity. Like the J_{nr} parameter, the binders with highly non-linear behavior are expected to exhibit a high amount of reduction in %Recovery when the stress level increased from 3.2 to 10 kPa.

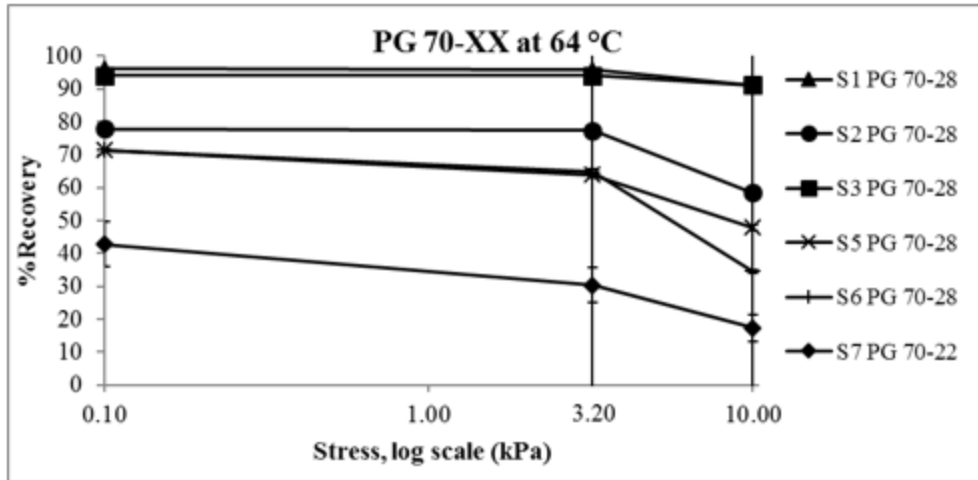


(a)

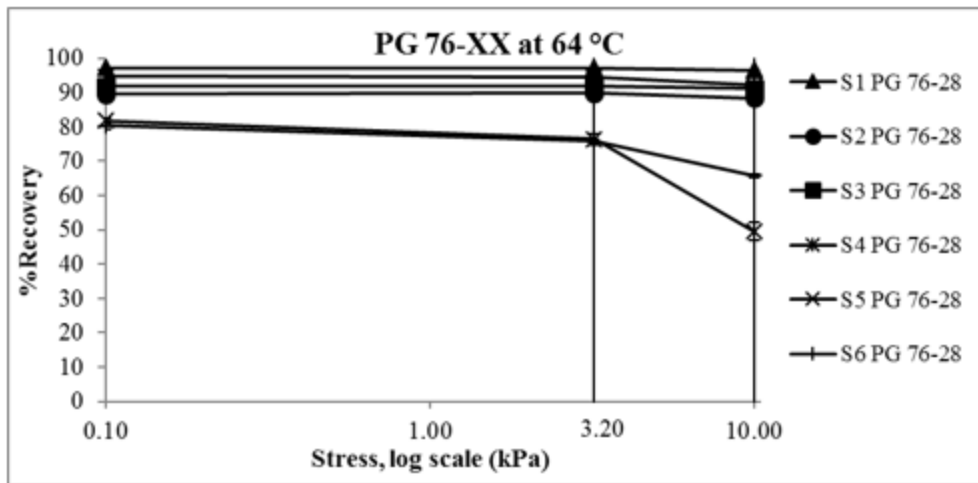


(b)

Figure 91. Change in J_{nr} value with stress levels at 64 °C: (a) PG 70-XX binders; (b) PG76-XX binders



(a)



(b)

Figure 92. Change in % Recovery with stress levels at 64 °C: (a) PG 70-XX binders; (b) PG 76-XX binders

Figures 93 (a) and 93 (b) show variations of the $J_{nr\ diff}$ and $\%R_{diff}$ values with a change in stress level for polymer-modified binders. The $J_{nr\ diff}$ and $\%R_{diff}$ between 10 kPa and 3.2 kPa stress levels were found to be higher than those between 3.2 kPa and 0.1 kPa stress levels. This indicates that the tested binders became more sensitive to stress level with an increase in the stress level from 3.2 to 10 kPa. Also, the PG 70-XX binders were observed to become more stress sensitive than the PG 76-XX binders, except the S5 PG 76-28 binder. The high polymer modification used to produce PG 76-XX binder is likely responsible for the lower stress sensitivity. Therefore, conducting the MSCR test at a stress level higher than 3.2 kPa will help to understand the stress sensitivity

and non-linearity of polymer-modified binders. Golalipour [111] suggested to use 10 kPa as an additional stress level for MSCR testing of polymer-modified binders to obtain a wider spectrum of binder behavior under different stress levels.

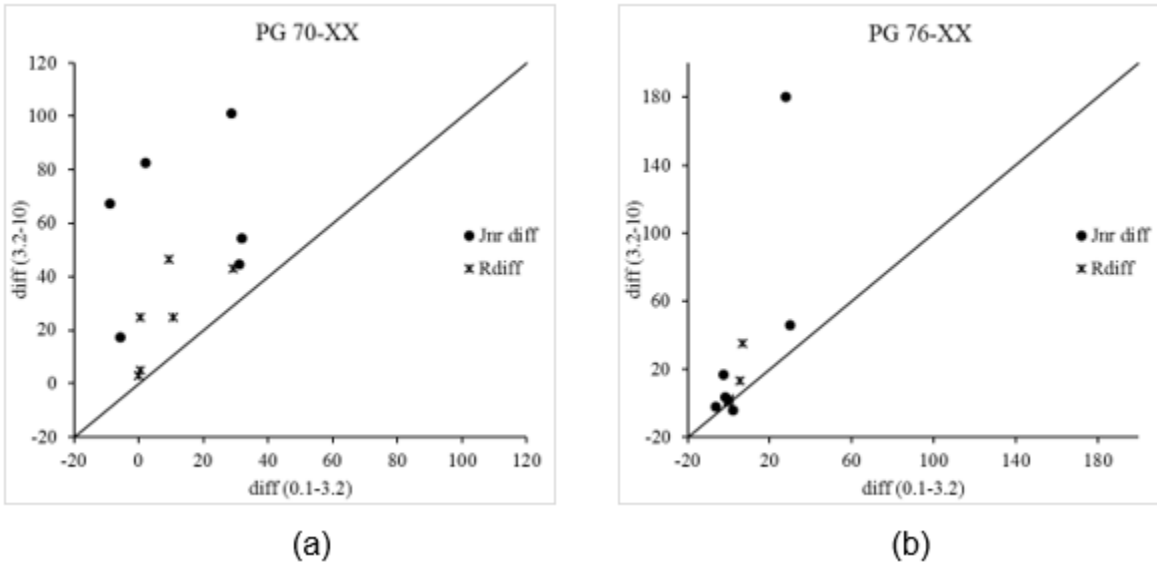
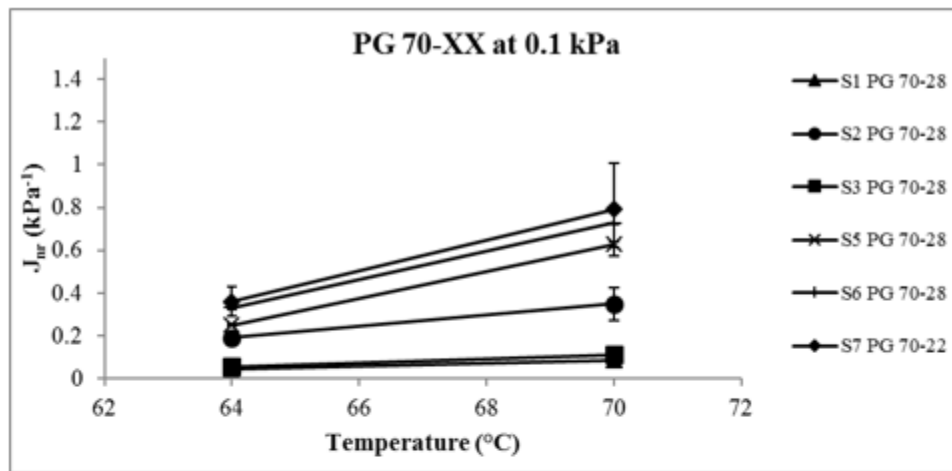


Figure 93. Plot of $J_{nr\ diff}$ and R_{diff} with increasing stress levels at 64 °C: (a) PG 70-XX binders; (b) PG 76-XX binders

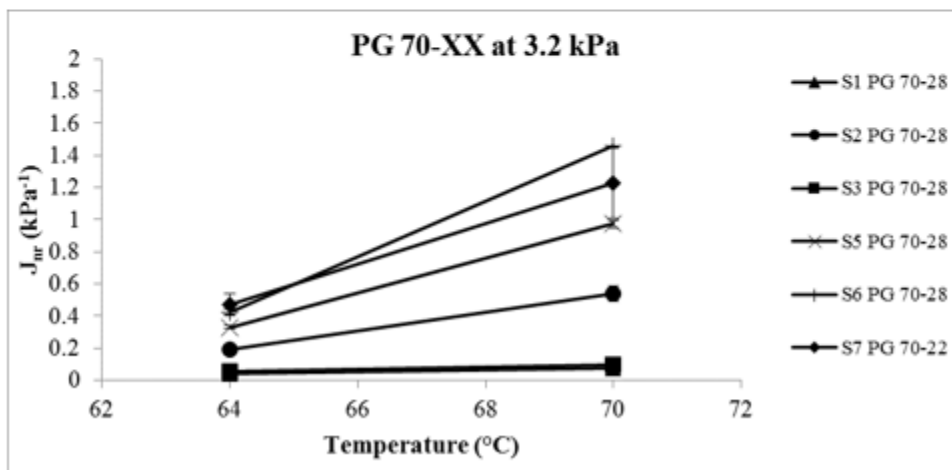
Effect of higher temperatures

The temperature sensitivity of the J_{nr} and %Recovery parameter of the PG 70-XX and PG 76-XX binders were evaluated by conducting MSCR tests at temperatures higher than 64 °C. Specifically, the PG 70-XX binders were tested at 70° C and the PG 76-XX binders were tested at 70° and 76 °C. Figures 94 (a) and 94 (b) present the variation of J_{nr} with temperature for the PG 70-XX binders and Figures 95 (a) and 95 (b) present the variation of J_{nr} with temperature for the PG 76-XX binders at 0.1 and 3.2 kPa stress levels, respectively. From Figures 94 and 95, it is evident that the J_{nr} values of the polymer-modified binders depend on the temperature. The J_{nr} values of both the binders were found to increase with an increase in temperature. For example, the J_{nr} value of the S6 PG 70-28 at 0.1 kPa stress level was found to increase from 0.33 to 0.73 kPa^{-1} when the temperature increased from 64° to 70 °C. The effect of the temperature change on the J_{nr} value was found to be more pronounced at 76 °C for PG 76-XX binders. A similar increasing trend of the J_{nr} with an increase in the temperature was observed by other researchers [169, 173, 175, 180]. Also, from Figures 94 and 95, the

differences between the J_{nr} values at 0.1 and 3.2 kPa stress levels were more significant at higher temperatures. Furthermore, the difference between J_{nr} values of asphalt binders of the same PG grade became more significant with an increase in temperature. For example, the J_{nr} values of the PG 76-XX binders from different sources were found to vary significantly from each other at 76 °C than that at 64° and 70 °C. According to Zhang et al. [173], the temperature sensitivity of the J_{nr} parameter can be correlated with the temperature sensitivity of rutting. Therefore, binders are expected to exhibit lower rutting resistance at higher temperature and vice versa.

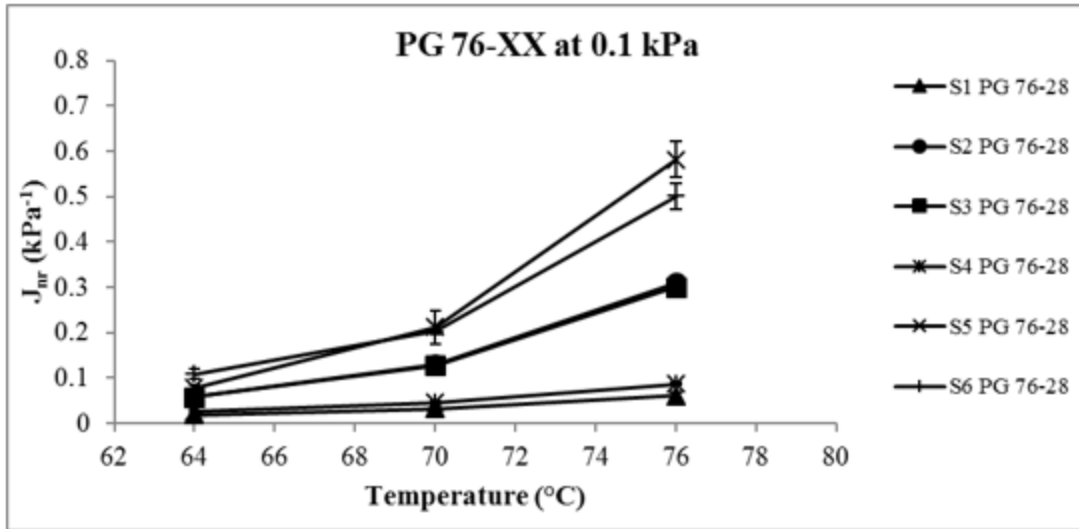


(a)

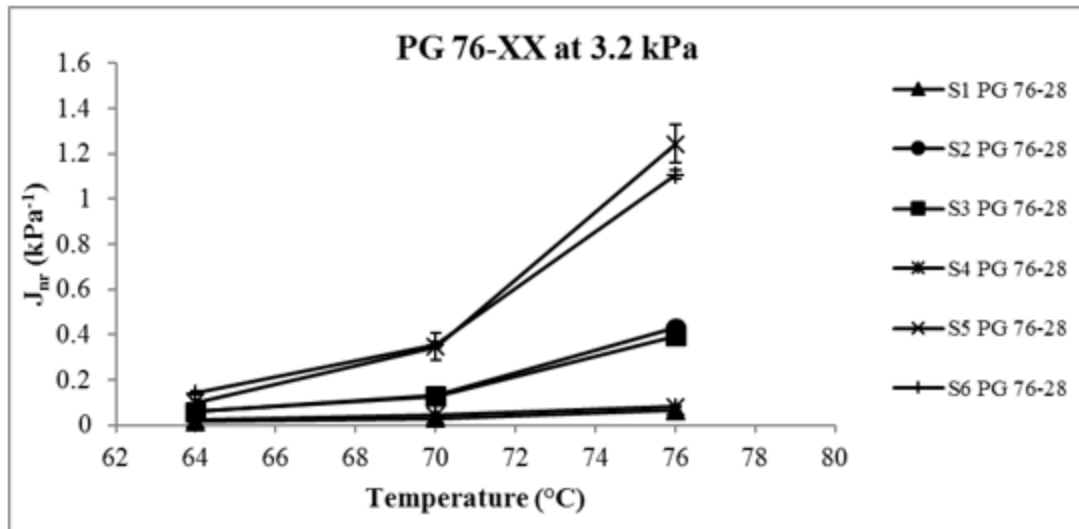


(b)

Figure 94. Changes in J_{nr} values with temperature for PG 70-XX binders: (a) 0.1 kPa stress level; (b) 3.2 kPa stress level



(a)

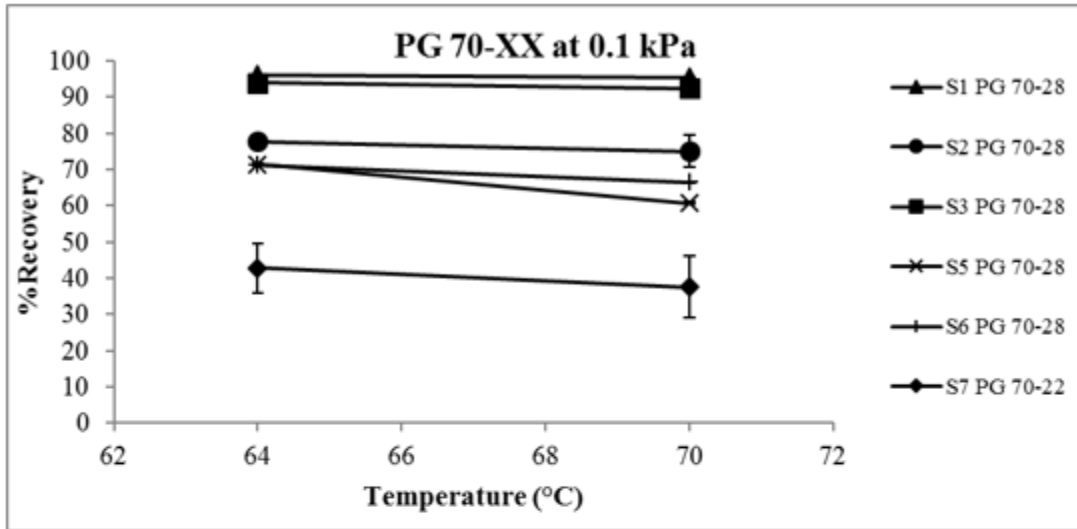


(b)

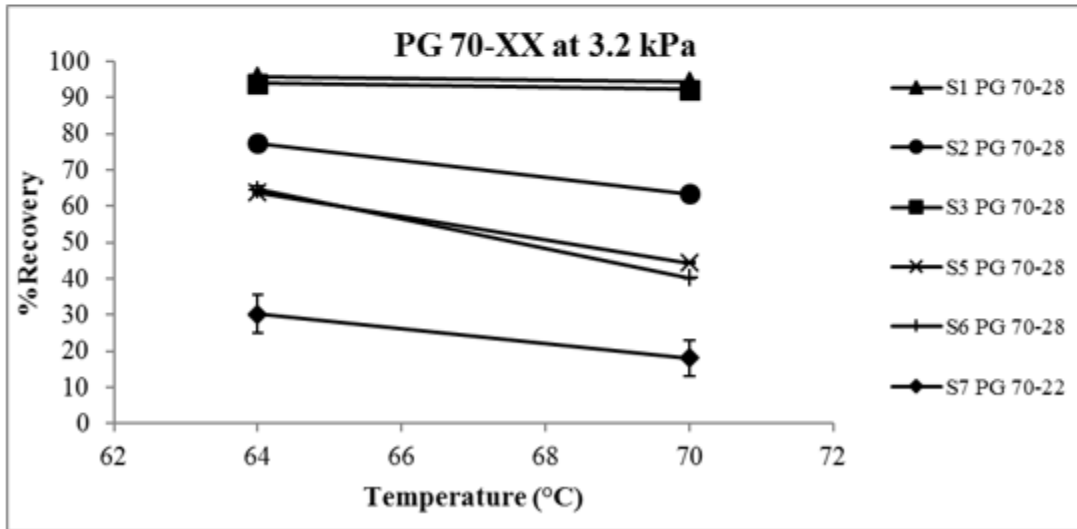
Figure 95. Changes in J_{nr} values with temperature for PG 76-XX binders: (a) 0.1 kPa stress level; (b) 3.2 kPa stress level

The variations in %Recovery with temperature are presented in Figures 96 (a) and 96 (b) for the PG 70-XX binders and in Figures 97 (a) and 97 (b) for the PG 76-XX binders at 0.1 and 3.2 kPa stress levels, respectively. Like J_{nr} parameter, %Recovery was found to exhibit temperature sensitivity for the both the PG 70-XX and PG 76-XX binders. The %Recovery was found to reduce with an increase in temperature for all tested binders. At 0.1 kPa stress level, the %Recovery of the S6 PG 70-28 binder was found to be

71.3% at 64 °C whereas it reduced to 66.5% at 70 °C. Previous studies have reported a similar temperature sensitivity of %Recovery of polymer-modified binders [61,67, 72].

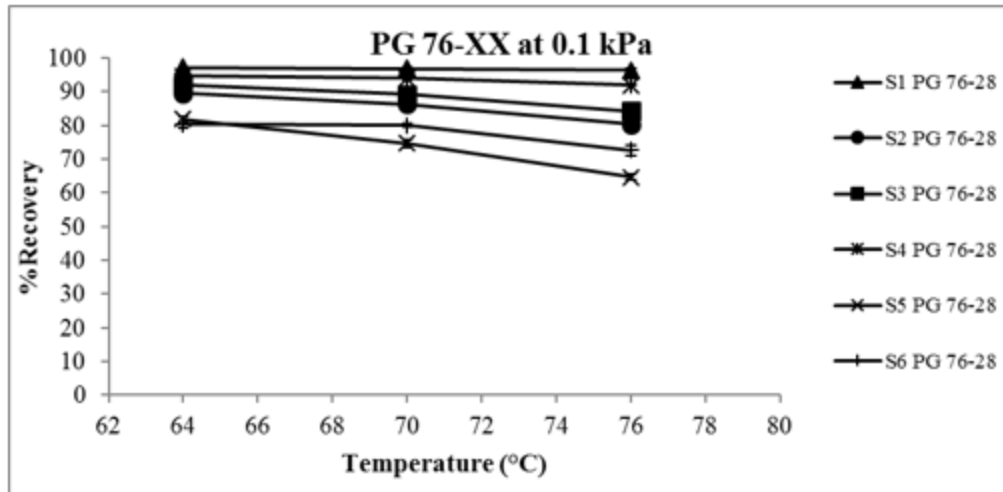


(a)

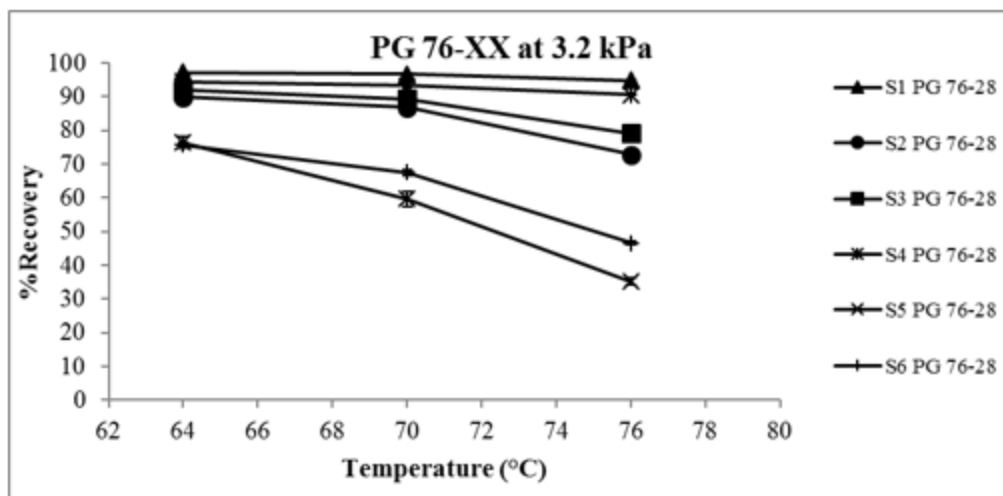


(b)

Figure 96.Changes in %Recovery with temperature for PG 70-XX binders: (a) 0.1 kPa stress level; (b) 3.2 kPa stress level



(a)

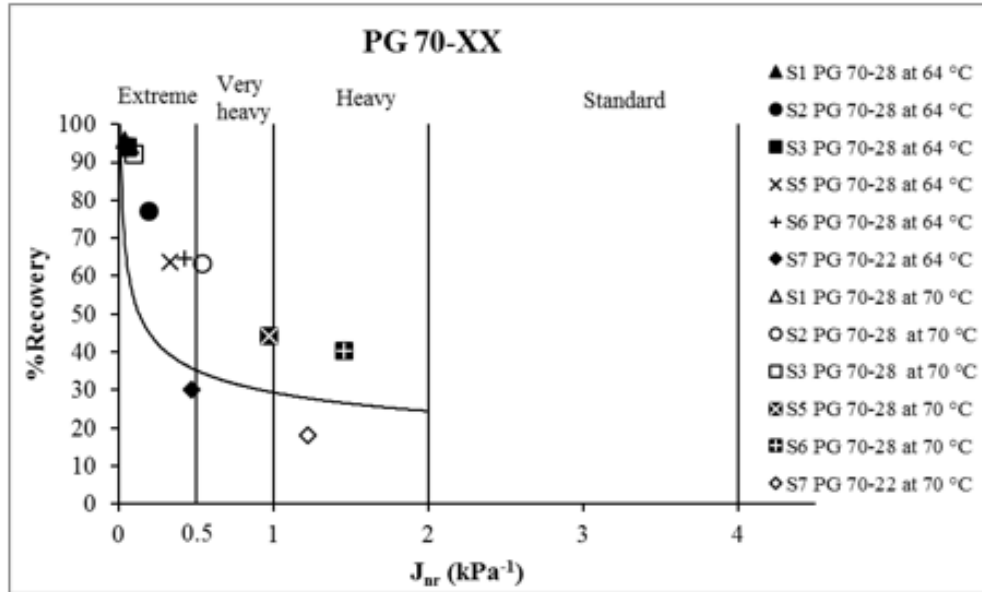


(b)

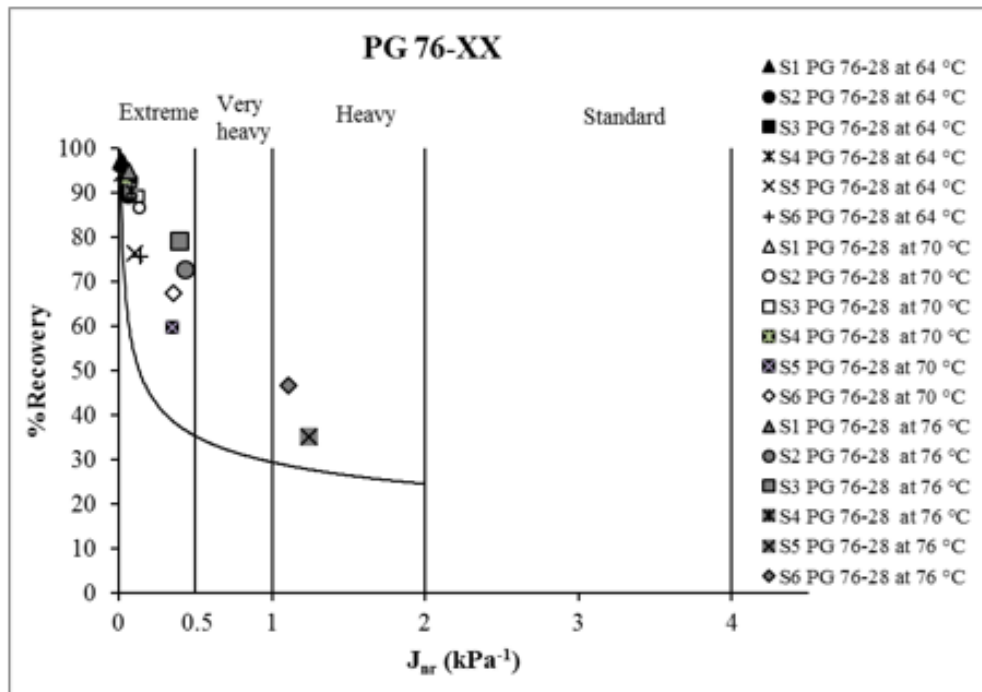
Figure 97. Changes in %Recovery with temperature for PG 76-XX binders: (a) 0.1 kPa stress level; (b) 3.2 kPa stress level

The polymer curve analyses of the PG 70-XX and PG 76-XX binders at higher temperature are presented in Figures 98 (a) and 98 (b). In Figure 98 (a), the J_{nr} values of the PG 70-XX binders at 64° and 70 °C are plotted against the corresponding %Recovery values. Likewise, in Figure 98 (b), the J_{nr} values of the PG 76-XX binders at 64°, 70° and 76 °C are plotted against the corresponding %Recovery values. As the J_{nr} values of the PG 70-XX binders increased with an increase in the temperature from 64° to 70°, the MSCR grades of the binders were found to reduce. For example, the MSCR grade of the S6 PG 70-28 binder was observed to be PG 64E-28 whereas the same

binder at 70 °C was found to reduce to PG 70H-28. This indicates that the binder can sustain extreme level of traffic at 64 °C but only heavy level of traffic at 70 °C, when used in an asphalt mixes.



(a)



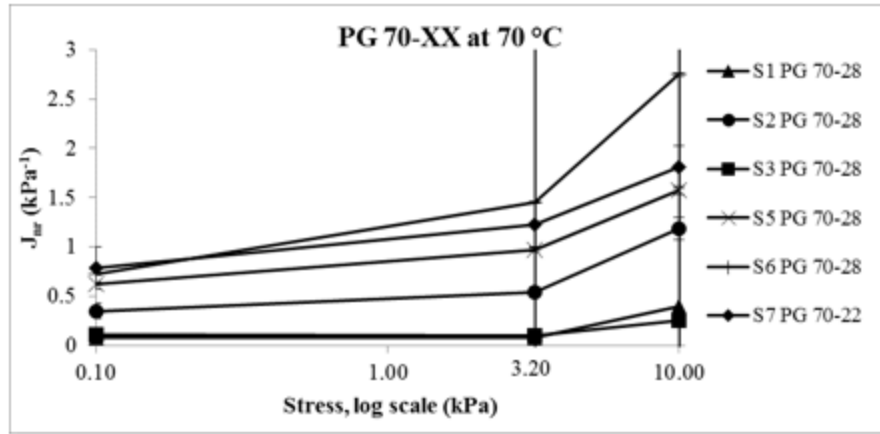
(b)

Figure 98. Polymer curve analyses at higher temperatures and 3.2 kPa stress level: (a) PG 70-XX binders; (b) PG 76-XX binders

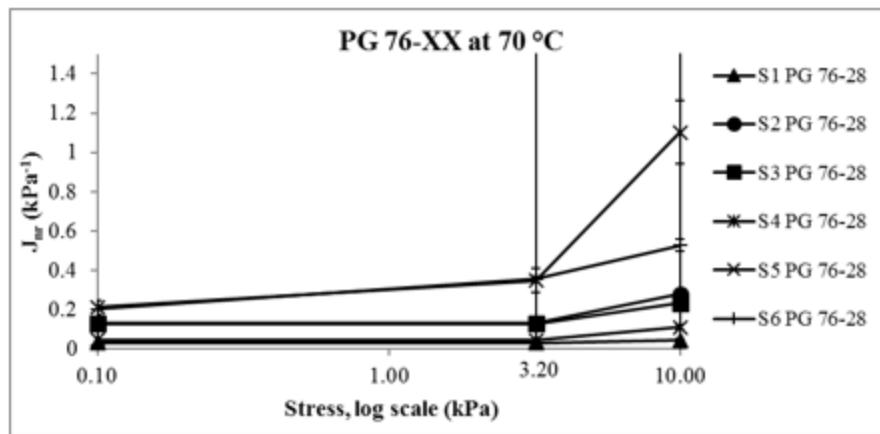
Therefore, the effect of an increase in temperature should be considered properly as the same binder can be graded differently at different temperatures. Stevens et al. (2015) reported that the effect of a single standard temperature drop (6 °C) might be equivalent to a single level increase in the traffic grade. However, the %Recovery requirement of all the PG 70-XX binders were found to meet the AASHTO TP 70 [164] criterion, except the S7 PG 70-22 binder. Although the PG 76-XX binders exhibited an increase in J_{nr} value with an increase in temperature, the effect of temperature change on MSCR grades was not significant. All PG 76-XX binders were found to meet the requirement for sustaining extreme traffic level at 64° and 70 °C. At 76 °C, only the PG 76-28 binders from S5 and S6 sources showed a reduced MSCR grade of PG 76H-28. Therefore, the PG 76-XX binders are expected to exhibit less temperature sensitivity than the PG 70-XX binders, as expected.

Combined effect of increased stress level and higher temperature

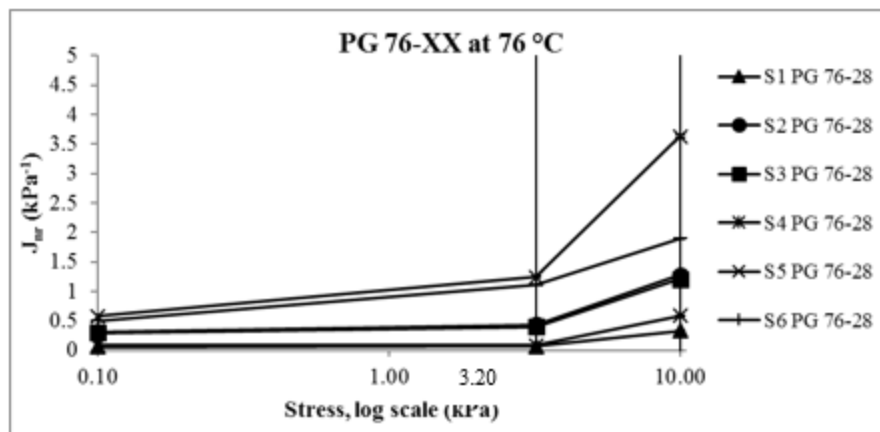
Figures 99 and 100 present the variation in the MSCR parameters of the PG 70-XX and PG 76-XX binders at different stress levels and temperatures higher than the standard procedure. As seen in Figure 99, the J_{nr} values were found to be almost independent of the stress levels up to 3.2 kPa, even at 70 °C for the PG 70-XX and at 76 °C for PG 76-XX binders. It is evident that at the first two stress levels, all the polymer-modified binders having the same continuous PG grade behaved very similarly. However, with an increase in the stress level to 10 kPa, the stress sensitivities of the PG 70-XX binders became clearer and the differences between the binders from different sources became prominent. However, at the 10 kPa stress level and higher temperature, the resistance to deformation of some of the binders dramatically decreased, which can be detected by a sharp increase in the J_{nr} values (Figure 99). Jafari et al [180] reported that this kind of sharp increase in the J_{nr} value might be due to the damage of the binder structure. Furthermore, the non-linear behavior of polymer-modified binders from different sources can be better understood from the combined effect of a higher testing temperature and a higher stress level. As suggested by previous studies, an additional stress level higher than 3.2 kPa, such as 10 kPa for MSCR testing, may be helpful to characterize the non-linear behavior of the binder as well as the rutting resistance of the polymer-modified binders [111, 180].



(a)

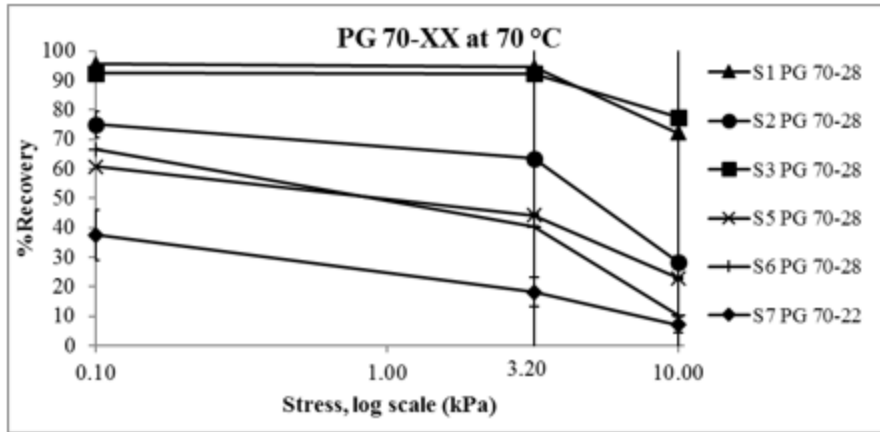


(b)

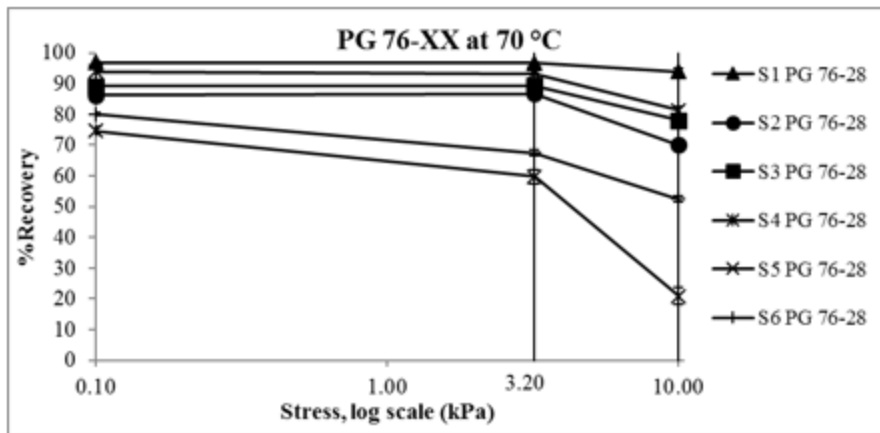


(c)

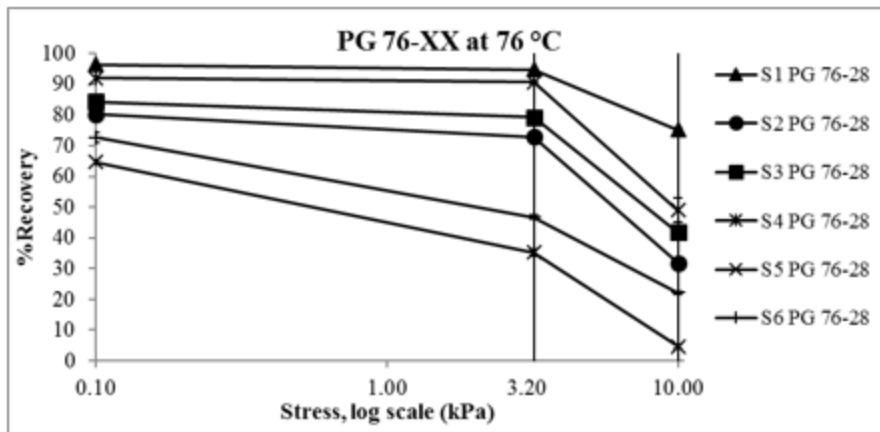
Figure 99. Changes in J_{nr} values with stress level: (a) PG 70-XX binders at 70 °C; (b) PG 76-XX binders at 70 °C; (c) PG 76-XX binders at 76 °C



(a)



(b)



(c)

Figure 100.Changes in %Recovery with stress levels: (a) PG 70-XX binders at 70 °C; (b) PG 76-XX binders at 70 °C; (c) PG 76-XX binders at 76 °C

7.1.3.2 RAP Binder Blends

The effect of the addition of RAP binders to the neat binder was evaluated using the MSCR test method. The MSCR tests were conducted on RTFO-aged binders' samples at 64 °C. Results of the J_{nr} (0.1 kPa), J_{nr} (3.2 kPa), $J_{nr\ diff}$, R_{100} and R_{3200} values and R_{diff} of the blended binders are presented in Table 35. The definition of the terms used in the table was presented in the Section 7.1.3.1.

Table 35. MSCR test results of 0%, 25%, 40% and 60% RAP1 and RAP2 binder blends

Binder type	Temp (°C)	J_{nr} (0.1 kPa) kPa^{-1}	J_{nr} (3.2 kPa) kPa^{-1}	$J_{nr\ diff}$ (0.1-3.2)	Stress sensitivity (meets AASTHO MP 19)	R_{100} (%)	R_{3200} (%)	R_{diff} (0.1-3.2)	%Recovery (meets AASTHO TP 70)	MSCR grade
PG 64-22	64	1.46	1.80	23.13	Yes	16.44	3.60	78.05	No	PG 64H-XX
PG 64-22-R1-25	64	1.55	1.77	14.73	Yes	10.55	2.77	73.69	No	PG 64H-XX
PG 64-22-R1-40	64	0.99	1.14	15.25	Yes	15.22	5.61	63.13	No	PG 64H-XX
PG 64-22-R1-60	64	0.38	0.43	12.68	Yes	26.01	16.33	37.21	No	PG 64E-XX
PG 64-22-R2-25	64	1.17	1.35	15.35	Yes	13.43	4.53	66.25	No	PG 64H-XX
PG 64-22-R2-40	64	0.63	0.71	14.00	Yes	19.86	10.36	47.82	No	PG 64V-XX
PG 64-22-R2-60	64	0.19	0.20	7.02	Yes	31.29	26.26	16.06	No	PG 64E-XX

Non-recoverable creep compliance (J_{nr})

The J_{nr} values measured for the RAP binder blends at the 0.1 kPa and 3.2 kPa stress levels at 64 °C are presented in Figure 101. As noted earlier, binder with a low J_{nr} value is expected to result in a mix with better rutting resistance. From Figure 101, it was observed that the J_{nr} value increased with an increase in the stress level from 0.1 to 3.2 kPa. For example, the J_{nr} value measured for the PG 64-22 binder was found to increase from 1.46 to 1.80 kPa^{-1} when the stress level changed from 0.1 to 3.2 kPa.

Also, from Figure 101, the J_{nr} values were observed to reduce with an increase in RAP binder content in the binder blends. As seen in Figure 101, the J_{nr} values of the PG 64-22 binder at the 3.2 kPa stress level was found to be 1.80 kPa^{-1} . It reduced to 1.77, 1.14 and 0.43 kPa^{-1} after incorporating 25%, 40% and 60% RAP1 binder, respectively. A similar reducing trend with an increase in RAP binder content was observed for RAP2 binder blends, as well. The PG 64-22-R2-25, PG 64-22-R2-40 and PG 64-22-R2-60 binders were found to exhibit J_{nr} values of 1.35, 0.71 and 0.20 kPa^{-1} at the 3.2 kPa stress level, respectively. As the J_{nr} values exhibited a reducing trend with increasing RAP binder, the binder blends are expected to exhibit a higher rutting resistance than the neat binders.

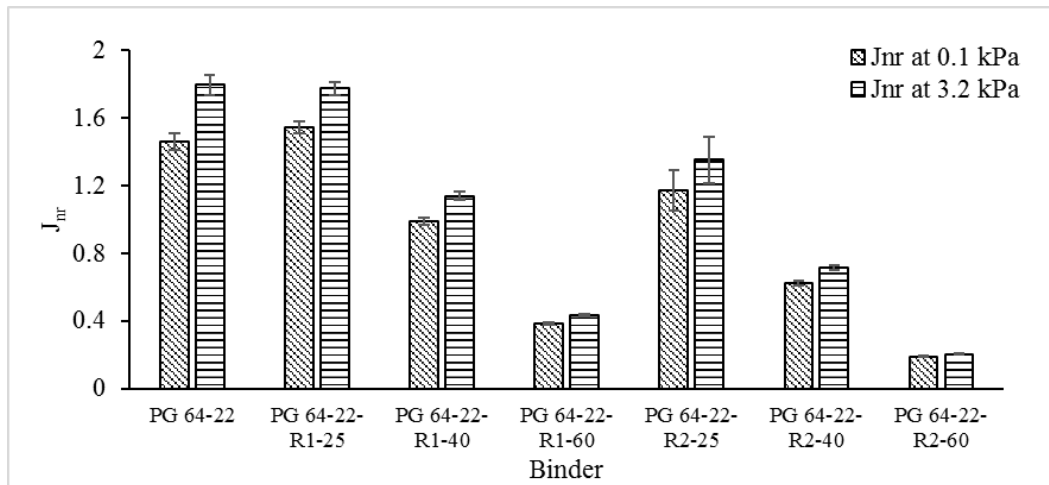


Figure 101. J_{nr} values of 0%, 25%, 40% and 60% RAP1 and RAP2 binder blends at $64 \text{ }^\circ\text{C}$

MSCR %Recovery

Figure 102 presents the %Recovery values obtained from MSCR tests conducted on RAP binder blends at $64 \text{ }^\circ\text{C}$. Relatively low %Recovery values were observed as the binders were not polymer-modified. As expected, the %Recovery values at the 3.2 kPa stress level were found to be lower than that measured at the 0.1 kPa stress level for all RAP binder blends. Also, from Figure 102, it was found that the %Recovery values reduced due to the addition of 25% RAP1 binder to the blend. However, for the PG 64-22-R1-40 and PG 64-22-R1-60 binders, the %Recovery showed an increasing trend with an increase in RAP binder content. A similar increasing trend of %Recovery was

also observed for RAP2 binder blends. Therefore, it can be concluded that the asphalt mixes produced with binder containing high RAP binder content are expected to exhibit a higher %Recovery at certain stress levels and temperatures than neat binders.

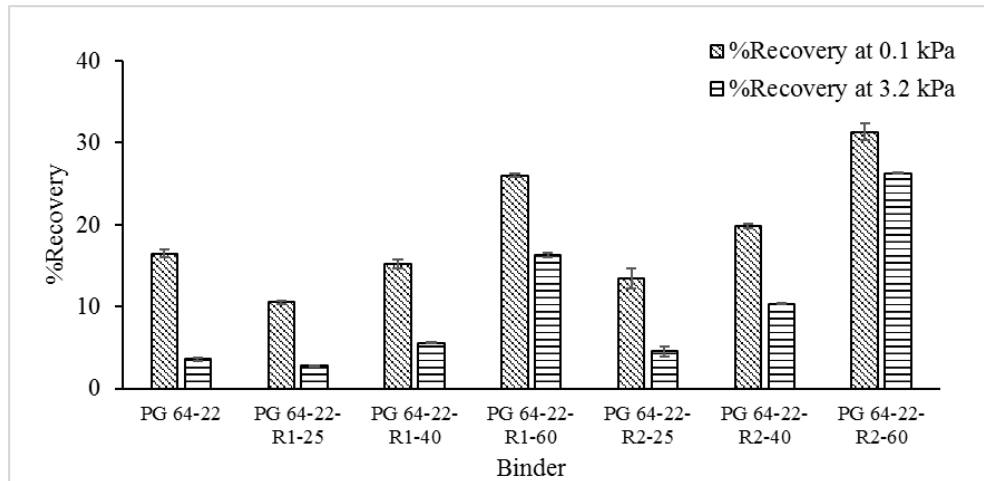


Figure 102. %Recovery values of 0%, 25%, 40% and 60% RAP1 and RAP2 binder blends at 64 °C

Stress sensitivity

Figures 103 and 104 present the $J_{nr\ diff}$ and R_{diff} for RAP binder blends while the stress level changed from 0.1 kPa to 3.2 kPa at 64 °C. It can be observed from Figure 103 that the $J_{nr\ diff}$ values for all the RAP binder blends met the AASHTO MP 19 [184] stress sensitivity criterion ($J_{nr\ diff} < 75\%$). The maximum $J_{nr\ diff}$ value was observed for the neat PG 64-22 binder (23.13%). The $J_{nr\ diff}$ values of the RAP binder blends were found to exhibit a reducing trend with an increase in the RAP binder. From Figure 103, the $J_{nr\ diff}$ values were found to reduce to 14.73%, 15.25% and 12.68% with the addition of 25%, 40% and 60% RAP1 binder, respectively. The RAP2 binder blends also exhibited a sharp reducing trend with an increase in RAP binder content. The $J_{nr\ diff}$ values for the PG 64-22-R2-25, PG 64-22-R2-40 and PG 64-22-R2-60 binders were observed to be 15.35%, 14.01% and 7.02%, respectively. Furthermore, from Figure 104, the R_{diff} values of the RAP binder blends exhibited a similar reducing trend as observed for $J_{nr\ diff}$ with an increase in RAP binder content. The R_{diff} values were found to decrease from 78.05% to 73.70%, 63.13% and 37.21% for the PG 64-22-R1-25, PG 64-22-R1-40 and PG 64-22-R1-60 binders, respectively. Therefore, it can be concluded that both MSCR

parameters, namely J_{nr} and %Recovery became less sensitive to stress level with an increase in the RAP binder to the binder blend.

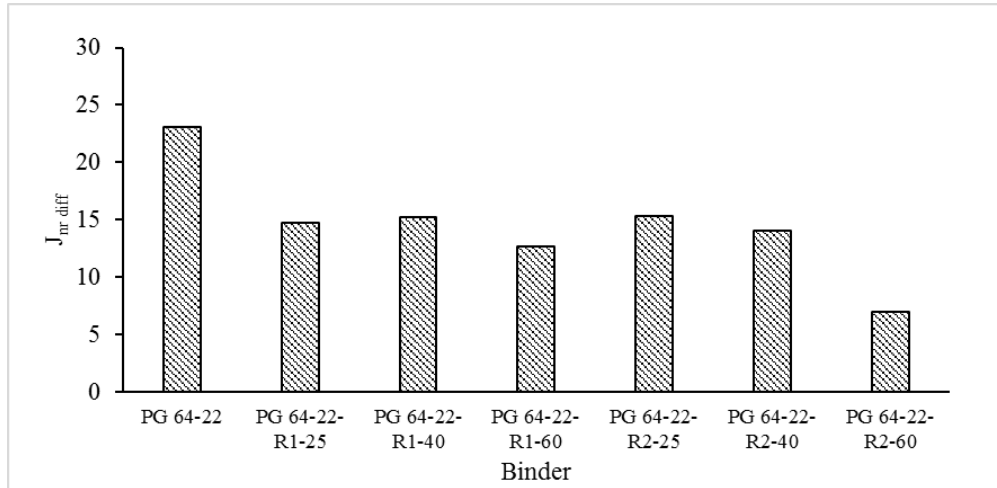


Figure 103. $J_{nr,diff}$ values of 0%, 25%, 40% and 60% RAP1 and RAP2 binder blends at 64 °C

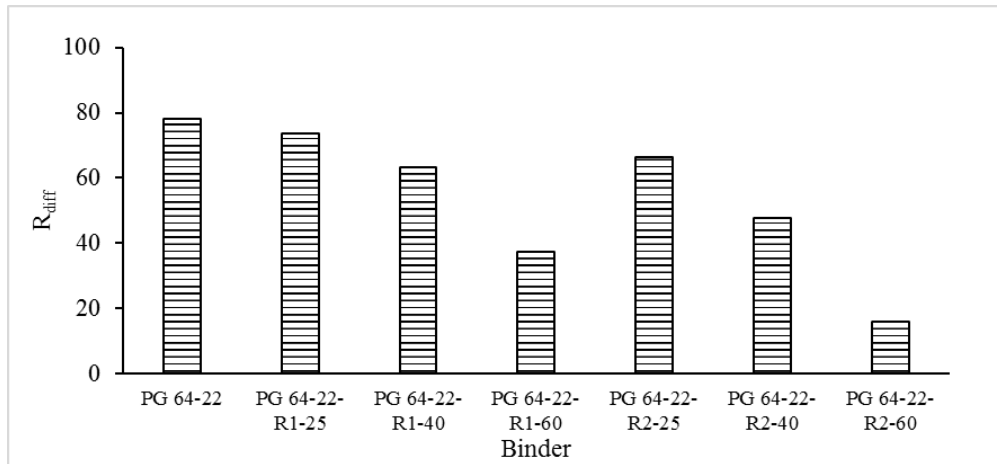


Figure 104. R_{diff} values of 0%, 25%, 40% and 60% RAP1 and RAP2 binder blends at 64 °C

Polymer method

The MSCR results, analyzed using polymer curve, for RAP binder blends are presented in Figure 105. From Figure 105, the data points for the RAP binder blends are clustered below the MSCR curve. This means that, these binders did not meet the %Recovery requirement proposed by AASHTO TP 70 [164]. A low %Recovery was expected, as

both the neat binder and RAP binders were not polymer-modified. The RAP binder blends are expected to perform better in rutting as the J_{nr} value reduced and %Recovery increased with an increase in the RAP binder content.

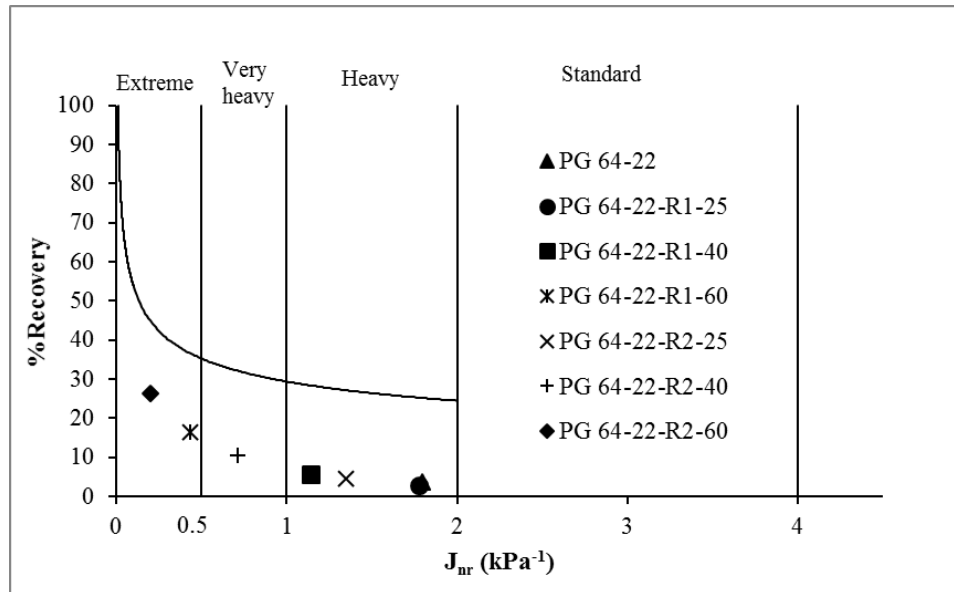


Figure 105. Polymer curve analysis for 0%, 25%, 40% and 60% RAP1 and RAP2 binder blends at 64 °C and 3.2 kPa stress level

MSCR grading system

Table 35 and Figure 105 present the MSCR grading of the RAP binder blends determined according to the AASHTO MP 19 [184] specification. The MSCR grade of the PG 64-22 binders was found to be PG 64H-XX. This means that the binder will be able to sustain heavy level of traffic at 64 °C without undergoing significant rutting, when used in asphalt mixes. Also, the equivalent MSCR grade of the PG 64-22-R1-25, PG 64-22-R1-40 binders were observed to be PG 64H-XX, the same grade as the neat binder. However, the MSCR grade of the PG 64-22-R1-60 binder was found to be PG 64E-XX, which is expected to sustain extreme level of traffic without exhibiting significant permanent deformation. The equivalent MSCR grades of the PG 64-22-R2-25, PG 64-22-R2-40 and PG 64-22-R2-60 binders were found to be PG 64H-XX, PG 64V-XX and PG 64E-XX, respectively. These results indicate that the MSCR grade of the neat binder is expected to increase with an increase in the amount of RAP binder in the blend.

Effect of increased stress level

The stress sensitivity of the RAP binder blends was determined at a higher stress level (10 kPa), in addition to the recommended stress levels in AASHTO TP 70 [164]. Table 36 presents the MSCR test results conducted on the RAP binder blends at three different stress levels and at 64 °C.

Figures 106 and 107 show the changes in J_{nr} and %Recovery values with an increase in the stress level at 64 °C. The J_{nr} value for the neat PG 64-22 binder was observed to increase significantly with a change in the stress level from 3.2 to 10 kPa.

Approximately 46% increase in J_{nr} value was observed when the stress level changed from 3.2 to 10 kPa. Also, a similar increase in J_{nr} value was observed for the other RAP binder blends. Therefore, it can be concluded that, the J_{nr} parameter of the RAP binder blends exhibited a higher stress sensitivity at 10 kPa stress levels than that at 0.1 and 3.2 kPa stress levels. Furthermore, the %Recovery of the RAP binder blends was found to exhibit sharp decrease with an increase in stress level from 3.2 to 10 kPa. As seen in Figure 107, the %Recovery value of the PG 64-22-R1-25 binder at 0.1, 3.2 and 10 kPa stress levels were 10.55%, 2.78%, and 0.17%, respectively. This indicates that the MSCR parameters of the RAP binder blends became overly stress sensitive with an increase in stress level.

Table 36.MSCR test results of 0%, 25%, 40% and 60% RAP1 and RAP2 binder blends at 64 °C and 0.1, 3.2 and 10 kPa

Binder type	Temp (°C)	J_{nr} (0.1 kPa) kPa^{-1}	J_{nr} (3.2 kPa) kPa^{-1}	J_{nr} (10 kPa) kPa^{-1}	J_{nr} diff (0.1-3.2)	J_{nr} diff (3.2-10)	R_{100} (%)	R_{3200} (%)	R_{10000} (%)	R_{diff} (0.1-3.2)	R_{diff} (3.2-10)
PG 64-22	64	1.46	1.79	2.63	23.13	46.54	16.44	3.61	-0.34	78.05	109.30
PG 64-22-R1-25	64	1.55	1.77	2.16	14.73	22.21	10.55	2.78	0.17	73.69	94.02
PG 64-22-R1-40	64	0.99	1.14	1.40	15.25	22.96	15.22	5.62	1.28	63.13	77.23
PG 64-22-R1-60	64	0.38	0.43	0.54	12.68	26.97	26.01	16.33	5.44	37.21	66.6
PG 64-22-R2-25	64	1.17	1.35	1.63	15.35	20.98	13.43	4.53	0.89	66.25	80.15
PG 64-22-R2-40	64	0.63	0.71	0.87	14.01	22.28	19.86	10.36	3.19	47.82	69.15
PG 64-22-R2-60	64	0.19	0.20	0.25	7.02	20.82	31.29	26.26	14.15	16.06	46.09

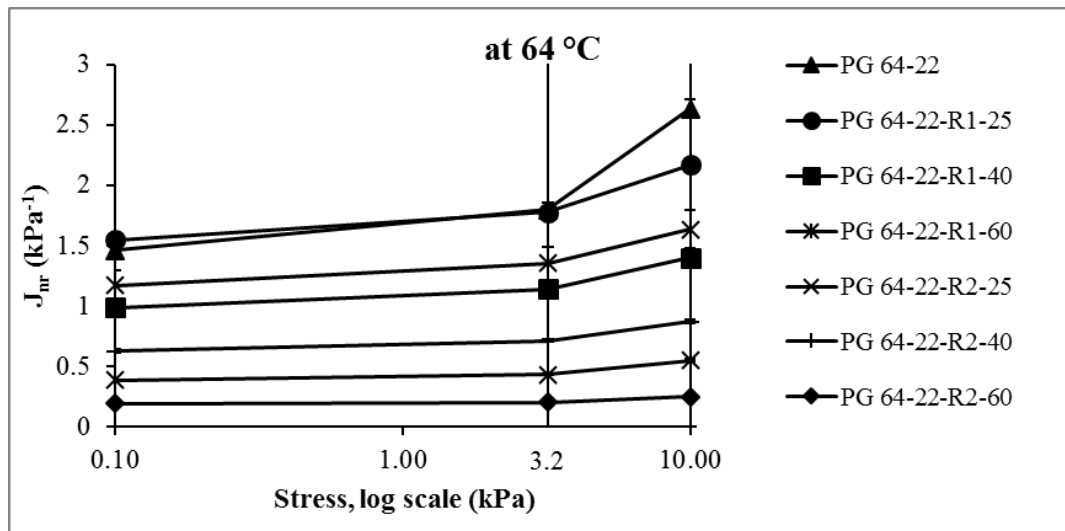


Figure 106.Changes in J_{nr} values with stress levels for 0%, 25%, 40% and 60% RAP1 and RAP2 binder blends at 64 °C

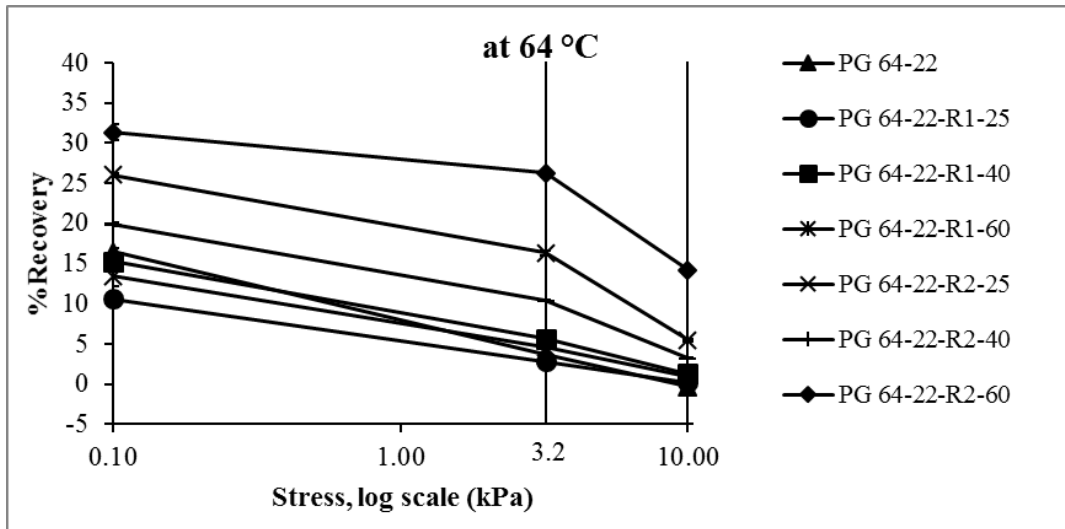


Figure 107.Changes in %Recovery values with stress levels for 0%, 25%, 40% and 60% RAP1 and RAP2 binder blends at 64 °C

Figures 108 and 109 present changes in the $J_{nr\ diff}$ and $\%R_{diff}$ values with a change in stress level for RAP binder blends, respectively. The $J_{nr\ diff}$ and $\%R_{diff}$ between 10 kPa and 3.2 kPa stress levels were found to be higher than those between 3.2 kPa and 0.1 kPa stress levels. This means that the RAP binder blends became more sensitive to stress levels, when the stress level changed from 3.2 to 10 kPa. Also, the neat binder was observed to exhibit higher stress sensitivity than the RAP binder blends.

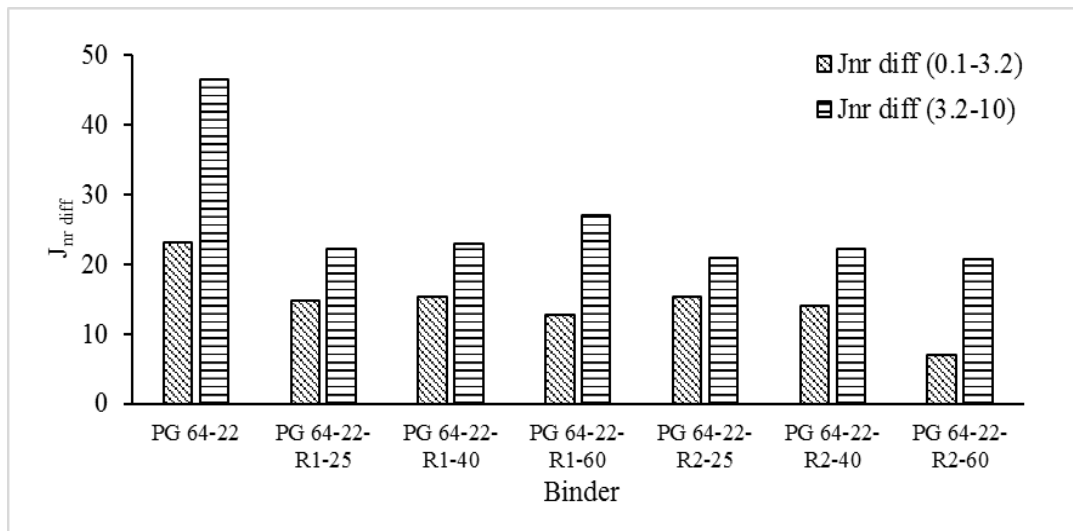


Figure 108.Variation in $J_{nr\ diff}$ with stress levels for 0%, 25%, 40% and 60% RAP1 and RAP2 binder blends at 64 °C

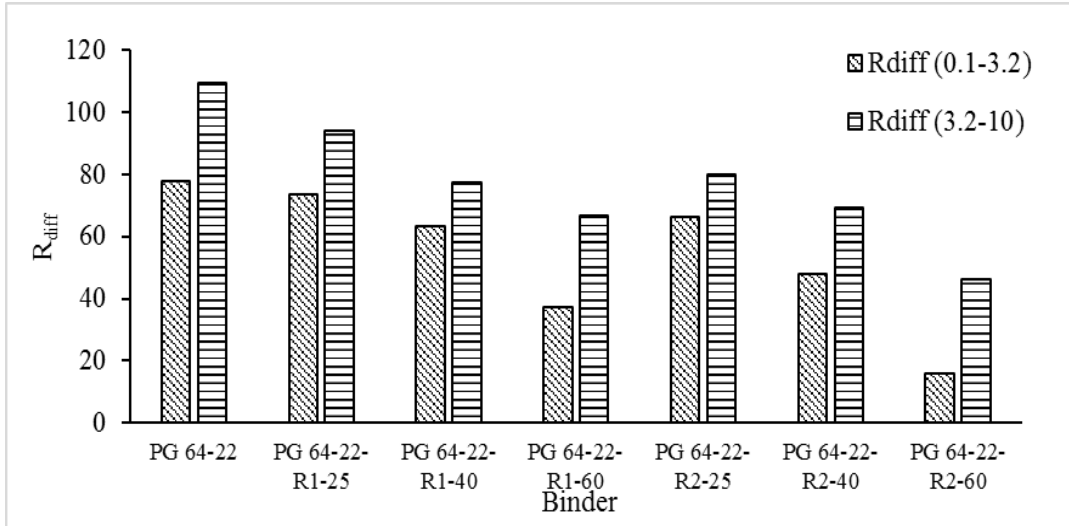
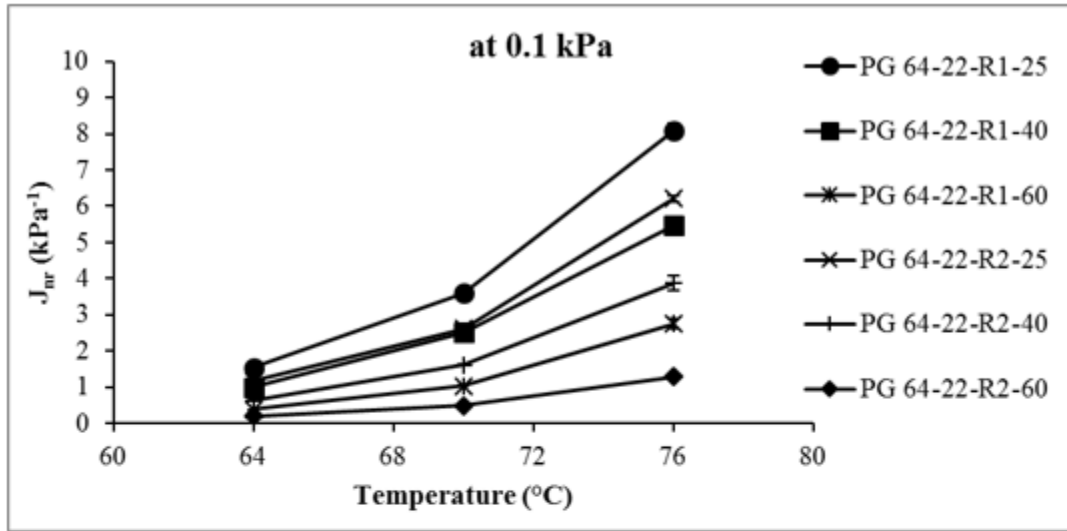


Figure 109. Variation in R_{diff} with stress levels for 0%, 25%, 40% and 60% RAP1 and RAP2 binder blends at 64 °C

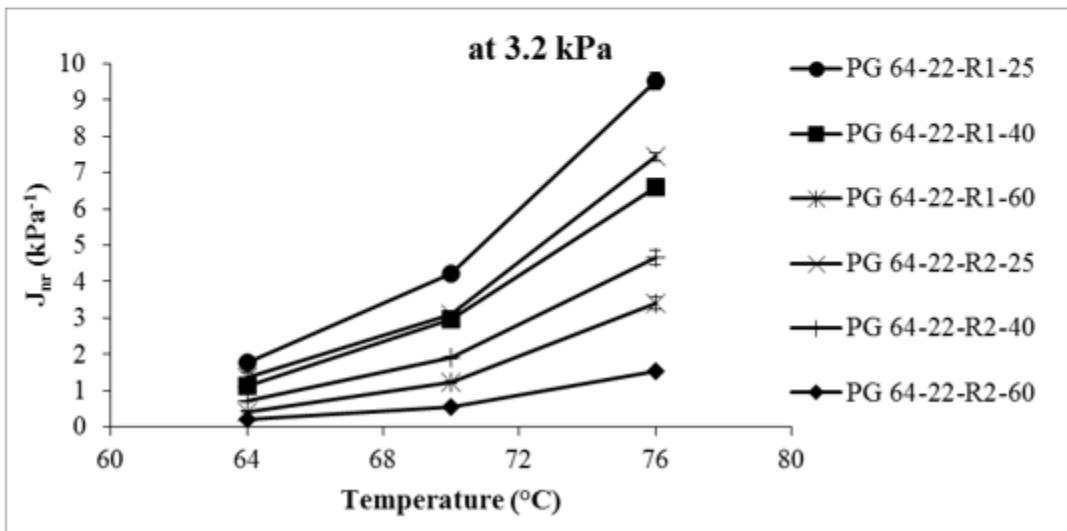
Effect of higher temperatures

To evaluate the temperature sensitivity of the MSCR parameters, the RAP binder blends were tested at temperatures (70° and 76 °C) higher than 64 °C. Figures 110 and 111 present the variation of J_{nr} and %Recovery values with temperature at 0.1 and 3.2 kPa stress levels, respectively. From Figure 110, it can be observed that the J_{nr} values exhibited an increasing trend with an increase in temperature. For example, the J_{nr} value of the PG 64-22-R1-25 binder at 3.2 kPa stress level was found to increase from 1.77 kPa⁻¹ to 4.21 and 9.53 kPa⁻¹ when the temperature increased from 64° to 70° and 76 °C, respectively. Also, from Figure 111, it is evident that the %Recovery reduced with an increase in temperature for all RAP binder blends. Furthermore, at 3.2 kPa stress level, the %Recovery for the PG 64-22-R1-25 binder was found to be 2.78% at 64 °C, whereas it reduced to 0.15% and -1.9% at 70° and 76 °C, respectively. The negative %Recovery implies that the binder underwent continuous deformation even after the removal of the load. Jafari et al. [180] reported that the negative recovery can result from a combination of high stress level and high temperature, if it caused the binders to enter the tertiary flow level. It can be interpreted that the structure of the binder might be damaged at this temperature. Figure 112 presents the polymer curve analysis of RAP binder blends at 70° and 76 °C. From Figure 112, it can be observed that the MSCR grade of the binder reduced with an increase in temperature. For example, the MSCR

grade of the PG 64-22-R1-60 binder was found to reduce from extreme to very heavy when the temperature increased from 64° to 70 °C. This means that the RAP binder blends are expected to become more susceptible to rutting with an increase in temperature.

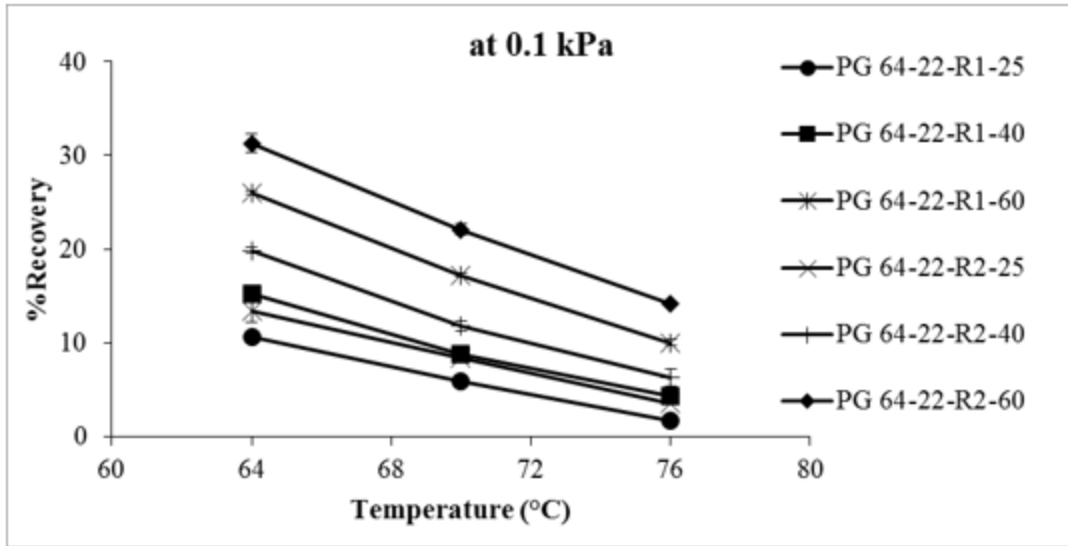


(a)

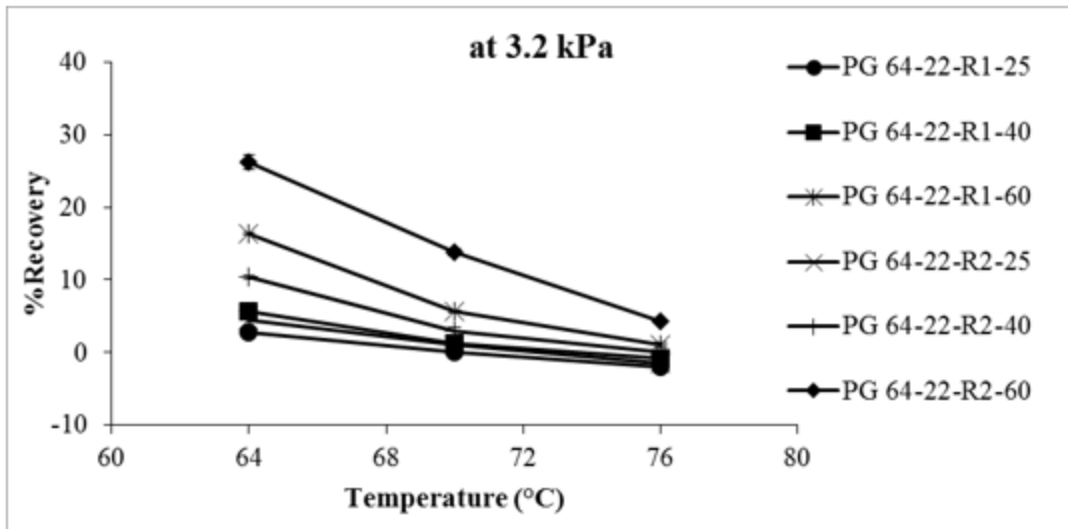


(b)

Figure 110. Changes in J_{nr} values with an increase in temperature for 25%, 40% and 60% RAP1 and RAP2 binder blends: (a) 0.1 kPa stress level; (b) 3.2 kPa stress level



(a)



(b)

Figure 111.Changes in %Recovery values with an increase in temperature for 25%, 40% and 60% RAP1 and RAP2 binder blends: (a) 0.1 kPa stress level; (b) 3.2 kPa stress level

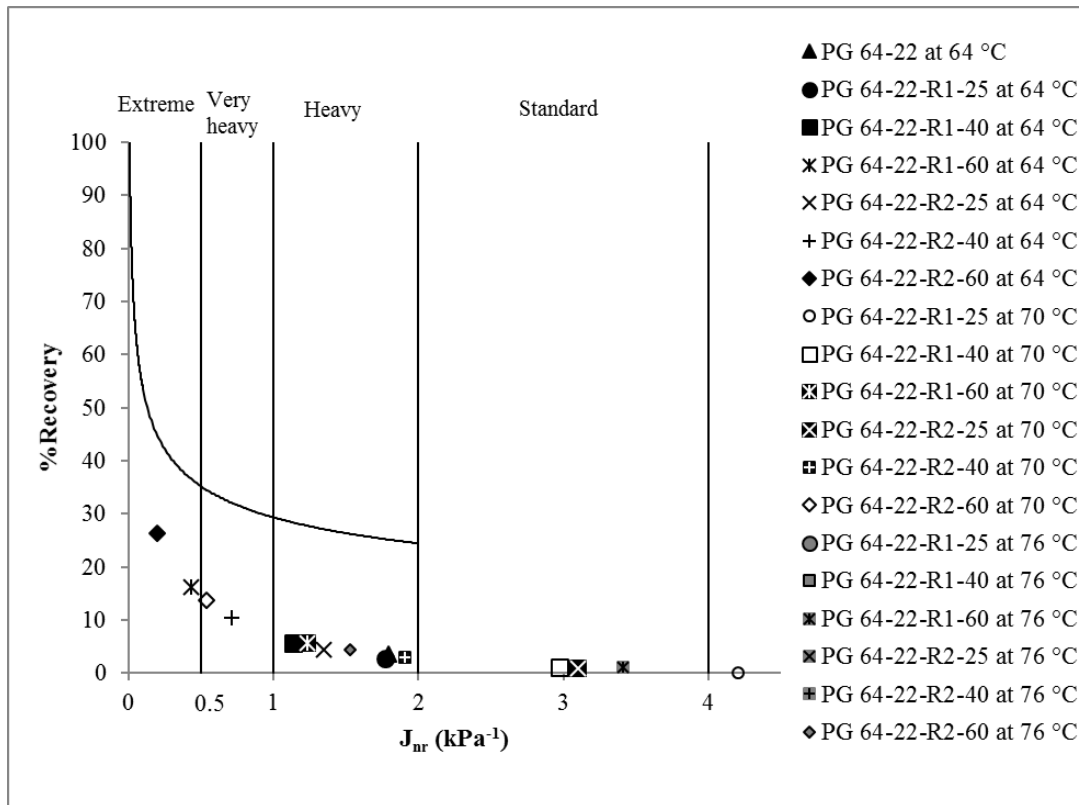
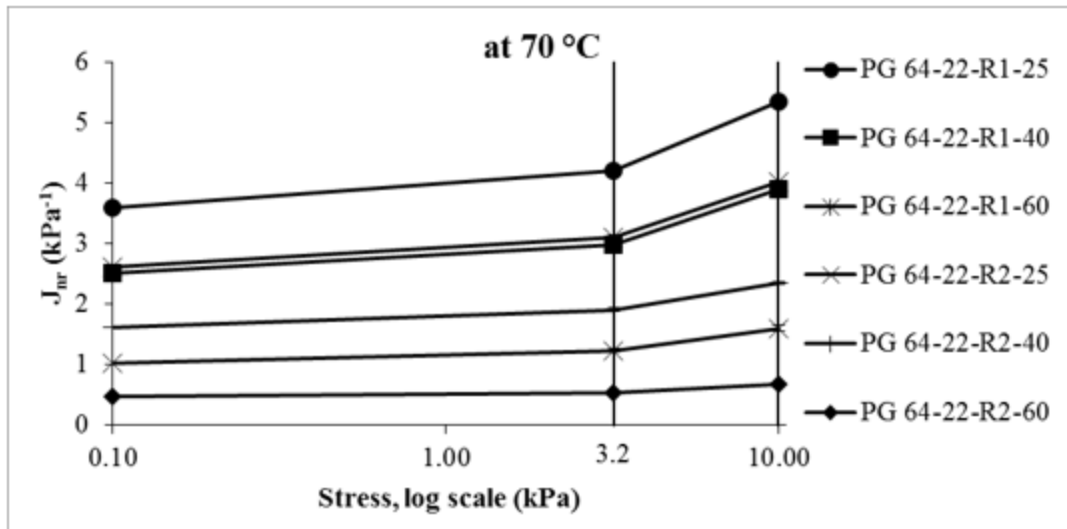


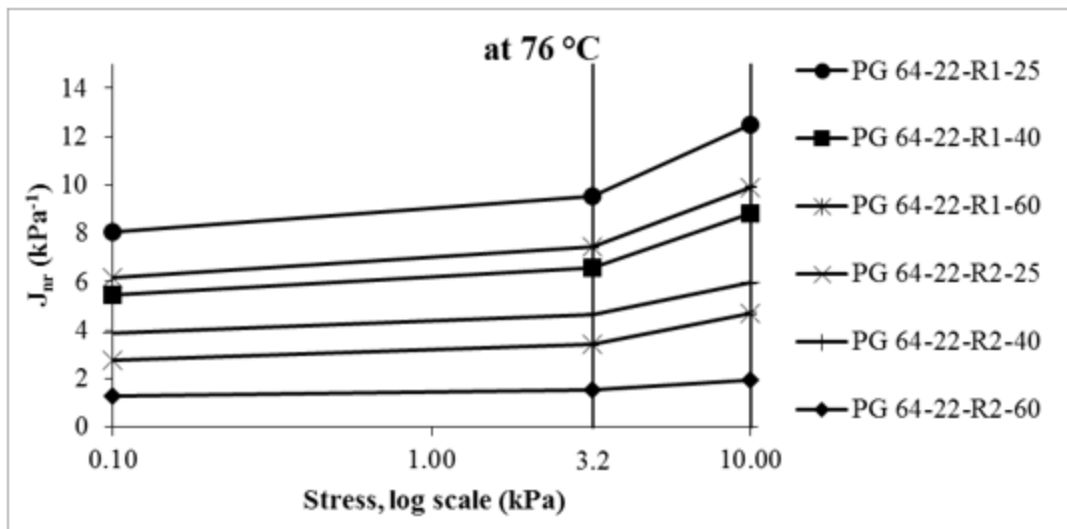
Figure 112. Polymer curve analysis for 0%, 25%, 40% and 60% RAP1 and RAP2 binder blends at different temperatures and 3.2 kPa stress level

Combined effect of increased stress level and higher temperature

Figures 113 and 114 present the changes in the MSCR parameters for RAP binder blends at higher stress levels and at higher temperatures than those used in conventional testing. As seen from Figures 113 and 114, the J_{nr} values increased and %Recovery values reduced with an increase in temperatures and stress levels. Also, at 70° and 76 °C, the stress sensitivities of the MSCR parameters of RAP binder blends became prominent with an increase in the stress level from 3.2 to 10 kPa. Except for the PG 64-22-R2-60 binder, all RAP binder blends exhibited a sharp reduction in %Recovery values at 76 °C temperature and 10 kPa stress level. Therefore, the non-linear behavior of the RAP binder blends became clearer at higher temperature and higher stress levels. This finding is expected to help understand the rutting behavior of the RAP binder blends, since the rutting itself is known to be a non-linear viscoelastic phenomenon observed in asphalt mixes.

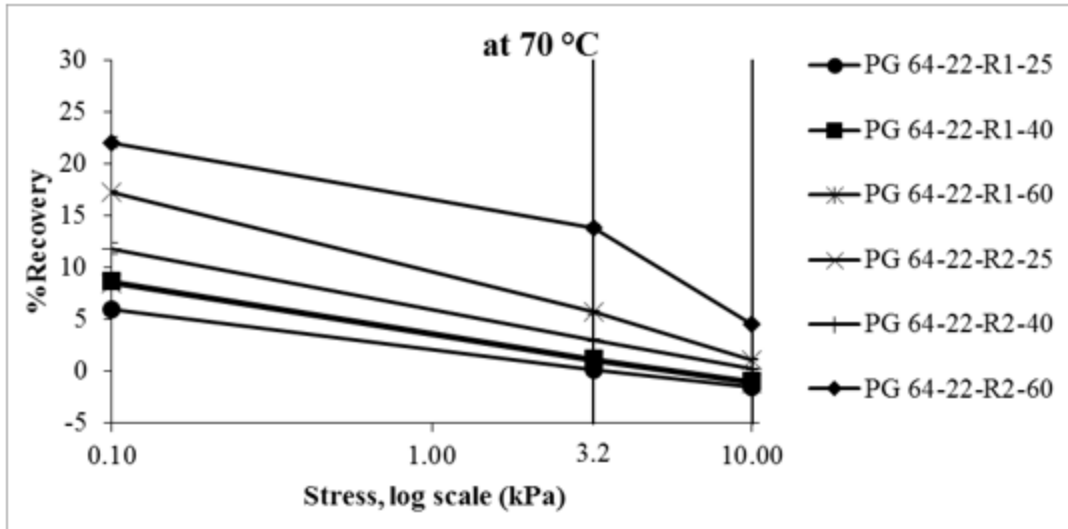


(a)

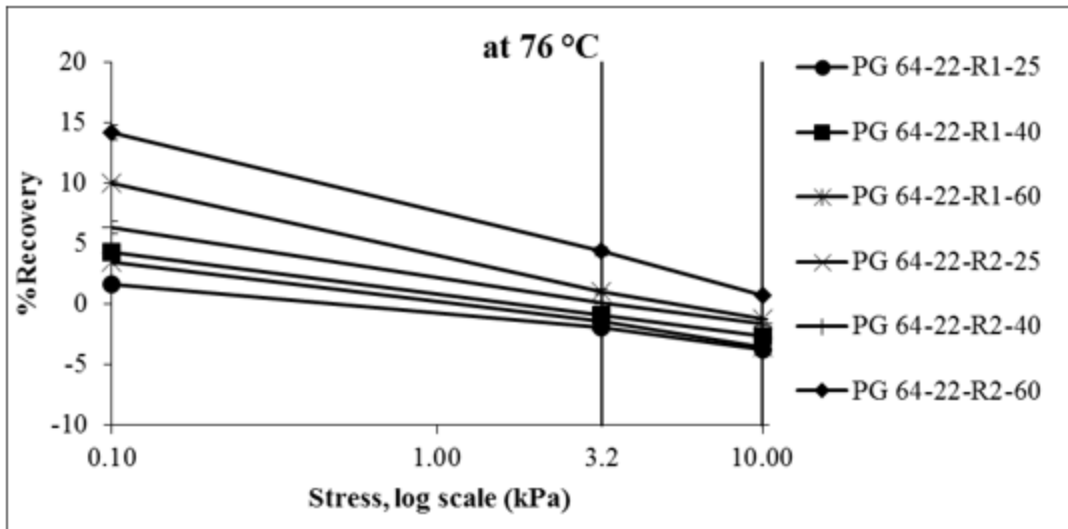


(b)

Figure 113. Changes in J_{nr} values with stress level for 25%, 40% and 60% RAP1 and RAP2 binder blends at 70° and 76 °C



(a)



(b)

Figure 114.Changes in %Recovery values with stress level for 25%, 40% and 60% RAP1 and RAP2 binder blends at 70° and 76 °C

7.1.4 Comparison of DSR and MSCR Test Results

7.1.4.1 Ranking of Binders

Polymer-modified binders

Tables 37 and 38 present the ranking of the polymer-modified binders based on their rutting performance determined from the DSR and MSCR tests. The binders were ranked based on the $|G^*|/\sin\delta$ value at corresponding high temperature. A lower $|G^*|/\sin\delta$ value was associated with less resistance to rutting in this ranking system. Also, the J_{nr} values from MSCR test at different temperatures and stress levels were used to rank the binders. A binder exhibiting the lowest J_{nr} value was considered to exhibit highest rut resistant behavior and vice versa. From Tables 37 and 38, the DSR and MSCR test methods were observed to rank the polymer-modified binders differently. For example, the S1 PG 70-28 binder was ranked the lowest rut resistant binder according to the DSR test results among all the PG 70-XX binders. However, the same binder ranked differently (highest resistance to rutting), based on the J_{nr} values. The ranks of the S2 PG 70-28, S2 PG 76-28 and S6 PG 70-28 binders were found to be similar for both ranking systems. Similar differences in ranking of binders, by different test methods, were reported by Zhang et al. [173]. The variations in sensitivity of the $|G^*|/\sin\delta$ and J_{nr} to binders' viscoelastic properties are assumed to be a primary reason for such differences in binders' ranking. Previous studies have reported better correlations between J_{nr} values and field rutting performance than the $|G^*|/\sin\delta$ values of asphalt binders [147, 170, 173]. Therefore, the MSCR-based ranking of binders is expected to predict the rutting resistance better than the DSR-based ranking. However, no significant differences were observed in the MSCR-based ranking at different temperatures and stress levels. Therefore, the MSCR results at 64 °C and 0.1 or 3.2 kPa can be used for ranking and selection of asphalt binders with respect to their rutting resistance using the MSCR method.

Table 37. Ranking of PG 70-XX binders with respect to rut performance

Binder	DSR ranking based on $ G^* /\sin\delta$	MSCR ranking based on J_{nr} 64 °C 0.1 kPa	MSCR ranking based on J_{nr} 64 °C 3.2 kPa	MSCR ranking based on J_{nr} 70 °C 0.1 kPa	MSCR ranking based on J_{nr} 70 °C 3.2 kPa
S1 PG 70-28	6	1	1	1	1
S2 PG 70-28	3	3	3	3	3
S3 PG 70-28	4	2	2	2	2
S5 PG 70-28	2	4	4	4	4
S6 PG 70-28	5	5	5	5	5
S7 PG 70-22	1	6	6	6	6

Table 38. Ranking of PG 76-XX binders with respect to rut performance

Binder	DSR ranking based on $ G^* /\sin\delta$	MSCR ranking based on J_{nr} 64 °C 0.1 kPa	MSCR ranking based on J_{nr} 64 °C 3.2 kPa	MSCR ranking based on J_{nr} 70 °C 0.1 kPa	MSCR ranking based on J_{nr} 70 °C 3.2 kPa	MSCR ranking based on J_{nr} 76 °C 0.1 kPa	MSCR ranking based on J_{nr} 76 °C 3.2 kPa
S1 PG 76-28	6	1	1	1	1	1	1
S2 PG 76-28	4	4	4	4	4	4	4
S3 PG 76-28	5	3	3	3	3	3	3
S4 PG 76-28	1	2	2	2	2	2	2
S5 PG 76-28	2	5	5	6	5	6	6
S6 PG 76-28	3	6	6	5	6	5	5

RAP binder blends

The ranking of the RAP binder blends based on the DSR and MSCR test results is presented in Table 39. The $|G^*|/\sin\delta$ values of the RAP binder blends at 64 °C were used to rank their rutting performance. Also, the J_{nr} values of the RAP binder blends at

different temperatures and stress levels were used in this ranking. Like the polymer-modified binders, the $|G^*|/\sin\delta$ and J_{nr} values ranked the binders differently. Based on the $|G^*|/\sin\delta$ results, the PG 64-22 binder ranked poorly with the lowest resistance to rutting. The same method ranked the PG 64-22-R1-40 binder superior, with the highest resistance to rutting. The PG 64-22-R2-60 binder and the neat binder were ranked as the binders with the highest and the lowest resistance to rutting based on the J_{nr} value at 64 °C and 3.2 kPa stress level, respectively. Based on these findings, it was concluded that the MSCR test results at 64 °C and 0.1 or 3.2 kPa stress levels can be used to rank binders effectively for their resistance to rutting.

Table 39. Ranking of the RAP binder blends with respect to rut performance

Binder	DSR ranking based on $ G^* /\sin\delta$	MSCR ranking based on J_{nr} 64 °C 0.1 kPa	MSCR ranking based on J_{nr} 64 °C 3.2 kPa	MSCR ranking based on J_{nr} 70 °C 0.1 kPa	MSCR ranking based on J_{nr} 70 °C 3.2 kPa	MSCR ranking based on J_{nr} 76 °C 0.1 kPa	MSCR ranking based on J_{nr} 76 °C 3.2 kPa
PG 64-22	7	6	7	-	-	-	-
PG 64-22-R1-25	3	7	6	6	6	6	6
PG 64-22-R1-40	1	4	4	4	4	4	4
PG 64-22-R1-60	4	2	2	2	2	2	2
PG 64-22-R2-25	5	5	5	5	5	5	5
PG 64-22-R2-40	6	3	3	3	3	3	3
PG 64-22-R2-60	2	1	1	1	1	1	1

7.1.4.2 Repeatability of Test Results

Tables 40 and 41 present the coefficient of variation (COV) for the results obtained from the DSR and MSCR tests conducted on the PG 70-XX and PG 76-XX binders, respectively. The COV values of the DSR tests were calculated based on the $|G^*|/\sin\delta$ values measured for three binder samples at their corresponding PG temperature. The COV values reported for the MSCR test at each stress level and testing temperature were calculated based on the J_{nr} values measured for three binder samples. The MSCR test was found to exhibit higher COV values than the DSR test for both binder types. The COV values of the DSR test were found to vary between 0.89% and 6.54%, whereas those for the MSCR test varied from 0.08% to 27.25%. Therefore, it can be concluded that the MSCR test is expected to exhibit higher variability than the DSR test. Gollalipour [111] also reported significantly higher variability of MSCR test parameters compared to the Superpave[®] parameters for the same binder.

Table 40. Coefficient of variation (CV) of the DSR and MSCR test of PG 70-XX binders

Binder	CV of DSR Test	CV of MSCR Test 64 °C 0.1 kPa	CV of MSCR Test 64 °C 3.2 kPa	CV of MSCR Test 70 °C 0.1 kPa	CV of MSCR Test 70 °C 3.2 kPa
S1 PG 70-28	3.21	6.24	6.44	4.39	4.56
S2 PG 70-28	0.89	3.03	2.80	21.85	9.06
S3 PG 70-28	1.95	1.95	1.92	3.56	3.60
S5 PG 70-28	1.00	2.35	3.41	5.89	6.31
S6 PG 70-28	2.79	2.33	4.16	0.26	0.36
S7 PG 70-22	1.82	19.07	14.26	27.25	17.86

Table 41. Coefficient of variation (CV) of the DSR and MSCR test of PG 76-XX binders

Binder	Coefficient of variation of DSR test	CV of MSCR Test 64 °C 0.1 kPa	CV of MSCR Test 64 °C 3.2 kPa	CV of MSCR Test 70 °C 0.1 kPa	CV of MSCR Test 70 °C 3.2 kPa	CV of MSCR Test 76 °C 0.1 kPa	CV of MSCR Test 76 °C 3.2 kPa
S1 PG 76-28	2.05	4.09	25.89	16.18	14.19	11.44	0.08
S2 PG 76-28	1.55	4.06	3.56	4.45	3.26	2.44	3.95
S3 PG 76-28	1.37	2.35	1.35	3.80	5.32	3.63	5.20
S4 PG 76-28	1.28	5.17	5.10	4.80	4.63	2.88	2.64
S5 PG 76-28	6.54	8.31	12.93	17.44	17.69	6.90	6.70
S6 PG 76-28	5.38	9.08	6.99	3.35	4.42	5.58	1.72

7.1.4.3 Subjective Comparison of DSR and MSCR Test Methods

A subjective comparison of DSR and MSCR test methods is presented in Table 42. This comparison is expected to help understand the suitability of the MSCR test in practice.

Table 42. Subjective comparison of the DSR and MSCR tests

DSR test	MSCR test
Simple test method	Simple DSR -based test method
Time consuming	Relatively less time consuming
Covers linear viscoelastic properties of the binders	Can be used to determine non-linear viscoelastic properties by adjusting stress level and temperature.
High repeatability and less variability	Higher variability than DSR test
Provides complex shear modulus and phase angle of binder	Determine non-recoverable creep compliance and %recovery of binders.
Cannot differentiate between polymer and non-polymer modified binders.	Differentiate between polymer and non-polymer-modified binders.

7.1.5 Summary

The results of the Superpave[®] and MSCR tests conducted on the polymer-modified binders and RAP binder blends are presented in this chapter. Although all of the polymer-modified binders were observed to meet the continuous high- and low-temperature PG grade specification requirements as labeled by the manufacturers, significant differences in the rheological properties determined by the MSCR test were observed for binders with the same PG grade. Based on the MSCR test results, the polymer-modified binders were observed to exhibit relatively low J_{nr} and high %Recovery values. This indicates a better rutting resistance of the binder when used in an asphalt mix. Also, the non-conventional MSCR tests conducted on the polymer-modified binders at higher stress levels and temperatures provided a better understanding of the non-linear behavior of the binders. Furthermore, the Superpave[®] and MSCR tests were found to help understand the improvement in the rutting performance of the binder blends containing RAP binder. The DSR and MSCR test methods were found to rank the rutting performance of both polymer-modified binders and those containing RAP binder differently. The MSCR-based ranking was found to correlate better with the field rutting performance.

7.2 TEST RESULTS OF ASPHALT MIXES

7.2.1 Introduction

As discussed in Chapter 6, a total of four asphalt mixes, namely MIX-1, MIX-2, MIX-3 and MIX-4 containing polymer-modified binders and RAP, were prepared in this study for testing. This chapter presents the rutting and moisture susceptibility evaluation of the asphalt mixes using a HWT device. A comparative analysis of these Superpave[®] and MSCR test methods considering the HWT rut data is discussed as well.

7.2.2 Volumetric Properties of Asphalt Mixes

Among the four asphalt mixes, two mixes (MIX-1 and MIX-2) were collected from a local plant and the other two mixes (MIX-3 and MIX-4) were prepared in the laboratory. The mix designs for all the mixes were provided by Silver Star Construction Co. The laboratory produced mixes were prepared by mixing different percentages of virgin

aggregates, virgin binder, and RAP, as recommended in the mix design reports. The prepared asphalt mixes were then used to prepare cylindrical samples using a Superpave® Gyratory Compactor (SGC) in accordance with the AASHTO T 31 [217] test method. Four specimens with air voids of $7.0 \pm 0.5\%$ were prepared for each mix type. The specimens were tested in a HWT device.

The MIX-1 specimens were prepared from a S4 mix, which composed of 42% of 5/8" chips, 18% of 3/16" screenings, 25% of manufactured sand and 15% of fine sand with a nominal maximum aggregate size (NMAS) of 12.5 mm. The design asphalt binder content of these specimens was 4.8%. The volumetric properties of the MIX-1 specimens satisfied the ODOT mix design requirements [218]. Tables 43 and 44 summarize the aggregates gradation and volumetric properties of MIX-1.

The MIX-2 specimens were prepared from a S3 mix, with a NMAS of 19 mm. This mix contained 25% RAP. The specimens were composed of 10% of 1" rock, 27% of 5/8" chips, 12% of screenings, 15% of manufactured sand and 11% of fine sand. The design asphalt binder content and the amount of binder replacement by RAP were 4.4% and 31.8%, respectively. A summary of the aggregates' gradation and volumetric properties of MIX-2 is presented in Tables 45 and 46.

The MIX-3 specimens were prepared from a S3 mix with a NMAS of 19 mm. This mix contained 35% RAP. The specimens were composed of 10% of 1" rocks, 27% of 5/8" chips, 19% of screening and 9% of manufactured sand. The design asphalt binder content and the amount of binder replacement by RAP were 4.5% and 44.4%, respectively. A summary of the aggregates' gradation and volumetric properties of MIX-3 is presented in Tables 47 and 48.

The MIX-4 specimens were prepared from a S4 mix with a NMAS of 12.5 mm. This mix contained 35% RAP. The specimens were composed of 10% and 20% of 5/8" chips from two different sources, 26% of manufactured sand 9% of fine sand. The design asphalt binder content and the amount of binder replacement by RAP were 4.8% and

41.7%, respectively. A summary of the aggregates' gradation and volumetric properties of the MIX-4 specimens is presented in Tables 49 and 50.

Table 43. Summary of aggregates' gradation of MIX-1

Blended material	% of each aggregate	
5/8" Chips	42	
3/16" Screens	18	
Man. Sand	25	
Sand	15	
Gradation (sieve size, mm)	%Passing	Required*
19	100	100
12.5	97	90-100
9.5	90	≤ 90
4.75	68	-
2.36	45	34-58
1.18	33	-
0.6	26	-
0.3	18	-
0.15	7	-
0.075	3.7	2-10

* ODOT specification (ODOT, 2012)

Table 44. Summary of aggregate properties and volumetric properties of MIX-1

Volumetric and aggregate properties	Values	Required*
G _{mm}	2.492	
G _{se}	2.691	
G _{sb}	2.671	
G _b	1.01	
Virgin Binder Type	PG 76-28	
Total Binder content (%)	4.8	
Virgin Binder Content (%)	4.8	
P _{ba}	0.28	
VMA (%)	14.7	min. 14.5
VFA (%)	72.8	72-77
DP	0.8	0.6-1.6
LA Abrasion (%)	24	max. 40
Micro Deval (%)	9.7	max. 25
Sand Equivalent (%)	93	min 50
Fractured Faces	100/100	min. 98/95
Tensile Strength Ratio	0.85	min. 0.8
Permeability (10 ⁻⁵ cm/s)	2	max. 12.5

* ODOT specification (ODOT, 2012)

Table 45. Summary of aggregates' gradation of MIX-2

Blended material	% of each aggregate	
1" Rock	10	
5/8" Chips	27	
3/16" Screens	12	
Man. Sand	15	
Sand	11	
Fine RAP	25	
Gradation (sieve size, mm)	% Passing	Required*
25	100	100
19	98	90-100
12.5	88	≤ 90
9.5	75	-
4.75	60	-
2.36	45	31-49
1.18	34	-
0.6	27	-
0.3	18	-
0.15	9	-
0.075	5.3	2-8

* ODOT specification (ODOT, 2012)

Table 46. Summary of aggregate properties and volumetric properties of MIX-2

Volumetric and aggregate Properties	Values	Required*
G_{mm}	2.528	
G_{se}	2.716	
G_{sb}	2.686	
G_b	1.01	
Virgin Binder Type	PG 64-22	
Total Binder content (%)	4.4	
Virgin Binder Content (%)	3	
P_{ba}	0.42	
VMA (%)	13.5	min. 13.5
VFA (%)	71.38	70-75
DP	1.4	0.6-1.6
LA Abrasion (%)	24	max. 40
Micro Deval (%)	9.7	
Sand Equivalent (%)	79	min 40
Fractured Faces	100/100	min. 85/80
Tensile Strength Ratio	0.83	min. 0.8
Permeability (10^{-5} cm/s)	0.2	max. 12.5

* ODOT specification (ODOT, 2012)

Table 47. Summary of aggregates' gradation of MIX-3

Blended material	% of each aggregate	
1" Rock	10	
5/8" Chips	27	
Man. Sand	19	
Sand	9	
Fine RAP	35	
Gradation (sieve size, mm)	%Passing	Required*
25	100	100
19	96	90-100
12.5	85	≤ 90
9.5	72	-
4.75	55	-
2.36	40	31-49
1.18	31	-
0.6	25	-
0.3	18	-
0.15	9	-
0.075	5.4	2-8

* ODOT specification (ODOT, 2012)

Table 48. Summary of aggregate properties and volumetric properties of MIX-3

Volumetric and aggregate properties	Values	Required*
G _{mm}	2.556	
G _{se}	2.754	
G _{sb}	2.707	
G _b	1.01	
Virgin Binder Type	PG 64-22	
Total Binder content (%)	4.5	
Virgin Binder Content (%)	2.5	
P _{ba}	0.64	
VMA (%)	13.5	min. 13.5
VFA (%)	69.9	70-75
DP	1.4	0.6-1.6
LA Abrasion (%)	24	max. 40
Micro Deval (%)	9.7	-
Sand Equivalent (%)	87	min 40
Fractured Faces	100/100	min. 85/80
Tensile Strength Ratio	0.86	min. 0.8
Permeability (10 ⁻⁵ cm/s)	5.5	max. 12.5

* ODOT specification (ODOT, 2012)

Table 49. Summary of aggregates' gradation of MIX-4

Blended material	% of each aggregate	
5/8" Chips	10	
5/8" Chips	20	
Man. Sand	26	
Sand	9	
Fine RAP	35	
Gradation (sieve size, mm)	%Passing	Required*
19	100	100
12.5	95	90-100
9.5	83	≤ 90
4.75	62	-
2.36	44	34-58
1.18	33	-
0.6	26	-
0.3	19	-
0.15	9	-
0.075	5.4	2-10

* ODOT specification (ODOT, 2012)

Table 50. Summary of aggregate properties and volumetric properties of MIX-4

Volumetric and aggregate properties	Values	Required*
G_{mm}	2.516	
G_{se}	2.72	
G_{sb}	2.691	
G_b	1.01	
Virgin Binder Type	PG 64-22	
Total Binder content (%)	4.8	
Virgin Binder Content (%)	2.8	
P_{ba}	0.4	
VMA (%)	14.7	min. 14.5
VFA (%)	72.1	72-77
DP	1.2	0.6-1.6
LA Abrasion (%)	24	max. 40
Micro Deval (%)	9.7	-
Sand Equivalent (%)	88	min. 40
Fractured Faces	100/100	min. 85/80
Tensile Strength Ratio	0.84	min. 0.8
Permeability (10^{-5} cm/s)	2.5	max. 12.5

* ODOT specification (ODOT, 2012)

7.2.3 Hamburg Wheel Tracking (HWT) Test Results

All the mix samples were tested at 50 °C using a HWT device under wet condition in accordance with the AASHTO T 324 test method [219]. Samples were tested up to 20,000 wheel passes or 20 mm rut depth, whichever reached first. The rut depths at 11 points on the specimen along the wheel-path were recorded automatically for each wheel pass and were saved in a Microsoft ACCESS database. The rut depths at the mid-point of the specimen (Point No. 6) were considered for analysis. The rut depths obtained from two sets of tests conducted on the same asphalt mix were averaged and used for further evaluation. It was observed that the moving steel wheels of the HWT device vibrate vertically on the rough specimen surface which introduces noise into the rut depth readings. The moving averages of the rut depth readings along the time axis were taken to remove this noise. Lu and Harvey [202] used the following Equations 8, 9 and 10 to calculate the moving averages of the HWT test results.

$$\bar{d}_t = 0.40d_t + 0.25d_{t+1} + 0.15d_{t+2} + 0.10d_{t+3} + 0.10d_{t+2} \quad (1 \leq t \leq 5) \dots \dots \dots (8)$$

$$\begin{aligned} \bar{d}_t = & 0.05d_{t-5} + 0.05d_{t-4} + 0.075d_{t-3} + 0.075d_{t-2} + 0.15d_{t-1} \\ & + 0.20d_t + 0.15d_{t+1} + 0.075d_{t+2} + 0.075d_{t+3} + 0.05d_{t+4} + 0.05d_{t+5} \end{aligned} \quad (5 < t < 19,995) \dots \dots \dots (9)$$

$$\bar{d}_t = 0.40d_t + 0.25d_{t-1} + 0.15d_{t-2} + 0.10d_{t-3} + 0.10d_{t-4} \quad (19,995 \leq t \leq 20,000) \dots \dots \dots (10)$$

The important performance parameters, namely post compaction deformation, creep slope, stripping slope, and stripping inflection point were determined from the HWT test results. The post compaction deformation observed instantaneously just after starting the test simulates the densification of asphalt mix owing to initial trafficking. Yildirim and Kennedy (2002) used the rut depth at 1,000 wheel passes as the post-compaction point. The linear region of the rut progression curve after post compaction point is called creep region which represents rutting due to plastic flow. The creep slope is defined as the rut depth per wheel pass in the creep region. The stripping inflection point is used to characterize the moisture-induced damage of the asphalt mix. The stripping slope was obtained by drawing lines between the stripping inflection point and

the final wheel pass. In this study, the creep and stripping slopes were defined as the number of passes per unit of rut depth for convenience.

7.2.4 Evaluation of Rutting and Resistance to Moisture-induced Damage of the Mixes

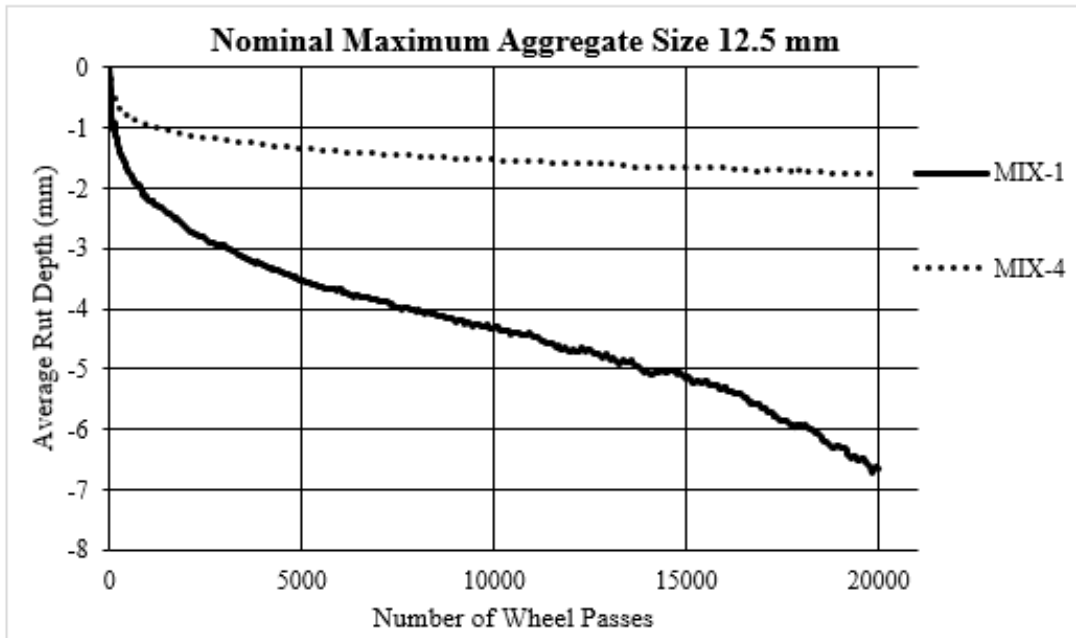
Figure 115 presents the average rut depth with respect to wheel passes for all asphalt mix specimens. Rut depths at 1,000, 5,000, 10,000, 15,000, and 20,000 passes for all four mix specimens are presented in Table 51. The performance parameters were determined from HWT curves and are presented in Table 52. From Figure 115, it was observed that the rut depths at 20,000 passes for all four mix specimens were less than 10 mm. However, only the MIX-1 specimens, which contained polymer-modified PG 76-28 binder, exhibited moisture-induced damage. None of the other three mixes containing RAP were found to exhibit moisture-induced damage during the test, since no stripping inflection points were observed.

The MIX-1 and MIX-4 specimens can be compared to examine the effects of polymer-modified binder and high RAP content on rut performance. From Figure 115 (a) and Table 51, it is evident that, although both the MIX-1 and MIX-4 specimens were S4 mixes with a NMAS = 12.5 mm, the MIX-4 specimens containing PG 64-22 and 35% RAP exhibited a lower rut depth compared to the MIX-1 specimens, which contained PG 76-28 binder without any RAP. The rut depths for the MIX-1 and MIX-4 specimens after 20,000 wheel passes were found to be 6.63 and 1.77 mm, respectively. Also, the creep slopes for the MIX-1 and MIX-4 specimens were found to be 5,458 and 28,986 passes/mm, respectively. Furthermore, the MIX-1 specimens exhibited a stripping inflection point at 16,100 passes with a stripping slope of 2,952 passes/mm. Therefore, it can be concluded that MIX-1, which contained polymer-modified PG 76-28 binder, is expected to exhibit higher rutting and moisture-induced damage than MIX-3, which contained PG 64-22 binder and 35% RAP.

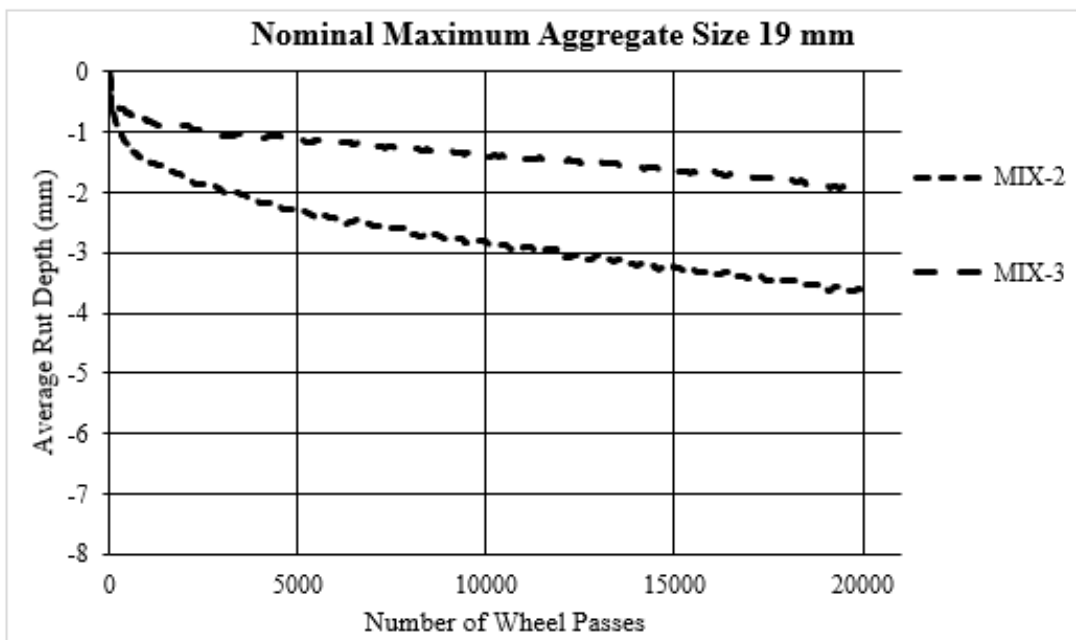
The effect of incorporating high amount of RAP in the mix on rutting performance can be evaluated by comparing the results of the HWT tests conducted on the MIX-2 and MIX-3 specimens. From Figure 115 (b) and Table 51, it can be observed that the

average rut depth for the MIX-2 specimens, which contained 25% RAP, was higher than those measured for the MIX-3 specimens, which contained 35% RAP. The post compaction deformations for the MIX-2 and MIX-3 specimens were found to be 1.49 and 0.89 mm, respectively. Also, the creep slopes for the MIX-2 and MIX-3 specimens were found to be 9,948 and 18,770 passes/mm, respectively. These results indicate that an asphalt mix containing high RAP content is expected to exhibit a higher rutting resistance. These observations agree with the findings reported by others [134, 135, 138].

The effect of aggregate gradation on the rut performance of asphalt mixes was evaluated using the HWT test results of the MIX-3 and MIX-4 specimens. From Table 51, the average rut depth measured for the MIX-3 (S3 mix) specimens was 1.95 mm, which was higher than the average rut depth measured (1.77 mm) for the MIX-4 (S4 mix) specimens. The creep slopes for the MIX-3 and MIX-4 specimens were found to be 18,770 and 28,986 passes/mm, respectively. This means that the S4 mix tested in this study is expected to perform better than the S3 mix in terms of rutting resistance.



(a)



(b)

Figure 115.HWT test results of the asphalt mixes: (a) NMAS= 12.5 mm; (b) NMAS= 19 mm

Table 51. Rut depths of asphalt mix specimens at different number of wheel passes

MIX ID	1000 Wheel passes	5000 Wheel passes	10000 Wheel passes	15000 Wheel passes	20000 Wheel passes
MIX-1	2.22	3.54	4.3	5.13	6.63
MIX-2	1.49	2.27	2.85	3.24	3.64
MIX-3	0.81	1.10	1.41	1.64	1.95
MIX-4	0.97	1.34	1.53	1.67	1.77

Table 52. Performance parameters of asphalt mix specimens obtained from the HWT tests

MIX ID	HWT indices Post- compacti on (mm)	HWT indices Creep slope (mm/Pass)	HWT indices Creep slope (Passes/mm)	HWT indices Stripping inflection point	HWT indices Stripping slope (mm/Pass)	HWT indices Stripping slope (Passes/m m)
	2.22	0.00018	5458	16100	0.00034	2952
MIX-2	1.49	0.00010	9948	N/A	N/A	N/A
MIX-3	0.81	0.00005	18770	N/A	N/A	N/A
MIX-4	0.97	0.00003	28986	N/A	N/A	N/A

7.2.5 Comparison of HWT, DSR and MSCR Test Results

Table 53 presents a comparison of the HWT, DSR, and MSCR test results. The amount of binder replacement by RAP for each mix, as mentioned in Section 7.2.2se, was used for this evaluation. The properties of the asphalt mixes were compared with the properties of corresponding equivalent RAP binder blends. For example, the HWT rut depth measured for the MIX-2 specimens (31.8% of binder replaced by RAP), was compared with the DSR and MSCR test results of the PG 64-22-R1-25 binder. The $|G^*|/\sin\delta$ values of the RTFO-aged binders at the corresponding high temperature were used for this comparison. Also, the J_{nr} values of the binders determined at 64 °C and 3.2 kPa stress level were used to compare with the HWT rut depths. Figure 116 presents a comparison of the DSR and HWT test results. It can be observed that the mixes with a NMA S = 12.5 mm, the HWT rut depth increased with a reduction in the

$|G^*|/\sin\delta$ value. A similar increasing trend of rut depth with a reduction in the $|G^*|/\sin\delta$ value was observed for asphalt mixes with a NMAS = 19 mm although the amount was not the same. Figure 117 presents a comparison of the MSCR and HWT tests results. From Figure 116, it can be observed that the HWT rut depth exhibited an increasing trend with an increase in J_{nr} value for asphalt mixes with an NMAS = 19 mm. However, asphalt mixes with a NMAS = 12.5 mm exhibited a completely opposite trend. The HWT rut depth was found to increase with a decrease in J_{nr} value. As mentioned in Section 7.2.2, the binder properties of the two mixes were different (one polymer-modified binder and another containing RAP binder). The sensitivity of the J_{nr} parameter to polymer modification may be the reason for this discrepancy. Other studies have reported that the J_{nr} at 3.2 kPa stress level correlated well with the HWT rut test results and can be used as a parameter for characterizing the rutting resistance of asphalt binders when used in a mix [173, 216]. Additional studies are needed on asphalt mixes used in Oklahoma to develop correlations between the DSR, MSCR and HWT test results.

Table 53. Comparison of HWT, DSR and MSCR test results

MIX ID	NMAS	Binder type	%Binder replacement	Rut depth (mm)	Equivalent RAP binder blend	$ G^* /\sin\delta$ (kPa)	J_{nr} (kPa^{-1})
MIX-1	12.5	PG 76-28	0.00	6.63	0	2.79	0.03
MIX-2	19	PG 64-22 + RAP	31.82	3.64	25	14.6	1.77
MIX-3	19	PG 64-22 + RAP	44.44	1.95	40	14.77	1.14
MIX-4	12.5	PG 64-22 + RAP	41.67	1.77	40	14.77	1.14

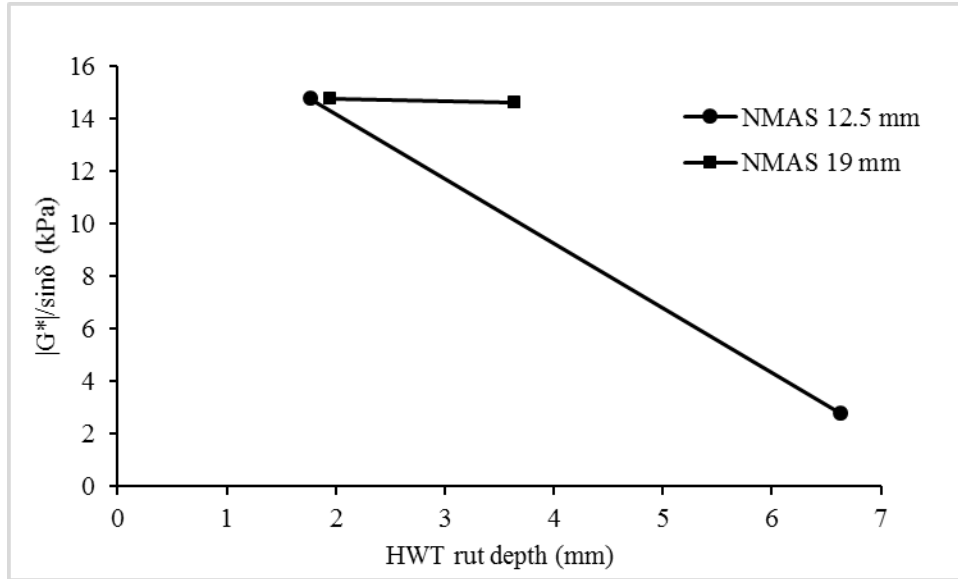


Figure 116. Comparison of DSR and HWT test results

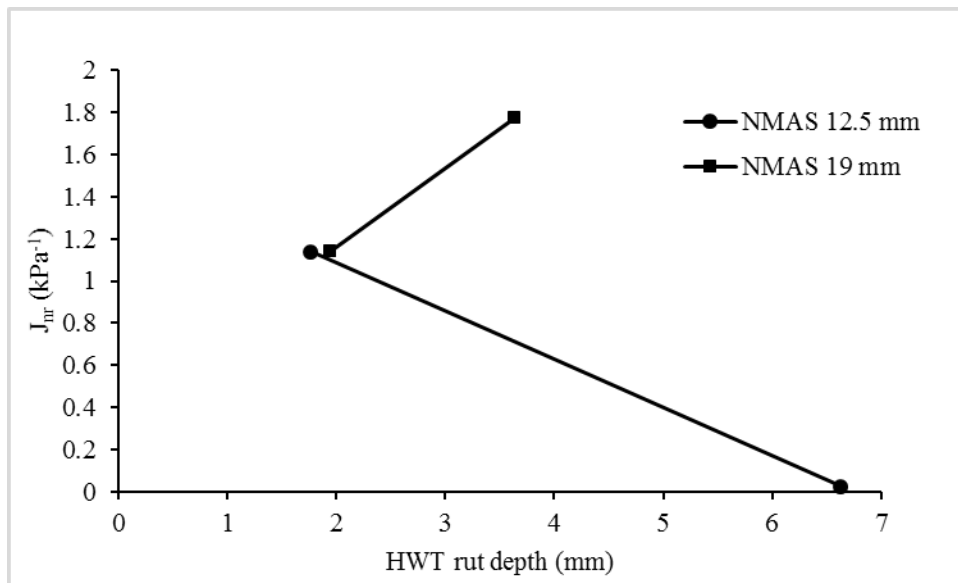


Figure 117. Comparison of MSCR and HWT test results

7.2.6 Summary

The results of the HWT tests conducted on asphalt mix specimens are presented in this chapter. Based on the HWT test results, the asphalt mixes with polymer-modified binder exhibited higher susceptibilities to rutting and moisture-induced damage than the asphalt mixes with RAP. Also, the HWT rut depths of the asphalt mixes was observed to reduce with an increase in the RAP content from 25% to 35%. Furthermore, the

rutting resistance of the S4 mix with 35% RAP was found to be better than that of the S3 mix with the same amount of RAP. Based on the comparison of the HWT, DSR and MSCR test results, the HWT rut depth was observed to increase with a reduction in the $|G^*|/\sin\delta$ value and with an increase in the J_{nr} value.

THIS PAGE IS LEFT INTENTIONALLY BLANK

CHAPTER 8

PART THREE LITERATURE REVIEW

8.1 INTRODUCTION

8.1.1 Background

One of the popular techniques to enhance asphalt pavement performance is the modifications use in the asphalt binder by utilizing materials such as polymer, lime, carbon black, fibers, and rubbers [220]. The use of polymer-modified asphalt binders has grown tremendously in North America due to the increasing stress on the highways from higher traffic volumes and heavier loads. The Strategic Highway Research Program (SHRP) on asphalt was carried out almost exclusively with unmodified asphalt cements, so the applicability of the Superpave Performance Graded (PG) AASHTO M320 specifications and test methods to modified binders was not validated.

Consequently, Departments of Transportation (DOT) in most of the states have added supplemental specifications, also known as “PG-Plus” tests, to identify the presence of polymers and modifiers. Louisiana is among the states that are currently using a PG-Plus specification. Separation of polymer, force ductility (AASHTO T300), and elastic recovery are the required tests for the Louisiana Department of Transportation and Development’s (LADOTD’s) PG-Plus specifications. The use of polymer modifiers in asphalt binders was found to be a promising technique to improve the performance of asphalt mixtures. However, an insight impact of polymer modifiers on asphalt binders relevant to the performance is yet to be researched [220].

Overview on Force Ductility Test

The force ductility test is used to estimate the asphalt binder potential for fatigue and thermal cracking, and/or raveling [221]. It was first introduced by Anderson and Wiley in 1976 [222] to indicate expected low temperature performance of asphalt binders by comparing their relative strength at low temperatures while being pulled at a fixed deformation rate [223]. Later, in 1985, Shuler [224-225] modified the test procedure to improve the precision and practicality, particularly for use with polymer modified asphalt

binders. Many agencies have adopted the rheology characterization methods. However, there are some agencies still using AASHTO T300 for characterizing polymer modified asphalt binders in which an asphalt binder sample is elongated typically at 4°C and 5 cm/min deformation rate until fragile fracture or reaching the elongation of at least 30 cm. AASHTO T300 specifies the force ratio (ratio of the force at the second peak to the force at the initial peak) to be reported. The first peak is related to the base asphalt and the second peak characterizes the polymer [224-225].

However, performing force ductility test is a time and material consuming process. It is subject to reproducibility difficulties and can exhibit significant variability at low to intermediate temperatures (4°-25°C) [221, 226, 227]. Besides variability in results, force ductility test requires the use of a ductility bath, which has several disadvantages including inconsistency of the testing sample geometry. Also, the force ductility test reflects the structure response of the sample not the material properties response. Most importantly, these tests are empirical [228] and often fail to accurately and comprehensively characterize the performance characteristics associated with polymer modified asphalt [227-228]. Many studies failed to correlate force ductility results with the asphalt binder performance. One of these studies is a study conducted by Tabatabaee [229]. No correlation was found between the force ductility results and the number of cycles to fatigue failure N_f which was calculated based on linear Amplitude Sweep LAS results at the intermediate grade temperature. It was also reported that force ductility test was not able to consistently detect the presence of the elastomeric modification. A survey was conducted of several state DOTs (such as Louisiana and Illinois) that specify force ductility test in their requirements; we observed the diversity of specifications in the force ductility test. Table 54 shows the PG plus requirements for performance graded asphalt binder (modified) for four different states.

Table 54 PG plus requirement for performance graded asphalt binder (modified) for four different states.

State	Criteria	Temp	Test Method	Requirements	Requirements	Requirements	Requirements	Requirements	Requirements	Requirements	Requirements
Illinois	(f2/f1)	4°C	T300	Binder (SB/SBS)	64-29	70-22	70-28	76-22	76-28		
Illinois	(f2/f1)	4°C	T300	Requirements	0.30 min	0.30 min	0.30 min	0.35 min	0.35 min		
Louisiana	(f2/f1)	4°C	T300	Binder	76-22 M						
Louisiana	(f2/f1)	4°C	T300	Requirements	0.30 min						
Louisiana	f2 in kg	4°C	T300	Binder	70-22 M						
Louisiana	f2 in kg	4°C	T300	Requirements	0.23 min						
Michigan	(f2/f1)	4°C	T 300	Binder	58-34 P	64-28 P	64-34 P	70-22 P	70-28 P	76-22 P	76-28 P
Michigan	(f2/f1)	4°C	T 300	Requirements	0.30 min	0.30 min	0.35 min	0.30 min	0.30 min	0.35 min	0.35 min
Oregon	(f2/f1)	4°C	ODOT TM 427	Binder	AC-15-5T R						
Oregon	(f2/f1)	4°C	ODOT TM 427	Requirements	0.30 min						

Figures 118 and Figure 119 were reported on the LTRC Project No. 11-2B [230]. It shows a visual of how the ductility test unclearly detects the second peak elongation force f_2 . Furthermore, it failed to detect it in some cases.

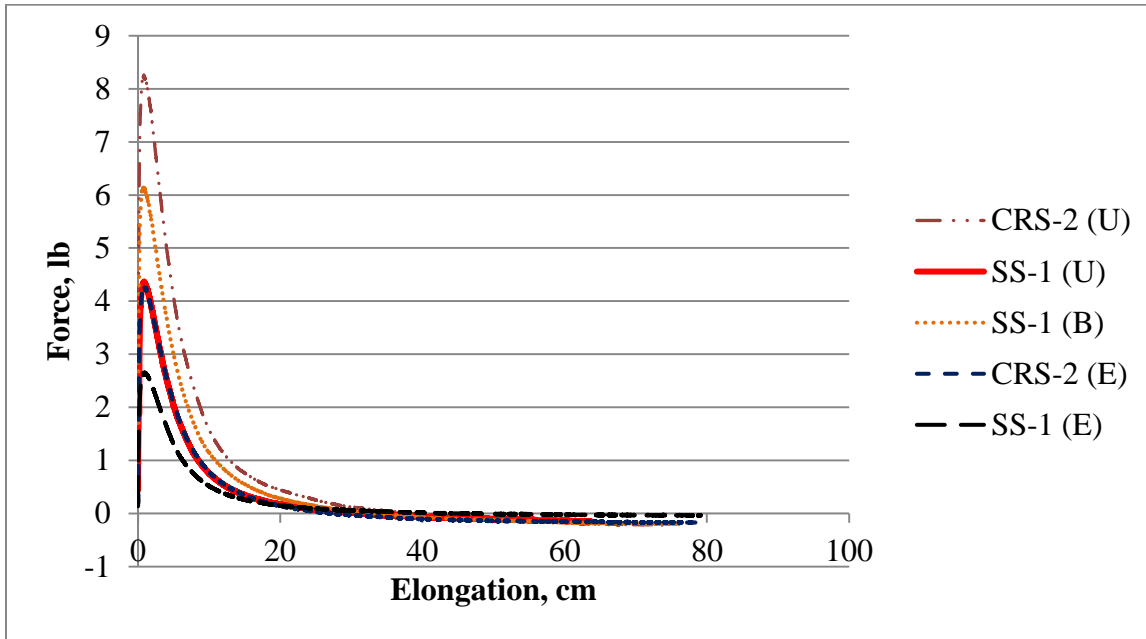


Figure 118. Force ductility results of non-polymer modified asphalt emulsion [230]

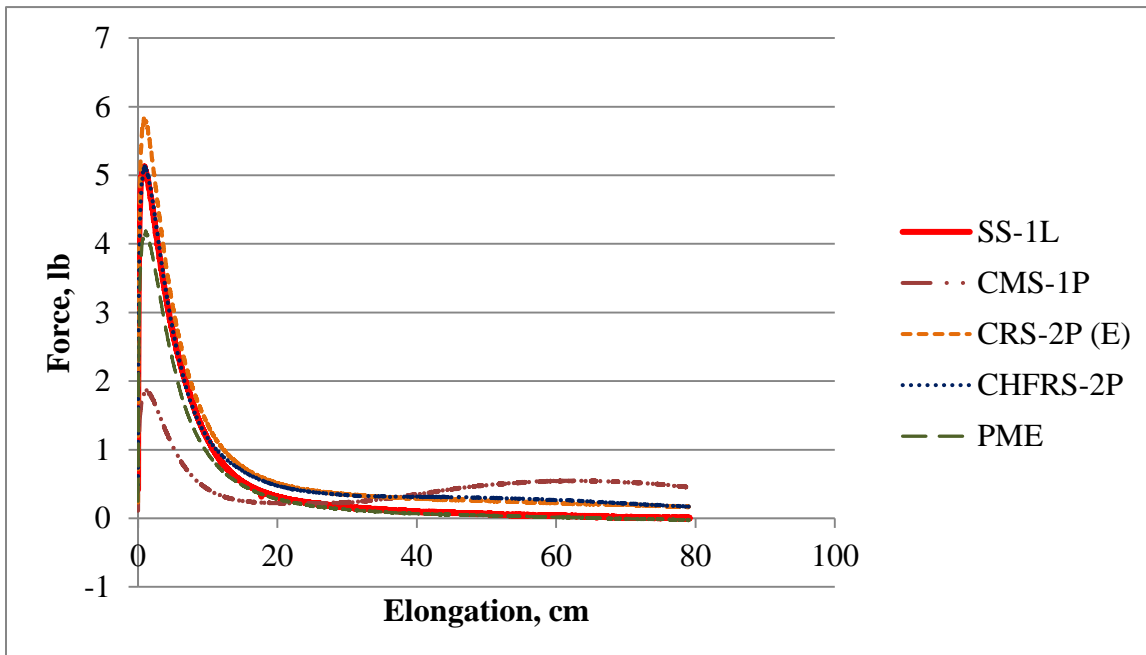


Figure 119. Force ductility results of polymer modified asphalt emulsion [230]

8.1.2 Overview on the Polymer Modified Asphalt Binder Characterization

Relating the polymer modified asphalt binder's properties to its molecular structure has become increasingly advocated. Simple shear is the most common method that has been used to generate most of the material's deformation. Characterizing the polymer's extensional flow behavior has historically been quite difficult because the deformations experienced by polymers during processing are both rapid and large [231]. Therefore, shear rheometers failed to differentiate between certain polymer's micro-structure features. One of the attempts to replace the simple shear methods was by the United States Federal Highway Administration when they proposed to replace AASHTO M 320-05 high temperature specifications and parameters, by the multi-stress creep recovery [232]. In NCHRP Project 9-10 [233], it was reported that linear binder tests ($G^*/\sin\delta$) which are performed in the LVE (linear visco-elastic) region such as high temperature tests of the current PG System do not correlate with high temperature mixture failure such as rutting unless the binder is a viscous fluid in those temperatures.

Therefore, to address mix failure accurately, non-linear binder properties should be evaluated. Multiple Stress Creep Recovery MSCR testing (AASHTO TP70) and the specifications (ASHTO MP19) were developed to describe binder properties in the non-linear range. The MSCR consists of a multiple stress-creep recovery. In its current form, it consists of 10 cycles of each stress level of 0.41 and 3.2 kPa; each cycle consists of 1 s of creep loading followed by 9 s recovery period [232]. There are two crucial parameters of the MSCR test: 1-The temperature of the test and 2-The applied shear stress [15]. It is now believed that MSCR based AASHTO MP19 provides asphalt binder specifications blind to modifications. Furthermore, some studies (NCHRP Project 9-10) do show that for some modifications, MSCR based high temperature grading is not significantly different than AASHTO M320. A new parameter J_{nr} has been developed, which is currently considered as a replacement for the parameter $G^*/\sin\delta$ at high temperatures. J_{nr} is the average of the non-recovered strain in every 10 cycles group over the applied stress appropriate for the group. However, when relating J_{nr} to the pavement rutting through the wheel tracking test results, the correlation between J_{nr} and the rutting depth exist just in the high stress levels of the MSCR test. As reported by

D'Angelo [2009a, 2009b], the linear viscoelastic description of the asphalt is not applicable when MSCR large shear stresses applied to the material.

Extensional flows have a high sensitivity towards the polymer's molecular microstructure, such as the polymer's long-chain branching [231]. Extensional rheometers can be much more accurate describing the polymer characteristics than the other type of rheological measurements mentioned above. In 2004, Sentmanat [231] developed the dual wind-up extensional rheometer "Sentmanat Extensional Rheometer" SER for short that achieved a truly uniform extensional deformation. Additionally, SER invests the fiber wind-up technique in applying the true strain rate to the specimen during the uniaxial extensional experiment. Furthermore, this fixture can convert a conventional rotational rheometer host system into a universal testing station capable of performing extensional melt rheology experiments, all within the controlled environment of the host system's environmental chamber. To this end, this study has been initiated to replace AASHTO T300 with an extensional deformation test using SER.

8.2 ADVANTAGES OF USING SER FOR CHARACTERIZATION OF POLYMER IN ASPHALTIC MATERIALS REPLACING FORCE DUCTILITY TESTS

- The SER fixture can be accommodated in currently used commercially available DSR models and will therefore replace the force ductilimeter with DSR.
- Less than 1 gm of materials is needed for the test.
- SER results reflect the material properties response.
- More four samples can be tested in 1 hour. The SER will provide Hencky strain rate, Elongation Viscosity, and it is more mechanistic.
- Most importantly, SER identifies polymer network (branching) through strain hardening measurements.

8.3 DESCRIPTION OF THE SER

As shown in Figure 120 and described in detail by Sentmanat [231], SER consists of a paired master, and slave wind-up drums mounted on bearing housed within a chassis, and mechanically coupled via termeshing gears. The rotational motion of the rheometer spindle drives the rotation of the drive shaft which results in the rotation of the master drum, and an equal opposite rotation of the slave drum, which causes the wound up of the two ends of the sample “secured by the clamps to the drums” onto the drums, rustling the sample stretched over an unsupported length, L_o .

For a constant drive shaft rotational rate, Ω , equal dimension wind-up drums R , and fixed unsupported length of the sample L_o , the applied Hencky strain rate to the sample can be expressed as [231]

$$\varepsilon_H = \frac{2\Omega R}{L_o} \dots \dots \dots (11)$$

The resistance of the sample to stretch in both drums, torque T , is measured by the torque transducer attached to the fixture which can be expressed as [231]

$$T(t) = 2RF(t) \dots \dots \dots (12)$$

For a constant strain rate experiment, the instantaneous cross-sectional area $A(t)$ can be expressed as [231]

$$A(t) = A_0 \exp [-\varepsilon_H t] \dots \dots \dots (13)$$

For a constant strain rate, the tensile stress function $\eta_E^+(t)$, can be expressed as [231]

$$\eta_E^+(t) = \frac{F(t)}{\varepsilon_H A(t)} \dots \dots \dots (14)$$

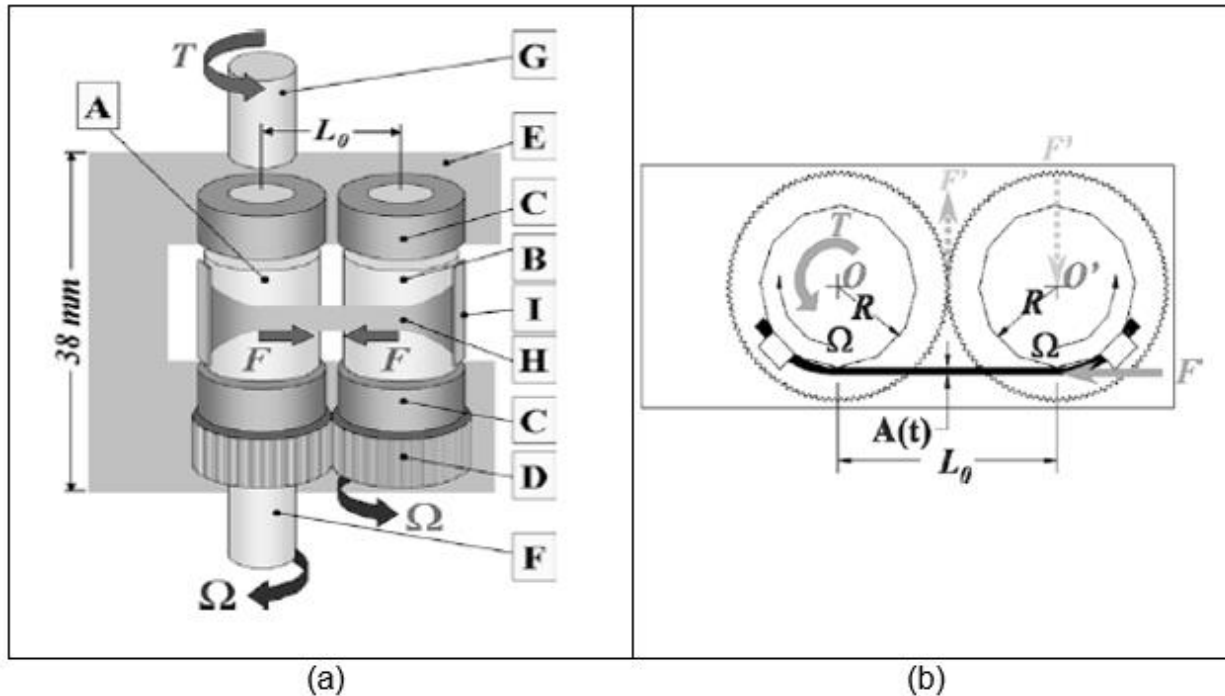


Figure 120. a) Side view of the Sentmanat Extensional Rheometer (SER) during Operation. Inside Squares: A. Master Drum, B. Slave Drum, C. Bearings, D. Intermeshing Gears, E. Chassis, F. Drive Shaft, G. Torque Shaft, H. Sample, I. Securing Clamps. b) Elevation the SER during an experiment. Symbols: L_0 Unsupported Length, Ω Drive Shaft Rotation Rate, T Torque, F Tangential Force.

8.4 VALIDATION OF SER RESULTS WITH PREVIOUS EXTENSIONAL RESULTS

8.4.1 Extension Experiment with Commercial poly-isobutylene (PIB) (BASF Oppanol (B15) [2])

Extensional experiments were performed at 23°C. The poly-isobutylene macular characteristics are as follows: macular number (M_n) of 44,000 and macular weight (M_w) of 88,000. The same material has been tested through uniaxial extension experiments by other independent laboratories [234-235]. Figure 121 shows the tensile stress curves results from the SER superposed with the stress growth results reported from the other laboratories. The agreement between the SER data and the data reported in the other studies can be observed through a variety of extensional rheometer technologies.

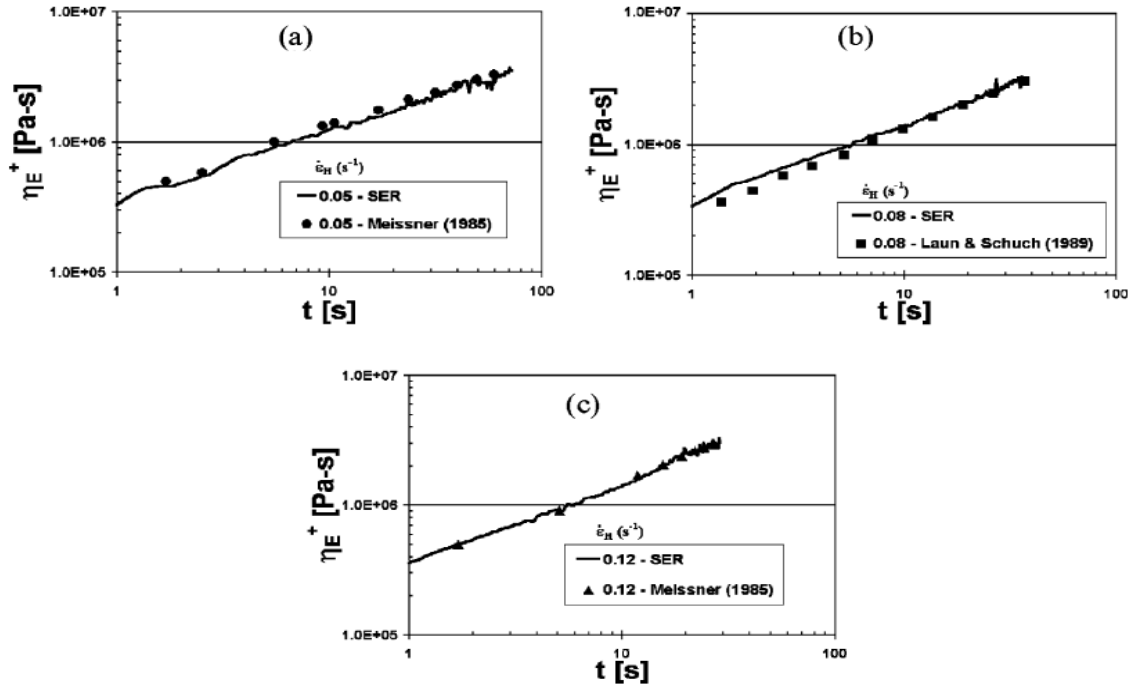


Figure 121. Comparison of tensile stress growth curves data from SER and another extensional rheometer technology [220]

8.4.2 Extensional Experiment with Natural Rubber [231]

Due to the extreme resilient of uncured natural rubber, it can be hard to characterize its rheological properties especially at room temperature. Therefore, the linear viscoelastic (LVE) properties of natural rubber can be a challengeable task to obtain by the simple shear method due to the slipping associate with the experiments of simple shear. Even though the relaxation modulus $G(t)$ of the LVE shear stress of natural rubber can be difficult to determine at room temperature without the use of the rheometer fixture sample bonding, it can be easily determined through the step extensional experiment with the SER. Figure 122 shows the LVE stress relaxation modulus for natural rubber NR-RSS2 using the SER.

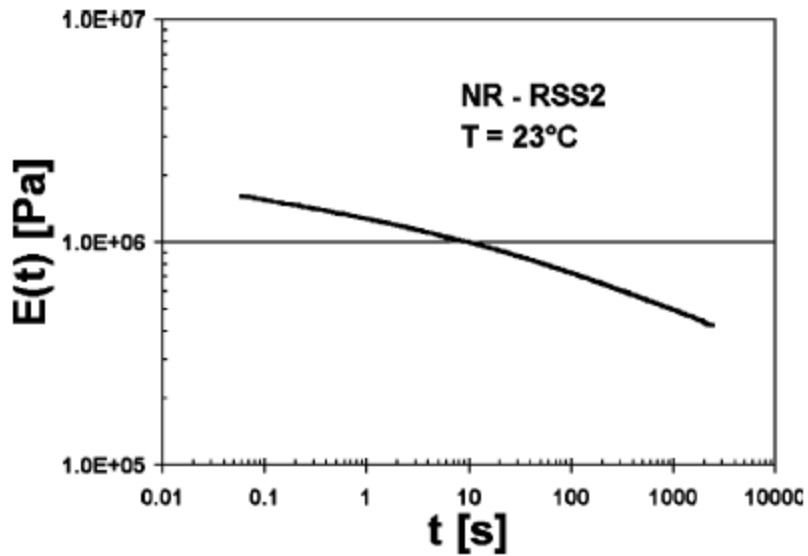


Figure 122. Extensional stress relaxation modulus for NR-RSS2 at 23°C [231]

Figure 123 indicates tensile stress growth curves plot for uncured NR-RSS2 at room temperature and constant Hencky strain rates ranging from 0.001 s^{-1} to 10 s^{-1} . Also included in the graph is a LVE stress relaxation modulus data plot from Figure 122 integrated with respect to time, which theoretically defines the LVE envelope of tensile stress growth behavior. Note the perfect agreement between the low-strain portion of all five tensile stress growth curves.

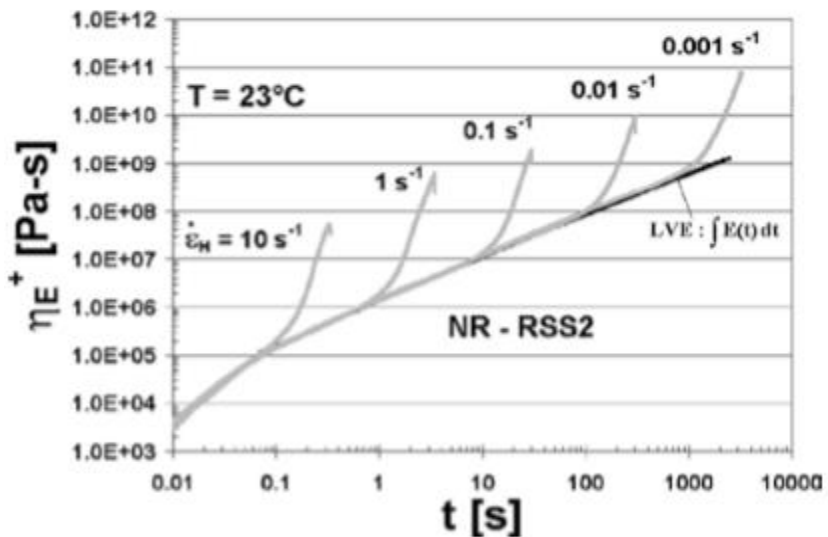


Figure 123. Tensile stress growth curves for NR-RSS2 for constant Hencky strain rates ranging from 0.001 s^{-1} to 10 s^{-1} .

8.4.3 Shear Rheology of Lupolen 1840H [236]

Figure 124 shows the extensional rheology of the transient extensional viscosity function $\eta_E^+(\varepsilon_H, t)$ for affinity LLDPE. The results were generated by a SER-HV-P01 mounted on Anton Paar MCR501 torsional rheometer. The solid line illustrates the linear viscoelastic envelop $\eta_E^+ = 3\eta^+$ generated from shear experiment with a cone and plate fixture. The similarity of results between the two methods can be observed.

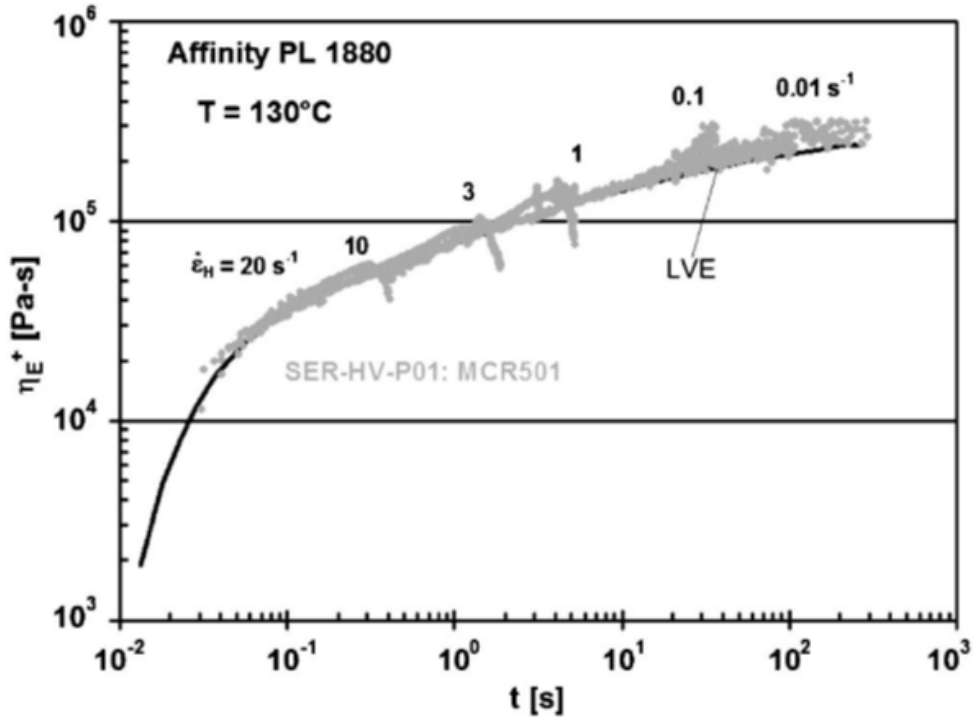


Figure 124. Tensile stress growth curves at 130°C for Affinity PL 1880 LLDPE obtained from the SER. Also shown LVE given by $\eta_E^+ = 3\eta^+$ generated by the cone and the plate measurements in start-up steady shear flow.

THIS PAGE IS LEFT INTENTIONALLY BLANK

CHAPTER 9

PART THREE METHODOLOGY

9.1 INTRODUCTION

In this study, the applicability of Sentmanat Extensional Rheometer (SER) to accurately detect the second peak elongation force was investigated. The effect of geometry, temperature, Table 55 and polymer on the elongation force were investigated. Sample preparation and the test procedure were developed for asphalt binders to be tested in the SER.

9.2 EXTENSIONAL TEST PARAMETERS

1. Sample geometry (Width, Thickness, and Area)
2. Test temperature
3. Extensional rate
4. Asphalt binder grade (PG)
5. Existence of Polymer

9.3 SELECTION OF ASPHALT BINDER GRADES

Three asphalt binder grades were chosen to be investigated in this study: PG 76-22, PG 64-22 and PG 58-28. PG 76-22 is a polymer modified binder, PG 64-22 and PG 58-28 are neat binders. The main objective of selecting the above-mentioned binder grades is to explore the hypothesis that the SER will detect the second peak elongation force in PG 76-22 but not in PG 64-22 accurately and PG 58-28 due to the polymer's modification.

The secondary objective is to investigate the accuracy of the SER in detecting the elongation force through verifying the principle rule that PG 76-22 should show greater first peak elongation force than PG 64-22, and PG 58-22 should display the least elongation force among the three binders.

9.4 SELECTION OF GEOMETRY

In this study, nine different geometries were chosen to investigate the effect of geometry in the second peak elongation force. Eight geometries were specified during the experimental plan stage. Then, the ninth geometry was added during the experimenting stage to improve the understanding of geometry's effect on the elongation force. The nine geometries are as follow:

1. (W= 5 mm x T= 0.6 mm) A= 3.0 mm²
2. (W= 7.5 mm x T= 0.4 mm) A = 3.0 mm²
3. (W= 6 mm x T= 0.6 mm) A= 3.6 mm²
4. (W= 9 mm x T= 0.4 mm) A= 3.6 mm²
5. (W= 5 mm x T= 0.83 mm) A= 4.2 mm²
6. (W= 6 mm x T= 0.83 mm) A= 5.0 mm²
7. (W= 8 mm x T= 0.72 mm) A= 5.8 mm²
8. (W= 9 mm x T= 0.72 mm) A= 6.5 mm²
9. (W= 10 mm x T= 0.83 mm) A= 3.6 mm²

9.5 SELECTION OF TEMPERATURE

In order to recommend the appropriate testing temperature for the newly developed test procedure, 4°C, 10°C and 16°C were chosen to be explored as testing temperatures. No testing temperature above 16°C was chosen because at higher temperature, lower viscosity of asphalt sample causes higher final strain. That exceeds the maximum recommended Hencky strain specified by the SER manufacturer, which is equal to 4 per drum.

9.6 EXPERIMENTAL PLAN

As mentioned earlier, PG 76-22, PG 64-22, and PG 58-28 were used in this study to verify SER results' reproducibility. One hundred twenty-two extensional deformation

tests were performed as shown in Table 55. Ninety-five tests out of the total 122 were performed in PG 76-22 polymer modified binder to investigate the capability of the SER to accurately detect the second peak elongation force. Eighty-three tests out of the 95 were performed at 4°C with nine different geometries to analyze the effect of the width and the thickness on the elongation force. The nine geometries were chosen according to the following categories:

1. Same initial areas with different width and thickness
2. Different initial areas with different width and different thickness
3. Different initial areas with different width but same thickness
4. Different initial areas with different thickness but same width

Ten replicates of each of the eight geometries were tested, then the ninth geometry was added with 3 replicates for more detailed investigation on the effect of width and thickness. Six samples of PG 76-22 were tested at 10°C using two geometries (three tests each). Six more samples were tested at 16°C using two geometries (three tests each) to investigate the temperature effect on the extensional deformation and its parameters.

Fifteen PG 64-22 samples were tested at 4°C with five different geometries and every geometry was tested three times to analyze the differences in elongation force behavior between modified and neat binders. Twelve PG 58-28 samples were prepared and tested at 4°C using four different geometries with three replicates for each geometry.

Table 55. Summary of materials and experimental plan

Sample Width W mm (+/- 0.25)	Sample Thickness T mm (+/-0.06)	Sample Area A mm² (+/- 0.39)	No. of Samples	Temperature	Binder
5	0.6	3.0	10	4°C	PG 76-22
7.5	0.4	3.0	10	4°C	PG 76-22
6	0.6	3.6	10	4°C	PG 76-22
9	0.4	3.6	10	4°C	PG 76-22
5	0.83	4.2	10	4°C	PG 76-22
6	0.83	5.0	10	4°C	PG 76-22
8	0.72	5.8	10	4°C	PG 76-22
8	0.72	5.8	3	10°C	PG 76-22
8	0.72	5.8	3	16°C	PG 76-22
9	0.72	6.5	10	4°C	PG 76-22
9	0.72	6.5	3	10°C	PG 76-22
9	0.72	6.5	3	16°C	PG 76-22
10	0.83	6.5	3	4°C	PG 76-22
7.5	0.4	3.0	3	4°C	64-22
7.5	0.4	3.0	3	4°C	58-28
9	0.72	6.5	3	4°C	64-22
9	0.72	6.5	3	4°C	58-28
6	0.83	5	3	4°C	64-22
6	0.83	5	3	4°C	58-28
8	0.72	5.8	3	4°C	64-22
9	0.4	3.6	3	4°C	64-22
6	0.6	3.6	3	4°C	58-28

9.7 SAMPLE PREPARATION

PG 76-22, PG 64-22 and PG 58-28 Samples were prepared using the following steps:

9.7.1 Preparing the Binder

- a. The binder in the main can was heated in the oven at 150°C for 45 minutes.
- b. Around 100 g of binder was placed in each of 5 different small metal cans to reduce the aging that occurs due to the repeated heating process as shown in Figure 125.
- c. The binder in one of the small cans was heated in the oven at 150°C for around 20 minutes until it liquefied.

9.7.2 Controlling the Sample Thickness

- a. The binder was poured in a 1 in diameter silicon mold to control the amount of binder needed as shown in Figure 126. Silicon was selected to be the molding material because asphalt does not adhere to silicon. The size of the mold was selected to be 1-in in diameter to simplify the thickness control process by reducing the amount of binder under the loads.
- b. The liquid binder that was poured in the silicon mold was left in room temperature for 15 to 20 minutes until it cooled down, so it could be removed from the silicon mold.
- c. In order to control the sample thickness, the sample was placed onto a silicon mat between two stainless steel plates with the exact desired thickness as shown in Figure 128. After few trials, 1.7 in was found to be

the suitable spacing dimension between the stainless-steel plates to allow the binder to spread to a uniform thickness.

- d. To block the adhesion between the asphalt sample and the glass plate from the next step, a minimum 2 in x 2 in silicon mat was placed over the sample overlapping with the stainless-steel plate as shown in Figure 129. The overlapping is to ensure that the silicon mat will not slip from the stainless-steel plates, and affect the sample's thickness control process. The other dimension of the silicon mat is to ensure that the sample was covered after spreading.
- e. In order to ensure a uniform distribution of the loads over the sample, a 2 in x 2 in thick glass plate was placed over the silicon mat, overlapping with the stainless-steel plates as shown in Figure 130.
- f. 20 lb of loads were placed over the thick glass plate. For the polymer modified binders' the loads were kept over the sample for 18 to 24 hours as shown in Figure 131. Several trials of 8, 12 and 14 hours were made but the sample's thickness increased by around 1 mm after removing the loads due to the increasing of the softening point as a result of polymer modification, which to increase its elastic properties [237-241]. As for the non-modified binders, the loads were kept over the sample for 10 to 12 hours.
- g. The loads were removed along with the glass plate and the silicon mat as shown in Figure 132.

9.7.3 Cutting the Sample to the Desired Dimensions

- a. The sample was placed in a refrigerator at 5°C for 1 to 2 minutes.

- b. The sample was removed carefully from the big silicon mat to a smaller 4 in x 4 in silicon mat.
- c. The sample was placed in a refrigerator at 5°C for 2 to 3 minutes. If the sample is left at 5°C for longer than 2 to 3 minutes the sample will crack during the cutting process as shown in Figure 133. If the sample is left at 5°C for less than 2 to 3 minutes, the sample will stick to the metal edge during the cutting process as shown in Figure 134.
- d. Immediately after removing the sample from the refrigerator, the sample was cut with a sharp metal edge to the desired dimensions as shown in Figure 135 and Figure 136. The sample was measured by a slide caliper to ensure the desired dimensions as shown in Figure 137.



Figure 125. The binder placed in to the small can

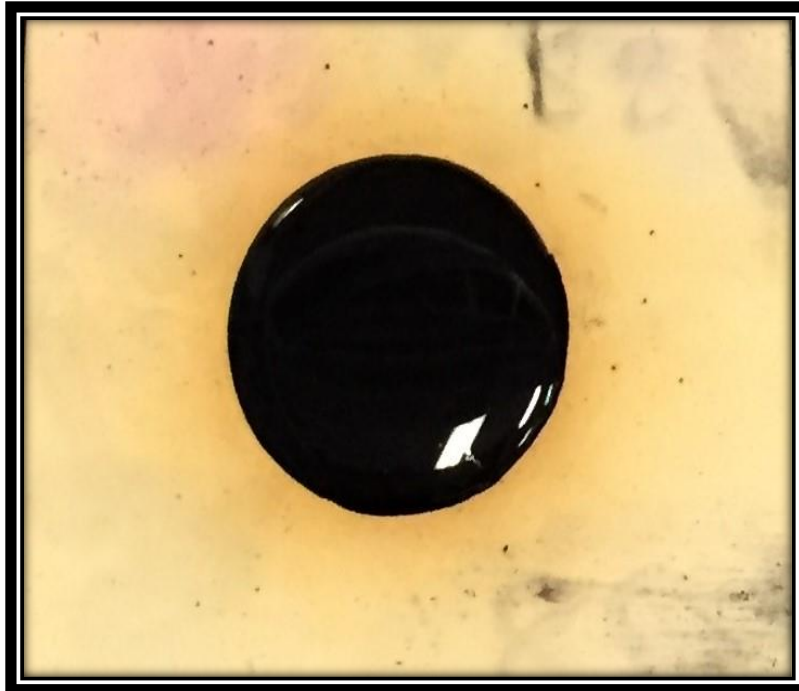


Figure 126.The binder poured in to the silicon mold



Figure 127.The binder was removed from the silicon mold

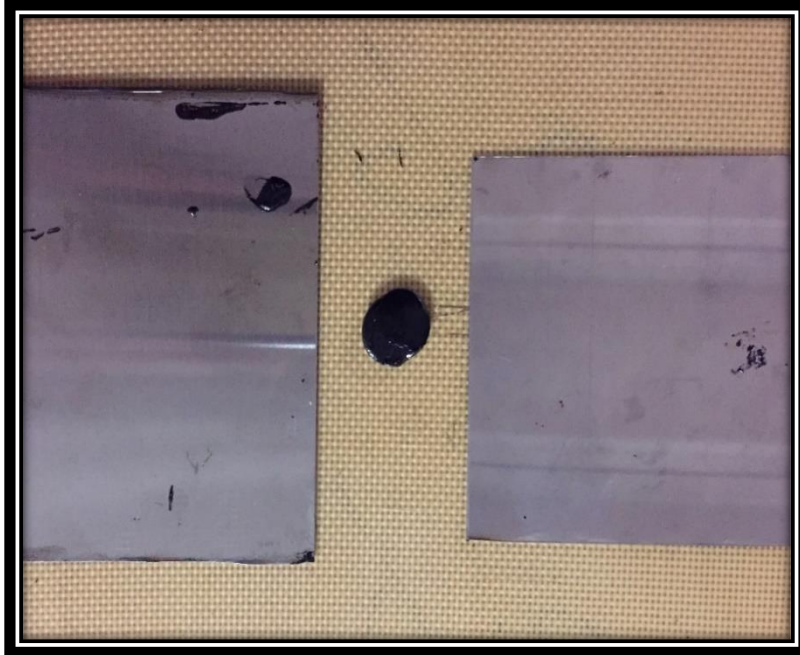


Figure 128. Binder placed between two stainless steel plates

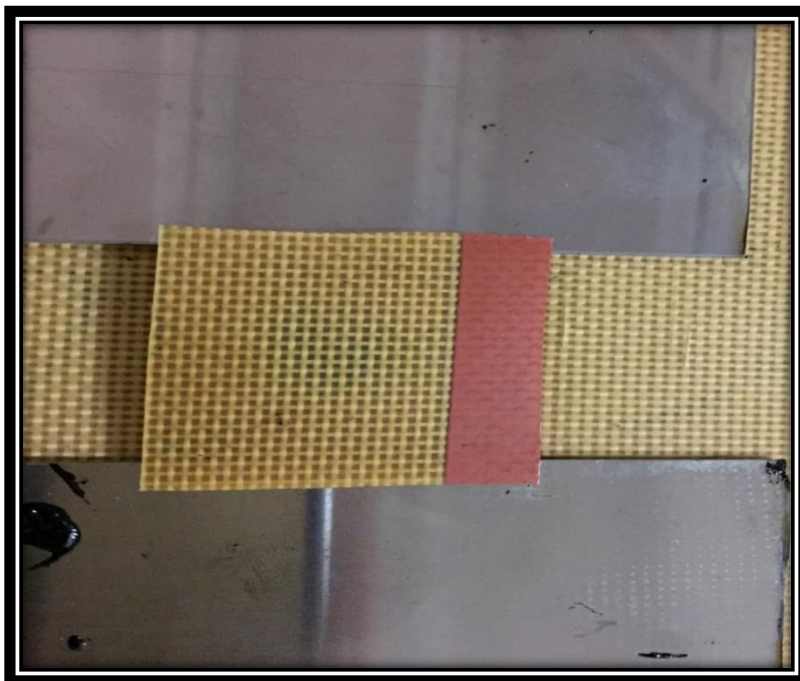


Figure 129. Silicon mat placed above the binder

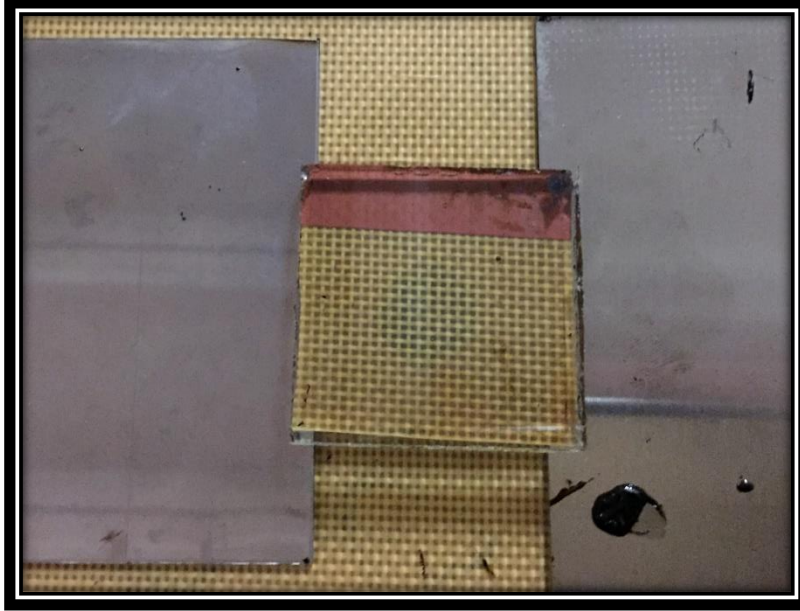


Figure 130. The thick glass placed over the silicon mat



Figure 131. The loads placed over the thick glass

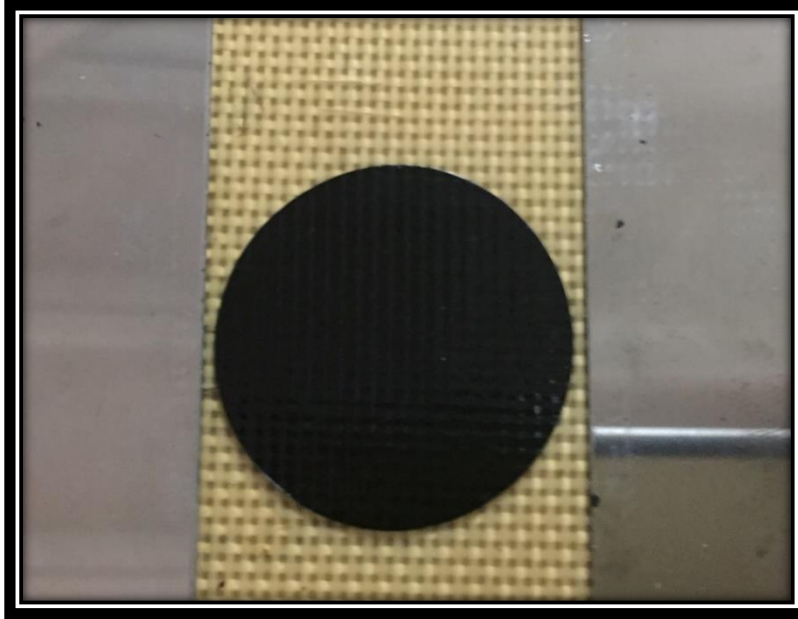


Figure 132. The binder's shape after removing the loads

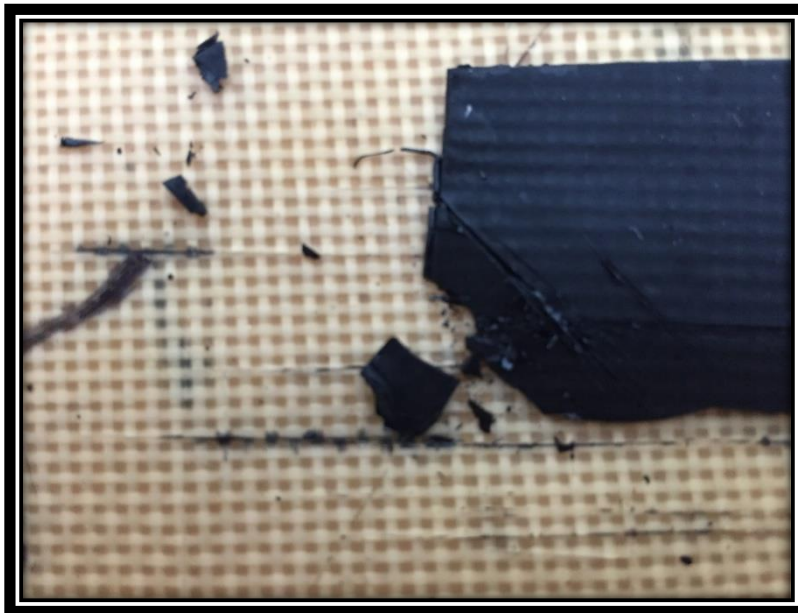


Figure 133. Cracked during the cutting process due to a long cooling period



Figure 134. Sticking to the metal edge due to a short cooling period



Figure 135. Cutting the binder to the desired length

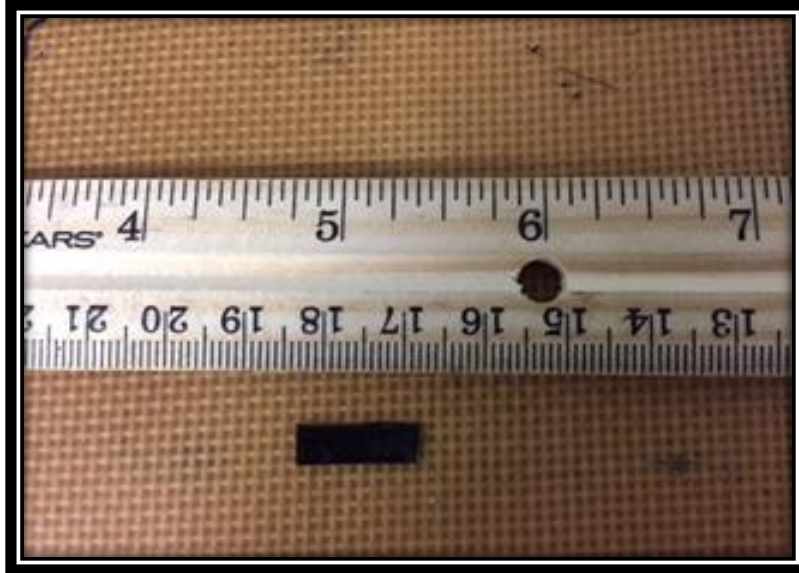


Figure 136. Sample with desired dimensions



Figure 137. Sample with desired dimensions

9.8 TEST PROCEDURE

Measurements were performed on a Universal Testing Platform model SER3-G, manufactured by Xpansion Instruments LLC. Connected to DSR model AR2000 Ex with an environmental chamber.

1. As shown in Figure 140, SER consists of paired master and slave wind-up drums connected to a drive shaft. Rotation of the drive shaft results in the rotation of the master drum and an equal and opposite rotation of the slave drum, which results in the stretching of the sample.
2. The sample was loaded and secured at each end by clamps as shown in Figure 141, and then the chamber was closed.
3. At the beginning, samples slipped several times during the tests because of the high stresses resulting from the solid tensile testing as shown in Figure 143.
4. Therefore, an ultra-thin double-sided adhesion tape with a thickness of 0.1 mm was placed into the drum prior to the sample loading to prevent the sample from slipping as shown in Figure 144.
5. As for the test parameters, as shown in Figure 146 the environmental control was set to 4°C, the soak time was 600 s, and the wait for temperature option was activated to ensure temperature equilibrium. The solid density was set to 1.0 g/cm³, and the melt density was set to 0.95 g/cm³. Final strain was 3.4 rad, with a strain rate of 0.1 s⁻¹. For more accurate measurements, the fast sampling option was activated.
6. Figure 143 shows the sample during the extensional deformation. Figure 148 shows the sample at the end of the test. Upon completion of the test, the sample was removed immediately, and the drums were carefully cleaned with a soft wipe, and paint thinner was used as needed.

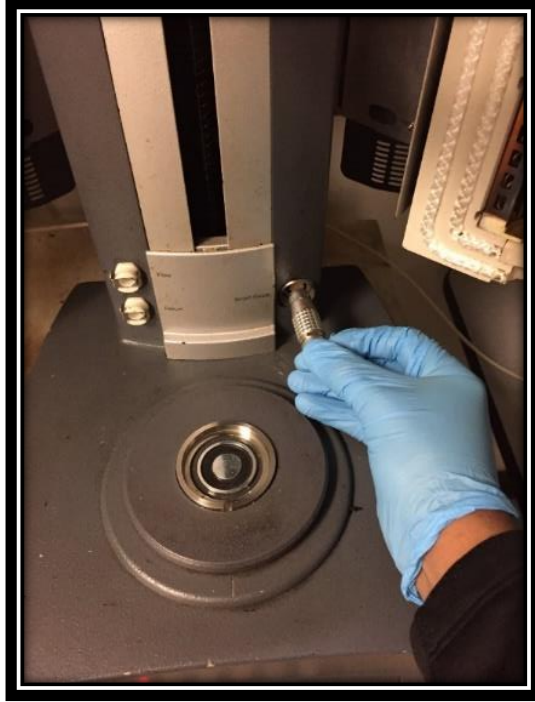


Figure 138. Inserting the smart swap.

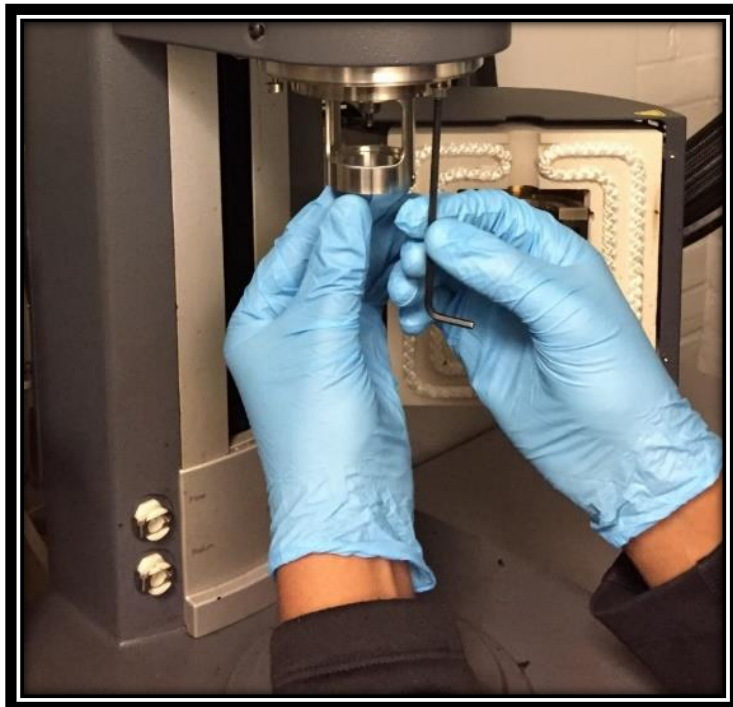


Figure 139. Fixing the SER bracket

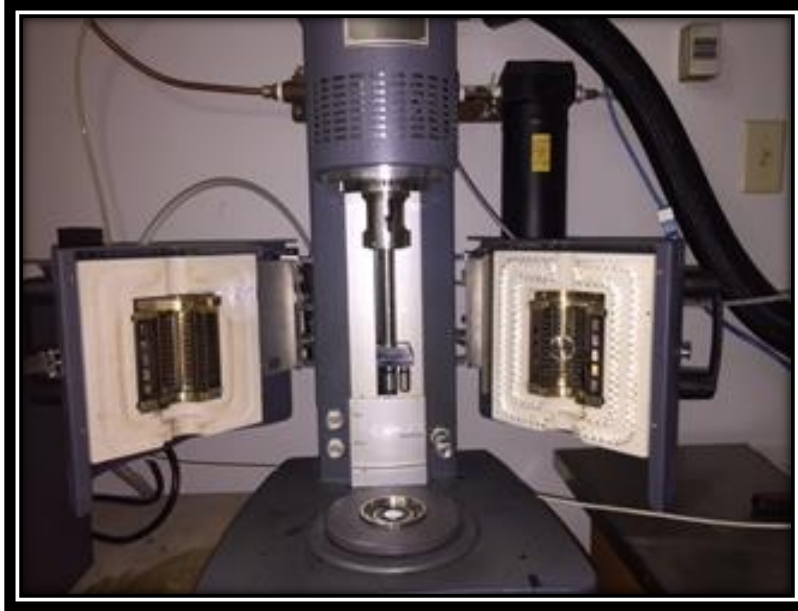


Figure 140. The SER fixture prior to the sample loading



Figure 141. SER fixture after loading the sample

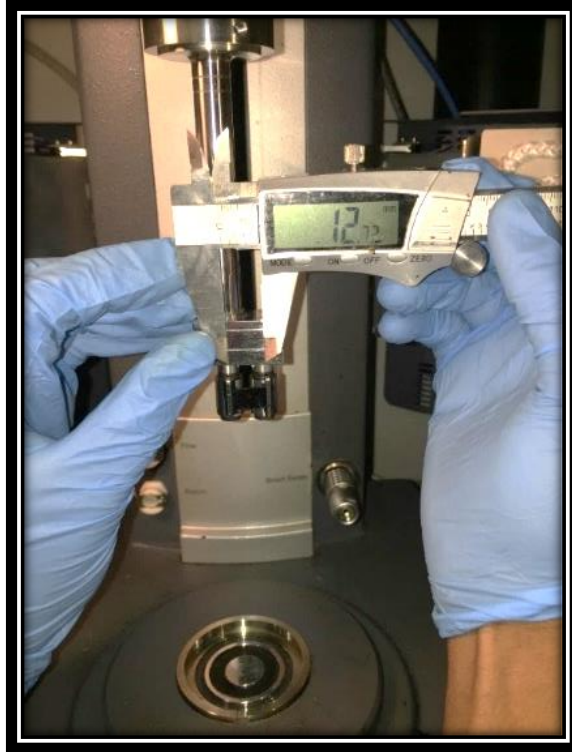


Figure 142.Length of the sample 12.75 mm

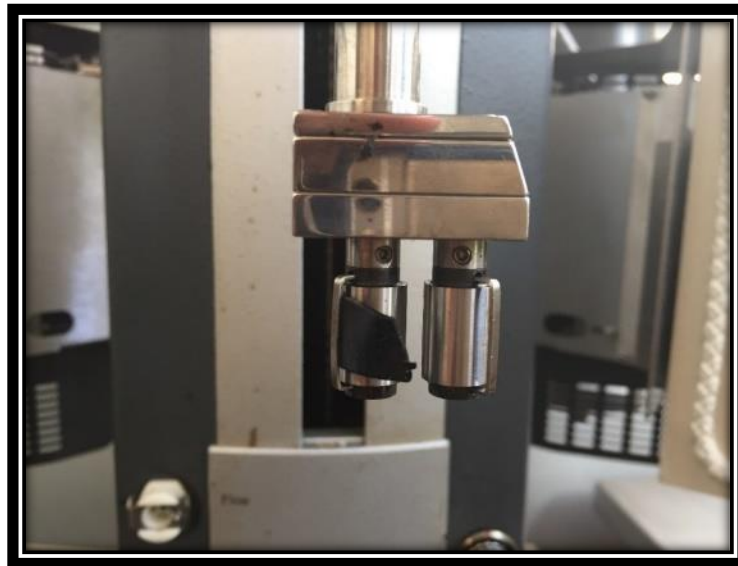


Figure 143.Clamps kicked out due to the hard stresses

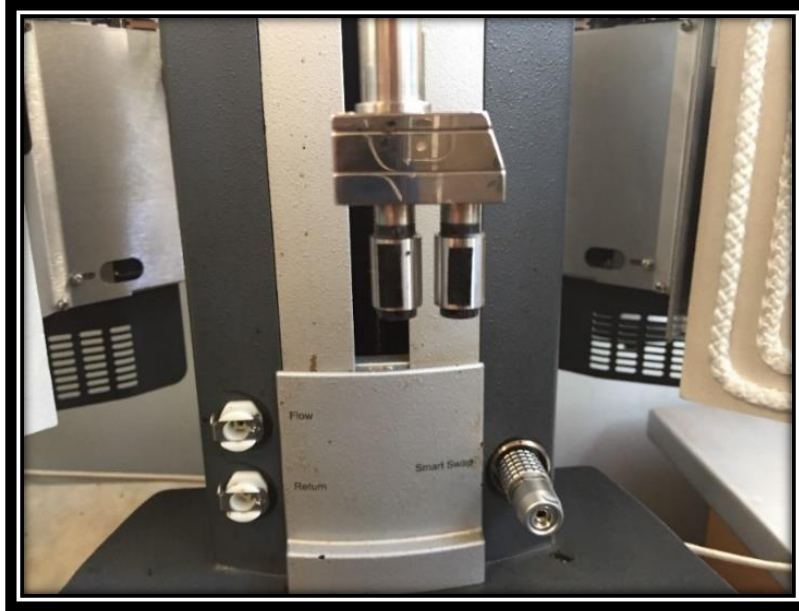


Figure 144. Double-sided adhesion tape fixed to the drums

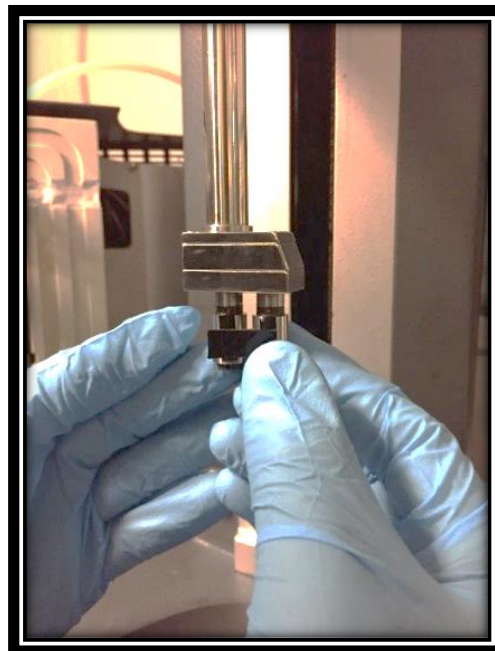


Figure 145. Loading the sample post to the double-side adhesion tape

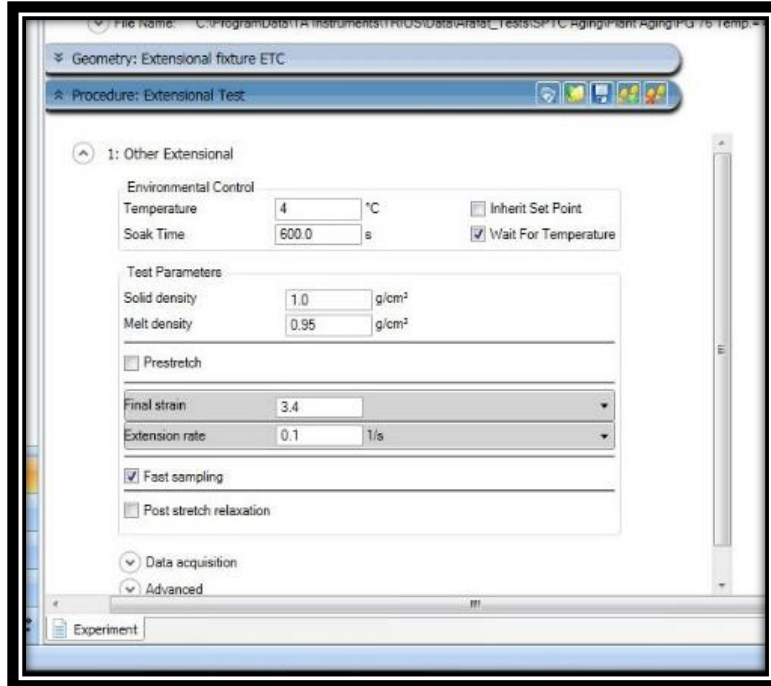


Figure 146. Software screenshot shows the test Parameter



Figure 147. Software screenshot shows the DSR control panel



Figure 148. Sample during the extensional deformation test



Figure 149. Sample after the end of the test

CHAPTER 10

PART THREE RESULTS AND DISCUSSIONS

10.1 SIMULATING SECOND AND FIRST PEAK ELONGATION FORCE

10.1.1 Introduction

Polymer modified binder is a non-homogeneous material [242]. The first part of the “elongation force vs. time” graph reflects the asphalt yielding due to the tensile force, so it is primarily due to the base asphalt’s behavior. The second part of the curve describes polymer behavior, so it depends on the polymer modification type and level of the [243].

One of the major objectives of this study was to simulate second peak elongation force of asphalt modified binders using Sentmanat Extensional Rheometer (SER).

In pursuit of this objective, PG 76-22, PG 64-22, and PG 58-28 samples were prepared to be tested in the SER according to the procedure described earlier. The results showed that SER can accurately detect the polymer effect in modified asphalt binder through simulating the second peak elongation force.

10.1.2 Simulating Second Peak Elongation Force

Three types of asphalt binders with three different geometries were illustrated in Figures 150 to 4.9. Binders were PG76-22, PG 64-22 and PG 58-22. Every binder was tested with three different geometries: $W = 9 \text{ mm} \times T = 0.72 \text{ mm}$, $W = 7.5 \text{ mm} \times T = 0.4 \text{ mm}$, and $W = 6 \text{ mm} \times T = 0.83 \text{ mm}$.

It can be observed from Figures 150 through Figure 158 that, PG 76-22 showed second peak elongation force for all the above mentioned three geometries. Comparatively, no second peak elongation force has been detected for PG 64-22 and PG 58-22. This demonstrates the above-mentioned statement: the second part of the Elongation Force vs Step Time curve describes the polymer’s behavior.

The general elongation force trend of PG 76-22 can be described as follow: Elongation force sharply increased immediately after starting the test until it reached the first peak elongation force F_1 . Then it started to decrease gradually for less than 2N until it reached the point of inflection F_m . As mentioned in Section 10.1.1, polymer modified binders are non-homogeneous material. Therefore, at the point of inflection, elongation force started to rise again due to the polymer yielding behavior until it reached the second peak elongation force. Immediately after that, the binder sample reached the final strain or the failure point 0 N, after which it can be described as sharp failure criteria. The time between the second peak elongation force and the final strain point is less than five seconds for all three geometries.

10.1.3 Simulating First Peak Elongation Force

As mentioned in Section 10.1.3, the first part of the Elongation Force vs Step Time curve reflects the asphalt yielding due to the tensile force. Hence, to evaluate the asphalt binder performance, the first peak elongation force is an important parameter to analyze.

It can be observed from Figures 150 to 158 that PG 64-22 showed less first peak elongation force than PG 76-22, and PG 58-28 showed less first peak elongation force than PG 64-22. This was expected because PG 76-22 has the highest stiffness among the three binders, and PG 58-28 has the lowest stiffness.

As for the failing criteria of PG 64-22 and PG 58-28, they are more ductile than PG 76-22. In the cases of PG 64-22 and PG 58-22, the time between the highest peak elongation force, which the first peak elongation force, and the final strain point is around 25 seconds. This variance of failing criteria is because of the polymer impact on the elongation force curve characteristics. The polymer inverts the elongation force at the point of inflection as shown in Figures 150, 153, and 156.

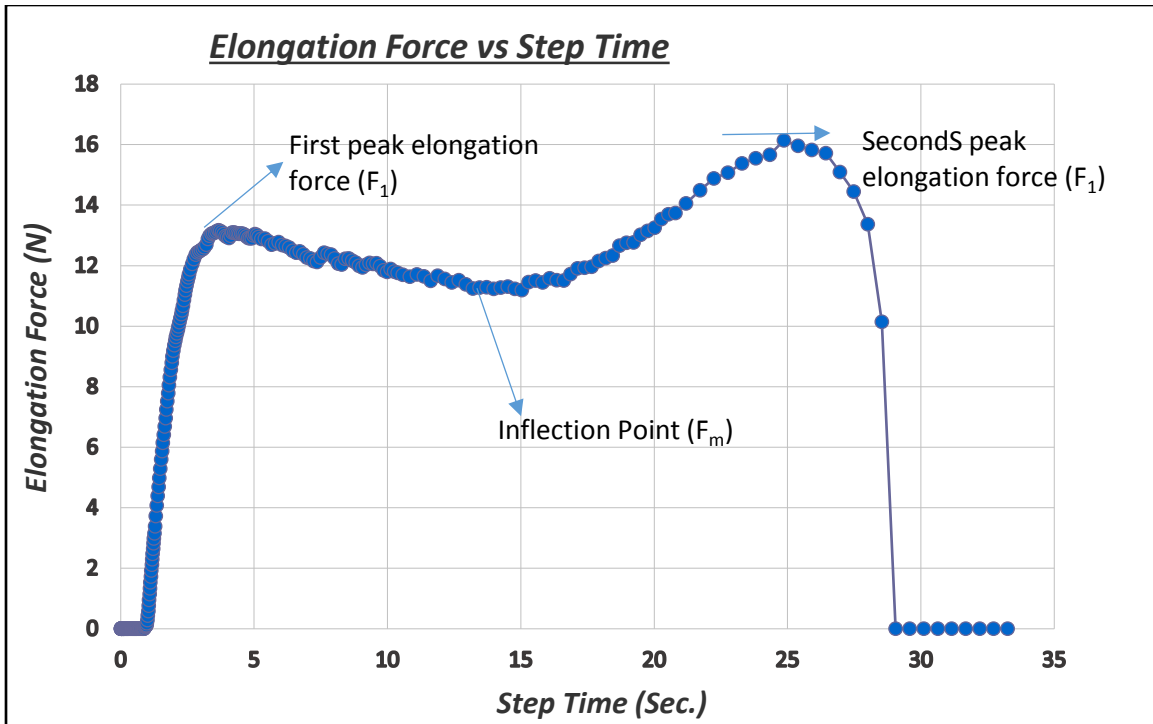


Figure 150. Elongation force vs. step time for PG 76-22 geometry of 9.0 mm x 0.72 mm

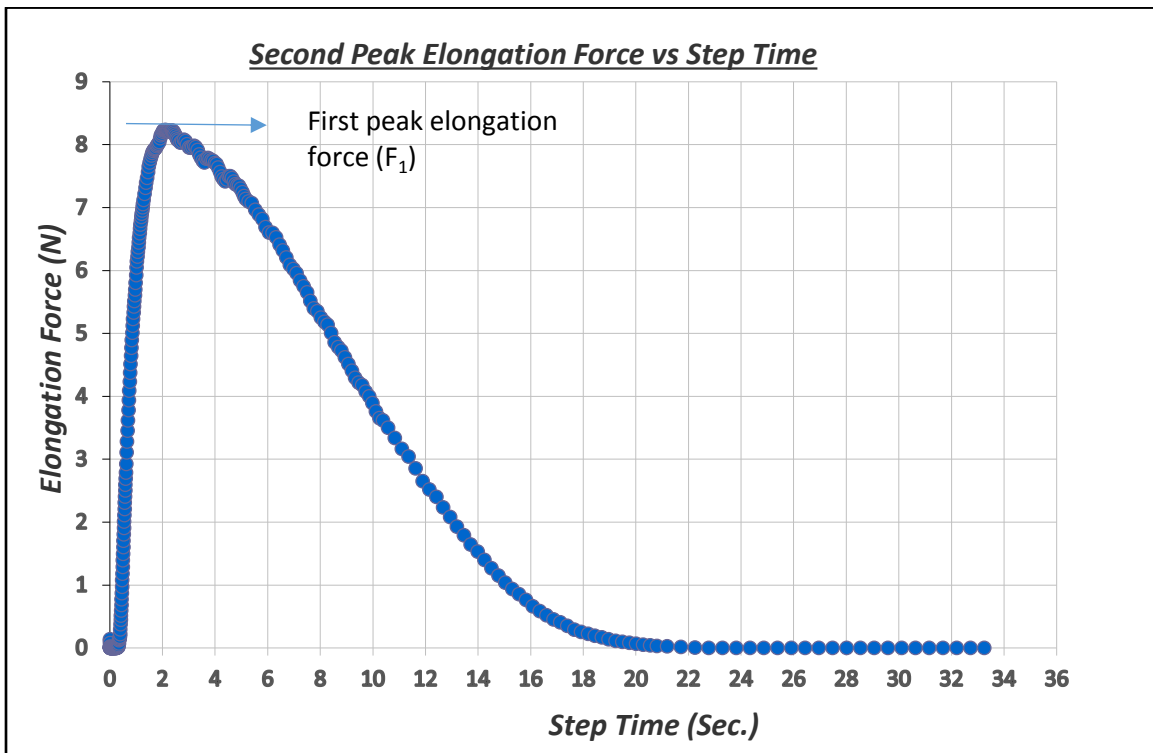


Figure 151. Elongation force vs. step time for PG 64-22 geometry of 9.0 mm x 0.72 mm

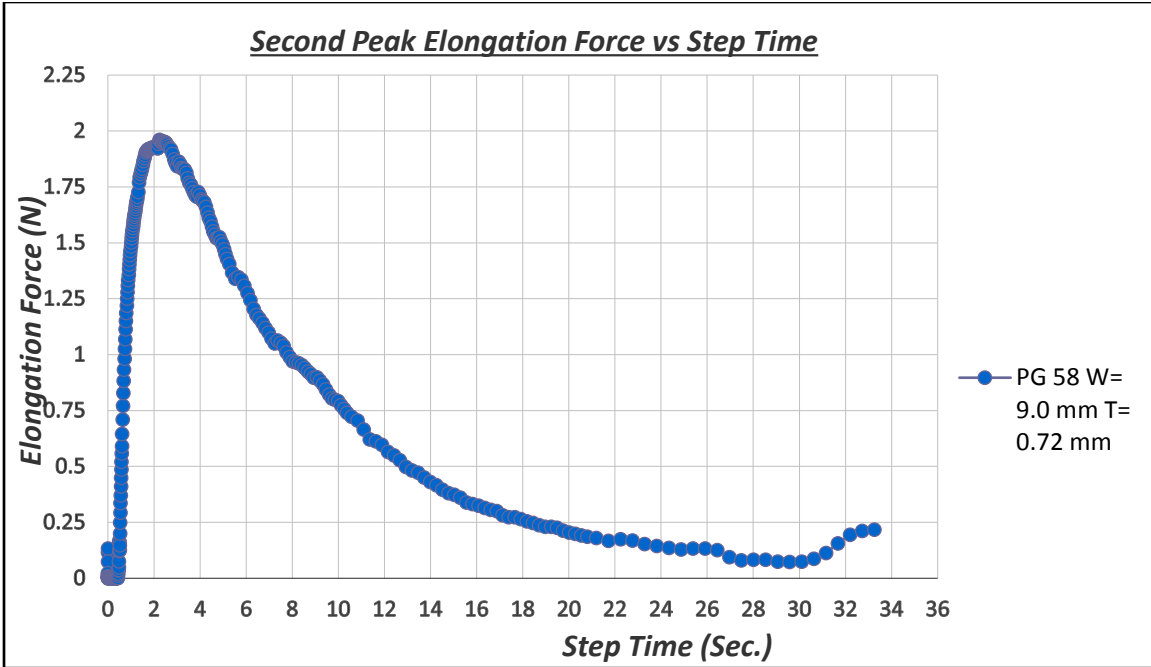


Figure 152. Elongation force vs. step time for PG 58-28 geometry of 9.0 mm x 0.72 mm

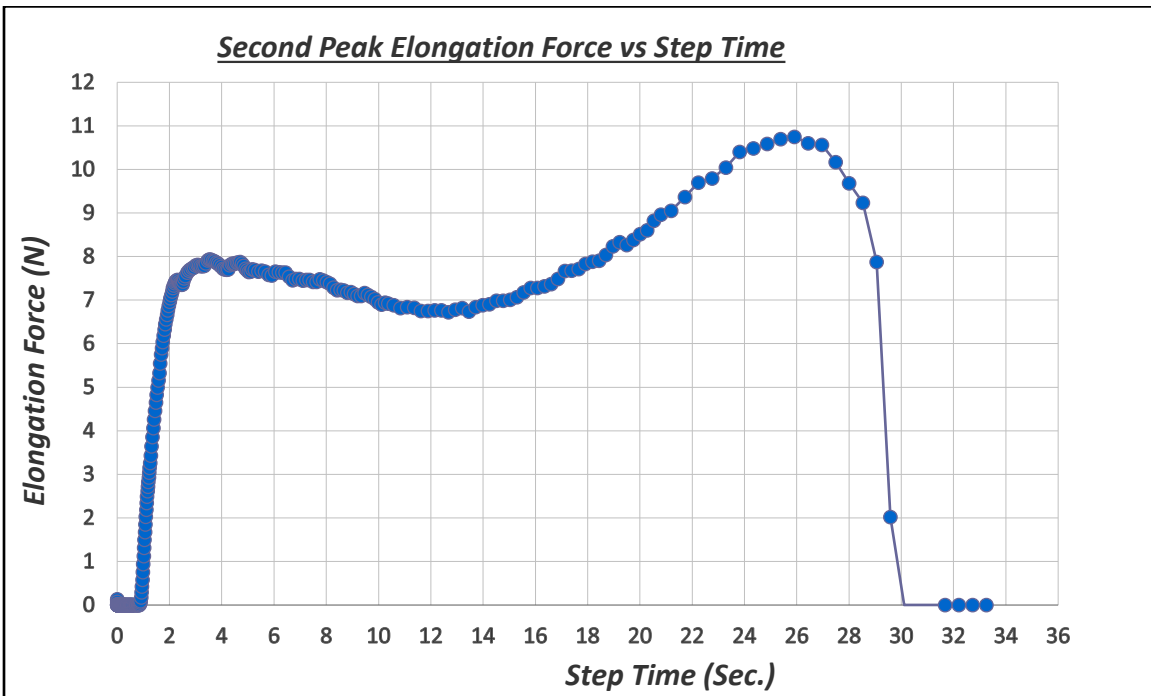


Figure 153. Elongation force vs. step time for PG 76-22 geometry of 6.0 mm x 0.83 mm

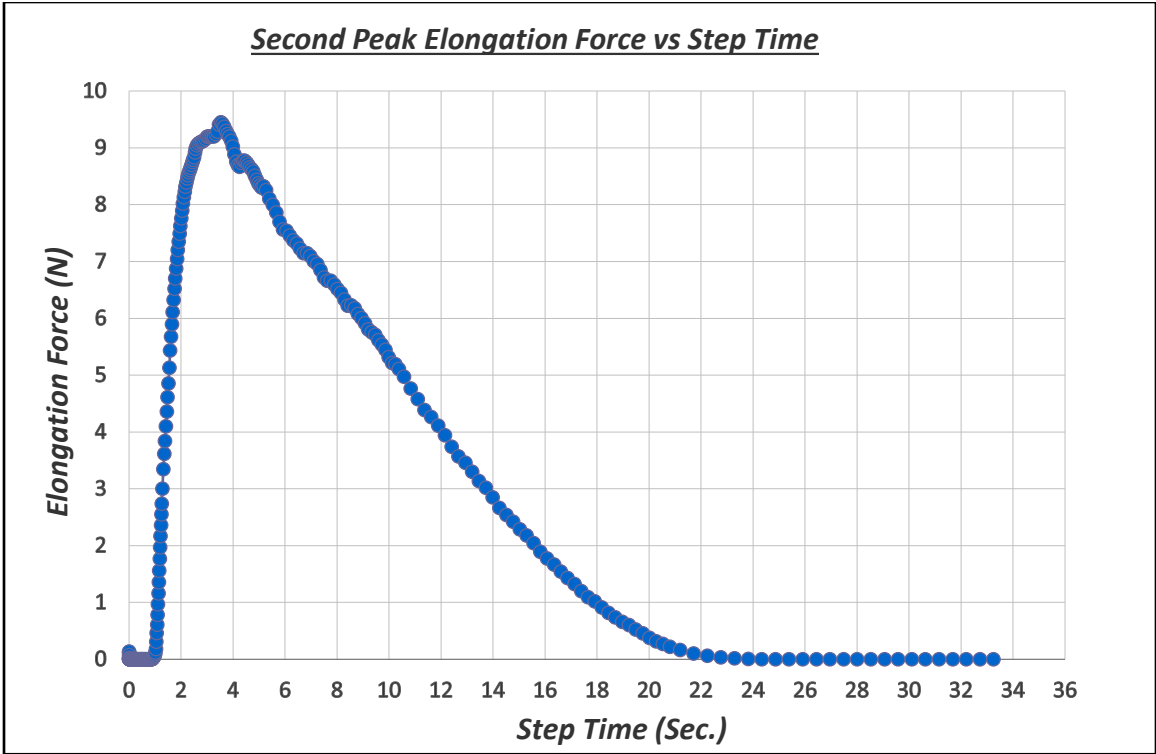


Figure 154. Elongation force vs. step time for PG 64-22 geometry of 6.0 mm x 0.83 mm

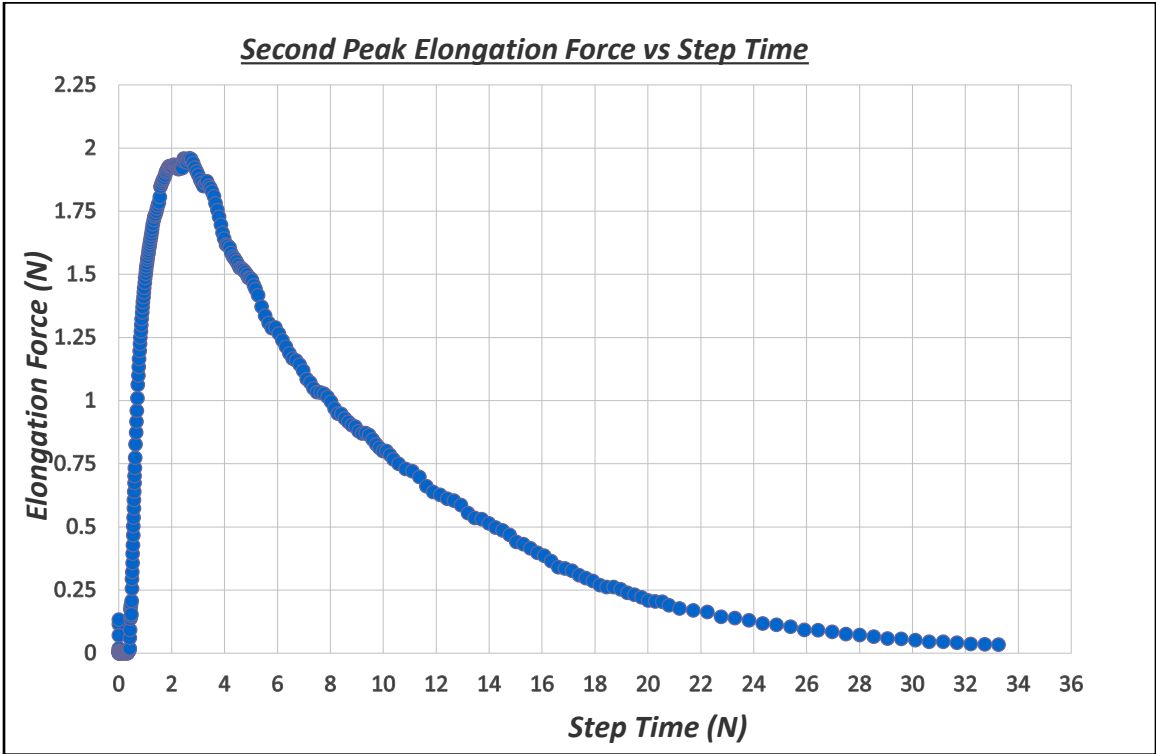


Figure 155. Elongation force vs. step time for PG 58-28 geometry of 6.0 mm x 0.83 mm

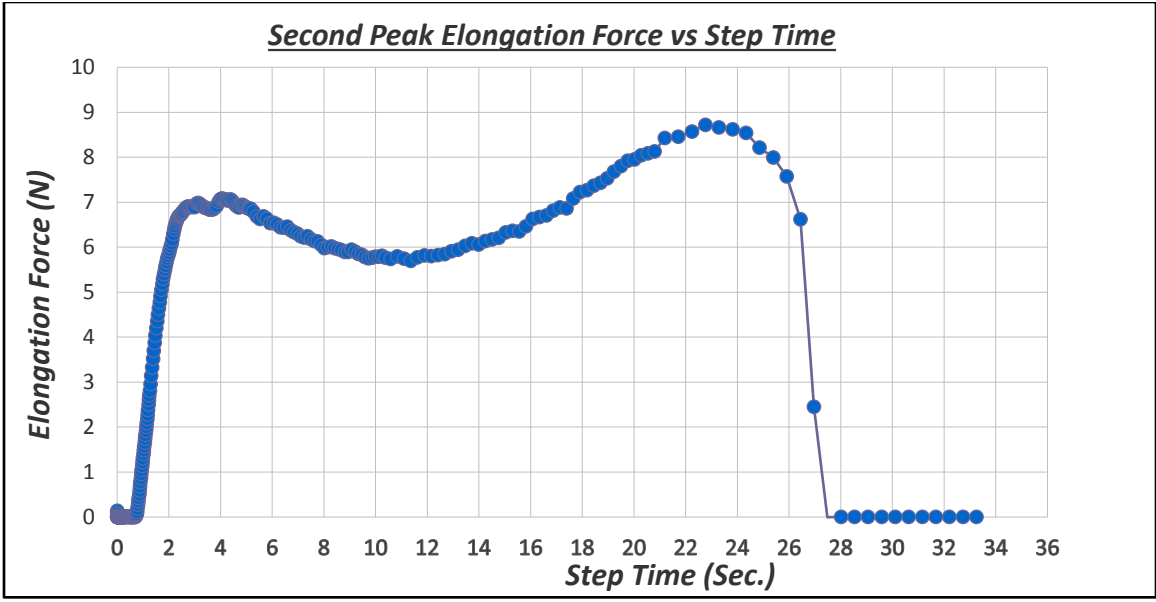


Figure 156. Elongation force vs. step time for PG 76-22 geometry of 7.5 mm x 0.4 mm

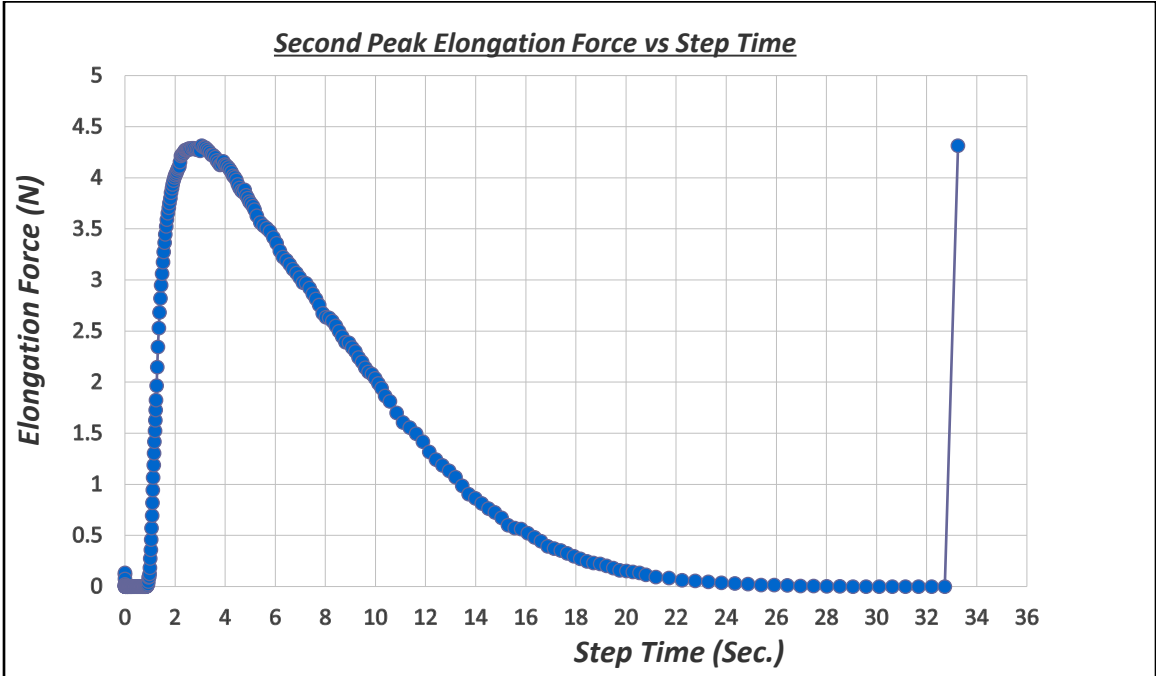


Figure 157. Elongation force vs. step time for PG 64-22 geometry of 7.5 mm x 0.40 mm

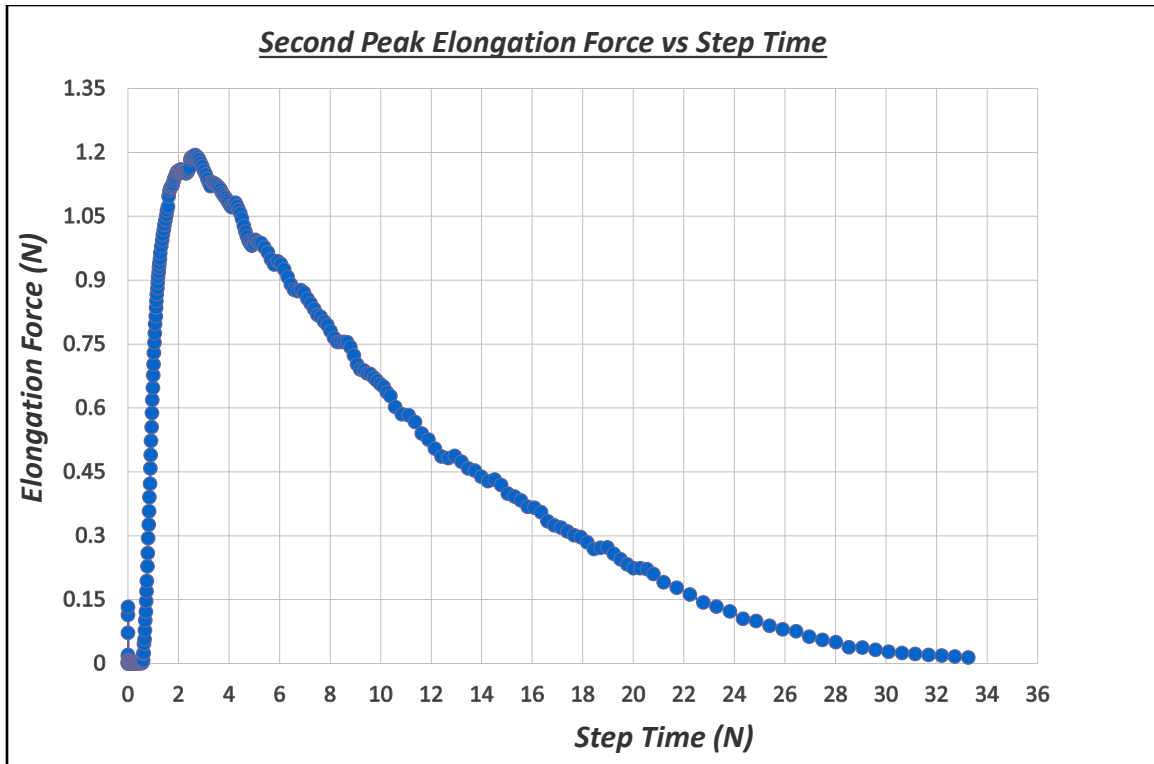


Figure 158. Elongation force vs. step time for PG 58-28 geometry of 7.5 mm x 0.40 mm

10.2 SELECTION OF GEOMETRY

10.2.1 Correlation between Sample Initial X-Sectional Area and Elongation Force

The potential effect of sample width and thickness on the elongation force was analyzed through four approaches: different initial cross-sectional areas, same initial cross-sectional areas with different geometries, different initial cross-sectional areas with the same width, and different initial cross-sectional areas with the same thickness.

10.2.1.1 *Correlation between Sample Initial X-Sectional Area and Second Peak Elongation Force*

Figure 159 demonstrates the correlation between the second peak elongation force F_2 and initial area for 122 samples. In general, as the initial area increases the second peak elongation force increases. It can be observed that each of the three initial areas

that have been tested with two different geometries have shown different F_2 values. For clearer results projection, an average of ten samples for every geometry was plotted in Figure 160 (except geometry $W= 10 \text{ mm} \times T= 0.83 \text{ mm}$ was tested three times as mentioned in Section 9.6). The R^2 value was found to be 0.85, which indicates the linear correlation between the second peak elongation force and the initial area. As for the same initial areas with different geometries, 3.0 mm^2 , 3.6 mm^2 , and 6.5 mm^2 , it can be clearly observed that as the initial area increases, the gap between the average second peak elongation force relatively increases. This indicates that the width and the thickness have different effects on the elongation force.

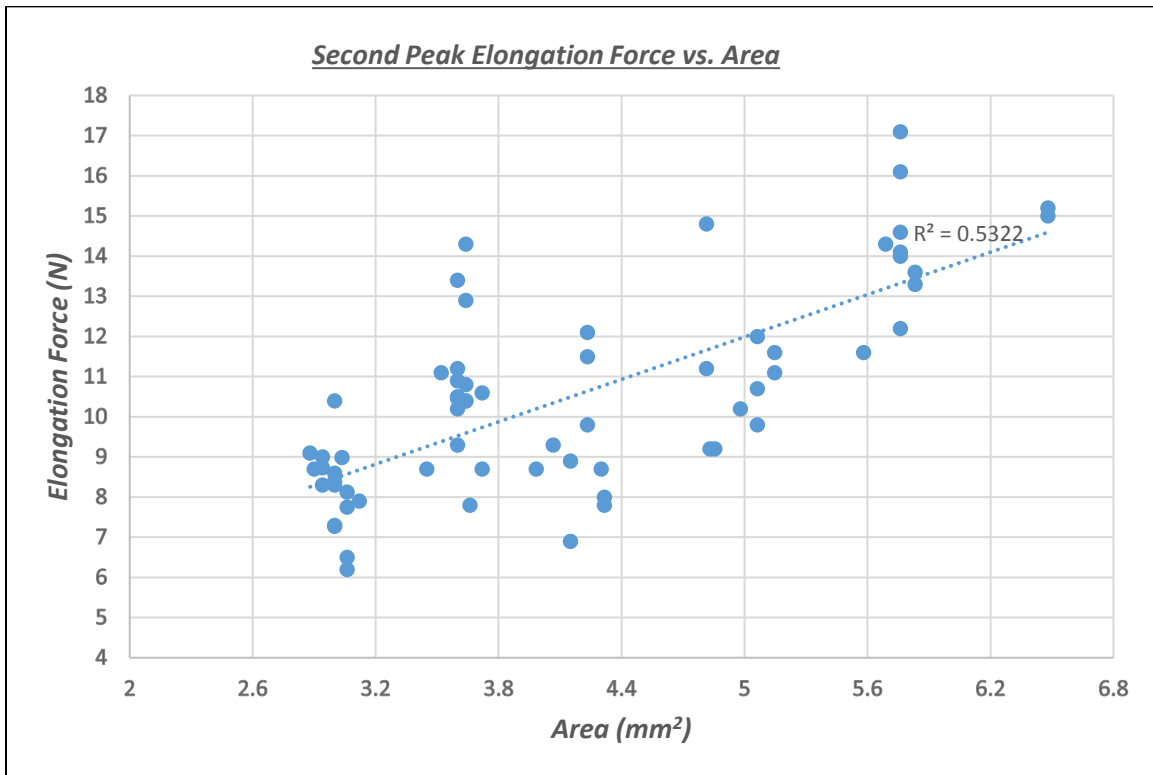


Figure 159. Second peak elongation force vs. initial area

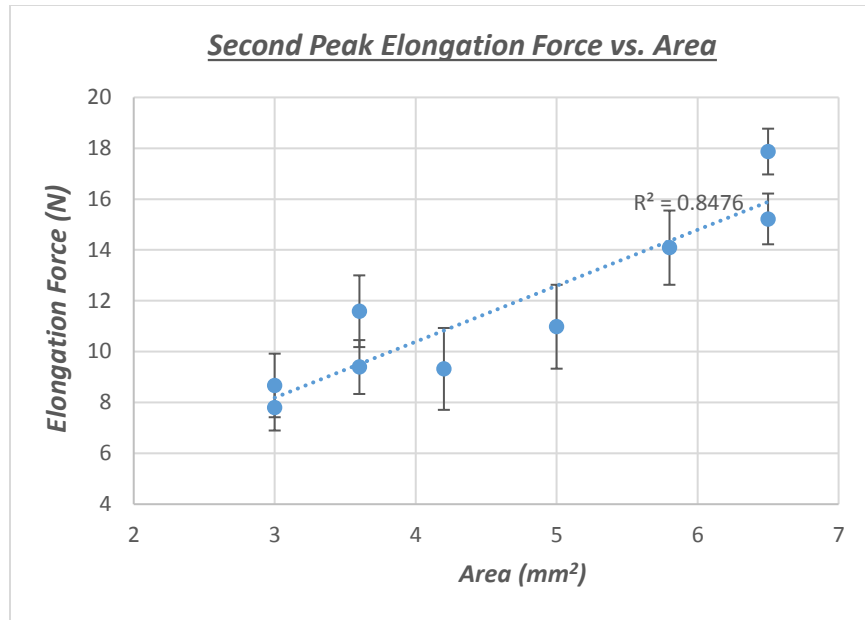


Figure 160. Average second peak elongation force vs. initial area

10.2.1.2 Correlation between Sample Initial X-Sectional Area and First Peak Elongation Force

Figure 161 shows the correlation between the first peak elongation force F_1 and the initial area. It can be observed that F_1 has almost the same increasing trend of F_2 been showed in Figure 159 but exhibits slightly lesser increase with respect to the initial area than F_2 . Figure 162 illustrates the average F_1 elongation force vs initial area. The R^2 value was found to be 0.84.

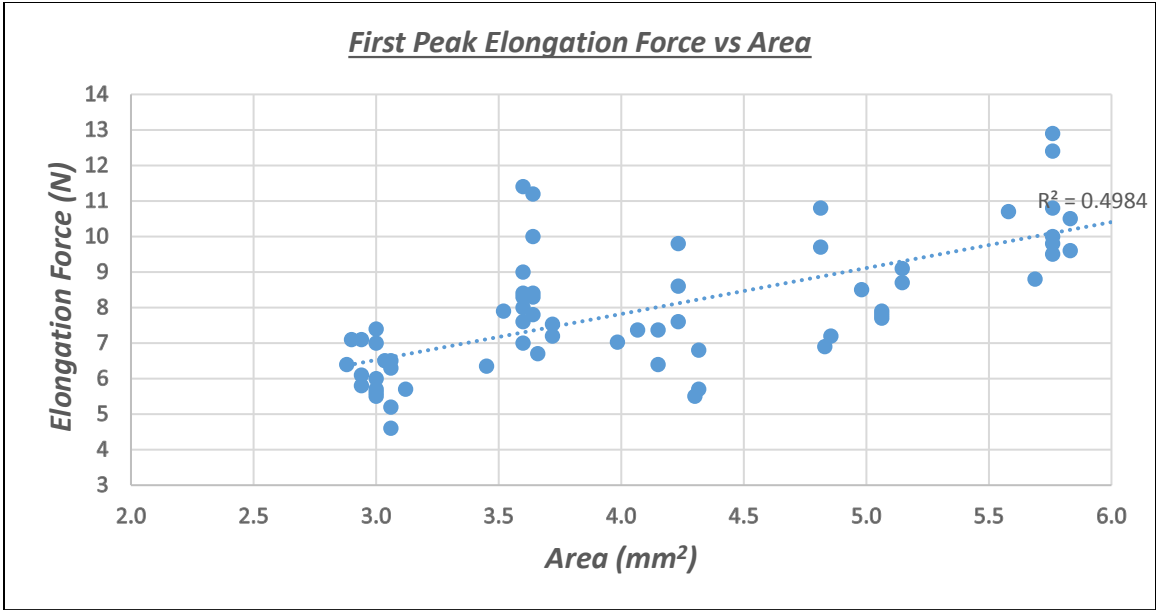


Figure 161. First peak elongation force vs. initial area

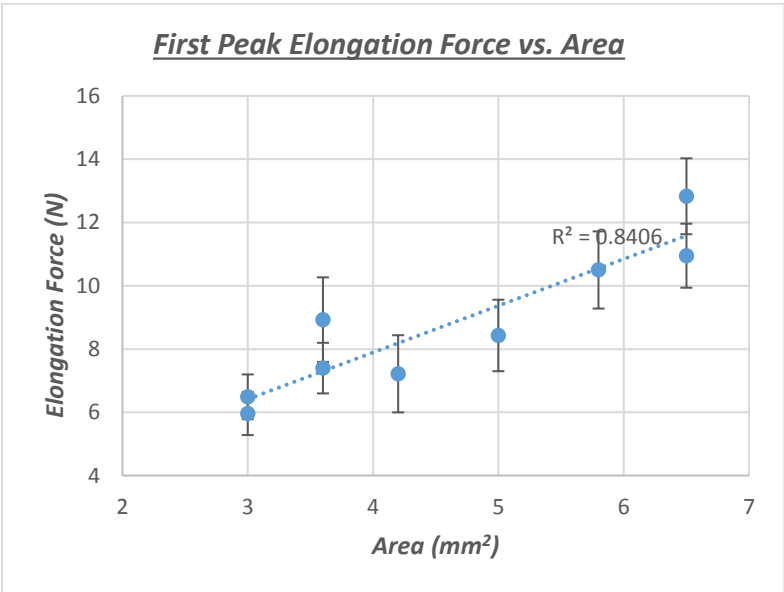


Figure 162. Average first peak elongation force vs. initial area

10.2.2 Width and Thickness Effect in the Elongation Force

10.2.2.1 *Width and Thickness Effect in the Second Peak Elongation Force*

In this study, the effect of the sample's geometry (the width and the thickness) on the average elongation force was investigated. Figure 163 shows the average second peak elongation force F_2 vs. width for three different selected initial areas. Every initial area has been tested with two different geometries. It can be observed that for the initial X-sectional area of 3.0 mm^2 , samples with dimensions of $5 \text{ mm} \times 0.6 \text{ mm}$ have shown an average F_2 of 7.8 N . As for the same initial area with dimensions of $7.5 \text{ mm} \times 0.4 \text{ mm}$ where the width increases by 50% , and the thickness decreases by 33% , average F_2 of 8.7 N was observed, with a force increment of 0.9 N . For the initial area of 3.6 mm^2 , the sample's dimensions of $6 \text{ mm} \times 0.6 \text{ mm}$ show average F_2 of 9.4 N . The same initial area with dimensions of $9 \text{ mm} \times 0.4 \text{ mm}$, with width increasing by 50% , and thickness decreases by 33% , has shown an average F_2 of 11.6 N with force increment of 2.2 N . For the initial area 6.5 mm^2 , the samples with dimensions of $9 \text{ mm} \times 0.72 \text{ mm}$ show average F_2 of 15.2 N . Finally, the samples with dimensions of $10.8 \text{ mm} \times 0.6 \text{ mm}$, with width increasing by 20% , and thickness decreasing by 20% , have shown an average F_2 of 17.9 N with an average force increment of 2.7 N .

Figure 163 illustrates F_2 for equal initial areas but different width. It can be observed that the second peak elongation force increases due to the increases in width. Also, It can be observed from Figure 163 that even though the thickness decreases, the width increases, and the initial cross-section area remains the same, all three tested initial areas have shown increasing in the average second peak elongation force.

To understand the effect of the thickness on the average elongation force, Figure 164 illustrates the average second peak elongation force vs. thickness for different initial areas. It can be observed how clearly the elongation force of the samples with the same initial areas decreases due to the increases in the sample's thickness and decreases in width.

Furthermore, Figure 165 illustrates the relation between the average F_2 and width for the samples with the same thickness but different widths. It can be observed that the force increment between the sample geometry of 5 mm x 0.6 mm and 6 mm x 0.6 mm is equal to 1.59 N, which is almost equal to the force increment between 5 mm x 0.83 mm and 6 mm x 0.83 mm, which is 1.66 N. As for the force increment between 6 mm x 0.6 mm and 10.8 mm x 0.6 mm, the average F_2 increases by 8.5N. In the case of the sample geometries 7.5 mm x 0.4 mm and 9 mm x 0.4 mm, the average F_2 increases by 2.92; this is due to the 1.5 mm increment of the width and, the relatively low thickness value of 0.4 mm. Moreover, it can be observed that at low thicknesses, the effect of the width on the average second peak elongation force behavior is more significant. For geometries 8 mm x 0.72 mm and 9 mm x 0.72 mm, it can be observed that average F_2 increases by just 1.13 N due to the limited percent increment of the width and the relatively high thickness value of 0.72 mm.

Figure 166 shows the correlation between F_2 , and thickness for equally width samples. It can be observed that the increasing of F_2 due to the increasing of thickness between the samples with a width of 6 mm is almost equal to the 5 mm width samples. For the samples with dimensions of 9 mm x 0.4 mm and 9 mm x 0.72 mm, the F_2 increment equal to 3.6 N, which is due to the relatively high width dimension of 9 mm.

The geometry 9 mm x 0.72 mm shows the lowest coefficient of variation among all the geometries by 6.6%. Among the eight geometries, the geometries 9 mm x 0.72 mm, and 10.8 mm x 0.60 mm show the highest two values of the average second peak elongation forces of 15.2 N and 18.2 N, respectively. However, the second mentioned geometry is almost at the SER recommended width threshold, which is equal to 12.7 mm. For the above mentioned details, geometry 9 mm x 0.72 mm was chosen to be the recommended geometry for the developed test method.

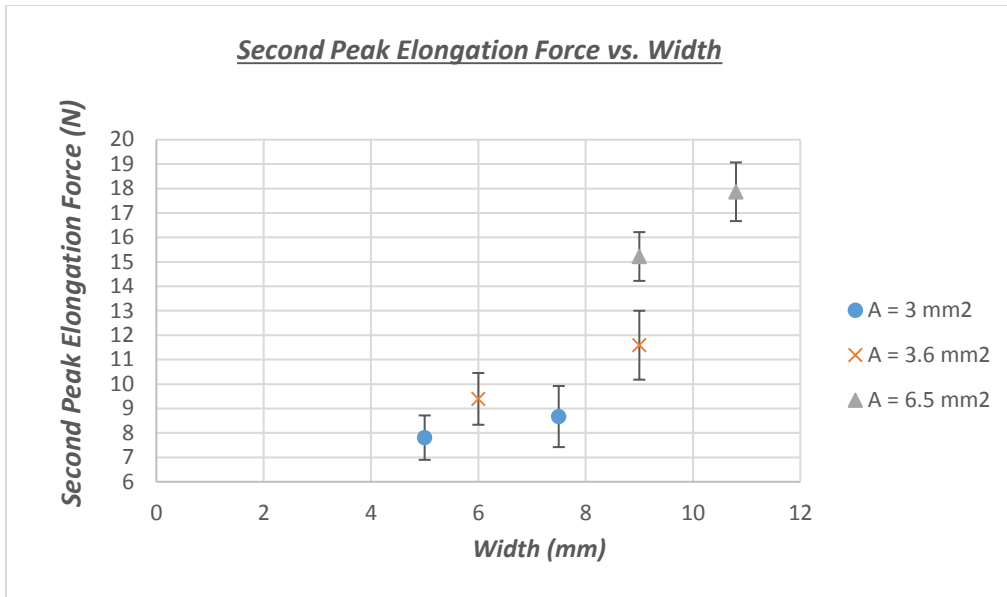


Figure 163. Average second peak elongation force vs. width

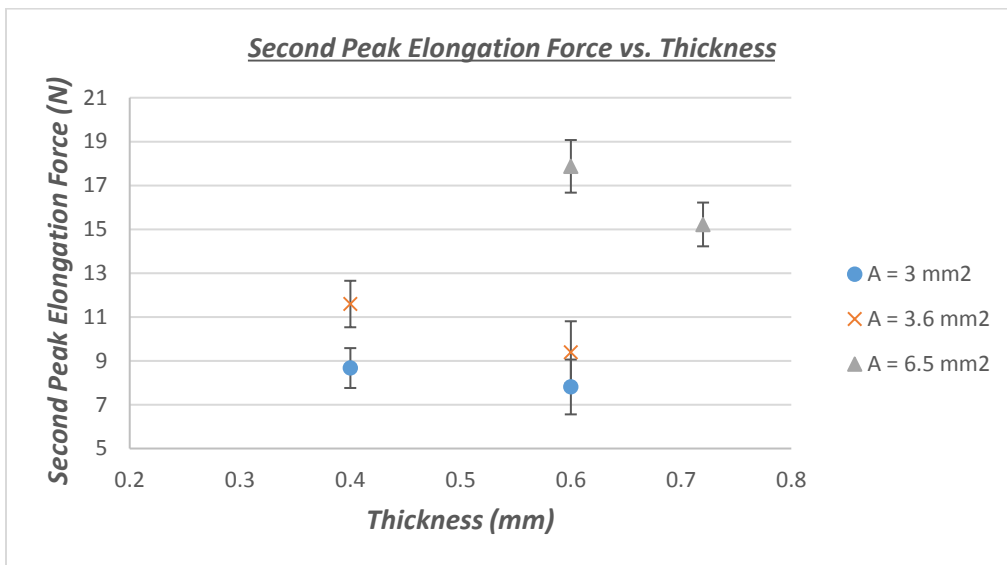


Figure 164. Average second peak Elongation force vs. thickness, for the different initial areas

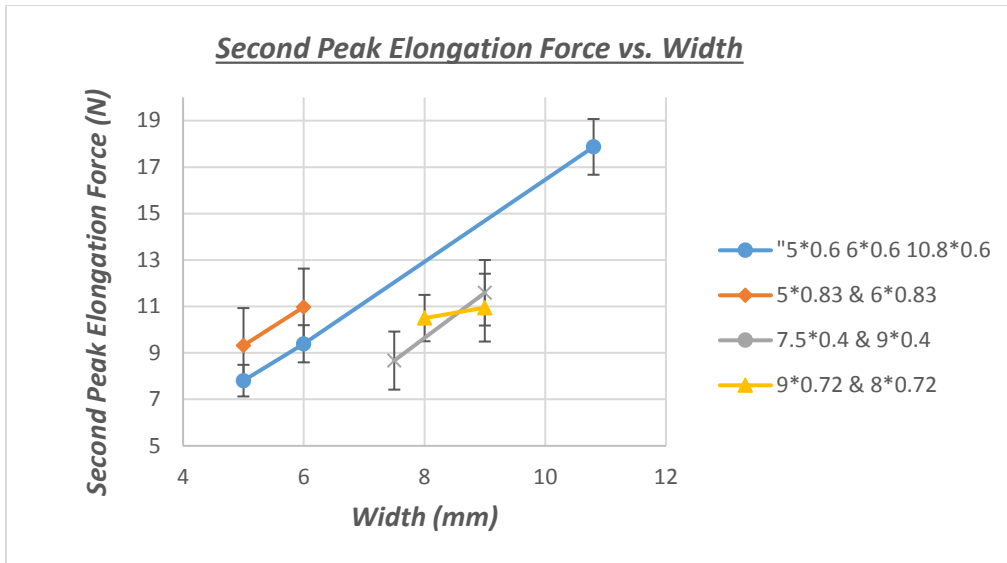


Figure 165. Average second peak elongation force vs. width, for the different thicknesses

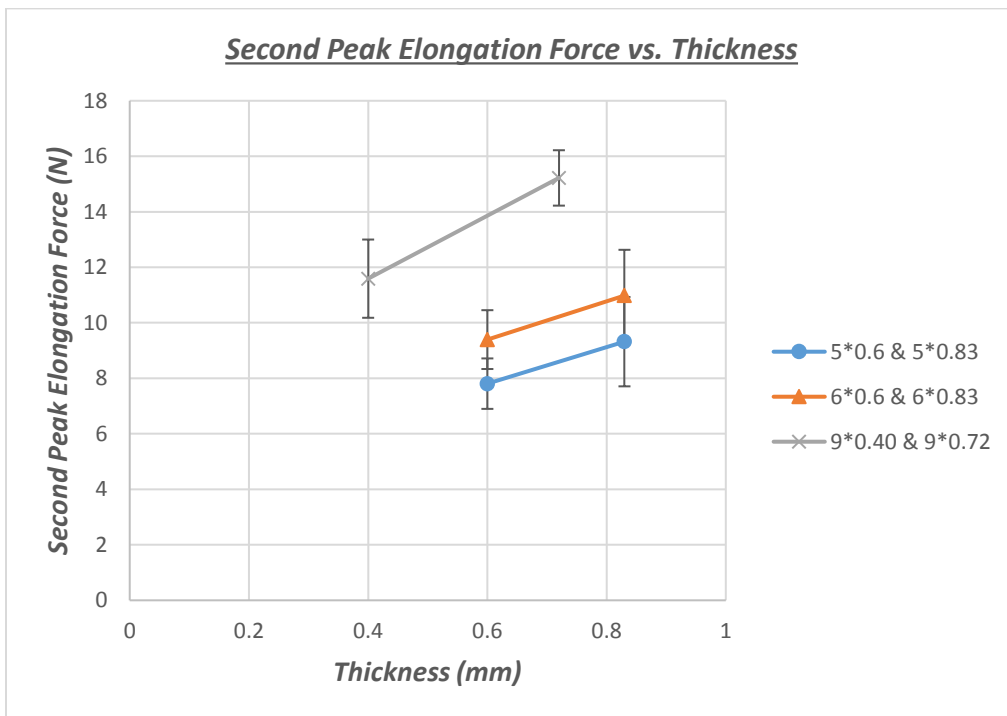


Figure 166. Average second peak elongation force vs. thickness, for different widths

10.2.2.2 Width and Thickness Effect in the First Peak Elongation Force

Figure 167 illustrates the average first peak elongation force F_1 vs width for the same above-mentioned initial areas: 3.0 mm^2 , 3.6 mm^2 , and 6.5 mm^2 . It can be observed that out of the twenty samples that were tested with an initial X-sectional area of 3.0 mm^2 , the ten samples with dimensions of $5 \text{ mm} \times 0.6 \text{ mm}$ show an average F_1 of 6.0 N . As for the ten samples with dimensions of $7.5 \text{ mm} \times 0.4 \text{ mm}$ with width increasing by 50%, and thickness decreasing by 33%, the average F_1 observed was 6.5 N with a force increment of 0.5 N , which is less by 0.4 N than the increment of F_2 of the same geometries mentioned in Section 10.2.2.1.

As for the initial area 3.6 mm^2 , the ten samples with geometry of $6 \text{ mm} \times 0.6 \text{ mm}$ show the average F_1 equals to 7.4 N . The samples with the dimension $9 \text{ mm} \times 0.4 \text{ mm}$ show an average F_1 of 8.9 N with force increment by 1.5 N , which is 0.7 N less than the F_2 increment mentioned in Section 10.2.2.1. For the initial area 6.5 mm^2 , samples dimension of $10.8 \text{ mm} \times 0.6 \text{ mm}$ show average F_1 of 12.8 N , as for samples dimension of $9 \text{ mm} \times 0.72 \text{ mm}$ show average F_1 equals to 10.9 N with force increases by 1.9 N , which is less than the increment of F_2 by 0.4 N . In general, the geometry effect is similar for F_1 , and F_2 but it is slightly less for F_1 than F_2 .

Figure 168 shows that for equal initial areas with different X-sectional dimensions, it can be observed that the average F_1 increases due to the increase in width even though the thickness decreases, and the initial area remains the same. It can also be observed that as the initial area increases the gap in average F_1 for equal initial areas with different dimensions increases.

Figure 169 illustrates the average F_1 vs. thickness for the different samples initial areas with the same width. Figure 170 shows the average F_1 vs. width for the different samples' initial areas with the same thickness but different width. For samples $5 \text{ mm} \times 0.6 \text{ mm}$ and samples $5 \text{ mm} \times 0.83 \text{ mm}$, with thickness increasing by 38%, the elongation force increases from 6 N to 7.2 N by percent increment of 20%. As for

samples 5 mm x 0.6 mm and samples 6 mm x 0.6 mm, with the width increasing by 20% but thickness staying the same, the elongation force's increase equals 23%. As for samples 6 mm x 0.6 mm and 6 mm x 0.83 mm, with the same thickness increment percent of 38%, elongation force increases from 7.4 N to 8.4 N by increment percent of 14%, which is less by 6% than the elongation force percent increment of the previous mentioned samples.

Overall, the above detailed analysis indicates that, the average second and first peak elongation forces increase due to the increasing of the sample's initial area, but the same initial areas with different dimensions derived different values of elongation force. In case of all samples with same initial areas but different dimensions, the elongation force increases due to the increase in width and decrease of thickness. The effect of the thickness in the average peak elongation force decreases due to the increasing of the width. We can also derive that second and first peak elongation forces have almost the same characteristics with respect to the sample initial X-sectional area. Therefore, the second peak elongation force is more sensitive towards the sample initial X-sectional area than the first peak elongation force.

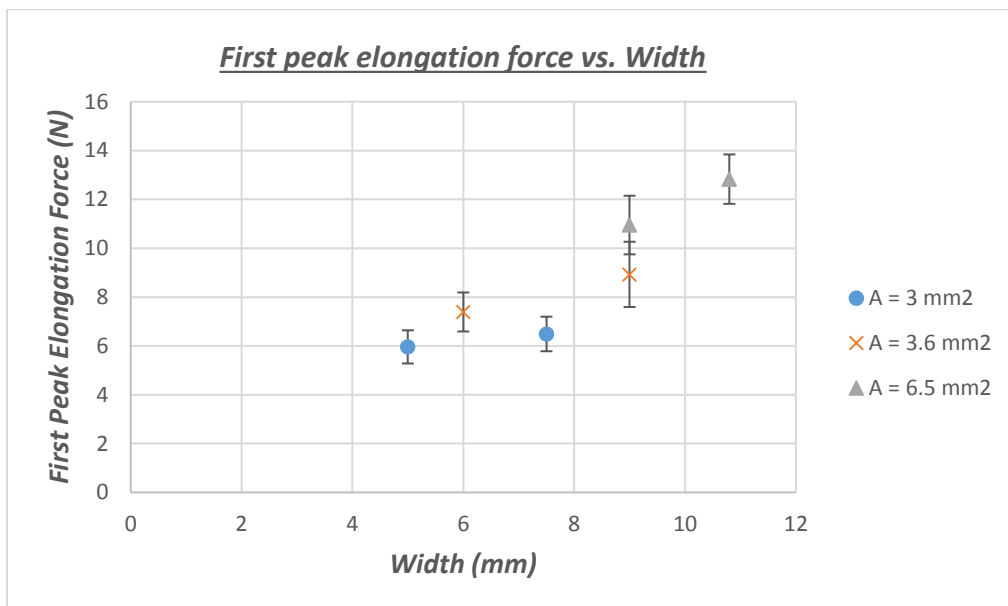


Figure 167. Average first peak elongation force vs. Width

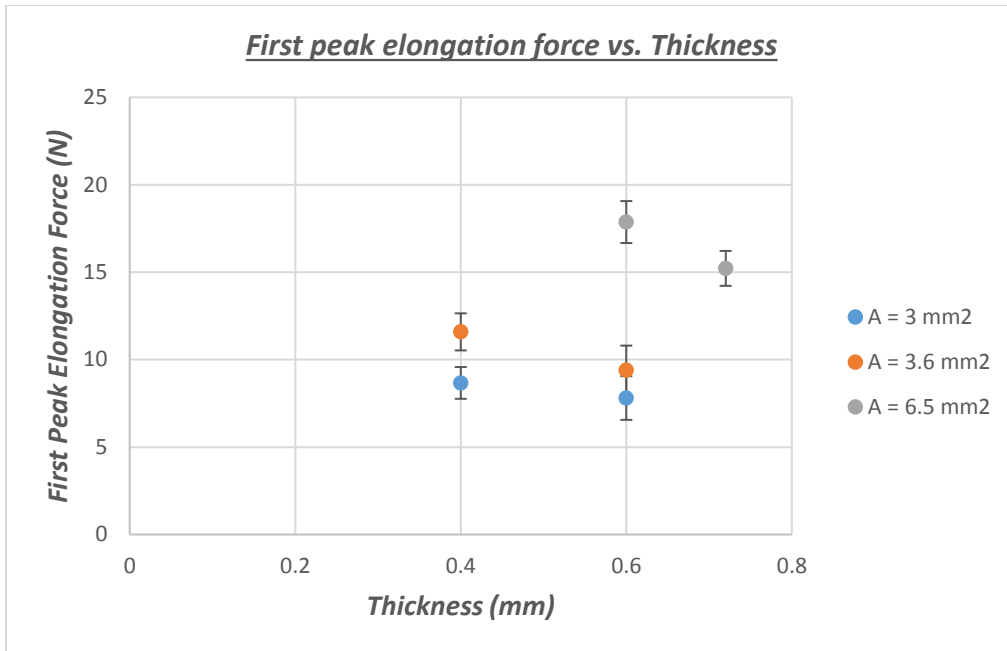


Figure 168. Average first peak elongation force vs. thickness

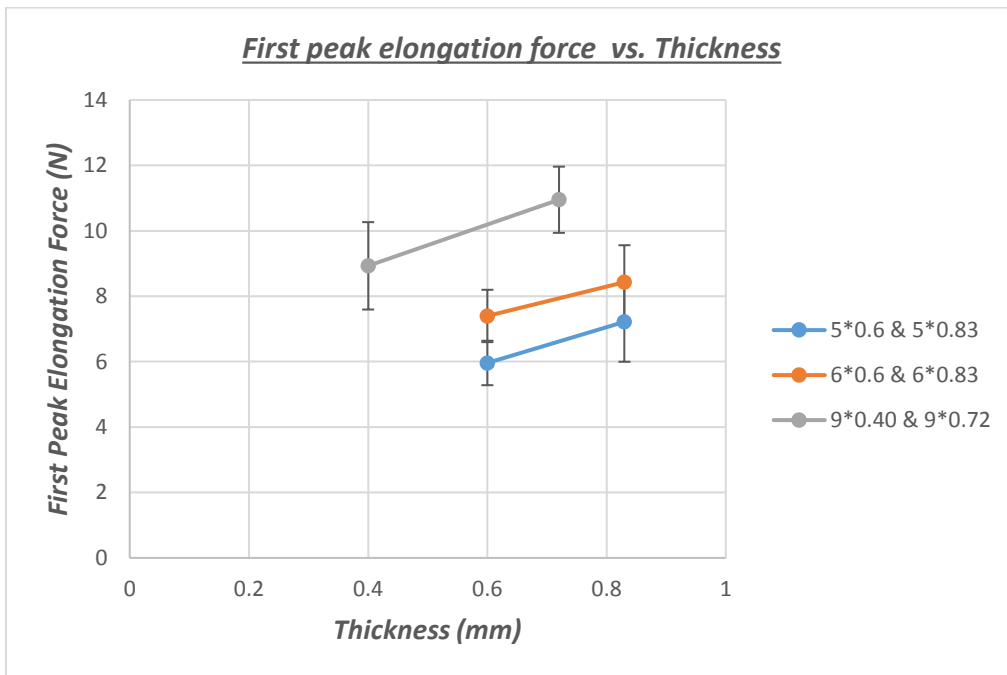


Figure 169. Average first peak elongation force vs. thickness

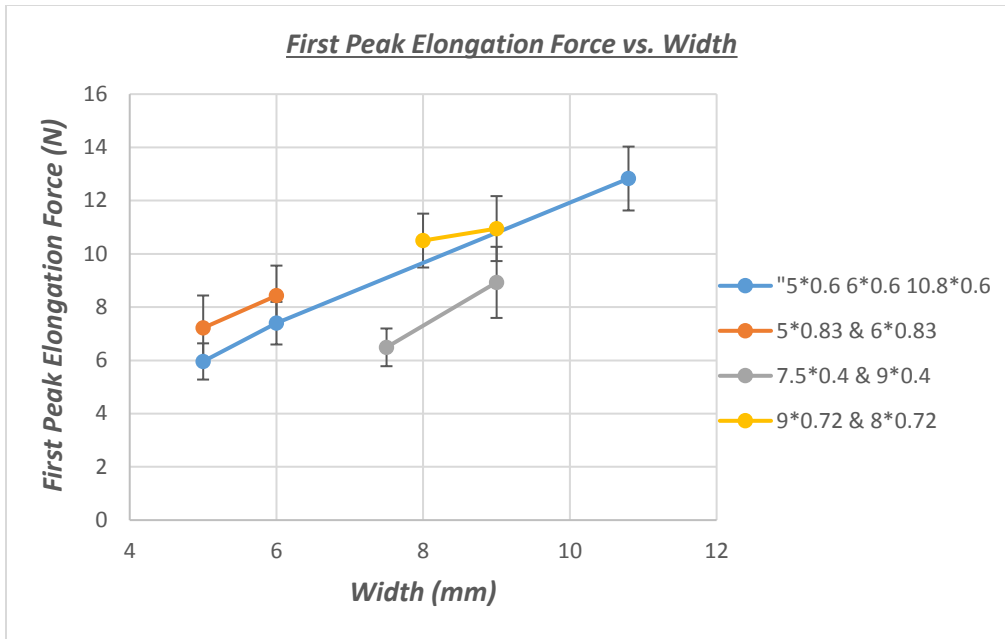


Figure 170. Average first peak elongation force vs. width

10.3 SELECTION OF A TEMPERATURE

10.3.1 Temperature Effect in the Second Peak Elongation Force

State of Louisiana is currently carrying out the force ductility test according to AASHTO T300, which specifies that the test shall be performed at a temperature of $4.0 \pm 0.5^\circ\text{C}$ ($39.2 \pm 1.0\text{ F}$). In order to evaluate the effect of temperature on the elongation force, two geometries, 8 mm x 0.72 mm and 9 mm x 0.72 mm, were tested at three different temperatures: 4°C , 10°C , and 16°C .

Figure 171 shows the correlation between the second peak elongation force and temperature for samples with an initial area of 5.8 mm^2 . Figure 172 shows the correlation between the average second peak elongation force and temperature for the samples with an initial area of 5.8 mm^2 . The second peak elongation force F_2 is almost linearly increased due to the temperature increase with R^2 values of 0.65 and 0.95 for F_2 and average F_2 , respectively. It can be observed from Figure 172 that the second peak

elongation force at 4°C was 14.1 N. At 10°C, elongation force decreases to 12.23 N, and for 16°C, elongation force was 7.7 N, which is the lowest among the three testing temperatures.

For the initial area of 6.5 mm², similar behavior was observed from Figure 173 and Figure 174, which illustrate the correlation between the second peak elongation force and average second peak elongation force with temperature, respectively. From Figure 174, the highest average second peak elongation force was found to be 15.22 N at 4°C. At 10°C, elongation force decreases to 13.6 N, as for 16°C, elongation force observed was 7.7 N. The R² value was 0.74 and 0.91 for F₂, and average F₂ respectively. In all the cases in this study, samples tested at 4°C (the lowest temperature among the three testing temperatures) exhibited the highest second peak elongation force.

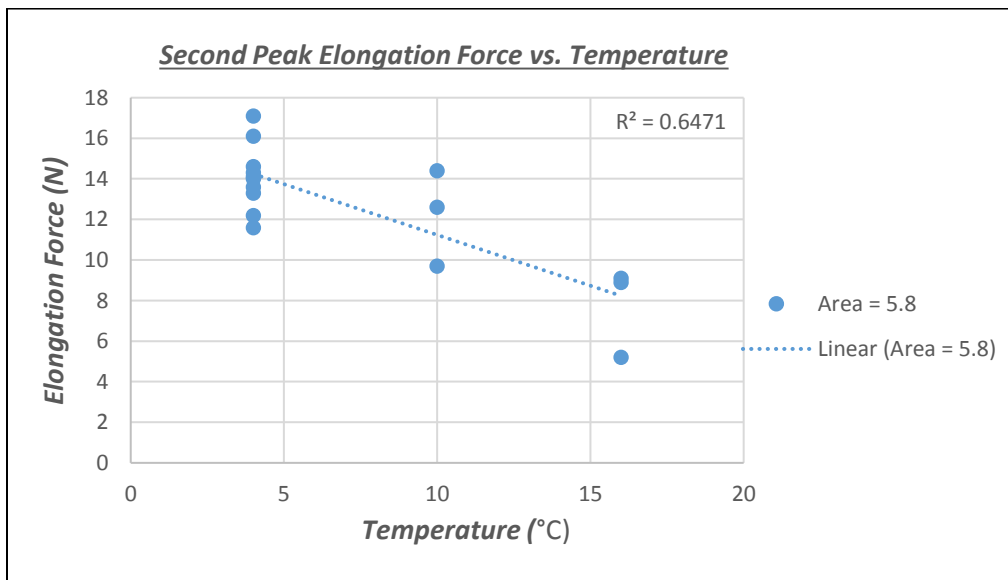


Figure 171. Second Peak Elongation Force vs. Temperature

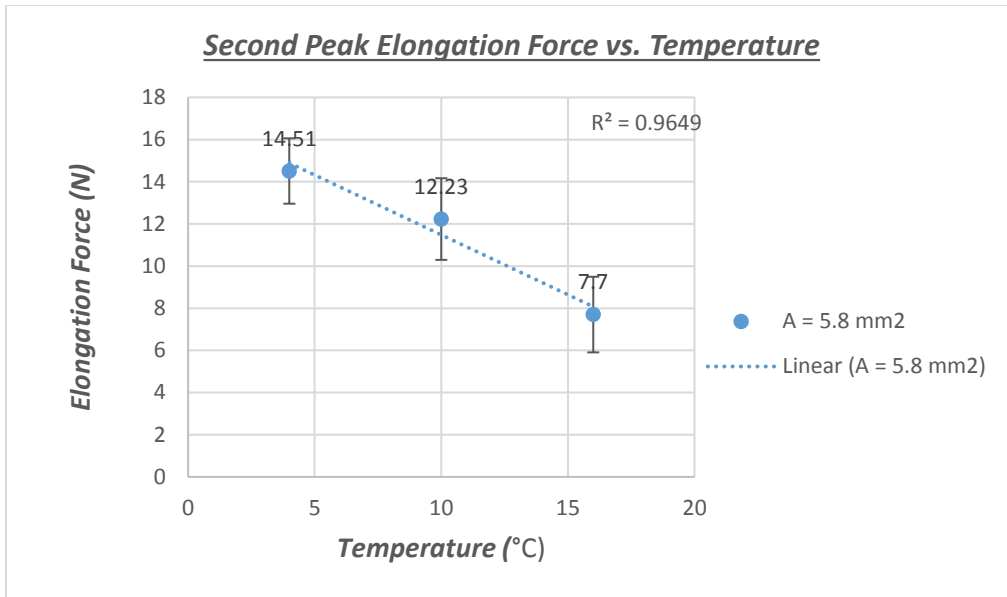


Figure 172. Average Second Peak Elongation Force vs. Temperature

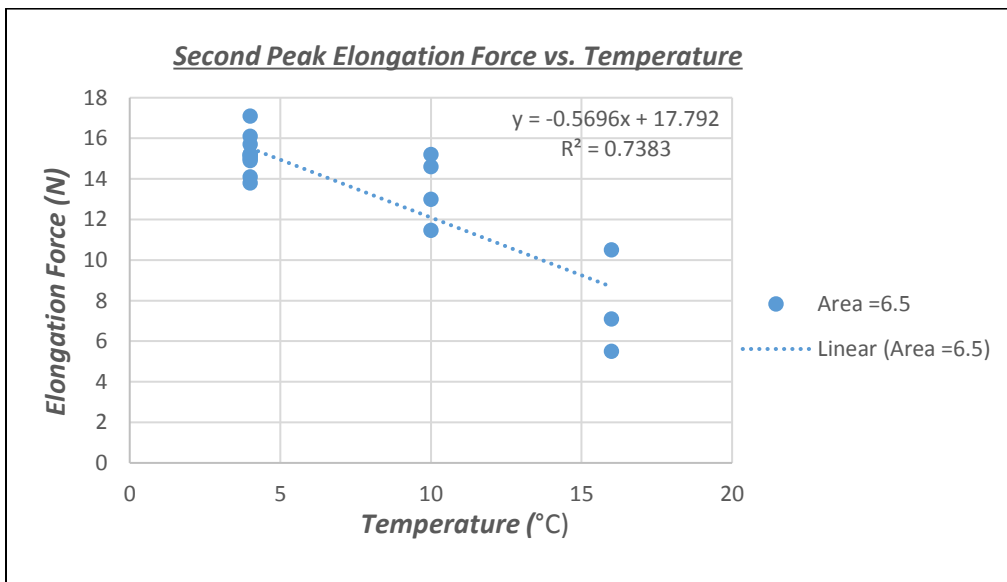


Figure 173. Second Peak Elongation Force vs. Temperature

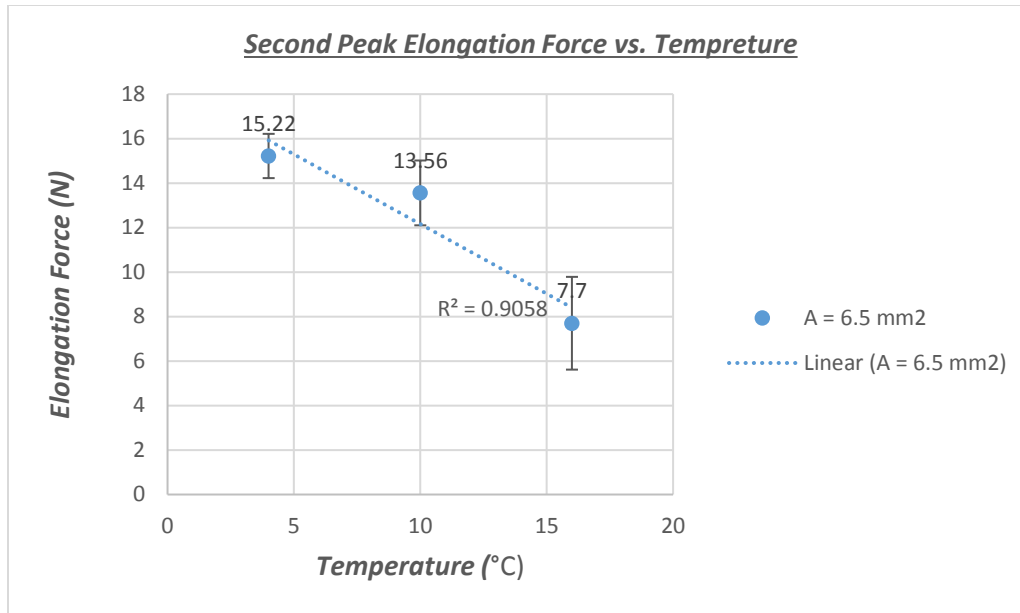


Figure 174. Average Second Peak Elongation Force vs. Temperature

10.3.2 Temperature Effect in the Elongation Force vs Step Time Curve Characteristics

Figures 175, 176, and 4-28 show the elongation force vs step time for geometry of 8 mm x 0.72 mm at 4°C, 10°C, and 16°C, respectively. Figures 178, 179, and 180 show the elongation force vs step time for geometry of 9 mm x 0.72 mm at 4°C, 10°C, and 16°C, respectively. It can be observed from Figures 175 to 180 that, the curve characteristics change due to the temperature changes. At 4°C the inflection point can be clearly determined. However, at 10°C, and 16°C the inflection points almost fully integrated with the first and second peak elongation forces. That is because of the increase of the asphalt resilience due to the temperature increment.

Furthermore, it can be observed that the failure criteria become more ductile with the temperature increment. For example, for geometry 8 mm x 0.72 mm the final test time was 26 seconds at 4°C. As for the same geometry, the final test time at 16°C was 33 seconds with 8 seconds increment than the 4°C. The same trend was observed for geometry 9 mm x 0.72 mm. From the above-mentioned discussions in sections 10.3.1

and 4.3.2, 4°C was selected to be the testing temperature for the developed extensional deformation test of asphalt binders.

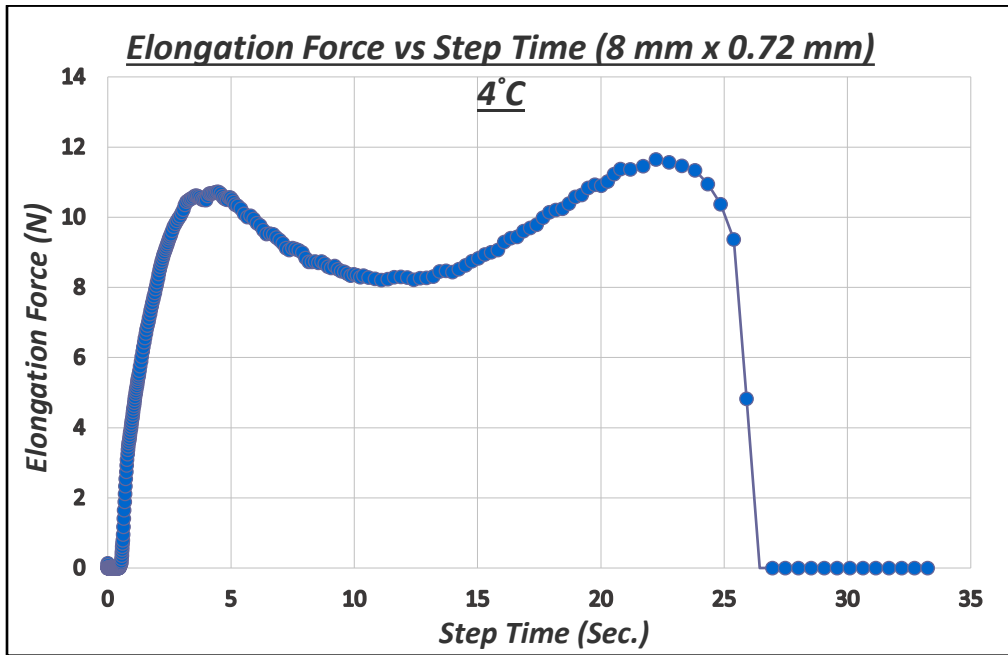


Figure 175. Elongation Force vs. Step Time for PG 76-22 geometry of 8 mm x 0.72 mm at 4°C

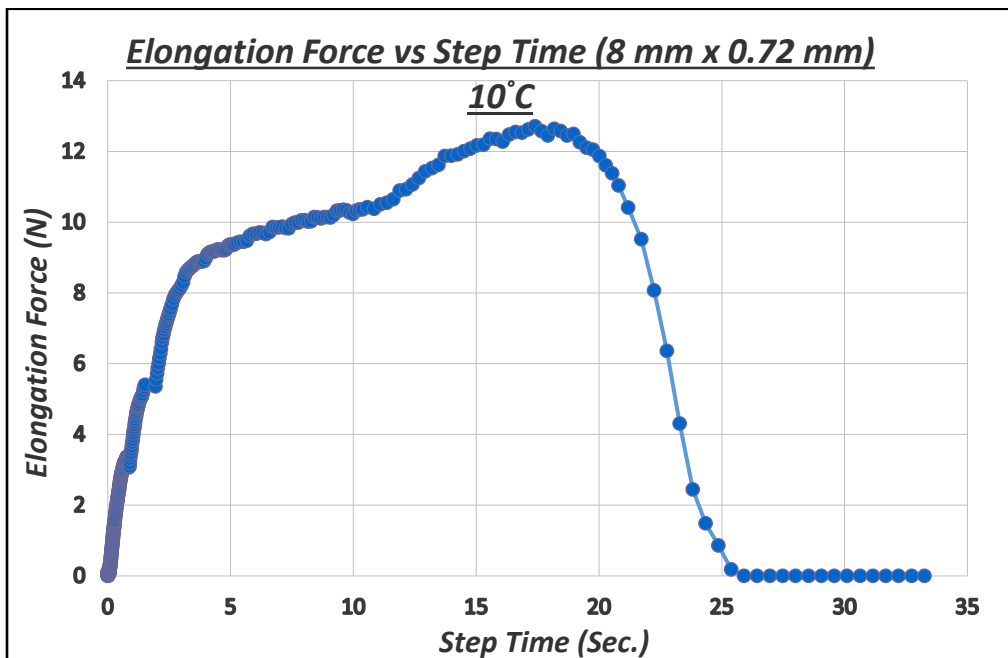


Figure 176. Elongation Force vs. Step Time for PG 76-22 geometry of 8 mm x 0.72 mm at 10°C

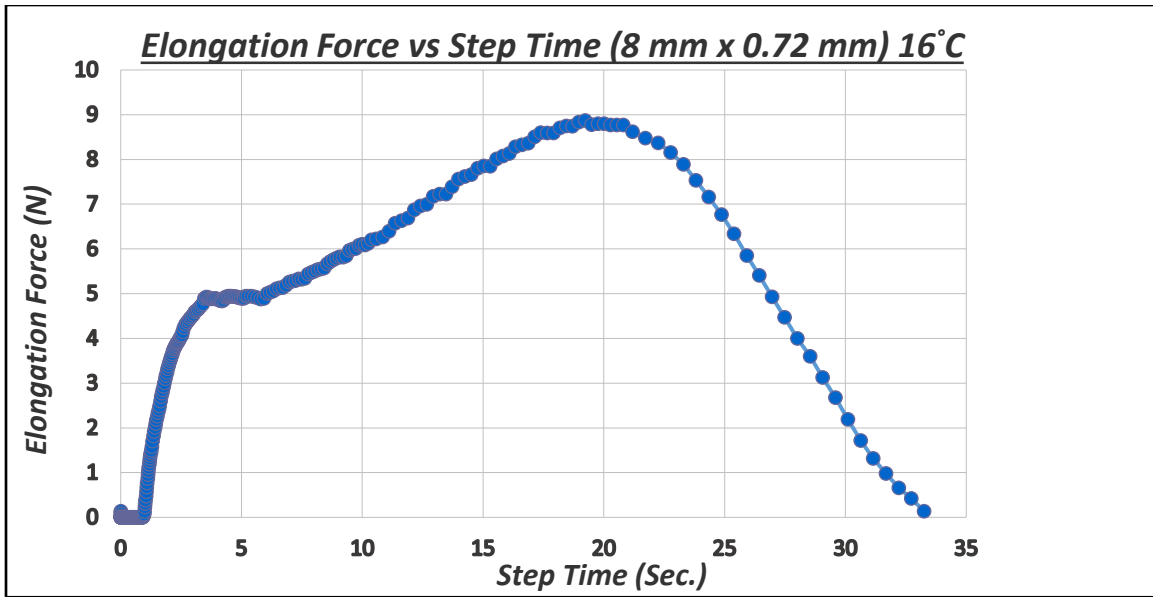


Figure 177. Elongation Force vs. Step Time for PG 76-22 geometry of 8 mm x 0.72 mm at 16°C

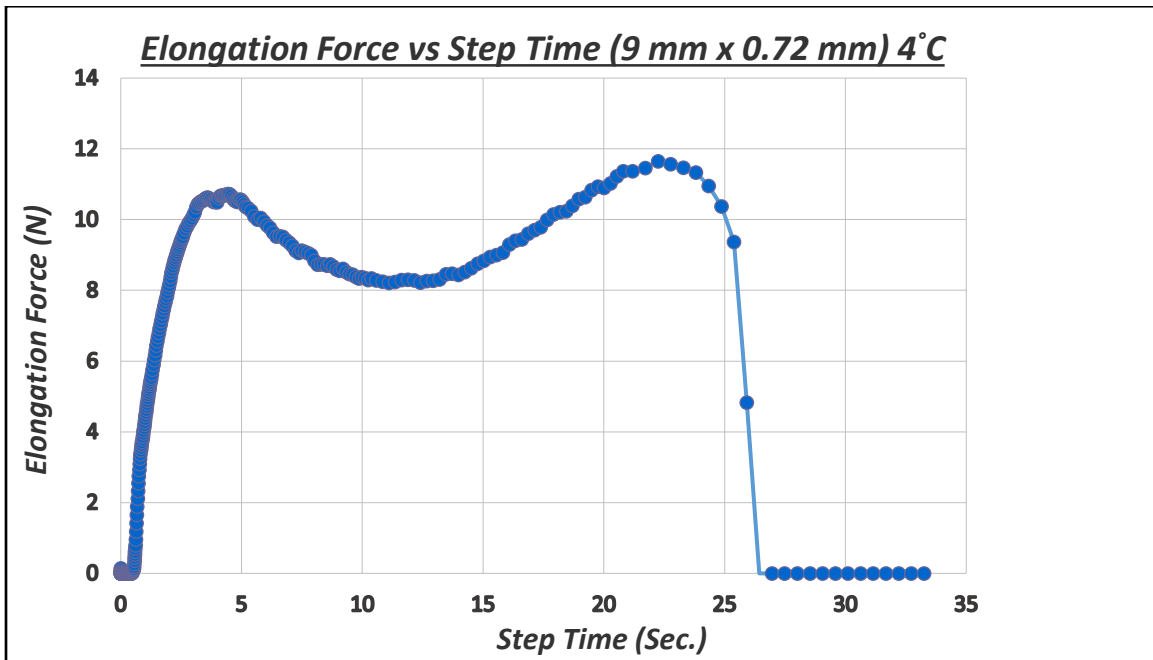


Figure 178. Elongation Force vs. Step Time for PG 76-22 geometry of 9 mm x 0.72 mm at 4°C

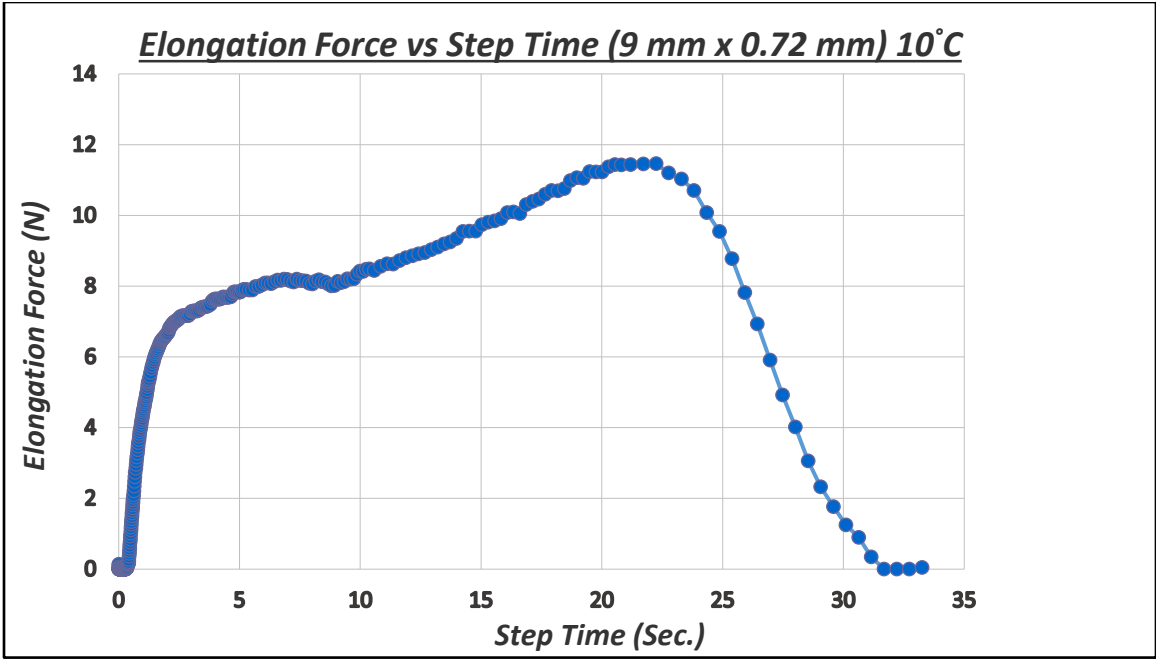


Figure 179. Elongation Force vs. Step Time for PG 76-22 geometry of 9 mm x 0.72 mm at 10°C

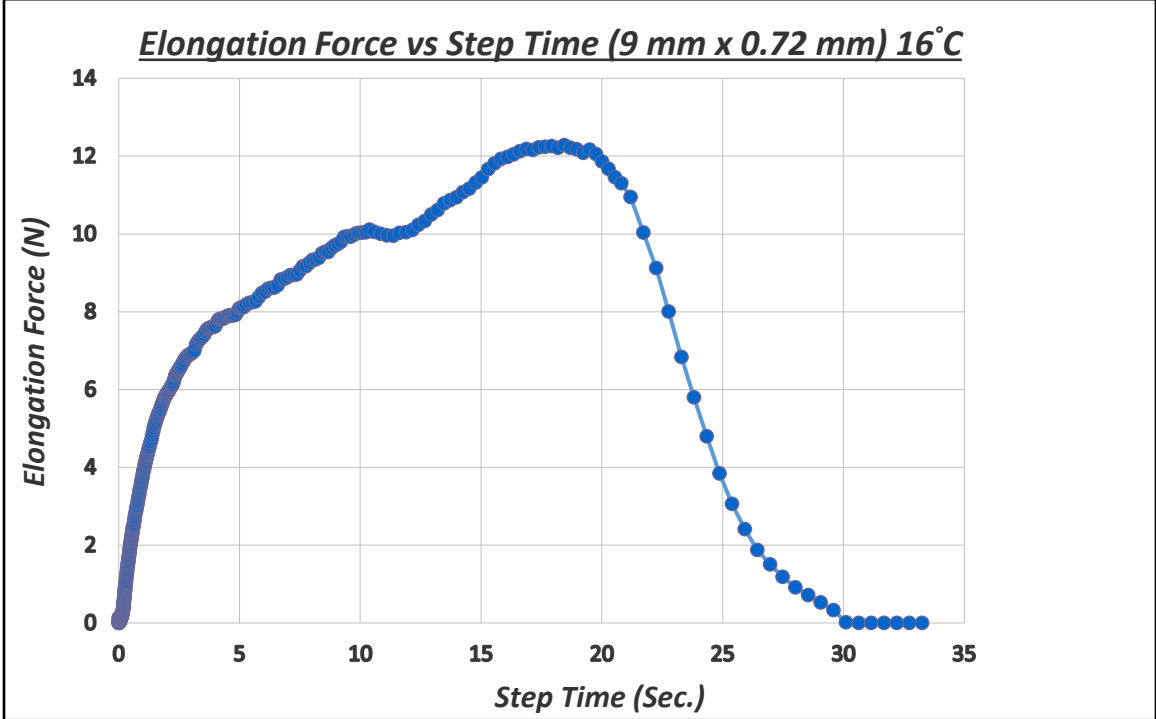


Figure 180. Elongation Force vs. Step Time for PG 76-22 geometry of 9 mm x 0.72 mm at 16°C

10.4 TEST PARAMETERS AND SPECIFICATIONS

As mentioned earlier, different parameters are used by different agencies for different asphalt materials in the current force ductility test (AASHTO 300). The commonly used parameters are F_2/F_1 and value of F_2 . Also, F_2 is defined by second peak force or by force at 30 cm elongation. Like the parameters, recommended specifications and testing temperature vary as well by different agencies.

Table 56 demonstrates the second peak elongation force results of the selected geometry, 9 mm x 0.72 mm (width x thickness). The lowest F_2 was 13.1 N and the highest F_2 was 17.1 N, with an average F_2 of 15.322 N, standard deviation of 0.998, and coefficient of variation of 6.55%. Table 56 also demonstrates that out of the ten samples, the lowest F_2/F_1 obtained was 1.17 and the highest F_2/F_1 obtained was 1.54 with an average of 1.4, and a standard deviation of 0.13.

The coefficient of variation for ten F_2 values is 6.19%, whereas coefficient of variation for F_2/F_1 values is 9.21%. The F_2 value has been chosen as a recommended force ductility parameter. The minimum F_2 value recommended is 14 N, which was lower than the lowest limit of 99% confidence interval (14.45N – 15.99 N). Also, minimum F_2/F_1 of 1.25 is recommended for PG76-22. This is also lower than the lowest value of 99% confidence interval (1.29-1.51).

The recommended temperature for the test remains to be 4°C as the conventional force ductility test. To avoid sample overlapping after a half rotation of each drum, the recommended final strain is 3.4 rad. Based on the findings of this study, the geometry of 9 mm x 0.72 mm was selected.

Table 56. Statistical analysis of the selected geometry

Sample No.	F₁ in N	F₂ in N	F₂/F₁
Sample1	12.2	15.2	1.25
Sample2	10.6	15	1.42
Sample3	10.1	15.1	1.5
Sample4	11.2	17.1	1.53
Sample5	9.7	14.9	1.54
Sample6	10.8	15.2	1.41
Sample7	9.2	14.1	1.53
Sample8	11.8	13.8	1.17
Sample9	11.5	15.7	1.37
Sample10	12.4	16.1	1.3
Average	10.95	15.22	1.40
Highest	12.4	17.1	1.54
Lowest	9.2	13.8	1.17
Stan. Dev.	1.07	0.94	0.13
Coefficient of Variation (%)	9.74	6.19	9.21
99% Conf. Interval	10.08- 11.82	14.45- 15.99	1.29- 1.51
No. of Sample Outside the Limits of 99% Confidence Int.	4	4	4
Recommended Value (Minimum)		14 N	1.25

CHAPTER 11

CONCLUSIONS AND RECOMMENDATIONS

11.1 PART ONE CONCLUSIONS AND RECOMMENDATIONS

The main objective of this study was to assess the feasibility of the adoption of the multiple stress creep recovery (MSCR) test method by the Arkansas State Highway and Transportation Department (AHTD) and Texas Department of Transportation (TxDOT). In order to achieve this objective, MSCR and Superpave tests were conducted on three types of performance grade (PG) binders (PG 64-22, PG 70-22, and PG 76-22) approved by AHTD and TxDOT. The effects of selected Warm Mix Asphalt (WMA) additives (Sasobit[®], Advera[®], and Evotherm[®]) and Reclaimed Asphalt Pavement (RAP) samples on MSCR parameters namely, the percent recovery (%R) and non-recoverable creep compliance (J_{nr}), were evaluated in this study.

Two types of polymer modified binders (PMBs) (PG 70-22 and PG 76-22) and one unmodified binder (PG 64-22) were collected from twelve different sources. The WMA additives were collected from three different suppliers: Sasobit[®] from Sasol Wax, Advera[®] from PQ Corporation, and Evotherm[®] from MeadWestavaco. Selective dosages, as recommended by the manufacturers, of these WMA additives were used in this study. Two types of coarse RAP samples, namely, RAP1 and RAP2, were collected from I-40 in Arkansas.

MSCR tests were conducted in accordance with AASHTO T 350. A total of 65 binder samples were tested in the laboratory. Of these, 8 were unmodified binders, 24 were PMBs, 27 were WMA-additive modified, and 6 were RAP-modified binders. All binder samples were tested at three stress levels (0.1 kPa, 3.2 kPa, 10 kPa) and at different temperatures. PG 64-22 binders with and without additives (WMA or RAP) was tested at 64°C. PG 70-22 binders with and without WMA additives were tested at two different temperatures (64°C and 70°C). And, PG 76-22 binders with and without WMA additives were tested at three different temperatures (64°C, 70°C, and 76°C). The MSCR test

results were then analyzed to grade these binders in accordance with the AASHTO M 332 specifications. Further, MSCR test results were analyzed by following the polymer method. The quadrant plot method (MSCR %R vs. Elastic Recovery) was also used for estimating the minimum MSCR %R values for AHTD and TxDOT.

11.1.1 Conclusions

11.1.1.1 Arkansas Binders' MSCR Data

Unmodified Binders and PMBs

PG 6-22:

- About 75% of the PG 64-22 binders were graded as PG 64S-22, which was followed by 25% of binders that were graded as PG 64H-22.
- At higher stress levels (10 kPa), about 87% of the PG 64-22 binders were showed negative %R values.
- All tested PG 64-22 binders were plotted under the AASHTO M 332 MSCR curve, indicating non-existence of polymers.

PG 70-22:

- At 64°C, 55% of binders were graded as PG 64E-22 and other 45% of the binders were graded as PG 64V-22.
- At 70°C, 22% of binders of these binders were graded as PG 70H-22, PG 70E-22 and PG 70S-22, and 33% of them were graded as PG 70V-22.
- At 64°C, about 55% of the tested PG 70-22 binders were plotted above the polymer curve, indicating the presence of polymers.
- Based on the quadrant plot, the suggested minimum MSCR %R values for PG 70-22 binders would be about 25%, without putting any suppliers or users at risk.

PG 76-22:

- At 64°C, all PG 76-22 were graded as PG 64E-22. At 70°C, about 22% and 78% of PG 76-22 were graded as PG 70V-22 and PG 70E-22, respectively.
- At 76°C, PG 76-22 were graded as PG 76E-22, PG 76V-22, PG 76H-22, and PG 76S-22.

- Per AASHTO M 332, PG 76-22 binders could be used at different locations on the basis of climate temperatures and traffic loading conditions.
- At 64°C and 3.2 kPa, the %R values of all PG 76-22 binders were above the polymer curve except PG 76-22 from source S1.
- Based on the quadrant plot, the suggested minimum MSCR %R values for PG 76-22 binders would be about 70%, which would put one supplier at risk but no user at risk. This supplier would have to make some adjustments so that the binder would meet the %R criterion.

Stress Sensitivity:

- At a testing temperature of 70°C, agencies may consider including a stress level between 3.2 kPa and 10 kPa for measuring the nonlinear properties of PG 70-22 binders.
- At a testing temperature of 64°C, agencies may consider the 10 kPa or higher stress levels for measuring the nonlinear properties of PG 70-22 binders.
- At a testing temperature of 70°C, a stress level of 12.8 kPa should be added to the MSCR standard procedure to measure the nonlinearity of SBS modified PG 76-22 binders.
- At a testing temperature of 76°C, agencies may consider a stress level between 3.2 kPa and 10 kPa for measuring the nonlinear properties of SBS modified PG 76-22 binders. The proposed limit of stress levels be also added to current MSCR test procedure for measuring the rutting properties of the SBS-modified binders in the nonlinear region at 76°C.

WMA-modified Binders

- Sasobit® and Advera® showed better MSCR grades than those of the unmodified binders.
- The effect of Evotherm® on the MSCR parameters of PG 64-22 varied from source to source.
- The addition of Sasobit® increased the %R and decreased the J_{nr} values of the PMBs.

- The effects of the Advera® and Evotherm® on the %R and J_{nr} values of PG 70-22 binders varied from source to source.
- The addition of Advera® and Evotherm® decreased the %R values and increased the J_{nr} values of the PG 76-22 binders.

RAP-modified Binders

- The addition of RAP increased the MSCR grade of the unmodified binders (PG 64-22).
- At 64°C, the MSCR grade of the 60% RAP modified binders and PMBs were similar.
- All RAP modified binders were plotted under the polymer curve.

11.1.1.2 Texas Binders' MSCR Data

PG 70-22:

- At 64°C, 75% of PG 70-22 binders were graded as PG 64V-22 and the other 25% of these binders were graded as PG 64E-22.
- At 70°C, 75% of PG 70-22 binders were graded as PG 70H-22, and 25% of these binders were graded as PG 70E-22.
- At 64°C and 3.2 kPa, all of the tested PG 70-22 binders were plotted above the polymer curve.
- Based on the quadrant plot, the suggested minimum MSCR %R values for PG 70-22 binders would be about 42%, which will put one supplier at risk but no user at risk.

PG 76-22

- At 64°C, all PG 76-22 binders would sustained greater than 30 million traffic load plus standing traffic as their MSCR grade was PG 64E-22.
- At 64°C and 3.2 kPa, the %R values of all PG 76-22 binders were plotted above the polymer curve.
- Based on the quadrant plot, the suggested minimum MSCR %R values for PG 76-22 binders would be about 55%; this would not put any suppliers or users at risk.

11.1.1.3 Superpave Test Data

- The addition of RAP increased the viscosity as well as the rutting resistance of the unmodified binders (PG 64-22).
- The addition of the Sasobit[®] significantly increased the rutting resistance of the PMBs, which is followed by Evotherm[®] and then Advera[®].
- The viscosity of all binders with Sasobit[®] and Evotherm[®] was lower than the unmodified binders and PMBs.
- Advera[®] increased the viscosity of the unmodified binders and PMBs.

11.1.2 Recommendations

Due to the limitation of resources and time, the research team could not attempt all necessary tasks. The followings are recommended for the future studies:

- Since the refinery did not provide any information about the specific amount of SBS modifier for making the PMBs, chemical analyses of these binders can be accomplished for a better understanding of the behavior of the binders.
- A few tested PMBs showed very low J_{nr} values at 10 kPa and at high temperatures. Thus, higher stress levels than 10 kPa are needed for characterizing the highly modified binders.
- In this study, only six sources were considered for recommending the MSCR %R values for TxDOT. More TxDOT' approved sources are needed to consider for MSCR testing before finalizing the MSCR %R values for TxDOT.
- The rutting resistance of the asphalt mix was not consider in this study. As a future study, rutting resistance of asphalt mixes can be considered for correlating with laboratory J_{nr} values.
- Unlike Sasobit[®], the effects of the Advera[®] and Evotherm[®] on the MSCR parameters varied from source to source. Thus, in the future study, other percentages of Advera[®] and Evotherm[®] are needed to consider for a better understanding the effects of these additives on the MSCR parameters.

11.2 PART TWO CONCLUSIONS AND RECOMMENDATIONS

The applicability of the MSCR test method to characterize the polymer-modified binders and RAP binder blends commonly used by DOTs in Oklahoma, Texas and New Mexico was evaluated in the present study. The experimental plan comprised of conducting the Superpave® and MSCR tests on the polymer-modified PG 70-XX and PG 76-XX binders from seven different sources. The effects of blending different amounts of RAP binders, namely 0%, 25%, 40% and 60% (by weight of the binder), with a PG 64-22 binder were evaluated using both the Superpave® and MSCR test methods. The MSCR tests were conducted on the RTFO-aged binder samples at 64 °C, in accordance with the AASHTO TP 70 (AASHTO, 2013) test method. Also, the MSCR tests were conducted at a higher stress level (10 kPa) and higher temperatures (70 °C and 76 °C) to determine the stress and temperature sensitivities of the tested binders. The results of the MSCR tests were analyzed using the AASHTO MP 19 (AASHTO, 2010) specification. Furthermore, the rutting and moisture susceptibilities of the asphalt mixes containing polymer-modified binders and high amounts of RAP were determined using the HWT test. The results of the DSR, MSCR and HWT tests were compared to evaluate relationships between binders' properties and performance of asphalt mixes. Based on the results and discussions presented in previous chapters, the following conclusions can be drawn:

11.2.1 Conclusions

- The MSCR parameters have potential to adequately characterize the rheological properties of polymer-modified binders. The J_{nr} and %Recovery parameters could successfully determine the effects of different amounts of RAP binder in the binder blends. Also, the MSCR parameters provide a better understanding of the stress and temperature sensitivities of polymer-modified binders and RAP binder blends.
- The %Recovery requirements proposed by AASHTO TP 70 (2013) were found to be adequate for differentiating the elastomeric polymer-modified binders from other binders used in this study. The polymer-modified PG 70-XX and PG 76-XX

binders (except S7 PG 70-22 binder) were found to satisfy the %Recovery requirements of AASHTO TP 70 (2013).

- It was found that the current MSCR test method is not sufficient to characterize the non-linear viscoelastic behavior of polymer-modified binders. A 10 kPa stress level can be added to the MSCR test method in conjunction with the 0.1 and 3.2 kPa stress levels to better characterize the non-linear viscoelastic behavior of polymer-modified binders. Such characterization is important as pavement rutting is known to be a non-linear phenomenon.
- The polymer-modified binders, which are produced to meet the Superpave® specifications, may not always satisfy the MSCR %Recovery requirements, depending on the types, and amounts of polymers used for binder modification.
- A pavement constructed with asphalt mix containing polymer-modified binders is expected to perform well in terms of rutting. The MSCR grades of all tested polymer-modified binders were found to be PG 64E-XX, indicating binders' ability to sustain extreme level of traffic at 64 °C. The results of the DSR and HWT tests were found to satisfy the specifications requirement for rutting.
- The responses to the permanent deformation of the binders having the same PG grade are expected to vary with the binder sources while other conditions (e.g., temperature and traffic) remain same. The J_{nr} and %Recovery parameters could identify the differences in the rheological properties of the polymer-modified binders of the same PG grades but from different sources.
- The MSCR grade of the S6 PG 70-28 binder was found to change from PG 64E-28 to PG 70H-28 with an increase in temperature from 64° to 70 °C. It is therefore critical that the “working” high temperature grade be established for the regional location of the pavement. LTPPBind is a software tool that can help establish a base high temperature for specific geographical regions. A higher base temperature grade may be required to better grade some binder blends with high RAP, higher polymer content, and other binder additives.
- The high-temperature PG grades of the RAP binder blends were observed to increase with an increase in the RAP binder content. No significant changes in the PG grades of the binder blends were observed after incorporating 25% RAP1

and RAP2 binders. However, the addition of 40% and 60% RAP1 binders resulted in an increase of two grades from the neat binder. Also, the high-temperature PG grades were found to increase by one and three grades after the addition of 40% and 60% RAP2 binders, respectively.

- The low-temperature PG grades of the RAP binder blends were found to exhibit an increasing trend with addition of RAP binder. The addition of 40% RAP1 binder to the binder blend resulted in a three grades bump of low-temperature PG grade. Also, the low-temperature PG grade of the PG 64-22 binder increased by one grade due to the addition of 60% RAP2 binder.
- The J_{nr} values were found to decrease and the %Recovery values were found to increase with an increase in the RAP binder content in the binder blends, indicating a higher rutting resistance than the neat binder.
- The MSCR grades of the RAP binder blends exhibited an increasing trend with an increase in amount of RAP binder. For example, the MSCR grade of the PG 64-22 binder was found to be PG 64H-22, which increased to PG 64E-XX after addition of 60% RAP1 and RAP2 binders. According to the AASHTO MP 19 (AASHTO, 2010) specification, a binder with an “extreme” grade is expected to sustain a traffic levels of greater than 30 million ESALs and standing traffics (< 20 km/h). Therefore, the 60% RAP1 and RAP2 binder blends can be used at places which experience extreme traffic and/or standing traffics, such as toll plazas, port facilities and intersections.
- From the HWT test results, the rutting resistance of the asphalt mixes was found to increase with an increase in the RAP content from 25% to 35%. As per ODOT specifications, the maximum allowable percent binder replacement by RAP for surface courses and other Superpave[®] mixes are 12% and 30%, respectively (ODOT, 2013). The ODOT may consider revising the allowable limit of binder replacement as both the RAP binder blends and asphalt mixes with high RAP content were found to exhibit an improved resistance to rutting.
- The negative %Recovery observed at higher stress levels and temperatures indicated a continuous deformation of the binder sample after the removal of creep load. Therefore, the stress and temperature sensitivities of the RAP binder

blends should be taken into consideration, although they are expected to exhibit a satisfactory rutting performance at high temperatures, based on the Superpave® test results.

- The DSR and MSCR test methods were found to rank the rutting performance of the polymer-modified binders differently. A similar dissimilarity in the ranking of binders based on the DSR and MSCR test methods were observed for the RAP binder blends. However, the MSCR-based ranking system is expected to predict the rutting performance of binders better than the DSR-based ranking.
- From the HWT test results, the rut depths for both types of asphalt mixes (NMAAS=12.5 mm and NMAAS= 19 mm) were found to increase with a reduction in the $|G^*|/\sin\delta$ values, although the level of increase was not the same. The HWT rut depths were found to exhibit an increasing trend with an increase in J_{nr} value for asphalt mixes with an NMAAS = 19 mm. However, the rut depths of asphalt mixes with a NMAAS = 12.5 mm were found to exhibit an opposite trend with J_{nr} value. The sensitivity of the J_{nr} parameter to polymer modification of binders were assumed to be the reason for this discrepancy.

11.2.2 Recommendations

The following recommendations were made based on the limitations and the scope of the present study:

- The Oklahoma DOT may consider improving its current MSCR database by including binders' results from all approved suppliers. A number of different polymers are currently being used by the asphalt binder refineries to achieve specification requirements. The effects of the types and amounts of the different polymers used by refineries located in Oklahoma on the performance of the binders were beyond the scope of the present study. A detailed rheological study using the MSCR test method is needed to characterize the polymer-modified binders with different types and amounts of polymers used in Oklahoma.
- The refineries located in Oklahoma, New Mexico and Texas are producing asphalt binders following the AASHTO M 320 (AASHTO, 2012) specification. A study is needed to find out the feasibility of changing the specification of binders'

production to AASHTO MP 19 (AASHTO, 2010) from AASHTO M 320 (AASHTO, 2012). Also, training of both users and producers on the MSCR test method and specification are necessary to help adopting this test method in Oklahoma, New Mexico and Texas.

- The present study provides an insight on the rutting resistance of asphalt mixes containing polymer-modified binders and high amount of RAP and its relation with the DSR and MSCR rutting parameters. However, a comprehensive study is needed to establish correlations between the performance of plant and laboratory produced asphalt mixes and the DSR and MSCR test results. Based on the results of field performance, the MSCR guidelines can be evaluated and updated, periodically.
- Oklahoma DOT could consider using high amount of RAP in asphalt mixes as they exhibited a higher rutting resistance. However, the low-temperature cracking and fatigue performance should be considered during the selection of an asphalt mix with high amount of RAP. A study is needed to optimize the amount of RAP to be added to asphalt mixes based on their overall performance.

11.2.3 Guidelines

- Communications between asphalt producers and specifying agencies is critical throughout the move from M 320 to M 332 adoptions.
- Review AI's MSCR-information for history and a basic understanding of MSCR.
- Obtain DSR equipment and software to perform and report MSCR test results.
- Train Technicians to perform and report results from AASHTO T 350 (replaced TP 70).
- Use LTPPBind software to determine what the base high temperature grade should be based on geographical regions. Consider a conservative estimate to cover more regions to prevent a proliferation of MSCR grades. e.g. PG 64.
- Create a database of test results from T 350. Use current AASHTO M 320 graded binders in common use. Compare to specifications in AASHTO M 332 (replaced MP 19). Determine MSCR grade according to M 332 specifications.

- If an elastomeric response is needed for some binders, $R_{3.2}$ is a feasible replacement for many of the common PG+ test methods for this characteristic. Setting the specification limit for $R_{3.2}$ will vary according to the chosen approach. One method is to use the curve in M 332's Appendix X1 Indications of Elastic Response. A second method is a stepped approach where the current M 320 grades are compared to the MSCR grades with $R_{3.2}$ and the PG+ test(s) plotted in four quadrants showing risks for Contractors and specifying Agencies. This method will ensure that the specifying Agency will get binders with few changes to production processes.
- Full adoption methods tend to fall into two approach types. (1) The specifying Agency fully adopts M 332's naming convention. This requires a similar effort as was done when the Penetration/Viscosity tests methods changed to M 320. (2) A translation table is set to only require testing according to M 332 but keep the M 320 naming convention. This allows fewer changes in Contract documents, mix designs, pay item descriptions, sampling guides, etc.
- As an interim approach, a partial adoption method can be used to simply replace PG+ tests with $R_{3.2}$.

11.3 PART THREE CONCLUSIONS AND RECOMMENDATIONS

11.3.1 Conclusions

In order to investigate the potential of Sentmanat Extensional Rheometer fixture as a replacement of the force ductility test (AASHTO T300), extensional deformation tests using a DSR-based SER fixture were performed for asphalt binders PG 76-22, PG 64-22, and PG 58-28.

This study focused on PG 76-22 in order to detect the second peak elongation force caused by the polymer modifications. In order to select the sample geometry, nine different geometries were investigated. Three temperatures, 4°C, 10°C, and 16°C, were used to determine the recommended test temperature. Based on the result presented in this study, the following conclusions can be drawn:

- A new test method was developed to fulfill the acknowledged gap in the current PG system and replace the force ductility test by exploring different potential extensional rheology parameters. Second peak elongation force was detected for PG 76-22 polymer modified binder.
- Sample preparation method was developed and simplified so it can be performed with easy access tools. Less than 1 g of the sample is needed, and less than 1 min is needed to perform the test after a temperature equilibrium soaking time of 10 min. The developed test procedure was kept limited to the fixture safety thresholds, and capabilities.
- The newly developed test parameters are F_2 and F_2/F_1 . The coefficient of variation for ten F_2 values is 6.19%, and coefficient of variation for F_2/F_1 values is 9.21%.
- A detailed analysis indicates that the average second peak and first peak elongation forces increase due to the increase of the sample's initial area, with R^2 values of 0.85 and 0.84, respectively. However, the same initial areas with different dimensions derived different values of elongation force. The elongation force of all samples with the same initial area but different dimensions increase due to the increase of width even though the thickness decreases.
- The second peak elongation force is almost linearly increasing due to the temperature increment, with R^2 value of 0.96 at 4°C, 10°C, and 16°C.
- Based on the study, the recommended test specifications are as follow: the selected geometry 9 mm x 0.72 mm. The F_2 value has been chosen as a recommended force ductility parameter. The minimum F_2 value recommended is 14 N, which was lower than the lowest limit of 99% confidence interval (14.45N – 15.99 N). Also, minimum F_2/F_1 of 1.25 is recommended for PG76-22. This is also lower than the lowest value of 99% confidence interval (1.29-1.51). The recommended temperature is 4°C, recommended strain rate 0.1 s^{-1} , and the recommended final strain is 3.4 rad.

11.3.2 Recommendations

The following recommendations have been made for implementation of this new test method:

- A standard method of test needs to be developed according to the DOTD/AASHTO/ASTM format.
- Reproducibility of inter-laboratory tests needs to be verified.
- More polymer modified binders need to be tested for confirming the specifications and passing/failing criteria.

THIS PAGE IS INTENTIONALLY BLANK

CHAPTER 12

IMPLEMENTATION/ TECHNOLOGY TRANSFER

12.1 PART ONE

12.1.1 Conferences and Other Presentations

12.1.1.1 Conferences

1. Rahaman, Z., Hossain, Z. (2017), “Non-recoverable Compliance and Recovery Behavior of Polymer-modified and Reclaimed Asphalt Pavement-blended Binders in Arkansas,” Transportation Research Board (TRB), Compendium of Papers, Volume: 96, January 8-12, 2017, Washington D.C.
2. Hossain, Z., Rahaman, M., Zaman, M., Ghosh, D., Hobson, K. “Investigation of Multiple Stress and Creep Recovery Properties of Polymer Modified Asphalt Binders”. Presented at International Airfield and Highway Pavements Conference, held in Miami, Florida, June 8, 2015.
3. Hossain, Z., and Rahaman, M. (2016). “Prediction of Fatigue and Rutting Behavior of the Polymer Modified Binders for Warm Mixes” an abstract submitted in the 2017 Geotechnical Frontiers to be held in Orlando, FL.

12.1.1.2 Other Presentations

1. Rahaman, M., and Hossain, Z. (2015). “Characterization of binders in the region using Multiple Stress Creep Recovery Test,” Presented at Create @State, Arkansas State University, Jonesboro, AR, April 7, 2015.
2. Rahaman, M., and Hossain, Z. (2015). “Multiple Stress Creep Recovery Analysis of Modified Binders in the SPTC Region,” Presented at Oklahoma Transportation Research Day, Oklahoma City, OK, October 20, 2015.
3. Rahaman, M. Z., Rashid, F., and Hossain, Z. (2016). “Realistic and Effective Characterization of Polymeric and Reclaimed Asphalt Binders Subjected to Extreme Weather Events.” To be presented at the 102nd Transportation

Research Committee Meeting and Engineering Conference, Little Rock, AR, April 5-6, 2016.

12.2 PART TWO

12.2.1 Implementation and Technology Transfer Workshop

A technology transfer workshop was organized and conducted on June 30, 2017 at ODOT's headquarters office in Oklahoma City. Participants from industry and ODOT personnel attended the workshop. Different aspects of the project, including implementation were discussed, after the presentation.

12.2.2 Peer-Reviewed Journal and Conference Papers

The research team has published/submitted one journal article and two proceedings papers and four poster presentations. Furthermore, test data from this project are integral part of a Master's thesis. The publication records of the research team related to the project are listed below:

12.2.2.1 Peer-Reviewed Journal Papers

1. Ali, S.A., Ghabchi, R., Rani, S., and Zaman, M. (2016). "Characterization of Effect of Polymer Modification, Poly-Phosphoric Acid and Aging on Asphalt Binder Using X-ray Diffraction (XRD)". Submitted to *Construction and Building Materials*.

12.2.2.2 Peer-Reviewed Conference Papers

1. Ali, S.A., Ghabchi, R., Rani, S., Zaman, M. and Parker, C. (2016). "A Laboratory Study of Rutting Susceptibility of Asphalt Mix Containing High RAP Content Using Rheological and Performance-based Test Methods". Submitted to *International Conference on Highway Pavements & Airfield Technology*, Philadelphia, Pennsylvania, will be held on August 27, 2017.

12.2.2.3 Other Presentations

1. Ali, S.A., Ghabchi, R., Rani, S., Zaman, M. and Parker, C. (2016). "Rutting Susceptibility Evaluation of RAP-Modified Asphalt using MSCR Method". Submitted to *15th International Conference of the International Association for*

Computer Methods and Advances in Geomechanics (15th IACMAG), Wuhan, China, will be held on October 19-23, 2017.

2. Ali, S.A., Rani, S., Ghabchi, R., and Zaman, M. (2015). "Development of Guidelines Toward Adopting the Multiple Stress Creep Recovery (MSCR) Test Method for Extreme Weather Conditions Prevailing in the Southern Plains." poster presented at 2015 Oklahoma Transportation Research Day, held at the Moore Norman Technology Center, OKC, OK. Date: October 20th, 2015.
3. Ali, S.A., Rani, S., Ghabchi, R., and Zaman, M. (2016). "Characterization of Rheological Properties of Polymer and RAP Modified Asphalt Binders Using Multiple Stress Creep and Recovery Method." Poster presented at the Graduate Student Research & Creativity Day, 2016, held at the University of Oklahoma, Norman, OK. Date: March 4th, 2016.
4. Ali, S.A., Rani, S., Ghabchi, R., and Zaman, M. (2016). " Evaluation of High Temperature Characteristics of Polymer and RAP Modified Asphalt Binders Using Multiple Stress Creep and Recovery Method." Poster presented at 2016 Oklahoma Transportation Research Day, held at the Moore Norman Technology Center, OKC, OK. Date: October 18th, 2016.
5. Ali, S.A., Ghabchi, R., Rani, S., and Zaman, M. (2016). "Characterization of Effect of Polymer Modification, Poly-Phosphoric Acid and Aging on Asphalt Binder Using X-ray Diffraction (XRD)". Poster presented at *Transportation Research Record 96th Annual Meeting*, Washington, D.C. Date: January 8-12, 2017.

12.3 PART THREE

12.3.1 Peer-Reviewed Journal and Conference Papers

The research team has published/submitted one journal article and one peer-reviewed conference proceeding. Furthermore, test data from this project are integral part of a Master's thesis. The publication records of the research team related to the project are listed below:

12.3.1.1 Peer-Reviewed Journal Papers

1. Mohammed Omer, W., and Wasiuddin, N. M. (2018). "Development of a Novel and DSR-Based Extensional Deformation Test Replacing Force Ductility Test (AASHTO 300)". Submitted to the Journal of Testing and Evaluation. Initially acceptance with reviewers' comments was received on January 22, 2018

12.3.1.2 Peer-Reviewed Conference Papers

1. Mohammed Omer, W., and Wasiuddin, N. M. (2018). "Development of a Novel and DSR-Based Extensional Deformation Test Replacing Force Ductility Test (AASHTO 300)". Presented at 97th Annual Meeting of the Transportation Research Board, Washington, D.C., 2018.

12.3.1.3 Other Presentations

1. Wasiuddin, N.M. (2016). "Replacement of Elastic Recovery Test and Force Ductility Tests by DSR-Based Tests", Presented at the Louisiana Transportation Conference, Baton Rouge, Feb. 28- Mar. 2, 2016.
2. Mohammed Omer, W., and Wasiuddin, N. M. (2018). "Development of a Novel and DSR-Based Extensional Deformation Test Replacing Force Ductility Test (AASHTO 300)". Presented at the SPTC Summer Symposium, Oklahoma City on August 15, 2017.

ACRONYMS, ABBREVIATIONS, AND SYMBOLS

AASHTO	American Association of State Highway and Transportation Officials
AI	Asphalt Institute
ALF	Accelerated Loading Facility
APA	Asphalt Pavement Analyzer
BBR	Bending Beam Rheometer
CR	Crumb Rubber
DCA	Dynamic Contact Angle
DOT	Departments of Transportation
DSR	Dynamic Shear Rheometer
ER	Elastic Recovery
EVA	Ethylene-Vinyl-Acetate
EVT	Equi-Viscous Temperature
ESAL	Equivalent Single Axle Load
FD	Forced Ductility
FHWA	Federal Highway Administration
FTIR	Fourier Transform Infrared
HMA	Hot Mix Asphalt
HWT	Hamburg Wheel Tracking
ILS	Inter-Laboratory Study
LTPP	Long-Term Pavement Performance
LSV	Low Shear Viscosity
LWT	Loaded Wheel Tester
MEPDG	Mechanistic-Empirical Pavement Design Guide
MSCR	Multiple Stress Creep Recovery
NCAT	National Center for Asphalt Technology
NCHRP	National Cooperative Highway Research Program
NEAUPG	North East Asphalt User Producer Group
NHDOT	New Hampshire Department of Transportation

NMDOT	New Mexico Department of Transportation
ODOT	Oklahoma Departments of Transportation
PAV	Pressure Aging Vessel
PG	Performance Grading
PURWheel	Purdue University Laboratory Wheel Tracking Device
RAS	Recycled Asphalt Shingles
RAP	Reclaimed Asphalt Pavement
RAP binder	Binder extracted from RAP
RCRT	Repeated Creep and Recovery Test
RLPD	Repeated Load Permanent Deformation
RTFO	Rolling Thin Film Oven
RV	Rotational Viscometer
S-VECD	Simplified Viscoelastic Continuum Damage
SBS	Styrene-Butadiene-Styrene
SEPS	Styrene-ethylene/propylene-styrene
SER	Sentmanat Extensional Rheometer
SFE	Surface Free Energy
SHRP	Strategic Highway Research Program
SEAUPG	Southeastern Asphalt User/Producer Group
Superpave®	Superior Performing Asphalt Pavements
TSR	Tensile Strength Ratio
TxDOT	Texas Department of Transportation
VDOT	Virginia Department of Transportation
ZSV	Zero-Shear Viscosity
J_{nr}	Non-recoverable creep compliance
$J_{nr \text{ diff}}$	Percent difference in J_{nr} values at two stress levels
%Recovery	MSCR percent recovery
η'	Storage viscosity

REFERENCES

PART ONE REFERENCES

- 1 Federal Highway Administration(FHWA). (2009). Highway Statistics 2009. Office of Highway Policy Information, Federal Highway Administration Washington, D.C. Available at: <http://www.fhwa.dot.gov/policy/ohpi/hss/index.cfm>. Last Accessed May 05, 2016.
- 2 Anderson, D., Youtcheff, J., Zupanick, M. (2016). Asphalt Binders. Transportation in the New Millennium, 2009. <http://onlinepubs.trb.org/onlinepubs/millennium/00006.pdf>. Last Accessed.
- 3 Anderson, D. A., Christensen, D. W., Bahia, H. U., Dongre, R., Sharma, M. G., Antle, C. E., Button, J. “Binder characterization and evaluation.” *Vol 3: Physical characterization*.
- 4 Anderson, D. A., Christensen, D. W., Bahia, H. U., Dongre, R., Sharma, M. G., Antle, C. E., Button, J. (1994) “Binder characterization and evaluation.” *Vol 3: Physical characterization. Strategic Highway Research Program*, National Research Council, Washington, D.C.
- 5 Golalipour, A. (2011). “Modification of multiple stress creep and recovery test procedure and usage in specification.” *Doctoral Dissertation*, University of Wisconsin-Madison, Wisconsin.
- 6 Bahia, H. U., Hanson, D. I., Zeng, M., Zhai, H., Khatri, M. A., Anderson, M. R. (2000). “A Project NCHRP 9-10 Superpave Protocols for Modified Asphalt Binders.” Draft Topical Report (Task 9), *Prepared for National Cooperative Highway Research Program*, Transportation Research Board, National Research Council, Washington, D.C.
- 7 Bahia, H. U., Hanson, D. I., Zeng, M., Zhai, H., Khatri, M. A., Anderson, R. M. (2001). “Characterization of Modified Asphalt Binders in Superpave Mix Design.” *Project No. 9-10 FY'96*, Transportation Research Board, Washington, D.C.
- 8 Bahia, H. U., Zhai, H., Zeng, M., Hu, Y., Turner. (2001). “Development of Binder Specification Parameters Based on Characterization of Damage Behavior.”

- Journal of the Association of Asphalt Paving Technologists*, Vol. 70, Louisville, Kentucky, pp. 442-470.
- 9 Anderson, M., D'Angelo, J., Walker, D. (2010). "MSCR: A better tool for characterizing high temperature performance properties". *Asphalt*, 25(2).
- 10 D'Angelo, J., Dongre, R. "Superpave binder specifications and their performance relationships to modified binders." *Proceedings Canadian Technical Asphalt Association*, Vol. 47, 2002, pp. 91-103.
- 11 D'Angelo, J. (2004). "Modified Binders and Superpave Plus Specifications." *Superpave Technical Issues*, Asphalt Institute, Lexington, KY.
- 12 D'Angelo, J., Dongre R. (2004). "Development of a Performance-Based Binder Specification in the United States." *Proceedings of 3rd Eurasphalt and Eurobitume Congress*, Vienna, Austria.
- 13 Kamel N. I., Bahia, H. U., Cho., D. W. (2004). "Critical laboratory evaluation of asphalt binders modified by refining processes." *Proceedings of Canadian Technical Asphalt Association*, Victoria, BC, Canada, pp. 57-76.
- 14 D'Angelo, J., Dongre, R., Reinke, G. (2006). "Evaluation of Repeated Creep and Recovery Test Method as an Alternative to SHRP+ Requirements for Polymer Modified Asphalt Binders." *Proceedings of the Fifty-First Annual Conference of the Canadian Technical Asphalt*, Prince Edward Island, Canada, pp. 143-162.
- 15 D'Angelo, J. A. (2009). "The relationship of the MSCR test to rutting." *Journal of Road Materials and Pavement Design*, Vol. 10(sup1), pp. 61-80.
- 16 D'Angelo, J. (2010). "New High Temperature Binder Specification Using Multi Stress Creep and Recovery." *Transportation Research Circular E-C147*, Washington, D.C, pp. 1-13.
- 17 Goodrich, J.L. (1988). "Asphalt and Polymer Modified Asphalt Properties Related to the Performance of Asphalt Concrete Mixes." *Proceedings of the Association of Asphalt Paving Technologists*, Vol. 57, pp. 116 – 175.
- 18 Airey, G.D. (1997). "Rheological Characteristics of Polymer Modified and Aged Bitumens." PhD Thesis, the University of Nottingham.

- 19 Shirodkar, P., Mehta, Y., Nolan, A., Dahm, K., Dusseau, R., McCarthy, L. (2012). "Characterization of creep and recovery curve of polymer modified binder." *Journal of Construction and Building Materials*, Vol. 34, pp. 504-511.
- 20 Mehta, Y., Nolan, A., DuBois, E., Zorn, S., Batten, E., Shirodkar, P. (2013). "Correlation between Multiple Stress Creep Recovery (MSCR) Results and Polymer Modification of Binder." *Final Report No. FHWA-NJ-2014-002*, New Jersey Department of Transportation, NJ.
<http://www.utrc2.org/sites/default/files/pubs/Final-MSCR-Polymer-Modification.pdf>.
- 21 Batten, E., Mehta, Y., Nolan, A., Zorn, S., Dahm, K. (2011). "Correlation between PG Plus, Superpave PG Specifications and Molecular Weight from GPC for Different Polymer Modified Binders." In *Geo-Frontiers Congress*.
- 22 Diehl, C. F. (2000). In *Proceedings of the 2nd Eurasphalt and Eurobitume Congress*, Vol.2, p.93.
- 23 Airey, G.D. (2003). "Rheological Properties of Styrene Butadiene Styrene Polymer Modified Road Bitumens." *Fuel*, Vol. 82, pp. 1709–1719.
- 24 Gina, M. H., Vivek, T., Jorge, Pi., Andre, S., Yetkin, Y., (2007). "Evaluation of Binder Tests for Identifying Rutting and Cracking Potential," Center for Transportation Infrastructure Systems." Research Report 0-4824-1. Conducted for Texas Department of Transportation.
- 25 Read, J., Whiteoak, D. (2003). "*The Shell Bitumen Handbook*." Fifth Edition, Edited by R. Hunter.
- 26 Mallick, R. B., Bergendahl, J., Pakula, M. (2009). "A Laboratory Study on CO2 Emission Reductions through the Use of Warm Mix Asphalt." Transportation Research Board 2009 Annual Meeting, Washington, D.C.
- 27 D'Angelo, J., Harm, E., Bartoszek, J., Baumgardner, G., Corrigan, M., Cowser, J., Harman, T., Jamshidi, M., Jones, W., Newcomb, D., Prowell, B., Sines, R., and Yeaton, B. (2008). "Warm-Mix Asphalt: European Practice." FHWA Report No. FHWA-PL-08-007, American Trade Initiatives, Alexandria, Virginia.

- 28 Cardone, F., Pannunzio, V., Virgili, A., Barbati, S. (2009). "An evaluation of use of synthetic waxes in warm mix asphalt." In *7th International RILEM Symposium on advanced testing and characterization of bituminous materials, Rhodes*.
- 29 Damm, K., Abraham, J., Butz, T., Hildebrand, G., Riebesehl. (2004). "Asphalt Flow Improvers As Intelligent Fillers for Hot Asphalts- A New Chapter in Asphalt Technology". Sasol Wax GmbH, Hamburg.
- 30 Anderson, R. M., Baumgardner, G., May, R., Reinke, G. (2008). "NCHRP 9-47: Interim Report: Engineering Properties, Emissions, and Field Performance of Warm Mix Asphalt Technologies." TRB, National Highway Research Council, Washington, D.C.
- 31 Button, J. W., Estakhri, C., Wimsatt, A. (2007). "A Synthesis of Warm-Mix Asphalt." Research Report FHWA/TX-07/0-5597-1, *Texas Transportation Institute*, College Station, TX.
- 32 Estakhri, C., Button, J., Alvarez, A. E. (2010). "Field and laboratory investigation of warm mix asphalt in Texas." Texas Transportation Institute. *The Texas A&M University*.
- 33 McDaniel, R., Anderson, R. M. (2001). "*Recommended use of reclaimed asphalt pavement in the Superpave mix design method.*" technician's manual (No. Project D9-12 FY'97).
- 34 Al-Qadi, I., Elseifi, M., Carpenter, S. (2007). "Reclaimed Asphalt Pavement." A Literature Review," Research Report FHWA-ICT-07-001, *Illinois Center for Transportation*, Rantoul, IL.
- 35 Swiertz, D., Emad, M., Hussain, B. (2001). "Estimating the effect of recycled asphalt pavements and asphalt shingles on fresh binder, low-temperature properties without extraction and recovery." *Transportation Research Record: Journal of the Transportation Research Board* 2208: 48-55.
- 36 Mallick, R. B., Karen A. O., Mingjiang T., Robert, F. "Why Not Use Rejuvenator for 100% RAP Recycling?." In *Transportation research board 89th annual meeting*, no. 10-1838.
- 37 Copeland, A. (2011). "*Reclaimed asphalt pavement in asphalt mixtures: state of the practice.*" No. FHWA-HRT-11-021.

- 38 Jones, C. L. (2008). "Summit on Increasing RAP Use in Pavements State's Perspective." *MoreRap Conference*, North Carolina Department of Transportation, Auburn, AL.
- 39 Anderson, M., D'Angelo, J., Walker, D. (2010). "MSCR: A Better Tool for Characterizing High Temperature Performance Properties." *The Magazine of the Asphalt Institute*, No.2, Asphalt Institute, Lexington, KY.
<http://www.asphaltmagazine.com/news/detail.dot?id=d90e7ce8-f127-4617-ac1d-7d788e2df710>. Accessed July 14, 2014.
- 40 Tabatabaee, H. A., Clopotel, C., Arshadi, A., Bahia, H. (2013). "Critical Problems with Using the Asphalt Ductility Test as a Performance Index for Modified Binders." *Transportation Research Record: Journal of the Transportation Research Board*, 2370, pp. 84-91.
- 41 Horan, B. (2010). "Multiple Stress Creep Recovery (MSCR) Binder Specification Implementation." Asphalt Institute (AI), *Southeastern Asphalt User-Producer Group (SEAUPG) Annual Meeting*, Oklahoma City, OK.
- 42 AASHTO M332-14: Standard Specification for Performance- Graded Asphalt Binder Using Multiple Stress Creep Recovery (MSCR) Test, AASHTO, Washington, D.C., 2014.
- 43 Buncher, M., Anderson, M., (2015) "MSCR Implementation across the Country." A Progress Report," PCCAS Binder Committee Meeting.,
http://www.pccas.org/uploads/3/3/0/0/3300836/2015-03_4_mscr_implementation_in_u.s._-_buncher-anderson.pdf. (Last Accessed January 22, 2016)
- 44 D'Angelo, J., Klutz, R., Dongre, R., Stephens, K., Zanzotto, L. (2007). "Revision of the Superpave High Temperature Binder Specification: The Multiple Stress Creep Recovery Test." *Journal of the Association of Asphalt Paving Technologists*, Vol. 76, pp. 123-162.
- 45 Zubeck, H., Lutfi, R., Saboundjian, S., Minassian, G., Ryer, J. (1999). "Constructability of polymer modified asphalt and asphalt-aggregate mixture in Alaska." *Final Report No. FHWA-AK-RD 99-1*, Alaska Department of Transportation and Public Facilities, Fairbanks, AK.

- 46 Anderson, R. M. (2011). "Northeast Asphalt User-Producer Group Interlaboratory Study to Determine the Precision of AASHTO TP 70 – The Multiple-Stress Creep-Recovery (MSCR) Test." *Report Prepared for the Northeast Asphalt User-Producer Group (NEAUPG)*, In cooperation with Federal Highway Administration, Asphalt Institute, Lexington, KY.
<http://www.asphaltinstitute.org/dotAsset/d5528c32-d102-4b9e-9b82-a993ca14d1fc.pdf>. Accessed July 15, 2014.
- 47 Anderson, R. M. (2011). "Southeast Asphalt User-Producer Group Interlaboratory Study to Determine the Precision of AASHTO TP70 – the Multiple-Stress Creep-Recovery (MSCR) Test." *Report Prepared for the Southeastern Asphalt User-Producer Group (SEAUPG)*, In cooperation with Federal Highway Administration, Asphalt Institute, Lexington, KY.
<http://www.asphaltinstitute.org/dotAsset/11e12e47-0fb7-4a57-b6bc-14d5307a5d81.pdf>. Accessed July 15, 2014.
- 48 Buncher, M., Anderson. M. (2015). "MSCR Implementation Across the Country." A progress Report. *PCCAS Binder Committee Meeting*, Reno, NV.
- 49 Anderson, M. (2007). "Evaluation of DSR Creep-Recovery Testing as a Replacement for PG Plus Tests." Asphalt Institute (AI), *Association of Modified Asphalt Producers (AMAP) Annual Meeting*, Boston, MA.
- 50 Horan, B. (2010). "Multiple Stress Creep Recovery (MSCR) Binder Specification Implementation." Asphalt Institute (AI), *Southeastern Asphalt User-Producer Group (SEAUPG) Annual Meeting*, Oklahoma City, OK.
- 51 Asphalt Institute Technical Advisory Committee. Guidance on the Use of the MSCR Test with the AASHTO M320 Specification. *Asphalt Institute (AI)*, Lexington, KY, December 2, 2010.
- 52 Anderson, M. (2010). "Understanding and Implementing the Multiple Stress Creep Recovery (MSCR) Test and Specification." *Association of Modified Asphalt Producers Annual Meeting*, Savannah, GA.
- 53 Gierhart, D. (2011). "Simple Talking Points for Sharing Why Your State Should Be Implementing MSCR." *Southeastern Asphalt User-Producer Group (SEAUPG) Web Meeting*, Asphalt Institute (AI), Lexington, KY.

- 54 Anderson, R. M. (2011). "Understanding the MSCR Test and its Use in the PG Asphalt Binder Specification." *Asphalt Institute (AI)*, Lexington, KY.
- 55 Horan, B. (2011). "Multiple Stress Creep Recovery (MSCR) Task Force." Asphalt Institute (AI), *Southeastern Asphalt User-Producer Group (SEAUPG) Annual Meeting*, Savannah, GA.
- 56 Anderson, M., Bukowski, J. (2012). "Using the Multiple-Stress Creep-Recovery (MSCR) Test." *North Central Asphalt User Producer Group Meeting*, Indianapolis, IN.
- 57 Anderson, M. (2012). "Evaluation of J_{nr} Criterion for Unmodified Asphalt Binders." *Asphalt Binder Expert Task Group Meeting*, Minneapolis, MN.
- 58 Harder, G. A. (2012). "Regional Implementation of the MSCR Test." Asphalt Institute (AI), *North East Asphalt User-Producer Group (NEAUPG) Meeting*, Philadelphia, PA.
- 59 Horan, B. (2012). "Multiple Stress Creep Recovery (MSCR) Task Force Overview and Recommendations." *Southeastern Asphalt User-Producer Group Meeting*, Asphalt Institute, Lexington, KY.
- 60 Asphalt Institute Technical Advisory Committee. Use of MSCR Recovery to Replace PG Plus Tests In the Southeast Asphalt User-Producer Group. Asphalt Institute (AI), Lexington, KY, April 24, 2012.
- 61 Anderson, M. (2012). "SEAUPG Evaluation of MSCR Recovery as a Replacement for PG Plus Tests." *Webinar*, Asphalt Institute, Lexington, KY.
- 62 Zhou, F., Li, H., Chen, P., Scullion, T. (2014). "*Laboratory Evaluation of Asphalt Binder Rutting, Fracture, and Adhesion Tests.*"
- 63 Asphalt Institute State MSCR Implementation Status Database, (<http://www.asphaltinstitute.org/specification-databases/state-mscr-implementation-status-database/>). Last accessed May 16, 2016.
- 64 DuBois, E., Mehta, Y., Nolan, A. (2014). "Correlation between multiple stress creep recovery (MSCR) results and polymer modification of binder." *Construction and Building Materials*, 65, 184-190.

- 65 Wasage, T. L. J., Stastna, J., Zanzotto, L. (2011). "Rheological analysis of multi-stress creep recovery (MSCR) test." *International Journal of Pavement Engineering*, 12(6), 561-568.
- 66 Domingos, M. D. I., Faxina, A. L. (2014). "Creep-Recovery Behavior of Modified Asphalt Binders with Similar High-Temperature Performance Grades." In *Transportation Research Board 93rd Annual Meeting* (No. 14-4666).
- 67 Santagata, E., Baglieri, O., Dalmazzo, D., Tsantilis, L. (2013). "Evaluation of the anti-rutting potential of polymer-modified binders by means of creep-recovery shear tests." *Materials and structures*, 46(10), 1673-1682.
- 68 Nejad, F. M., Gholami, M., Naderi, K., Rahi, M. (2001). "Evaluation of rutting properties of high density polyethylene modified binders." *Materials and Structures*, 1-11.
- 69 Shenoy, A. Refinement of the Superpave[®] specification parameter for performance grading of asphalt. *Journal of transportation engineering*, 127(5), 357-362.
- 70 Laukkanen, O. V., Soenen, H., Pellinen, T., Heyrman, S., Lemoine, G. "Creep-recovery behavior of bituminous binders and its relation to asphalt mixture rutting." *Materials and Structures*, 1-15.
- 71 Davidson, T., Nolan, A., Mehta, Y. (2014). "A Study to Evaluate the Effects of SBS Polymer Modification on the True Grade of an Asphalt Binder." In *Geo-Hubei 2014 International Conference on Sustainable Civil Infrastructure*.
- 72 Hafeez, I., Kamal, M. A. (2014). "Creep Compliance: A Parameter to Predict Rut Performance of Asphalt Binders and Mixtures." *Arabian Journal for Science and Engineering*, 39(8), 5971-5978.
- 73 Zoorob, S. E., Castro-Gomes, J. P., Oliveira, L. P., O'Connell, J. (2012). "Investigating the multiple stress creep recovery bitumen characterization test." *Construction and Building Materials*, 30, 734-745.
- 74 Zhang, J., Walubita, L. F., Faruk, A. N., Karki, P., Simate, G. S. (2015). "Use of the MSCR test to characterize the asphalt binder properties relative to HMA rutting performance." A laboratory study. *Construction and Building Materials*, 94, 218-227.

- 75 Stevens, R., Stempihar, J., Underwood, B. S. (2015). "Evaluation of Multiple Stress Creep and Recovery (MSCR) Data for Arizona." *International Journal of Pavement Research and Technology*, 8(5), 337.
- 76 Hurley, G. C., Prowell, B.D. (2005). "Evaluation of Sasobit for Use in Warm Mix Asphalt". National Center for Asphalt Technology, Auburn University.
- 77 Hurley, G. C., Prowell, B. D. (2006). "Evaluation of Evotherm[®] for use in warm mix asphalt." *NCAT report*, 2, 15-35.
- 78 Kim, H., Lee, S. J., Amirkhanian, S. N. (2010). "Effects of warm mix asphalt additives on performance properties of polymer modified asphalt binders." *Canadian Journal of Civil Engineering*, 37(1), 17-24.
- 79 Ziari, H., Babagoli, R. (2015). "Evaluation of Fatigue and Rutting Behavior of Asphalt Binder Containing Warm Additive." *Petroleum Science and Technology*, 33(17-18), 1627-1632.
- 80 Akisetty, C., Xiao, F., Gandhi, T., Amirkhanian, S. (2011). "Estimating correlations between rheological and engineering properties of rubberized asphalt concrete mixtures containing warm mix asphalt additive." *Construction and Building Materials*, 25(2), 950-956.
- 81 Morea, F., Marcozzi, R., Castaño, G. (2012). "Rheological properties of asphalt binders with chemical tensoactive additives used in Warm Mix Asphalts (WMAs)." *Construction and Building Materials*, 29, 135-141.
- 82 Mannan, U. A. (2012). "Effect of Recycled Asphalt Shingles (RAS) on Physical and Chemical Properties of Asphalt Binders." (Doctoral dissertation, The University of Akron).
- 83 Wu, S., Zhang, K., Wen, H., DeVol, J., Kelsey, K. (2015). "Performance Evaluation of Hot Mix Asphalt Containing Recycled Asphalt Shingles in Washington State." *Journal of Materials in Civil Engineering*, 28(1), 04015088.
- 84 Hossain, Z., Zaman, M., Ghosh, D. (2015). "Creep compliance and percent recovery of Oklahoma certified binder using the multiple stress recovery (MSCR) method." Report No. FHWA-OK-14-19). *Federal Highway Administration, Oklahoma Department of Transportation, Oklahoma*.

- 85 Hossain, Z., Zaman, M., Ghosh, D. (2015). “Creep Compliance and Percent Recovery of Oklahoma Certified Binders Using the Multiple Stress Creep Recovery (MSCR) Method.” (No. FHWA-OK-14-19).
- 86 Ghosh, D. (2014). “Characterization of Oklahoma Certified Binders Using Multiple Stress Creep Recovery Method.” *Master of Science Thesis, The University of Oklahoma, Norman.*
- 87 Rahaman, M. (2016). “Creep and Recovery Behavior of Polymeric and Chemically Treated Asphalt Binders.” *Master of Science Thesis, Arkansas State University, Jonesboro.*
- 88 Anderson, M., (2010). “Using the Multiple-Stress Creep-Recovery (MSCR) Test,” presented at the Association of Modified Asphalt Producers Annual Meeting, Savannah, GA. AMAP, Avon, OH, -unpublished.
- 89 D’Angelo, J. (2010). “The multiple stress creep recovery (MSCR) procedure.” *Technical brief, Office of the Pavement Technology, Federal Highway Administration, Washington, D.C, pp. 11-38.*
- 90 Anderson, M., (2010). “Using the Multiple-Stress Creep-Recovery (MSCR) Test.” presented at the Association of Modified Asphalt Producers Annual Meeting, Savannah, GA, 2010, AMAP, Avon, OH, -unpublished.
- 91 Hossain, Z., Ghosh, D., Zaman, M., Hobson, K. (2015). “Use of the Multiple Stress Creep Recovery (MSCR) Test Method to Characterize Polymer-Modified Asphalt Binders.” *ASTM Journal of Testing and Evaluation, 44(1S):1-4.*
- 92 Asphalt Institute Technical Advisory Committee. Use of MSCR Recovery to Replace PG Plus Tests In the Southeast Asphalt User-Producer Group. Asphalt Institute (AI), Lexington, KY, April 24, 2012.
- 93 Colbert, B., You, Z. (2012). “The properties of asphalt binder blended with variable quantities of recycled asphalt using short term and long term aging simulations.” *Construction and Building Materials, 26(1), 552-557.*
- 94 Akisetty, C. K., Lee, S. J., Amirkhanian, S. N. (2009). “High temperature properties of rubberized binders containing warm asphalt additives.” *Construction and Building Materials, 23(1), 565-573.*

- 95 D'Angelo, J., R. Dongré. (2006). "Development of a High Temperature Performance Based Binder Specification in the United States." Proc., 10th International Conference on Asphalt Pavements, Quebec City, Quebec, Canada.
- 96 D'Angelo, J. A., Dongre, R. N. (2009). "Practical Use of Multiple Stress Creep and Recovery Test: Characterization of Styrene–Butadiene–Styrene Dispersion and Other Additives in Polymer-Modified Asphalt Binders." In Transportation Research Record: Journal of the Transportation Research Board, No. 2126, Transportation Research Board of the National Academies, Washington, D.C., pp. 73–82.
- 97 Delgadillo, R., Nam, K., Bahia, H. U. (2006). "Why Do We Need to Change $G^*/\sin \delta$ and How?" Road Materials and Pavement Design, Vol. 7, No. 1, pp. 7–27.
- 98 Delgadillo, R. A., Cho, D. W., Bahia, H. U. (2006). "Nonlinearity of Repeated Creep and Recovery Binder Test and Relationship with Mixture Permanent Deformation." In Transportation Research Record: Journal of the Transportation Research Board, No. 1962, Transportation Research Board of the National Academies, Washington, D.C., pp. 3–11.
- 99 Dreessen, A., Planche, J. P., Gandel, V. (2009). "A New Performance Related Test Method for Rutting Prediction: MSCRT. In Advanced Testing and Characterization of Bituminous Materials." Vol. 2. (A. Loizos, M. N. Partl, T. Scarpas, and I. L. Al-Qadi, eds.), CRC Press, Taylor & Francis Group, London.
- 100 Jafari, M., Babazadeh, A., Aflaki, S. (2015). "Effects of Stress Levels on Creep and Recovery Behavior of Modified Asphalt Binders with the Same Continuous Performance Grades." *Transportation Research Record: Journal of the Transportation Research Board*, (2505), 15-23.
- 101 Kvasnak, A., et al., (2010a). "Evaluation of warm mix asphalt field demonstration." Nashville, Tennessee. Auburn, AL. NCAT Report 10-01 National Center for Asphalt Technology.
- 102 Jamshidi, A., Hamzah, M. O., You, Z. (2013). "Performance of warm mix asphalt containing Sasobit®: state-of-the-art." *Construction and Building Materials*, Vol. 38, pp. 530-553.

- 103 Zaumanis, M., Haritonovs, V. (2010). "Research on properties of warm mix asphalt." Scientific Proceedings of Riga Technical University, Series 2: Architecture and Construction Science, Vol. 11, 2010, pp. 77-84.
- 104 Kheradmand, B., Muniandy, R., Hua, L. T., Yunus, R. B., Solouki, A. (2014). "An overview of the emerging warm mix asphalt technology." International Journal of Pavement Engineering, 15(1), 79-94.
- 105 King, G. N., King, H. W. (1988). "Polymer modified bitumen: Laboratory evaluation, construction Guidelines and field experience." 3rd International Road Federation Middle East Regional Meeting, Riyadh, Saudi Arabia.
- 106 Xiao F., Amirkhanian S. N., Putman B. J. (2010). "Evaluation of rutting resistance in warm mix asphalts containing moist aggregate." Trans Res Rec: J Trans Res Board 2010;2180 (-1):75–84.
- 107 McDaniel, R. S., Shah, A. (2003a). "Use of Reclaimed Asphalt Pavement (RAP) Under Superpave Specifications." Journal of the Association of Asphalt Paving Technologists, Vol. 72, pp. 226-252.
- 108 Li, X., Marasteanu, M., Williams, R. C., Clyne, T. R. (2008). "Effect of RAP Proportion and Type and Binder Grade on the Properties of Asphalt Mixtures." Transportation Research Record, No. 2051, Journal of the Transportation Research Board, Washington, D.C., pp. 90-97.

PART TWO REFERENCES

109. Maccarrone, S., Holleran, G., and Gnanaseelan, G. P. (1995). "Properties of Polymer Modified Binders and Relationship to Mix and Pavement Performance (with Discussion and Closure)." *Journal of the Association of Asphalt Paving Technologists*, 64, 209-240.
110. Airey, G. D. (2002). "Rheological Evaluation of Ethylene Vinyl Acetate Polymer Modified Bitumens." *Construction and Building Materials*, 16(8), 473-487.
111. Gopalipour, A. (2011). "Modification of Multiple Stress Creep and Recovery Test Procedure and Usage in Specification." *Master Thesis, University of Wisconsin-Madison, Wisconsin*.
112. Khadivar, A., and Kavussi, A. (2013). "Rheological Characteristics of SBR and NR Polymer Modified Bitumen Emulsions at Average Pavement Temperatures." *Construction and Building Materials*, 47, 1099-1105.
113. Bahia, H. U., Hanson, D. I., Zeng, M., Zhai, H., Khatri, M. A., and Anderson, M. R. (2001). "NCHRP Report 459, Characterization of Modified Asphalt Binders in Superpave Mix Design." Prepared for *National Cooperative Highway Research Program*, Transportation Research Board, National Research Council, Washington, D.C.
114. Collins, J. H., Bouldin, M. G., Gelles, R., and Berker, A. (1991). "Interpretation of Dynamic Mechanical Test Data for Paving Grade Asphalt Cements." In *Proceedings of the Association of Asphalt Paving Technologists*, 60, 43-69.
115. Sargand, S. M., and Kim, S. S. (2001). "Performance Evaluation of Polymer Modified and Unmodified Superpave Mixes." In *Second International Symposium on Maintenance and Rehabilitation of Pavements and Technological Control*, Auburn, AL.
116. Chen, J. S., Liao, M. C., and Tsai, H. H. (2002) "Evaluation and Optimization of the Engineering Properties of Polymer-Modified Asphalt." *Practical Failure Analysis*, 2(3), 75-83.

117. Diehl, C. F. (2000). "Ethylene-Styrene Interpolymers for Bitumen Modification." In *Proceedings of the Papers submitted for review at 2nd Eurasphalt and Eurobitume Congress, Held 20-22 September 2000, Barcelona, Spain., 2*, 93.
118. Airey, G. D. (2011). "Factors Affecting the Rheology of Polymer Modified Bitumen. Polymer Modified Bitumen-Properties and Characterization." *Woodhead Publishing Limited, Oxford*, 238-263.
119. Elseifi, M. A., Flintsch, G. W., and Al-Qadi, I. L. (2003). "Quantitative Effect of Elastomeric Modification on Binder Performance at Intermediate and High Temperatures." *Journal of Materials in Civil Engineering, ASCE, 15(1)*, 32-40.
120. Zhu, J., Birgisson, B., and Kringos, N. (2014). "Polymer Modification of Bitumen: Advances and Challenges." *European Polymer Journal, 54*, 18-38.
121. Airey, G. D. (2003). "Rheological Properties of Styrene Butadiene Styrene Polymer Modified Road Bitumens". *Fuel, 82*, 1709-1719.
122. Read, J.; and Whiteoak, D. (2003). "The Shell Bitumen Handbook". Fifth Edition, *Thomas Telford Publishing, Heron Quay, London*.
123. Airey, G. D. (2004). "Fundamental Binder and Practical Mixture Evaluation of Polymer Modified Bituminous Materials." *International Journal of Pavement Engineering, 5(3)*, 137-151.
124. Yildirim, Y. (2007). "Polymer Modified Asphalt Binders." *Construction and Building Materials, 21*, 66–72.
125. Kumar, P., Mehndiratta, H. C., and Singh, K. L. (2010). "Comparative study of rheological behavior of modified binders for high-temperature areas." *Journal of Materials in Civil Engineering, ASCE, 22(10)*, 978–984.
126. Xiao, F., Amirkhanian, S., Wang, H., and Hao, P. (2014). "Rheological Property Investigations for Polymer and Polyphosphoric Acid Modified Asphalt Binders at High Temperatures." *Construction and Building Materials, 64*, 316-323.
127. Rahi, M., Fini, E. H., Hajikarimi, P., and Nejad, F. M. (2014). "Rutting Characteristics of Styrene-Ethylene/Propylene-Styrene Polymer Modified Asphalt." *Journal of Materials in Civil Engineering, ASCE, 27(4)*, 04014154.

128. Hansen, K. R., and Copeland, A. (2013). "Annual Asphalt Pavement Industry Survey on Recycled Material and Warm-Mix Asphalt Usage: 2009–2012." *No. IS-138*, National Asphalt Pavement Association, 5100 Forbes Blvd., Lanham, MD 20706.
129. Daniel, J., Pochily, J., and Boisvert, D. (2010). "Can More Reclaimed Asphalt Pavement Be Added? Study of Extracted Binder Properties from Plant-Produced Mixes with up to 25% Reclaimed Asphalt Pavement." *Transportation Research Record: Journal of the Transportation Research Board*, 2180, 19-29.
130. Kim, S., Sholar, G. A., Byron, T., and Kim, J. (2009). "Performance of Polymer-Modified Asphalt Mix with Reclaimed Asphalt Pavement." *Transportation Research Record: Journal of the Transportation Research Board*, 2126(1), 109-114.
131. Colbert, B., and You, Z. (2012). "The Properties of Asphalt Binder Blended with Variable Quantities of Recycled Asphalt Using Short Term and Long Term Aging Simulations." *Construction and Building Materials*, 26(1), 552-557.
132. Bernier, A., Zofka, A., and Yut, I. (2012). "Laboratory Evaluation of Rutting Susceptibility of Polymer-Modified Asphalt Mixtures Containing Recycled Pavements." *Construction and Building Materials*, 31, 58-66.
133. Hossain, Z., Buddhalla, A., O'Rear, A. O., Zaman, M., Laguros, J. L., and Lewis, S. (October 1-3, 2012). "Recycled Asphalt Pavement in new Asphalt Mixes: State of the Practice." In *2nd International symposium on Asphalt Pavement and Environment*, Fortaleza, Brazil.
134. Boriack, P., Katicha, S., and Flintsch, G. (2014). "Laboratory Study on Effects of High Reclaimed Asphalt Pavement and Binder Content: Stiffness, Fatigue Resistance, and Rutting Resistance." *Transportation Research Record: Journal of the Transportation Research Board*, 2445, 64-74.
135. Ghabchi, R., Barman, M., Singh, D., Zaman, M., & Mubarak, M. A. (2016). "Comparison of Laboratory Performance of Asphalt Mixes Containing Different Proportions of RAS and RAP." *Construction and Building Materials*, 124, 343-351.

136. Oklahoma Department of Transportation (ODOT), (2013). "Oklahoma Department of Transportation Special Provision for Reclaimed Asphalt Pavement and Shingles." *SP No. 708-21*, Oklahoma Department of Transportation, http://www.odot.org/c_manuals/specprov2009/oe_sp_2009-708-21.pdf.
137. West, R., Kvasnak, A., Tran, N., Powell, B., and Turner, P. (2009). "Testing of Moderate and High Reclaimed Asphalt Pavement Content Mixes: Laboratory and Accelerated Field Performance Testing at The National Center for Asphalt Technology Test Track." *Transportation Research Record: Journal of the Transportation Research Board*, 2126, 100-108.
138. Hong, F., Chen, D. H., and Mikhail, M. (2010). "Long-term Performance Evaluation of Recycled Asphalt Pavement Results from Texas: Pavement Studies Category 5 Sections from the Long-Term Pavement Performance Program." *Transportation Research Record: Journal of the Transportation Research Board*, 2180, 58-66.
139. Ghabchi, R., Singh, D., & Zaman, M. (2014). "Evaluation of Moisture Susceptibility of Asphalt Mixes Containing RAP and Different Types of Aggregates and Asphalt Binders Using the Surface Free Energy Method." *Construction and Building Materials*, 73, 479-489.
140. Sabouri, M., Bennert, T., Daniel, J. S., and Kim, Y. R. (2015). "Fatigue and Rutting Evaluation of Laboratory-Produced Asphalt Mixtures Containing Reclaimed Asphalt Pavement." *Transportation Research Record: Journal of the Transportation Research Board*, 2506, 32-44.
141. Choi, Y. T., and Kim, Y. R. (2013). "Development of Calibration Testing Protocol for Permanent Deformation Model of Asphalt Concrete." *Transportation Research Record: Journal of the Transportation Research Board*, 2373, 34-43.
142. McGennis, R. B., Shuler, S., and Bahia, H. U. (1994). "Background of Superpave Asphalt Binder Test Methods." *Office of Technology Applications, Federal Highway Administration*.

143. Delgadillo, R., Cho, D. W., and Bahia, H. (2006). "Part 1: Bituminous Materials: Nonlinearity of Repeated Creep and Recovery Binder Test and Relationship with Mix Permanent Deformation." *Transportation Research Record: Journal of the Transportation Research Board*, 1962(1), 3-11.
144. Anderson, D. A., Christensen, D. W., Bahia, H. U., Dongre, R., Sharma, M. G., Antle, C. E., and Button, J. (1994). "Binder Characterization and Evaluation. Volume 3: Physical Characterization." *Strategic Highway Research Program, National Research Council*, Washington, DC.
145. Bahia, H. U., and Anderson, D. A. (1995). "Strategic Highway Research Program Binder Rheological Parameters: Background and Comparison with Conventional Properties." *Transportation research record; Journal of Transportation Research Board*, 1488, 32-39.
146. AASHTO T 315 (2012). "Standard Method of Test for Determining the Rheological Properties of Asphalt Binder Using a Dynamic Shear Rheometer (DSR)." *American Association of State Highway and Transportation Officials*, Washington, D.C.
147. Bahia, H. U., Zhai, H., Zeng, M., Hu, Y., and Turner, P. (2001). "Development of Binder Specification Parameters Based on Characterization of Damage Behavior." *Journal of the Association of Asphalt Paving Technologists*, 70, 442-470.
148. AASHTO T 301 (2013). "Standard Method of Test for Elastic Recovery Test of Asphalt Materials by Means of a Ductilometer." *American Association of State Highway and Transportation Officials*, Washington, D.C.
149. ASTM D 5801 (2012). "Standard Test Method for Toughness and Tenacity of Bituminous Materials." *ASTM International*, West Conshohocken, PA, www.astm.org.
150. AASHTO T 300 (2011). "Standard Method of Test for Force Ductility Test of Asphalt Materials." *American Association of State Highway and Transportation Officials*, Washington, D.C.
151. Kamel, N. I., Bahai, H. U., and Cho, D. W. (2004). "Critical Laboratory Evaluation of Asphalt Binders Modified by Refining Processes." In

- Proceedings of the Forty-Ninth Annual Conference of the Canadian Technical Asphalt Association (CTAA)-Montreal, Quebec, 57-76.*
152. Shenoy, A. (2001). "Refinement of The Superpave Specification Parameter for Performance Grading of Asphalt." *Journal of Transportation Engineering*, 127(5), 357-362.
 153. Dongré, R., and D'Angelo, J. (2003). "Refinement of Superpave High-Temperature Binder Specification Based on Pavement Performance in the Accelerated Loading Facility." *Transportation Research Record: Journal of the Transportation Research Board*, 1829, 39-46.
 154. Carreau, P. J., MacDonald, I. F., and Bird, R. B. (1968). "A Nonlinear Viscoelastic Model for Polymer Solutions and Melts—II." *Chemical Engineering Science*, 23(8), 901-911.
 155. Dongré, R., D'Angelo, J. and Reinke, G. (2004). "New Criterion for Superpave High-Temperature Binder Specification." *Transportation Research Record: Journal of the Transportation Research Board*, 1875, 22-32.
 156. Diefenderfer, S. (2006). "Detection of Polymer Modifiers in Asphalt Binder". *VTRC 06-R18*, Virginia Department of Transportation, 1401 East Broad Street, Richmond, VA 23219, USA.
 157. Zoorob, S. E., Castro-Gomes, J. P., Oliveira, L. P., and O'Connell, J. (2012). "Investigating the Multiple Stress Creep Recovery Bitumen Characterization Test." *Construction and Building Materials*, 30, 734-745.
 158. Domingos, M. D. I., and Faxina, A. L. (2015). "Susceptibility of asphalt binders to rutting: literature review." *Journal of Materials in Civil Engineering, ASCE*, 28(2), 04015134.
 159. Bahia, H. U., Hanson, D. I., Zeng, M., Zhai, H., Khatri, M. A., and Anderson, M. R. (2000). "A Project NCHRP 9-10 Superpave Protocols for Modified Asphalt Binders." Draft Topical Report (Task 9), Prepared for *National Cooperative Highway Research Program*, Transportation Research Board, National Research Council, Washington, D.C.
 160. D'Angelo, J., Dongre, R., and Reinke, G. (2006). "Evaluation of Repeated Creep and Recovery Test Method as an Alternative to SHRP+ Requirements

- for Polymer Modified Asphalt Binders.” In *Fifty-First Annual Conference of the Canadian Technical Asphalt Association (CTAA)*, Charlottetown Prince Edward Island, Canada.
161. D’Angelo, J. (2010). “New High-Temperature Binder Specification Using Multistress Creep and Recovery.” *Development in Asphalt, Transportation Research Circular, E-C147*, Transportation Research Board, Washington, DC, 1-13.
 162. Reinke, G. (2010). “Use of Hamburg Rut Testing Data to Validate the Use of J_{nr} as A Performance Parameter for High-Temperature Permanent Deformation.” *Development in Asphalt, Transportation Research Circular, E-C147*, Transportation Research Board, Washington, DC, 14-24.
 163. D’Angelo, J. and Dongr’e, R. (2009). “Practical Use of Multiple Stress Creep and Recovery Test Characterization of Styrene-Butadiene-Styrene Dispersion and Other Additives in Polymer-Modified Asphalt Binders.” *Transportation Research Board: Journal of the Transportation Research Board, 2126*, 73-82.
 164. AASHTO TP 70 (2013). “Standard Method of Test for Multiple Stress Creep Recovery (MSCR) Test of Asphalt Binder Using a Dynamic Shear Rheometer (DSR)”. *American Association of State Highway and Transportation Officials*, Washington, D.C.
 165. Tabatabaee, N., and Tabatabaee, H. A. (2010). “Multiple Stress Creep and Recovery and Time Sweep Fatigue Tests.” *Transportation Research Record: Journal of the Transportation Research Board, 2180(1)*, 67-74.
 166. Adorjányi, K., and Füleki, P. (2011). “Performance Evaluation of Bitumens at High Temperature with Multiple Stress Creep Recovery Test.” *Hungarian Journal of Industry and Chemistry, 39(2)*, 195-199.
 167. Wasage, T. L. J., Stastna, J., and Zanzotto, L. (2011). “Rheological analysis of multi-stress creep recovery (MSCR) test.” *International Journal of Pavement Engineering, 12(6)*, 561-568.
 168. Shirodkar, P., Mehta, Y., Nolan, A., Dahm, K., Dusseau, R. and McCarthy, L. (2012). “Characterization of Creep and Recovery Curve of Polymer Modified Binder.” *Construction and Building Materials, 34*, 504-511.

169. Mehta, Y., Nolan, A., DuBois, E., Zorn, S., Batten, E., and Shirodkar, P. (2013). "Correlation between Multiple Stress Creep Recovery (MSCR) Results and Polymer Modification of Binder." *FHWA-NJ-2014-002*, New Jersey Department of Transportation, Bureau of Research.
170. DuBois, E., Mehta, Y., and Nolan, A. (2014). "Correlation Between Multiple Stress Creep Recovery (MSCR) Results and Polymer Modification of Binder." *Construction and Building Materials*, 65, 184-190.
171. Mohseni, A., and Azari, H. (2014). "High-temperature Characterization of Highly Modified Asphalt Binders and Mixtures." *Transportation Research Record: Journal of the Transportation Research Board*, 2444(1), 38-51.
172. Domingos, M. D. I., and Faxina, A. L. (2014). "Creep-Recovery Behavior of Asphalt Binders Modified with SBS and PPA." *Journal of Materials in Civil Engineering, ASCE*, 26(4), 781-783.
173. Zhang, J., Walubita, L. F., Faruk, A. N., Karki, P., and Simate, G. S. (2015). "Use of the MSCR Test to Characterize the Asphalt Binder Properties Relative to HMA Rutting Performance—A Laboratory Study." *Construction and Building Materials*, 94, 218-227.
174. Hossain, Z., Ghosh, D., Zaman, M., and Hobson, K. (2015). "Use of the Multiple Stress Creep Recovery (MSCR) Test Method to Characterize Polymer-Modified Asphalt Binders," *Journal of Testing and Evaluation, ASTM*, DOI:10.1520/JTE20140061. ISSN 0090-3973.
175. Stevens, R., Stempihar, J., and Underwood, B. S. (2015). "Evaluation of Multiple Stress Creep and Recovery (MSCR) Data for Arizona." *International Journal of Pavement Research and Technology*, 8(5), 337.
176. AASHTO T 350 (2014). "Standard Specification for Performance-Graded Asphalt Binder Using Multiple Stress Creep Recovery (MSCR) Test." *American Association of State Highway and Transportation Officials*, Washington, D.C.
177. AASHTO M 332 (2014). "Standard Specification for Performance-Graded Asphalt Binder Using Multiple Stress Creep Recovery (MSCR) Test."

- American Association of State Highway and Transportation Officials*, Washington, D.C.
178. AASHTO M 320 (2010). "Standard Specification for Performance-Graded Asphalt Binder." *American Association of State Highway and Transportation Officials*, Washington, D.C.
 179. Yang, X., and You, Z. (2015). "High Temperature Performance Evaluation of Bio-Oil Modified Asphalt Binders Using the DSR and MSCR Tests." *Construction and Building Materials*, 76, 380-387.
 180. Jafari, M., Babazadeh, A., and Aflaki, S. (2015). "Effects of Stress Levels on Creep and Recovery Behavior of Modified Asphalt Binders with the Same Continuous Performance Grades." *Transportation Research Record: Journal of the Transportation Research Board*, 2505, 15-23.
 181. Laukkanen, O. V., Soenen, H., Pellinen, T., Heyrman, S., and Lemoine, G. (2015). "Creep-recovery behavior of bituminous binders and its relation to asphalt mixture rutting." *Materials and Structures*, 48(12), 4039-4053.
 182. Saboo, N., and Kumar, P. (2016). "Analysis of Different Test Methods for Quantifying Rutting Susceptibility of Asphalt Binders." *Journal of Materials in Civil Engineering*, ASCE, 04016024.
 183. Anderson, R. M. (2011). "Understanding the MSCR Test and its Use in the PG Asphalt Binder Specification." In *Webinar, Asphalt Institute (AI)*, Lexington, KY.
 184. AASHTO MP 19 (2010). "Standard Specification for Performance-Graded Asphalt Binder Using Multiple Stress Creep Recovery (MSCR) Test." *American Association of State Highway and Transportation Officials*, Washington, D.C.
 185. Asphalt Institute Guidance Document (2010). "Implementation of the Multiple-Stress Creep-Recovery (MSCR) Test and Specification." *Asphalt Institute*, Lexington, KY, www.asphaltinstitute.org.
 186. Anderson, M. (2012(a)). "Evaluation of J_{nr} Criterion for Unmodified Asphalt Binders." In *Asphalt Binder Expert Task Group Meeting*, Minneapolis, MN.

187. Anderson, M. (2014). "Introduction to the Multiple-Stress Creep-Recovery (MSCR) Test and its Use in the PG Binder Specification." In *54th Annual Idaho Asphalt Conference*, Moscow, Idaho.
188. Anderson, M. (2015). "Implementation of the MSCR Test and Specification: Questions, Clarifications, and Emphasis." In *Asphalt Binder ETG Meeting*, Oklahoma City, Ok.
189. Gierhart, D. (2011). "Simple Talking Points for Sharing Why Your State Should Be Implementing MSCR." In *Southeastern Asphalt User-Producer Group (SEAUPG) Web Meeting, Asphalt Institute (AI)*, Lexington, KY.
190. Anderson, m. (2012(b)). "SEAUPG Evaluation of MSCR Recovery as a replacement for PG Plus Tests." In *Webinar, Asphalt Institute*, Lexington, KY.
191. Horan, B. (2012). "Multiple Stress Creep Recovery (MSCR) Task Force Overview and Recommendations." In *Southeastern Asphalt User-Producer Group Meeting, Asphalt Institute*, Lexington, KY.
192. Zipf, K. (2014). "Grading Asphalt Binders with the Multiple Stress Creep Recovery Test AASHTO TP-70 and MP-19." *Delaware Department of Transportation (DelDOT)*, Dover, DE.
193. Corun, R. (2015). "Multiple Stress Creep Recovery Test for Asphalt Binders." *PAPA Regional Technical Workshop*, Breinigsville, PA.
194. Anderson, M., R. (2013). "Northeast Asphalt User-Producer Group Second Inter Laboratory Study to Determine the Precision of ador70 – the Multiple Stress Creep-Recovery (MSCR) Test." *Asphalt Institute*, Lexington, KY.
195. Anderson, M., R. (2012(c)). "Southeast Asphalt User-Producer Group Inter Laboratory Study to Determine the Precision of AASHTO TP70 – the Multiple Stress Creep-Recovery (MSCR) Test." *Asphalt Institute*, Lexington, KY.
196. Asphalt Institute (2016). "State MSCR Implementation Status." *Asphalt Institute*, Lexington, KY, www.asphaltinstitute.org .
197. Miller, T., Ksaibati, K., and Farrar, M. (1995). "Using Georgia Loaded-Wheel Tester to Predict Rutting." *Transportation Research Record: Journal of the Transportation Research Board*, 1473, 17-24.

198. Choubane, B., Page, G., and Musselman, J. (2000). "Suitability of Asphalt Pavement Analyzer for Predicting Pavement Rutting." *Transportation Research Record: Journal of the Transportation Research Board*, 1723, 107-115.
199. Cooley, L. A., Kandhal, P. S., Buchanan, M. S., Fee, F., and Epps, A. (2000). "Loaded Wheel Testers in The United States: State of The Practice." *Transportation Research Circular, E-C016*, Transportation Research Board, Washington, DC.
200. Corte, J. F. (2001). "Development and Uses of Hard-grade Asphalt and of High-Modulus Asphalt Mixes in France." *Transportation Research Circular, 503*, Transportation Research Board, Washington, DC, 12-31.
201. Kandhal, P. S., and Cooley, L. A. (2002). "Evaluation of Permanent Deformation of Asphalt Mixtures Using Loaded Wheel Tester." *Asphalt Paving Technology*, 71, 739-753.
202. Lu, Q., and Harvey, J. (2006). "Evaluation of Hamburg wheel-tracking Device Test with Laboratory and Field Performance Data." *Transportation Research Record: Journal of the Transportation Research Board*, 1970, 25-44.
203. Grebenshikov, S., and Prozzi, J. (2011). "Enhancing Mechanistic-Empirical Pavement Design Guide Rutting-Performance Predictions with Hamburg Wheel-Tracking Results." *Transportation Research Record: Journal of the Transportation Research Board*, 2226, 111-118.
204. Walubita, L., Zhang, J., Das, G., Hu, X., Mushota, C., Alvarez, A., and Scullion, T. (2012). "Hot-mix Asphalt Permanent Deformation Evaluated by Hamburg Wheel Tracking, Dynamic Modulus, and Repeated Load Tests." *Transportation Research Record: Journal of the Transportation Research Board*, 2296, 46-56.
205. Howard, I. L., and Doyle, J. D. (2013). "Rutting and Moisture Damage Wheel Tracking Comparison of Laboratory and Field Compacted Asphalt Concrete." In *Green Streets, Highways, and Development 2013@ sAdvancing the Practice*, ASCE, 106-116.

206. Sel, I., Yildirim, Y., and Ozhan, H. B. (2014). "Effect of Test Temperature on Hamburg Wheel-Tracking Device Testing." *Journal of Materials in Civil Engineering, ASCE*, 26(8), 04014037.
207. Brown, E. R., Kandhal, P. S., Roberts, F. L., Kim, Y. R., Lee, D. Y., and Kennedy, T. W. (2009). "Hot Mix Asphalt Materials, Mixture Design, and Construction." *NAPA Research and Education Foundation*, Lanham.
208. AASHTO T 319 (2015). "Standard Method of Test for Quantitative Extraction and Recovery of Binder from Asphalt Mixtures." *American Association of State Highway and Transportation Officials*, Washington, D.C.
209. AASHTO T 240 (2013). "Standard Method of Test for Effect of Heat and Air on a Moving Film of Asphalt (Rolling Thin-Film Oven Test)." *American Association of State Highway and Transportation Officials*, Washington, D.C.
210. AASHTO R 28 (2012). "Standard Practice for Accelerated Aging of Asphalt Binder Using a Pressurized Aging Vessel (PAV)." *American Association of State Highway and Transportation Officials*, Washington, D.C.
211. AASHTO T 316 (2013). "Standard Method of Test for Viscosity Determination of Asphalt Binder Using Rotational Viscometer." *American Association of State Highway and Transportation Officials*, Washington, D.C.
212. AASHTO T 313 (2013). "Standard Method of Test for Determining the Flexural Creep Stiffness of Asphalt Binder Using the Bending Beam Rheometer (BBR)." *American Association of State Highway and Transportation Officials*, Washington, D.C.
213. AASHTO T 269 (2014). "Standard Method of Test for Percent Air Voids in Compacted Dense and Open Asphalt Mixtures." *American Association of State Highway and Transportation Officials*, Washington, D.C.
214. Pavement Interactive. "Laboratory Wheel Tracking Devices." Website: <http://www.pavementinteractive.org/article/laboratory-wheel-tracking-devices/>
215. Hossain, Z., Zaman, M., Solanki, P., Ghabchi, S., Singh, D. V., David, A., and Lewis, S. (2013). "Implementation of MEPDG for Asphalt Pavement with RAP Final Report." *OTCREOS10.1-45-F*, Oklahoma Transportation Center, Midwest City, Oklahoma.

216. D'Angelo, J., R. Kluttz, R., Dongre, K. Stephens and L. Zanzotto. (2007). "Revision of the Superpave High Temperature Binder Specification: The Multiple Stress Creep Recovery Test." *Asphalt Paving Technology*, 76, 123.
217. AASHTO T 312 (2015). "Standard Method of Test for Preparing and Determining the Density of Asphalt Mixture Specimens by Means of the Superpave Gyratory Compactor." *American Association of State Highway and Transportation Officials*, Washington, D.C.
218. Oklahoma Department of Transportation (ODOT), (2012). "Oklahoma Department of Transportation Special Provision for Plant Mix Bituminous Bases and Surfaces (Superpave)." *SP No. 708-26*, Oklahoma Department of Transportation, http://www.odot.org/c_manuals/specprov2009/oe_sp_2009-708-26.pdf.
219. AASHTO T 324 (2014). "Standard Method of Test for Hamburg Wheel-Track Testing of Compacted Hot Mix Asphalt (HMA)." *American Association of State Highway and Transportation Officials*, Washington, D.C.

PART THREE REFERENCES

220. Gogoi, R., Biligiri, K. P, Das N. C. (2015). "Performance prediction analyses of styrene-butadiene rubber and crumb rubber materials in asphalt road applications". *Materials and Structures*, Vol. 49, No. 9, pp. 3479–3493.
221. Anderson, M. (2003) "Force Ductility Testing of Asphalt Binders." *Asphalt Magazine of the Asphalt Institute*, Vol. 18, No. 2.
222. Shuler, T. S., Adams, C. K., Lamborn M. (1985). "Asphalt-Rubber Binder Laboratory Performance." Texas State Department of Highways and Public Transportation (SDHPT) Research Report 347-1F, Texas Transportation Institute, College Station, Texas.
223. Shuler, T. S., Collins, J. P., Kirkpatrick, J. H. (1987). "Polymer-Modified Asphalt Properties Related to Asphalt Concrete Performance." *Asphalt Rheology: Relationship to Mixture ASTM STP 941*, pp. 179-193.
224. King, G., H., King, R. D., Pavlovich, A. L. Epps, Prithvi, K. (1998). "Additives in Asphalt." 75th Anniversary Historical Review of the Association of Asphalt Paving Technologists.
225. Glover, C. J., Davison, R. R., Domke, C. H., Ruan, Juristyarini, Y. Y., Knorr, P. D., Jung., S. H. (2005). "Development of a New Method for Assessing Asphalt Binder Durability with Field Validation." Texas Transportation Report No. 0-1872-2.
226. D'Angelo, J. (2005). "Development of Standard Practice for Superpave Plus Specifications." North-East Asphalt User/Producer Group (NEAUPG) Conference, Burlington, VT.
227. Airey, G. D. (2004). "Fundamental Binder and Practical Mixture Evaluation of Polymer Modified Bituminous Materials." *International Journal of Pavement Engineering*, Vol. 5(3), pp. 137-151.
228. Takamura, K. (2005). "Pavement Preservation Using the SBR Latex Modified Asphalt Emulsion. BASF Corporation". International Latex Conference, Charlotte, NC.

229. Tabatabaee, H., Clopotel, C. A., Arshadi, Bahia, H. (2013). "Critical Problems with Using the Asphalt Ductility Test as a Performance Index for Modified Binders." *Transportation Research Record: Journal of the Transportation Research Board*, Vol. 2370, pp. 84–91.
230. Nazimuddin, W., Ashani, S. S., Islam, R. M. (2014). "Evaluation of Dynamic Shear Rheometer Test for Emulsions." Publication LTRC Project No. 11-2B. Louisiana Department of Transportation.
231. Sentmant, M. L. (2004). "Miniature universal platform: from extensional melt rheology to solid state deformation behavior." *Journal of Rheologica Acta*, Vol. 43, No. 6, pp. 657-669.
232. Wasage, T. L., Stastna, J., Zanzotto, L. (2011). "Rheological analysis of multi-stress creep recovery (MSCR) test." *International Journal of Pavement Engineering*, Vol. 12, No. 6, pp. 561–568.
233. Bahia, H., Hanson, D. I., Zeng, M. H., Zahi, M. A., Anderson, R. M. (2001). "NCHRP Report 459: *Characterization of Modified Asphalt Binders in Superpave Mix Design*." Transportation Research Board, Washington D. C. http://onlinepubs.trb.org/onlinepubs/nchrp/nchrp_rpt_459-a.pdf.
234. Newsprints. *Chemical & Engineering News*, Vol. 63, No. 23, 1985, p. 80.
235. Laun, H. M., Schuh, H. (1989). "Transient Elongational Viscosities and Drawability of Polymer Melts." *Journal of Rheology*, Vol. 33, No. 1, pp. 119–175.
236. Sentmanat, M., Wang, B. N., Mckinley, G. H. (2005). "Measuring the transient extensional rheology of polyethylene melts using the SER universal testing platform." *Journal of Rheology*, Vol. 49, No. 3, pp. 585–606.
237. Navarro, F. J., Partal, P., M-Boza, F., Gallegos, C. (2005). "Influence of crumb rubber concentration on the rheological behavior of a crumb rubber modified bitumen." *Energy Fuels*. Vol. 19, pp. 1984–1990.
238. Al-Abdul-Wahhab, H., Al-Amri, G. (1991). "Laboratory evaluation of reclaimed rubber asphaltic concrete mixes." *JMater Civil Eng*. Vol. 3(3), pp. 189–203.

239. Albayati, A. H., Mohammed, H. K. (2011). "Influence of styrene butadiene rubber on the mechanical properties of asphalt concrete mixtures." *Al-Qadisiya J Eng Sci*. Vol. 4(3), pp. 258–274.
240. Khadivar, A., Kavussi, A. (2013). "Rheological characteristics of SBR and NR polymer modified bitumen emulsions at average pavement temperatures." *Constr Build Mater*. Vol. 47, pp. 1099–1105.
241. Tamimi, A. A., Zubaidy, I. A. H. A., Upadhye, A., Ali, L. (2014). Evaluation of sustainable asphalt mixture. *Study Civil Eng Archit*. Vol. 3, pp. 41–47.
242. Chen, J. C., Lio, M. C., Shian, M. S. (2002). "Asphalt Modified by Styrene-Butadiene-Styrene Triblock Copolymer: Morphology and Model." *Journal of Materials in Civil Engineering*, Vol. 14, No. 2, pp. 224-229.
243. Read, J., Whiteoak, D. "The Shell Bitumen handbook." Thomas Telford, 2003.

APPENDIX

This study recommended F_2/F_1 and F_2 as the new developed extensional test parameters, but the true material properties can also be obtained from the stress vs. strain curve and the modulus curve. The following paragraphs discuss on the stress-strain curves and elaborate why the final recommendations are still based on F_2/F_1 and F_2 .

Figure A-1, A-2, and A-3 show the elongation force vs. step time, the true stress vs. Hencky strain, and the engineering stress vs. Hencky strain, respectively. It can be observed from Figure A-2 that, for the first part of the curve the true stress was relatively low comparing with the second part. That is because at the start of the test the initial area was 6.5 mm^2 , but with the stretching of the sample the area decreases therefore, the stress increases until it reaches the second peak in which the force starts dropping, subsequently, the stress drops.

For Figure A-3, the engineering stress has a similar trend of the elongation force, that is because the area is constant so, the only inconstant in the stress equation is the elongation force.

Figure A-4 and Figure A-5 show the elastic modulus, based on the true stress, vs. step time and the elastic modulus, based on engineering stress, vs. stress time, respectively. From Figure A-4, it can be observed very clearly that the PG 76-22 has two distinct elastic moduli. The first elastic modulus at the first part of the curve is related to the asphalt binder which is equal to 2.9 MPa. As for the elastic modulus obtained at the second part of the curve is related to the polymer, which is equal to 4.3 MPa.

It can also be observed from Figures 1 and 4 that, the elongation force curve has the same trend of the elastic modulus curve, but there is an insignificant time differences for the peak points as follow: for the elongation force, the step time of the first peak is 4.6 s, as for the modulus, the step time of the first peak is 2.4 s, with time difference of 2.2 s. As for the second part of the curve, the elongation force second peak step time is 25.9

s, but the elastic modulus second peak step time is 26.9 s with time difference of 1 second. That is because the area calculation is theoretical so, insignificant variation expected.

So, the elongation force curve (Figure A-1) and the modulus curve (based on true stress and Hencky strain in Figure A-5) exhibit very similar material trends with a first peak and an increased second peak. This study recommends F_2/F_1 and F_2 parameters for the newly developed test because forces are actual in this case whereas, for modulus curve, stresses are derived from theoretically calculated area. Figures A-1 to A-5 and Table A-1 were prepared from one sample of the selected geometry.

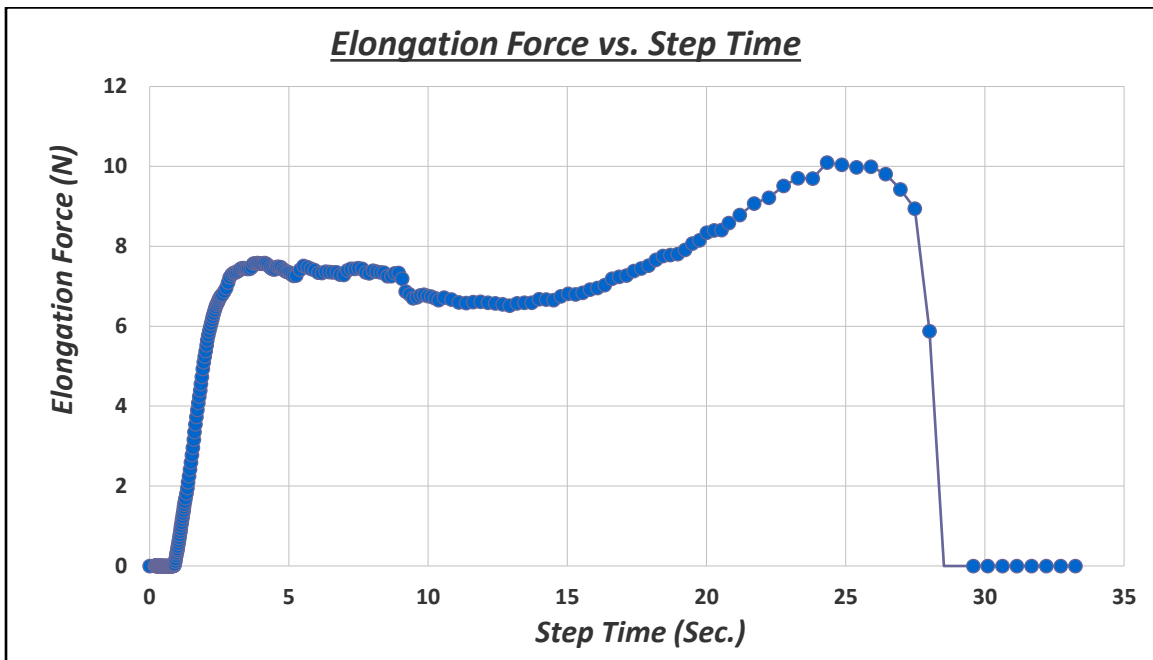


Figure A-1. Elongation Force vs. Step Time for PG 76-22 geometry of 9 mm x 0.72 mm at 4°C.

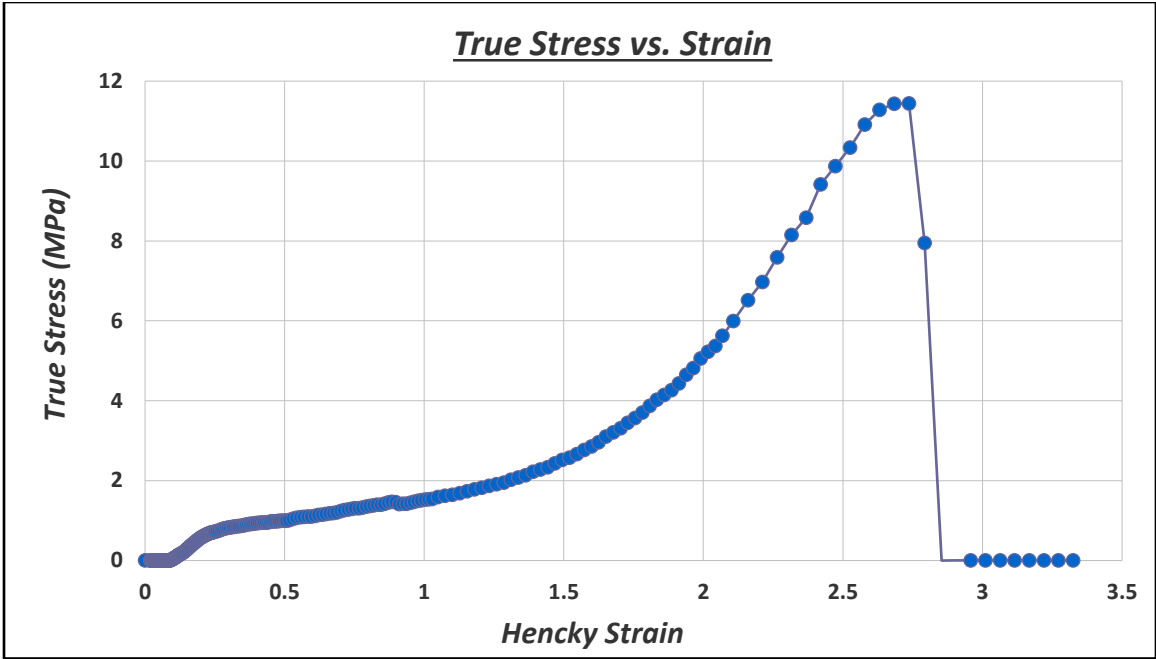


Figure A-2. True Stress vs. Hencky Strain for PG 76-22 geometry of 9 mm x 0.72 mm at 4°C.

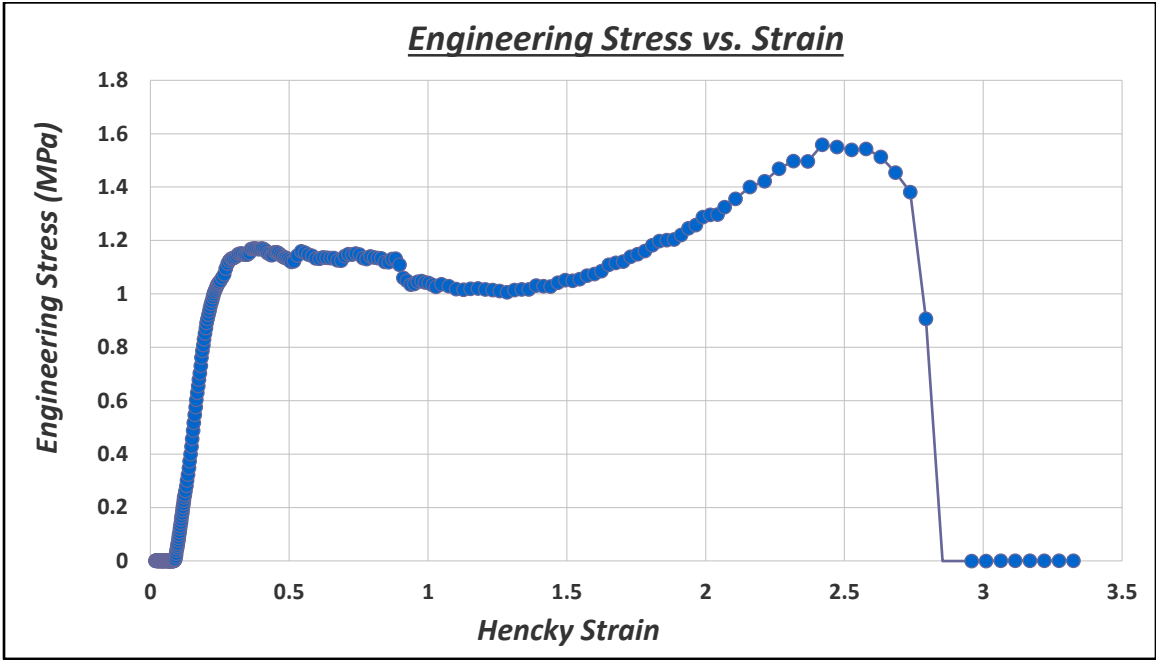


Figure A-3. Engineering Stress vs. Hencky Strain for PG 76-22 geometry of 9 mm x 0.72 mm at 4°C.

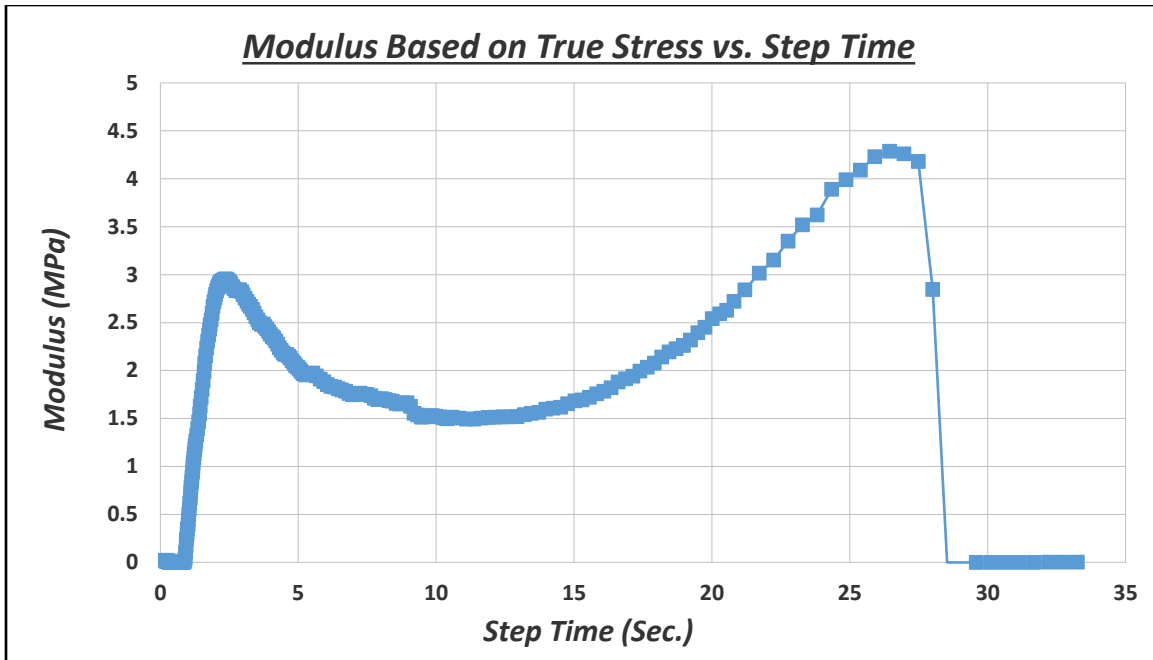


Figure A-4. Elastic Modulus based on true stress vs. Step Time for PG 76-22 geometry of 9 mm x 0.72 mm at 4°C.

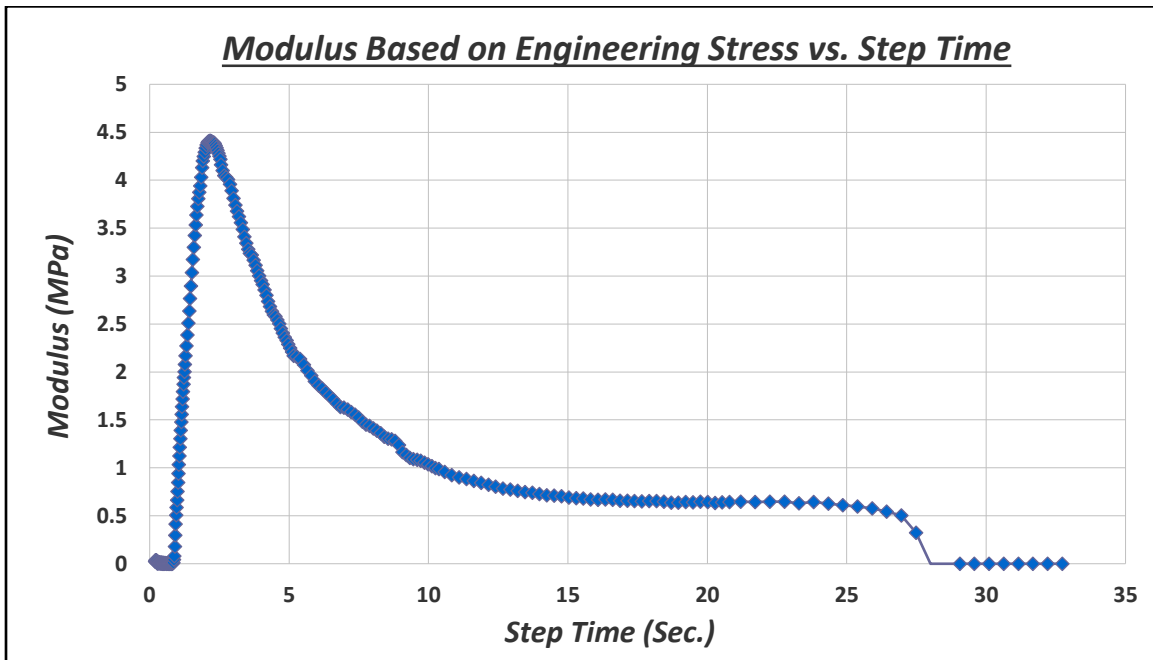


Figure A-5. Elastic Modulus based on Engineering Stress vs. Step Time for PG 76-22 geometry of 9 mm x 0.72 mm at 4°C.

Table A-1. Typical test results extracted from a SER

Number of result	Step time	Temperature	Hencky strain	Hencky rate	Stress	Elongation viscosity	Velocity	Displacement	Elongation Force
	s	°C		1/s	Pa	Pa.s	rad/s	rad	N
1.	0.000	3.967	0.0000	0.0003	0.00E+00	0.0E+00	0.0003	-18.276	0.000
2.	0.001	3.967	0.0000	0.0003	1.22E+03	4.0E+06	0.0004	-18.276	0.016
3.	0.002	3.967	0.0000	0.0080	8.66E+03	1.1E+06	0.0099	-18.276	0.116
4.	0.003	3.967	0.0001	0.0366	1.04E+04	2.9E+05	0.0452	-18.276	0.140
5.	0.004	3.967	0.0001	0.0687	6.15E+03	8.9E+04	0.0847	-18.276	0.082
6.	0.005	3.967	0.0002	0.0875	2.06E+03	2.4E+04	0.1079	-18.276	0.028
7.	0.006	3.967	0.0003	0.0937	2.81E+02	3.0E+03	0.1155	-18.275	0.004
8.	0.007	3.967	0.0004	0.0943	7.47E+01	7.9E+02	0.1163	-18.275	0.001
9.	0.008	3.967	0.0005	0.0938	4.22E+02	4.5E+03	0.1157	-18.275	0.006
10.	0.009	3.967	0.0006	0.0943	6.92E+02	7.3E+03	0.1163	-18.275	0.009
11.	0.010	3.967	0.0007	0.0959	6.70E+02	7.0E+03	0.1182	-18.275	0.009
12.	0.011	3.967	0.0008	0.0972	4.98E+02	5.1E+03	0.1199	-18.275	0.007
13.	0.012	3.967	0.0009	0.0978	4.52E+02	4.6E+03	0.1206	-18.275	0.006
14.	0.013	3.967	0.0010	0.0985	4.23E+02	4.3E+03	0.1215	-18.275	0.006
15.	0.014	3.967	0.0011	0.0992	3.08E+02	3.1E+03	0.1224	-18.274	0.004
16.	0.015	3.967	0.0012	0.0994	2.75E+02	2.8E+03	0.1225	-18.274	0.004
17.	0.016	3.967	0.0013	0.0993	3.09E+02	3.1E+03	0.1225	-18.274	0.004
18.	0.017	3.967	0.0014	0.0991	3.85E+02	3.9E+03	0.1222	-18.274	0.005
19.	0.018	3.967	0.0015	0.0991	4.71E+02	4.8E+03	0.1221	-18.274	0.006
20.	0.019	3.967	0.0016	0.0994	4.68E+02	4.7E+03	0.1226	-18.274	0.006
21.	0.020	3.967	0.0017	0.0999	3.90E+02	3.9E+03	0.1231	-18.274	0.005
22.	0.021	3.967	0.0018	0.1002	3.03E+02	3.0E+03	0.1236	-18.274	0.004
23.	0.022	3.967	0.0019	0.1003	2.34E+02	2.3E+03	0.1237	-18.273	0.003
24.	0.023	3.967	0.0021	0.1003	2.24E+02	2.2E+03	0.1236	-18.273	0.003
25.	0.024	3.967	0.0022	0.1000	2.47E+02	2.5E+03	0.1234	-18.273	0.003
26.	0.025	3.967	0.0023	0.0999	3.11E+02	3.1E+03	0.1232	-18.273	0.004
27.	0.026	3.967	0.0024	0.1005	2.20E+02	2.2E+03	0.1239	-18.273	0.003
28.	0.027	3.967	0.0025	0.1012	-1.13E+00	-1.1E+01	0.1248	-18.273	0.000
29.	0.028	3.967	0.0026	0.1012	-1.24E+02	-1.2E+03	0.1247	-18.273	-0.002
30.	0.029	3.967	0.0027	0.1005	-6.75E+01	-6.7E+02	0.1239	-18.273	-0.001
31.	0.030	3.967	0.0028	0.0997	1.12E+02	1.1E+03	0.1229	-18.272	0.001
32.	0.031	3.967	0.0029	0.0994	2.29E+02	2.3E+03	0.1226	-18.272	0.003

Number of result	Step time	Temperature	Hencky strain	Hencky rate	Stress	Elongation viscosity	Velocity	Displacement	Elongation Force
33.	0.032	3.967	0.0030	0.0991	3.42E+02	3.4E+03	0.1222	-18.272	0.005
34.	0.033	3.967	0.0031	0.0994	3.68E+02	3.7E+03	0.1226	-18.272	0.005
35.	0.034	3.967	0.0032	0.0996	3.33E+02	3.3E+03	0.1228	-18.272	0.004
36.	0.035	3.967	0.0033	0.0996	3.48E+02	3.5E+03	0.1228	-18.272	0.005
37.	0.036	3.967	0.0034	0.0995	3.87E+02	3.9E+03	0.1227	-18.272	0.005
38.	0.037	3.967	0.0035	0.0998	3.66E+02	3.7E+03	0.1231	-18.272	0.005
39.	0.038	3.967	0.0036	0.0998	3.61E+02	3.6E+03	0.1231	-18.271	0.005
40.	0.039	3.967	0.0037	0.0999	3.59E+02	3.6E+03	0.1232	-18.271	0.005
41.	0.040	3.967	0.0038	0.1003	2.92E+02	2.9E+03	0.1237	-18.271	0.004
42.	0.042	3.967	0.0039	0.1005	1.46E+02	1.5E+03	0.1239	-18.271	0.002
43.	0.044	3.967	0.0042	0.0998	2.87E+02	2.9E+03	0.1231	-18.271	0.004
44.	0.046	3.967	0.0044	0.1001	2.61E+02	2.6E+03	0.1234	-18.270	0.003
45.	0.048	3.967	0.0046	0.1009	1.99E+01	2.0E+02	0.1245	-18.270	0.000
46.	0.050	3.967	0.0048	0.1000	6.84E+01	6.8E+02	0.1233	-18.270	0.001
47.	0.052	3.967	0.0050	0.0995	2.83E+02	2.8E+03	0.1227	-18.270	0.004
48.	0.054	3.967	0.0052	0.0998	2.73E+02	2.7E+03	0.1231	-18.269	0.004
49.	0.056	3.967	0.0054	0.0997	2.72E+02	2.7E+03	0.1230	-18.269	0.004
50.	0.058	3.967	0.0056	0.0994	4.21E+02	4.2E+03	0.1226	-18.269	0.006
51.	0.060	3.967	0.0058	0.0998	4.01E+02	4.0E+03	0.1231	-18.269	0.005
52.	0.062	3.967	0.0060	0.1007	1.91E+02	1.9E+03	0.1242	-18.268	0.003
53.	0.065	3.967	0.0062	0.1003	1.14E+02	1.1E+03	0.1237	-18.268	0.002
54.	0.067	3.967	0.0064	0.0998	2.91E+02	2.9E+03	0.1231	-18.268	0.004
55.	0.069	3.967	0.0066	0.1003	1.67E+02	1.7E+03	0.1237	-18.268	0.002
56.	0.071	3.967	0.0068	0.1001	1.48E+02	1.5E+03	0.1234	-18.267	0.002
57.	0.073	3.967	0.0070	0.0992	3.89E+02	3.9E+03	0.1223	-18.267	0.005
58.	0.075	3.967	0.0072	0.0995	4.77E+02	4.8E+03	0.1227	-18.267	0.006
59.	0.077	3.967	0.0074	0.1004	2.51E+02	2.5E+03	0.1238	-18.267	0.003
60.	0.079	3.967	0.0076	0.0995	4.16E+02	4.2E+03	0.1227	-18.266	0.006
61.	0.081	3.967	0.0078	0.1002	3.68E+02	3.7E+03	0.1235	-18.266	0.005
62.	0.083	3.967	0.0080	0.1007	1.33E+02	1.3E+03	0.1242	-18.266	0.002
63.	0.085	3.967	0.0082	0.0999	2.48E+02	2.5E+03	0.1232	-18.266	0.003
64.	0.087	3.967	0.0085	0.1003	2.50E+02	2.5E+03	0.1236	-18.265	0.003
65.	0.089	3.967	0.0087	0.1012	-8.79E+01	-8.7E+02	0.1248	-18.265	-0.001
66.	0.091	3.967	0.0089	0.0999	3.78E+01	3.8E+02	0.1232	-18.265	0.001
67.	0.093	3.967	0.0091	0.0990	3.84E+02	3.9E+03	0.1220	-18.265	0.005

Number of result	Step time	Temperature	Hencky strain	Hencky rate	Stress	Elongation viscosity	Velocity	Displacement	Elongation Force
68.	0.095	3.967	0.0093	0.0993	4.38E+02	4.4E+03	0.1225	-18.264	0.006
69.	0.097	3.967	0.0095	0.0998	3.62E+02	3.6E+03	0.1231	-18.264	0.005
70.	0.099	3.967	0.0097	0.0997	4.07E+02	4.1E+03	0.1229	-18.264	0.005
71.	0.101	3.967	0.0099	0.1003	3.27E+02	3.3E+03	0.1237	-18.264	0.004
72.	0.103	3.967	0.0101	0.1013	-2.22E+01	-2.2E+02	0.1248	-18.263	0.000
73.	0.106	3.967	0.0103	0.1001	8.37E+01	8.4E+02	0.1234	-18.263	0.001
74.	0.108	3.967	0.0105	0.1000	2.09E+02	2.1E+03	0.1233	-18.263	0.003
75.	0.110	3.967	0.0107	0.1003	6.00E+01	6.0E+02	0.1237	-18.263	0.001
76.	0.112	3.967	0.0109	0.0995	2.25E+02	2.3E+03	0.1227	-18.262	0.003
77.	0.114	3.967	0.0111	0.0992	4.26E+02	4.3E+03	0.1223	-18.262	0.006
78.	0.116	3.967	0.0113	0.0997	4.00E+02	4.0E+03	0.1229	-18.262	0.005
79.	0.118	3.967	0.0115	0.1000	3.32E+02	3.3E+03	0.1233	-18.262	0.004
80.	0.120	3.967	0.0117	0.1003	2.43E+02	2.4E+03	0.1237	-18.261	0.003
81.	0.122	3.967	0.0119	0.1008	8.31E+01	8.2E+02	0.1242	-18.261	0.001
82.	0.125	3.967	0.0122	0.1002	7.89E+01	7.9E+02	0.1235	-18.261	0.001
83.	0.129	3.967	0.0127	0.1001	1.75E+02	1.8E+03	0.1234	-18.260	0.002
84.	0.133	3.967	0.0131	0.0996	2.50E+02	2.5E+03	0.1228	-18.260	0.003
85.	0.137	3.967	0.0135	0.1002	1.66E+02	1.7E+03	0.1235	-18.259	0.002
86.	0.141	3.967	0.0139	0.0998	2.73E+02	2.7E+03	0.1230	-18.259	0.004
87.	0.145	3.967	0.0143	0.0998	2.62E+02	2.6E+03	0.1231	-18.258	0.003
88.	0.150	3.967	0.0147	0.1004	1.92E+02	1.9E+03	0.1238	-18.258	0.003
89.	0.154	3.967	0.0151	0.1000	1.47E+02	1.5E+03	0.1233	-18.257	0.002
90.	0.158	3.967	0.0155	0.0999	1.93E+02	1.9E+03	0.1231	-18.257	0.003
91.	0.162	3.967	0.0159	0.0997	3.48E+02	3.5E+03	0.1230	-18.256	0.005
92.	0.166	3.967	0.0163	0.0999	2.90E+02	2.9E+03	0.1232	-18.256	0.004
93.	0.170	3.967	0.0167	0.1005	1.73E+02	1.7E+03	0.1240	-18.255	0.002
94.	0.174	3.967	0.0172	0.1000	1.53E+02	1.5E+03	0.1233	-18.255	0.002
95.	0.178	3.967	0.0176	0.1001	1.82E+02	1.8E+03	0.1234	-18.254	0.002
96.	0.182	3.967	0.0180	0.0997	2.65E+02	2.7E+03	0.1229	-18.254	0.003
97.	0.186	3.967	0.0184	0.0998	3.00E+02	3.0E+03	0.1230	-18.253	0.004
98.	0.190	3.967	0.0188	0.1006	1.30E+02	1.3E+03	0.1240	-18.253	0.002
99.	0.195	3.967	0.0192	0.0999	1.78E+02	1.8E+03	0.1232	-18.252	0.002
100.	0.199	3.967	0.0196	0.1000	1.43E+02	1.4E+03	0.1233	-18.252	0.002
101.	0.203	3.967	0.0200	0.0998	2.75E+02	2.8E+03	0.1230	-18.251	0.004
102.	0.207	3.967	0.0204	0.0996	3.39E+02	3.4E+03	0.1227	-18.251	0.004

Number of result	Step time	Temperature	Hencky strain	Hencky rate	Stress	Elongation viscosity	Velocity	Displacement	Elongation Force
103.	0.211	3.967	0.0208	0.1005	1.99E+02	2.0E+03	0.1240	-18.250	0.003
104.	0.215	3.967	0.0213	0.1002	1.41E+02	1.4E+03	0.1235	-18.250	0.002
105.	0.219	3.967	0.0217	0.1002	6.96E+01	6.9E+02	0.1235	-18.249	0.001
106.	0.223	3.967	0.0221	0.0990	4.86E+02	4.9E+03	0.1221	-18.249	0.006
107.	0.227	3.967	0.0225	0.1000	3.96E+02	4.0E+03	0.1233	-18.248	0.005
108.	0.231	3.967	0.0229	0.1013	-8.10E+01	-8.0E+02	0.1250	-18.248	-0.001
109.	0.236	3.967	0.0233	0.0994	2.00E+02	2.0E+03	0.1226	-18.247	0.003
110.	0.240	3.967	0.0237	0.0995	3.28E+02	3.3E+03	0.1227	-18.247	0.004
111.	0.244	3.967	0.0241	0.1000	4.17E+02	4.2E+03	0.1233	-18.246	0.005
112.	0.248	3.967	0.0245	0.1007	2.25E+01	2.2E+02	0.1241	-18.246	0.000
113.	0.252	3.967	0.0249	0.1004	-1.77E+01	-1.8E+02	0.1238	-18.245	0.000
114.	0.256	3.967	0.0253	0.0993	3.20E+02	3.2E+03	0.1224	-18.245	0.004
115.	0.260	3.967	0.0258	0.0997	3.49E+02	3.5E+03	0.1229	-18.244	0.005
116.	0.264	3.967	0.0262	0.1003	2.25E+02	2.2E+03	0.1237	-18.244	0.003
117.	0.268	3.967	0.0266	0.1001	1.69E+02	1.7E+03	0.1235	-18.243	0.002
118.	0.272	3.967	0.0270	0.1002	1.15E+02	1.1E+03	0.1236	-18.243	0.001
119.	0.277	3.967	0.0274	0.0993	4.22E+02	4.3E+03	0.1224	-18.242	0.006
120.	0.281	3.967	0.0278	0.1005	1.40E+02	1.4E+03	0.1239	-18.242	0.002
121.	0.285	3.967	0.0282	0.0997	3.28E+02	3.3E+03	0.1230	-18.241	0.004
122.	0.291	3.967	0.0288	0.1000	2.29E+02	2.3E+03	0.1234	-18.240	0.003
123.	0.299	3.967	0.0297	0.1002	2.04E+02	2.0E+03	0.1235	-18.239	0.003
124.	0.307	3.967	0.0305	0.0996	3.36E+02	3.4E+03	0.1228	-18.238	0.004
125.	0.315	3.967	0.0313	0.1005	9.55E+01	9.5E+02	0.1239	-18.237	0.001
126.	0.324	3.971	0.0321	0.0995	3.15E+02	3.2E+03	0.1227	-18.236	0.004
127.	0.332	3.971	0.0329	0.1006	1.10E+02	1.1E+03	0.1241	-18.235	0.001
128.	0.340	3.971	0.0337	0.0994	3.14E+02	3.2E+03	0.1226	-18.234	0.004
129.	0.348	3.971	0.0346	0.1003	2.58E+02	2.6E+03	0.1237	-18.233	0.003
130.	0.356	3.971	0.0354	0.0997	2.03E+02	2.0E+03	0.1230	-18.232	0.003
131.	0.365	3.971	0.0362	0.1002	2.59E+02	2.6E+03	0.1235	-18.231	0.003
132.	0.373	3.971	0.0370	0.1002	9.72E+01	9.7E+02	0.1235	-18.230	0.001
133.	0.381	3.971	0.0378	0.0998	3.28E+02	3.3E+03	0.1230	-18.229	0.004
134.	0.389	3.971	0.0387	0.1000	1.97E+02	2.0E+03	0.1233	-18.228	0.003
135.	0.397	3.971	0.0395	0.1000	2.79E+02	2.8E+03	0.1233	-18.227	0.004
136.	0.406	3.971	0.0403	0.1000	1.78E+02	1.8E+03	0.1233	-18.226	0.002
137.	0.414	3.971	0.0411	0.1000	2.91E+02	2.9E+03	0.1233	-18.225	0.004

Number of result	Step time	Temperature	Hencky strain	Hencky rate	Stress	Elongation viscosity	Velocity	Displacement	Elongation Force
138.	0.422	3.971	0.0419	0.1003	3.18E+00	3.2E+01	0.1237	-18.224	0.000
139.	0.430	3.971	0.0428	0.0995	4.30E+02	4.3E+03	0.1227	-18.223	0.006
140.	0.438	3.971	0.0436	0.1004	3.49E+01	3.5E+02	0.1238	-18.222	0.000
141.	0.446	3.971	0.0444	0.0996	4.13E+02	4.1E+03	0.1228	-18.221	0.005
142.	0.455	3.971	0.0452	0.1005	1.04E+02	1.0E+03	0.1239	-18.220	0.001
143.	0.463	3.971	0.0460	0.0996	2.69E+02	2.7E+03	0.1228	-18.219	0.003
144.	0.471	3.971	0.0469	0.1002	2.76E+02	2.8E+03	0.1236	-18.218	0.004
145.	0.479	3.971	0.0477	0.1000	1.88E+02	1.9E+03	0.1232	-18.217	0.002
146.	0.487	3.971	0.0485	0.1000	2.30E+02	2.3E+03	0.1233	-18.216	0.003
147.	0.496	3.971	0.0493	0.0998	2.82E+02	2.8E+03	0.1231	-18.215	0.004
148.	0.504	3.971	0.0501	0.1003	1.74E+02	1.7E+03	0.1236	-18.214	0.002
149.	0.512	3.971	0.0509	0.0997	3.71E+02	3.7E+03	0.1229	-18.213	0.005
150.	0.520	3.971	0.0518	0.1005	1.52E+02	1.5E+03	0.1239	-18.212	0.002
151.	0.528	3.971	0.0526	0.0995	2.92E+02	2.9E+03	0.1226	-18.211	0.004
152.	0.537	3.971	0.0534	0.1004	2.54E+02	2.5E+03	0.1237	-18.210	0.003
153.	0.545	3.971	0.0542	0.1000	5.93E+01	5.9E+02	0.1233	-18.209	0.001
154.	0.553	3.971	0.0550	0.0998	4.66E+02	4.7E+03	0.1230	-18.208	0.006
155.	0.561	3.971	0.0559	0.1003	8.94E+01	8.9E+02	0.1236	-18.207	0.001
156.	0.569	3.971	0.0567	0.0996	4.61E+02	4.6E+03	0.1228	-18.206	0.006
157.	0.578	3.971	0.0575	0.1006	2.94E+01	2.9E+02	0.1241	-18.205	0.000
158.	0.586	3.971	0.0583	0.0995	3.30E+02	3.3E+03	0.1227	-18.204	0.004
159.	0.594	3.971	0.0591	0.1004	1.63E+02	1.6E+03	0.1238	-18.203	0.002
160.	0.602	3.971	0.0600	0.0998	2.61E+02	2.6E+03	0.1231	-18.202	0.003
161.	0.610	3.971	0.0608	0.0999	2.64E+02	2.6E+03	0.1232	-18.201	0.003
162.	0.623	3.971	0.0620	0.1001	2.23E+02	2.2E+03	0.1234	-18.199	0.003
163.	0.639	3.971	0.0636	0.1001	2.79E+02	2.8E+03	0.1234	-18.197	0.004
164.	0.655	3.971	0.0653	0.1000	3.14E+02	3.1E+03	0.1233	-18.195	0.004
165.	0.672	3.971	0.0669	0.1000	3.08E+02	3.1E+03	0.1232	-18.193	0.004
166.	0.688	3.971	0.0686	0.0999	2.32E+02	2.3E+03	0.1232	-18.191	0.003
167.	0.705	3.971	0.0702	0.1000	2.16E+02	2.2E+03	0.1233	-18.189	0.003
168.	0.721	3.971	0.0718	0.1002	2.48E+02	2.5E+03	0.1235	-18.187	0.003
169.	0.737	3.977	0.0735	0.0998	2.93E+02	2.9E+03	0.1230	-18.185	0.004
170.	0.754	3.977	0.0751	0.1000	2.58E+02	2.6E+03	0.1234	-18.183	0.003
171.	0.770	3.977	0.0768	0.0999	2.52E+02	2.5E+03	0.1232	-18.181	0.003
172.	0.786	3.977	0.0784	0.1001	1.94E+02	1.9E+03	0.1234	-18.179	0.002

Number of result	Step time	Temperature	Hencky strain	Hencky rate	Stress	Elongation viscosity	Velocity	Displacement	Elongation Force
173.	0.803	3.977	0.0800	0.1002	2.15E+02	2.1E+03	0.1235	-18.177	0.003
174.	0.819	3.977	0.0817	0.0999	3.08E+02	3.1E+03	0.1232	-18.175	0.004
175.	0.836	3.977	0.0833	0.0997	4.18E+02	4.2E+03	0.1230	-18.173	0.005
176.	0.852	3.977	0.0849	0.0999	6.56E+02	6.6E+03	0.1231	-18.171	0.008
177.	0.868	3.977	0.0866	0.1000	5.03E+02	5.0E+03	0.1233	-18.169	0.006
178.	0.885	3.977	0.0882	0.0984	1.41E+03	1.4E+04	0.1214	-18.167	0.017
179.	0.901	3.977	0.0898	0.0943	6.44E+03	6.8E+04	0.1163	-18.165	0.079
180.	0.918	3.977	0.0913	0.0939	1.18E+04	1.3E+05	0.1158	-18.163	0.144
181.	0.934	3.977	0.0928	0.0897	2.27E+04	2.5E+05	0.1106	-18.161	0.277
182.	0.950	3.977	0.0943	0.0922	3.11E+04	3.4E+05	0.1136	-18.160	0.379
183.	0.967	3.977	0.0958	0.0908	4.04E+04	4.5E+05	0.1119	-18.158	0.493
184.	0.983	3.977	0.0973	0.0884	5.18E+04	5.9E+05	0.1089	-18.156	0.630
185.	0.999	3.977	0.0987	0.0851	6.66E+04	7.8E+05	0.1049	-18.154	0.809
186.	1.016	3.977	0.1001	0.0836	8.35E+04	1.0E+06	0.1031	-18.152	1.013
187.	1.032	3.977	0.1014	0.0815	1.02E+05	1.3E+06	0.1005	-18.151	1.241
188.	1.049	3.977	0.1028	0.0808	1.23E+05	1.5E+06	0.0996	-18.149	1.485
189.	1.065	3.977	0.1041	0.0808	1.43E+05	1.8E+06	0.0996	-18.148	1.730
190.	1.081	3.977	0.1054	0.0810	1.63E+05	2.0E+06	0.0999	-18.146	1.973
191.	1.098	3.977	0.1067	0.0814	1.83E+05	2.3E+06	0.1004	-18.144	2.211
192.	1.114	3.977	0.1081	0.0819	2.03E+05	2.5E+06	0.1010	-18.143	2.442
193.	1.131	3.977	0.1094	0.0823	2.22E+05	2.7E+06	0.1015	-18.141	2.669
194.	1.147	3.977	0.1108	0.0827	2.41E+05	2.9E+06	0.1020	-18.139	2.891
195.	1.163	3.983	0.1121	0.0831	2.59E+05	3.1E+06	0.1025	-18.138	3.107
196.	1.180	3.983	0.1135	0.0837	2.77E+05	3.3E+06	0.1032	-18.136	3.317
197.	1.196	3.983	0.1149	0.0840	2.95E+05	3.5E+06	0.1036	-18.134	3.522
198.	1.212	3.983	0.1163	0.0844	3.12E+05	3.7E+06	0.1040	-18.132	3.721
199.	1.229	3.983	0.1176	0.0844	3.29E+05	3.9E+06	0.1041	-18.131	3.920
200.	1.245	3.983	0.1190	0.0847	3.46E+05	4.1E+06	0.1044	-18.129	4.116
201.	1.262	3.983	0.1204	0.0846	3.63E+05	4.3E+06	0.1043	-18.127	4.312
202.	1.286	3.983	0.1225	0.0852	3.88E+05	4.5E+06	0.1051	-18.125	4.598
203.	1.319	3.983	0.1253	0.0860	4.19E+05	4.9E+06	0.1061	-18.121	4.963
204.	1.352	3.983	0.1281	0.0866	4.50E+05	5.2E+06	0.1068	-18.118	5.307
205.	1.384	3.983	0.1310	0.0876	4.79E+05	5.5E+06	0.1081	-18.114	5.635
206.	1.417	3.983	0.1339	0.0897	5.04E+05	5.6E+06	0.1106	-18.111	5.916
207.	1.450	3.983	0.1368	0.0886	5.30E+05	6.0E+06	0.1093	-18.107	6.195

Number of result	Step time	Temperature	Hencky strain	Hencky rate	Stress	Elongation viscosity	Velocity	Displacement	Elongation Force
208.	1.483	3.983	0.1397	0.0895	5.55E+05	6.2E+06	0.1103	-18.104	6.471
209.	1.516	3.983	0.1427	0.0902	5.79E+05	6.4E+06	0.1112	-18.100	6.727
210.	1.548	3.991	0.1456	0.0909	6.01E+05	6.6E+06	0.1121	-18.096	6.966
211.	1.581	3.991	0.1486	0.0913	6.22E+05	6.8E+06	0.1126	-18.093	7.191
212.	1.614	3.991	0.1516	0.0921	6.42E+05	7.0E+06	0.1136	-18.089	7.399
213.	1.647	3.991	0.1547	0.0927	6.61E+05	7.1E+06	0.1143	-18.085	7.592
214.	1.679	3.991	0.1577	0.0933	6.78E+05	7.3E+06	0.1151	-18.081	7.767
215.	1.712	3.991	0.1608	0.0937	6.95E+05	7.4E+06	0.1155	-18.078	7.933
216.	1.745	3.991	0.1638	0.0927	7.12E+05	7.7E+06	0.1142	-18.074	8.106
217.	1.778	3.991	0.1669	0.0921	7.32E+05	7.9E+06	0.1136	-18.070	8.305
218.	1.810	3.991	0.1699	0.0925	7.51E+05	8.1E+06	0.1141	-18.066	8.499
219.	1.843	3.991	0.1729	0.0925	7.70E+05	8.3E+06	0.1141	-18.063	8.690
220.	1.876	3.991	0.1760	0.0934	7.88E+05	8.4E+06	0.1152	-18.059	8.868
221.	1.909	3.991	0.1790	0.0939	8.05E+05	8.6E+06	0.1158	-18.055	9.026
222.	1.942	3.996	0.1821	0.0946	8.21E+05	8.7E+06	0.1166	-18.051	9.172
223.	1.974	3.996	0.1852	0.0947	8.35E+05	8.8E+06	0.1168	-18.047	9.308
224.	2.007	3.996	0.1883	0.0948	8.50E+05	9.0E+06	0.1169	-18.044	9.441
225.	2.040	3.996	0.1914	0.0950	8.64E+05	9.1E+06	0.1171	-18.040	9.570
226.	2.073	3.996	0.1945	0.0948	8.79E+05	9.3E+06	0.1169	-18.036	9.702
227.	2.105	3.996	0.1977	0.0949	8.93E+05	9.4E+06	0.1171	-18.032	9.831
228.	2.138	3.996	0.2008	0.0952	9.08E+05	9.5E+06	0.1173	-18.028	9.958
229.	2.171	3.996	0.2039	0.0952	9.22E+05	9.7E+06	0.1174	-18.024	10.080
230.	2.204	3.996	0.2070	0.0952	9.36E+05	9.8E+06	0.1174	-18.021	10.200
231.	2.236	3.996	0.2101	0.0951	9.50E+05	1.0E+07	0.1172	-18.017	10.325
232.	2.269	3.996	0.2132	0.0951	9.64E+05	1.0E+07	0.1173	-18.013	10.449
233.	2.302	3.996	0.2164	0.0956	9.78E+05	1.0E+07	0.1179	-18.009	10.567
234.	2.335	3.996	0.2195	0.0962	9.91E+05	1.0E+07	0.1186	-18.005	10.668
235.	2.368	4.004	0.2227	0.0966	1.00E+06	1.0E+07	0.1191	-18.001	10.760
236.	2.400	4.004	0.2258	0.0965	1.01E+06	1.0E+07	0.1190	-17.997	10.847
237.	2.433	4.004	0.2290	0.0970	1.02E+06	1.1E+07	0.1196	-17.993	10.926
238.	2.466	4.004	0.2322	0.0971	1.03E+06	1.1E+07	0.1197	-17.990	11.002
239.	2.499	4.004	0.2354	0.0974	1.04E+06	1.1E+07	0.1201	-17.986	11.073
240.	2.531	4.004	0.2386	0.0976	1.05E+06	1.1E+07	0.1204	-17.982	11.136
241.	2.564	4.004	0.2418	0.0979	1.06E+06	1.1E+07	0.1207	-17.978	11.191
242.	2.613	4.004	0.2466	0.0975	1.08E+06	1.1E+07	0.1202	-17.972	11.278

Number of result	Step time	Temperature	Hencky strain	Hencky rate	Stress	Elongation viscosity	Velocity	Displacement	Elongation Force
243.	2.679	4.004	0.2530	0.0974	1.10E+06	1.1E+07	0.1202	-17.964	11.408
244.	2.744	4.013	0.2593	0.0961	1.12E+06	1.2E+07	0.1185	-17.956	11.574
245.	2.810	4.013	0.2656	0.0967	1.15E+06	1.2E+07	0.1192	-17.948	11.777
246.	2.875	4.013	0.2720	0.0982	1.16E+06	1.2E+07	0.1211	-17.940	11.889
247.	2.941	4.013	0.2784	0.0986	1.18E+06	1.2E+07	0.1216	-17.933	11.970
248.	3.007	4.013	0.2849	0.0992	1.19E+06	1.2E+07	0.1224	-17.925	12.020
249.	3.072	4.013	0.2914	0.0992	1.20E+06	1.2E+07	0.1223	-17.916	12.059
250.	3.138	4.013	0.2979	0.0986	1.22E+06	1.2E+07	0.1216	-17.908	12.117
251.	3.203	4.012	0.3044	0.0992	1.23E+06	1.2E+07	0.1223	-17.901	12.174
252.	3.269	4.012	0.3109	0.0999	1.24E+06	1.2E+07	0.1232	-17.892	12.192
253.	3.334	4.012	0.3175	0.1003	1.25E+06	1.2E+07	0.1236	-17.884	12.186
254.	3.400	4.012	0.3241	0.1008	1.25E+06	1.2E+07	0.1243	-17.876	12.156
255.	3.465	4.012	0.3307	0.1006	1.26E+06	1.2E+07	0.1241	-17.868	12.112
256.	3.531	4.012	0.3373	0.1004	1.26E+06	1.3E+07	0.1238	-17.860	12.096
257.	3.596	4.012	0.3438	0.0999	1.27E+06	1.3E+07	0.1232	-17.852	12.078
258.	3.662	4.012	0.3503	0.0979	1.29E+06	1.3E+07	0.1207	-17.844	12.141
259.	3.727	4.012	0.3568	0.0995	1.30E+06	1.3E+07	0.1226	-17.836	12.224
260.	3.793	4.012	0.3633	0.1009	1.31E+06	1.3E+07	0.1244	-17.828	12.200
261.	3.858	4.012	0.3700	0.1016	1.31E+06	1.3E+07	0.1253	-17.820	12.132
262.	3.924	4.012	0.3766	0.1015	1.31E+06	1.3E+07	0.1252	-17.811	12.044
263.	3.990	4.015	0.3833	0.1003	1.31E+06	1.3E+07	0.1236	-17.803	12.002
264.	4.055	4.015	0.3898	0.0994	1.32E+06	1.3E+07	0.1226	-17.795	12.019
265.	4.121	4.015	0.3963	0.1000	1.33E+06	1.3E+07	0.1233	-17.787	12.030
266.	4.186	4.015	0.4029	0.1001	1.34E+06	1.3E+07	0.1234	-17.779	12.028
267.	4.252	4.015	0.4095	0.1006	1.35E+06	1.3E+07	0.1241	-17.771	12.010
268.	4.317	4.015	0.4161	0.1004	1.35E+06	1.3E+07	0.1238	-17.763	11.974
269.	4.383	4.011	0.4226	0.1005	1.36E+06	1.4E+07	0.1239	-17.755	11.962
270.	4.448	4.011	0.4292	0.1001	1.37E+06	1.4E+07	0.1234	-17.747	11.935
271.	4.514	4.011	0.4357	0.0981	1.38E+06	1.4E+07	0.1210	-17.739	11.986
272.	4.579	4.011	0.4422	0.0992	1.40E+06	1.4E+07	0.1223	-17.731	12.073
273.	4.645	4.011	0.4487	0.1004	1.41E+06	1.4E+07	0.1238	-17.723	12.071
274.	4.710	4.011	0.4553	0.1006	1.42E+06	1.4E+07	0.1240	-17.714	12.047
275.	4.776	4.006	0.4619	0.1002	1.42E+06	1.4E+07	0.1235	-17.706	12.024
276.	4.842	4.006	0.4684	0.0993	1.43E+06	1.4E+07	0.1224	-17.698	12.037
277.	4.907	4.006	0.4749	0.0991	1.45E+06	1.5E+07	0.1221	-17.690	12.089

Number of result	Step time	Temperature	Hencky strain	Hencky rate	Stress	Elongation viscosity	Velocity	Displacement	Elongation Force
278.	4.973	4.006	0.4814	0.0997	1.46E+06	1.5E+07	0.1229	-17.682	12.119
279.	5.038	4.006	0.4880	0.1004	1.47E+06	1.5E+07	0.1238	-17.674	12.117
280.	5.104	4.006	0.4946	0.1010	1.48E+06	1.5E+07	0.1246	-17.666	12.081
281.	5.169	4.006	0.5012	0.1010	1.48E+06	1.5E+07	0.1245	-17.658	12.019
282.	5.267	4.003	0.5111	0.0998	1.49E+06	1.5E+07	0.1230	-17.646	11.995
283.	5.399	4.003	0.5241	0.0992	1.52E+06	1.5E+07	0.1224	-17.630	12.082
284.	5.530	4.003	0.5372	0.1007	1.54E+06	1.5E+07	0.1242	-17.613	12.066
285.	5.661	4.006	0.5504	0.1002	1.55E+06	1.5E+07	0.1236	-17.597	11.999
286.	5.792	4.006	0.5634	0.0996	1.58E+06	1.6E+07	0.1229	-17.581	12.035
287.	5.923	4.006	0.5766	0.1010	1.59E+06	1.6E+07	0.1245	-17.565	12.000
288.	6.054	4.006	0.5899	0.1010	1.60E+06	1.6E+07	0.1246	-17.549	11.874
289.	6.185	4.006	0.6030	0.0989	1.62E+06	1.6E+07	0.1220	-17.532	11.860
290.	6.316	4.006	0.6160	0.1000	1.65E+06	1.7E+07	0.1233	-17.516	11.960
291.	6.447	4.001	0.6291	0.1008	1.67E+06	1.7E+07	0.1243	-17.500	11.911
292.	6.578	4.001	0.6423	0.1002	1.68E+06	1.7E+07	0.1236	-17.484	11.865
293.	6.709	4.001	0.6555	0.1013	1.69E+06	1.7E+07	0.1249	-17.468	11.779
294.	6.840	3.999	0.6688	0.1014	1.69E+06	1.7E+07	0.1250	-17.451	11.633
295.	6.971	3.999	0.6821	0.1005	1.70E+06	1.7E+07	0.1239	-17.435	11.533
296.	7.103	3.999	0.6951	0.0989	1.73E+06	1.8E+07	0.1219	-17.419	11.610
297.	7.234	3.998	0.7082	0.1008	1.76E+06	1.7E+07	0.1243	-17.403	11.600
298.	7.365	3.998	0.7214	0.1002	1.77E+06	1.8E+07	0.1236	-17.386	11.540
299.	7.496	3.998	0.7345	0.1005	1.79E+06	1.8E+07	0.1240	-17.370	11.519
300.	7.627	3.994	0.7477	0.1014	1.80E+06	1.8E+07	0.1251	-17.354	11.412
301.	7.758	3.994	0.7610	0.1011	1.80E+06	1.8E+07	0.1246	-17.337	11.273
302.	7.889	3.994	0.7742	0.0992	1.82E+06	1.8E+07	0.1223	-17.321	11.246
303.	8.020	3.983	0.7872	0.1007	1.85E+06	1.8E+07	0.1242	-17.305	11.283
304.	8.151	3.983	0.8005	0.1013	1.85E+06	1.8E+07	0.1248	-17.289	11.162
305.	8.282	3.983	0.8137	0.0999	1.87E+06	1.9E+07	0.1232	-17.273	11.103
306.	8.413	3.981	0.8268	0.1011	1.89E+06	1.9E+07	0.1246	-17.256	11.069
307.	8.544	3.981	0.8401	0.1015	1.89E+06	1.9E+07	0.1251	-17.240	10.915
308.	8.675	3.981	0.8534	0.1000	1.90E+06	1.9E+07	0.1234	-17.224	10.828
309.	8.806	3.981	0.8664	0.0996	1.93E+06	1.9E+07	0.1228	-17.208	10.903
310.	8.938	3.981	0.8795	0.1007	1.95E+06	1.9E+07	0.1242	-17.191	10.857
311.	9.069	3.981	0.8927	0.0997	1.97E+06	2.0E+07	0.1230	-17.175	10.818
312.	9.200	3.981	0.9058	0.1004	2.00E+06	2.0E+07	0.1238	-17.159	10.838

Number of result	Step time	Temperature	Hencky strain	Hencky rate	Stress	Elongation viscosity	Velocity	Displacement	Elongation Force
313.	9.331	3.978	0.9190	0.1011	2.01E+06	2.0E+07	0.1247	-17.143	10.754
314.	9.462	3.978	0.9322	0.1008	2.02E+06	2.0E+07	0.1243	-17.126	10.651
315.	9.593	3.978	0.9453	0.0989	2.04E+06	2.1E+07	0.1219	-17.110	10.653
316.	9.724	3.969	0.9584	0.1008	2.08E+06	2.1E+07	0.1243	-17.094	10.690
317.	9.855	3.969	0.9716	0.1011	2.08E+06	2.1E+07	0.1246	-17.078	10.582
318.	9.986	3.969	0.9848	0.1004	2.10E+06	2.1E+07	0.1237	-17.062	10.513
319.	10.117	3.969	0.9980	0.1010	2.11E+06	2.1E+07	0.1245	-17.045	10.447
320.	10.248	3.969	1.0113	0.1009	2.12E+06	2.1E+07	0.1244	-17.029	10.342
321.	10.379	3.969	1.0244	0.0999	2.14E+06	2.1E+07	0.1232	-17.013	10.298
322.	10.576	3.969	1.0440	0.0997	2.20E+06	2.2E+07	0.1230	-16.989	10.400
323.	10.838	3.967	1.0702	0.1001	2.26E+06	2.3E+07	0.1235	-16.956	10.384
324.	11.100	3.967	1.0966	0.1008	2.29E+06	2.3E+07	0.1243	-16.924	10.244
325.	11.362	3.962	1.1228	0.0998	2.35E+06	2.4E+07	0.1231	-16.891	10.262
326.	11.625	3.963	1.1491	0.1001	2.40E+06	2.4E+07	0.1234	-16.859	10.196
327.	11.887	3.963	1.1754	0.1006	2.45E+06	2.4E+07	0.1240	-16.827	10.138
328.	12.149	3.969	1.2015	0.0991	2.52E+06	2.5E+07	0.1222	-16.794	10.173
329.	12.411	3.969	1.2277	0.1003	2.60E+06	2.6E+07	0.1237	-16.762	10.206
330.	12.673	3.968	1.2540	0.1008	2.65E+06	2.6E+07	0.1242	-16.730	10.134
331.	12.935	3.964	1.2803	0.0993	2.71E+06	2.7E+07	0.1224	-16.697	10.091
332.	13.197	3.964	1.3064	0.0998	2.81E+06	2.8E+07	0.1231	-16.665	10.210
333.	13.460	3.965	1.3325	0.1003	2.89E+06	2.9E+07	0.1236	-16.633	10.229
334.	13.722	3.969	1.3588	0.0992	2.95E+06	3.0E+07	0.1224	-16.600	10.178
335.	13.984	3.969	1.3848	0.0999	3.09E+06	3.1E+07	0.1231	-16.568	10.376
336.	14.246	3.97	1.4110	0.0999	3.18E+06	3.2E+07	0.1232	-16.536	10.394
337.	14.508	3.97	1.4372	0.1001	3.25E+06	3.2E+07	0.1235	-16.504	10.349
338.	14.770	3.97	1.4632	0.0988	3.40E+06	3.4E+07	0.1218	-16.472	10.554
339.	15.032	3.98	1.4893	0.0995	3.52E+06	3.5E+07	0.1227	-16.440	10.648
340.	15.295	3.986	1.5154	0.1000	3.63E+06	3.6E+07	0.1233	-16.407	10.703
341.	15.557	3.986	1.5415	0.0991	3.76E+06	3.8E+07	0.1222	-16.375	10.805
342.	15.819	3.994	1.5676	0.0993	3.91E+06	3.9E+07	0.1224	-16.343	10.931
343.	16.081	3.994	1.5936	0.0996	4.07E+06	4.1E+07	0.1228	-16.311	11.104
344.	16.343	3.997	1.6197	0.0990	4.21E+06	4.3E+07	0.1221	-16.279	11.182
345.	16.605	4.007	1.6457	0.0999	4.38E+06	4.4E+07	0.1232	-16.247	11.338
346.	16.867	4.007	1.6717	0.0989	4.55E+06	4.6E+07	0.1220	-16.215	11.471
347.	17.130	4.01	1.6977	0.0990	4.74E+06	4.8E+07	0.1221	-16.183	11.634

Number of result	Step time	Temperature	Hencky strain	Hencky rate	Stress	Elongation viscosity	Velocity	Displacement	Elongation Force
348.	17.392	4.009	1.7236	0.0992	4.97E+06	5.0E+07	0.1223	-16.151	11.897
349.	17.654	4.009	1.7497	0.0995	5.15E+06	5.2E+07	0.1226	-16.118	12.005
350.	17.916	4.008	1.7759	0.0999	5.30E+06	5.3E+07	0.1232	-16.086	12.025
351.	18.178	4.01	1.8018	0.0980	5.55E+06	5.7E+07	0.1208	-16.054	12.289
352.	18.440	4.01	1.8276	0.0989	5.83E+06	5.9E+07	0.1219	-16.022	12.565
353.	18.702	4.012	1.8536	0.0998	6.05E+06	6.1E+07	0.1231	-15.990	12.712
354.	18.965	4.008	1.8796	0.0983	6.30E+06	6.4E+07	0.1212	-15.958	12.895
355.	19.227	4.008	1.9055	0.0995	6.57E+06	6.6E+07	0.1227	-15.926	13.113
356.	19.489	4.006	1.9316	0.0998	6.80E+06	6.8E+07	0.1231	-15.894	13.218
357.	19.751	4.006	1.9577	0.0984	7.03E+06	7.1E+07	0.1213	-15.862	13.304
358.	20.013	4.004	1.9835	0.0991	7.41E+06	7.5E+07	0.1222	-15.830	13.673
359.	20.275	4.002	2.0095	0.0992	7.69E+06	7.8E+07	0.1223	-15.798	13.828
360.	20.537	4.002	2.0356	0.0998	7.93E+06	7.9E+07	0.1231	-15.766	13.885
361.	20.800	3.992	2.0615	0.0985	8.29E+06	8.4E+07	0.1214	-15.734	14.153
362.	21.193	3.989	2.1007	0.0997	8.70E+06	8.7E+07	0.1230	-15.686	14.276
363.	21.717	3.987	2.1526	0.0990	9.39E+06	9.5E+07	0.1220	-15.622	14.625
364.	22.241	3.98	2.2048	0.0995	1.00E+07	1.0E+08	0.1227	-15.557	14.802
365.	22.766	3.978	2.2570	0.0999	1.07E+07	1.1E+08	0.1232	-15.493	15.006
366.	23.290	3.982	2.3093	0.0993	1.14E+07	1.1E+08	0.1224	-15.428	15.137
367.	23.814	3.977	2.3616	0.1007	1.20E+07	1.2E+08	0.1241	-15.364	15.199
368.	24.339	3.978	2.4144	0.1007	1.24E+07	1.2E+08	0.1242	-15.299	14.896
369.	24.863	3.989	2.4673	0.1005	1.28E+07	1.3E+08	0.1239	-15.234	14.548
370.	25.387	3.993	2.5204	0.1028	1.30E+07	1.3E+08	0.1267	-15.168	14.011
371.	25.911	3.993	2.5746	0.1036	1.24E+07	1.2E+08	0.1277	-15.101	12.683
372.	26.436	3.998	2.6293	0.1052	1.13E+07	1.1E+08	0.1297	-15.034	10.905
373.	26.960	3.999	2.6865	0.1225	7.83E+06	6.4E+07	0.1511	-14.963	7.155
374.	27.484	3.987	2.7482	0.1016	-5.09E+03	-5.0E+04	0.1252	-14.887	-0.004
375.	28.009	3.982	2.8006	0.1000	-7.59E+02	-7.6E+03	0.1233	-14.823	-0.001
376.	28.533	3.978	2.8530	0.1000	9.23E+02	9.2E+03	0.1233	-14.758	0.001
377.	29.057	3.967	2.9055	0.1000	5.74E+01	5.7E+02	0.1233	-14.693	0.000
378.	29.581	3.973	2.9579	0.1000	2.85E+02	2.8E+03	0.1233	-14.629	0.000
379.	30.106	3.975	3.0103	0.1000	6.68E+02	6.7E+03	0.1233	-14.564	0.000
380.	30.630	3.971	3.0627	0.1000	-5.84E+01	-5.8E+02	0.1233	-14.499	0.000
381.	31.154	3.968	3.1152	0.1000	1.53E+03	1.5E+04	0.1233	-14.435	0.001
382.	31.679	3.964	3.1676	0.1000	1.49E+03	1.5E+04	0.1233	-14.370	0.001

Number of result	Step time	Temperature	Hencky strain	Hencky rate	Stress	Elongation viscosity	Velocity	Displacement	Elongation Force
383.	32.203	3.953	3.2200	0.1000	3.10E+03	3.1E+04	0.1233	-14.306	0.002
384.	32.727	3.954	3.2725	0.1000	1.74E+03	1.7E+04	0.1233	-14.241	0.001
385.	33.251	3.953	3.3249	0.1000	2.01E+03	2.0E+04	0.1233	-14.176	0.001